Glutathione metabolism and proteome analysis of ectomycorrhizal fungi in response to heavy metal stress

A thesis

Submitted in fulfilment of the requirements for the award of the degree of

DOCTOR OF PHILOSOPHY

IN

BIOTECHNOLOGY

By

Shikha Khullar

(Regn. No. 901400002)

Under the supervision of

Dr. M. Sudhakara Reddy

Professor

Department of Biotechnology

Thapar Institute of Engineering and Technology

Patiala-147004,

Punjab (India)

November 2020

CERTIFICATE

This is to certify that the thesis entitled **"Glutathione metabolism and proteome analysis of ectomycorrhizal fungi in response to heavy metal stress"** submitted by **Ms. Shikha Khullar** in fulfilment of the requirements for the award of the degree of **Doctor of Philosophy** in Biotechnology, Thapar Institute of Engineering and Technology, Patiala is an authentic record of candidates own independent and original research work carried out by her under my supervision and guidance.

It is also to certify that the matter embodied in this thesis has not been submitted to any other university or institute for the award of any degree.

Dr. M. Sudhakara Reddy

(Professor)

Department of Biotechnology

Thapar Institute of Engineering and Technology

Patiala-147004, Punjab, India

DECLARATION

I, hereby declare that the work presented in this thesis entitled **"Glutathione metabolism and proteome analysis of ectomycorrhizal fungi in response to heavy metal stress"** in fulfilment of the requirement for the award of the Degree of **Doctor of Philosophy** in the Department of Biotechnology, Thapar Institute of Engineering and technology , Patiala, is an authentic record of my own independent and original work carried under the supervision of **Dr. M. Sudhakara Reddy**, Professor, Department fo Biotechnology, Thapar Institute of Engineering and Technology, Patiala, India. The material embodied in this thesis has nt been submitted in parts or full in any other university or institute for the award of any degree in India or abroad.

Shikha Khullar

Shikha Khullar

(Regn No. 901400002)

Place: PATIALA

Date: 20 Feb, 2020

ACKNOWLEDGEMENT

It is easy to dream a project; it is difficult to initiate it and it is impossible to successfully lead to its final stage of completion without the presence of some important and indispensable people. This PhD was never a one man's job. Other than commitment, dedication and hard work, it demanded an extensive guidance, generous academic, financial and emotional support. In pursuit of this academic endeavour, I feel that I have been singularly fortunate because inspiration, guidance, direction, cooperation, love and care- all came my way in abundance. I feel nostalagic when I look back into the last five years and find it difficult to put into words the never-ending support and encouragement of everyone throughout these years. I take an opportunity to extend my heart felt gratitude to all those who allowed and enabled me to transform my academic dream into a successful doctoral thesis.

First and foremost, I acknowledge the grace of ***Almighty God*** *who paved my way through all the problems and provided me with the strength required to make this thesis a materiality.*

Humbly, with a profound sense of gratitude, I acknowledge my supervisor, ***Dr. M. Sudhakara Reddy,*** *Professor, Department of Biotechnology, Thapar Institute of Engineering and Technology, Patiala, for his expertise guidance, kindness, motivation and patience. His intelligent ideas, confidence imbibing attitude, splendid discussions and endless endeavour has helped me a lot in building up my personality and passion for research. No words can express my sincere and deep sense of reverence for him. Much thanks to you sir for being my beacon of light. It is to you I commit this work…*

It is my privilege to thank ***Prof. Prakash Gopalan****, Director TIET, Patiala, for providing all the amenities for the successful completion of my work. I also express my gratitude to* ***Dr. Rafat Siddique*** *Professor and Dean of Research and Sponsored Projects for providing motivating research environment during my stay in the institute.*

My sincere gratitude to my research committee members ***Dr. Vikar Handa, Dr. Manoj Baranwal*** *and* ***Dr. Haripada Bhunia*** *for their valuable suggestions, patient advice and insightful comments during the progress monitoring presentations of my PhD work, which incented me to widen my research from various perspectives.*

*I am also thankful to **Dr. Moushumi Ghosh**, Professor and Head, Department of Biotechnology, TIET, Patiala for providing all the facilities for my research work. I am also grateful to **Dr. Anil Kumar**, Professor and Head, TIFAC-CORE for his guidance, support and help and for providing me with necessary infrastructure, equipments and facilities required for my research work.*

*I also express my profound gratitude to **Dr. M. Vasundhara**, for her invaluable suggestions, constant support and guidance throughout my PhD.*

I would take this opportunity to thank all the faculty members of Department of Biotechnology, TIET, Patiala for their constant encouragement.

*A very special thanks to the non-teaching staff **Soni ji, Joga ji, Mrs. Manjula, Babban ji and Lallan ji** for their selfless services, cooperation and help. They made each and ever work convenient and effortless.*

*I acknowledge **Department of Biotechnology, Govt. of India** for sponsoring the research project (BT/PR8339/BCE/8/1045/2013) to carry out the present work.*

*Both my families withstood all the pressure of this longish period of work with great determination and concern by my side. I find it difficult to pen down my deepest sense of indebtedness towards my parents and all other family members, who soulfully provided me their constant support and right impetus to undertake the challenge of this proportion, like all other spheres of life, that I cannot measure, but will always treasure. My indubitable gratitude for the never-ending love and support of my father **Mr. Arun Kumar**, mother **Mrs. Neena Khullar**. My father is my backbone and mother is my pillar of strength. To them, I owe my wonderful today and dream-filled future.*

*I also express my sincere gratitude to my father-in-law **Mr. Anil Gupta** and mother-in-law **Mrs. Vandana Gupta,** for their understanding and patience during this phase, without which this completion would not have been possible. I consider myself lucky to have such a supporting and loving family, standing behind me with their love and care.*

*This endeavour of mine would not have seen light without the constant support of my husband **Mr. Abhay Gupta**. I feel lacunae of words to express my most heartfelt and cordial*

thanks for his constant support and encouragement, and for always having faith in me. I can proudly say that its not 'me' but its 'we', who have together achieved this milestone.

Words fail me to express my gratitude towards my loving brother ***Manurag Khullar****. I could not have asked for anything more than what I got in him. My heartfelt appreciation to his unsolicited cooperation and cheery assistance. His abundant affection, unflagging love and support were the constant source of inspiration for me.*

Sincere thanks to my grandparents, my uncle ***Rajeev Khullar****, aunt* ***Neeraj Khullar*** *and my beloved* ***Urvashi*** *and* ***Raghav,*** *who never failed to give me a boost, and made my life better in every possible way.*

I am thankful to my friends ***Harleen, Preetinder, Srishti, Charu, Nehakshi, Tania, Supriya, Shilpi, Manvi*** *and* ***Sumedha*** *for encouraging me in every endeavour of my life.*

I also express my deep gratitude to my friends and my lab-mates ***Bharti Thakur*** *and* ***Tanveer Kaur*** *for their great support, creating a friendly working atmosphere and giving me the moments to be cherished lifelong. Life at TIET has been an enjoyable experience with them. I an also grateful to my lab-mates* ***Arkadeep Mukhejee, Sumit Joshi, Amanpreet Kaur*** *and* ***Saloni*** *for their help and support.*

A very warm thanks to my lovely juniors, ***Radhika, Anuja, Tania, Alisha, Prabhleen, Eetika*** *for making a remarkable work team. More than juniors you were my friends and siblings.*

It has been a great privilege to spend these years in ***Thapar University, Patiala****. Thank you for providing me an opportunity to perform the research activities and an environment for my all-round growth.*

Last but not the least I would like to acknowledge one and all, who have helped me either directly or indirectly during my research work.

Date: 20 Feb, 2020

Place: PATIALA

Shikha Khullar

(Shikha Khullar)

LIST OF PUBLICATIONS

The following publications are the outcome of present research work.

1. **Khullar S, Reddy MS.** 2020. Arsenic toxicity and its mitigation in ectomycorrhizal fungus *Hebeloma cylindrosporum* through glutathione biosynthesis. Chemosphere. 240:124914. (***Impact factor: 5.108***)
2. **Khullar S, Sudhakara Reddy M**. 2019. Cadmium and arsenic responses in the ectomycorrhizal fungus *Laccaria bicolor*: glutathione metabolism and its role in metal (loid) homeostasis. Environmental Microbiology Reports. 11:53-61. **(*Impact factor: 2.874*)**
3. **Khullar S, Reddy MS**. 2019. Cadmium induced glutathione bioaccumulation mediated by γ-glutamylcysteine synthetase in ectomycorrhizal fungus *Hebeloma cylindrosporum*. BioMetals. 32:101-110. **(*Impact factor: 2.455*)**
4. **Khullar S, Reddy MS.** 2019. Ectomycorrhizal diversity and tree sustainability. InMicrobial Diversity in Ecosystem Sustainability and Biotechnological Applications. (pp. 145-166). Springer, Singapore.
5. **Khullar S, Reddy MS.** 2018. Ectomycorrhizal fungi and its role in metal homeostasis through metallothionein and glutathione mechanisms. Current Biotechnology. 7:231-241.

LIST OF CONFERENCES

1. **Khullar S, Reddy MS.** 2017. Ectomycorrhizal fungi and their role in heavy metal detoxification. In International conference on emerging trends in biotechnology for waste conversion (ETBWC-2017), XIV Annual convention of biotech research society India, CSIR-NEERI, Nagpur.
2. **Khullar S, Reddy MS.** 2016. Characterization of glutathione synthesizing genes in ectomycorrhizal fungus *Laccaria bicolor*. In National conference on Emerging trends in fungal biology and plant protection, Centre of advanced study in botany Banaras Hindu University, Varanasi.
3. **Khullar S, Reddy MS.** 2016. Metal homeostasis in ectomycorrhizal fungus *Hebeloma cylindrosporum* through glutathione biosynthesis. In National conference on fungal biotechnology, Birla Institute of Scientific Research, Jaipur
4. **Khullar S, Reddy MS.** 2016. γ-glutamylcysteine Synthetase - the key ingredient of metal homeostasis in ectomycorrhizal fungi *Laccaria bicolor* and *Hebeloma cylindrosporum.* In National conference on Basic and Applied researchs in Plants and microbes, Department of Botany, Punjabi University, Patiala

ABSTRACT

Ectomycorrhizal (ECM) fungi hold a potential role in bioremediation of heavy metal polluted areas because of its metal accumulation and detoxification properties. However, the incomplete information about the molecular response of these fungi restricts its potential applications. The present study focuses on scrutinizing the ECM fungi for its potential role in heavy metal detoxification and understanding the molecular mechanisms involved in its tolerance. ECM fungi, *Laccaria bicolor* and *Hebeloma cylindrosporum* when exposed to increasing concentrations of cadmium (Cd) and arsenic (As), accumulated the metal(loid) intracellularly, inducing the glutathione biosynthesis pathway. The genes coding for glutathione (GSH) biosynthesis enzymes, γ-glutamylcysteine synthetase (*γ-GCS*) and glutathione synthetase (*GS*) were highly regulated by Cd and As stress. Both Cd and As coordinately upregulated the expression of both *γ-GCS* and *GS* genes, thus resulting in increased *γ-GCS* and *GS* protein expressions and enzyme activities, with substantial increase in intracellular GSH. Functional complementation of the two genes (*γ-GCS* and *GS*) in their respective yeast mutants ($gsh1^{\Delta}$ and $gsh2^{\Delta}$) further validated the role of both enzymes in mitigating Cd and As toxicity. These findings clearly highlight the potential importance of GSH antioxidant defense system in regulating Cd and As induced responses and its detoxification in ECM fungus *L. bicolor* and *H. cylindrosporum*. Further, the proteomic analysis of ECM fungi in response to Cd stress provides deep insight into the mechanisms of Cd toxicity and the response of ECM fungi in mitigating it. The comparative proteomic analysis of *L. bicolor* reported 997 differentially expressed proteins under Cd stress. The KEGG annotation of these differentially expressed proteins revealed that Cd induced toxicity in ECM fungi by altering various metabolisms like carbohydrate metabolism, nucleotide metabolism, energy metabolism, lipid metabolism and genetic information processing like DNA replication, DNA repair, transcription, translation, protein folding and chromosome metabolism. In defense, the ECM fungi confront the Cd induced toxicity by up-regulating the enzymes involved in oxidative response including glutathione metabolism, inducing signaling pathway and increase the amino acid and protein biosynthesis. These observations provide deep understanding of the Cd toxicity mechanisms and highlight the biomarkers for Cd toxicity in *L. bicolor*. This study also provides the reference dataset on fungal proteome changes under Cd stress.

TABLE OF CONTENTS

LIST OF TABLES

LIST OF FIGURES

ABBREVIATIONS

1DGE	One dimensional gel electrophoresis
2DGE	Two dimensional gel electrophoresis
%	Percent
°C	Degree centigrade
µg	Microgram
µl	Microlitre
µM	Micromolar
γ-GC	γ- glutamylcysteine
γ-GCS	γ- glutamylcysteine synthetase
ABC	ATP binding cassette
ADP	Adenosine di-phosphate
ANOVA	Analysis of Variance
ARE	Antioxidant response element
As	Arsenic
As(III)	Arsenite
As(V)	Arsenate
ATP	Adenosine tri-phosphate
ATSDR	Agency for Toxic Substances and Disease Registry
BLAST	Basic local alignment search tool
Bp	Base pair
BSA	Bovine serum albumin
BSR	Base excision repair
Ca	Calcium
$CaCl_2$	Calcium chloride
Cd	Cadmium
cDNA	Complementary deoxyribonucleic acid
Ct	Comparative threshold
Cu	Copper
Cys	Cystein
Da	Dalton
DNA	Deoxyribonucleic acid

dNTP	2’-deoxynucleoside-5’-triphosphate
DTNB	5,5'-dithio-bis-[2-nitrobenzoic acid]
DTT	Dithiothreitol
ECM	Ectomycorrhiza
EDTA	Ethylenediamine-tetra acetic acid
ESI	Electron spray ionization
EtBr	Ethidium Bromide
EV	Empty vector
et al.	et alii
g	Gram
GK	γ-glutamyl kinase
GO	Gene ontology
GR	Glutathione reductase
GRE	Glucocorticoid responsive element
GS	Glutathione synthetase
GSH	Glutathione
GSSG	Oxidised glutathione
HSE	Heat shock element
HSP	Heat shock protein
IC	Inhibitory concentration
IARC	International agency for research on cancer
IPTG	Isopropyl β-D-1-thiogalactopyranoside
K	Potassium
KEGG	Kyoto Encyclopedia of Genes and Genomes
Kg	Kilogram
KPE	Potassium phosphate and EDTA
kV	Kilo volt
l	Litre
LA	Luria Agar
LB	Luria-Bertani
LC	Liquid chromatography
M	Molar
m/z	Mass-to-charge ratio

MAPK	Mitogen activated protein kinase
Mg	Magnesium
mg	Milligram
min	Minutes
ml	Millilitre
mM	Millimolar
mm	Millimetre
MMN	Modified Melin-Norkans medium
MMR	Mismatch repair
MRE	Metal response element
mRNA	Messenger RNA
MRP	Multidrug resistance proteins
MS	Mass spectroscopy
MSMS	Tandem mass spectroscopy
MT	Metallothionein
NADP	Nicotinamide adenine dinucleotide phosphate
NaOH	Sodium Hydroxide
Ni	Nickel
NCBI	National Centre for Biotechnology Information
NER	Nucleotide excision repair
NTP	National Toxicology Program
nm	Nanometre
O.D	Optical Density
ORF	Open reading frame
P	Phosphorus
PAGE	Poly acrylamide gel electrophoresis
Pb	Lead
PC	Phytochelatin
PCR	Polymerase chain reaction
PEG	Polyethylene glycol
pH	Potential of hydrogen
pI	Isoelectric point
Pi	Inorganic phosphorus

ppm	Parts per million
psi	Pounds per square inch
Q-TOF	Quadrupole Time-of-Flight
RNA	Ribonucleic acid
ROS	Reactive oxygen species
rpm	Revolutions per minute
RT	Reverse transcriptase
S	Sulphur
SD	Standard deviation
SD media	Synthetic defined
SDS	Sodium dodecyl sulphate
sec	Second(s)
SOD	Superoxide dismutase
TBE	Tris/Borate/EDTA
TCA	Trichloro acetic acid
TE	Tris-EDTA
TNB	5’-thiol-2-nitrobenzoic acid
U	Unit
Ura	Uracil
USEPA	United States Environmental Protection Agency
UV	Ultra violet
V	Volts
w/v	Weight by volume
X-gal	5-Bromo-4-chloro-3-indolyl-β-galactoside
YPD	Yeast extract-peptone-dextrose
YRE	yAP-1 response elements
Zn	Zinc

CHAPTER 1
INTRODUCTION

Heavy metal(loid)s (HMs) represent major environmental hazards to human health. Heavy metal(loid)s like cadmium, arsenic, lead, mercury, zinc etc., are continuously being mobilized into the biosphere through both natural processes like volcanoes, erosion, weathering of metalliferous rocks and anthropogenic activities like combustion of fossil fuels, mining and industry, use of phosphate fertilizers, sewage sludge, dust from smelters, bad agricultural practices etc. Metal polluted soil is the major source of heavy metals in the environment. The excess heavy metals in soil, gets accumulated into the plants thus entering the food chain. Amongst all heavy metals, arsenic (As), cadmium (Cd), chromium (Cr), mercury (Hg) and lead (Pb) possess the highest degree of toxicity. Arsenic and cadmium have been placed in the list of "Group-1 carcinogens" by IARC (International Agency for Research on Cancer) (IARC, 2019). Arsenic has been ranked first in the toxicity and as the most hazardous metalloid in the environment by the Agency for Toxic Substances and Disease Registry (ATSDR-Agency for toxic substances and Disease Registry, 2017) with cadmium holding the 7th rank. These heavy metal(loid)s are highly toxic to living organisms affecting various physiological processes (John *et al.,* 2009). These heavy metals enter inside the cell through the same transport system as essential ions and alter various cellular and molecular activities. Inside the cell, they induce toxicity through different mechanisms. Firstly, they generate reactive oxygen species (ROS) due to their ionophoretic property, leading to oxidative stress and induction of antioxidant defense mechanisms. Secondly, HMs having similarity with the nutrient cations, compete with nutrient molecules to enter inside cell, thus interfering with various cellular mechanism, e.g. As and Cd show similarity with P and Zn, respectively and use their transporters to enter inside cell. Inside the cell, these HMs displaces essential cations from their specific binding sites leading to cellular malfunctioning (Singh *et al.,* 2011). Thirdly, HMs show high affinity for the sulfhydryl group (-SH) of various functional proteins, thus disrupting their structure, function and rendering them inactive (Tchounwou *et al.,* 2012). Most commonly affected molecular metabolisms under HM stress are energy metabolism, carbohydrate metabolism, ATP synthesis, glutathione metabolism, response to oxidative stress, DNA replication and repair, protein metabolism and signal transduction pathway (Yang *et al.,* 2015; Zhang *et al.,* 2015; Jin *et al.,* 2016).

Although there are many conventional methods like soil replacement, vitrification, encapsulation, electro-kinetics, soil washing, immobilization etc., to detoxify these heavy metals but they are tedious, expensive, applicable on small scale (Khalid *et al.,* 2017). Bioremediation using plants and microorganisms have proven to be more efficient and cost-effective method to remediate heavy metals. Mycorrhizas are the class of rhizospheric microorganisms that grow in close proximity with the plant roots, forming a symbiotic association with the root cells. They are cosmopolitan and abundant, even in the highly degraded areas. They protect the host plant from various biotic and abiotic stress. Broadly, there are two types of mycorrhizal fungi depending on whether the fungus colonize the intercellular space of roots (Ectomycorrhizal) or develop inside the cortical cells of roots (Endomycorrhizal). The ectomycorrhizal (ECM) fungi do not penetrate inside the host cell, instead forms an intracellular network of hyphae known as Hartig's net (Bonfante and Genre, 2010). The Hartig's net is the region of juxtaposition where the exchange of nutrients, water, and other components between both fungi and plant roots takes place (Balestrini and Bonfante, 2014; Henke *et al.,* 2015). In contrast to host dependent endomycorrhizas, ectomycorrhizas have dual lifestyle. They can live both in symbiosis with the plant roots and as facultative saprotrophes in soil (Martin and Nehls, 2009). When in soil, ECM fungi depend on their host plant for carbohydrates, whereas under laboratory conditions, they can be cultured without host (Van Der Heijden *et al.,* 2015). Therefore, ECM fungi are gaining more interest. The ECM fungi are known to benefit the host plant by improving nutrient and water uptake, improves plant growth and protects against various stresses like drought, salinity, pests and toxic metal(loid)s (Leung *et al.,* 2013). Extensive studies have been carried to implicate their use in bioremediation of heavy metals (Cejpková, *et al.,* 2016; Xu *et al.,* 2018). The ECM fungi possess multifarious defence mechanisms against heavy metal(loid)s toxicity (Bellion *et al.,* 2006). The metal tolerance mechanisms can be broadly classified as 'Avoidance' and 'Tolerance'. In 'Avoidance', the ECM fungi prevent the uptake of heavy metal(loid)s into the cytosol by extracellular chelation through extruded ligands like tricarboxylic acid, oxalic acid (Xu *et al.,* 2015) or by biosorption of these metal(loid)s to the fungal cell wall through chitin and glucosamine (Bellion *et al.,* 2006) or by increasing the metal efflux (Majorel *et al.,* 2014). However, inspite of the restricted entry of these metals, 20-30% of metal still enters the cytosol (Fernández-Fuego *et al.,* 2017). Further, the metal(loid)s accumulated in the cytosol are detoxified by synthesizing thiol rich ligands like glutathione (γ-Glu–Cys–Gly, GSH) and metallothioneins (small cysteine-rich proteins, MTs) (Bellion *et al.,* 2006; Reddy *et al.,* 2016). MTs and GSH are the key molecules in ECM fungi responsible heavy metal homeostasis. MTs

are low molecular weight cysteine rich proteins coded by specific genes, whereas GSH is a non-protein thiol synthesized enzymatically.

Glutathione play an important role in metal(loid) scavenging due to the high affinity of metal(loid)s to its thiol (-SH) group and as a precursor of phytochelatins (PCs). Glutathione a tripeptide (γ-glutamyl-cysteinyl-glycine) is the most abundant non-protein thiol present in the living system (Pócsi *et al.,* 2004). GSH provides dual protection to the cells under HM stress. Firstly, it acts as metal scavenger to sequester HMs metals away from the functional organelles. It sequesters the toxic metal(loid)s (X) by forming non-toxic $(GSH)_nX$ conjugates, which are further compartmentalized into the vacuoles through ABC (ATP-binding cassette) transporters (Schlunk *et al.,* 2015). Both cadmium and arsenic show high affinity for the thiol (–SH) group of glutathione. Thus, forming a metal(loid)-$(GSH)_2$ complex, which gets subsequently sequestered into the vacuoles (Verbruggen *et al.,* 2009). GSH is biosynthesized in two sequential ATP dependent reactions, mediated by two enzymes γ-glutamylcysteine synthetase (*γ-GCS*; E.C.6.3.2.2) and glutathione synthetase (*GS*; E.C.6.3.2.3). In the first step γ-glutamylcysteine synthetase catalyzes the formation of γ-glutamylcysteine using L-glutamate and L-cysteine, followed by the second step catalyzed by glutathione synthetase, where L-glycine is added to the C-terminal of γ-glutamylcysteine, forming glutathione. Studies have reported the induction of GSH biosynthesis pathway by different heavy metal(loid)s like As, Cd, Hg and Cr (Thorsen *et al.,* 2007; Jozefczak *et al.,* 2012).

In many ECM fungi like *Laccaria bicolor, Hebeloma cylindrosporum, Pisolithus albus, Suillus luteus, S. himalayensis* etc., metallothioneins have been found highly expressive under copper stress (Ramesh *et al.,* 2009; Reddy *et al.,* 2014, 2016; Nguyen *et al.,* 2017; Kalsotra *et al.,* 2018). However, very little expression of MTs have been reported under cadmium stress. It has been hypothesized that Cd detoxification in ECM fungi might be operated through glutathione chelation as the concentrations of GSH in ECM fungi are reported in millimolar range in response to Cd stress (Courbot *et al.,* 2004). These observations show that different mechanisms are induced by different metal(loid)s in ECM fungi. Therefore, the molecular analysis of the response of ECM systems under metal stress is a prerequisite so that the fungi can be implicated further for bioremediation.

Proteomics has recently emerged as a powerful tool to study the response of cell, tissue or organism under different conditions. It is practically intricate, as it involves the analysis and characterization of overall protein signatures of the genome. Most of the functional information

of genes is characterize by their translated proteins. The proteomic analysis provides complete characterization of cell's proteome including protein expression, structure, functions, interactions and modifications under a particular situation. Although very complex, but proteomics is the most significant methodology to assimilate the actual gene function. It provides complete information about the fluctuations in the gene expression under two different conditions. Moreover, in comparison to transcriptomic analysis, where the microarray chips provide information regarding the mRNA expression levels under different conditions, proteomic analysis is considered more relevant. The genomic and transcriptomic studies do not always correlate with the actual gene expression because the mRNA is not always translated into proteins and also it may undergo various post-translational modifications. Therefore, proteomic analysis provides more relevant dataset than transcriptomics. The complete proteomic analysis revolves around the separation of proteins by either sodium dodecyl sulfate polyacrylamide gel electrophoresis (SDS-PAGE), 2-dimensional gel electrophoresis (2DGE) or Liquid chromatography (LC) followed by their digestion into smaller fragments and identification through Mass spectroscopy (MS) or tandem mass spectroscopy (MS/MS).

Differential proteomic analysis is a powerful tool to study the effect of various biotic as well as abiotic stresses on living systems. There are few studies on plants (Cvjetko *et al.*, 2014; Borges *et al.*, 2019), bacteria (Khan *et al.*, 2017; Zhai *et al.*, 2017) and yeast (Ilyas *et al.*, 2016), where the response of biological system to heavy metal stress was revealed through proteomic analysis. However, till date there is no report on studying the response of ectomycorrhizal fungi to heavy metals through proteomics.

The present study focuses on studying the effect of As and Cd on ECM fungi, *Laccaria bicolor* and *Hebeloma cylindrosporum* and providing the molecular insight into the mechanisms involved in mitigating the toxic effect of Cd and As with special emphasis on GSH biosynthesis. The present study concentrates on studying the response of ECM fungi to Cd and As and to investigate the role of glutathione metabolism in its mitigation. Also, the fact that the mechanisms involved in Cd toxicity and the response of ECM fungi- *L. bicolor* in mitigating Cd have not been investigated till date, prompted us to investigate the entire proteome of *L. bicolor* under Cd stress. The present research work focuses on the fulfilment of following objectives:

1. Cloning and characterization of γ-glutamylcysteine synthetase (*γ-GCS)* and glutathione synthetase (*GS)* genes involved in the glutathione biosynthesis

2. Heterologous expression of glutathione biosynthesis genes in yeast mutants
3. Proteomic analyses of ectomycorrhizal fungi in response to metal stress

CHAPTER 2

REVIEW OF LITERATURE

2.1 Heavy metals and their modes of toxicity

Heavy metals (HMs) are the naturally occurring metallic elements (both metals and metalloids) characterized with high atomic weight and specific density greater than 5 g cm^{-3}. In 1997, a chemistry professor- Stephen Hawkes defined HMs as 'metals with insoluble sulfides and hydroxides, whose salts produce colored solution in water and whose complexes are usually colored' (Hawkes, 1997). They are consistently present in the earth's crust in the form of sulfide and oxide ores. They cannot be degraded or destroyed but can be transformed from one form to another (Figure 2.1).

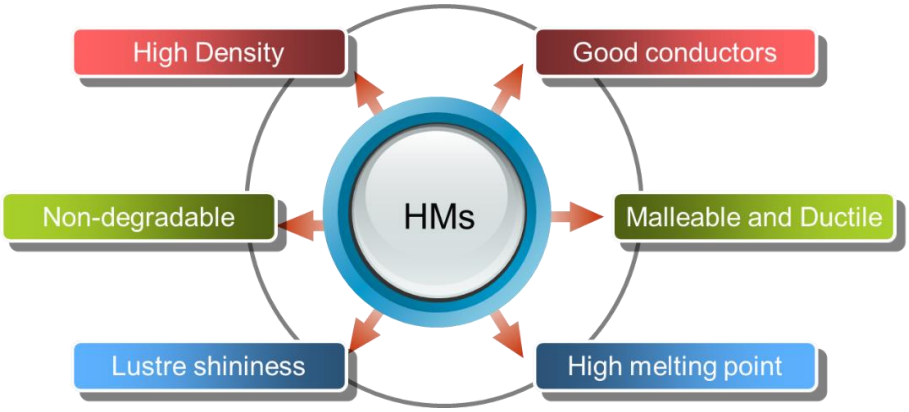

Figure 2.1: Physical properties of heavy metals

Although most of the HMs are highly noxious, few HMs are required for certain biochemical and physiological functions in trace amount. Such HMs are known as essential HMs (Alloway, 2012). Copper (Cu), Cobalt (Co), Chromium (Cr), Iron (Fe), Magnesium (Mg), Manganese (Mn), Molybdenum (Mo), Nickel (Ni), Selenium (Se) and Zinc (Zn) are few heavy metals that are essential micro-nutrients for various functions in living systems. They are important component of many key enzymes and play significant role in various oxidation-reduction reactions. They are also involved in various other biochemical processes like: formation of protein structures, regulation of osmotic pressure, maintaining the ionic balance etc (Alloway, 2012). Our body mass constitutes of 0.01% of these heavy metals mainly – iron, zinc, lead and copper. However, the same essential elements when present in elevated concentrations lead to the formation of free radicals and reactive oxygen species with detrimental consequences to

the cell, affecting their structural and functional properties. The ectopic binding of excess metals to various proteins disturb their structures and function (Hänsch and Mendel, 2009).

On the other hand, heavy metals like Aluminum (Al), Antimony (Sb), Arsenic (As), Barium (Ba), Beryllium (Be), Cadmium (Cd), Gallium (Ga), Germanium (Ge), Gold (Au), Indium (In), Lead (Pb), Lithium (Li), Mercury (Hg), Nickel (Ni), Platinum (Pt), Silver (Ag), Strontium (Sr), Tellurium (Te), Thallium (Tl), Tin (Sn), Titanium (Ti), Vanadium (V), Uranium (U), have no biological function and are considered non-essential heavy metals (Tchounwou *et al.,* 2012). Inside the biological system, they affect various cellular components and organelles like cell membrane, mitochondria, endoplasmic reticulum, lysosome, nuclei and various enzymes involved in detoxification, metabolism and damage repair (Wang and Shi, 2001). Most of them are carcinogenic (arsenic, cadmium, mercury, cobalt, nickel, antimony) (Kim *et al.,* 2015), mutagenic (arsenic, vanadium), allergic (nickel), teratogenic (arsenic), disrupting endocrine (copper, selenium, silver, zinc), causing osteoporosis (cadmium), damaging nervous system (mercury, lead, manganese, thallium, tin), hepatoxic/nephrotoxic (cadmium, manganese, mercury) and affecting the immune system (lead) (Tchounwou *et al.,* 2012; Koller and Saleh, 2018). These heavy metal ions displace the naturally binding essential metal ions from the biomolecules, thus disrupting their structure and activity and causing various deficiency symptoms. The heavy metals also lead to the production of free radicals and reactive oxygen species by autoxidation and Fenton reaction, thus causing oxidative stress inside the cell. Many studies claim that oxidative deterioration of biomolecules is mainly due to the binding of heavy metals to the DNA and nuclear proteins, thus causing DNA damage and conformational changes that leads to carcinogenesis, cell cycle modulation and apoptosis (Beyersmann and Hartwig, 2008; Flora *et al.,* 2008). According to USEPA (United States Environmental Protection Agency) and IARC (International Agency for Research on Cancer) these heavy metals are characterized as ‘known’ or ‘probable’ human carcinogens based on epidemiological and experimental studies revealing a strong association between metal exposure and cancer incidence in humans and animals. Arsenic, cadmium, lead, mercury and chromium have been listed into the twenty most hazardous substances by the ‘Agency for Toxic Substances and Disease Registry (ATSDR, 2012) and United States Environmental Protection Agency (USEPA, 2018). The common sources of these HMs in environment and their effects on living systems have been summarized in Table 2.1.

Table 2.1: Sources of heavy metals in environment and their harmful effect on humans

S. No.	Heavy Metal	Sources	Effect on humans
1	Arsenic	Pesticides, fungicides, metal smelters	Cancer, bronchitis, dermatitis, poisoning
2	Cadmium	Welding, electroplating, fertilizers, pesticides, Cd and Ni batteries, nuclear fission plant	Renal disfunction, lung disease, lung cancer, bone defects (osteomalacia, osteoporosis), increase blood pressure, kidney damage, bronchitis, gastrointestinal disorder
3	Mercury	Pesticides, batteries, paper industry,	Tremors, gingivitis, acrodynia, spontaneous abortion, nervous breakdown, protoplasm poisoning
4	Chromium	Mines, mineral sources	Nervous damage, fatigue, irritability
5	Lead	Paint, pesticides, smoking, automobile emission, mining, burning of coal	Mental retardation, developmental delay, fatal infant encephalopathy, congenital paralysis, sensor neural deafness, nervous damage, epilepticus, liver, kidney, gastrointestinal damage

The toxicity of HMs depends upon various factors like dosage, chemical species, route of exposure, age, genetics, gender and nutritional status of exposed individual (Tchounwou *et al.*, 2012). The toxicological properties of HMs include:

- Persistence - long residual and half life
- Soil residence time - >1000 years
- Acute toxicity – in plants, animals and microorganisms
- Bioaccumulation and biomagnification
- Chronic and sub-lethal effect at low-concentrations
- Synergistic effects
- Teratogenic and carcinogenic properties.

Amongst all heavy metals, arsenic, cadmium, chromium, mercury and lead possess the highest degree of toxicity. Arsenic, cadmium and chromium have been placed in the list of "Group-1

carcinogens" by IARC (IARC, 2019). Arsenic (As) has been ranked first in the toxicity and as the most hazardous metalloid in the environment by the Agency for Toxic Substances and Disease Registry (ATSDR, 2017) with cadmium holding the 7th rank. These heavy metal(loid)s are highly toxic to living organisms affecting various physiological processes (John *et al.*, 2009).

2.1.1 Cadmium

Cadmium is the metallic compound with atomic number- 48, relative atomic mass- 112.41, placed in group IIB of periodic table with oxidation state +2. It is silver-white with blue-ting, usually odorless. It occurs naturally in the earth's crust and in ocean water and is emitted in the environment due to both natural and anthropogenic activities (Friberg, 2018). In the earth's crust, cadmium usually appears in association with ores of zinc, lead and copper forming complex oxides, sulfides and carbonates (ATSDR, 2008). It is extracted as the by-product of zinc and lead mining and smelting.

It has been widely used in industries due to its special properties of being a) excellent corrosion resistance, low melting temperature, high ductility and high thermal and electrical conductivity (Friberg, 2018; National Resources Canada, 2007). According to the U.S Geological survey, the main use of cadmium has been found in nickel-cadmium batteries (83%), pigments (8%), coating and plating (7%), stabilizers for plastic (1.2%) and others including photovoltaic devices, semiconductors and non-ferrous alloys (0.8%) (US Geological Survey, 2009).

Cadmium is one of the most toxic elements found in earth's crust. It has been ranked seventh in the list of most hazardous elements by ATSDR (ATSDR, 2017). Many research agencies have classified cadmium as a potential carcinogen to humans including NTP (National Toxicology Program) (https://ntp.niehs.nih.gov/ntp/roc/content/profiles/cadmium.pdf), USEPA (https://cfpub.epa.gov/ncea/iris/iris_documents/documents/subst/0141_summary) WHO (World health organization) and IARC (https://monographs.iarc.fr/wp-content/uploads/2018/06/mono100C-8.pdf). Under section 112 of the "Clean Air Act", cadmium and its compounds have been included in the list of 189 hazardous air pollutants (EPA, 2007). Not only in air, cadmium has also been designated as the hazardous substance under Section 311 of "The Clean Water Act". Due to its toxicity, long half-life and high solubility, cadmium has been designated as the non-essential heavy metal.

Cadmium contaminates the environment either due to natural activities like volcanic eruptions, sea spray, weathering of Cd-containing rocks, mobilization of cadmium previously deposited into soils, sediments, landfills or due to the anthropogenic activities like mining and smelting, combustion of fossil fuels, waste incineration and release from municipal landfills. Cadmium rich sludge can pollute surface water as well as soil. Phosphatic fertilizers are also the major source of cadmium in soil (Satarug *et al.,* 2003).

2.1.1.1 Sources and effect of cadmium on living systems

Cadmium emitted into the soil and water through various natural and anthropogenic activities is retained there for several decades. It gets strongly adsorbed to the organic matter present in the soil. The plants growing on these contaminated areas uptake these cadmium molecules and mobilize them into various parts. In the aquatic ecosystems, cadmium gets bioaccumulated in mussels, oysters, shrimps, lobsters and fish (Campbell, 2007; Ibemenuga, 2013). Therefore, human beings get exposed to cadmium through the consumption of contaminated food, drinking contaminated water, inhaling cadmium particles from ambient air, cigarette smoking or from contaminated soil and dust (Nawrot *et al.,* 2010). Tobacco leaves are natural bio-accumulators of large amount of cadmium. Therefore, cigarettes are a major source of cadmium exposure in humans (Marano *et al.,* 2012). Smoking one pack a day can imbibe 5 to 10 times of cadmium consumed through regular diet. Tobacco smokers consume almost 1.7 μg of cadmium per cigarette (Ganguly *et al.,* 2018). The non-smokers usually get exposed to cadmium often through plant and sea driven foods. Ingesting contaminated foodstuffs like cereals, grains, fruits, leafy vegetables as well as contaminated beverages is the major source of cadmium in humans (Jackson and Alloway, 2017; Mandlate *et al.,* 2017; Wang *et al.,* 2019). As per "The Agency for Toxic Substances and Disease Registry", in USA, more than 500,000 workers get exposed to cadmium toxicity each year (Bernard, 2008).

Cadmium has been implicated in promoting various diseases in living systems. In plants, cadmium toxicity causes retardation in photosynthesis, chlorosis, rolling of leaves, stunting, decreased leaf conductance and impairs the CO_2 uptake by plants (Andresen and Küpper, 2013; Benavides *et al.,* 2005;). Cadmium interferes with the uptake and transport of various essential elements like Ca, Mg, P, K and water by the plants (Perfus-Barbeoch *et al.,* 2002). Cadmium also inhibits nitrate reductase activity in plants leading to poor absorption of nitrates and affects nitrogen fixation and ammonia assimilation in plants (Gouia *et al.,* 2000; Garg and Aggarwal, 2011). Cadmium toxicity also affects the plasma membrane permeability in plants, causing

reduction in water uptake (Singh and Tewari, 2003). It also affects the ATPase activity, indices lipid peroxidation, inhibits chlorophyll biosynthesis and reduces the activity of enzymes involved in CO_2 fixation (Benavides *et al.,* 2005; Andresen and Küpper, 2013; Xue *et al.,* 2013; Shanying *et al.,* 2017). Insufficiency of cadmium detoxification in some plants disturbs the redox-control of the cell, thus inhibits the plant growth and stimulates secondary metabolites leading to cell death (Schutzendubel and Polle, 2002).

In mammals, cadmium has been classified as a human carcinogen, resulting in various types of cancers like cancer of lungs, prostate, pancreas, kidney and breast (Verougstraete *et al.*, 2003; Hartwig, 2018; IARC, 2018; Kolluru *et al.,* 2019). Apart from being carcinogenic, cadmium exposure also various defects in human body including, cardiovascular, developmental, gastrointestinal, neurological, renal, reproductive and respiratory (Bernard, 2008). Airborne cadmium ions cause chronic toxicity resulting in proteinuria and lung emphysema, skin ulcers and cancer (Bonnell, 1955; Friberg, 2018). The disease Itai-Itai has also been associated with cadmium exposure (Kobayashi *et al.,* 2009; Aoshima, 2016). Cadmium contamination also effects the microbial population present in the soil. Excessive amount of cadmium in soil disrupts the homeostasis of soil by interfering with the control mechanisms on the genetic level and damaging the metabolic pathways, often resulting in the cell apoptosis (Wyszkowska *et al.*, 2013).

2.1.1.2 Mode of toxicity

The mechanisms involved in cadmium induced toxicity are multifactorial. Cadmium has been implicated in increasing the oxidative stress, replacing essential metals, promoting apoptosis, inhibiting DNA repair and inducing genotoxicity in the cells.

a) Oxidative stress:

The principal molecular basis underlying the cadmium cytotoxicity is the induction of oxidative stress. Cadmium is a bivalent cation and is redox-inactive, therefore it cannot generate free radicals directly. However, numerous studies have reviewed the production of ROS after Cd exposure (Joseph 2009; Thévenod 2009; Cuypers *et al.,* 2010; Rani *et al.,* 2014; Nath *et al.,* 2015). There are many explanations to this indirect generation of oxidative stress in the cells. First possible explanation to this is the depletion of cell's major antioxidants (glutathione) under cadmium stress leading to oxidative stress (Ercal *et al.,* 2001; Lopez *et al.,*

2006). Another possible reason is the replacement of redox-active elements. Cd replaces Fe in various proteins, thus increasing the cellular concentration of free redox active metal like iron and copper. These redox-active metals undergo Fenton reactions leading to the free radical synthesis (Dorta *et al.,* 2003; Watanabe *et al.,* 2003; Cuypers *et al.,* 2010). These free radicals and ROS inside the cell can lead to disruption of macromolecules- protein degradation, DNA cross-linking and membrane peroxidation (Thévenod 2009). The cadmium mediated ROS also induces mitophagy (mitochondrial apoptosis) (Wei *et al.,* 2015, Yan *et al.,* 2016) and causes mitochondrial dysfunction (Belyaeva, 2018) by affecting the mitochondrial membrane potential and electron transfer chain (Yeh *et al.,* 2009). The imbalance created in redox system affects both damaging (apoptosis and uncontrolled cell proliferation) and repair process by activating several signaling cascades. Therefore, oxidative stress plays an important in acute Cd poisoning and carcinogenicity. (Cuypers *et al.,* 2010).

b) Genotoxicity:

Cadmium induces toxicity by altering the cell proliferation, differentiation, cell cycle progression, DNA synthesis, apoptosis and various cellular mechanisms (Aimola *et al.,* 2012; Rani *et al.,* 2014). Cadmium also causes genomic instability by inhibiting the DNA repair mechanism of cell (Giaginis *et al.,* 2006; Hartwig 2018). Cadmium does not interact directly with the DNA, however, the reactive oxygen species (ROS) generated in response to Cd interfere with DNA processing and repair, thus causing DNA damage. DNA damage includes a range of lesions- DNA breaks in both single and double strand, DNA base modifications, DNA sugar lesions, DNA-protein crosslinks and abasic sites (Cadet and Wagner, 2014). Cd has been reported of impairing all major DNA repair pathways including base excision repair (BER), nucleotide excision repair (NER) and DNA mismatch repair (MMR) (Giaginis *et al.,* 2006), thus leading to genomic instability and cadmium induced carcinogenicity. Apart from DNA damage, Cd also provoked clastogenic effects in the cell such as micronuclei formation and chromosomal aberrations (Beyersmann and Hartwig, 2008; Filipič, 2012; Nersesyan *et al.,* 2016; Hartwig, 2018). Cadmium also affects the cell cycle control mechanisms and apoptosis. Cadmium has been known to interfere with the structure and function of p53-zinc binding domain (involved in tumor suppression) (Schwerdtle *et al.,* 2010). All these factors together contribute to cadmium carcinogenicity.

2.1.2 Arsenic

Arsenic is a ubiquitous metalloid with atomic number: 33, atomic mass: 74.92 and belongs to group VA. It exists in four oxidation states -3, 0, +3, +5. The chemical and physical properties of As are intermediate between a metal and non-metal, therefore it is often categorized as a semi-metal or a metalloid. Arsenite (AsIII) and Arsenate (AsV) are the two predominant oxidation states under reducing and oxygenated conditions respectively (IARC, 2018a). It is the 20th most common element found in earth's crust and occurs both naturally and anthropogenically in nature. It has been used widely in pharmaceuticals, wood preservation, metallurgical, glass making, agriculture chemicals and in semi-conductor industries (Sun, 2010).

Arsenic (As) has been ranked first in the toxicity and as the most hazardous metalloid in the environment by the ATSDR (ATSDR, 2017). Arsenic and its compounds have been classified as "Carcinogenic to humans" by IARC, mostly responsible for lung, bladder, liver, kidney and skin cancer (IARC, 2018). World Health organization, USEPA, Health Canada and European Union (EU) has restricted the amount of arsenic in drinking water to 10 mg/l. Still there are millions of people across the world especially in India, Bangladesh, Thailand, Argentina, Nepal, Poland, China, Mexico and USA who are in exposure to the concentrations of As much higher than the prescribed value (greater than 100 mg/l) (Argos *et al.,* 2010; Cho *et al.,* 2011; Bundschuh *et al.,* 2012; Rodríguez-Lado *et al.,* 2013; Diwakar *et al.,* 2015; Komorowicz and Barałkiewicz, 2016; Bhowmick *et al.,* 2018; Pinter *et al.,* 2018).

2.1.2.1 Sources and effects of Arsenic

Geogenic activities occurring inside the aquifers are the major cause of arsenic mobility into the environment. The use of these As polluted tube-wells for irrigation further pollutes the agricultural topsoil (Casentini *et al.,* 2011). Other anthropogenic activities like mining, use of pesticides, burning of fossil-fuels, coal combustion, tobacco and use of arsenic laden irrigation water are the major cause of arsenic exposure to living systems.

Arsenic toxicity in plants affects plant biomass, grain yield, seed germination, plant height, leaf area and photosynthesis (Srivastava and Sharma, 2013; Farooq *et al.,* 2016). Arsenic accumulates inside the plants, thus entering the food chain and posing high threat to human beings. Human beings are exposed to As through ingestion of contaminated food, drinking

water from As-rich ground strata (bore or well), seafood or inhaling As ambient air (Abdul *et al.*, 2015; Taylor *et al.*, 2017). Arsenic toxicity in humans leads to various types of cancers like cancer of lungs, urinary bladder, kidney, skin, liver and prostate (Kuo *et al.*, 2017; Smith *et al.*, 2017; Koutros *et al.*, 2018). Apart from cancer, As exposure also leads to many other notorious diseases like neurological disorders, skin lesions, arsenical-keratosis, leukaemia, diabetes, liver damage, peripheral vascular diseases, black foot disease, gastrointestinal disturbances, renal diseases and various reproductive problems (Jomova *et al.*, 2011).

2.1.2.2 Modes of toxicity

Arsenic exposure is highly carcinogenic and may cause various health intimidations. The arsenic toxicity levels and mechanisms are strongly dependent upon the chemical speciation in the environment (Wang *et al.*, 2015). In general, the toxicity of different As species is in the order: dimethylarsinous acid (DMA(III)) > monomethylarsonous acid (MMA(III)) > arsenite (As(III)) > arsenate (As(V)) > dimethylarsinic acid (DMA(V)) > monomethylarsonic acid (MMA(V)) (Petrick *et al.*, 2000; Hirano *et al.*, 2004; Wang *et al.*, 2015). In environment, arsenic mainly exists in two forms: pentavalent arsenate (As(V)) and trivalent arsenite (As(III)). Both are easily taken up by the plants and microorganisms, thus entering the food chain. Inside the cell, As(V) is readily converted to As (III) (Finnegan and Chen, 2012)

Arsenate (As(V)) is the main As species present in the oxic conditions of aerobic soil. Since As and P belong to same chemical group (Group 15 (VA) of periodic table), both exhibit similar chemical and geochemical properties. As(V) being analogous to Pi, enters the plants as a hitchhiker through the phosphorous transporters and thereby pose high threat to the plant establishment (Wu *et al.*, 2011). As(V) competes with phosphate (PO_4^{3-}) in various enzymatic reactions, thus inhibiting both phosphorylation and oxidative phosphorylation and interfering with the cellular mechanisms (Bhattacharjee *et al.*, 2008). As(V) also interferes with the phosphorous metabolism in ATP cycle by incorporating into the phosphorylated compounds (Levy *et al.*, 2005; Wang *et al.*, 2015). Arsenite (As(III)) on the other hand is more toxic than arsenate. It is the thiol reactive compound causing toxicity by blocking the sulfhydryl (-SH) group in various cellular proteins like pyruvate dehydrogenase and 2-oxoglutarate dehydrogenase leading to production of ROS causing membrane degradation and cell death (Lloyd and Oremland, 2006).

Oxidative carbon metabolism, amino acid metabolism, protein formation, nitrogen and Sulphur assimilation are also affected by As exposure (Finnegan and Chen, 2012). In plants, As damages the cellular membranes causing electrolyte leakage (Singh *et al.*, 2006). The arsenic exposure also enhances the lipid peroxidation leading to oxidative stress (Altikat *et al.*, 2015). Still the exact mechanism through which arsenic causes toxicity is unknown.

2.2 Remediation of heavy metals

There are more than 5 million sites covering more than 20 million hector of land globally, in which the soil is contaminated with different heavy metal(loids) (He *et al.*, 2015b; Liu *et al.*, 2018). These heavy metals impair the natural ecosystem, enters the food chain, thus damaging human health. Due to their pervasive and persistent nature, they do not biodegrade, instead they bioaccumulate into the environment with time, therefore, it becomes difficult to remediate them from environment. There are various in-situ and ex-situ techniques, that have been developed over time to clean up or restore heavy metal contaminated soil like soil washing, soil flushing, surface capping, electrokinetic extraction, vitrification, solidification and phytoremediation and bioremediation (Liu *et al.*, 2018). The selection of the suitable remediation technique depends upon the site characteristics like- soil type, soil pH, geographical location, types of co-contaminants, depth, water content, particle size and clay content etc (Diagne *et al.*, 2015).

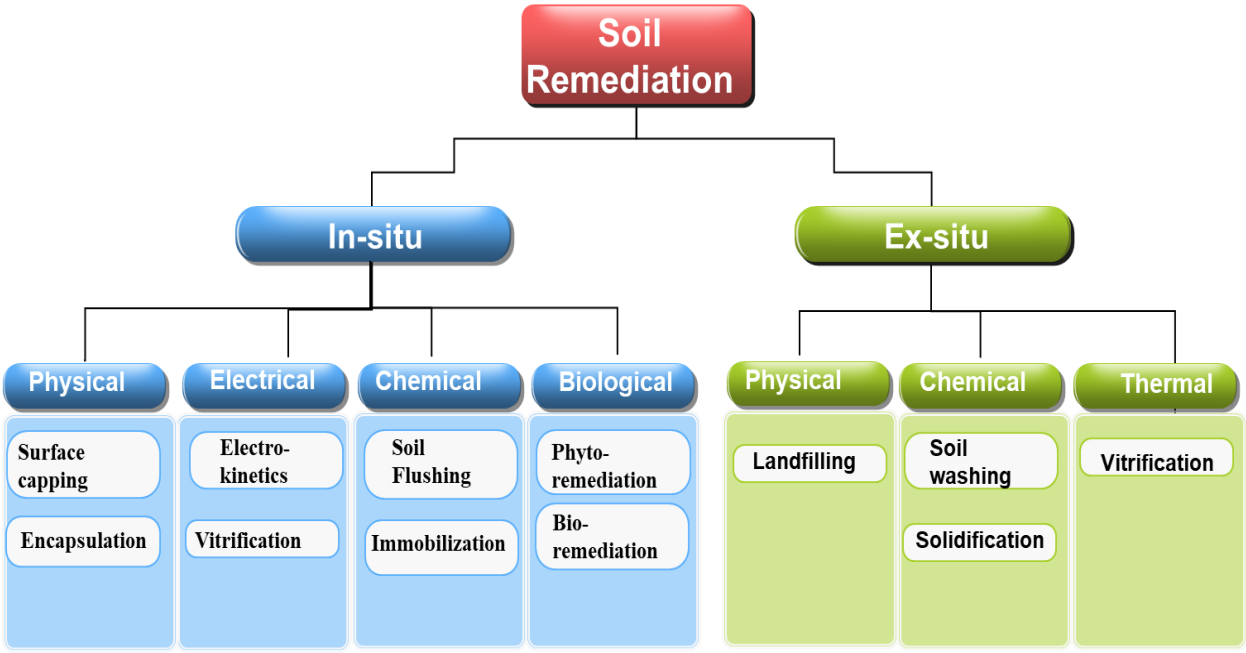

Figure 2.2: Different methods of heavy metal remediation form contaminated soil

The heavy metal remediation techniques can be classified into five categories: Physical, Chemical, Electrical, Biological and Thermal (Figure. 2.2). These technologies vary significantly in cost and effectiveness in field practices (Khalid *et al.,* 2017). The in-situ methods of soil remediation include; soil replacement/soil capping, encapsulation, immobilization, soil washing/ soil flushing, electro-kinetics, vitrification, phytoremediation and bioremediation.

a) **Soil replacement/Soil capping:** Soil replacement refers to replacing/partly replacing the contaminated soil by non-contaminated soil. This dilutes the concentration of heavy metals in soil, leading to increased soil fertility (Khalid *et al.,* 2017). The replaced soil can be further treated or dumped at another barren place. Douay *et al.,* (2008) reported improvement in vegetation and soil quality by replacing the garden soil contaminated with Pb and Cd with non-contaminated soil. Whereas in soil capping, the surface of the contaminated land is covered with a layer of material like clay, concrete, asphalt, and high-density polyethylene etc, to form a stable, protection surface. Although effective but these techniques are very laborious, costly and appropriate only with small areas (Khalid *et al.,* 2017).
b) **Encapsulation:** Encapsulation involves mixing of contaminated soil with products like concrete, lime, asphalt, calcium aluminate cement (CAC), or immobilizing agents like polyvinyl alcohol, chitosan, alginate, agar, polyurethanes and polyacrylamide. The contaminated soil becomes immobilized and thus prevent the contamination of surroundings. The carboxylic group of alginate mediates efficient sorption of metal ions and makes it an excellent encapsulation agent (Kuang *et al.,* 2015). Alginate encapsulated microparticles efficiently remoced Cd, Zn and Cu in synthetic medium (Bertagnolli *et al.,* 2016). Encapsulation in nanoparticles is gaining a lot of interest these days. Metallic nanoparticles (NPs) of Fe (Park *et al.,* 2000), Ni (Hou and Gao, 2003) and Co (Tripp *et al.,* 2002) are of great interest due to their magnetic, optical and electrochemical properties. Carbon encapsulated magnetic NPs have proven to be promising candidates for efficiently removing heavy metals from waste water (Pyrzyńska and Bystrzejewski, 2010; Haham *et al.,* 2015).
c) **Immobilization:** In immobilization, the precipitating/stabilizing chemicals or organic materials are incorporated into the contaminated soil to induce physiochemical interactions between the immobilizing agent and heavy metals in-order to reduce their mobility (Tajudin *et al.,* 2016). The wide range of materials are used for immobilization

like- carbonates (lime), phosphates (ammonium phosphate, bone meal, apatite and hydroxyapatite), alkalines (calcium hydroxide and fly ash), clay, bauxite, red mud, greensand, goethite, silica gel, vermiculite, zeolite and organic matters like- chitosan, peat, starch xanthate, compost, manure, biochar, activated carbon etc (Mahar *et al.,* 2015; Huang *et al.,* 2016; Seshadri *et al.,* 2017; Waterlot *et al.,* 2017; Liu *et al.,* 2018). Apart from these, low cost industrial residues like industrial eggshell (Soares *et al.,* 2015), termitaria (Anoduadi *et al.,* 2009), red mud (Smičiklas *et al.,* 2014) also hold potential in immobilizing HMs from soil (Khalid *et al.,* 2017). Khan *et al.,* (2015) used farm yard manure to immobilize Fe, Cr, Ni, Mn and Pb, and di-ammonium phosphate for stabilizing Cd, Cu and Zn from soil. These soil amendments induce HMs precipitation, complexation and surface adsorption, thus reducing their bioavailability and leaching potential. The soil treated with immobilization can be used for growing plants. This is an effective and affordable method to temporarily fix heavy metals in less contaminated farmland soils (Liu *et al.,* 2018).

d) Soil washing/Soil flushing: The basic principle of both techniques is the extraction of heavy metals from the soil matrix by solubilizing them into various reagents and extractants like EDTA, EDDS, organic acids, humic substances, surfactants and cyclidextrins, that can leach HMs from soil (Kulikowska *et al.,* 2015). However, soil washing is an ex-situ process whereas soil flushing is an in-situ process. In soil washing the contaminated soil is dug-out and mixed with the suitable extractant, depending upon the type of soil and metal. The heavy metals in soil may undergo precipitation, ions-exchange, adsorption or chelation and gets transferred into the liquid phase (Ferraro *et al.,* 2015). The separated soil is then again backfilled into the original site. Wei *et al.,* (2016) used phosphoric acid, oxalic acid and Na_2EDTA to wash soil and enhance the As and Cd removal efficiencies. It is a rapid method and completely remediates the soil. Owing to its high efficiency, it is considered one of the most effective soil remediation technique applicable on limited areas.

e) Electrokinetics: Electrokinetics works on the principle that the low-density direct current electricity is applied using electrodes inserted into the ground (in-situ)/ in electrolytic tank (ex-situ), the cations in the contaminated soil migrates towards the cathode whereas the anions migrate towards anode, to establish an electric field (Habibul *et al.,* 2016). Heavy metals present in the soil are separated either through electrophoresis, electroplating, co-precipitation, electric seepage, electro-migration or ion exchange resin complexation, thus decontaminating the soil (Rosestolato *et al.,*

2015; Fu *et al.,* 2017). Rosestolato *et al.,* (2015) remediated approx. 400 kg of soil using in less than 3 months using electrokinetic remediation. Various factors effecting the remediation of heavy metals through electro-kinetics include- type of HMs, concentration of metals, soil type, soil pH, organic content, type of electrolyte used etc (Figueroa *et al.,* 2016). Lee *et al.,* (2016) isolated As, Cu, Zn and Pb using KH_2PO_4 as anolyte. Suzuki *et al.,* (2014) also reported efficient Pb and Cd remediation using electrokinetics by adding ethylene diamine disuccinate. Mao *et al.,* (2016) used electrokinetic phytoremediation to lower soil pH thus enhancing the dissolution of Pb, As and Cs in soil. Electro-kinetic remediation is economically effective, easy to install and do not abolish the original nature of soil.

f) Vitrification: It is a thermal remediation technique that restricts the mobility of heavy metal(loids) in soil by applying high temperature and transforming them into glass like solids (Liu *et al.,* 2018). Vitrification can be done both in-situ and ex-situ. In in-situ vitrification, electric current is passed through vertically inserted array of electrodes into the contaminated soil. The heavy metals are encapsulated into the glassy matrix, while the organic contaminants get destroyed. However, ex-situ vitrification is done in various stages – excavation, mixing, pretreatment, melting, feeding and casting of melted products. There are three types of vitrification depending upon the source of energy: electrical vitrification, thermal vitrification and plasma vitrification. Dellisanti (2009) efficiently cleaned tons of Pb and Zn contaminated ceramic waste by heating upto 1850 ℃. Navarro *et al.,* (2013) vitrified Ag-Pb waster using solar technology. The main limitation of vitrification is the potential of soil to melt so as to pass the current through it. Soils with high alkaline content are usually poor conductors of electricity. This technique can be applied on small scale and can be highly expensive. Moreover, the processed soil is no longer suitable for agricultural purposes.

All the above techniques are highly expensive, laborious and time consuming. However, bioremediation using plants/microorganisms is more cost effective, non-invasive and provides permanent solution.

g) Phytoremediation: Phytoremediation is the process of growing plants on the contaminated soil either to remove heavy metals (phytoextraction and phytovolatilization) or to stabilize them into harmless state (phytoimmobilization and phytostabilization) (Figure 2.3) (Liu *et al.,* 2018). Phytoremediation is an environment friendly, operationally simple, aesthetically preferable, non-invasive, energy efficient, economically viable, cost-effective and widely accepted technology for soil

remediation from heavy metals (Mahar *et al.,* 2016). Unlike other physical, chemical and electrical remediation methods that irreversibly alters the soil properties, phytoremediation on the other hand improves the physical, chemical and biological qualities of contaminated soil. Hyperaccumulator plants and macrophytes, are the key plants responsible for heavy metal remediation from soil and water. These plants can tolerate high concentrations of HMs, grow well in metalliferous soil and have tendencies to efficiently absorb metal ions from soil and translocate them to aerial parts. Till date approximately 721 species of plants have been identified as metal hyperaccumulators (Reeves *et al.,* 2018). *Arabidopsis thaliana, Brassica juncea* and *Chara canescens* are capable of up-taking heavy metals and transferring them to gaseous state, followed by their release into the atmosphere (Verbruggen *et al.,* 2009). However, most of the hyperaccumulators are metal-selective, limited to native habitats, slow growth rate, have shallow roots and low biomass (Chaney and Baklanov, 2017). To reduce 1 mg/kg Cd from a contaminated soil, hyperaccumulator requires 15 years (Li *et al.,* 2012). These factors make phytoremediation an inefficient and impractical technique.

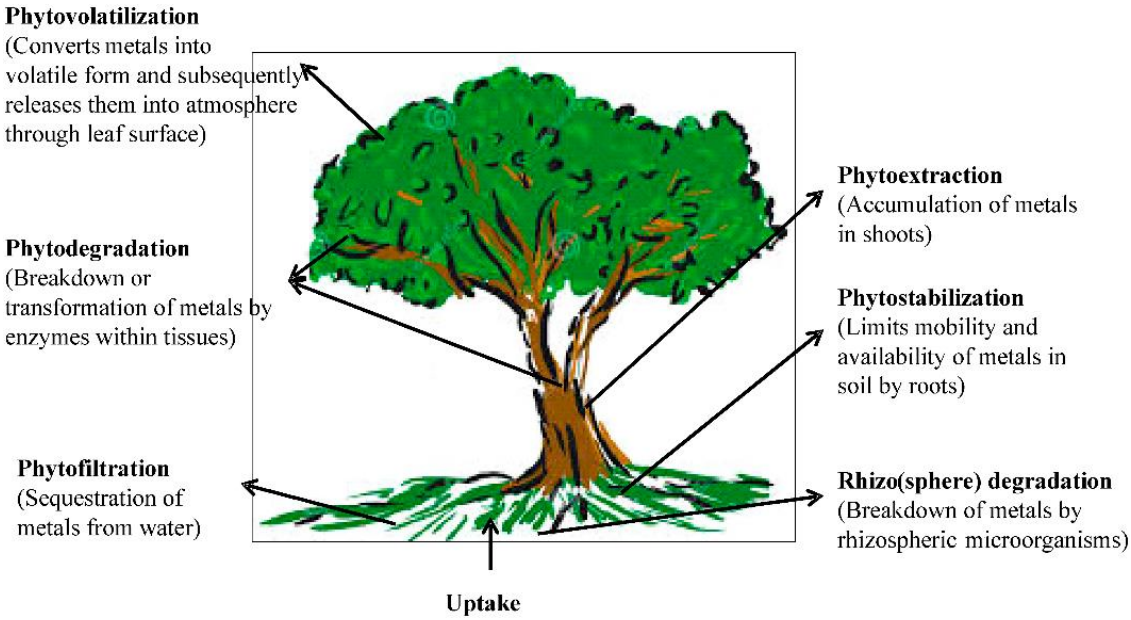

Figure 2.3: Different processes involved in phytoremediation of heavy metals (Dixit *et al.,* 2015)

h) Microbial remediation: Microbial remediation is the process of detoxification and rehabilitation of contaminated soil with the use of microbes. It is one of the most innovative and promising technology for removal and recovery of heavy metals from contaminated areas. Many microorganisms have developed specialized metabolic

capabilities using their molecular machineries to survive and perform well even in the heavy metal polluted habitats. They have developed different detoxification mechanisms to cope up with different heavy metals like- biosorption, bioaccumulation, biotransformation, bioleaching and biomineralization, thus proving themselves to be potent candidates for heavy metal remediation both in-situ and ex-situ. Rhizospheric microorganisms are the most suitable candidates for bioremediation with abilities to bioaccumulate heavy metals from contaminated soil and protect the host plant. These include various bacteria, fungi, algae, protozoa, arthropods and nematodes (Mendes *et al.,* 2013). In case of fungi, ascomycetes and basidiomycetes are the most reported candidates for HM detoxification (Narendrula-Kotha and Nkongolo, 2017). An extensive study has been performed on fungi of genera *Penicillium, Rhizopus, Suillus* and *Aspergillus* for their potential role in HM removal from soil and aqueous solution (Liu *et al.,* 2017; Kalsotra *et al.,* 2018). Most commonly isolated bacteria in HM contaminated sites includes *Actinobacteria, Proteobacteria* and *Firmicutes*, commonly from genera *Bacillus, Pseudomonas* and *Arthrobacter* (Pires *et al.,* 2017). One of the most potential microorganisms found in the rhizosphere are mycorrhizal fungi. They form a symbiotic association with the plant roots, thus protecting them from various biotic and abiotic stresses (Bonfante and Genre, 2010). Mycorrhizas possess inherent novel remediation properties for HMs in soil, therefore can act as good metal accumulators. They can survive well in poor nutrient soil, loaded with heavy metals. Thus, microbial remediation serves as a most easy, safe and effective technology for remediation and rehabilitation of contaminated soil.

2.3 Mycorrhizas

Mycorrhizal fungi are mutualistic root symbionts with heterogeneous fungal taxas that thrive in the rhizospheric soil. In this association, both plant and fungi assist each other with various nutritional and non-nutritional benefits (Bonfante and Genre, 2010). Mycorrhizae forms a dense filamentous network that draw water and nutrients from the deeper soil and delivers to the plant roots, thus accelerating plant growth and root development. It is estimated that every kilometer of soil contains at least 200 km of fungal strands, accessing the smallest pore of the soil (Bonneville *et al.*, 2009). Apart from providing nutrition, mycorrhizal fungi also protect the plant from drought and salinity, pests and pathogens, heavy metal toxicity and extreme environments (Smith and Smith, 2015). In exchange to all these benefits, the mycorrhizae are

awarded with photosynthates or carbohydrates like glucose by the plants. The fungi utilize these carbohydrates for its growth and synthesis of glycoprotein glomalin which is released into the soil improving the soil structure and organic content (Wu *et al.*, 2014). In the soil, the mycorrhizal hyphae form an extensive network of wood-wide web, which connect all surrounding plant communities promoting horizontal nutrition transfer (Harrison, 2005). They are the source of carbon to many achlorophyllous heterotrophic plants. Alpines and boreal zones, tropical forests, grasslands and croplands are the most commonly mycorrhizal colonized areas (Selosse and Roy, 2009).

These mycorrhizal fungi are more than 450 million years old. About 80% of all land plants with more than 92% plant families are mycorrhizal (Wang and Qiu, 2006). They are most prevalent symbionts involving about 6000 fungal species in the Glomeromycotina, Ascomycotina, and Basidiomycotina and 240,000 plant species (Bonfante, 2003). Mycorrhizas are cosmopolitan and abundant even in the highly degraded areas. They are classified into 5 groups based on their characteristic interact with the host cells (Table 2.2). Among the five associations, arbuscular mycorrhizas (AM) and ectomycorrhizas (ECM) are the two most abundant associations. Orchid, ericoid and arbutoid mycorrhizas are confined to the genera within the Orchidaceae, Ericaceae and Arbutoideae families, respectively (Brundrett, 2017). Arbuscular, orchid, ericoid and arbutoid mycorrhizas establish an intracellular symbiosis by penetrating their hyphae into the root cells, whereas the ectomycorrhizal hyphae remain extracellular (Bonfante and Genre, 2010). Till date mycorrhizas have garnered vast attention owing to the new genetic, cellular and molecular techniques along with the genome sequencing of various mycorrhizal plants and fungi (Martin *et al.*, 2008).

Table 2.2: Classification of different types of mycorrhiza based on fungal Texas and plant species along with their characteristic features.

Mycorrhiza Type	**Fungal Texas**	**Plant Host**	**Features**
Arbuscular-Mycorrhiza	Glomeromycota	Angiosperms Gymnosperms Pteridophytes Lower plants	• Fungus penetrates the cortical cells of roots of vascular plants forming arbuscules

			• help plants in capturing phosphorus, sulfur, nitrogen and micronutrients from soil • found in 80% of vacuolar plants
Ecto-Mycorrhiza	Ascomycota Basisiomycota Zygomycota	Woody trees: Pinaceae Fagaceae Dipterocarpaceae Caesalpinoidaceae	• fungus don't penetrate the plant cells, instead forms an intercellular hypha called Hartig net • found in 2% plant species • forms 40 µM thick hyphae mantle around the root surface • protect host plant from various biotic and abiotic stresses
Orchid Mycorrhiza	Basidiomycota	Orchidaceae	• association between roots of plants orchidaceae and variety of fungi • during germination, orchid seeds receive carbon from their fungal symbionts • fungus develop structures called pelotons within the root cortex of orchids
Ericoid Mycorrhiza	Ascomycota	Ericaceae	• association between members of Ericaceae family and various fungi • highly adopted to acidic and nutrient deprived soil including boreal forests, bogs and heathlands

			• Molecular clock estimated these associations to be approximately 140 million years old
Arbutoid Mycorrhiza	Basidiomycota	Arbutoideae	• fungal association between plants of family arbutoideae and basidiomycetes • fungus forms intracellular coils within the cortical cells, intercellular hartig net and outer mantle sheath • fungus induces a pinnate-crutiate branching pattern with host lateral roots

Among different types of mycorrhizas, ectomycorrhizas hold a great interest due to their dual lifestyle. In soil, they form symbiotic association with the host plant, depending on plants for carbohydrates, whereas under laboratory conditions, they can live as facultative saprotrophs and can be cultured on suitable media. Therefore, they hold potential application in bioremediation.

2.4 Ectomycorrhiza

Ectomycorrhiza is a symbiotic association of fungi to the plant roots, where the fungi ensheath its hyphae around the root tip forming the thick hyphae mantle of nearly 40 µm. Inside the mantle, the hyphae penetrate the cell wall and grow in between epidermal cells and cortical cells. They never penetrate inside the cell lumen of roots, hence forming a Hartig net (Figure 2.4). This Hartig net is the region of juxtaposition where exchange of water, nutrients and other components between both fungi and the plant roots takes place (Bonfante and Genre, 2010; Balestrini and Bonfante, 2014; Henke *et al.*, 2015).

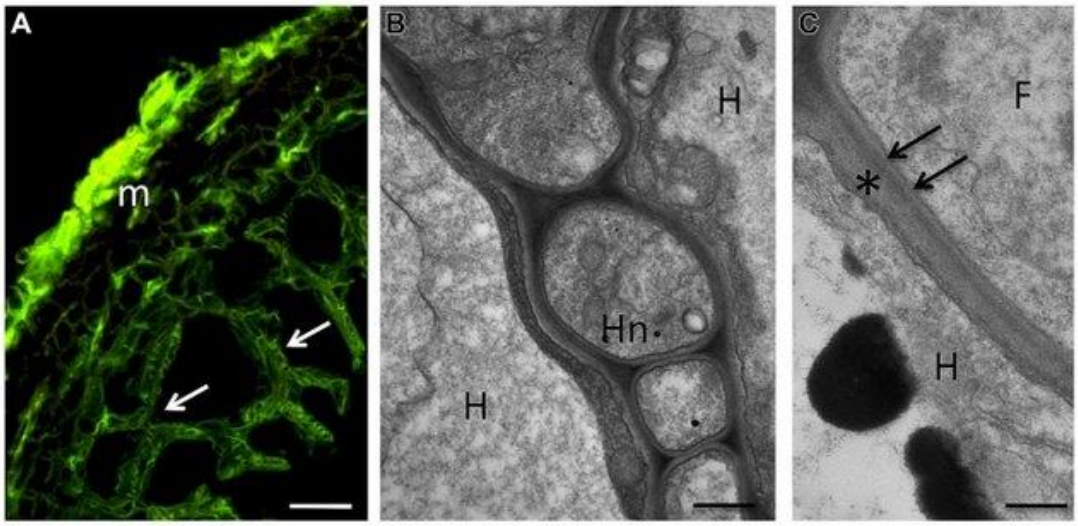

Figure 2.4: The hyphae of ECM fungi colonizing epidermal and cortical cell layer (A) The confocal micrograph of ECM *Tuber melanosporum* colonizing hazelnut, indicating the mantle (m) formed by the dense hyphae and Hartig net (arrows) surrounding epidermal and cortical cells. (B) Hartig net (Hn) (C) Magnification of the contact zone between plant (*) and fungal cell wall (arrows). F-fungus; H-Host cell. (Balestrini and Bonfante, 2014).

On the other end outside the fungal mantle, hyphae extend into the soil called extraradical mycelium and acts like an extension to the plant roots so as to have access to the nutrients from deeper parts in soil. In pine seedlings, extraradical mycelium of *Pisolithus tinctorius* contributes 99% of the nutrient-absorbing surface of roots (Rousseau *et al.,* 1992). Thus, ectomycorrhizal fungi provide water, mineral and nutrients to the plant and are rewarded with the photosynthates or stored carbohydrates by the host plant (Figure 2.5) (Martin and Nehls, 2009; Bonfante and Genre, 2010). These fungi have a dual lifestyle, form symbiosis with the plant roots and as facultative saprotrophs in soil (Martin and Nehls, 2009). At laboratory conditions they can be cultured without host (unlike AMF), but under field conditions they depend on their host for carbohydrates (Van Der Heijden *et al.*, 2015).

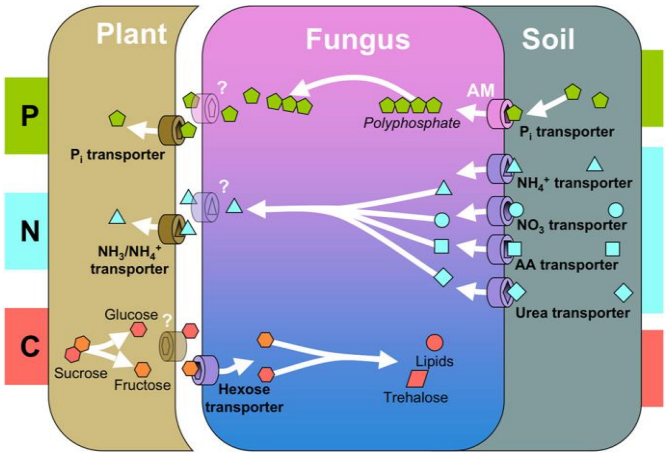

Figure 2.5: Nutrient exchange mechanism between ECM fungi and their host plant (Bonfante and Genre, 2010)

Ectomycorrhizal fungi belong to the family of Basidiomycota (252 genera), Ascomycota (84 genera) and Mucoromycota-Endogonales (Van Der Heijden *et al.,* 2015). More than 10,000 fungal species have been estimated to form ectomycorrhiza with the host plants (Finlay, 2008). They can form a visible reproductive structure of epigeous mushroom and hypogeous truffles at the feet of trees they colonize. The most popular edible mushrooms 'Tuber fungus", deadly caps destroying angels "*Amanita*" also belongs to ectomycorrhizas. Trees hosts for ectomycorrhizal fungi include families like Pinaceae, Fagaceae, Betulaceae, Dipterocarpaceae and Caesalpinoidaceae, distributed in the sub-tropic, temperate and boreal forests (Smith and Read, 2010). Birch (*Betula*), dipterocarp (*Pakaraimaea*), beech (*Fagus*), Willows (*Salix*), Pine (*Pinus*), Oaks (*Quercus*), eucalypts (*Eucalyptus*) are the common host species for ectomycorrhizal symbiosis (Chen *et al.,* 2015; Hrynkiewicz *et al.,* 2015; Murata *et al.,* 2015; Brearley *et al.,* 2016; García-Guzmán *et al.,* 2017; Horton *et al.,* 2017; Kaiser *et al.,* 2017)

It has been estimated that more than 50,000 plant species are involved in ectomycorrhizal association. Most of the ectomycorrhizas have colonized northern temperate forest soils, whereas arbuscular mycorrhizas are commonly found in tropical forests. Agaricomycetes were found to be the most dominant class of ectomycorrhizal fungi in the soil (Buée *et al.,* 2009). Ascomycetes have been reported showing higher stress tolerance as compared to basidiomycetes. Many authors have observed the dominance of ascomycetes in heavily polluted areas whereas basidiomycetes were observed in less polluted and control plots. The genera *Phialophora, Phialocephala, Leptodontidium* and many other ascomycetes have been reported to have adaptive metal tolerance (Colpaert *et al.,* 2011). Similarly many

basidiomycetes have also been reported to have complete defense mechanisms against heavy metals like *Laccaria bicolor* (Reddy *et al.,* 2014), *Hebeloma cylindrosporum* (Ramesh *et al.,* 2009), *Pisolithus albus* (Reddy *et al.,* 2016), *Suillus bovinus* (Ruytinx *et al.,* 2013), *Suillus luteus* (Nguyen *et al.,* 2017), *Suillus himalayensis* (Kalsotra *et al.,* 2018) *Paxillus involutus* (Bellion *et al.,* 2007), *Amanita strobiliformis* (Osobovva *et al.,* 2011) etc.

2.4.1 *Laccaria bicolor*

Laccaria bicolor is an ectomycorrhizal fungus widely used as a soil inoculant in various agricultural and horticultural practices with a variety of tree species like red pines, jack pines, black spruce, Oregon pine, Poplar, etc. (Heller *et al.,* 2008; Felten *et al.,* 2009; Plett *et al.,* 2011). They belong to Phylum: Basidiomycota - Class: Agaricomycetes - Order: Agaricales and Family: Hydnangiaceae. *L. bicolor* grows gregariously in the temperate zone of the globe including temperate and boreal forests of North America, Great lake region in West Virginia and Northern Europe (Mueller and Gardes, 1991; Selosse *et al.,* 1998). It is edible but not much palatable and grows usually in mixed birch and pine woods. They are small tan colored mushrooms with lilac gills (Figure 2.6). The gills are faintly purplish to pinkish in color. The mushroom cap is 2-4.5 cm broad, flat to convex, often incurved at the margins in various shades of ochraceous buff and tan. The fibrillose flesh is whitish, tinged with pink having no apparent smell or taste. The microscopic analysis reveal that the spores are white, nearly round with thin spines and 4-spored basidia. The mushroom stem is 3-10 cm long and almost 1 cm thick with slightly swollen from base. *L. bicolor* is a carnivorous fungus that can catch and kill insects specially springtails (Klironomos and Hart, 2001).

L. bicolor is the first ectomycorrhizal fungus to have its whole genome sequences (Martin *et al.,* 2008). The genome is approximately 65 mega bases long with estimate 20,000 protein coding genes (Martin and Selosse, 2008). The fungus has a dual saprotrophic and biotrophic lifestyle. The genome of *L. bicolor* lacks enzymes involved in degradation of plant cell wall however, possess enzymes involved in degradation of other polysaccharides. Thus, they can also live as saprotrophs in soil (Martin *et al.,* 2008).

Figure 2.6: Picture of *L. bicolor* showing mushroom cap, lilac gills and stem while growing in soil (Source: https://www.first-nature.com/fungi/laccaria-bicolor.php)

L. bicolor is known to support forest growth and sustainability by providing growth limiting nutrients to their host plant. It stimulates lateral root formation in the host plant (*Poplar* and *Arabidopsis*), thus providing access to the otherwise inaccessible areas of soil (Felten *et al.,* 2009; Plett *et al.,* 2014). In field studies, it has proven to efficiently colonize and improve the survival of red pines, black spruce, Douglas-fir and jack pines (Quoreshi and Timmer, 2000; Selosse *et al.,* 2000; Podila *et al.,* 2002; Felten *et al.,* 2009). It secretes various endocellulases like β-1,4 endoglucanase (Zhang *et al.,* 2018), lipochitooligosaccharides (Cope *et al.,* 2019) and small-secreted proteins (Pellegrin *et al.,* 2019) to form symbiotic association with host plants. *L. bicolor* is commercially used in French nurseries to inoculate Douglas-fir seedlings, so as to obtain high-performance planting material for reforestation.

2.5.2 *Hebeloma cylindrosporum*

Hebeloma cylindrosporum is a mushroom forming ectomycorrhizal fungus. It belongs to Phylum: Basidiomycota, Class: Agaricomycetes, Order: Agaricales and Family: Cortinariaceae. It was first isolated and identified by a French mycologist Henri Romagnesi (Romagnesi, 1965). Its mushroom cap is almost 2-4 cm wide, convex in beginning but later gets flattened. Its slightly papilliform with margins slightly striated and incurved. The cuticles are viscous with smooth brown color in center with lighter edges (Figure 2.7). The cylindrical mushroom stem is usually very long of slightly lighter color than the mushroom cap. The flesh

is thin, whitish with no smell. It has been reported to occur in Europe mainly from Norway to Finland in north and to Spain in south. It is mostly precured in autumn season until mid-winter, before frost from the mixed forests with pines, oaks and sandy soil (Gryta *et al.*, 1997; Marmeisse *et al.*, 2004). It grows in basins of plains and rivers but not in mountains. It is abundant in forest stands, developing on sand dunes with little organic matter mostly along the Mediterranean and Atlantic coast (Contu, 1991). It is mostly associated with different pine trees, mainly reported with *Pinus pinaster* (Torres-Aquino *et al.*, 2017). *H. cylindrosporum* is a saprotroph and can utilize soil organic nitrogen (Kohler *et al.*, 2015). It is the ectomycorrhizal fungus with smallest genome sequenced so far. The genome of *H. cylindrosporum* consists of 38 mega bases with 15382 predicted protein coding genes (Kohler *et al.*, 2015). The genome retains diverse genes coding for enzymes active on polysaccharides (cellulose, hemicellulose, pectin) and lignins (Peroxidases) (Doré *et al.*, 2015; Kohler *et al.*, 2015). The fungi have few genes coding for cell wall degrading enzymes but have retained a diverse array of genes coding for other lignocellulose degrading enzymes (Kohler *et al.*, 2015).

Figure 2.7: *H. cylindrosporum* showing mushroom hat, cuticles and long stem (Source: http://www.mykologie.net/index.php/houby/podle-morfologie/lupenate/item/1442-hebeloma-cylindrosporum).

One of the most remarkable feature of *H. cylindrosporum* is that its entire life cycle (including fruit body formation) can be reproduced in laboratory under axenic conditions using defined medium and can be genetically transformed using *Agrobacterium tumerfacins* (Debaud and Gay, 1987; Combier *et al.,* 2003). Therefore, *H. cylindrosporum* represents a good model to perform in-depth studies on ectomycorrhizal systems.

2.5 Mycorrhizal interaction with Heavy metals

Mycorrhizas are an integral and functional part of plant roots. They colonize the plant roots and extend their extensive network of hyphae into the surrounding environment. These hyphae penetrate deep into the soil, fetching the low mobility nutrients like P, N, Cu, Zn etc., for the host plant. They play an important role in promoting plant growth and health through nutrient exchange, water cycling and proving tolerance to biotic as well as abiotic stresses in exchange for plant fixed carbohydrates (Bonfante and Genre, 2010; Smith and Read, 2010).The experimental field application of these mycorrhizal fungi have proven to increase the overall productivity and biomass in many crops including fruits, legumes, cereals and trees (Hashem *et al.,* 2016; Mo *et al.,* 2016; Bona *et al.,* 2017; Grelet *et al.,* 2017;). They are well known for their role in alleviating heavy metal toxicity in the host plant. They act like a buffer to protect the host plant from heavy metal toxicity. The ECM fungus *Paxillus ammoniavirescens* increased the biomass of *Betula pubescens,* protecting it from heavy metals like Cu, Zn, As, Cd, Hg and Pb leading to lower oxidative stress (Fernández-Fuego *et al.,* 2017). Similarly, in Popular clones, the inoculation of plants with both ecto and endomycorrhizal fungi increased the plant biomass whereas limiting the accumulation of Zn, Cu, Pb and Cr (Phanthavongsa *et al.,* 2017). Also, *Tuber borchii* Vitt. innoculated with *Cistus creticus* L. protected it form Zn, Pb and Cr stress (Sabella *et al.,* 2016). ECM fungus *Pisolithus albus* accumulated Cd and Cu, protecting the host *Eucalyptus tereticornis* from metal stress (Reddy *et al.,* 2016). *Pisolithus* sp., *Cenococcum geophilum*, *Laccaria laccata* protected Japanese red pine and Oak in copper mine tailing (Zong *et al.,* 2015)

However, the response to mycorrhizal fungi to different heavy metals depends upon the plant species, fungal isolate and the associated heavy metal (Ferrol *et al.,* 2016). Although mycorrhizal fungi are well known for their ability to filter the transfer of HMs from soil to plant roots, but in many cases they have been reported of enhancing the metal accumulation in the host plant (Leung *et al.,* 2010). In a study by Orłowska, (2012), different mycorrhizal fungi (*Rhizophagus intraradices*, *Funneliformis geosporum*, *Rhizophagus clarus*, *Glomus* sp.)

inoculated with *Plantago lanceolate* plant showed differential response to different heavy metals. The mycorrhizal inoculation inhibited the transfer of arsenic and lead to the host plant whereas enhanced the uptake of zinc and cadmium in *P. lanceolate*. Similar observations were recorded in case of sunflower plant inoculated with *Rhizophagus irregularis* and *Funneliformis mosseae*. The *Rhizophagus irregularis* enhances the cadmium phytoextraction by sunflower plant whereas the *Funneliformis mosseae* promoted Cd and Zn phytostabilitization in soil (Hassan *et al.,* 2013). Also, in case of *Limonium sinuatum*, inoculation of plant with *Glomus mosseae* and *G. intraradices* increased the total Pb and Cd accumulation in roots by 3 folds higher than the non-mycorrhizal plant (Sheikh-Assadi *et al.,* 2015).

Different mycorrhizal fungi accumulate different metals under different conditions. When exposed to different metals, *Imleria badia* accumulated Ag, Cd, Zn and Cl whereas *Amanita muscaria* accumulated V (Cejpkova *et al.,* 2016). Similarly, in a different study, exposure of different fungi to different metals showed that *Agaricus campestris* accumulated Ni, Cr and Cd, whereas *Macrolepiota procera* accumulated Pb and *Boletus edulis* accumulated Hg (Širić *et al.,* 2017). Therefore, the mycorrhizal fungi show different response to different metals.

2.6 Ectomycorrhizal fungi and the mechanism of HM detoxification

ECM fungi have proven to protect the plants against heavy metal stresses. The presence of ECM symbionts at plant roots significantly reduces the heavy metal uptake (Degola *et al.,* 2015; Reddy *et al.,* 2016). ECMs are not only capable of surviving under metalliferous soil but also promote the growth of host plant under metal stress. ECM fungi modulate the heavy metal transfer into the host plants. The fungal mantle acts as an effective barrier or filter for the heavy metals to enter into the plant cells (Figure 2.2). The heavy metal concentration decreases from the rhizomorphs - hyphae mantle – cortical cells to vascular tissues. This has been clearly demonstrated in case of *Pinus sylvestris* colonized with *Suillus luteus* under zinc stress, where the concentration of zinc declined from 12,830 µg/g in rhizomorph to 2040-3820 µg/g in hyphal mantle, to 280-675 µg/g in cortical cells to 430 µg/g in the vascular tissues (Turnau *et al.,* 2001). Similar results were reported in case of Cu and Mn by Turnau *et al.,* (2001), where the Cu concentration decreased from 420 µg/g in rhizomorphs to 17 µg/g in hyphal mantle and 6 µg/g in vascular tissues and Mn concentrations decreased from 490 µg/g in rhizomorphs to 88 µg/g in hyphal mantle, to 13-26 µg/g in cortical cells and 14 µg/g in vascular tissues (Turnau *et al.,* 2001). *Betula pendula* seedlings inoculated with ECM fungi reduced the concentration of Cu and Pb in the above ground parts of plant, thus protecting the plant from elevated metal

stress (Bojarczuk and Kieliszewska-Rokicka, 2010). Similar results have been reported in *Pinus sylvestris*, where the plants inoculated with *Suillus luteus*, *Suillus bovinus*, *Scleroderma citrinum, Amanita muscaria and Lactarius rufus* showed better plant protection and nutrient uptake, transferring less Cd, Cu, Pb and Zn to the above ground plants than non-mycorrhizal plants (Adriaensen *et al.,* 2005, 2006; Krupa and Kozdroj, 2007; Krznaric *et al.,* 2009).

Colpaert *et al.,* (2011) reported development of adaptive heavy metal tolerance in different ECM fungi isolated from metal polluted areas. *Suillus luteus* and *Suillus bovinus* isolated from metal polluted areas showed better tolerance to heavy metals like Zn, Cu and Cd when colonized with *Pinus sulvestris* than the same fungus isolated from non-polluted areas (Adriaensen *et al.,* 2005, 2006; Krznaric *et al.,* 2009; Colpaert *et al.,* 2011). Similar observations have also been made with *Pisolithus tinctorius*, *Pisolithus albus* and *Cenococcum geophilum,* where the isolates from metal polluted areas showed higher metal tolerance than isolates from non-polluted areas (Egerton-Warburton and Griffin, 1995; Goncalves *et al.,* 2009; Jourand *et al.,* 2010). These fungi have developed polygenic mechanisms to cope with heavy metals in the soil, thus protecting their host plant. These mechanisms can be broadly classified into two categories: Avoidance and Tolerance.

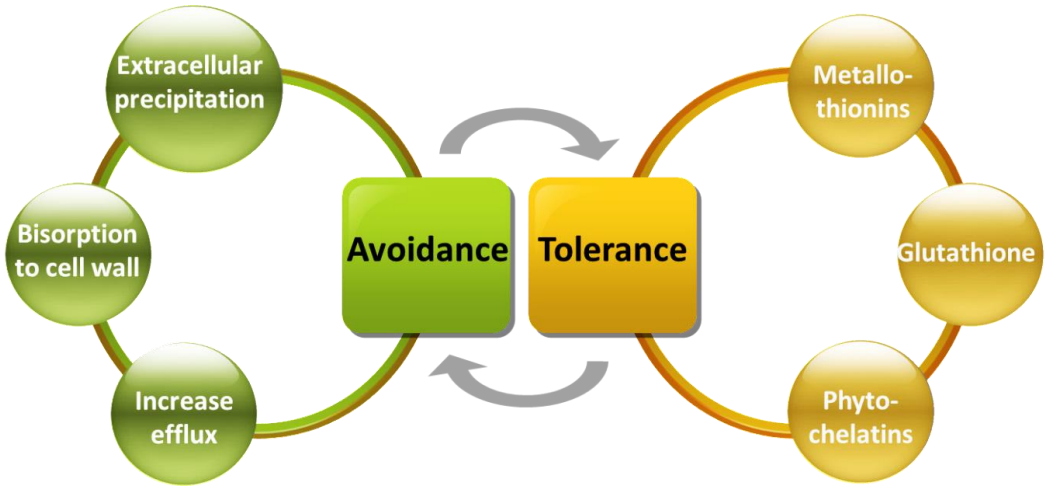

Figure 2.8: Polygenic response of ECM fungi to heavy metals either through avoidance or through tolerance.

In "Avoidance": the ECM fungi restrict the entry of heavy metals through extracellular precipitation by excreting di/tricarboxylic acids and oxalic acids, by bisorption of metal ions to the cell wall through chitin and glucosamine or by increasing the cellular efflux (Figure 2.8). In spite of the restricted entry of these heavy metals, 20-30% of heavy metals could still be

found in the cytosol and vacuoles (Blaudez *et al.,* 2000; Fernández-Fuego *et al.,* 2017). The heavy metals that enter inside the cell are chelated intracellularly through various thiol rich compounds like metallothioneins (MTs), glutathione (GSH) and phytochelatin (PCs) known as "Tolerance" mechanisms (Figure 2.8). Heavy metals have high affinity for the thiol group (-SH) of these chelators and forms metal-MT, metal-(GSH) complex, which actively gets transported into the vacuoles (Sharma *et al.,* 2016) (Figure 2.9). The role of ECM fungi in metal homeostasis has been clearly reviewed by Bellion *et al.,* (2006), Colpaert, (2011), Luo *et al.,* (2014), etc.

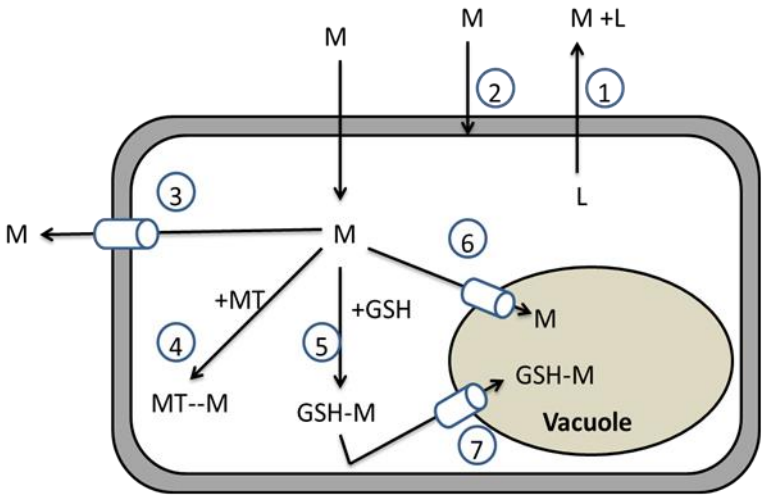

Figure 2.9: Mechanisms of heavy metal tolerance in ECM fungi. 1) extracellular chelation by secreted ligands 2) cell wall binding 3) enhanced efflux 4) intracellular chelation by metallothioneins (MT) 5) intracellular chelation by glutathione (GSH) 6) subcellular compartmentation 7) compartmentation of GSH-M in vacuoles.

2.6.1 Biosorption to Cell wall

Cell wall is the first barrier to the heavy metal toxicity. Fungal cell wall, being rich in polysaccharides and glycoproteins, exhibit excellent metal binding properties (Georgescu *et al.,* 2019). The fungal cell wall being negatively charged (due to anionic glucan and chitin) offers multiple active sites for heavy metal binding (Bellion *et al.,* 2006; Anahid *et al.,* 2011). The polysaccharides present in fungal cell wall – chitin and chitosan have been well characterized for their metal sequestration potential. The chitin molecules present in the fungal cell wall have been characterized for their efficient binding to Cd molecules forming the Chitin-Cadmium complex in *Neurospora crassa* (Bhanoori and Venkateswerlu, 2000). The role of

polysaccharide α-(1,3)-D-glucan and β-(1,3)-glucanase in Pb, Cd and Ca biosorption has also been characterized in *Boletus edulis* and *Neurospora crassa* through GPC, NMR and FTIR analysis (Sowjanya and Mohan, 2009; Choma *et al.*, 2018). The potential metal-binding sites on the fungal surface includes- free carboxyl groups, amino groups, hydroxyl groups, phosphate and mercapto groups of cell wall polysaccharides, proteins and lipids (Dhankhar and Hooda, 2011). Different mechanisms responsible for metal binding to the fungal surface are adsorption, ion-exchange, surface complexation, chelation, precipitation and crystallization (Figure 2.10). In a recent study on *Pleurotus ostreatus* under Cd stress, the SEM-EDX and FTIR characterization revealed that the biosorption of Cd on the fungal wall was due to the ion-exchange process along with the complexation of functional groups (Georgescu *et al.*, 2019).

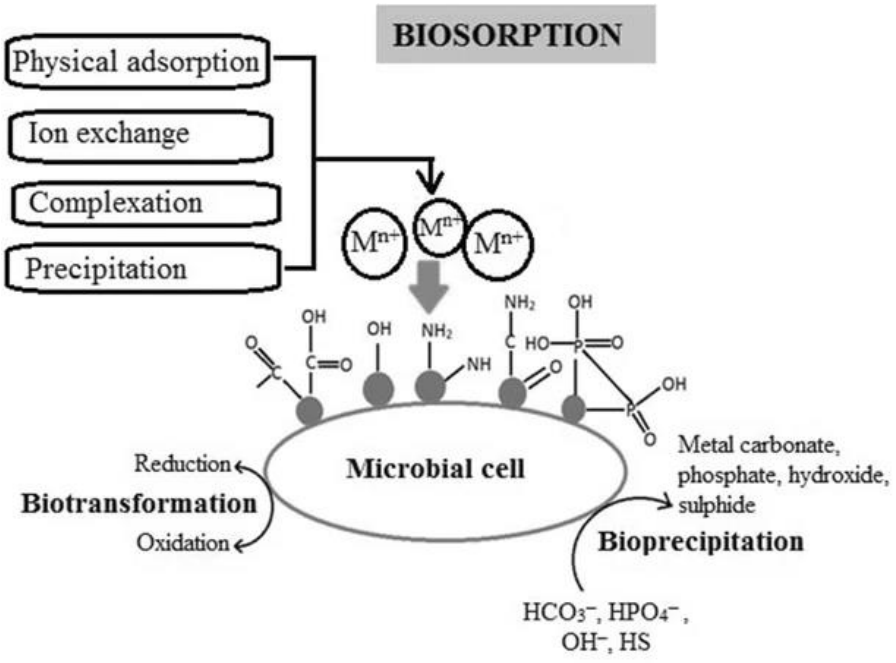

Figure 2.10: Mechanisms involved in heavy metal biosoption to fungal cell wall (Hansda *et al.*, 2016)

There are many reports on the metal biosorption tendencies of different fungi. *Phanerochaete chrysosporiun* adsorbs As, Cd and Cr (Rudakiya *et al.*, 2018), *Hebeloma crustuliniforme* adsorbs Cd and Zn (Frey *et al.*, 2000), *Amanita rubescens* (Sari and Tuzen, 2008), *Aspergillus niger* adsorbed Cd and Ni, *Trichoderma* for Cd (Bazrafshan *et al.*, 2016) etc.

2.6.2 Metal efflux

The reduced uptake of heavy metals by ECM fungi is due to the induction of efflux mechanism under heavy metal stress. Majorel *et al.,* (2014) reported low accumulation of Ni in *P. albus* tissues, under exposed to high Ni concentrations, due to the metal efflux mechanisms. Similar observations were made in *S. bovinus*, *P. involutus* and *H. cylindrosporum*, where the increase in metal efflux resulted in low metal accumulation in the fungal tissue. This metal exclusion in fungal symbionts results in lower metal influx by the host plant, thus protecting from metal stress (Blaudez *et al.*, 2000; Blaudez and Chalot 2011; Ruytinx *et al.*, 2013). In contrast to the above observations, few studies have reported increase in metal bioaccumulation in both ECM and its associated host when exposed to high metal stress (Ma *et al.,* 2014; Širić *et al.,* 2016). ECM fungus *Paxillus involutus* significantly increased the net Cd influx in the root apical region of *Populus canescens* when exposed to high cadmium stress (Ma *et al.*, 2014).

ECM fungi have been reported of secreting various exudates in the rhizosphere in response to metal stress. These exudates like oxalic acid, formic acid, malic acid and succinic acid can alter the bioavailability of toxic metals in the rhizosphere, thus protecting the host plant from metal toxicity (Meharg 2003; Bellion *et al.,* 2006; Ray and Adholeya 2009; Colpaert *et al.,* 2011; Targhetta *et al.,* 2013). Johansson *et al.,* (2008) reported oxalate exudation in six ECM fungi, *Hebeloma velutipes, Piloderma byssinum, Paxillus involutus, Rhizopogon roseolus, Suillus bovinus* and *Suillus variegatus*, when exposed to Pb, Cd and As stress (Johansson *et al.,* 2008). In addition of fungal exudates, ECM fungi also induce plant exudates in the rhizosphere. *Pinus tabulaeformis* when colonized with ECM fungus *Xerocomus chrysenteron*, showed enhanced activity of soluble proteins and acid phosphatases in root exudates than their non-mycorrhizal roots under Cu and Cd stress (Zheng *et al.,* 2009). Bellion *et al.,* (2006), reported upto 85% reduction in Cd uptake by oxalic acid exudation in cadmium stressed *Paxillus involutus*. In a similar study Shi *et al.,* (2018), reported 99% removal of chromium Cr(VI) by *Pisolithus* sp. by secreting H^+ ions and organic acids. The H^+ ions secreted by *Pisolithus* sp. reduced the pH of medium, thus reducing Cr(VI). After 12 days treatment with *Pisolithus* sp., it was observed that 75% Cr was removed due to extracellular reduction and 24% was removed by adsorption on cell wall (Shi *et al.*, 2018).

2.6.3 Intracellular chelation

Inspite of the all the extracellular mechanisms, the ECM fungi still accumulate metal ions into its cytosol. The accumulation of these metal ions into the fungal cytosol has been reported in many studies on *Macrolepiota procera, Agaricus campestris, Boletus edulis, Agaricus macrosporus, Pisolithus albus, Aspergillus niger,* etc. (Mukherjee *et al.,* 2010; Melgar *et al.,* 2016; Reddy *et al.,* 2016; Širić *et al.,* 2017). ECM fungi have developed an intense intracellular mechanism to cope with the heavy metals accumulated inside the cell, thus preventing their transfer to host plant. ECM fungi synthesize various thiol rich ligands like metallothioneins and glutathione in response to metal stress. Heavy metals having high affinity for the thiol group of these ligands bind them forming a strong metal-MT or metal-$(GSH)_2$ complex, rendering them nontoxic and subsequently sequestering into the vacuoles (Sousa *et al.,* 2015), thus protecting the host plant from metal stress. The heavy metal tolerance mechanism in ECM plants depends on various factors like type of plant, ECM strain and the type of heavy metal.

2.6.3.1 Metallothioneins

Metallothioneins are intracellular, low molecular weight (usually below 7 kDa), cysteine rich (up to 33%) proteins having high affinity for binding metals and xenobiotics. They lack aromatic amino acids. They also protect cells by trapping reactive oxygen species (ROS). MTs are heterogeneous proteins with diverse amino acid and nucleotide sequences. They are named metallothionein for the ability of their thiol group to bind metal, resulting in a metalloprotein complex which is accumulated into vacuole and later released as metallic complex (Diaz *et al.,* 2006). Apart from metal chelation, MTs are also induced under oxidative stress and salt stress. Metallothioneins are characterized with recurring C-X-C motifs in their primary structure (Figure 2.11) (Reddy *et al.,* 2014; Kalsotra *et al.,* 2018). There are total nine conserved cysteine motifs reported till date, which include- C-X-C, C-X-C-X-C, X-X-C-X-X, X-C-C-X, C-X-C-C, C-C-X-C, C-C-C, C-C-X-C-C and C-X-C-X-C-X-C, where X is any amino acid other than cysteine (Ziller and Fraissinet-Tachet, 2018). Among these nine motifs, only C-X-C motif is common to all MTs, whereas others are species specific.

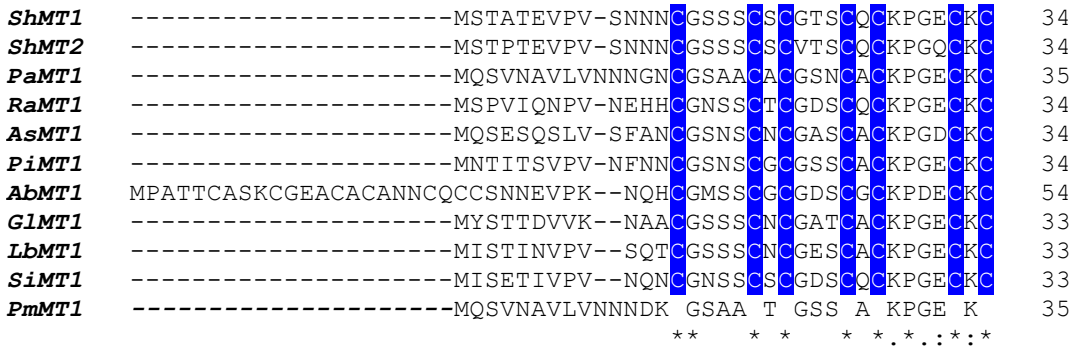

Figure 2.11: Multiple sequence alignment of MT genes isolated from different fungal sources highlighting conserved C-X-C motifs: *Suillus himalayensis* (ShMT1: KY775394, ShMT2: KY775395), *Pisolithus albus* (PaMT1: AJO67962), *Russula atropurpurea* (RaMT1: AHA31882), *Amanita strobiliformis* (AsMT1: AGO04615), *Paxillus involutus* (PiMT1: AAS19463), *Agaricus bisporus* (AbMT1), *Ganoderma lucidum* (GlMT1: ABP02008), *Laccaria bicolor* (LbMT1: AH143933), *Serendipita indica* (SiMT1: ACT83730), *Pisolithus microcarpus* (PmMT1: ESTN25) (Kalsotra *et al.*, 2018).

Metallothioneins bind both essential as well as non-essential heavy metals like copper, cadmium, zinc, arsenic, lead, mercury, silver and forming metal-thiolate complex resulting in metal homeostasis and metal detoxification (Ramesh *et al.,* 2009; Reddy *et al.,* 2014). They form γ-mercaptide bonds with the metal. MT genes are induced by the same metal ions that bind to the MT protein, thus providing a direct activation of the defense mechanism (Waalkes and Goering, 1990). The most common inducers of metallothioneins are Zn, Cu, Cd and Hg. Among these copper and zinc are the primary inducers of metallothioneins.

2.6.3.1.1 Classification of metallothioneins

Numerous studies have reported the presence of metallothioneins in almost all organisms including prokaryotes, fungi, sea urchins, mammals to plants. UniProt data till date records 15 metallothionein families and 38 subfamilies including vertebrates (12), mollusc (4), crustacean (3), echinodermata (2), diptera (2), nematoda (2), ciliate (1), fungi (6), prokaryota (1) and plant (5) (Released: 20th December, 2019) (UniProt, 2019).

Metallothioneins are classified into 3 classes based on their heterogeneous amino acid sequence. Class I metallothioneins comprises of all metallothioneins having sequence similarity with horse kidney MTs. MTs from various vertebrates and mammals fall in this class. Class II metallothioneins consists of all MTs with sequence different from that of Class I

metallothioneins. They mainly include metallothioneins from plant, fungi, yeast and nonvertebrate animals. Class III metallothioneins are basically phytochelatins, which is an entirely different class now (Binz and Kägi, 1999). So broadly we can say that metallothioneins can be classified into two classes Class I and Class II. In case of plants, Class II is further classified into four types based on the distribution of cysteine motifs on both N-terminal and C-terminal domain (Robinson *et al.*, 1993).

A new functional classification system has been proposed by Palacios *et al.,* (2011), in which metallothioneins are classified into two groups Cu-thioneins and Zn-thioneins based on their metal binding ability (Palacios *et al.,* 2011). Zn-thioneins (also Cd-thioneins) are those which form a homometallic Zn-MT or Cd-MT complexes when exposed to zinc or cadmium-enriched media. They exhibit high degree of folding with expected stoichiometry. But when exposed to copper-supplemented media, they form various heteronuclear complexes like Zn-MT/Cu-MT with a lower degree of folding and high thiol group oxidation resulting in disulfide formation. Similarly, Cu-thioneins forms homometallic Cu-MT complexes when exposed to copper-enriched media and shows heteronuclear complexes of Cu/Zn-MT when exposed to zinc supplemented media. Cu-thioneins when exposed to cadmium-supplemented media, forms heterometallic complex of Cd-MT containing sulfide ligands (S^{2-}) (Palacios *et al.*, 2011). Two MTs in *Saccharomyces cerevisae Cup1* and *Crs5* are identified as Cu-thioneins and Zn-thioneins respectively, where *Cup1* isoform has been classified as the strict Cu-thionein and *Crs5* can be defined as a dual metal binding MT more expressive for zinc than copper. Most of the Zn-thioneins exhibit dual behavior (Pagani *et al.*, 2007). In different organisms MTs occur in different isoforms, depending on their different metal binding tendencies. One organism can code for many MTs having differential expression for different metals.

2.6.3.1.2 Structure of metallothioneins

MTs in its apoform (native form without metal ions) are devoid of any tertiary structures. When exposed to metal ions, MTs bind the metal coordinates and form metal-thiolate clusters. Hence, we can say that metallothioneins undergo metal-induced protein folding (Ngu and Stillman, 2009). Since different metal ions require different coordinate geometry, depending on whether they are monovalent or divalent, a single MT protein can be folded into different three-dimensional conformations. Hence, the three-dimensional structure of the metallothionein depends upon the metal ion bound to it. In case of plants, mammals and other higher organisms, metal-MT complexes are reported of having two-domain structure (C-terminal α-domain and

N-terminal β-domain). The α-domain consists of 11 cysteine molecules and can bind 4 divalent metal ions ($M_4(Cys)_{11}$), whereas β-domain consists of 9 cysteine molecules which can bind 3 divalent metal ions ($M_3(Cys)_9$) (Figure 2.12 A,B) (Blindauer and Leszczyszyn, 2010).

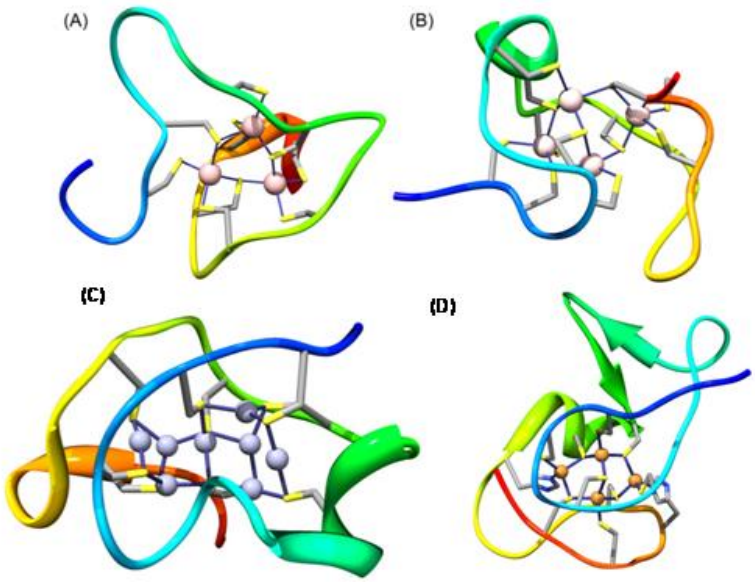

Figure 2.12: Structure of metal-MT complex in different organisms. Mammalian MTs have two domains α and β-domain A) β-domain in mammalian MTs showing Cd3(Cys)9 complex B) α-domain in mammalian MTs showing Cd4(Cys)11 complex C) *S. cerevisiae* Cu8-Cup1, showing the Cu8(Cys)10 complex D) *S. elongatus* Zn4–SmtA, showing the Zn4(Cys)9(His)2 complex (Capdevila *et al.*, 2012).

In case of lower organisms like bacteria, yeast, fungi single domain MTs have been reported. *Neurospora crassa, Agaricus bisporus, Saccharomyces cerevisae, Synechococcus* are reported of having a single domain metallothioneins (Figure 2.12 C,D) (Blindauer *et al.*, 2001; Cobine *et al.*, 2004; Calderone *et al.*, 2005). Metallothionein from *Neurospora crassa* has 25 amino acid residues containing seven cysteines. These seven cysteines can coordinate six Cu^+ atoms forming $Cu_6(Cys)_7$ complex (Cobine *et al.*, 2004). *Cup1* of *Saccharomyces cerevisae* consists of ten cysteine residues which can coordinate 8 Cu^+ ions forming $Cu_8(Cys)_{10}$ complex. Bacterial zinc metallothionein *SmtA* has also been reported in cynobacteria *Synechococcus* forming $Zn_4(Cys)_9(His)_2$ complex. This is for the first time that metallothioneins have been reported of having Histidine molecules. Inspite of diversities, a conserved sequence segment has been reported in mammals, sea-urchins and many single domain MTs, which clearly signals for the common ancestry.

2.6.3.1.3 Metalation by metallothioneins

Inspite of devoting more than three decades on the study of metallothioneins, the information on true mechanisms involved in the metalation process are still incomplete. Metalation can be achieved either by binding of metals to the apo-MT or by the substitution of metalated-MT with the metal with higher binding constant (Li and Otvos, 1998). There are three reasons behind this paucity, firstly the metalation reactions are generally fast to be completed in milliseconds, secondly metallothioneins are very sensitive to oxidation and thirdly lack of proper chromophores (Ngu and Stillman, 2009). Earlier studies on Co^{2+} metalation with metallothioneins concluded that the initial binding of the cobalt ions to metallothioneins occur randomly followed by rearrangement to form unique metal-thiolate clusters (Ejnik *et al.,* 2002) but recently Ngu and Stillman (2009) reported the metalation process using arsenic instead of copper and zinc by electrospray ionization mass spectrometry (ESI-MS). As metalation process is slow and takes minutes to process, whereas copper and zinc metalation occur in milliseconds. The process explains that metals are bound in a non-cooperative manner to the MT peptide. As the first As ion binds to the MT, the rate constant value for the second As ion decreases and the process becomes slow. Similarly, the rate constant keep on decreasing as the metal ions keep on binding and the process becomes slow. The rate constant for binding first As is 6.8 times greater than that for the last As. So, it can be observed that the rate binding values depend upon the number of binding sites in the MT peptide. Since single domain MTs have lesser metal binding sites than double-domain MTs, the metalation process in single domains is slower than in double domains (Ngu and Stillman, 2009).

2.6.3.1.4 Regulation of Metallothionein genes

MT genes are mostly induced under stress conditions like heavy metal stress, oxidative stress, heat shock, etc. Copper, zinc and cadmium are the most active inducers of metallothioneins. Many studies have reported high expression of MT genes under copper and zinc stress (Reddy *et al.,* 2014). The regulation of MT genes occurs mainly at transcription level but some of the post-transcription, translation and post-translation regulations may also occur. Large number of the regulatory sequences are present on the 5' promoter region of MTs. They include various cis-acting elements like metal response elements (MREs), antioxidant response elements (AREs), glucocorticoid responsive elements (GREs), cAMP response elemnts (CREs), TPA response elements (TREs), Interferon response elements (IRE), heat shock elements (HSEs), etc located in the promoter region (Guirola *et al.,* 2012; Ziller and Fraissinet-Tachet, 2018).

When exposed to metal stress, metal transcription factor-1(MTF-1) binds MREs and induces the metallothionein expression. Hence, we can say that MT genes are regulated at transcriptional level (Park *et al.,* 2013). The transcriptional regulators of MTs can also be used as biomarkers of cell metal toxicity (Lu *et al.,* 2018).

2.6.3.1.5 Metallothioneins and ectomycorrhizal fungi

It is very essential to study the role of metallothioneins in ECM fungi, since they thrive on the metal polluted soil and possess a significant role in bioremediation. Although many reports are available till date on metallothionein genes isolated from prokaryotic bacteria (Jan *et al.,* 2014), plants (Shukla *et al.,* 2016), animals (Davis and Cousins, 2000) and fungal species (Reddy *et al.,* 2016) etc., but not much have been reported in ECM fungi.

The metal binding tendency of metallothioneins varies for different metals and host species. Different metallothionein isoforms express differentially in different ECM fungi in response to different metals. In case of *Amanita strobiliformis*, three isoforms of metallothionein genes (*AsMT1, AsMT2, AsMT3*) have been characterized. Among these *AsMT1* was up-regulated in the presence of copper and silver, *AsMT2* in the presence of cadmium and *AsMT3* by zinc (Hložková *et al.,* 2016). Reddy *et al.,* (2014) characterized two (*LbMT1 and LbMT2*) out of six putative metallothionein genes in *Laccaria bicolor* genome and reported their differential expression to copper, cadmium and zinc stress. The expression of both *LbMT1 and LbMT2* were found to increase as a function of increasing external copper concentration, whereas only *LbMT1* responded to cadmium. The expression of both the genes was unaffected by zinc (Reddy *et al.,* 2014). Kalsotra *et al.,* (2018) also identified two MT genes in *Suillus himalayensis* (*ShMT1* and *ShMT2*), both genes were highly expressive under copper stress but not under cadmium stress. Further, the functional complementation of both *ShMT1* and *ShMT2* genes in yeast mutants *cup1* (*S. cerevisiae* mutant for copper), *zrc1* (*S. cerevisiae* mutant for zinc) and *yap1* (*S. cerevisiae* mutant for cadmium) through drop assay on SD media supplemented with heavy metal. The results clearly demonstrated the role of *ShMT1* and *ShMT2* genes in providing copper and zinc tolerance (Figure 2.13). However, poor tolerance was recorded for cadmium (Figure 2.13) (Kalsotra *et al.,* 2018).

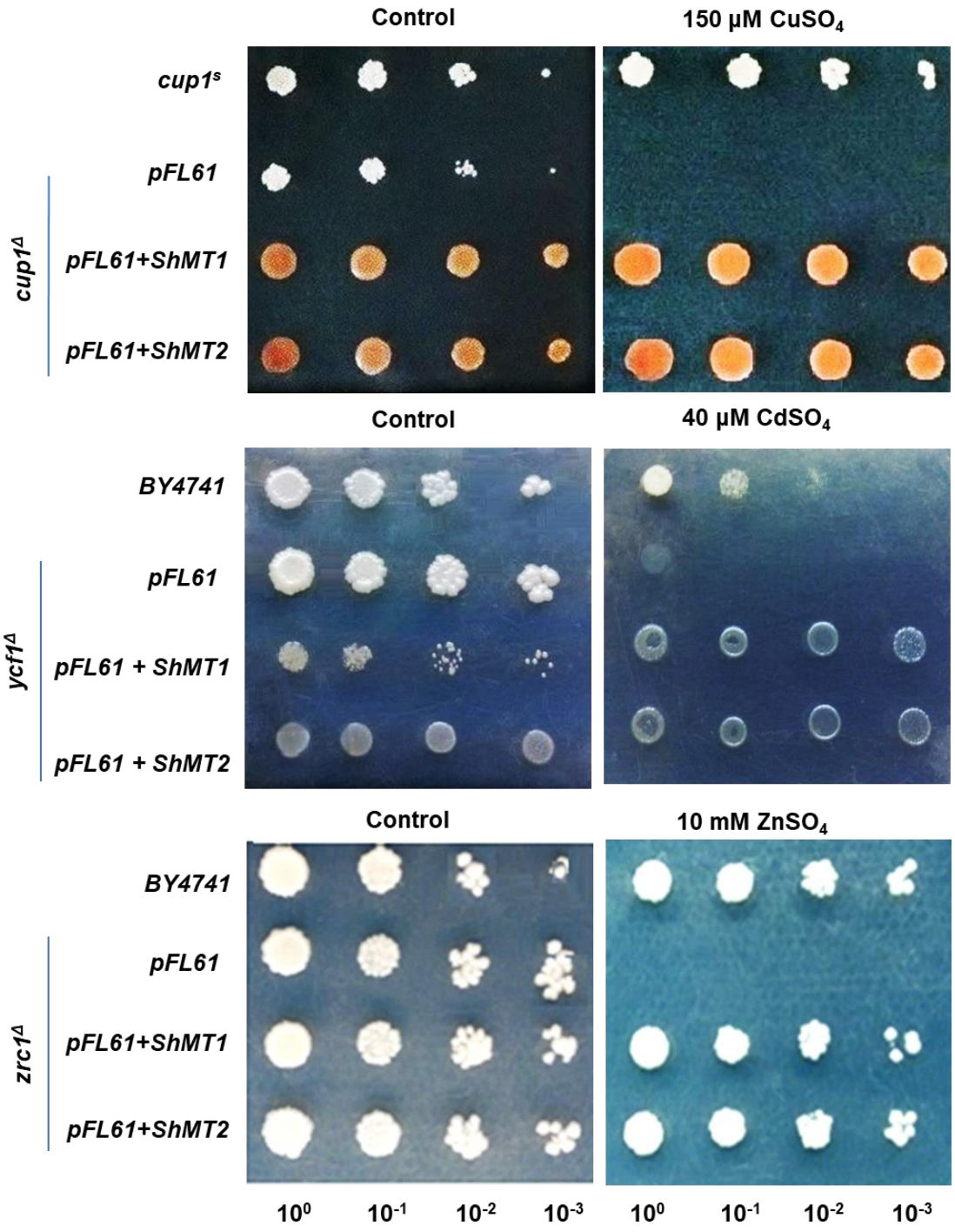

Figure 2.13: Functional complementation of *Saccharomyces cerevisiae* mutants, *cup1*$^{\Delta}$, *ycf1*$^{\Delta}$ and *zrc1*$^{\Delta}$ on selective media. Mutant strains were transformed with empty vector (EV) pFL61, or vector containing *ShMT1* and *ShMT2*. Diluted transformant cultures were spotted on SD-Ura medium with or without metal supplement as indicated. Wild-type strains *cup1*^{S} and BY4741 transformed with EV were used as positive controls (Kalsotra *et al.*, 2018).

Also, in case of *Hebeloma mesophaeum*, three MT isoforms (*HmMT1*, *HmMT2*, *HmMT3*) have been identified and characterized, among which *HmMT1* was induced by zinc and cadmium whereas *HmMT2* was induced by silver (Sácký *et al.*, 2014). In case of *Hebeloma cylindrosporum* two metallothionein genes (*HcMT1* and *HcMT2*) have been characterized, where *HcMT1* was expressive only in response to copper and *HcMT2* was expressive in response to both cadmium and copper (Ramesh *et al.*, 2009). The expression level of both *HcMT1* and *HcMT2* genes in response to different concentrations of cadmium and copper also analyzed by RT-PCR analysis. The *HcMT1* transcription was induced by copper and *HcMT2* transcription was induced by cadmium (Ramesh *et al.*, 2009). This clearly shows that different isoforms of MT genes express differentially to different metals in different ECM fungi.

In other studies, on *Pisolithus albus* (Reddy *et al.*, 2016) and *Paxillus involutus* (Bellion *et al.*, 2007), one metallothionein coding gene *PaMT1* and *PiMT1*, respectively was identified in each, which were induced by both cadmium and copper stress. Nguyen *et al.*, (2017) characterized two highly conserved MT genes *SlMTa* and *SlMTb* in *Suillus luteus*. The heterologous expression of these genes in yeast mutants successfully rescued them from Cu toxicity but could not survive Cd and Zn. Therefore, both *SlMTa* and *SlMTb* were classified as Cu-thioneins.

Lorenzo-Gutiérrez *et al.*, (2019) characterized MT gene (*mt1*) isolated from *Fusarium oxysporum*. The expression of *mt1* gene was highly activated under Zn exposure. However, the *Fusarium oxysporum* strain mutated with *mt1* gene, showed high sensitivity to Cu, Cd, and Zn. The *mt1* mutant strain also displayed poor resistance to macrophage killing and were more prone to oxidative stress due to low induction in of *gapdh* and *prx* genes. This observation highlights the fact that the absence of *mt1* gene impairs the fungal defense system against reactive oxygen species, Cu and Cd. Many other metallothionein isoforms were also identified in other ECM fungi as listed in Table 2.3.

Table 2.3: Differential expression of different metallothionein isoforms in ECM fungi in response to different metal stress.

S.No.	Ectomycorrhizal fungi	Metallothionein genes	Inducing metal	References
1.	*Fusarium oxysporum*	*Mt1*	Zinc	Lorenzo-Gutiérrez *et al.,* (2019)
2.	*Suillus luteus*	*SlMTa*	Copper	Nguyen *et al.,* (2017)
		SlMTb	Copper	
3.	*Pisolithus albus*	*PaMT1*	Copper, cadmium	Reddy *et al.,* (2016)
4.	*Laccaria bicolor*	*LbMT1*	Copper, cadmium	Reddy *et al.,* (2014)
		LbMT2	Copper	
5.	*Amanita strobiliformis*	*AsMT1a*	Silver	Osobová *et al.,* (2011)
		AsMT1b	Silver, cadmium	
		AsMT1c	Silver, copper	
6.	*Amanita strobiliformis*	*AsMT1*	Silver, copper	Hložková *et al.,* (2016)
		AsMT2	Cadmium	
		AsMT3	Zinc	
7.	*Hebeloma cylindrosporum*	*HcMT1*	Copper	Ramesh *et al.,* (2009)
		HcMT2	Cadmium, copper	
8.	*Hebeloma mesophaeum*	*HmMT1*	Zinc, cadmium	Sácký *et al.,* (2014)
		HmMT2	Silver	
		HmMT3	Silver	
9.	*Russula atropurpurea*	*RaZBP1*	Zinc	Leonhardt *et al.,* (2014)
		RaZBP2	Zinc	
10.	*Paxillus involutus*	*PiMT*	Cadmium, Copper	Bellion *et al.,* (2007)

2.6.3.2 Glutathione

Glutathione (GSH) is a tripeptide (L-γ-glutamyl-L-cysteinyl-glycine) (307 Da) composed of 3 amino-acids, glutamate, cysteine and glycine. It is synthesized endogenously and plays an important part in various cellular processes (Townsend, 2007).

Glutathione is the most abundant non-protein thiol present in living systems. The normal glutathione concentration in yeast and fungi is approximately 10 mM (Pócsi *et al.,* 2004). Gluathione production has been reported in both prokaryotes and eukaryotes. Bacteria (Smimova and Oktyabrsky, 2005), algae (Chen *et al.,* 2012), yeast (Ilyas and Rehman, 2015), fungi (Pócsi *et al.,* 2004), plants (Noctor *et al.,* 2012), mammals (Bhowmick *et al.,* 2015) all produce glutathione. Glutathione plays multiple roles in the cell; it is an efficient redox buffer (Foyer and Noctor, 2005), xenobiotic detoxifier (Cummins *et al.,* 2011), sulphur assimilator (Kopriva, 2006), heavy metal detoxifier (Cobbett, 2000), cell signaling component (Foyer and Noctor, 2005), and antioxidant (Mittova *et al.,* 2003). Glutathione functions as an antioxidant in two ways: firstly, it oxidizes its thiol group in the presence of reactive oxygen species leading to the formation of oxidized glutathione (GSSG); secondly, it acts as a substrate for the enzymes like glutathione peroxidase which scavenges peroxides using glutathione as the reducing factor. Glutathione is a key component in metal scavenging, due to the high affinity of metals for its thiol (-SH) group and also as a precursor of phytochelatins (PCs). It bind heavy metals forming a metal-$(GSH)_n$ complex, which is further compartmentalized into the vacuoles through various ATP-binding cassette (Outten *et al.,* 2017).

2.6.3.2.1 Biosynthesis of glutathione

The biosynthesis of GSH consists of 2 sequential ATP dependent reactions mediated by two enzymes γ-glutamylcysteine synthetase (γ-GCS; E.C.6.3.2.2) and glutathione synthetase (GS; E.C.6.3.2.3) (Figure 2.7). Firstly, γ-glutamylcysteine (γ-GC) is formed from $_L$-glutamate and $_L$-cysteine by γ-glutamylcysteine synthetase and then glycine is added to the C-terminal of γ-GC by glutathione synthetase (GS) forming Glutathione (Figure 2.14). Both the reactions require ATP as substrate. The γ-GCS is a rate limiting enzyme for GSH synthesis. In cell the γ-GCS activity is enhanced by Cd ions and the expression of genes in GSH biosynthesis pathways is stimulated by As, Cd, Hg, Cr (Vido *et al.,* 2001; Thorsen *et al.,* 2007).

In plants, γ-GC is restricted to plastids, whereas GS is localized in cytosol (Wachter *et al.,* 2005). Two important factors affecting GSH synthesis are sulfur availability and γ-GCS activity (rate limiting). During metal toxicity both factors increase in order to meet the desired GSH demand for detoxification and survival (Jozefczak *et al.,* 2012). The GSH synthesis in cell is controlled by the feedback inhibition, where GSH itself act as an inhibitor to γ-GCS activity. During metal stress, GSH inside the cell is oxidized and consumed in phytochelatin

synthesis, resulting in depleting cellular GSH level which results in releasing the feedback inhibition and increasing GSH synthesis (Hibi *et al.*, 2004).

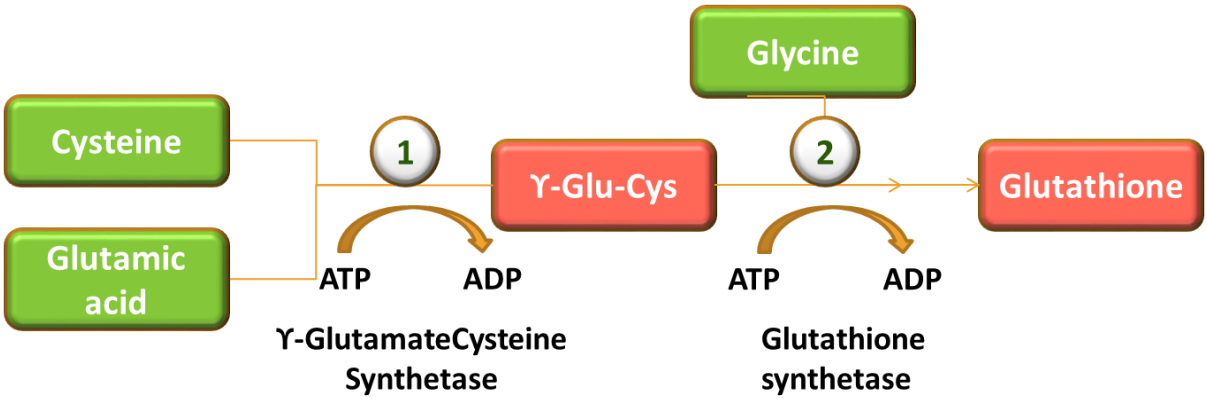

Figure 2.14: Biosynthesis of glutathione - two step reaction catalyzed by two ATP dependent enzymes γ-glutamatecysteine synthetase and glutathione synthetase.

Recently, studies have reported two more pathways named F-pathway and P-pathway for glutathione production in different organisms (Figure 2.15) (Tang *et al.*, 2015). Few organisms lacking genes for *γ-GCS* and *GS* were reported of producing glutathione. This observation threw light on the new pathway known as F-pathway for the synthesis of glutathione. In few strains of Gram-positive bacteria *Listeria monocytogenes, Streptococcus agalactiae, Streptococcus thermophilus* and *Pasteurella multocida* a novel bifunctional enzyme GshF was identified (Gopal *et al.*, 2005; Janowiak and Griffith, 2005; Vergauwen *et al.*, 2006). GshF functions both as γ-GCS and GS and performs complete synthesis of glutathione.

The third pathway identified is P-pathway. Bioinformatic analysis of some glutathione producing strains of yeast and *Escherichia coli* revealed the absence of gene coding for *γ-GCS* but presence of *GS* in their genome. This observation gave rise to a new compensatory pathway for glutathione production. The gene *Pro1* in proline biosynthesis pathway encodes γ-Glutamyl kinase (GK) which catalyzes the formation of γ-glutamylphosphate which reacts with cysteine to form γ-glutamylcysteine. Glutathione synthetase catalyzes the addition of glycine to produce glutathione (Figure 2.15).

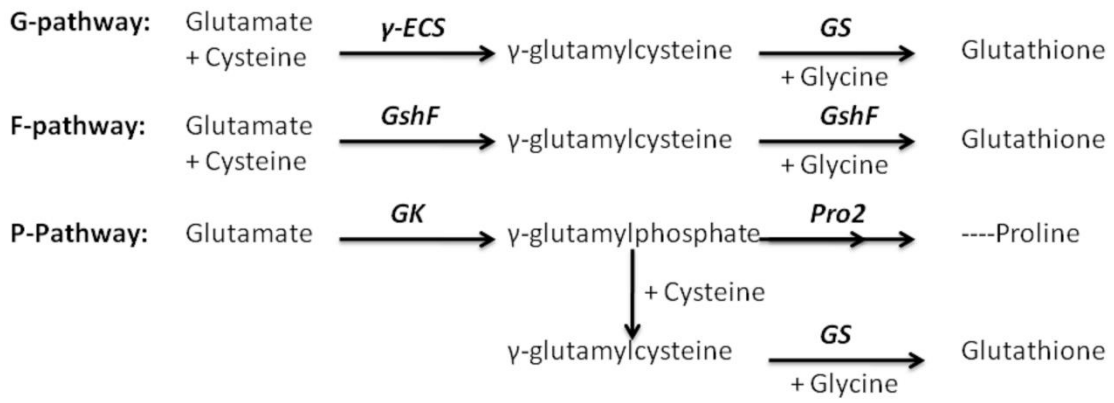

Figure 2.15: Different pathways of glutathione production. G-pathway involves two enzymes γ-GCS and GS, F-pathway involves only one enzyme GshF and P-pathway involves glutamyl kinase (GK) and glutathione synthetase (GS).

2.6.3.2.2 Glutathione and heavy metal detoxification

Glutathione has a dual protection mechanism. It acts as a metal scavenger during metal homeostasis and as an antioxidant during oxidative stress. As an antioxidant, it reacts non-enzymatically with different ROS. Cells under heavy metal stress generated ROS such as hydrogen peroxide (H_2O_2), superoxides ($O_2^{\bullet -}$) and hydroxyl radicals (•OH) which are the major contributors of oxidative damage to membrane lipids, proteins, nucleic acids and cellular organelles (Hernández *et al.,* 2015). Glutathione in cell is present in both reduced-GSH and oxidized-GSSG. In reduced state, the thiol group of cysteine has the tendency to donate an electron to the unstable ROS like H_2O_2 and free radicals and neutralize them, but GSH itself becomes reactive and reacts with another reactive GSH to form oxidized GSSG (Pócsi *et al.,* 2004). This electron transfer is mediated by an enzyme glutathione peroxidase (Margis *et al.,* 2008). Glutathione reductase (a FAD-containing protein) further converts this GSSG to GSH using NADPH as an electron donator (Marty *et al.,* 2009; Noctor *et al.,* 2012), thus maintaining the redox balance (Figure 2.16). The ratio of reduced to oxidized glutathione (GSH/GSSG) in a cell is used as a measure of cellular toxicity or oxidative stress. The GSH/GSSG plays an important role in maintaining cell homeostasis. Qualitative and quantitative alterations in this ratio are considered as the indices of oxidative damage. If the ratio favors GSSG production, it signifies that the apoptosis may have triggered (Shakhristova *et al.,* 2016). Many studies have reported the role of GSH in mitigating oxidative stress.

Ilyas and Rehman (2014) reported the increased GSH levels when in *Candida tropicalis* in response to As, Cd and Cr. However, the decline in GSH concentration was observed under Cu and Pb stress due to GSH degradation. The stressed cells had more GSSG than GSH. However, the GSH/GSSG ratio increased significantly under Cd and Cu stress in contrast to As, Pb and Cr. Similar results were observed in *Saccharomyces cerevisiae*, where the GSH biosynthesis was induced under As stress (Thorsen *et al.*, 2007).

The active role of GSH in mitigating metal toxicity has also been highlighted in various plants. GSH and its metabolic enzymes were actively induced under metal stress (Hossain *et al.*, 2012). In plants, glutathione is the key thiol responsible for relief against Cd, As and Hg toxicity and controlling the cellular redox homeostasis (Hernandez *et al.*, 2015). In *Brassica juncea*, increased GSH production was reported in response to Cd, Zn and Ni (Asgher *et al.*, 2014; Barrameda-Medina *et al.*, 2014; Khan and Khan, 2014; Khan *et al.*, 2016; Per *et al.*, 2016). Similar observations were made for *Triticum aestivum* (Khan *et al.*, 2015) and *Lycium chinense* (Guan *et al.*, 2015) where the GSH production increased in response to Cd stress. Arsenic induced GSH production was reported in *Pteris vittata* (Sakai *et al.*, 2010) and *Oryza sativa* (Dixit *et al.*, 2016).

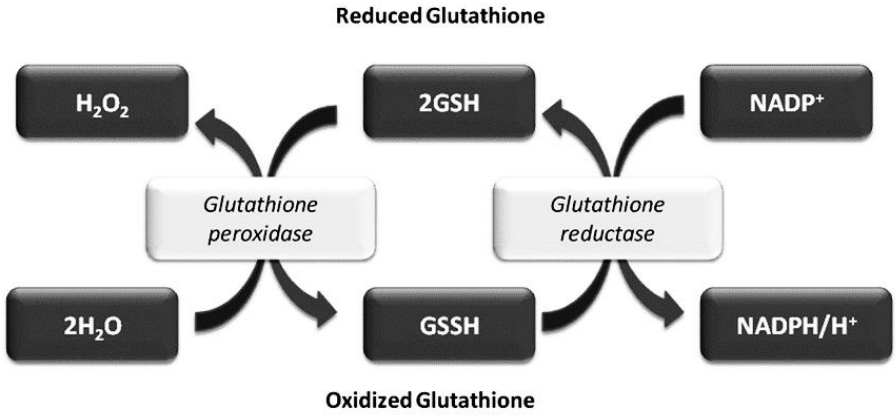

Figure 2.16: Glutathione in alleviating oxidative stress by hydrogen peroxide. Role of glutathione peroxide and glutathione reductase in maintaining cellular redox homeostasis

Glutathione act as sequester for various heavy metals and xenobiotics like fungicides, insecticides etc. The GSH bind these toxic metal/xenobiotics (X) forming a non-toxic GSH-X complex. This conjugation is catalyzed by the enzyme Glutathione-S-transferase. These GSH-X conjugates are then transported to vacuoles through the ABC (ATP-binding cassette)

transporters (Schlunk *et al.,* 2015). The MRP (multidrug resistance related protein) transporters of ABC type undergo ATP hydrolysis to transport these conjugates across the vacuolar membrane (Klein *et al.,* 2002). The two ABC transporters, ABCC1 and ABCC2 have been identified as the major GSH-X complex transporters (Song *et al.,* 2014). The sequestration of Cd and Pb by GSH has been characterized using Infrared Rays (IR) and protonic Nuclear Magnetic Resonance (NMR) (Jacquart *et al.,* 2017; Bottari *et al.,* 2020). Due to the strong metal binding property of GSH, it is becoming the molecular probe of choice in preparation of sensors for heavy metal ion detection (Zhang *et al.,* 2019).

2.6.3.2.3 Regulation of Glutathione synthesis

As explained earlier, glutathione is synthesized in a two-step process, where synthesis of gamma glutamylcysteine is the rate limiting step. Hence, the key regulator of glutathione synthesis is the gene coding for *γ-GCS*. Like metallothioneins, *γ-GCS* gene expression is also regulated on the transcriptional level. *γ-GCS* in its promoter region carries AREs like sequences that match 11 out of 12 positions (Wu and Moye-Rowley, 1994). Two transcription factors, yAP-1 and Met-4, controls the expression of *γ-GCS* gene. Under stress conditions, cellular glutathione gets depleted, which further activate yAP-1 and Met-4 target gene through oxidation of thioredoxin (which otherwise downregulate the yAP-1 mediated response) (Wheeler *et al.,* 2003). In case of yeast, yAP-1 response elements (YREs) were recognized by yAP-1 protein (Wu and Moye-Rowley, 1994). Hence, we can say that when an organism is exposed to stress, glutathione is depleted and oxidized thioredoxin is accumulated, which leads to the activation of yAP-1/Met-4 dependent transcriptional response of *γ-GCS* (Wheeler *et al.,* 2003).

2.6.3.2.4 Glutathione in ectomycorrhizal fungi

Many ECM fungi have been reported of producing glutathione in response to heavy metal stress. Courbot *et al.,* (2004) reported no metallothionein but the increase in glutathione concentration in *Paxillus involutus* in response to cadmium stress (Courbot *et al.,* 2004). Similar results were observed in case of *Laccaria laccata* (Gallie *et al.,* 1993). Glutathione production in mycorrhizal fungi is mainly triggered by cadmium and arsenic stress followed by chromium, lead and copper (Ilyas and Rehman, 2015). Numerous studies have now confirmed the dominant role of glutathione as a cadmium chelator. *Glomus mosseae* also produced glutathione in response to cadmium whereas no glutathione was reported under lead

stress (Garg and Aggarwal, 2011). *Funneliformis mosseae* was also reported to have increased glutathione levels in response to cadmium and arsenic (Degola *et al.*, 2015). *Phanerochaete chrysosporium* and *Penicillium chrysogenum* also clearly demonstrated the role of glutathione as an intracellular cadmium chelator (Xu *et al.*, 2015; Xu *et al.*, 2016). Putative genes encoding for the γ-glutamylcysteine synthetase and glutathione synthetase have been reported in the genome of *Laccaria bicolor*, *Hebeloma cylindrosporum*, *Paxillus involutus* (Bellion *et al.*, 2006). However, the detailed information on the cellular response of ECM fungi towards the trace metals and heavy metal pollutants is still incomplete and therefore restricts its successful execution in soil remediation. Since ectomycorrhizal fungi lives in close association with the plants in metal polluted areas and are the most potential candidates for bioremediation of heavy metals therefore, it is necessary to study the cellular and molecular response of these fungi to metal stress.

2.7 Proteomic analysis: technology and methods

'Proteomics' involves the application of different technologies for identification and quantification of the whole proteome present in cell, tissue or organism. It studies the structure and function of proteins on large scale, in complex biological samples. The proteomic analysis is commonly used for: a) protein identification, b) proteome profiling, c) comparative analysis of the protein expression in two or more samples, d) localization and identification of post-translational modifications, e) protein-protein interaction studies f) protein-nucleic acid interactions (Chandramouli and Qian, 2009; Zhang *et al.*, 2014). Proteins are the functional unit of an organism. Therefore, most of the functional information of the genes resides in its proteome. Proteome of a cell includes a complex dynamic range which comprises of various processes like protein phosphorylation, protein trafficking, protein localization and protein-protein interactions. Genomics and transcriptomic studies do not always correlate with the gene expression because mRNA is not always translated into protein. Since single mRNA transcript can code for several proteins and post translational modifications can immensely modify the function of proteins. Therefore, proteomic analysis provides exact information about the expression of each gene under certain circumstance. However, proteomic analysis is more complex than genomics and transcriptomics due to the rapid changes in protein function and abundance caused by altered gene expression, multiple post-translational and post-transcriptional modifications, protein hydrophobicity and hydrophilicity (Zhang *et al.*, 2014;

Garcia 2018). The proteome of a cell fluctuates from time to time, from cell to cell and in response to external conditions.

With the invent of mass spectroscopy (MS), the proteomic analysis has become easier and more convenient. It is the most important tool used for identifying, characterizing and quantifying the proteins and their post translational modifications with high throughput at larger scale. The complete proteomic analysis revolves around three steps (i) isolation of total proteins, (ii) protein separation, (iii) identification and quantification by mass spectrometry.

2.7.1 Protein separation

There are different methods of protein separation, which include:

a) Gel based methods of protein separation: The proteins are separated on poly acrylamide gel through either sodium dodecyl sulfate polyacrylamide gel electrophoresis (SDS-PAGE), two-dimensional gel electrophoresis (2DE) or two-dimensional differential gel electrophoresis. The proteins are separated on the basis of their molecular weight and their isoelectric point, followed by their digestion and identification through mass spectroscopy (Chevalier *et al.*, 2010; Rabilloud *et al.*, 2010; Magdeldin *et al.*, 2014).
b) Chromatography based protein separation: These are the conventional methods of protein separation and purification. They include, liquid chromatography, ion-exchange chromatography and affinity chromatography (Shishkova *et al.*, 2016; Liu *et al.*, 2019). The proteins can be easily digested to peptides, which are more easily separated by liquid chromatography, rapidly analyzed and is much cost-effective than gel-based proteomics (Di Palma *et al.*, 2012).

Both Gel-based and chromatography-based techniques are widely used these days for comparative analysis of protein expressions under different conditions. There are many studies where the differentially expressed proteins were analyzed using 2D gel electrophoresis. These techniques are widely used in studying the response of different plants and organisms to various biotic and abiotic stresses like metal stress, salt stress, soil conditions, microbial infestation etc.

Liu *et al.*, (2020) and Long *et al.*, (2019) used 2DE to identify proteins involved in salt tolerance in mangrove plant *Kandelia obovate, Medicago sativa* and *Medicago truncatula*. Yang *et al.*, (2015) identified 83 differentially expressed proteins in *Populus yunnanensis* leaves when

exposed to Cd stress, through 2DE. Similarly, 53 differentially expressed proteins were identified in *Kandelia candel* roots under Cd stress through 2DE (Weng *et al.*, 2013). Ahsan *et al.*, (2008) used 2DGE to identify 37 differentially expressed proteins in rice roots under As stress. Szajko *et al.*, (2020) studied the effect of fungal infestation on different potato cultivars using 2DE and LC-MS analysis.

However, the protein differentiation in gel-based separation is not unequivocal. Moreover, only the high abundance proteins can be identified through 2DGE, low abundance proteins may be hidden inside the gel and might be non-detectable. Also, the proteins with extreme isoelectric values 4>pI>9 as well as very high (>200 kDa) and very low (<10 kDa) molecular weight or hydrophobic in nature are usually undetectable under 2DGE. The 2DGE is also very tedious, time consuming and requires extensive manual handling. Therefore, these days the Gel-free proteomics is trending in many studies (Baiwir *et al.*, 2018).

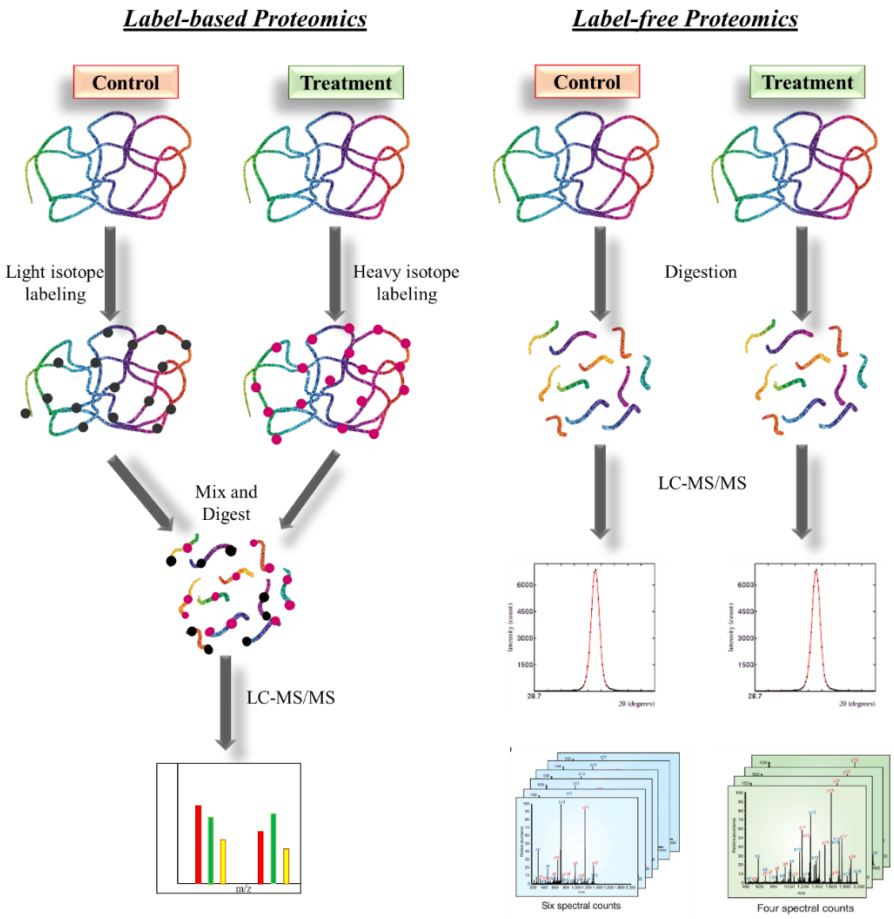

Figure 2.17: Schematic diagram discriminating between Label-based proteomics and Label-free proteomics.

Different techniques have been developed to quantify the separated proteins. The most commonly used are label based quantification and label free quantification. Isotope-coded affinity tag (ICAT), stable isotope labeling with amino acids in culture (SILAC), isobaric tag for relative and absolute quantitation (iTRAQ), have been recently developed for quantitative proteomic analysis. In contrast to this, the label free shortgun proteomics quantifies proteins based upon their signal intensity and spectral counting (Neilson *et al.*, 2011; Baiwir *et al.*, 2018) (Figure 2.17). These techniques have been widely used to study the response of different plants and organisms under heavy metal stress (Table 2.4).

2.7.2 Protein mass spectroscopy

The proteins/peptides separated by Gel-based or Gel-free approaches are then introduced into the mass spectrophotometer for its quantitative and qualitative analysis. The basic principle behind mass spectroscopy is the generation of multiple ions from the protein (sample) under investigation, followed by their separation according to their mass/charge (m/z) ratio. The detector then records the relative abundance of each ion with respective to their m/z ratio in a graph known as mass spectrum. These spectra provide information about the mass of particles, their isotopic signature, chemical identity and helps in predicting their structure. For mass spectroscopic analysis of a protein sample, the chromatographically separated proteins are introduced into the ionization chamber, where they are ionized and fragmented. The positively charged ions are then deflected into the magnetic field and separated according to their mass/charge ratio. The ions with same m/z will be deflected at the same range. The deflected ions are then detected by the detector capable of detecting the charged particles. The output is displayed as a spectrum plotting signal intensity as the function of m/z ratio. Further the ions can be identified by correlating its mass to the known data or through the characteristic fragmentation pattern. The mass spectrometer mainly consists of three components: an ionizer, a mass analyzer and a detector (Figure 2.18).

- Ionizer: It ionizes the sample (protein/peptide) into positive charged fragments or ions. Different ionizers are used under different conditions depending upon the type of analyte. Ionizers can be classified broadly into two categories: Hard ionizer and soft ionizers. Hard ionizers impart very high energy to the analyte molecules, thus invoking high fragmentation (eg. Electron ionization (EI)). Soft ionizers on the other hand imparts very little energy generating positive ions with very less fragmentation. The

soft ionizers include: fast atom bombardment (FAB), electron spray ionization (ESI), chemical ionization (CI), matrix-assisted laser desorption/ionization (MALDI) and atmospheric-pressure chemical ionization (APCI). Apart from these photoionizers (ionization using high energy photons), thermospray, desorption/ionization on silicon (DIOS), spark ionizers and thermal ionizers are also used to for fragmentation and ionization.

- Mass analyzer: Mass analyzer separates the fragments ions according to their m/z ratio. They accelerate the movement of ions by applying the electric or magnetic field and deflect them towards the detector on the basis of m/z ratio. Ions with lower m/z will be deflected faster than the ions with higher m/z. However, the ions with same charge will be separated on the basis of their mass. There are different types of analyzers based upon their deflection tendencies:
    - Time-of-flight (TOF) mass analyzer: use electric field to accelerate ions and measures the time they required to reach the detector
    - Quadrupole mass analyzer: it consists of four cylindrical rods aligned parallel to each other. The ions are separated on the basis of the stability of their trajectories in the oscillating electric or magnetic fields applied to the rods. The movement of ions in quadrupole will depend upon the voltage generated between the rods. Therefore, it also acts as mass filter.
    - Ion traps: in this mass analyzer, the ions are first trapped between the electrodes and then sequentially ejected. There are many types of ion trappers which include: three-dimensional quadrupole ion trap, cylindrical ion trap, linear quadrupole ion trap, orbitrap
- Detector: The deflected ions are then received by the detector. The detector then records the ion intensity by measuring the charge induced or current produced as the ions reaches its surface. The most commonly used detector is the electron multiplier. Other detectors commonly used are Faraday cups, ion-to photon detectors, microchannel plate detectors. Since the signal received by the detector is usually very low, therefore, these detectors amplify the signal and makes it recordable.

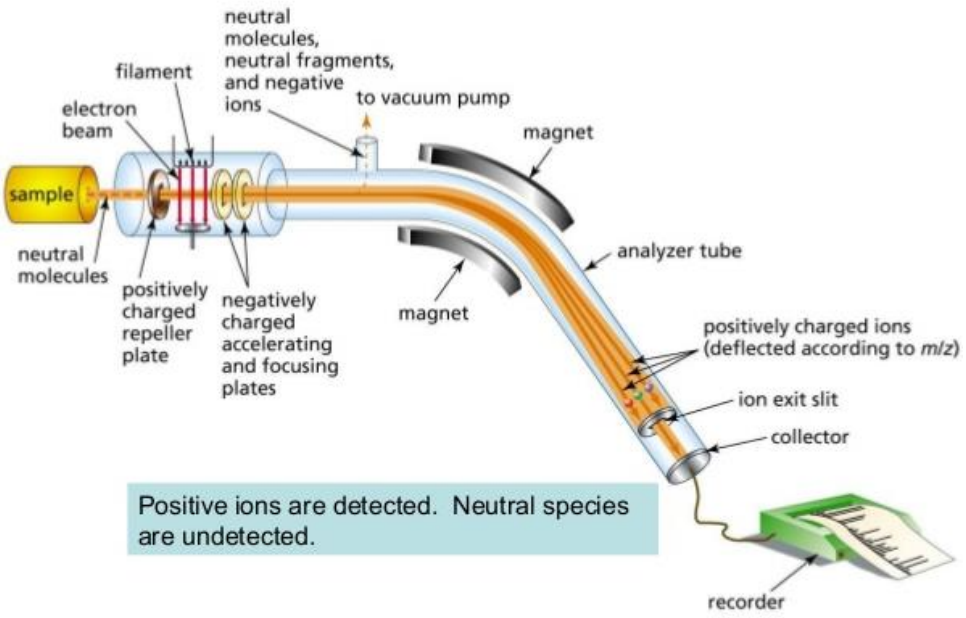

Figure 2.18: Various steps involved in mass spectroscopic analysis of a protein.

- Tandem mass spectroscopy: In this spectroscopy, two or more mass spectrometers are coupled so as to increase their ability to analyze with more precision. It is commonly used for analyzing biomolecules like proteins and peptides. In this, the ionized molecules are separated on the basis of their m/z ratio in first mass spectrometer. The separated ions are then selected and passed into a collision chamber, where they are further split into smaller fragment ions using various techniques like collision-induced dissociation, photodissociation or ion-molecule reaction. The fragmented ions are then again introduced into second mass spectrometer, where they are again separated according to their m/z ratio and detected (Figure 2.19). The additional fragmentation step in tandem mass spectroscopy helps in separating and identifying ions that otherwise have similar m/z ratios in normal mass spectrophotometer. The technique is widely used now a days to study the relative protein quantification under different conditions (Zhang *et al.*, 2017).

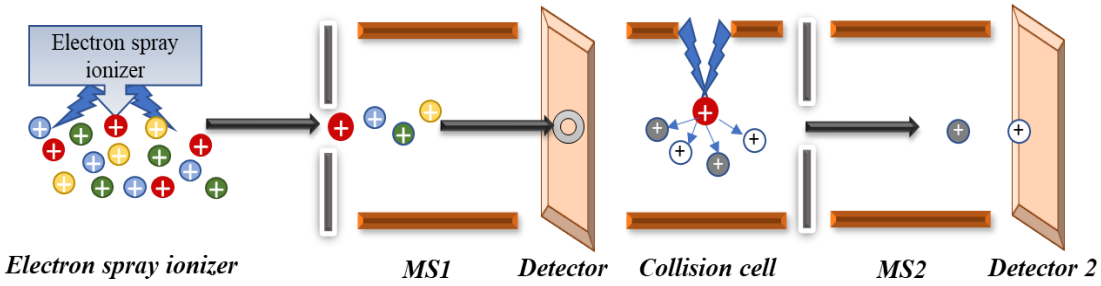

Figure 2.19: Steps involved in tandem mass spectroscopy

Mass spectroscopy has been developed to study the complex proteins with higher sensitivity. It has wide application in analytical laboratories to study the physical, chemical and biological properties of different compounds. It shows excellent specificity in characterizing the fragmentation patterns, identifying the unknown compounds, analyze the molecular weight, calculating the isotopic abundance of elements and resolving their chemical composition.

2.7.3 Protein microarray

Apart from these, protein microarrays or chips have also been developed for rapid and high-throughput protein expression analysis. It is a new emerging class of proteomics, which can be used to detect, identify proteins, track protein interactions and activities and determine their function from very small concentration in large number of samples. There are mainly three types of protein microarray: analytical protein microarray, functional protein microarray and reverse-phase protein microarray (Aslam *et al.*, 2016). They are very rapid, automated, economical and highly sensitive techniques for protein analysis.

2.8 Proteomic analysis under heavy metal stress

Although the transcriptomic analysis of gene expression at the mRNA level made a huge contribution to our understanding on different effects of heavy metals on living systems. But the level of mRNA not always correlate with the levels of final protein products. Therefore, the prediction of proteins from their mRNA transcripts does not give the true analysis. The mRNA transcripts undergo various post translational regulations like nuclear export, transcription stability, mRNA localization, translation regulation and protein degradation (Pradet-Balade *et al.*, 2001). However, the proteomic analysis provides precise picture of the protein networks and various metabolic pathways involved in metal induced toxicity, cellular detoxification and tolerance mechanisms against heavy metal toxicity.

The power of proteomics in providing deeper insight into the heavy metal responses has been recently realized in different plants like *Arabidopsis thaliana, Populus tremula, Populus yunnanensis, Kandelia candel, rice, Sorghum, Amaranthus hybridus, tomatoes, Brachypodium distachyon* (Lee *et al.,* 2010; Semane *et al.,* 2010; Weng *et al.,* 2013; Lin *et al.,* 2015; Yang *et al.,* 2015; Jin *et al.,* 2016; Roy *et al.,* 2016; Cheng *et al.,* 2018; Borges *et al.,* 2019), in algae *Sargassum fusiforme* (Zhang *et al.,* 2015), bacteria *Lactobacillus plantarum, E. coli* (Khan *et al.,* 2017; Zhai *et al.,* 2017), yeast *Rhodotorula mucilaginosa* (Ilyas *et al.,* 2016) etc.

The proteomic analysis of the organisms under metal stress helps in identifying the proteins potentially involved in metal tolerance, metal accumulation and regulation of metal responses. Thus, providing deep understanding of the mechanisms involved in metal tolerance and accumulation and metabolic changes induced by metal stress.

In hyperaccumulator *Chlamydomonas reinhardtii*, Cd stress up-regulated the expression of proteins involved in glutathione metabolism, ATP metabolism, response to oxidative stress and protein folding (Gillet *et al.,* 2006).

Jin *et al.,* (2016), reported increased expression of the proteins involved in energy metabolism, protein metabolism, signal transduction and stress and defense, leading to enhanced Cd tolerance in *Amaranthus hybridus* under Cd stress. However, the expression of structural proteins involved in cell wall, microRNA, were down-regulated under Cd stress.

Roy *et al.,* (2016) studied the effect of Cd stress on *Sorghum bicolor* leaves. Cd stress induced major changes in the level of proteins involved in carbohydrate metabolism, transcriptional regulation, translation and stress response. However, the ATP synthesis, carbon fixation and protein synthesis were inhibited under Cd stress.

The proteomic analysis of the response of *Populus yunnanensis* to Cd stress revealed the up-regulation in defense-response proteins, photosynthesis and energy associated proteins, antioxidant enzymes, heat shock proteins, MAPK signaling and plant cell wall synthesis. Thus, providing defense against Cd stress (Yang *et al.,* 2015).

The prompt increase in antioxidative response including glutathione biosynthesis, TCA and PPP cycle for generating ATP, NADH and NADPH was reported in proteomic analysis of *Kendelia candel* roots exposed to Cd stress (Weng *et al.,* 2013). The proteomic analysis of rice

roots in response to As stress revealed that glutathione plays a central role in mitigating As stress (Ahsan *et al.,* 2008).

Zhai *et al.,* (2017) identified the key proteins and metabolic pathways responsible for Cd tolerance in *Lactobacillus plantarum*. Cd stress altered the proteins involved in energy metabolism, purine and pyrimidine metabolism, lipid metabolism, amino acid metabolism, global stress response, cell wall binding, and membrane transportation. The induced biosynthesis of hydrophobic amino acids enhanced the surface hydrophobicity of cell thus protecting the cells from Cd induced protein damage.

Zhang *et al.,* (2015) studied the response of brown algae *Sargassum fusiforme* to Cd stress through comparative proteomic analysis. The proteins involved in carbohydrate metabolism, energy metabolism, amino acid metabolism, nucleotide metabolism, stress and defense, transport and catabolism were significantly down-regulated under Cd stress. However, the most Cd sensitive pathway was energy metabolism. Most of the proteins involved in energy metabolism like photosynthesis, oxidative phosphorylation, ATP synthetase were significantly down-regulated under Cd stress.

However, to our knowledge no report is available on comparative proteomic analysis of ECM fungi in response to Cd stress. Since, these ECM fungi thrive in metal polluted areas, have high tolerance for metal toxicity and are good metal-accumulators, they hold high potential for their application in HM bioremediation. Therefore, knowing the internal mechanisms of these fungi in response to HMS is a need of an hour. Therefore, the present study focuses on studying the metabolic response of ECM fungus *L. bicolor* to Cd stress.

Table 2.4: Use of proteomic analysis to study the response to heavy metals (2010-2020).

S. No.	Heavy metal	Plant/organism	Proteomics methodology	Major findings	References
1	Cr	*Streptomyces* sp.	2D-nanoUPLC-ESI-MSI/MSI	Induction in expression of molecular biosynthesis, energy generation, protein folding, stress response, transcription, DNA supercoiling, DNA repair and replication, oxidation-reduction process.	Bonilla *et al.,* (2020)
2	Cd	*Solanum lycopersicum*	Label free LC-MS/MS	DAPs associated to cell wall, redox and stress response.	Borges *et al.,* (2019)
3	Ag	*Nicotiana tabacum*	2DE, MALDI-TOF/TOF MS/MS	Affected photosynthesis metabolism, enhanced energy production	Štefanić *et al.,* (2019)
4	Cd	*Brachypodium distachyon*	2D-DIGE, MALDI-TOF/TOF-MS	DAPs in energy and carbon metabolism, photosynthesis/respiration, stress and defense, protein folding and degradation and amino acid metabolism.	Cheng *et al.,* (2018)
5	Cd	*Lactobacillus plantarum*	iTRAQ LC/LC-MS/MS	Low abundance of proteins involved in carbohydrate metabolism, global stress response, phosphotransferase system, two-component system, membrane protein and cell surface proteins. And higher abundance of proteins involved in amino-acid metabolism, nucleic acid metabolism and extracellular proteins.	Zhai *et al.,* (2017)

6	Cd	*Escherichia coli*	2DE, LC-ESI, QTOF, MS	Down-regulation in carbohydrate metabolism and up-regulation in SOD activity.	Khan *et al.*, (2017)
7	As, Cd	*Rhodotorula mucilaginosa*	2DE, IAF labeling, MALDI-TOF-MS	Differentially affected ATP synthesis, protein degradation/synthesis and metabolism of xylose and chitin	Ilyas *et al.*, (2016)
8	Cd	*Sorghum bicolor*	2DE, MALDI-TOF MS/MS	Major changes in proteins of carbohydrate metabolism, transcriptional regulation, translation and stress response. Cd stress inhibited carbon fixation, ATP production and protein synthesis.	Roy *et al.*, (2016)
9	Cd	*Amaranthus hybridus*	2DE, TOF	Increased expression of proteins involved in energy metabolism, protein metabolism, signal transduction, stress and defense and down-regulation in mechanisms involved in synthesis of cell wall and micro RNAs.	Jin *et al.*, (2016)
10	Cd	*Populus yunnanensis*	2DE, MALDI-TOF, MS/MS	Induction in defense response molecules, energy associated proteins, photosynthesis, antioxidant enzymes, heat shock proteins, MAPK signaling pathway and cell wall synthesis	Yang *et al.*, (2015)
11	Cu	*Allium cepa*	2DE, MALDI-TOF-TOF MS	Differentially expressed proteins involved in defensive response, protein synthesis, transcriptional regulation, cell cycle, cell wall synthesis, DNA replication and repair	Qin *et al.*, (2015)
12	Cd	*Oryza sativa*	Native PAGE, LC-MS/MS	Proteins involved in energy metabolism and glutathione metabolism were up-regulated	Lin *et al.*, (2015)

13	Cd	*Sargassum fusiforme*	2DE, MALDI-TOF/TOF MS	Differentially expressed proteins involved in carbohydrate metabolism, energy metabolism, genetic information processing, molecular chaperons and HSP	Zhang *et al.,* (2015)
14	Al	*Glycine max*	LC-MS/MS (Gel free proteomics)	Decrease in energy metabolism, protein synthesis/degradation, glycolysis, lipid metabolism, transcriptional regulation,	Mustafa *et al.,* (2015)
15	Cu	*Streptococcus pnemoniae*	2DE, MALDI-TOF/TOF MS	Differentially expressed proteins involved in call wall synthesis, protein biosynthesis, purine and pyrimidine metabolism, nitrogen compound metabolic process	Guo *et al.,* (2015)
16	Cu	*Acidithiobacillus ferrooxidans*	2D-nano, ICPL, LC-ESI-MS/MS	Up-regulation of proteins involved in efflux pumps, histidine synthesis, cysteine production. Down-regulation of proteins involved in outer membrane porin, ionic transporters	Almárcegui *et al.,* (2014)
17	Cu	*Oryza sativa*	2DE, MALDI-TOF/TOF-MS	Up-regulation in proteins involved in antioxidant defense, carbohydrate metabolism, nucleic acid metabolism, protein transport, protein folding and stabilization and cell wall synthesis	Song *et al.,* (2014)
18	Ur, Cr, Cd	*Caulobacter crescentus*	LC-MS/MS (Gel free proteomics)	Cell signaling and amino-acid metabolism was up-regulated under all three metals, decreasing electron transport and cell motility. Uranium up-regulated phytase,	Yung *et al.,* (2014)

				Cr up-regulated HSPs and outer membrane receptors and Cd up-regulated efflux pumps and oxidative stress response	
19	Cd	*Brassica juncea*	2DE LC MS/MS	Alterations in expression of enzymes involved in antioxidant responses, ATP synthase subunits, carbonic anhydrase and Calvin cycle.	D'Alessandro *et al.,* (2013)
	Cd	*Kandelia candel*	2DE, MALDI-TOF MS/MS	The proteins involved in oxidative stress response were promptly induced under Cd stress	Weng *et al.,* (2013)
20	Al	*Rhodotorula taiwanensis*	2DE, MALDI-TOF/TOF-MS	Decreased in abundance of proteins involved in DNA transcription, translation, DNA defense, Golgi function and glucose metabolism and increased abundance of malate dehydrogenase and intracellular citrates	Wang *et al.,* (2013)
21	Cd	*Glycine max L.*	2DE, LC-MS/MS, MALDI-TOF MS	Activation of energy metabolism, photosynthesis, antioxidant enzymes like SOD, APX, CAT, molecular chaperons under Cd stress.	Hossain *et al.,* (2012)
22	Cd	*Glycine max L.*	2DE, LC-MS/MS	Activated proteins involved in Cd-chelation, lignin biosynthesis under Cd stress	Ahsan *et al.,* (2012)
23	Cd	*T. aestivum*	2DE, MALDI-TOF MS	Most of the up-regulated proteins were involved in metal detoxification and anti-oxidant process (acsorbate peroxidase and glutathione-s-transferase)	Wang *et al.,* (2011)

24	Cd	*Phytolacca Americana*	2DE, MALDI-TOF, MS/MS	Predominantly proteins involved in photosynthesis, and sulfur metabolism and glutathione metabolism were up-regulated. Other up-regulated proteins were attributed to transcription, translation and molecular chaperons	Zhao *et al.,* (2011)
25	Cd	*Oryza Sativa*	2DE, MALDI-TOF, MS	Antioxidants like GST, APX, NADH-ubiquinone oxidoreductase up-regulated in response to CD stress	Lee *et al.,* (2010)

CHAPTER 3

MATERIALS & METHODS

3.1 Biological Materials

3.1.1 Ectomycorrhizal fungi

Two ectomycorrhizal (ECM) fungi used in this study were *Laccaria bicolor* strain S238N and *Hebeloma cylindrosporum* strain h7. The monokaryotic strain h7 of *H. cylindrosporum* was obtained from single spore germination (Debaud and Gay, 1987). Both the strains were maintained on modified Melin-Norkran's medium (MMN) (Melin,1953) supplemented with Heller's micronutrients at 25˚C in dark (Figure 3.1) (Appendix I).

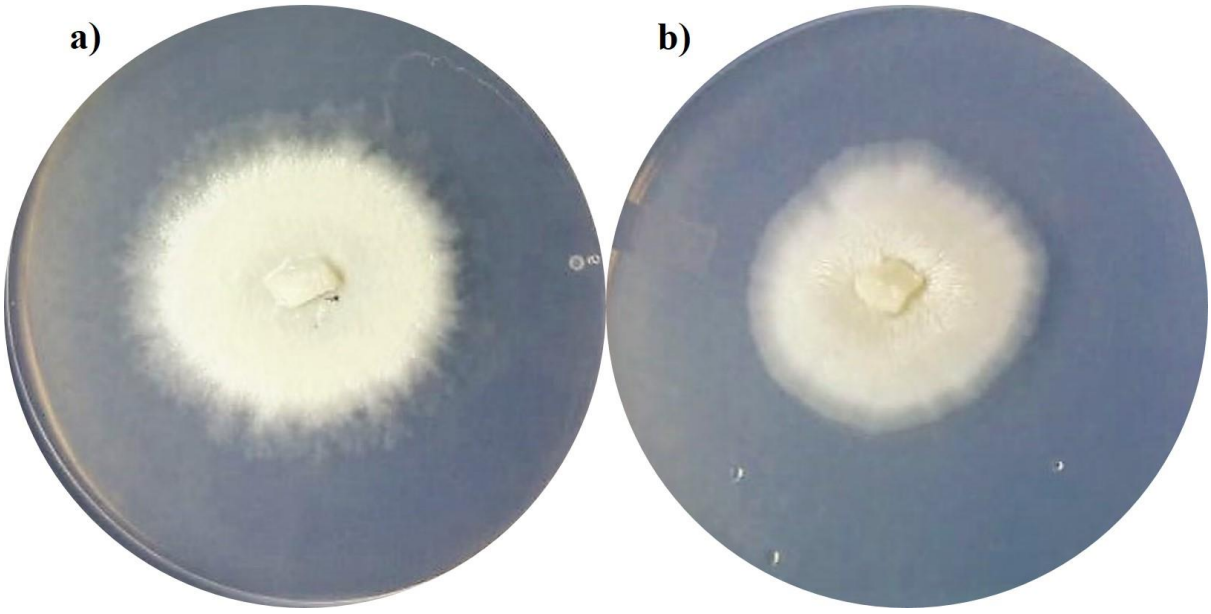

Figure 3.1: Cultures of a) *L. bicolor* and b) *H. cylindrosporum* grown on MMN agar plates at 25˚C for 14 days.

3.1.2 Bacterial Culture

Escherichia coli DH10β cells "MAX Efficiency DH10β Competent Cells" (Invitrogen, California, USA) were maintained on Luria agar medium (Appendix I) at 37˚C. The culture was further preserved at -80˚C in the form of glycerol stocks.

3.1.3 Yeast Cultures

Two *Saccharomyces cerevisiae* mutants *gsh1*$^{\Delta}$ (Y07097) (BY4741; MATa; ura3Δ0; leu2Δ0; his3Δ1; met15Δ0; YJL101c::kanMX4) and *gsh2*$^{\Delta}$ (Y01740) (BY4741; MATa; ura3Δ0; leu2Δ0; his3Δ1; met15Δ0; YOL049w::kanMX4), which are deficient of γ-glutamylcysteine synthetase (*γ-GCS*) and glutathione synthetase (*GS*) genes, respectively, were procured from Indian Institute of Science Education and Research, Mohali, Punjab, India. *Saccharomyces cerevisiae* BY4741 stain was used as wild type. All the cultures were maintained on YPD medium (Appendix I) at 30˚C in dark conditions and stored at -80˚C in the form of glycerol stocks. For the functional complementation studies, the transformed cells were selected by growing them on complete synthetic defined (SD) medium (Appendix I) without uracil (DO supplement -Ura; Cat. No. 630416), (Takara, CA, USA)

3.1.4 Heavy metals

Heavy metal(loids) cadmium (Cd) and arsenic (As) were used in the present study. Cd was used as cadmium sulphate octahydrate ($3CdSO_4.8H_2O$) and As was used as di-sodium hydrogen arsenate heptahydrate ($Na_2HAsO_4.7H_2O$). Both metals were procured from Sigma Aldrich (Missouri, USA)

3.2 Methods

3.2.1 Tolerance of ECM fungi to heavy metals Cd and As

The response of ECM fungi, *L. bicolor* and *H. cylindrosporum* to different concentrations of Cd and As was assessed by growing them in liquid MMN medium supplemented with various concentrations of Cd and As. Liquid MMN medium with Heller's micronutrients (Appendix I) was prepared and dispensed 50 ml in each 250 ml Erlenmeyer flasks (pH 5.6). The flasks were then autoclaved at 121˚C, 15 psi for 15 minutes. Each flask was inoculated with four freshly grown mycelial discs of 7 mm diameter each and incubated at 25˚C in dark for 2 days. In order to avoid immediate stress and to allow mycelium to initiate growth, the metals were supplemented two days after fungal inoculation. After two days, different concentrations of Cd ($3CdSO_4.8H_2O$: 0, 3, 6, 9, 12, 15 μM) and As ($Na_2HAsO_4.7H_2O$: 0, 5, 10, 12, 15 mM) were supplemented in different flasks. The flasks were again incubated at 25˚C in dark for 14 days. After 14 days, the mycelium was harvested and washed with 0.9% saline water and 0.1 M

EDTA followed by three washings with distilled water. The harvested mycelium was then dried at 60˚C for 24 hours and the dry weight was recorded.

3.2.2 Metal(loid) accumulation by ECM fungi

The total content in ECM fungi, *L. bicolor* and *H. cylindrosporum* when exposed to different concentrations of Cd and As was measured using atomic absorption spectroscopy. The mycelium was stressed with different concentrations of Cd and As for 14 days (Section 3.2.1). After 14 days, the mycelium was harvested and washed with 0.1 M EDTA water followed by three washings with distilled water. The washed mycelium was then dried at 60˚C for 24 hours. The dried mycelium from each metal(loid) stress was digested with nitric acid/perchloric acid (3:1) in a round bottom flask using the following protocol:

1. To 100 mg of dried mycelium, 20 ml of concentrated $HNO_3/NClO_4$ mixture (3:1) was added
2. The acidified samples were then incinerated on electric heater in an acid proof digestion chamber having fume exhaust system, at 100℃ for one hour.
3. The heating temperature was then raised gradually till 180℃ and the samples were digested until the sample turns colorless and fumes turn white.
4. The white residue after digestion was allowed to cool at room temperature and then dissolved in HCl (50%).
5. The solution was then filtered through the Whatman filter paper no.1.
6. The volume was raised to 50 ml with HCl (50%).
7. The concentration of Cd and As in each sample was then measured using atomic absorption spectroscopy (GBS 932AA, GBC Scientific Equipment Pvt. Ltd., USA).

3.2.3 Glutathione produced in response to metal(loid) stress

In order to check the total amount of glutathione produced by *L. bicolor* and *H. cylindrosporum* in response to both Cd and As, both fungi were grown on MMN agar plates overlaid with cellophane sheets for 14 days at 25˚C. The cellophane sheets were then transferred on MMN media supplemented with increasing concentrations of both Cd ($CdSO_4$: 0, 10, 20, 30, 40 µM) and As (Na_2HAsO_4: 0, 3, 6, 9, 12, 15, 20 mM) for 48 hours. After 48 hours, the mycelium was scrapped from the cellophane sheets and crushed with liquid nitrogen. Total glutathione was

estimated from these crushed samples by enzymatic recycling in two steps: Cell extract preparation and GSH detection, as per the method described in Rahman *et al.,* (2006).

Cell extract preparation:

1. Cell extract was prepared by homogenizing liquid nitrogen crushed mycelium in sulfosalicylic acid-Triton-X solution (0.6% sulfosalicylic acid and 0.1% Triton-X solution in 0.1 M Potassium phosphate buffer with 5 mM EDTA disodium salt at pH 7.5 (KPE)).
2. The homogenized samples were then centrifuged at 8000 g for 10 min at 2-4°C.
3. The clear supernatant was collected and used for total glutathione estimation.

GSH detection:

The amount of glutathione produced by the mycelium under various stress conditions was quantified spectrophotometrically by enzymatic recycling method, using the sulfhydryl reagent 5,5'-dithio-bis(2-nitrobenzoic acid) (DTNB) to form the yellow colored derivative 5'-thio-2-nitrobenzoic acid (TNB) measurable at 412 nm.

1. The cell extract (100 µl) was mixed with 700 µl of KPE buffer (0.1 M Potassium phosphate buffer with 5 mM EDTA disodium salt at pH 7.5). (Blank was set as KPE buffer without cell extract).
2. Added 120 µl of freshly prepared DTNB and GR (Glutathione reductase) mix (Ratio1:1).
3. The mixture was kept at room temperature for 30 seconds.
4. Then, 60 µl of β-NADPH (2 mg β-NADPH in 3 ml KPE buffer) was added to the above mix and the absorbance was measured at 412 nm.
5. The amount of glutathione produced was measured using the GSH (Sigma, cat. no. G-4251) standard curve prepared using the same procedure.

3.2.4 Determination of γ-GCS and GS activity

γ-GCS and GS activity was /assayed according to Ruiz *et al.,* (2003) and Sengupta *et al.,* (2012).

1. The liquid nitrogen crushed samples of *L. bicolor* and *H. cylindrosporum* stressed with different concentrations of Cd (0, 10, 20, 30, 40 µM) and As (0, 5, 10, 15, 20 mM) were homogenized with lysis buffer consisting of 100 mM Tris-HCl (pH 8.0), 10 mM $MgCl_2$ and 1 mM DTT.
2. The homogenate was then centrifuged at 8000 g for 10 min (2-4˚C).
3. The supernatant collected after centrifugation was used for γ-GCS and GS assay.
4. γ-GCS activity was assayed by mixing 100 µl of supernatant with 500 µl of assay mix consisting of 100 mM Hepes (pH 8.0), 50 mM $MgCl_2$, 5 mM ATP, 5 mM phosphoenolpyruvate, 5 mM DTT, 20 mM glutamate, 1 mM cysteine, and 10 U/ml pyruvate kinase.
5. The mixture was then incubated at 37˚C for 60 minutes followed by addition of 100 µl of 50% TCA to stop the reaction.
6. The mixture was again centrifuged, and the supernatant was used for phosphate estimation by phosphomolybdate method.
7. The total phosphorus release by the enzyme was measured by phosphomolybdate method using Hydrazine sulphate and ascorbic acid as the reducing agents (Katewa and Katyare, 2003).
8. The amount of phosphate released is directly proportional to the enzyme activity of γ-GCS.
9. For GS activity the same assay was performed replacing glutamate and cysteine with 1 mM glycine and 0.5 mM γ-glutamylcysteine in assay mix.

3.2.5 Isolation of total RNA from ECM fungi

The total RNA was isolated from both *L. bicolor* and *H. cylindrosporum* using the "QIAzol Lysis Reagent" (Qiagen, Hilden, Germany). Both cultures were grown on MMN-agar plates overlaid with cellophane sheets for 21 days at 25˚C in dark. The fully-grown mycelium was then scrapped aseptically and crushed using liquid nitrogen. The powdered mycelium so obtained was then used for isolation of total RNA using the following protocol:

1. To 100 mg of liquid crushed mycelium, 1 ml of QIAzol lysis reagent was added and mixed thoroughly by vortexing.
2. The mixture was then incubated at room temperature for 5 minutes, to permit the complete dissociation of nucleoprotein complexes.

3. The mixture was then centrifuged at 12000 g for 10 minutes (4˚C), to remove cell debris.
4. The supernatant so obtained was collected in a new vial and mixed with 0.2 ml of ice-cold chloroform.
5. Both supernatant and chloroform were mixed thoroughly and incubated at room temperature for 2-3 minutes.
6. For phase separation, the tubes were centrifuged at 12000 g for 15 minutes (4˚C). The uppermost aqueous phase containing RNA was then carefully transferred to new tube.
7. For precipitating RNA, 0.5 ml of ice-cold isopropanol was added to the aqueous phase and mixed thoroughly. The vials were incubated at -20˚C for 30-60 minutes for successful precipitation.
8. The tubes were then centrifuged at 12000 g for 10 minutes (4˚C) and the supernatant was carefully aspirated and discarded. RNA pellet was visible as gel-like white pellet at bottom of the tube.
9. The RNA pellet was then washed with 1 ml of ice-cold 75% ethanol and centrifuged at 7500 g for 5 minutes (4˚C). The supernatant was carefully removed, and RNA pellet was air-dried.
10. The RNA pellet was dissolved in 30-50 µl of RNase-free water and stored at -80˚C for further use.

3.2.6 Qualitative and quantitative analysis of isolated RNA

The total RNA was then analyzed for its purity and quantity. The qualitative analysis of RNA was achieved through “Electrophoresis” on non-degrading agarose-gel and the quantitative analysis was achieved using nanodrop “NanoDrop™ 1000” (Thermo Fisher Scientific, Massachusetts, USA).

Agarose gel electrophoresis: 0.8-1.0% agarose gel (w/v) was prepared in 0.5 X TBE buffer pH 8.0 (Appendix I). Ethidium bromide (EtBr) was added to the gel, just prior to pouring, to visualize the nucleic acids. Total RNA was loaded into the wells using 6 X loading buffer (Appendix I) and run at 70 V for 45 minutes. DNA ladder was run along to determine the size. The RNA migration was tracked using bromophenol blue in loading buffer. The migrated gel was then visualized on a U.V transilluminator at 312 nm.

Nanodrop Spectrophotometer: The total RNA was quantified by placing the sample drop on Nanodrop 1000 spectrophotometer (Thermo Scientific, USA) and measured the absorbance of the sample at 260 nm. The purity of the sample from contaminating proteins or polysaccharides was evaluated by calculating the ratio between absorbance at 260/280 nm and absorbance at 260/230 nm, respectively. Pure RNA samples indicated value of $O.D_{260/280nm}$ close to 2.0.

3.2.7 Complementary DNA (cDNA) synthesis

Total RNA isolated from both *L. bicolor* and *H. cylindrosporum* was used for synthesizing cDNA using "PrimeScript 1st strand cDNA Synthesis Kit, (Takara, CA, USA)" as per the manufacturer's instructions:

1. To 5 µg of total RNA added 1µl of oligo dT Primers (50 µM), 1 µl of dNTP mixture (10 mM) and RNase-free water to raise the volume to 10 µl.
2. Incubated the mixture at 65˚C for 5 minutes and then immediately cooled on ice.
3. To the above mixture added 4 µl PrimeScript Buffer (5x), 20 U of RNase inhibitor, 100-200 U of PrimeScript reverse transcriptase (RT) and RNase free water for volume makeup upto 20 µl.
4. Mixed gently and the reaction was carried out at 42˚C for 1 hour to robust extension capability of template with complex secondary structure.
5. Heated the mixture at 70˚C for another 10 minutes to stop the reaction and inactivate enzymes followed by cooling the mixture. The cDNA was stored at -20˚ for further use.
6. cDNA was verified by amplifying the housekeeping genes such as α-actin and β-tubulin.

3.2.8 PCR amplification of *γ-GCS* and *GS*

The two genes involved in glutathione biosynthesis - γ-glutamylcysteine synthetase (*γ-GCS*) and glutathione synthetase (*GS*) were amplified from the cDNA of both *L. bicolor* and *H. cylindrosporum* through polymerase chain reaction (PCR). Gene specific primers were designed for both *γ-GCS* and *GS* genes, using the sequences retrieved from JGI portal (http://genome.jgi.doe.gov/) (Table 3.1). Specific restriction sites were added to the 5' end of each primer (underlined: Table 3.1). PCR amplification of *γ-GCS* gene was carried out in a 25 µl reaction consisting of 1 X reaction buffer, 2 µl (dNTPs, 2mM), 1 µl (forward primer, 10 µM), 1 µl (reverse primer, 10 µM), template DNA (cDNA) (100 ng), 1.5 U *Taq* polymerase

and nuclease free water to make 25 µl. The PCR program was set as: initial denaturation at 95°C for 5 min followed by 30 cycles of 1 min at 94°C, 1 min at 62°C, 1 min at 72°C and a final extension at 72°C for 8 min. The amplified products were visualized on 1.0% agarose gel using ethidium bromide staining.

Table 3.1: List of primers used for complete genes amplification and qPCR analysis. The restriction sites added to the 5' end of primers are underlined.

Gene	Primer	Sequence (5'-3')
Primers for complete gene synthesis		
Lbγ-GCS	Lbnde1F	GGAATTCCATATGGATGGGCCTCTTGTATCTCGGCA
	Lbxho1R	CCGCTCGAGCGGCATTTCATCTATGGCCAGCAATAG
LbGS	Lbbam2F	CGGGATCCCGATGACAATAGAGCCGTTTGACATCCC
	Lbeco2R	CGGAATTCCGATCCACCAACAGCAGCGAATCTAAC
Hcγ-GCS	Hcnde1F	GGAATTCCATATGGATGGGTCTTCTTTATCTCGGAAC
	Hcnot1R	ATAAGAATGCGGCCGCCGGGAATTTGGGCATAAAG
HcGS	Hcnde2F	GGAATTCCATATGATGGCATCGACTTTCGACTTTGCC
	Hcnot2R	ATAAGAATGCGGCCGCCACCAAGAGCAATGAATCC
Primers for qPCR analysis		
Lb α-actin	LactF	TGGAAGCGTAATGGGGAAGT
	LactR	CAGTGTTGGTGATGTGCGAA
Lb β-tubulin	LtubF	CCCACGTTGCCATTTTCTCA
	LtubR	CATGCGGTTCTTGGGTTGAA
Lbadenosin	LakF	TCATCACTGGCCATCATCGA
kinase	LakR	TAGTAGAACTTCGCGCCCTC
Lbγ-GCS	LG1F	GCATGCAATGTTTCTGACGC
	LG1R	CGACAATCCACATCAGCGAG
LbGS	LG2F	TTCAAGAGGTGCTAGCCCAA
	LG2R	TCTAAACCCCACATGGCCAT
Hc α-actin	HactF	GTACAAGCGCTCGTGAACAT
	HactR	GATACTCTCGTCCAGTGGCA
Hc β-tubulin	HtubF	CGCTACTAACCCTCAAACGC
	HtubR	CCATCACGGTGGACACTAGT
	HakF	CGGTGTTGAATCTGCTCTCG

Hcadenosin kinase	HakR	ATTTGTTGAAGTTGGGCGCT
Hcγ-GCS	HG1F	ACATTCCAAGCTTGCAACGT
	HG1R	TCGACATCAGCGAGGTATCC
HcGS	HG2F	CGTGGACCAGCTCGAAAATT
	KG2R	AGGCGAAGGAAAGAGGGAAA

3.2.9 Gene purification, digestion and ligation

Purification: The amplified genes (*Lbγ-GCS, LbGS, Hcγ-GCS* and *HcGS*) were then purified using "GeneJET PCR Purification Kit (Thermo Fisher Scientific, Massachusetts, USA)" as per the manufacturer's instructions. The purified gene products were eluted in deionized water in a clean vial.

Digestion: The purified genes (*Lbγ-GCS, LbGS, Hcγ-GCS* and *HcGS*) along with pFL61 plasmid were subjected to double digestion at restriction sites added to their 5' end (Table 3.1) using their respective restriction enzymes (Figure 3.2) in a 50 µl reaction (Table 3.2).

Table 3.2: Composition of restriction digestion reaction

Component	**Concentration**
Gene/ Plasmid DNA	1 µg
Restriction enzyme I	1 µl
Restriction enzyme II	1 µl
Digestion buffer (10X)	5 µl
Deionized water	To make 50 µl

The reaction mixture was mixed well and incubated at 37˚C for 3-4 hours. The digested genes and plasmids were loaded on 0.8% agarose gel and purified using "GeneJET Gel Extraction Kit". The purified digested genes and plasmid were eluted into deionized water.

Ligation: The genes (*Lbγ-GCS, LbGS, Hcγ-GCS* and *HcGS*) were then ligated into their respectively digested pFL61 plasmids in the ratio 3:1 (3-times insert in 1-time plasmid) using the T4 DNA ligase (Figure 3.2) in the following reaction mixture (Table 3.3):

Table 3.3: Composition of ligation reaction

Component	Concentration
Digested gene insert	75 ng
Digested plasmid	25 ng
T4 DNA ligase	1 µl
Ligation buffer (10X)	2 µl
Deionized water	To make 20 µl

The reaction mixture was properly mixed and incubated at 4˚C overnight.

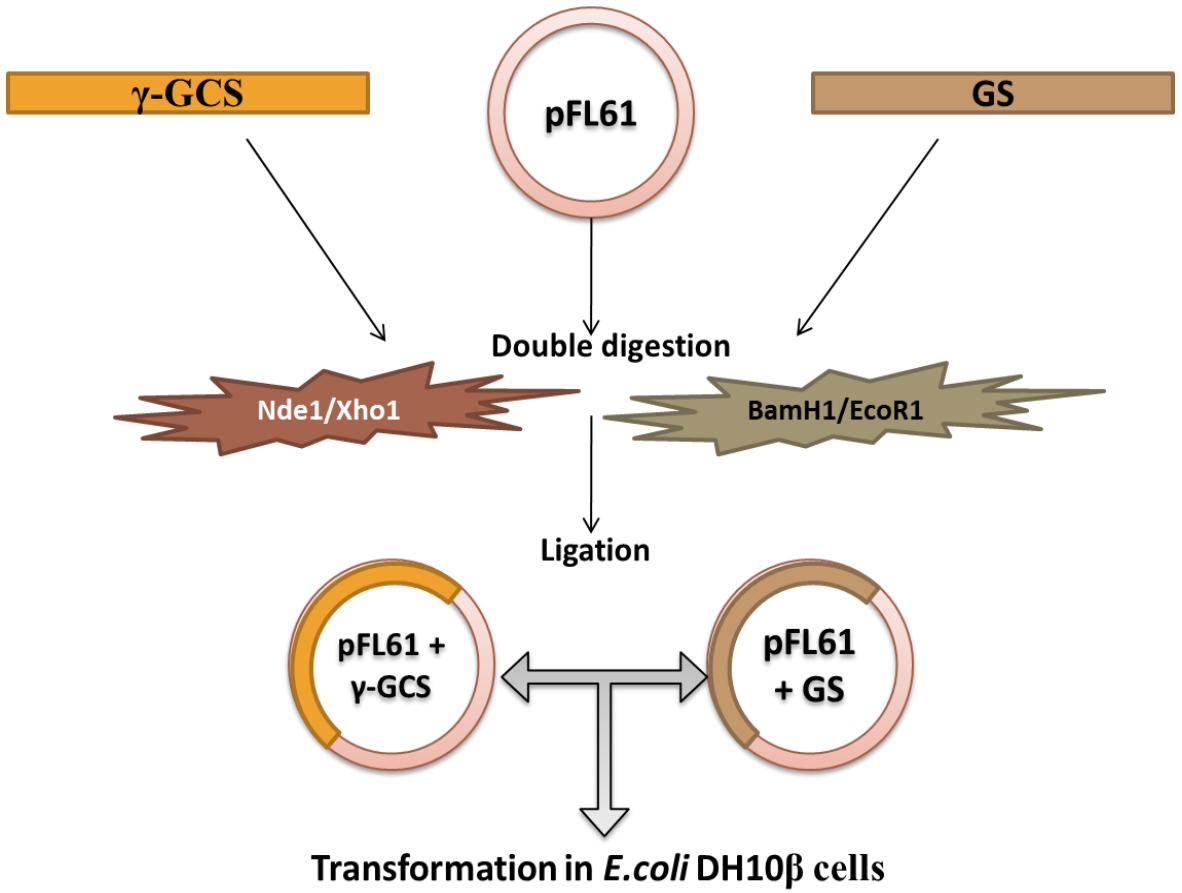

Figure 3.2 Schematic diagram highlighting the process of double digestion, ligation and transformation.

3.2.10 Cloning of ligated glutathione genes in *E. coli* DH10β

The ligated genes (pFL61+*Lbγ-GCS*, pFL61+*LbGS*, pFL61+*Hcγ-GCS* and pFL61+*HcGS*) were then transformed into *E. coli* DH10β competent cells through heat shock method:

Competent cell preparation:

1. The *E. coli* DH10β cells were inoculated in 20 ml LB medium (Appendix I) and incubated overnight at 37˚C with vigorous shaking.
2. The overnight grown culture (100 µl) was then used to inoculate 50 ml LB, incubated at 180 rpm for 3-4 hours (till the absorbance at 600nm reached 0.5).
3. Transferred the culture into 50 ml Oakridge tubes and incubated on ice for 20 minutes.
4. The cells were then centrifuged at 8000 g for 15 minutes (4˚C) and the supernatant was discarded.
5. The *E. coli* pellet was then suspended in 10 ml of ice cold 0.1M $CaCl_2$ and incubated on ice for 15 minutes, followed by centrifugation at 8000 g for 15 minutes (4˚C).
6. The supernatant was discarded, and pellet was again dissolved in 1 ml of ice cold 0.1 M $CaCl_2$. The cells were then incubated overnight at 4˚C.

Bacterial cell transformation

1. To 100 µl of freshly prepared competent cells, 5 µl of ligated product was added and mixed gently. The mixture was then incubated on ice for 30 minutes to initiate plasmid binding to cell.
2. The cells were then exposed to heat shock for exactly 2 minutes at 42˚C in a still water bath, followed by rapid transfer to ice for 2-3 minutes.
3. 1 ml of LB was then added to each tube and incubated at 37˚C for 1 hour.
4. After 1 hour, the tubes were centrifuged and 900 µl of LB was discarded. The pellet was then resuspended in remaining 100 µl LB and spread on LA + Amp or LA + Amp + X-Gal + IPTG plates.
5. The plates were then incubated at 37˚C for 16 hours. After 16 hours, the positive clones for each transformation (pFL61+*Lbγ-GCS*, pFL61+*LbGS*, pFL61+*Hcγ-GCS* and pFL61+*HcGS*) were screened using colony PCR.

Colony PCR for screening of positive clones

1. The pin tip colony from each transformant was dissolved in 10 µl H_2O and lysed by heating at 97˚C for 5 minutes.

2. 3 µl of lysed cells were used as template to run the PCR in a 25 µl reaction consisting of 1X reaction buffer, 2 µl dNTPs (2 mM), 1 µl forward primer (10 µM), 1 µl reverse primer (10 µM), 1.5 U *Taq* polymerase and nuclease free water to make 25 µl.
3. The PCR was run in a thermocycler with the following program: 95°C for 5 min followed by 30 cycles of 30 sec at 94°C, 30 sec at 55°C, 30 sec at 72°C and final extension at 72°C for 7 min.
4. The positive clone for each gene (pFL61+*Lbγ-GCS,* pFL61+*LbGS,* pFL61+*Hcγ-GCS* and pFL61+*HcGS*) was selected based on the amplified product visualized on 1.0% agarose gel using ethidium bromide staining.

3.2.11 Isolation of Plasmid DNA

The plasmid DNA was isolated from the positive *E. coli* clone of each pFL61+*Lbγ-GCS,* pFL61+*LbGS,* pFL61+*Hcγ-GCS* and pFL61+*HcGS* obtained after transformation by alkaline lysis method as given below:

1. The positive clones were inoculated in 20 ml LB broth and incubated overnight at 37˚C with constant shaking.
2. 2 ml of the freshly grown culture was centrifuged at 12000 g for 1 minute and the supernatant was discarded.
3. To the pellet, 200 µl of ice-cold solution I (50 mM glucose, 10 mM EDTA in 25 mM Tris-HCl (pH 8)) was added and mixed vigorously by vortexing till the pellet was completely dispersed in the solution.
4. Added 200 µl of freshly prepared solution II (0.2N NaOH with 1% SDS) and mixed the content by gently inverting the tubes five to ten times. The tubes were then incubated on ice for 2-3 minutes.
5. To the above mixture, 300 µl of ice-cold solution III (3M potassium acetate with 11.5 ml glacial acetic acid in deionized water) was added and mixed by inverting the tubes 5-10 times. The mixture was then incubated on ice for 5-10 minutes.
6. The mixture was then centrifuged at 12000 g for 10 minutes (4˚C) and the supernatant was carefully transferred to fresh tube.
7. The plasmid DNA was then precipitated from the supernatant by adding equal amount of isopropanol and mixing well.
8. The tubes were then incubated at -20˚C for 1 hour to facilitate precipitation, followed by centrifugation at 12,000 g for 10 minutes (4˚C).

9. The supernatant was discarded, and the pellet was washed with 400 µl of 70% ethanol. The tubes were then centrifuged at 8500 g for 5 minutes.
10. The pellet so obtained was air dried by inverting the tubes on paper towel and dissolved in 30-50 µl of DNase free water.
11. The isolated plasmid was then visualized on 0.8% agarose gel using agarose gel electrophoresis (Section 3.2.6) and quantified on nanodrop.

3.2.12 Yeast transformation

For the functional characterization of genes, the plasmid isolated from their respective *E. coli* positive clones (pFL61+*Lbγ-GCS,* pFL61+*LbGS,* pFL61+*Hcγ-GCS* and pFL61+*HcGS*) were transformed into *S. cerevisiae* mutants. Two *S. cerevisiae* mutants $gsh1^{\Delta}$ (BY4741; MATa; ura3Δ0; leu2Δ0; his3Δ1; met15Δ0; YJL101c::kanMX4) and $gsh2^{\Delta}$ (BY4741; MATa; ura3Δ0; leu2Δ0; his3Δ1; met15Δ0; YOL049w::kanMX4) were transformed with *pFL61+Lbγ-GCS/pFL61+Hcγ-GCS* and *pFL61+LbGS/pFL61+HcGS,* respectively using the Lithium acetate method (Gietz and Schiestl, 2007) as described below:

1. 20 ml of YPD medium (Appendix I) was inoculated with *S. cerevisiae* mutants $gsh1^{\Delta}$ and $gsh2^{\Delta}$ and incubated overnight at 30˚C with constant shaking at 200-250 rpm. The $absorbance_{600nm}$ of the overnight grown culture was measured.
2. A new 40 ml YPD flask was inoculated with the overnight culture such that the $absorbance_{600nm}$ becomes 1.0 and the final volume becomes 50 ml.
3. The flask was then incubated at 30˚C for 3-4 hours at 200 rpm such that the $absorbance_{600nm}$ reaches 2.0.
4. The culture with $absorbance_{600nm}$ 2.0 was then transferred into 50 ml falcon tube and centrifuged at 3000 g for 5 minutes. The supernatant was discarded, and the pellet was washed with 20 ml of distilled water (autoclaved), followed by centrifugation at 3000 rpm for 5 minutes.
5. The pellet was again resuspended in 1 ml of distilled water and transferred to 1.5 ml eppendorf tube.
6. The tubes were again centrifuged, and the supernatant was discarded. The pellet was again dissolved in 1 ml of distilled water.
7. Make 100 µl aliquots from the above 1 ml solution to make competent cells. Centrifuge the aliquots for 30 seconds and discard the supernatant.
8. To the pellet in each tube, add the following mixture:

(*Before using, salmon sperm DNA was denatured by heating at 100˚C for 5 minutes)

PEG 3500 (50% w/v)	240 µl
Lithium acetate (1M)	36 µl
Salmon sperm DNA (10 mg/ml) *	10 µl
Plasmid DNA	5 µl
Distilled water	To make 360 µl

9. An aliquot without plasmid DNA was kept as negative control and with only pFL61 was used as positive control.
10. For *gsh1*$^{\Delta}$ cells, plasmid DNA used were *pFL61+Lbγ-GCS* and *pFL61+Hcγ-GCS*, whereas for *gsh2*$^{\Delta}$, the plasmid used were *pFL61+LbGS* and *pFL61+HcGS*.
11. The pellet was dissolved properly, and the mixture was incubated at 42˚C for 1 hour, followed by centrifugation at 3000 g for 30 seconds.
12. The supernatant was discarded, and the pellet was resuspended in 1 ml of YPD media, followed by incubation at 30˚C for 1 hour. After 1 hour, the tubes were again centrifuged at 3000 g for 30 seconds.
13. The pellet was washed with 1 ml distilled water (autoclaved) and centrifuged at 3000 g for 30seconds.
14. The pellet was again suspended in 1 ml water, followed by spreading on SD-Ura plates supplemented with and without metal(loid) (As: 100 µM and Cd: 40 µM). The plates were then incubated at 30˚C for 2 days.
15. After 2 days the positive clones were selected by colony PCR followed by plasmid isolation.

3.2.13 Yeast Colony PCR

1. Pin heads of colonies were picked using sterile toothpicks and dissolved in 10 µl of NaOH (20 mM).
2. The tubes were then heated at 98˚C for 30 minutes and then immediately transferred on to ice.
3. The tubes were then spinned on table top spinner for 30 seconds.
4. 3 µl of the supernatant obtained after spinning was used as a template to run PCR in a 25 µl reaction as described in section 3.2.10.
5. The PCR products were then visualized on 1% agarose gel under U.V light.

3.2.14 Functional complementation assay

The function characterization of both *γ-GCS* and *GS* genes isolated from *L. bicolor* and *H. cylindrosporum* was achieved by expressing both genes in their respective yeast mutants *gsh1*$^{\Delta}$ and *gsh2*$^{\Delta}$. The positive clones of *gsh1*$^{\Delta}$ carrying pFL61, pFL61+*Lbγ-GCS*, pFL61+*Hcγ-GCS* and *gsh2*$^{\Delta}$ carrying pFL61, pFL61+*LbGS*, pFL61+*HcGS* along with wild type BY4741 were grown on SD-Ura medium at 30˚C. The cultures were then characterized using two tests- drop test and liquid medium test.

3.2.14.1 Drop test:

1. All the transformants along with wild type BY4741 were inoculated in SD-Ura broth and incubated at 30˚C for 48 hours with constant shaking at 210 rpm.
2. After 48 hours, the absorbance of each culture was measured at 600 nm. The absorbance of each culture was adjusted to 1.0.
3. Each culture with absorbance 1.0 was then serially diluted up to 10^{-4} (10^{0}, 10^{-1}, 10^{-2}, 10^{-3}, 10^{-4}).
4. 5 µl of each serial dilution was then spotted as a drop on SD-Ura plates supplemented with and without metal(loid) i.e., $CdSO_4$: 40 µM and Na_2HAsO_4: 100 µM.
5. The plates were then sealed and incubated at 30˚C for 48 hours. After 48 hours, the growth on each plate was monitored and photographed.

3.2.14.2 Liquid assay:

1. All the transformants along with wild type BY4741 were inoculated in different flasks containing 50 ml of SD-Ura medium and incubated at 30˚C with constant shaking till the absorbance at 600 nm reached 0.05.
2. The cultures were then supplemented with different concentrations of Cd (0, 20, 40, 60, 80 µM) and As (0, 50, 100, 150, 200 µM).
3. All the flasks were then incubated at 30˚C with constant shaking at 210 rpm for 24 hours.
4. After 24 hours, the growth of each culture under different stresses was recorded as absorbance at 600 nm.

3.2.15 Expression of *γ-GCS* and *GS* by real time PCR (RT-PCR) analysis

The effect of Cd and As on the expression of both genes *γ-GCS* and *GS* in *L. bicolor* and *H. cylindrosporum* was analyzed using real time PCR.

1. *L. bicolor* and *H. cylindrosporum* were grown on MMN plates overlaid with cellophane sheets for 14 days. After 14 days, both cultures were stressed with different concentrations of Cd (0, 10, 20, 30, 40 µM) and As (0, 5, 10, 15, 20 mM) and incubated at 25˚C for 48 hours.
2. After 48 days, the stressed mycelium was scrapped and crushed using liquid nitrogen.
3. The total RNA was isolated from the liquid nitrogen crushed samples of both *L. bicolor* and *H. cylindrosporum* using the protocol described in section 3.2.5.
4. Complementary DNA (cDNA) was synthesized using 5 µg of each RNA sample as described in section 3.2.7.
5. The gene expression analysis of both *γ-GCS* and *GS* was performed using the SYBR Green JumpStart Taq ReadyMix (Sigma-Aldrich) in a 25 µl reaction mixture (Table 3.4)

   Table 3.4: Reaction composition for real time PCR analysis

Component	Concentration
SYBR Green master mix	12.5 µl
Forward Primer (10 mM)	1.0 µl
Reverse Primer (10 mM)	1.0 µl
cDNA template (20 folds diluted)	1.0 µl
Water	To make 25 µl

6. The qPCR reaction was performed in a mastercycler® ep realplex real-time PCR system (Eppendorf, Germany) using the following PCR program- initial denaturation at 95˚C for 2 minutes, followed by 40 cycles of 95˚C for 15 seconds, 55˚C for 15 seconds and 68˚C for 20 seconds.
7. To confirm that there were no traces of DNA present in RNA extracts, PCR was performed with non-reverse-transcribed RNA samples as control
8. The relative expression of all four genes *Lbγ-GCS, LbGS, Hcγ-GCS* and *HcGS* was calculated by the comparative threshold (Ct) method using α-actin, β-tubulin and adenosine kinase as housekeeping reference genes (Primers- Table: 3.1).

9. The Norm-Finder analysis of all three housekeeping genes was performed by method described by Andersen *et al.,* (2004) and it was observed that α-actin showed minimum stability value. Therefore, α-actin was further used as the reference gene for comparative analysis.
10. The amplification efficiency of genes was calculated by the equation $E=[10^{(-1/slope)}]-1$. The E values so obtained were in a range from 1.25 to 1.75.
11. The values were further used to calculate Ct1 value where Ct1=Cte X [log(1+E)/log2]. The Ct1 value was calculated for each sample and then the comparative expression level of the genes was given by the formula $2^{-\Delta\Delta Ct}$, where ΔΔCT was calculated by subtracting the baseline's ΔCT to the sample's ΔCT and where the baseline represents the expression level of the control (Livak and Schmittgen 2001).
12. All qRT-PCR measurements were performed on RNA extracted from three independent biological samples (experimental replicates), and for each RNA extract three technical replicates were performed.

3.2.16 Sequence analysis of *γ-GCS* and *GS* genes

Both *γ-GCS* and *GS* genes were amplified from the cDNA of *L. bicolor* and *H. cylindrosporum* using the gene specific primers synthesized in table 3.1. The amplified genes *Lbγ-GCS, LbGS, Hcγ-GCS* and *HcGS* were then ligated into pMD20 vector using the "Mighty TA cloning kit (Takara, CA, USA)". The ligated products were then transformed into *E. coli* DH10β cells by the heat shock method as described in section 3.2.10. The positive clones were then selected by colony PCR followed by plasmid isolation. The genes were then sequenced using the M13 primers by chain termination method, using an Applied Biosystems automatic sequencer (DNA sequencing facility, Department of biochemistry, South campus, Delhi university, New Delhi, India). The sequences so obtained were then submitted to GenBank of NCBI (Table 3.5) (Appendix-II) and further analyzed using various bioinformatic tools.

Table 3.5: List of sequences submitted to NCBI with accession number.

S. No.	Gene Name	Accession No.
1	*Lbγ-GCS*	MF766455
2	*LbGS*	MF766456
3	*Hcγ-GCS*	MH892339

4	*HcGS*	MK617301

The open reading frame (ORF) of all the four sequences was identified using the ORF finder (https://www.ncbi.nlm.nih.gov/orffinder/). The selected ORF was then subjected to BLASTX (https://blast.ncbi.nlm.nih.gov/Blast.cgi) for searching the homologous sequences. The homologous sequences so obtained were then aligned using Clustal Omega (https://www.ebi.ac.uk/Tools/msa/clustalo/). The evolutionary relationship of genes was further studied by constructing their phylogenetic tree. Maximum parsimony phylogenetic tree with 1000 bootstraps was constructed using MEGA 7.0 software. The molecular weight and pI of the identified protein sequences was calculated using ExPASy (https://web.expasy.org/compute_pi/). The protein domains were identified using Interpro (http://www.ebi.ac.uk/interpro/sequence-search). Various conserved domains like catalytic domains, ATP binding domains, glycosylation sites, phosphorylation sites were identified using Motif-Scan and ATPint (crdd.osdd.net/raghava/atpint/index.html). The secondary structure of protein was predicted using PSSpred (http://zhanglab.ccmb.med. umich.edu/ PSSpred), where all the possible a-helix, b-sheets and coils were identified.

3.2.17 Comparative proteomic analysis of *L. bicolor* in response to Cd stress.

The response of ECM fungus *Laccaria bicolor* to Cd stress and the mechanisms involved in Cd toxicity were studies using the comparative proteomic analysis. *L. bicolor* was grown on MMN medium for 14 days at 25°C. After 14 days, half of the plates were supplemented with 40 µM of Cd and allowed to grow for another 48 hours. After 48 hours, the mycelium was precured from both stressed (LbCd-40) and unstressed (LbCd-0) plates and crushed with liquid nitrogen. The crushed samples were further used for proteomic analysis using the steps mentioned below (Figure 3.3):

- Isolation of total proteins from both Lbcd-0 and LbCd-40
- Qualitative analysis of isolated proteins using SDS-PAGE
- In-solution digestion of isolated proteins using Trypsin
- Separation of digested peptides using liquid chromatography
- Mass spectroscopic analysis using ECI-qTOF MS/MS system
- Identification and quantification of peptides
- Comparative analysis of data LbCd-40: LbCd-0

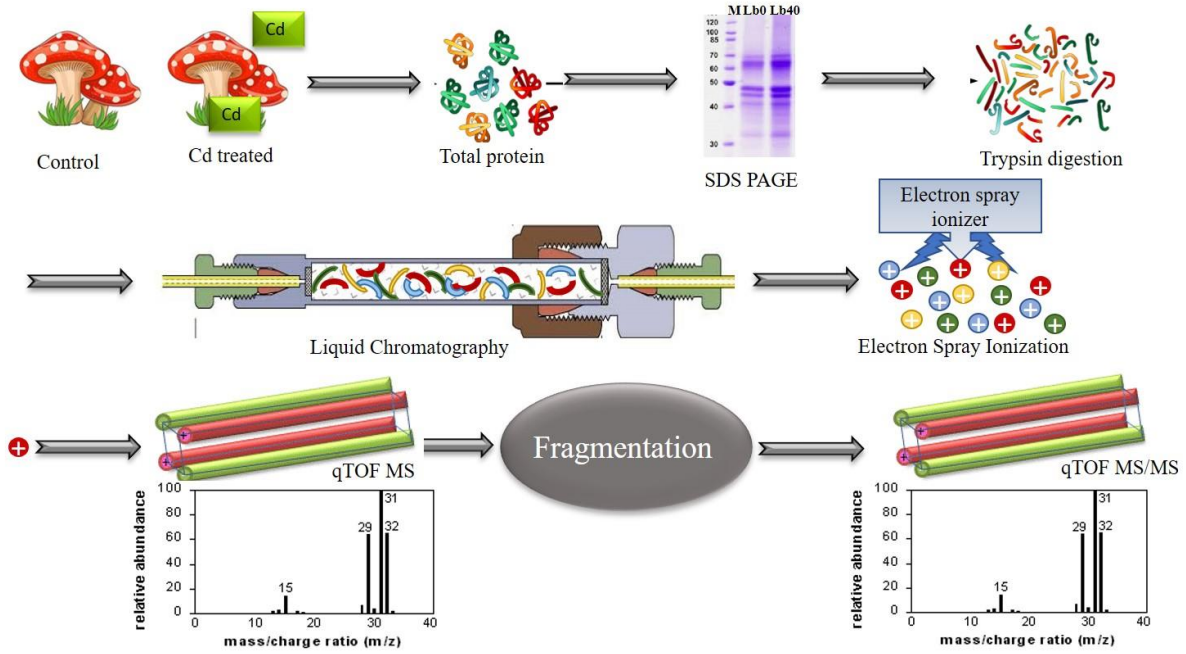

Figure 3.3: Total proteome analysis of ECM fungus *L. bicolor* in response to Cd stress using Liquid chromatography-ESI-qTOF-MS/MS analysis.

3.2.17.1 Isolation of total protein from *L. bicolor*

The proteomic response of ECM fungus *L. bicolor* to Cd stress was studied by isolating the total proteins from the liquid nitrogen crushed samples of *L. bicolor* both with and without Cd stress. The *L. bicolor* culture was grown on MMN plates overlaid with cellophane sheets at 25˚C for 14 days. After 14 days, the cellophane sheets were transferred on to liquid MMN medium supplemented with and without Cd (40 µM) for 48 hours. The mycelium from both samples was then scrapped and crushed using liquid nitrogen. Total proteins were then isolated from the liquid nitrogen crushed samples using the following protocol:

1. 1 ml of lysis buffer containing 50 mM ammonium bicarbonate pH8, 1% SDS and 5 µl protease inhibitor cocktail was added to 500 mg of liquid nitrogen crushed mycelium, and mixed by vigorous vortexing.
2. The mixture was then sonicated in Ultrasonic bath sonicator for 15 minutes at 4°C with intermediate mixing.
3. The mixture was then centrifuged at 5000g for 5 minutes at 4°C, and the supernatant containing proteins was precured in a separate tube.

4. The isolated proteins were then purified using ReadyPrep™ 2-D Cleanup Kit (BioRad) as per the manufacturer's instructions.
5. The purified proteins were then dissolved in 50 mM ammonium bicarbonate+ 0.1% SDS and quantified using Bradford assay (Section 3.2.17.2)
6. The protein integrity was checked by visualizing them through SDS-PAGE (3.2.17.3).

3.2.17.2 Protein quantification using Bradford assay

The total proteins isolated were then quantifies using the protocol described by Bradford (1976).

1. Firstly, six dilutions of BSA (1 mg/ml) were serially dilutes to 1000, 500, 250, 125, 62.5, 31.25 µg/µl.
2. 100 µl of each dilution along with the unknown proteins (LbCd-0 and LbCd-40) were distributed in separate test tubes. Two tubes were prepared with 100 µl water for setting 'Blank'.
3. To each tube 3 ml of Bradford reagent (Appendix I) was added and the tubes were mixed by either inversion or vortexing.
4. The tubes were then incubated at room temperature for at least 5 minutes.
5. The absorbance of each sample was recorded at 595 nm.
6. The values for each protein standard were plotted on a graph (concentration vs absorbance). The linear graph so obtained was used to measure the quantity of LbCd-0 and LbCd-40.

3.2.17.3 Qualitative analysis of proteins using SDS-PAGE

1. Gel casting:
    - The glass plates were assembled with spacers placed in between the plates.
    - The plates were then fixed on the gel casting assembly
    - Firstly, the 12% separating gel (resolving gel) (Appendix I) was prepared and poured immediately into the glass plates till $3/4^{th}$ of the space is filled.
    - A layer of butanol was poured on the top of separating gel so as to kill bubbles and avoid gel oxidation.
    - The gel was allowed to solidify.

- Once the separating gel solidifies, layer of butanol is removed and comb is inserted between the glass plates on top.
- The remaining 1/4th of the plates is then filled with 4% stacking gel (Appendix I) and allowed to solidify.
- Once the gel stacking gel solidifies, remove the comb and the gel is ready for SDS-PAGE.

2. Poly acrylamide gel electrophoresis:
    - The casted gel is then placed into the electrophoresis tank filled with tank buffer (Appendix I).
    - The 20 µg of protein sample is then mixed with 5 µl of loading dye and loaded into the wells.
    - Suitable molecular weight marker was also loaded in a separate well.
    - The plates were then connected to electrodes and the electrophoresis was run at 100V till the tracking dye reaches the other end.
3. Gel Staining:
    - The acrylamide gel was then precured by removing the glass plates and placed in a staining box.
    - Staining solution (Appendix I) was poured on top of the gel till the gel is completely immersed.
    - The box was then placed on the gel rocker for 2-4 hours.
4. Destaining:
    - The stained gel is then washed with deionized water.
    - The stained gel was then immersed in destaining solution (Appendix I) for 8-10 hours.
    - The destaining solution was changed in between till the gel is completely destained and the bands are clearly visible.

3.2.17.4 Label free LCMS Q-TOF analysis

The total protein isolated in section 3.2.17 was then subjected to in-solution digestion followed by HPLC, label free quantitation, Q-TOF for mass spectroscopy analysis and protein identification by Sandor Speciality Diagnostics Pvt Ltd, Hyderabad, Telangana using the following protocol:

1. For in-solution digestion, 100 µg of the isolated total protein was diluted with 50 mM of NH_4HCO_3 and treated with 100 mM DTT at 95˚C for 1 hour.
2. After 1 hour the sample was cooled and 250 mM IDA was added and incubated at room temperature in dark for 45 minutes.
3. The sample was then digested with trypsin and incubated overnight at 37˚C.
4. The digested sample was then vacuum dried and dissolved in 50 µl of 0.1% formic acid in water.
5. The sample was then centrifuged at 10000 g for 10 minutes. The supernatant was carefully collected in a separate tube.
6. 10 µl of the digested sample was then injected into the Liquid chromatography system "ACQUITY UPLC system (Waters, UK) using the column UPLC BEH C18) (150 mm X 2.1 mm X 1.7 µm) (Waters, UK) in order to achieve the protein separation. A gradient elution program was run for the chromatographic separation with mobile phase A (0.1% formic Acid in water), and mobile phase B (0.1% formic acid in acetonitrile) using the program mentioned in Table 3.6.

   Table 3.6: Liquid chromatography- Gradient elution program

S. No	Time	Flow	%A	%B	Curve
1	Initial	0.300	98.0	2.0	Initial
2	1.00	0.300	98.0	2.0	6
3	30.00	0.300	50.0	50.0	6
4	32.00	0.300	50.0	50.0	6
5	40.00	0.300	20.0	80.0	6
6	45.00	0.300	20.0	80.0	6
7	50.00	0.300	98.0	2.0	6
8	55.00	0.300	98.0	2.0	6
9	60.00	0.300	98.0	2.0	6

7. Three runs per sample were carried out for label free quantitation.
8. The peptides separated by LC were then directed to Waters Synapt G2 Q-TOF (Waters, UK) for MS and MSMS analysis. Samples were analyzed in positive mode using the operation parameters mentioned in Table 3.7.

Table 3.7: Operational parameters for Q-TOF MSMS analysis

Experimental Instrument Parameters	
Polarity	ES+
Analyzer	Resolution mode
Capillary (kV)	3.5000
Source Temperature (˚C)	150
Sampling Cone	45
Extraction Cone	4.5
Source Gas Flow (ml/min)	30
Desolvation Temperature (˚C)	350
Cone Gas flow (l/hour)	30
Desolvation Gas flow (l/hour)	800
Acquisition	
Acquisition time	60 minutes
Source	ES
Acquisition polarity	Positive
Analyzer mode	Resolution
TOF MS	
Da Range	50 Da to 1500 Da
Scan Time	0.5 seconds
Data Format	Continuum
Collision Energy (Low)	
Collision Energy (Trap)	On-6 V
Collision Energy (Transfer)	On-6 V
Collision Energy (High)	
Ramp Trap Collision Energy	On-20 V to 45 V
Ramp Transfer Collision Energy	Off
Cone voltage	
Cone Voltage	40 V

9. The raw data precured was then processed by Mass Lynx 4.1 (Waters, UK).
10. The individual peptide's MSMS spectra were then matched to the database sequence for protein identification on PLGS software 3.0.2 (Waters, UK). The source of the

sample being Basidiomycota Proteins for samples: LBCD_0 and LBCD_40 the protein database was downloaded from UniProt database (Basidiomycota Proteins) and used for searching the proteins present in the sample. 3 run of each sample was processed using the search parameters in the software (Table 3.8).

Table 3.8: Search parameters for PLGS software

Search Parameters:	
Peptide tolerance (ppm)	50
Fragment tolerance (ppm)	100
Min no. of fragment matches for peptides	2
Min no. of fragment matches for proteins	5
Min no. of peptide matches for proteins	2
Missed Cleavages	1
Modification	Carbamidomethyl c, Oxidation m
Database	UniProt: Basidiomycota
Search engine	PLGS

3.3 Statistical analysis

All the experiments were performed in triplicates. The data were analyzed by analysis of variance and the means were compared with Tukey's test at $P < 0.05$. All the analyses were performed by using Graph Pad Prism 5.1 software.

CHAPTER 4

RESULTS & DISCUSSION

4.1 Screening of ectomycorrhizal fungi for their tolerance to Cd and As

Studying the physiological response of ectomycorrhizal (ECM) fungi, *Laccaria bicolor* and *Hebeloma cylindrosporum* to different concentrations of cadmium (Cd) and arsenic (As) is a prerequisite for molecular and genetic analysis. It provides the information about the threshold toxic concentration of each metal(loid) and its tolerance level in ECM fungi. The ECM fungi, *L. bicolor* and *H. cylindrosporum* were subjected to different concentrations of Cd and As. The tolerance of the fungi was recorded as the biomass recovered after stress. With the increase in external metal(loid) concentration, the growth of both *L. bicolor* and *H. cylindrosporum* was adversely affected.

In case of Cd, the increase in external metal concentration significantly decreased the mycelium growth. For *L. bicolor*, the half minimum inhibitory concentration (IC_{50}: concentration of Cd at which the biomass is reduced to 50%) of Cd was recorded at ~8 µM. At 9 µM, the mycelium growth was reduced to 45%, whereas at 12 µM, only 7% of the biomass was obtained, which got reduced to 4.8% at 15 µM (Figure 4.1) (Table 4.1). Similarly, in case of *H. cylindrosporum*, the half minimum inhibitory concentration of Cd was recorded at 8 µM. At 6 µM, the growth was reduced to 70%, whereas at 9 µM, the growth was reduced to 46% and at 12 µM, only 5.4% biomass was recovered, which further got reduced to 4.4% at 15 µM (Figure 4.1) (Table 4.1).

Similar observations have been recorded in case of As, where with increase in external concentrations, the fungal biomass was adversely affected (Figure 4.2). In case of *L. bicolor*, at 3 mM of external As, the mycelium growth was reduced to 72.4%, at 6 mM it was reduced to 58.9%. Half minimum inhibitory concentration (IC_{50}) was recorded at ~7 mM, which was further reduced to 34.4% at 9 mM, 27.1% at 12 mM and 21.6% at 15 mM. Similarly, in case of *H. cylindrosporum*, when exposed to 3 mM of external As, the growth was reduced to 84.9% and at 6 mM, it was reduced to 62.5%. The IC_{50} for As was recorded at ~8 mM. Further, increasing the As concentration to 9 mM resulted in biomass reduction to 44.4 %, followed by 31.7 % at 12 mM and 24.8 % at 15 mM (Table 4.2).

Table 4.1: Tolerance of *L. bicolor* and *H. cylindrosporum* to Cd. Effect of external Cd concentration was recorded as the dry weight (mg) precured after 48 hours of metal stress in a 50 ml MMN broth supplemented with different concentrations of Cd.

Cadmium concentration (µM)	Dry Weight (mg/50 ml culture)	
	L. bicolor	***H. cylindrosporum***
0	72.00±3.21a	42.5±0.940a
3	59.66±2.56b	32.8±2.496b
6	50.68±1.89c	30.2±1.554c
9	32.33±2.15d	19.5±1.650d
12	5.33±0.245e	2.3±1.589e
15	3.50±0.11e	1.9±0.075e

Values (Mean±SD) sharing a common letter within the column are not significantly different at P<0.05 (n=3).

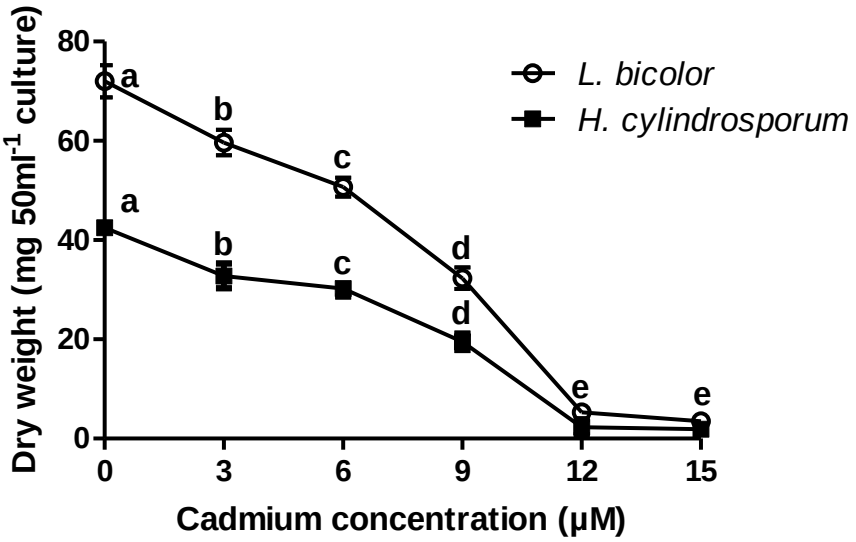

Figure 4.1: Effect of different concentrations of Cd on the growth of *L. bicolor* and *H. cylindrosporum* recorded as dry weight of mycelium precure after 48 hours of metal stress. Values sharing a common letter within the fungal strain are not significantly different at P<0.05 (n=3). Error bars are ± SD.

Table 4.2: Tolerance of *L. bicolor* and *H. cylindrosporum* to As. Effect of external As concentration was recorded as the dry weight (mg) precured after 48 hours of metal(loid) stress in a 50 ml MMN broth supplemented with different concentrations of As.

Arsenic Concentration (mM)	**Dry weight (mg/50 ml culture)**	
	L. bicolor	***H. cylindrosporum***
0	68.5±2.56a	48.60±1.072a
3	49.6±2.41b	41.30±1.320b
6	40.4±1.99c	30.40±1.150c
9	23.6±1.58d	21.60±1.890d
12	18.6±0.95e	15.40±1.265e
15	14.8±0.88e	12.10±1.690e

Values (Mean±SD) sharing a common letter within the column are not significantly different at P<0.05 (n=3)

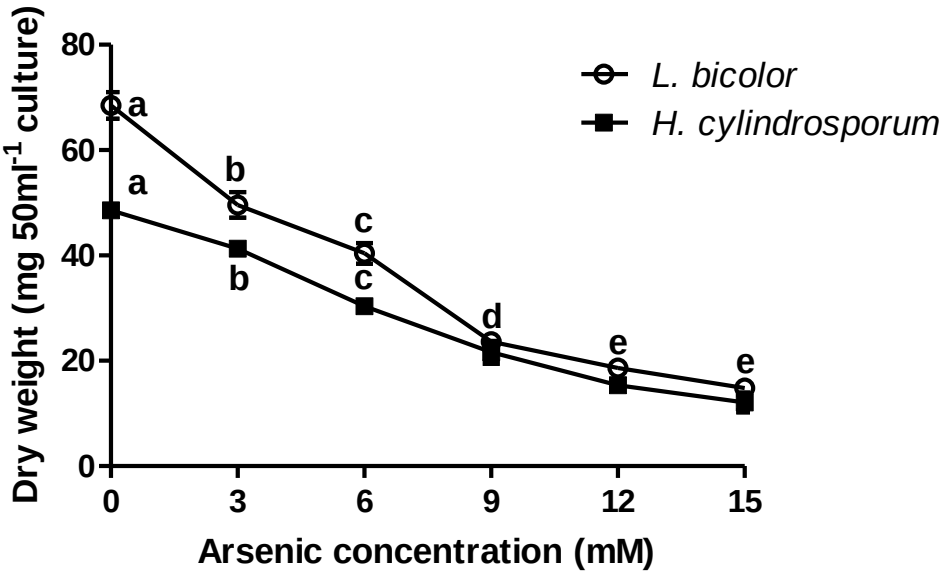

Figure 4.2: Effect of different concentrations of As on the growth of *L. bicolor* and *H. cylindrosporum* recorded as dry weight of mycelium precure after 48 hours of metals stress. Values sharing a common letter within the fungal strains are not significantly different at P<0.05 (n=3). Error bars are ± SD.

These results suggest that increasing the external metal(loid) concentration, the mycelium growth was retarded. The IC_{50} values of Cd recorded for *L. bicolor* and *H. cylindrosporum* are quite comparable to that of other ECM fungi, *Cenococcum geophilum, Paxillus involutus, Suillus luteus* and *Suillus himalayensis*. The IC_{50} value for *Cenococcum geophilum* was recorded at 9 µM, whereas that for *Paxillus involutus* and *Suillus luteus* it was recorded at 2.2 µM and 0.4 µM respectively (Hartley *et al.,* 1997). The IC_{50} value of *S. himalayensis* when exposed to Cd was recorded at 10 µM (Kalsotra *et al.,* 2018) and that of *Pisolithus albus* was recorded at 25 µM of Cd (Reddy *et al.,* 2016). Different ECM fungal strains showed different levels of tolerance to different heavy metals. Krznaric *et al.,* (2009) isolated different strains of *Suillus luteus* form *Pinus Sylvestris* grown in Cd contaminated and non-contaminated areas. The IC_{50} value of these species varied from 19 µM to 154 µM Cd. This difference in tolerance is due to the adaptation of fungal species isolated from metal(loid) contaminated areas (Krznaric *et al.,* 2009).

The response of both *L. bicolor* and *H. cylindrosporum* to As stress is also comparable to some of the already studied metal(loid) tolerant fungal systems. The IC_{50} value of As recorded for *Hymenoscyphus ericae* isolated from uncontaminated soil was at 1.33 mM, whereas the same fungus isolated from mine area showed IC_{50} at 13.3 mM As (Sharples *et al.,* 2001). However, the growth of *Suillus variegatus, Hebeloma crustuliniforme* and *Cenoccum geophilum* was completely inhibited at 8 mM of As stress (Chen and Tibbett, 2007). The growth of *Aspergillus oryzae* isolated from As-contaminated soil showed 50% inhibition at 8 mM As and complete inhibition at 13 mM of As (Liang *et al.,* 2018). Since different fungi responds differently to different heavy metals, therefore it is important to study the tolerance level of ECM fungi to each metal(loid) before its application.

4.2 Metal(loid) accumulation in ECM fungi

ECM fungi have developed diverse mechanisms for heavy metal(loid) tolerance, which includes cell wall binding, metal(loid) efflux or intracellular chelation through ligands. Bioaccumulation and biomethylation have been suggested as the key detoxification mechanisms in microbes existing in Cd and As polluted areas (Su *et al.,* 2011; Singh *et al.,* 2015). Therefore, to study the molecular mechanism involved in metal(loid) detoxification, it is prerequisite to investigate the metal(loid) accumulation in *L. bicolor* and *H. cylindrosporum*, when exposed to increasing concentrations of Cd and As. Both fungi were stressed with different concentrations of Cd and As for 48 hours followed by their washing and digestion

with nitric acid/perchloric acid. The metal(loid) content in the fungal biomass was measured using the atomic absorption spectroscopy.

With increase in external metal(loid) concentration, the metal(loid) accumulation in both *L. bicolor* and *H. cylindrosporum* increased (Figure 4.3). When exposed to Cd stress, the metal uptake in *L. bicolor* increased up to 9 µM Cd stress and decreased thereafter. The metal accumulation of 0.224 µg/mg dry mycelium was observed at 3 µM Cd stress followed by 0.784 µg/mg at 6 µM and 0.869 µg/mg at 9 µM. Further, increasing the metal concentration became lethal causing the fungus to stop growing and thus reducing the metal uptake to 0.615 µg/mg at 12 µM and 0.396 µg/mg at 15 µM. Similar observations were made in case of *H. cylindrosporum*, where the metal uptake increased till 9 µM of Cd stress followed by its decrease at 12 µM and 15 µM (Table 4.3).

Table 4.3: Metal accumulation in *L. bicolor* and *H. cylindrosporum* when exposed to different concentrations of Cd for 48 hours.

Cadmium concentration (µM)	**Cadmium uptake (µg/mg dry mycelium)**	
	L. bicolor	***H. cylindrosporum***
3	0.224±0.0245e	0.314±0.095e
6	0.784±0.0085b	0.649±0.025c
9	0.869±0.0156a	0.946±0.023a
12	0.615±0.0696c	0.745±0.055b
15	0.396±0.0420d	0.490±0.012d

Values (Mean±SD) sharing a common letter within the column are not significantly different at $P<0.05$ (n=3)

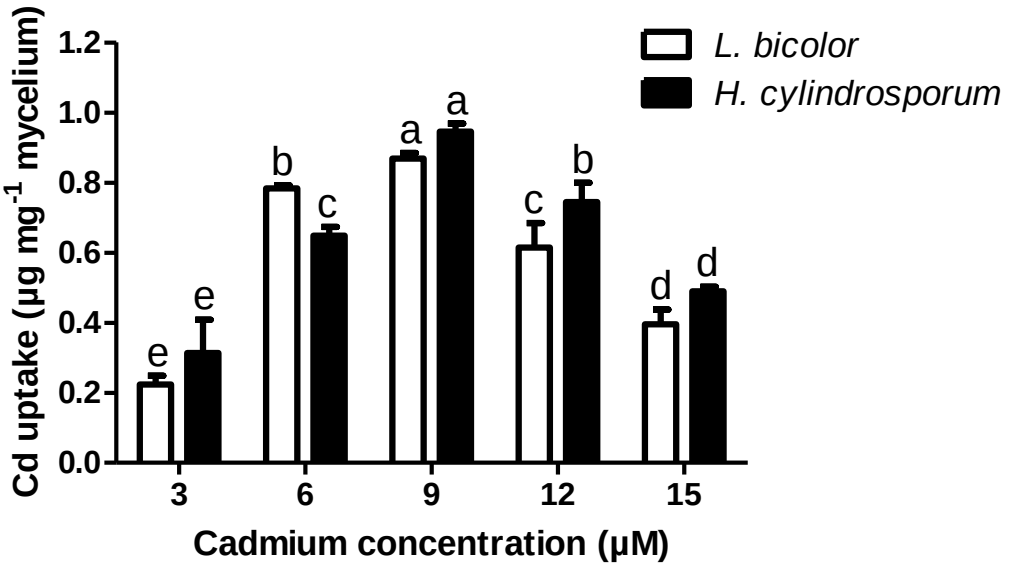

Figure 4.3: The metal accumulation in *L. bicolor* and *H. cylindrosporum* when exposed to different concentrations of Cd. Values sharing a common letter within the fungal strain are not significantly different at $P<0.05$ (n = 3).

In case of As, the metal accumulation in both fungi increased as a function of external As concentration (Figure 4.4). In *L. bicolor*, the As content of 0.07 µg/mg was observed at 3 mM stress, which further increased to 0.137 µg/mg at 6 mM, 0.46 µg/mg at 9 mM, 0.52 µg/mg at 12 mM and 0.667 µg/mg at 15 mM. Similar observations were made in case of *H. cylindrosporum*, where 0.6 µg/mg of As was accumulated when fungus was exposed to 3 mM of external As. The accumulation further increased to 0.21 µg/mg at 6 mM, 0.45 µg/mg at 9 mM, 0.52 µg/mg at 12 mM and 0.76 µg/mg at 15 mM of external As stress (Table 4.4).

Table 4.4: Metal(loid) accumulation in *L. bicolor* and *H. cylindrosporum* when exposed to different concentrations of As for 48 hours.

Arsenic concentration (mM)	**Arsenic uptake (µg/mg dry mycelium)**	
	L. bicolor	***H. cylindrosporum***
3	0.0710±0.0089e	0.06±0.012e
6	0.1370±0.0394d	0.21±0.068d
9	0.4600±0.0520c	0.45±0.031c

12	0.5200±0.0458b	0.52±0.096b
15	0.6670±0.0258a	0.76±0.021a

Values (Mean±SD) sharing a common letter within the column are not significantly different at P<0.05 (n=3).

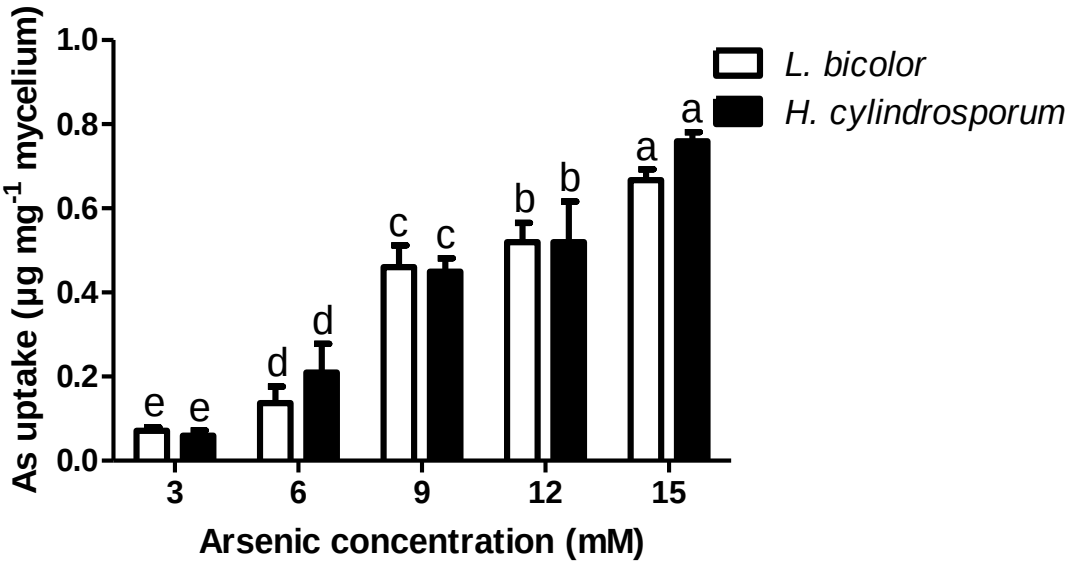

Figure 4.4: Metal(loid) accumulation in *L. bicolor* and *H. cylindrosporum* when exposed to different concentrations of As. Values sharing a common letter within the fungal strain are not significantly different at P<0.05 (n = 3).

Previous studies reveal that different ECM fungi responds differently to various toxic metals. In a study by Širić *et al.,* (2017), ten ECM fungi when exposed to Pb, Cd and Hg, showed different metal accumulation patterns. *Macrolepiota procera* was more efficient in accumulating Pb, whereas *Agaricus campestris* was efficient in accumulating Cd and *Boletus edulis* was efficient in accumulating Hg (Širić *et al.,* 2017). *Agaricus macrosporus* accumulated Cd (Melgar *et al.,* 2016) and *Pisolithus albus* accumulated Cd and Cu (Reddy *et al.,* 2016). The increase in As accumulation has also been reported in *Aspergillus niger* (Mukherjee *et al.,* 2010), *Serpula himantioides* and *Trametes versicolor* (Adeyemi, 2009). Borovička *et al.,* (2019) also reported high accumulation of Cd in *Cystoderma carcharias* isolated from smelter-polluted sites.

Both *L. bicolor* and *H. cylindrosporum* substantially accumulated both Cd and As when exposed to different concentrations. The observation throws light on the fact that both *L. bicolor* and *H. cylindrosporum* accumulate Cd and As inside their cellular bodies and are tolerant to them at a wide range. Therefore, there might be some internal mechanisms contributing to their sequestration and detoxification.

4.3 Total GSH production in response to Cd and As

The role of glutathione in Cd and As tolerance has been reported in many plants, mammals, yeast and fungi (Ilyas and Rehman, 2015; Bianucci *et al.,* 2017). The comparative proteomic analysis of As induced differentially expressed proteins in rice plant revealed that glutathione played a central role under As stress (Ahsan *et al.,* 2008). Therefore, for better understanding the molecular response of *L. bicolor* and *H. cylindrosporum* to Cd and As, total glutathione produced in response to each stress was recorded.

Total GSH produced by both *L. bicolor* and *H. cylindrosporum* when exposed to different concentrations of Cd and As was measured using the enzymatic recycling method (Rahman *et al.,* 2006). The readings were recorded as mM of glutathione produced per 100 mg of mycelium. The amount of glutathione produced by both fungi increased with increase in external metal(loid) stress.

A linear increase in GSH production was recorded when both fungi were exposed to increasing concentrations of Cd (Figure 4.5). *L. bicolor* when exposed to 10 µM Cd, produced 0.573 mM of GSH i.e., almost 6.36 times more than the GSH produced by mycelium without stress. The proportion increased as the external Cd concentration was increased. At 20 µM Cd, the GSH production increased by 9.8 times which increased to 13.8 times at 30 µM and 15.9 times at 40 µM. Similarly, in *H. cylindrosporum,* 10 µM Cd stress resulted in 3 times increase in GSH production as compared to the control. When the stress increased to 20 µM, the GSH production increased 6.55 times, which was further elevated to 7.23 times at 30 µM and 7.34 times at 40 µM of external Cd (Table 4.5).

Table 4.5: Total GSH production in *L. bicolor* and *H. cylindrosporum* when exposed to increasing concentrations of Cd for 48 hours. The amount of GSH produced is recorded as mM of GSH per 100 mg of mycelium.

Cadmium Concentration (µM)	**Total GSH (mM/100 mg mycelium)**	
	L. bicolor	***H. cylindrosporum***
0	0.090±0.011e	0.115±0.025c
10	0.573±0.089d	0.346±0.059b
20	0.882±0.065c	0.754±0.031a
30	1.244±0.148b	0.832±0.041a
40	1.436±0.126a	0.845±0.055a

Values (Mean±SD) sharing a common letter within the column are not significantly different at P<0.05 (n=3).

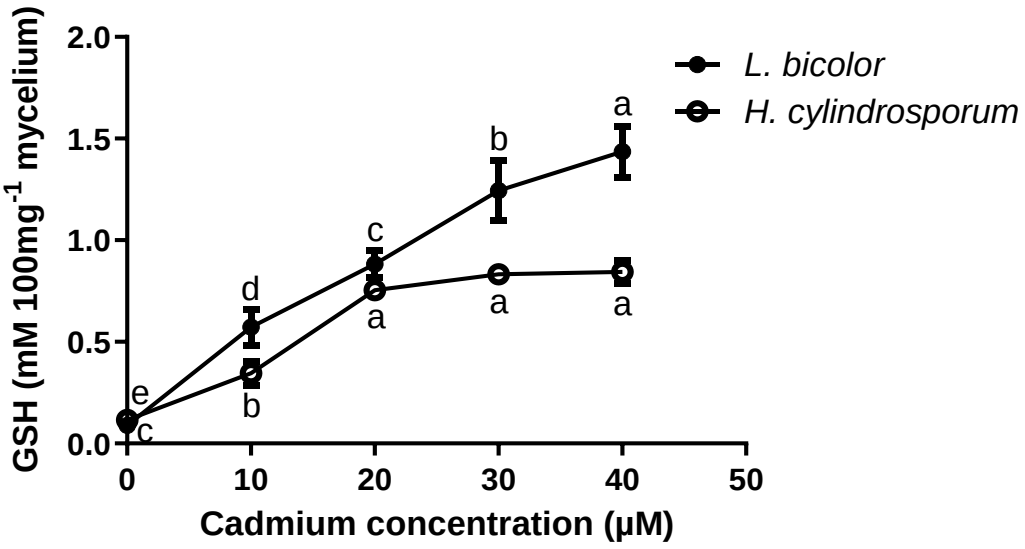

Figure 4.5: Total glutathione production in *L. bicolor* and *H. cylindrosporum* when exposed to Cd stress for 48 hours. Values plotted are mM of GSH produced per 100 mg of liquid nitrogen crushed stressed fungi. Values sharing a common letter within the fungal strain are not significantly different at P<0.05 (n = 3).

Similar observations were made when both fungi were exposed to increasing concentrations of As (Figure 4.6). When *L. bicolor* was exposed to 3 mM of external As, the total GSH content increased by 5.07 times. Further, increasing the As concentration to 6 mM, the GSH concentration increased to 10.64 times followed by 12.27 times increase at 9 mM As. Increasing the As stress to 12 mM and 15 mM, sparingly increased the GSH concentration in *L. bicolor*. In *H. cylindrosporum*, at 3 mM As stress, the GSH production was increased by 5.23 times. At 6 mM As, the GSH production was 10.48 times more than the control which was further increased to 11.30 and 12.19 times at 9 mM and 12 mM As respectively. Further, increasing the As stress to 15 mM did not increased the GSH production in *L. bicolor* (Table 4.6).

Table 4.6: Total GSH production in *L. bicolor* and *H. cylindrosporum* when exposed to increasing concentrations of As for 48 hours. The amount of GSH produced is recorded as mM of GSH per 100 mg of liquid nitrogen crushed mycelium.

Arsenic Concentration (mM)	**Total GSH (mM/100 mg mycelium)**	
	L. bicolor	***H. cylindrosporum***
0	0.122±0.056c	0.119±0.022c
3	0.619±0.047b	0.623±0.097b
6	1.299±0.082a	1.248±0.078a
9	1.498±0.041a	1.345±0.105a
12	1.518±0.091a	1.451±0.075a
15	1.583±0.054a	1.467±0.062a

Values (Mean±SD) sharing a common letter within the column are not significantly different at $P<0.05$ (n=3).

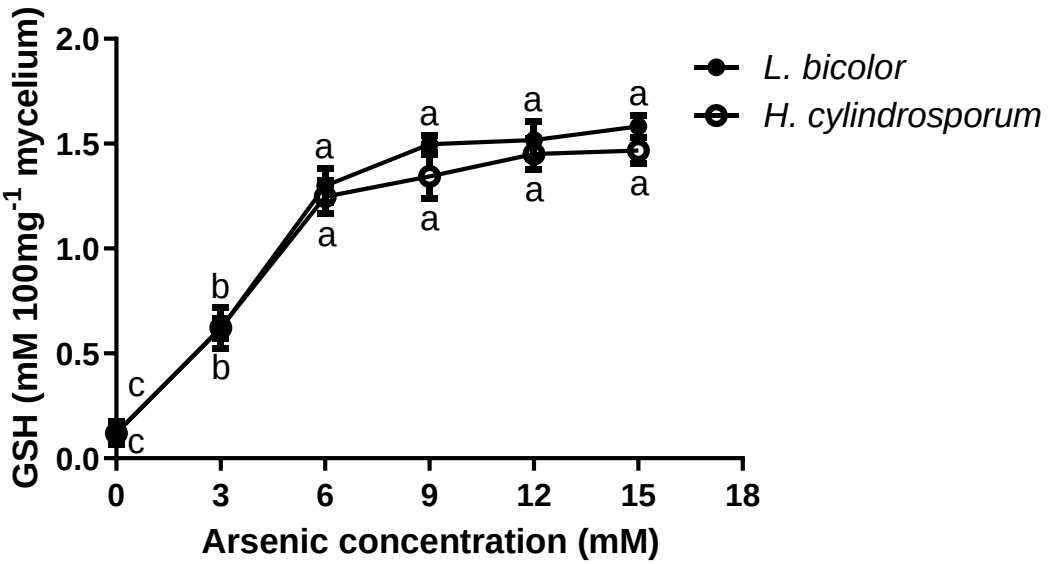

Figure 4.6: Total glutathione production in *L. bicolor* and *H. cylindrosporum* when exposed to As stress for 48 hours. Values plotted are mM of GSH produced per 100 mg of liquid nitrogen crushed stressed fungi. Values sharing a common letter within the fungal strain are not significantly different at $P<0.05$ (n = 3).

The amount of GSH produced in ECM fungi is directly proportional to the external metal(loid) stress. GSH production increases with increase in external metal(loid) stress. The amount of glutathione produced by *L. bicolor* (1.44 nmol/mg; 1.58 nmol/mg) and *H. cylindrosporum* (0.84 nmol/mg, 1.47 nmol/mg) in response to Cd and As, respectively are quite comparable to that of *Paxillus involutus* where 1.2 nmol/mg GSH was produced when stressed with 64 µM Cd (Courbot *et al.,* 2004) and *P. chrysosporium* where 2.5 nmol/mg GSH was produced at 162 µM Cd (Xu *et al.,* 2016).

When exposed to intracellular Cd and As, glutathione provides a dual protection mechanism. It acts both as an antioxidant and as a metal(loid) scavenger. As an antioxidant, glutathione reduces the free radicals generated by Cd and As stress, thus, neutralizing their harmful effects and itself gets oxidized to GSSG (Davison *et al.,* 2003). Glutathione also reduces pentavalent As to trivalent As (Muñiz Ortiz *et al.,* 2009). Both trivalent As and Cd are sulfhydryl reactive metals having high affinity for the (-SH) group of glutathione (Delalande *et al.,* 2010). They bind glutathione forming As-$(GSH)_3$ and Cd-$(GSH)_2$ complex, which actively gets transported to vacuoles through the ABC transporters (Klein *et al.,* 2002; Adamis *et al.,* 2007; Leslie, 2012; Outten *et al.,* 2017). The metal-GSH conjugate has been identified in various mammals, plants

and fungi, when exposed to heavy metals (Pickering *et al.,* 2000; Cánovas *et al.,* 2004; Thomas, 2009; Verbruggen *et al.,* 2009). However, it is worth noting that the ABC proteins serve as metal(loid) transporters only when metal(loid) is complexed with the thiol group (Zhao *et al.,* 2009). Therefore, when exposed to Cd and As, the active glutathione present inside the cell gets immediately utilized, leading to the induction in glutathione biosynthesis pathway (Davison *et al.,* 2003; Xu *et al.,* 2014).

The increase in glutathione production in response to Cd has been reported in plants (Semane *et al.,* 2007; Yadav, 2010; Garg and Aggarwal, 2011; Liang *et al.,* 2016; Xu *et al.,* 2020), mammals (Zhou *et al.,* 2019; Del Águila-Vargas *et al.,* 2020), yeast (Adamis *et al.,* 2007; Pluskal *et al.,* 2016;) and few fungi, *Paxillus involutus, Phanerochaete chrysosporium* (Courbot *et al.,* 2004; Xu *et al.,* 2016). However, in case of As, the studies are limited to few plants like *Arabidopsis thaliana*, *Nicotiana tabacum* (Degola *et al.,* 2015; Aborode *et al.,* 2016), mammals (Muñiz Ortiz *et al.,* 2009) and yeast, *Candida tropicalis, Saccharomyces cerevisiae* (Thorsen *et al.,* 2007; 2012; Ilyas and Rehman, 2016). A remarkable 2.7-fold increase in intracellular GSH concentration was observed in *Candida tropicalis* when exposed to As and 2-fold increase under Cd stress (Ilyas and Rehman, 2016). However, the study is still fragmentary in ECM systems. To our knowledge till date no data is available on studying the response of ECM fungi to As stress and to provide the molecular insight into the glutathione biosynthesis pathway in response to As stress. The present study clearly indicates the prompt increase in glutathione production in both *L. bicolor* and *H. cylindrosporum* when stressed with external Cd and As.

4.4 Enzyme activity of γ-GCS and GS in response to metal(loid) stress

Glutathione biosynthesis is a two steps reaction mediated by two ATP dependent enzymes, γ-glutamylcysteine synthetase (γ-GCS) and glutathione synthetase (GS). The function of both enzymes (γ-GCS and GS) isolated from ECM fungi, *L. bicolor* (Lbγ-GCS and LbGS) and *H. cylindrosporum* (Hcγ-GCS and HcGS) in Cd and As tolerance has been corroborated by monitoring their enzyme activity in response to heavy metals stress. Since both γ-GCS and GS are ATP dependent enzymes, they liberate one molecule of inorganic phosphate by converting ATP to ADP, every-time they catalyze the synthesis of γ-glutamylcysteine and glutathione, respectively. Therefore, the amount of inorganic phosphate released per minute per mg of protein is directly proportional to the enzyme activity of γ-GCS and GS.

When exposed to increasing concentrations of Cd, the activity of all the four enzymes Lbγ-GCS, LbGS, Hcγ-GCS and HcGS increased (Figure 4.7, Figure 4.8). At the initial Cd stress of 10 µM, the activity of both Lbγ-GCS and Hcγ-GCS increased by 3 folds (0.768 µmol and 0.745 µmol of Pi released per mg protein per min) as compared to the control (0.260 µmol and 0.246 µmol of Pi released per mg protein per min), whereas the activity of LbGS and HcGS increased by 2.2 and 1.77 folds, respectively. Increasing the Cd concentration to 20 µM, increased the enzyme activity of Lbγ-GCS by 3.13 folds and that of Hcγ-GCS by 3.62 folds, whereas the activity of LbGS and HcGS was increased by 2.7 folds as compared to control. Further, increasing the Cd stress to 30 µM, escalated the enzyme activity of Lbγ-GCS by 3.3 folds and that of Hcγ-GCS by 3.9 folds, whereas the activity of LbGS and HcGS was increased by 2.9 and 3.5 folds respectively. At 40 µM Cd, the enzyme activity of Lbγ-GCS and Hcγ-GCS was increased by 3.8 and 4.3 folds respectively whereas that of LbGS and HcGS was increased by 3.1 and 3.58 folds respectively (Table 4.7, Table 4.8).

Table 4.7: Effect of different concentrations of Cd on the activity of Lbγ-GCS and LbGS in ECM fungus *L. bicolor*. The activity was measured as the amount of inorganic phosphorous released by the enzymes using ATP per mg of isolated protein per minute.

Cadmium concentration (µM)	**Pi (µmol/mg protein/min)**	
	Lbγ-GCS	**LbGS**
0	0.260±0.023c	0.30±0.011d
10	0.768±0.8088b	0.68±0.045c
20	0.814±0.079b	0.82±0.034b
30	0.849±0.074b	0.86±0.053b
40	0.981±0.164a	0.94±0.195a

Values (Mean±SD) sharing a common letter within the column are not significantly different at $P<0.05$ (n=3).

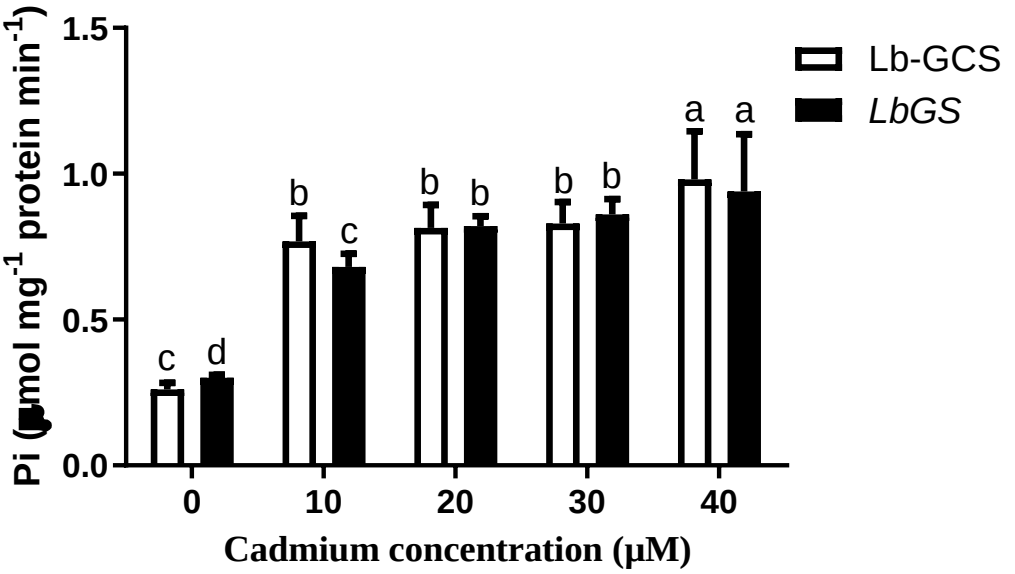

Figure 4.7: Effect of different concentrations of Cd on the activity of Lbγ-GCS and LbGS in ECM fungus *L. bicolor*. The activity was measured as the amount of inorganic phosphorous released by the enzymes using ATP per mg of isolated protein per minute. Values sharing a common letter within the enzyme are not significantly different at P<0.05. Error bars are ± SD.

Table 4.8: Effect of different concentrations of Cd on the activity of Hcγ-GCS and HcGS in ECM fungus *H. cylindrosporum*. The activity was measured as the amount of inorganic phosphorous released by the enzymes using ATP per mg of isolated protein per minute.

Cadmium concentration (µM)	**Enzyme activity Pi (µmol/mg protein/min)**	
	Hcγ-GCS	**HcGS**
0	0.246±0.031e	0.255±0.054d
10	0.745±0.088d	0.451±0.095c
20	0.890±0.077c	0.687±0.078b
30	0.960±0.085b	0.893±0.051a
40	1.065±0.096a	0.915±0.036a

Values (Mean±SD) sharing a common letter within the column are not significantly different at P<0.05.

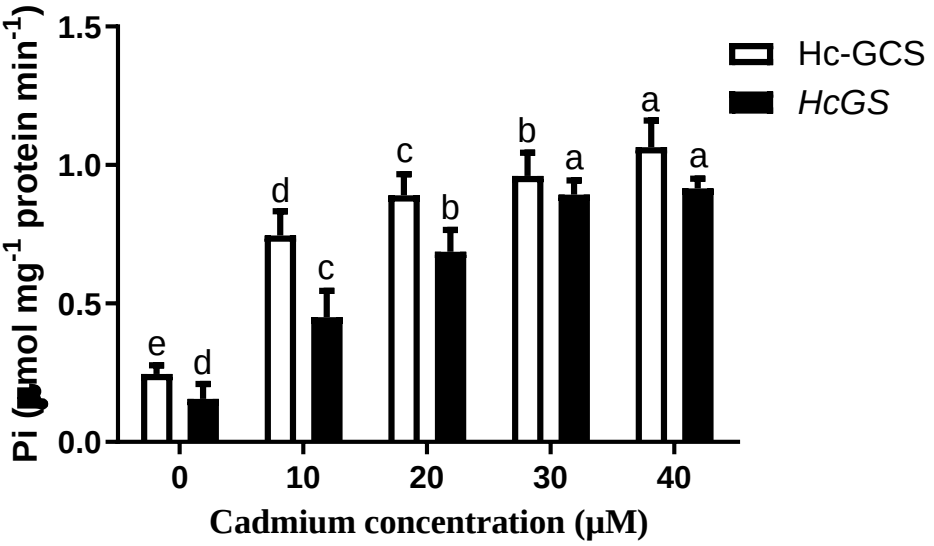

Figure 4.8: Effect of different concentrations of Cd on the activity of Hcγ-GCS and HcGS in ECM fungus *H. cylindrosporum*. The activity was measured as the amount of inorganic phosphorous released by the enzymes using ATP per mg of isolated protein per minute. Values sharing a common letter within the enzyme are not significantly different at $P<0.05$ (n = 3). Error bars are ± SD.

Similar observations were made when both *L. bicolor* and *H. cylindrosporum* were subjected to As stress. The activity of both enzymes, Lbγ-GCS, Hcγ-GCS, LbGS and HcGS increased in response to the external As stress (Figure 4.9, Figure 4.10). When the mycelium was stressed with 5 mM of As, the activity of Lbγ-GCS was increased by 2 folds (0.34 to 0.68 µmol of Pi released per mg protein per min) and that of Hcγ-GCS was increased by 3 folds (0.30 to 0.88 µmol of Pi released per mg protein per min). The enzyme activity of LbGS and HcGS was also reported to be increased by 2.4 and 2.78 times respectively. Further, increasing the As stress to 10 mM, also increased the enzyme activity of Lbγ-GCS, Hcγ-GCS, LbGS and HcGS by 2.3, 3, 2.8 and 3 folds respectively. The pattern continued even at 20 mM of As stress when the activity of Lbγ-GCS, Hcγ-GCS, LbGS and HcGS increased by 2.8 folds, 3.9 folds, 4.1 folds and 4.2 folds respectively (Table 4.9, Table 4.10).

Table 4.9: Effect of different concentrations of As on the activity of Lbγ-GCS and LbGS in ECM fungus *L. bicolor*. The activity was measured as the amount of inorganic phosphorous released by the enzymes using ATP per mg of isolated protein per minute.

Arsenic Concentration (mM)	Pi (µmol/mg protein/min)	
	Lbγ-GCS	LbGS
0	0.34±0.011e	0.24±0.018e
5	0.68±0.056d	0.59±0.022d
10	0.79±0.060c	0.68±0.045c
15	0.85±0.057b	0.87±0.059b
20	0.97±0.089a	0.99±0.094a

Values (Mean±SD) sharing a common letter within the column are not significantly different at P<0.05 (n=3).

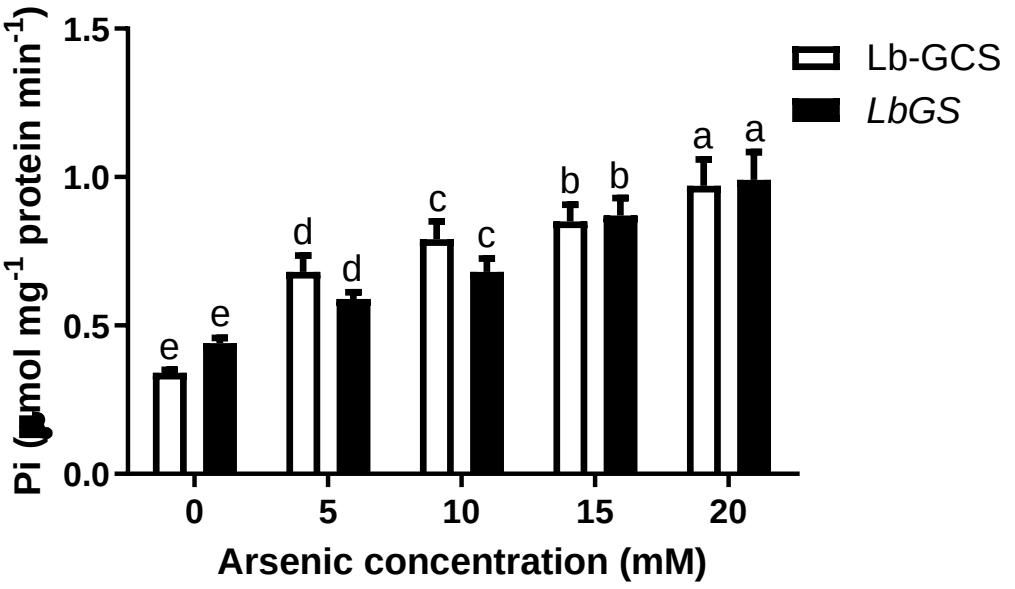

Figure 4.9: Effect of different concentrations of As on the activity of Lbγ-GCS and LbGS in ECM fungus *L. bicolor*. The activity was measured as the amount of inorganic phosphorous released by the enzymes using ATP per mg of isolated protein per minute. Values sharing a common letter within the enzyme are not significantly different at P<0.05 (n = 3). Error bars are ± SD.

Table 4.10: Effect of different concentrations of As on the activity of Hcγ-GCS and HcGS in ECM fungus *H. cylindrosporum*. The activity was measured as the amount of inorganic phosphorous released by the enzymes using ATP per mg of isolated protein per minute.

Arsenic concentration (mM)	Enzyme activity Pi (µmol/mg protein/min)	
	Hcγ-GCS	**HcGS**
0	0.30±0.035d	0.28±0.021d
5	0.88±0.052c	0.78±0.042c
10	0.92±0.022c	0.84±0.033c
15	1.01±0.041b	0.98±0.068b
20	1.18±0.095a	1.15±0.085a

Values (Mean±SD) sharing a common letter within the column are not significantly different at P<0.05.

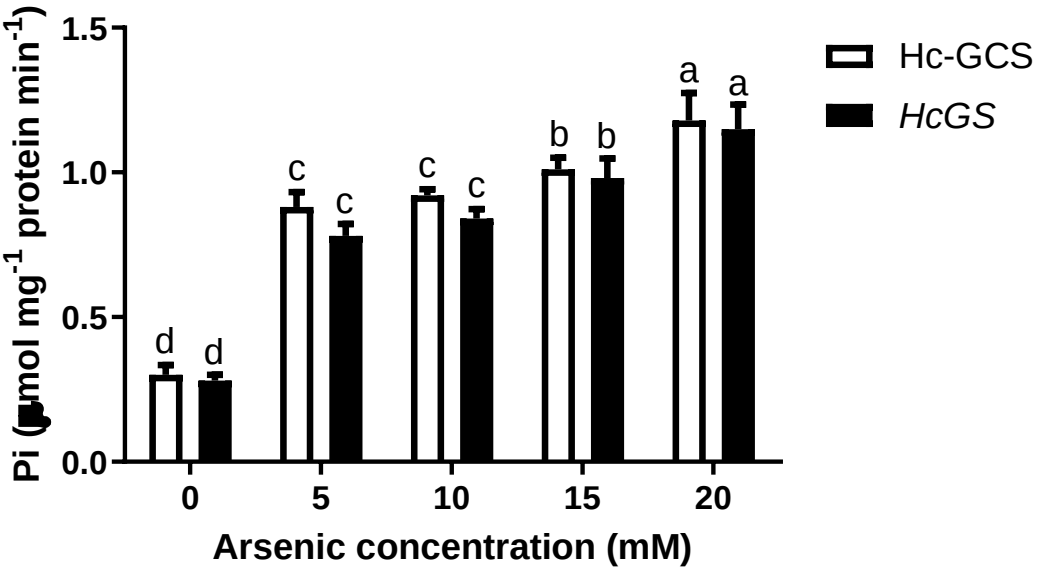

Figure 4.10 Effect of different concentrations of As on the activity of Hcγ-GCS and HcGS in ECM fungus *H. cylindrosporum*. The activity was measured as the amount of inorganic phosphorous released by the enzymes using ATP per mg of isolated protein per minute. Values sharing a common letter within the enzyme are not significantly different at P<0.05(n = 3). Error bars are ± SD.

The increase in enzyme activity of γ-GCS and GS has also been reported in various mammals (Shukla *et al.,* 2000; Wang *et al.,* 2008) and plants (Pickering *et al.,* 2000; Dhankher *et al.,* 2002), *S. agalactiae* (Janowiak and Griffith, 2005). *Brassica chinensis* when exposed to 10 µM Cd stress elevated the γ-GCS activity from 0.7 µmol Pi/mg protein/min to 1.6 µmol Pi/mg protein/min (Lou *et al.,* 2017).

4.5 Total RNA isolation from ECM fungi

The total RNA was isolated *L. bicolor* and *H. cylindrosporum* using the QIAzol reagent. The isolated RNA was then analyzed on 1% agarose gel electrophoresis at 70 V and then visualized on U.V transilluminator (Figure 4.11). The isolated RNA was also quantified by using nanodrop and the purity was checked by calculating its absorbance at 260/280 nm (Table 4.11).

Table 4.11: Concentration of total RNA isolated from *L. bicolor* and *H. cylindrosporum*.

Fungus	Total RNA concentration (ng/µl)	$A_{260/280}$
L. bicolor	1586	2.05
H. cylindrosporum	1441	2.07

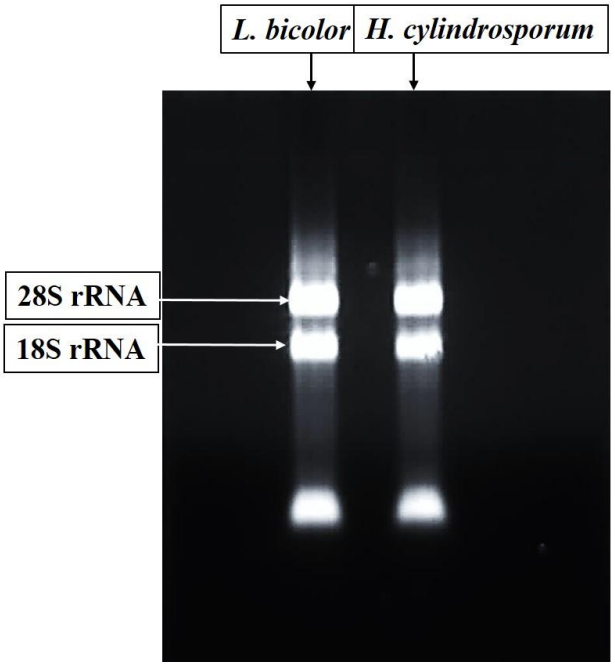

Figure 4.11: Total RNA isolated form *L. bicolor* and *H. cylindrosporum*, highlighting 28S rRNA and 18S rRNA.

4.6 cDNA synthesis and amplification of *γ-GCS* and *GS* genes

Five µg total RNA was used for cDNA synthesis. Both cDNAs were examined by amplifying the housekeeping actin and tubulin genes for both *L. bicolor* and *H. cylindrosporum* using the primers mentioned in Table 3.1 (Figure 4.12). The cDNA so obtained was used as template for amplification of both *γ-GCS* (*Lbγ-GCS* and *Hcγ-GCS*) and *GS* (*LbGS* and *Hc*GS) genes (Figure 4.13). The amplified genes visualized on 1.0% agarose gel were of approximate sizes: *Lbγ-GCS*- 1.9 Kb; *LbGS*- 1.6 Kb, *Hcγ-GCS*: 2.0 Kb and *HcGS*-1.6 Kb (Figure 4.13).

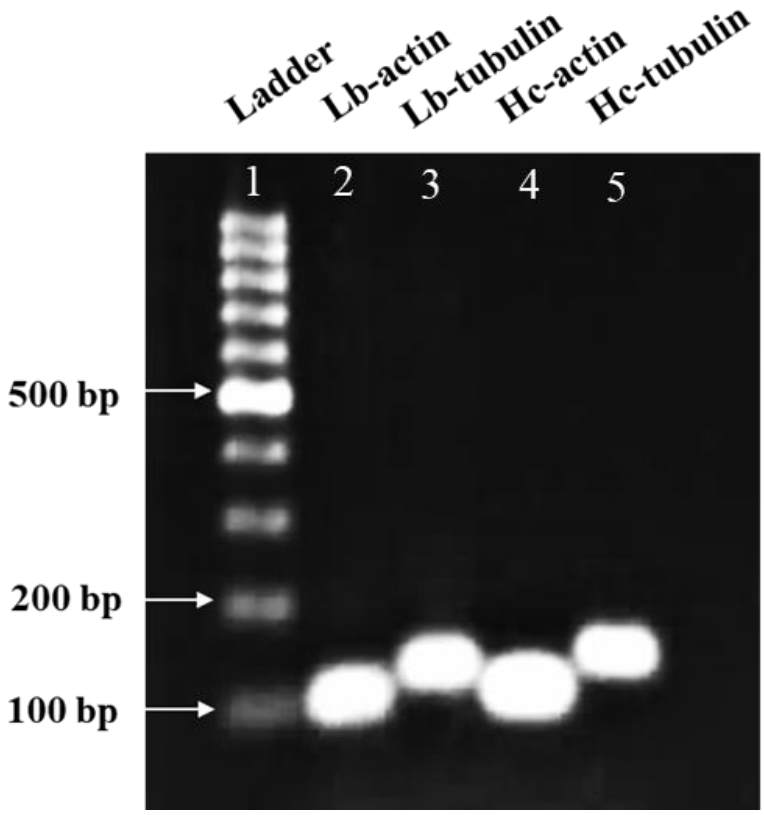

Figure 4.12: Amplification of α-actin and β-tubulin genes form the cDNA of *L. bicolor* (*Lb-actin* (Lane 2) and *Lb-tubulin* (Lane 3)) and *H. cylindrosporum* (*Hc-actin* (Lane 4) and *Hc-tubulin* (Lane 5)) using the gene specific primers. Lane 1: 100 bp ladder.

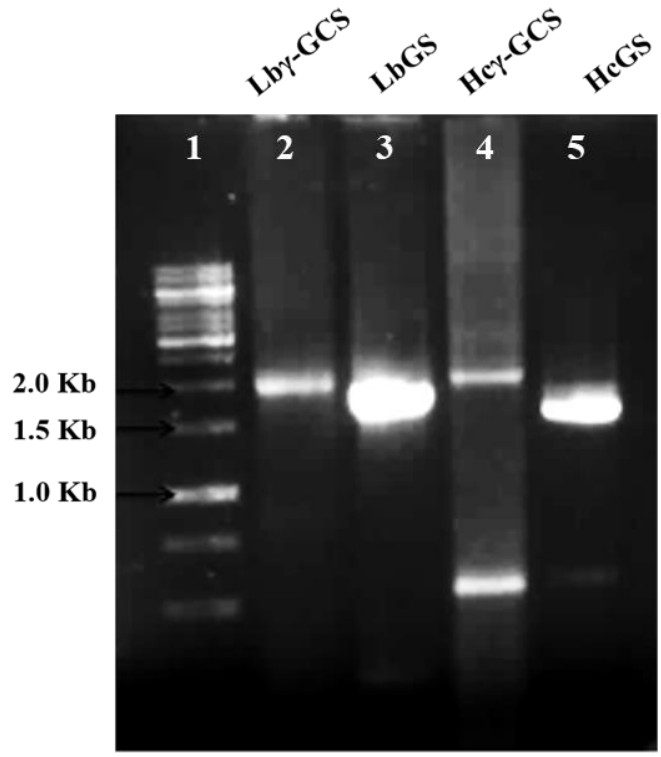

Figure 4.13: Amplification of *γ-GCS* and *GS* genes form *L. bicolor* (*Lbγ-GCS* (Lane 2) and *LbGS* (Lane 3)) and *H. cylindrosporum* (*Hcγ-GCS* (Lane 4) and *HcGS* (Lane 5)) using their respective cDNAs and gene specific primers. Lane 1: 1Kb ladder.

4.7 Gene sequencing and sequence analysis

The amplified genes were ligated into pMD-20 vector using "The Mighty TA-cloning Kit" (Takara, CA, USA) and sequenced. The inserts in the plasmids were sequenced by chain termination method (Sanger *et al.,* 1977) using Applied Biosystems automatic sequencer (DNA sequencing facility, Department of Biochemistry, South campus, Delhi university, New Delhi, India). The coding sequences so obtained were of length: *Lbγ-GCS*: 1854 bp, *LbGS:* 1593 bp, *Hcγ-GCS*: 2040 bp and *HcGS*: 1641 bp. All the four sequences were submitted to NCBI database under the accession numbers: MF766455, MF766456, MH892339, MK617301 for *Lbγ-GCS*, *LbGS*, *Hcγ-GCS* and *HcGS*, respectively (Appendix-II). The sequences so obtained were further characterized using various bioinformatic tools.

4.7.1 *Lbγ-GCS*

The *Lbγ-GCS* cDNA contained 1854 bp ORF encoding 617 amino acids (Figure 4.14) with predicted molecular mass of 70.56 kDa and pI 5.31.

atg ggc ctc ttg tat ctc ggc act cct ttg cct tgg gat gaa gct aaa aaa tat gct gac

M G L L Y L G T P L P W D E A K K Y A D

cat gtg cga acc cat gga atc act cag ttc ctt cat att tgg gat cga ttg aag gac aga

H V R T H G I T Q F L H I W D R L K D R

act ggc gac gag cta cta tgg ggc gat gag atc gaa tat atg gtg gta gcc ttc gat gaa

T G D E L L W G D E I E Y M V V A F D E

caa gaa aag agt gca aaa ctc tca ttg agg caa acg gaa att ctc gca aaa ctc agt gat

Q E K S A K L S L R Q T E I L A K L S D

ata gtc cat gac att tct gct ggc tta cgt tac gag gtc gac aca ttg atg tta tta aca

I V H D I S A G L R Y E V D T L M L L T

gat cat ttc agc gtc gct gtg ccg aac ttc cac cca gag tat gga cga tac atg ctt gag

D H F S V A V P N F H P E Y G R Y M L E

tct acc cca ggt tct ccc tac act ggc tat att caa gat ctc ttg tcg gtt gag tgc aat

S T P G S P Y T G Y I Q D L L S V E C N

atg cga tac aga cga gct ctt gct cgt aaa cat ctc aag ccg aat gaa ata cct ttg acc

M R Y R R A L A R K H L K P N E I P L T

ttt act tcg ttt cct ctt ttg ggt gtg caa ggt cac ttt acg gaa cca tat ttc aat cca

F T S F P L L G V Q G H F T E P Y F N P

aac gat gct gtt tca agt cat agc ttt ttt tta ccc gaa gaa atc acg aat ccg cat gca

N D A V S S H S F F L P E E I T N P H A

cgc ttc ccc acc ctt acg gcc aat atc agg agt cga aga ggt tcc aag gtt gca atc aat

R F P T L T A N I R S R R G S K V A I N

tta cca att ttt ttc gac gag aag acc cct cgt cca ttt gtc gac cca acg att ccc tgg

L P I F F D E K T P R P F V D P T I P W

gac cgc aac att tac aaa gaa gat tca gat gcg aag aat ggt gca gcc ctc ccc gat cac

D R N I Y K E D S D A K N G A A L P D H

att tat ctt gac gcg atg ggc ttt gga atg gga tgt tgc tgc ctt caa ctc act ttc cag

I Y L D A M G F G M G C C C L Q L T F Q

gca tgc aat gtt tct gac gcc agg cgc ctg tat gat ggt ttg att cct att ggc cct atc

A C N V S D A R R L Y D G L I P I G P I

ttg ctg gcg ttg acg ggg gcc agc cct ata tgg cgt ggg tac ctc gct gat gtg gat tgt

L L A L T G A S P I W R G Y L A D V D C

cga tgg aac gtt att gcc ggc agt gtc gat gat cgc acg gag gaa gag cgt ggc ttg aag

R W N V I A G S V D D R T E E E R G L K

gtg att cca aag tct cgt tac gac agc gtt gat ctg tac atc tca aac gat gga ttc aac

V I P K S R Y D S V D L Y I S N D G F N

cga ccc gag tat aac gat aac tat ttg ccg tac gac gaa tct att tac gac cgc ctg cgc

R P E Y N D N Y L P Y D E S I Y D R L R

gca cat gga atc gat gat ttg ctc tca aag cac atg tcg cac ctc ttc ata cgc gac cct

A H G I D D L L S K H M S H L F I R D P

ctt gtc gtt ttc tca gaa aca atc aac caa gat gac acg tcc agc agt gat cat ttt gag

L V V F S E T I N Q D D T S S S D H F E

aat ata caa tca acc aac tgg cag act ctc cga ttc aaa ccc cct ccg ccc aac tca ccg

N I Q S T N W Q T L R F K P P P P N S P

att ggc tgg cgt gtt gaa ttt cgt agc atg gag gtt caa ata acg gat ttc gag aat gcc

I G W R V E F R S M E V Q I T D F E N A

gct ttc gct gta ttt gtt gtg ctg ctt tca cgc gct atc ctt agt ttc aat ctt aat ctc

A F A V F V V L L S R A I L S F N L N L

tac att cca ata tcg aag gtc gac gag aat atg gcc acg gct cag cgt agg gac gcc gct

Y I P I S K V D E N M A T A Q R R D A A

gcg aaa gcg aag ttc cat ttt aga aaa gac gta tac cca ccc ggc cga agt gga gcg tca

A K A K F H F R K D V Y P P G R S G A S

agc gag gag tat gag gaa atg agc atg gac gaa atc atc aat ggc aag ggg gac aat ttc

S E E Y E E M S M D E I I N G K G D N F

cca gga ctc ctg cga ctt att tat gcc tat att gac acg tta gat atc gag ccg cga gag

P G L L R L I Y A Y I D T L D I E P R E

```
ttg gca aag gta ggg agt tat cta gat ctc att aga cgg cgg gcc aac gga tct ctc ata
 L   A   K   V   G   S   Y   L   D   L   I   R   R   R   A   N   G   S   L   I
act cct gca act tgg atc aga aat ttc gta cgg tcg cac ccg act tat aaa cac gac tcg
 T   P   A   T   W   I   R   N   F   V   R   S   H   P   T   Y   K   H   D   S
gtt gtt tca cag gaa att aat tac gat cta ttg ctg gcc ata gat gaa atg tga
 V   V   S   Q   E   I   N   Y   D   L   L   L   A   I   D   E   M   -
```

Figure 4.14: The nucleotide (lower case) and deduced amino acid (upper case) sequence of *Lbγ-GCS* cDNA.

The protein was then identified by looking for its homologous sequences in NCBI database using BLASTX tool (https://blast.ncbi.nlm.nih.gov/Blast.cgi). The data revealed that *Lbγ-GCS* showed homology with glutamate-cysteine ligase or γ-glutamylcysteine synthetase proteins isolated from various basidiomycetes as summarized in Table 4.12 and Figure 4.15. The homologous sequences so obtained were then selected for multiple sequence analysis so as to identify the conserved domains.

Description	Max Score	Total Score	Query Cover	E value	Per. Ident	Accession
gamma glutamylcysteine synthetase [Laccaria bicolor S238N-H82]	1196	1196	99%	0.0	100.00%	XP_001877753.1
hypothetical protein K443DRAFT_127343 [Laccaria amethystina LaAM-08-1]	972	1137	97%	0.0	95.38%	KIK09975.1
glutamate-cysteine ligase catalytic subunit [Crucibulum laeve]	960	960	99%	0.0	76.31%	TFK44334.1
glutamate-cysteine ligase catalytic subunit [Dendrothele bispora CBS 962.96]	959	959	99%	0.0	76.70%	THV05006.1
Glutamate--cysteine ligase [Termitomyces sp. J132]	956	956	99%	0.0	78.96%	KNZ72047.1
hypothetical protein GALMADRAFT_268698 [Galerina marginata CBS 339.88]	953	953	99%	0.0	75.75%	KDR75147.1
glutamate-cysteine ligase catalytic subunit [Coprinopsis cinerea okayama7#130]	951	951	99%	0.0	73.16%	XP_001830305.2
glutamate-cysteine ligase [Moniliophthora roreri MCA 2997]	949	949	99%	0.0	75.54%	ESK96650.1
Glutamate--cysteine ligase [Leucoagaricus sp. SymC.cos]	946	946	99%	0.0	79.01%	KXN90986.1
hypothetical protein M413DRAFT_441977 [Hebeloma cylindrosporum h7]	943	943	99%	0.0	74.55%	KIM45296.1
hypothetical protein CVT24_003415 [Panaeolus cyanescens]	939	939	99%	0.0	74.62%	PPQ98707.1
glutamate-cysteine ligase catalytic subunit [Coprinopsis marcescibilis]	939	939	99%	0.0	73.53%	TFK26502.1
hypothetical protein CVT25_014505 [Psilocybe cyanescens]	936	936	99%	0.0	74.29%	PPQ68044.1
hypothetical protein EST38_g4569 [Psathyrella aberdarensis]	935	935	99%	0.0	74.14%	RXW21302.1
gamma glutamylcysteine synthetase [Agaricus bisporus var. bisporus H97]	930	930	99%	0.0	73.57%	XP_006460756.1
hypothetical protein AGABI1DRAFT_71066 [Agaricus bisporus var. burnettii JB137-S8]	929	929	99%	0.0	73.57%	XP_007328121.1
glutamate-cysteine ligase catalytic subunit [Cylindrobasidium torrendii FP15055 ss-10]	925	925	99%	0.0	72.55%	KIY74336.1

Figure 4.15: BLASTX analysis showing protein sequences homologous to *Lbγ-GCS*

Table 4.12: Homologous sequences retrieved from BLASTX analysis of *Lbγ-GCS* for multiple sequence analysis.

S. No	Organism	Accession no.	Gene	Percent Identity
1	*Laccaria amethystina*	KIK09975	glutamate-cysteine ligase	95.38%
2	*Crucibulum leave*	TFK44334	glutamate-cysteine ligase	76.31%
3	*Dendrothele bispora*	THV05006	glutamate-cysteine ligase	76.70%
4	*Agaricus bisporus*	XP_006460756	glutamylcysteine synthetase	73.57%
5	*Gymnopus luxurians*	KIK67150	glutamate-cysteine ligase	71.67%
6	*H. cylindrosporum*	MH892339	glutamylcysteine synthetase	67.56%
7	*Serendipita indica*	CCA66352	glutamate-cysteine ligase	62.04%
8	*Fistulina hepatica*	KIY44398	glutamate-cysteine ligase	67.21%
9	*Rhodotorula sp.*	KWU43246	glutamate-cysteine ligase	59.58%
10	*Paxillus rubicundulus*	KIK91183	glutamate-cysteine ligase	70.51%

The multiple sequence alignment of these sequences revealed many domains that were found to be conserved in most of the basidiomycetes. The amino acid sequence from 261-617 have been identified as the conserved catalytic unit of γ-GCS family. The amino acids 22-71 have been identified as the conserved S1 RNA binding site. Most of the predicted ATP binding sites in Lbγ-GCS sequence were also found to be highly conserved (Table 4.13). The unique ATP binding sites including amino acid sequence 110-124 "FHPEYGRYMLE", 199-217 "HARFPTLTANIRSRRGSKV", 261-276 "IYLDAMGFGMGCCCLQ" and 311-325 "WRGYLADVDCRWNVI" were found to be conserved throughout the nine selected basidiomycetes (Table 4.13).

N-glycosylation motifs in Lbγ-GCS were also predicted at amino acid 283 (NVSD) and 576 (NGSL) along with cAMP phosphorylation site RRGS at amino acid 212. These sites were also found to be highly conserved among basidiomycetes.

Table 4.13: Multiple sequence alignment of Lbγ-GCS with other basidiomycetes indicating conserved domains identified for their potential role in ATP binding. The *L. bicolor* γ-GCS gene MF766455 were aligned with different basidiomycetes, *Rhodotorula* KWU43246, *Serendipita indica* CCA66352, *Daedalea quercina* EPT04524, *Paxillus rubicundulus* KIK91183, *Pisolithus microcarpus* KIK27695, *Fistulina hepatica* KIY44398, *Gymnopus luxurians* KIK67150, *Agaricus bisporus* XP_006460756, *Hebeloma cylindrosporum* KIM45296 and the conserved ATP domains were identified.

γ-GCS Conserved ATP binding domains				
Organism	**110-124**	**199-217**	**261-276**	**311-325**
Rhodotorula	FHPEYGRYMLESTPG	HVRFPTLTANIRRRR*GS*KV	IYMDAMGFGMGCCCLQ	FRGWLSDVDCRWDVI
S. indica	FHPEYGRFMLESTPG	HARFPTLTANIRKRR*GS*KV	IYMDAMGFGMGCCCLQ	WRGYIADVDCRWNVI
D. quercina	FHPEYGRFMLESTPG	HARFPTLTANIRRRR*GS*KV	IYMDAMGFGMGCCCLQ	WRGYIADVDCRWDVI
P. rubicundulus	FHPEYGRYMLESTPG	HARFPTLTANIRTRRRSKV	IYMDAMGFGMGCCCLQ	WRGYLADVDCRWNVI
P. microcarpus	FHPEYGRYMLESTPG	HARFPTLTSNIRSRRESKV	IYMDAMGFGMGCCCLQ	WRGYLADVDCRWNVI
F. hepatica	FHPEYGRYMLESTPG	HIRFPTLTANIRRRR*GS*KV	IYMDAMGFGMGCCCLQ	WRGYISDVDCRWNVI
G. luxurians	FHPEYGRYMLESTPG	HARFPTLTANIRSRR*GS*KV	IYMDAMGFGMGCCCLQ	WRGYLSDVDCRWNVV
A. bisporus	FHPEYGRYMLESTPG	HARFPTLTANIRTRR*GS*KV	VYMDAMGFGMGCCCLQ	WRGYLADVDCRWNVV
L. bicolor	FHPEYGRYMLESTPG	HARFPTLTANIRSRR*GS*KV	IYLDAMGFGMGCCCLQ	WRGYLADVDCRWNVI
H. cylindrosporum	FHPEYGRYMLESTPG	HARFPTLTANIRRRR*GS*KV	IYLDAMGFGMGCCCLQ	WRGYLADVDCRWNVI
	********:********	* ******:*** ** ***	:*:**************	:**:::******:*:

The evolutionary history of *Lbγ-GCS* was studied by comparing various *γ-GCS* genes through the maximum parsimony phylogenetic tree constructed using MEGA software. The tree formed three different classes of γ-GCS proteins clustered separately as basidiomycetes, mucoromycetes and ascomycetes showing their common evolutionary history (Figure 4.16).

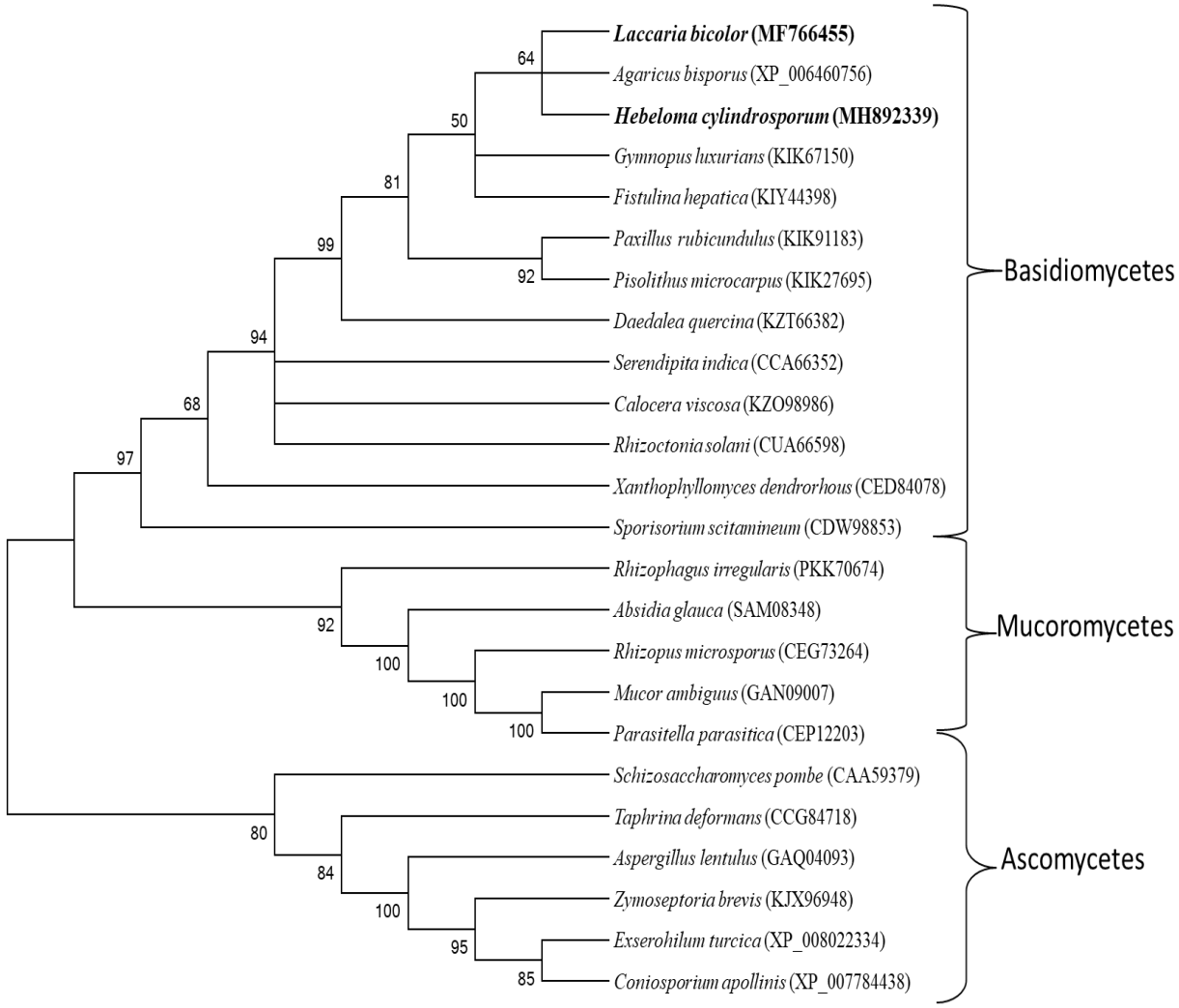

Figure 4.16: The maximum parsimony tree for Lbγ-GCs and Hcγ-GCS constructed using MEGA 7. γ-GCS enzymes from three different classes of fungi were clustered separately into basidiomycetes, mucoromycetes and ascomycetes, showing their common evolutionary history. The tree was constructed using 1000 bootstrap test. Accession number of each protein has been mentioned in parenthesis.

Further, the Lbγ-GCS protein was predicted as a transmembrane protein with three domains: amino acids 1 to 459 as non-cytoplasmic domain, 460 to 482 as transmembrane domain and 483 to 617 as cytoplasmic domain (Phobius prediction: http://phobius.sbc.su.se/cgi-bin/predict.pl).The secondary structure prediction revealed that the protein Lbγ-GCS can be classified as a mixed protein composed of 34.5% helix, 57.7% loops and 7.78% strands (Figure 4.17).

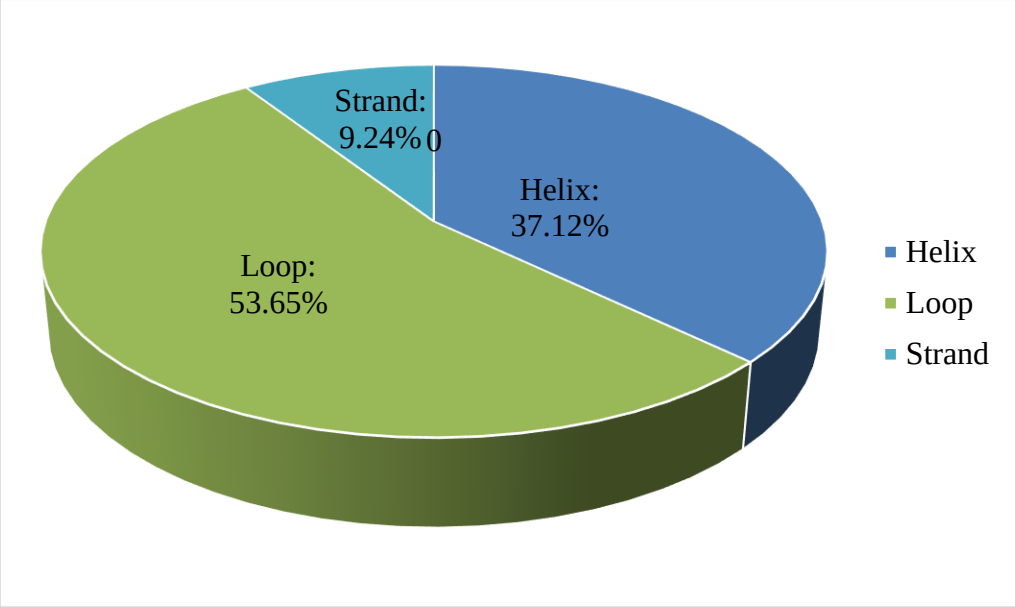

Figure 4.17: Secondary structure composition of Lbγ-GCS indicating percentage proportion of helix, loops and strands involved in protein confirmation.

4.7.2 *LbGS*

The sequence analysis of *LbGS* cDNA reveals that the gene ORF consists of 1593 base pairs encoding 531 amino acids protein (Figure 4.18) with the predicted molecular weight of 58.9 kDa and pI 5.59.

```
atg aca aca gaa ccg ttt gac atc cct agc tgg ccc cca tca ctc aca ccc att caa ttg
 M   T   T   E   P   F   D   I   P   S   W   P   P   S   L   T   P   I   Q   L
gag gcg ttg aca cta tat gcc act aca tat gca cta tcc cac ggg cta ctt tat ctt ctg
 E   A   L   T   L   Y   A   T   T   Y   A   L   S   H   G   L   L   Y   L   L
cca ggc cca cta cca gca ata tca agc gcg gcc atc cac gct cct ttc tct ctt ttc cca
 P   G   P   L   P   A   I   S   S   A   A   I   H   A   P   F   S   L   F   P
tca cct ttt cct cga aag ctt ttt gaa gct gga cag aga atc cag agg act tac aat gtc
 S   P   F   P   R   K   L   F   E   A   G   Q   R   I   Q   R   T   Y   N   V
ctt tac gcg aga atc gcg atg gat gaa gag ttt ttg gat agg gtc atg gga aca gag acg
 L   Y   A   R   I   A   M   D   E   E   F   L   D   R   V   M   G   T   E   T
ggt gtg ggc aag gtc gat gac ttt att ggg caa ttg tgg act ggg tgg aag cag ttg agg
 G   V   G   K   V   D   D   F   I   G   Q   L   W   T   G   W   K   Q   L   R
```

gat gag ggg ctt gct cag cac ctg cat ctt ggc cta ttt cgt tcc gac tac ctt ctc cac

D E G L A Q H L H L G L F R S D Y L L H

acc cta ccg aac cag cca ctt tct atc aag cag gtc gag ttc aat acc atc tcc gtg tcg

T L P N Q P L S I K Q V E F N T I S V S

ttc gca tgt cta tcc caa aag ata tct gag ctt cat agg tac ctc tta tcg tca acg caa

F A C L S Q K I S E L H R Y L L S S T Q

tat tac aac tgc tct gca caa ctc aaa ccc gag aac ttg ccg cca aac cgg acc atc tct

Y Y N C S A Q L K P E N L P P N R T I S

ggc cta gca gaa ggg ctt gca gta ggg cat aaa gcc tat aac gtt caa ggg tct cga ata

G L A E G L A V G H K A Y N V Q G S R I

cta ttt gtc gtt caa ccc gga gaa cgc aat gtt ttt gac caa cga tgg ctc gag tac gag

L F V V Q P G E R N V F D Q R W L E Y E

ctg ctg gaa cag cat tcc atc cac att gtc cgc caa act ttt gaa gaa ctc gct cat tcg

L L E Q H S I H I V R Q T F E E L A H S

gcc atc gta gac ccg cac aca tcc atc ctc cgc gtt tcc tgc tct acg gac att cac cca

A I V D P H T S I L R V S C S T D I H P

tca ggt tcc att gag ata tcc aca gta tat tat cgc gcg ggg tat atg ccc aat gaa tac

S G S I E I S T V Y Y R A G Y M P N E Y

cca acc cct gcg cac tac gcc act cgt ttc ctt ctc gaa cga tcc aaa gca atc aaa tgt

P T P A H Y A T R F L L E R S K A I K C

cct act atc gcc ctc cag cta gct ggt ggg aaa aaa gtt caa gag gtg cta gcc caa cct

P T I A L Q L A G G K K V Q E V L A Q P

ggt gtt ctt gag cgc ttc tta cgc gac gag aaa agg tat ggc aaa gac ggc ata ttc tcc

G V L E R F L R D E K R Y G K D G I F S

gaa cac gaa gtc aac gag cta cgg tcc acc ttc atg gcc atg tgg ggt tta gac gtg ggg

E H E V N E L R S T F M A M W G L D V G

gaa aat ctc cta acg gcc gat tat gac tcc atc gca tct gga aaa gag gga ttc gga gtc

E N L L T A D Y D S I A S G K E G F G V

```
ctc aaa gct aga gat gac gca cat gcg tta gtg ctc aag ccg cag agg gaa ggt ggc ggc
 L   K   A   R   D   D   A   H   A   L   V   L   K   P   Q   R   E   G   G   G
aat aac gtc tat aaa gaa gca att cct gct ttc ctg gac agc cta ccg ccg caa gaa cgc
 N   N   V   Y   K   E   A   I   P   A   F   L   D   S   L   P   P   Q   E   R
cag gct tgg att gcg atg gaa ttg att gtc cct cct gag ggc act gga aac tac ctc gtt
 Q   A   W   I   A   M   E   L   I   V   P   P   E   G   T   G   N   Y   L   V
cgc gcc gga aca att cag gcg gag agt caa gca gcg gcg aag gct gat gtc gtc agc gag
 R   A   G   T   I   Q   A   E   S   Q   A   A   A   K   A   D   V   V   S   E
ctt ggg atc ttt ggc tat gcg ctg ttt ggg ggc gag tct agg gaa atc aaa gaa aag gaa
 L   G   I   F   G   Y   A   L   F   G   G   E   S   R   E   I   K   E   K   E
gtc gga tgg tta gtc aga acc aag ggg aag gac agc gat gag ggt ggc gtt gca act gga
 V   G   W   L   V   R   T   K   G   K   D   S   D   E   G   G   V   A   T   G
ttt tct gtg tta gat tcg ctg ctg ttg gtg gat
 F   S   V   L   D   S   L   L   L   V   D
```

Figure 4.18: The nucleotide (lower case) and deduced amino acid (upper case) sequence of *LbGS* cDNA.

The nucleotide sequence so obtained was analyzed by using BLASTX (https://blast.ncbi.nlm.nih.gov/Blast.cgi) program for homologous protein sequences. The data revealed that LbGS showed homology with glutathione synthetase proteins isolated from various basidiomycetes (Figure 4.19). LbGS showed 95.86% homology with the glutathione synthetase gene isolate from *Laccaria amethystine* followed by 75.90% homology with *Crucibulum laeve* and 74.62% with *Hebeloma cylindrosporum* (Table 4.14).

Description	Max Score	Total Score	Query Cover	E value	Per. Ident	Accession
glutathione synthetase [Laccaria bicolor]	1066	1066	100%	0.0	100.00%	AVX28162.1
hypothetical protein K443DRAFT_674506 [Laccaria amethystina LaAM-08-1]	1031	1031	100%	0.0	95.86%	KIK06216.1
glutathione synthase [Crucibulum laeve]	815	815	99%	0.0	75.90%	TFK40501.1
hypothetical protein GALMADRAFT_220520 [Galerina marginata CBS 339.88]	799	799	99%	0.0	75.24%	KDR82535.1
hypothetical protein M413DRAFT_69714 [Hebeloma cylindrosporum h7]	786	786	98%	0.0	74.62%	KIM43057.1
hypothetical protein CVT26_000911 [Gymnopilus dilepis]	781	781	99%	0.0	73.62%	PPQ65891.1
glutathione synthetase [Hebeloma cylindrosporum]	771	771	98%	0.0	72.01%	QDD67718.1
hypothetical protein CVT25_010739 [Psilocybe cyanescens]	769	769	96%	0.0	73.74%	PPQ78736.1
hypothetical protein CVT24_004470 [Panaeolus cyanescens]	743	743	99%	0.0	70.24%	PPQ63610.1
Glutathione synthetase [Termitomyces sp. J132]	736	736	98%	0.0	70.34%	KNZ73319.1
Glutathione synthetase [Hypsizygus marmoreus]	716	716	93%	0.0	70.36%	RDB14681.1
hypothetical protein M378DRAFT_72735 [Amanita muscaria Koide BX008]	683	683	99%	0.0	64.90%	KIL67776.1
hypothetical protein AGABI1DRAFT_59176 [Agaricus bisporus var. burnettii JB137-S8]	679	679	99%	0.0	64.73%	XP_007329727.1
hypothetical protein AGABI2DRAFT_224431 [Agaricus bisporus var. bisporus H97]	679	679	99%	0.0	64.92%	XP_006462797.1
hypothetical protein AMATHDRAFT_78746 [Amanita thiersii Skay4041]	673	673	99%	0.0	63.19%	PFH54004.1
glutathione synthase [Obba rivulosa]	661	661	98%	0.0	64.46%	OCH89932.1
Glutathione synthetase large chain [Sparassis crispa]	657	657	98%	0.0	64.14%	XP_027616359.1

Figure 4.19: BLASTX analysis showing protein sequences homologous to *LbGS*

Table 4.14: Homologous sequences retrieved from BLASTX analysis of *LbGS* for multiple sequence analysis.

S. No.	Organism	Accession No.	Gene	Percent identity
1	*Laccaria amethystina*	KIK06216	Glutathione synthetase	95.86%
2	*Crucibulum leave*	TFK40501	Glutathione synthase	75.90%
3	*Hebeloma cylindrosporum*	MK617301	Glutathione synthetase	74.62%
4	*Hypsizygus marmoreus*	RDB14681	Glutathione synthetase	70.36%
5	*Termitomyces sp*	KNZ73319	Glutathione synthetase	70.34%
6	*Obba rivulosa*	OCH89932	Glutathione synthetase	64.46%
7	*Lentinula edodes*	GAW08968	Glutathione synthase	62.74%
8	*Armillaria gallica*	PBK99639	Glutathione synthase	61.33%
9	*Coniophora puteana*	XP_007768870	Glutathione synthase	57.75%

The multiple sequence alignment of these homologous sequences revealed various conserved domains. Amino acids 15-530 have been identified as the conserved eukaryotic glutathione synthetase catalytic domain with ATP binding domain. A conserved glycine rich domain 'LVLKPQREGGGNNVYK' involved in ATP binding has been observed between 410 and

425 amino acids along with "KQVEFNTISSSF", "LQLAGGKKVQ" and "DEGGVAAGFSVLDS" at amino acid 150-161, 325-334 and 513-526, respectively (Table 4.15). Other predicted ATP binding amino acids E153, K331, Y424, E480, K508, E514 were also found to be conserved throughout 10 selected basidiomycetes. Two N-glycosylation sites in LbGS protein was predicted at amino acid 183 (NCSA) and at 196 (NRTI). Both sites were found to be conserved in GS proteins isolated from different basidiomycetes. Three putative Protein Kinase C phosphorylation sites were also predicted at amino acid site 148 (SIK), 165 (SQK) and 393 (SGK).

Table 4.15: Multiple sequence alignment highlighting conserved domains in LbGS genes identified for their potential role in ATP binding. The LbGS protein MF766456 was aligned with *Coniophora puteana* XP_007768870, *Lentinula edodes* GAW08968, *Obba rivulosa* OCH89932, *Armillaria gallica* PBK99639, *Laccaria amethystina* KIK06216, *Crucibulum leave* TFK40501, *Hebeloma cylindrosporum* MK617301, *Hypsizygus marmoreus* RDB14681, *Termitomyces* KNZ73319 and the conserved ATP binding domains were identified.

Organism	**LbGS - ATP binding domains**			
Coniophora puteana	KQVEFNTISSSF	LQLAGGKKVQ	LVLKPQREGGGNNVYK	DEGGVAAGFSVLDS
Lentinula edodes	KQVEFNTISSSF	LQLAGGKKVQ	LVLKPQREGGGNNVYK	NEGGVATGFSVLDS
Obba rivulosa	KQVEFNTISSSF	LQLAGGKKVQ	LVLKPQREGGGNNIYK	NEGGVAAGFSVLDS
Armillaria gallica	KQVEFNTISSSF	LQLAGGKKVQ	LVLKPQREGGGNNVYK	NEGGIAAGFSVLDS
Laccaria bicolor	KQVEFNTISVSF	LQLAGGKKVQ	LVLKPQREGGGNNVYK	DEGGVATGFSVLDS
L. amethystina	KQVEFNTISVSF	LQLAGGKKVQ	LVLKPQREGGGNNVYK	DEGGVATGFSVLDS
C. laeve	KQVEFNTISVSF	LQLAGGKKVQ	LVLKPQREGGGNNVYK	NEGGVATGFSVLDS
H. cylindrosporum	KQVEFNTISVSF	LQLAGGKKVQ	LVLKPQREGGVNNVYK	NEGGVATGFSVLDS
H. marmoreus	KQVEFNTISVSF	LQLAGGKKIQ	LVLKPQREGGGNNIYK	DEGGVATGFSVLDS
Termitomyces	KQVEFNTISVSF	LQLAGGKKIQ	LVLKPQREGGGNNVYK	DEGGVATGFSVLDS
	********* **	********:*	********** **:*:	:***:*:*******

The phylogenetic analysis was performed using maximum parsimony method on the basis of genetic distance of 18 GS proteins from different fungal species using MEGA 7 software. The GS proteins were clustered into three groups- basidiomycetes, mucoromycetes and ascomycetes based upon their evolutionary relations (Figure 4.20). Seven GS proteins from basidiomycetes clustered themselves using the same branch with LbGS being most related to *Laccaria amethystina* GS protein.

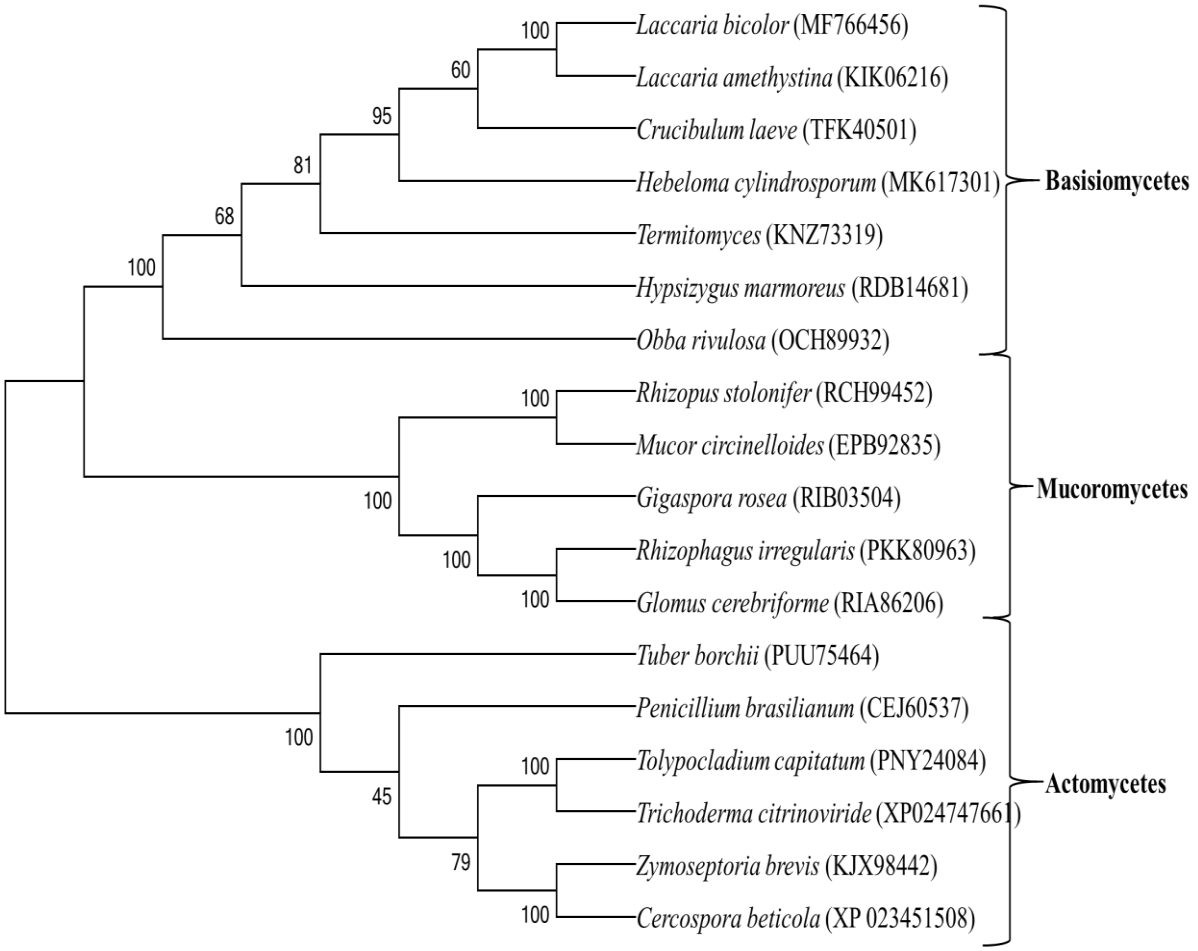

Figure 4.20: The maximum parsimony tree for LbGC and HcGS constructed using MEGA 7. Glutathione synthetase enzymes from three different classes of fungi were clustered separately into basidiomycetes, mucoromycetes and ascomycetes, showing their common evolutionary history. The tree was constructed using 1000 bootstrap test. Accession number of each protein has been mentioned in parenthesis.

The secondary structure prediction of the LbGS protein revealed that the protein is a non-cytoplasmic protein with aminoacids 77-85 being transmembrane domain. The protein is

predicted as a mixed composition with 38.04% helix, 14.88% strands and 47.08% loops (Figure 4.21).

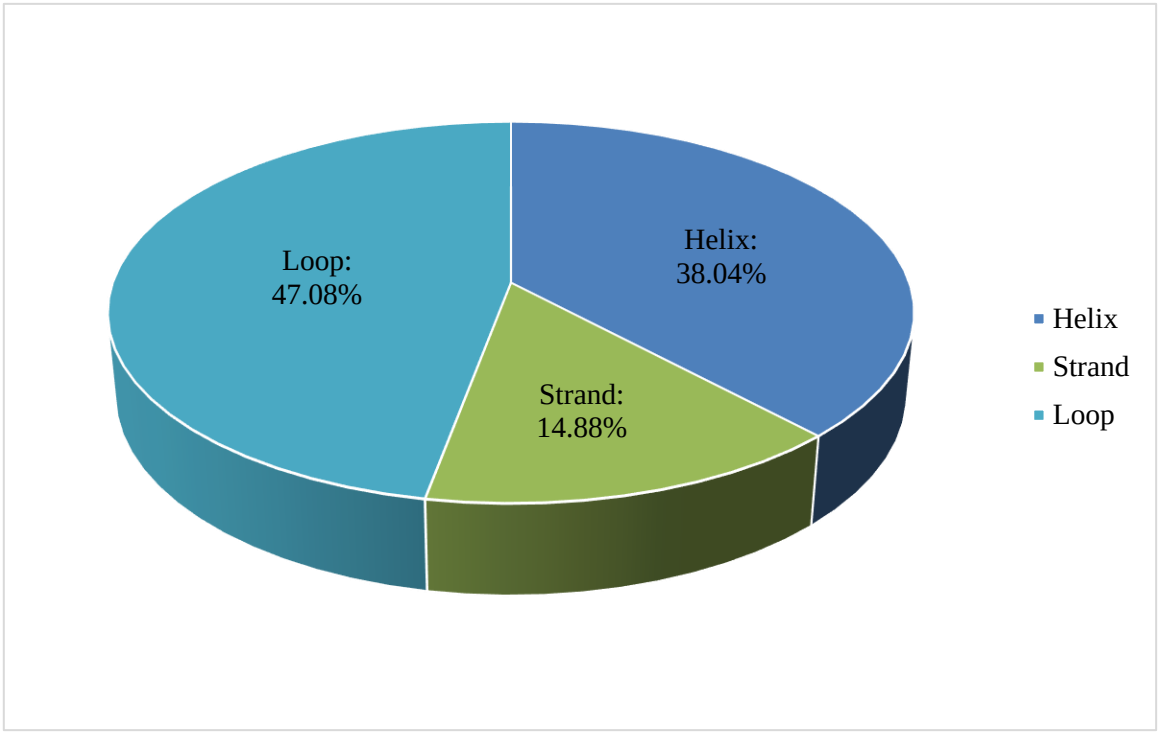

Figure 4.21: Secondary structure composition of LbGS indicating percentage proportion of helix, loops and strands involved in protein confirmation.

4.7.3 *Hcγ-GCS*:

The full-length cDNA sequences of *Hcγ-GCS* consists of 2040 bp long open reading frame encoding 679 amino acids (Figure 4.22) with predicted molecular weight of 78.09 kDa and pI of 6.6.

```
atg ggt ctt ctc tat ctc gga act ccg ttg gtc tgg gac gag gct aaa aag tac gcc gat
 M   G   L   L   Y   L   G   T   P   L   V   W   D   E   A   K   K   Y   A   D
cat gta cga agt cat ggg atc acc caa ttt ctt cat ata tgg gac cgc cta aag gac agg
 H   V   R   S   H   G   I   T   Q   F   L   H   I   W   D   R   L   K   D   R
caa ggt gat gaa ctg ctc tgg ggt gac gag att gaa tat atg gtg gtc tcc ttc gat gct
 Q   G   D   E   L   L   W   G   D   E   I   E   Y   M   V   V   S   F   D   A
aag gaa aaa aat gca aag tta tcc ttg cga cag caa gag att ttg gaa aaa att aac tct
```

K E K N A K L S L R Q Q E I L E K I N S

gcc gtc gac gac atc tcc gct ggg gct cca aac aac gtt tgt gta ccc aag ttc cac cca

A V D D I S A G A P N N V C V P K F H P

gag tat ggc cgc tac atg ctc gaa tct acc ccc ggc gcc ccg tat acc ggt tct att cct

E Y G R Y M L E S T P G A P Y T G S I P

gat ctg ttg tcg gtt gaa aat aac atg cga tac agg cga aac ctc gcc cgc aag cat ctc

D L L S V E N N M R Y R R N L A R K H L

aat cct aac gaa ata ccc att aca atc act tcc ttc ccg cga ctg ggc gtt ccg ggc aat

N P N E I P I T I T S F P R L G V P G N

tta cgg aac cct tct atg atc cat gcg acg ccg tct cca gcc aca gtc tat ttc tat cag

L R N P S M I H A T P S P A T V Y F Y Q

aag aaa tca caa acc cgc acg cac gtt tcc cga ccc tgt act gct aat att aga cgg cga

K K S Q T R T H V S R P C T A N I R R R

agg ggg tca aag gtt gcg atc aat ctc ccg att tac ttt gac gaa aaa acg cct cga cct

R G S K V A I N L P I Y F D E K T P R P

ttc att gac ccc act ata cca tgg gat cgt gcg ata tac cca gaa gat tca gag gca aag

F I D P T I P W D R A I Y P E D S E A K

cgt ggg gca gct ttg cct gat cat ata tac ctg gac gct atg ggt ttc ggc atg ggt tgt

R G A A L P D H I Y L D A M G F G M G C

tgc tgt ctt caa tta aca ttc caa gct tgc aac gtt gcc gat gct cgg aga atg tat gat

C C L Q L T F Q A C N V A D A R R M Y D

ggg ttg atc cca atc gga cct ctt ctt ttg gca ttg aca gct gcg agc cct atc tgg agg

G L I P I G P L L L A L T A A S P I W R

gga tac ctc gct gat gtc gac tgt cgt tgg aac gtt atc gca gga agc gtt gac gac cga

G Y L A D V D C R W N V I A G S V D D R

acc gag gaa gaa cgt ggc ttg aaa ccc att gaa aga aag caa ttc cgg acc gaa gtc tcg

T E E E R G L K P I E R K Q F R T E V S

tta cga cag cgt cat ctc tac att tcg gac gat tgg gtt aat cgt cca gaa tat aac gac

L R Q R H L Y I S D D W V N R P E Y N D

aac ccc att acc tta cga cga gaa cat tta caa ccg ttt gcg cac aca cgg cac atc tct

N P I T L R R E H L Q P F A H T R H I S

cac ctt ttc att cgt gac cct ctt gta gtc ttc tcc gag acg ata gat caa gac gac act

H L F I R D P L V V F S E T I D Q D D T

tcc agc agc gat cac ttc gag aat atc caa tcg aca aac tgg caa act ctc cgc ttt aaa

S S S D H F E N I Q S T N W Q T L R F K

ccg cca cca cca aat tca ccg atc gga tgg agg gtt gaa ttc cga tcc atg gag gtt caa

P P P P N S P I G W R V E F R S M E V Q

atg acg gac ttt gag aat gcc gca ttt gcg gtc ttt gtc gtg ctc ctc tct cga gcc atc

M T D F E N A A F A V F V V L L S R A I

ttt gcc ttc aac ctc aat ttt tat atc ccg ata tcc aaa gtc gac gaa aat atg gct agg

F A F N L N F Y I P I S K V D E N M A R

gca cag caa agg gat gct tcg gct tca aag aag ttt ttc ttt aag aag gac gta tat gca

A Q Q R D A S A S K K F F F K K D V Y A

acg ggc cga agt gcg acc atc gag cgc tgc aat caa tcc ttc ggg cgc cag aac acc tcc

T G R S A T I E R C N Q S F G R Q N T S

gcc atg aag tgt acc gcg gaa gaa aga caa aaa atg aag aat tgt ttt cct cct cca cct

A M K C T A E E R Q K M K N C F P P P P

ctt ccc gag aat ggt ttc gca tat cgc ggt cca gta gaa gat gaa tac gaa gaa atg act

L P E N G F A Y R G P V E D E Y E E M T

atg aaa gaa att atg aac gga aag ggc gat aat ttc cct ggt ttg ctt gca ctt gtg gat

M K E I M N G K G D N F P G L L A L V D

gcc tat cta gag acg ctg gaa att gag ctc cgg gat atg gag aag ata cag caa tat cta

A Y L E T L E I E L R D M E K I Q Q Y L

gac ttt gtc cga cgt cgt tct gac gga aga ctc ctg acc cca gcg acg tgg atc cgg aat

D F V R R R S D G R L L T P A T W I R N

ttt gtc acg tct cat cct gac tac aga aag gat tcg gtt gtt tct caa acc atc aac tac

```
 F   V   T   S   H   P   D   Y   R   K   D   S   V   V   S   Q   T   I   N   Y

gat cta tta gta gct gtg gat gaa atc gaa cga ggg gtt cgt cgg gcg cct gat ctt ctt

 D   L   L   V   A   V   D   E   I   E   R   G   V   R   R   A   P   D   L   L

ccg gct gat tac agg ggt gga gac aag gat aca agg gac cct ttg ata ttt att ttt taa

 P   A   D   Y   R   G   G   D   K   D   T   R   D   P   L   I   F   I   F   -
```

Figure 4.22: The nucleotide (lower case) and deduced amino acid (upper case) sequence of *Hcγ-GCS* cDNA.

Hcγ-GCS sequence obtained was then subjected to BLASTX analysis to identify the homologous sequences (Figure 4.23). The putative Hcγ-GCS protein showed maximum homology with most of the basidiomycetes displaying 74%, 71%, 70%, 69% and 68% sequence similarity with the γ-GCS protein sequence form *Crucibulum laeve* (TFK44334) *Coprinopsis cinerea* (XP001830305), *Armillaria gallica* (PBK91420), *Agaricus bisporus* (XP006460756) and *Laccaria bicolor* (XP001877753), respectively (Table 4.16).

	Description	Max Score	Total Score	Query Cover	E value	Per. Ident	Accession
☑	gammaglutamyl cysteine synthetase 1 [Hebeloma cylindrosporum]	1366	1366	99%	0.0	100.00%	AZS52301.1
☑	hypothetical protein M413DRAFT_441977 [Hebeloma cylindrosporum h7]	1083	1083	95%	0.0	86.49%	KIM45296.1
☑	hypothetical protein GALMADRAFT_268698 [Galerina marginata CBS 339.88]	1005	1005	98%	0.0	76.83%	KDR75147.1
☑	hypothetical protein CVT24_003415 [Panaeolus cyanescens]	969	969	98%	0.0	73.06%	PPQ98707.1
☑	glutamate-cysteine ligase catalytic subunit [Crucibulum laeve]	968	968	98%	0.0	74.16%	TFK44334.1
☑	hypothetical protein CVT25_014505 [Psilocybe cyanescens]	953	953	95%	0.0	75.19%	PPQ68044.1
☑	hypothetical protein HYPSUDRAFT_83574 [Hypholoma sublateritium FD-334 SS-4]	945	945	98%	0.0	72.46%	KJA27880.1
☑	LOW QUALITY PROTEIN: hypothetical protein CVT26_003726 [Gymnopilus dilepis]	942	942	98%	0.0	71.55%	PPR07703.1
☑	glutamate-cysteine ligase catalytic subunit [Coprinopsis cinerea okayama7#130]	938	938	98%	0.0	71.01%	XP_001830305.2
☑	glutamate-cysteine ligase catalytic subunit [Dendrothele bispora CBS 962.96]	932	932	98%	0.0	70.93%	THV05006.1
☑	glutamate-cysteine ligase [Moniliophthora roreri MCA 2997]	926	926	98%	0.0	70.40%	ESK96650.1
☑	glutamate-cysteine ligase catalytic subunit [Armillaria gallica]	911	911	98%	0.0	69.60%	PBK91420.1
☑	glutamate-cysteine ligase catalytic subunit [Coprinopsis marcescibilis]	911	911	98%	0.0	68.81%	TFK26502.1
☑	glutamate-cysteine ligase catalytic subunit [Armillaria solidipes]	907	907	98%	0.0	69.44%	PBK73874.1
☑	Glutamate--cysteine ligase [Hypsizygus marmoreus]	905	905	98%	0.0	70.44%	RDB24730.1
☑	probable gamma-glutamylcysteine synthetase [Armillaria ostoyae]	905	905	98%	0.0	69.30%	SJK97449.1
☑	glutamate-cysteine ligase catalytic subunit [Gymnopus androsaceus JB14]	904	904	98%	0.0	68.09%	KAE9411198.1

Figure 4.23: BLASTX analysis showing protein sequences homologous to *Hcγ-GCS*

Table 4.16: Homologous sequences retrieved from BLASTX analysis of *Hcγ-GCS* for multiple sequence analysis.

S.No.	Organism	Accession No.	Gene	Percent identity
1	*Crucibulum leave*	TFK44334	glutamate-cysteine ligase	74.16%
2	*Coprinopsis cinereal*	XP_001830305	glutamate-cysteine ligase	71.01%
3	*Agaricus bisporus*	XP_006460756	gamma-glutamylcysteine synthetase	68.62%
4	*Laccaria bicolor*	XP_001877753	gamma-glutamylcysteine synthetase	67.56%
5	*Gymnopus luxurians*	KIK67150	glutamate-cysteine ligase	66.52%
6	*Daedalea quercina*	KZT66382	glutamate-cysteine ligase	63.85%
7	*Fistulina hepatica*	KIY44398	glutamate-cysteine ligase	62.95%
8	*Serendipita indica*	CCA66352	gamma-glutamylcysteine synthetase	58.50%

The multiple sequence alignment of different homologous sequences revealed many domains that were found to be conserved in many fungi. Amino acids 249–649 were identified as a conserved glutamylcysteine synthetase catalytic subunit and amino acids 26–84 were identified as 30S ribosomal proteinS1 (Table 4.17). Both the sequences were found to be highly conserved.

Most of the predicted ATP binding domains in the primary sequence of Hcγ-GCS protein were found to be conserved. This includes amino acids 188–204 ‘‘HVSRPCTANIRRRRGSK’’, amino acids 249–268 ‘‘IYLDAMGFGMGCCCLQLTFQ’’, amino acids 299–316 ‘‘WRGYLADVDCRWNVIAGS’’ (Table 4.18). N-glycosylation motifs were also predicted at amino acid site 511 (NQSF) and 518 (NTSA) along with the various Protein kinase C (PKC) phosphorylation sites at amino acid 68 (SLR), 217 (TPR), 340 (SLR), 364 (TLR), 416 (TLR), 486 (SKK), 501 (TGR) and 560 (TMK).

Table 4.17: Multiple sequence alignment of various γ-GCS protein sequences isolated from different basidiomycetes indicating conserved 30S ribosomal protein S1 binding site.

30S ribosomal protein S1 Conserved domains	
Organism	**Conserved sequence**
Serendipita indica	GITQLLNIWNRYKARSGDKLLWGDEIEYIVVAFDD
Daedalea quercina	GITQFLNIWDRTKDRCGDELLWGDEIEYFVVSFDN
Hebeloma cylindrosporum	GITQFLHIWDRLKDRQGDELLWGDEIEYMVVSFDA
Fistulina hepatica	GITQFLHTWDRLKDRHGDVLLWGDEIEYMVVSFDK
Gymnopus luxurians	GITQFLHTWDRLKDKNGDELLWGDEIEYMVVYLDD
Laccaria bicolor	GITQFLHIWDRLKDRTGDELLWGDEIEYMVVAFDE
Agaricus bisporus	GITQFLHIWDRLKDRTGDELLWGDEVEYLVISLDD
Crucibulum laeve	GITQFLHIWDRLKDRTGDELLWGDEIEYMVVSFDN
Coprinopsis cinereal	GITQFLHIWDRLKDRSGDELLWGDEVEYMVVSFDN
	:*:*. *:* * : ** ***:**:*: :*

Table 4.18: Multiple sequence alignment of Hcγ-GCS protein with γ-GCS proteins isolated from different basidiomycetes highlighting the conserved ATP and substrate binding domains.

Organism	**Conserved ATP and substrate binding domains**		
S. indica	HARFPTLTANIRKRRGSK	IYMDAMGFGMGCCCLQITFQ	WRGYIADVDCRWNVISGAVDDRT
D. quercina	HARFPTLTANIRRRRGSK	IYLDAMGFGMGCCCLQLTFQ	WRGYIADVDCRWDVISGCVDDRT
H.cylindrosporum	THVSRPCTANIRRRRGSK	IYMDAMGFGMGCCCLQVTFQ	WRGYLADVDCRWNVIAGSVDDRT
F. hepatica	HIRFPTLTANIRRRRGSK	IYMDAMGFGMGCCCLQLTFQ	WRGYISDVDCRWNVIAGSVDDRT
G. luxurians	HARFPTLTANIRSRRGSK	IYMDAMGFGMGCCCLQLTYQ	WRGYLSDVDCRWNVVAGSVDDRT
L. bicolor	HARFPTLTANIRSRRGSK	IYLDAMGFGMGCCCLQLTFQ	WRGYLADVDCRWNVIAGSVDDRT

A. bisporus	HARFPTLTANIRTRRGSK	VYMDAMGFGMGCCCLQLTFQ	WRGYLADVDCRWNVVAGSVDDRT
C. leave	HARFPTLTANIRTRRRSK	IYMDAMGFGMGCCCLQLTFQ	WRGYLADVDCRWNVIAGSVDDRT
C. cinerea	HARFPTLTSNIRSRRESK	IYMDAMGFGMGCCCLQLTFQ	WRGYLADVDCRWNVIAGSVDDRT
	::: ****:*******	*:*:**************:**	****::******:*::*.*****

The evolutionary history of Hcγ-GCS was studied by maximum parsimony phylogenetic tree constructed using MEGA software. The Phylogenetic tree forms three different clusters of basidiomycetes, mucoromycetes and ascomycetes each sharing common evolutionary history (Figure 4.16).

Further, the secondary structure prediction of the Hcγ-GCS protein revealed that the protein is a transmembrane protein with three membrane domains: N-terminal from amino acid 1 to 446 forms a non-cytoplasmic domain; amino acids from 447 to 469 are embedded in the membrane forming a transmembrane domain and at the C-terminal from amino acid 470 to 679 forms a cytoplasmic domain. The structural composition of the protein is mixed with 33.3% helix, 10.2% strands and 56.6% loops (Figure 4.24)

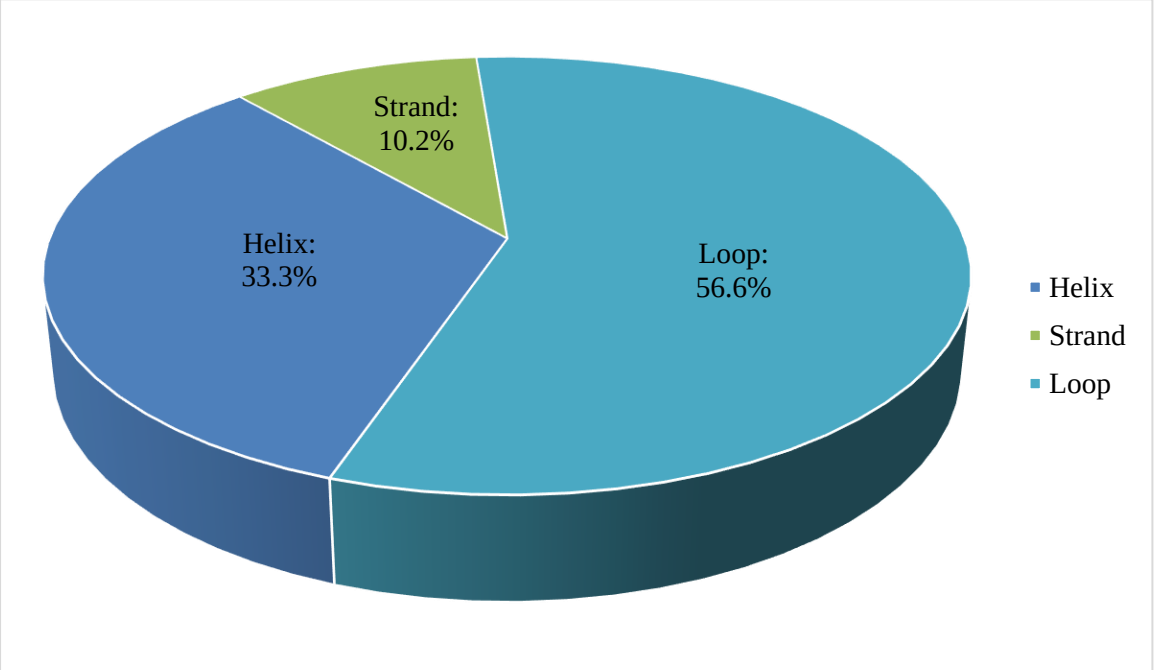

Figure 4.24: Secondary structure composition of Hcγ-GCS protein indicating percentage proportion of helix, loops and strands involved in protein confirmation.

4.7.4 *HcGS*

The full-length cDNA of *HcGS* gene consists of 1641 base pair long open reading frame encoding 546 amino acids (Figure 4.25) with predicted molecular weight 60.46 kDa and pI of 5.39.

```
atg gca tcg act ttc gac ttt gcc agt tgg ccg cca tct ttg acc gtg gac cag ctc gaa
 M   A   S   T   F   D   F   A   S   W   P   P   S   L   T   V   D   Q   L   E
aat ttg acg tta tac gca acg tca tac gcc cta tcg cac ggt gct ttg tat cta cca cca
 N   L   T   L   Y   A   T   S   Y   A   L   S   H   G   A   L   Y   L   P   P
gct gaa cca caa ccg act gtc ccc agc gct gct atc cat gca ccg att tcc ctc ttt cct
 A   E   P   Q   P   T   V   P   S   A   A   I   H   A   P   I   S   L   F   P
tcg cct ttc cct cgt cag ctc tat gaa caa ggc cgc cgg ata caa cgc aca tac aac gtc
 S   P   F   P   R   Q   L   Y   E   Q   G   R   R   I   Q   R   T   Y   N   V
ttg tat tct cgg atc gcg atg gat acc gaa ttt ctg gac aag ata atg ggg gcg gaa gaa
 L   Y   S   R   I   A   M   D   T   E   F   L   D   K   I   M   G   A   E   E
gga gtt ggc aag gtc gac gat ttt atc ggc cag ctt tgg aga ggt tgg aaa aag cta aga
 G   V   G   K   V   D   D   F   I   G   Q   L   W   R   G   W   K   K   L   R
gat gct ggg ctt gcc caa gta cgc ccc ttt tct cga gag ggg acc gta atg cgt ctg atc
 D   A   G   L   A   Q   V   R   P   F   S   R   E   G   T   V   M   R   L   I
tca ggg caa ccc ctc cat ctt ggt ctt ttt cgc tca gat tac ctt ctt cat gca cca cgc
 S   G   Q   P   L   H   L   G   L   F   R   S   D   Y   L   L   H   A   P   R
aat gag ccg tta tcc atc aag caa gtg gaa ttt aac acc atc tct gtg tct ttt ggg ggt
 N   E   P   L   S   I   K   Q   V   E   F   N   T   I   S   V   S   F   G   G
cta tct caa aaa acg tcg gag ctg cat cga tac ttg cta gcc gcg aca gat tac tac aat
 L   S   Q   K   T   S   E   L   H   R   Y   L   L   A   A   T   D   Y   Y   N
agt tca tcc tac tta aag ccg gac aac ttt cca tcg aat gat tca atc gca ggg ctg gca
 S   S   S   Y   L   K   P   D   N   F   P   S   N   D   S   I   A   G   L   A
cag ggt ttg gcg gag gcc cat aag gct tac gat gtc gaa ggc tcg cgg atc ctc ttc gtc
 Q   G   L   A   E   A   H   K   A   Y   D   V   E   G   S   R   I   L   F   V
```

gtc caa tca ggc gag cgg aat gtt ttc gac caa agg ctt ttg gaa tac gaa ttg ctc gaa

V Q S G E R N V F D Q R L L E Y E L L E

aag cat tcc att cgg att ata cgg caa acc ttc agc gaa ttg gcc ctc tct gcc tct gtg

K H S I R I I R Q T F S E L A L S A S V

gat cca tca aca tgt gtt cta cga ata gca cgg tcc cca gat ctc caa cct tcg ggt tca

D P S T C V L R I A R S P D L Q P S G S

atc gaa att tcg acg gtg tat ttc cgt gcc gga tat atg ccg cat gat tac cac act ccg

I E I S T V Y F R A G Y M P H D Y H T P

gcg cat tat gac act cgt ttt ctt ctc gag agt tca aag gcg atc aaa tgc cca aca att

A H Y D T R F L L E S S K A I K C P T I

gcc ctc cag ctg gcc ggt gga aag aaa gtc cag gaa gtg ttg acg caa gca ggc atg ctc

A L Q L A G G K K V Q E V L T Q A G M L

gag cgc ttt tta tct gac gag aaa aag tac ggg aag aat att gct agt atg cag gac att

E R F L S D E K K Y G K N I A S M Q D I

gat gag ctg agg gca agc ttt atg gga atg tgg gtt ctg gac gtc agt gaa gat ttg tta

D E L R A S F M G M W V L D V S E D L L

acg cca gat tac gca gct cag gca gct ggt tct gag gaa ttc ggg gtt cga aaa gcc aga

T P D Y A A Q A A G S E E F G V R K A R

gat ctt gca caa tcg ccg gtc ctc aaa cca cag cgc gaa gga ggt ggt aac aat gtt tac

D L A Q S P V L K P Q R E G G G N N V Y

aag gag tca ata cct ggc ttc ctt gat gcc ctg gcg ccc caa gaa cgg cag gct tgg att

K E S I P G F L D A L A P Q E R Q A W I

gcc atg gaa ttg atc gac gca ccg gaa aat gca gga aac tat ctt gtc cga gcc ggc tca

A M E L I D A P E N A G N Y L V R A G S

acg gat tct caa agc caa acc cca gtt aaa acc gac gtt gtg agc gag ttg ggt att ttt

T D S Q S Q T P V K T D V V S E L G I F

ggg tgg gca ctg ttt ggt gga cca gac aaa agc att gat gag cgt gag gtg gga tgg ttg

G W A L F G G P D K S I D E R E V G W L

```
gta cgg act aaa ggg aaa gac atc aat gaa ggt ggc gtc gca acc ggc ttc tcg gtc ttg
 V   R   T   K   G   K   D   I   N   E   G   G   V   A   T   G   F   S   V   L
gat tca ttg ctc ttg gtg tag
 D   S   L   L   L   V   -
```

Figure 4.25: The nucleotide (lower case) and deduced amino acid (upper case) sequence of *HcGS* cDNA.

The cDNA sequence was further identified by looking for its homologous sequences in BLASTX analysis (Figure 4.26). The HcGS protein showed homology with glutathione synthetase protein sequences from different basidiomycetes displaying 72%, 71%, 67% and 65% sequence similarity with *Laccaria bicolor*, *Crucibulum laeve*, *Termitomyces* and *Hypsizygus marmoreus* respectively (Table 4.19).

Description	Max Score	Total Score	Query Cover	E value	Per. Ident	Accession
glutathione synthetase [Hebeloma cylindrosporum]	1122	1122	99%	0.0	100.00%	QDD67718.1
hypothetical protein M413DRAFT_69714 [Hebeloma cylindrosporum h7]	1054	1054	99%	0.0	95.62%	KIM43057.1
hypothetical protein GALMADRAFT_220520 [Galerina marginata CBS 339.88]	861	861	99%	0.0	77.01%	KDR82535.1
hypothetical protein CVT25_010739 [Psilocybe cyanescens]	811	811	96%	0.0	75.80%	PPQ78736.1
hypothetical protein CVT24_004470 [Panaeolus cyanescens]	805	805	99%	0.0	72.71%	PPQ63610.1
hypothetical protein CVT26_000911 [Gymnopilus dilepis]	805	805	99%	0.0	72.53%	PPQ65891.1
hypothetical protein K443DRAFT_674506 [Laccaria amethystina LaAM-08-1]	791	791	99%	0.0	72.01%	KIK06216.1
glutathione synthase [Crucibulum laeve]	787	787	99%	0.0	71.43%	TFK40501.1
glutathione synthetase [Laccaria bicolor]	771	771	99%	0.0	72.01%	AVX28162.1
Glutathione synthetase [Termitomyces sp. J132]	726	726	98%	0.0	66.79%	KNZ73319.1
hypothetical protein AGABI1DRAFT_59176 [Agaricus bisporus var. burnettii JB137-S8]	694	694	99%	0.0	64.05%	XP_007329727.1
hypothetical protein AGABI2DRAFT_224431 [Agaricus bisporus var. bisporus H97]	691	691	99%	0.0	63.87%	XP_006462797.1
hypothetical protein M378DRAFT_72735 [Amanita muscaria Koide BX008]	684	684	99%	0.0	61.90%	KIL67776.1
hypothetical protein AMATHDRAFT_78746 [Amanita thiersii Skay4041]	678	678	99%	0.0	60.85%	PFH54004.1
Glutathione synthetase [Hypsizygus marmoreus]	677	677	93%	0.0	65.62%	RDB14681.1
glutathione synthase [Obba rivulosa]	672	672	98%	0.0	62.75%	OCH89932.1
Glutathione synthetase large chain [Sparassis crispa]	665	665	98%	0.0	62.04%	XP_027616359.1

Figure 4.26: BLASTX analysis showing protein sequences homologous to *LbGS*

Table 4.19: Homologous sequences retrieved from BLASTX analysis of *HcGS* for multiple sequence alignment

S. No.	Organism	Accession No.	Gene	Percent identity
1	*Crucibulum leave*	TFK40501.1	glutathione synthase	71.43%
2	*Laccaria bicolor*	AVX28162.1	glutathione synthetase	72.01%
3	*Termitomyces*	KNZ73319.1	glutathione synthetase	66.79%
4	*Hypsizygus marmoreus*	RDB14681.1	glutathione synthetase	65.62%
5	*Obba rivulosa*	OCH89932.1	glutathione synthase	62.75%
6	*Coprinopsis cinerea*	XP_001836000	glutathione synthase	59.64%
7	*Lentinula edodes*	GAW08968.1	glutathione synthase	58.87%

The multiple sequence alignment of the above sequences revealed various conserved domains including the ATP binding domain from amino acid 167-181 "KQVEFNTISVSFGGL", substrate binding domain from amino acid 237-345 and few mentioned in Table 4.20. Few N-glycosylation sites in HcGS were predicted at amino acid 21 (NLTL), 200 (NSSS), 213 (NDSI) and PKC phosphorylation sites were predicted at amino acid 165 (SIK), 182 (SQK), 263 (SIR), 331 (SSK). All these sites were also found to be conserved amongst the six aligned sequences.

Table 4.20: Multiple sequence alignment of HcGS protein with GS protein sequences isolated from different basidiomycetes highlighting the conserved ATP and substrate binding domains.

Organisms	HcGS conserved domains			
L. edodes	IHAPISLFPTPFPR	LHLGLFRSDYLLH	KQVEFNTISSSFGAL	VLKPQREGGGNNVYK
C. cinerea	IHAPLSLVPSPFPR	LHLGLFRSDYLLH	KQVEFNTISISFGCL	VLKPQREGGGNNVYK
O. rivulosa	IHAPLALFPSPFPR	LHLGLFRSDYLMH	KQVEFNTISSSFGSL	VLKPQREGGGNNIYK
H. marmoreus	IHAPLSLFPSPFPR	LQLGLFRSDYLVH	KQVEFNTISVSFASL	VLKPQREGGGNNIYK
Termitomyces	IHAPLALFPSPLPR	LHLGLFRSDYLIH	KQVEFNTISVSFGSL	VLKPQREGGGNNVYK
H. cylindrosporum	IHAPISLFPSPFPR	LHLGLFRSDYLLH	KQVEFNTISVSFGGL	VLKPQREGGGNNVYK

C. laeve	IHAPLSLFPSPFPR	LQLGLFRSDYLLH	KQVEFNTISVSFGAL	VLKPQREGGGNNVYK
L. bicolor	IHAPFSLFPSPFPR	LHLGLFRSDYLLH	KQVEFNTISVSFACL	VLKPQREGGGNNVYK
	****::*.*:*:**	*:**********:*	********* **. *	************:**

The Phylogenetic tree constructed for different glutathione synthetase genes forms three different clusters of basidiomycetes, mucoromycetes and ascomycetes each sharing common evolutionary history (Figure 4.20).

Further, the secondary structure analysis of the HcGS protein reveals that the protein is a non-cytoplasmic protein with mixed composition of 37.18% Helix, 14.47% Strands and 48.35% Loops (Figure 4.27).

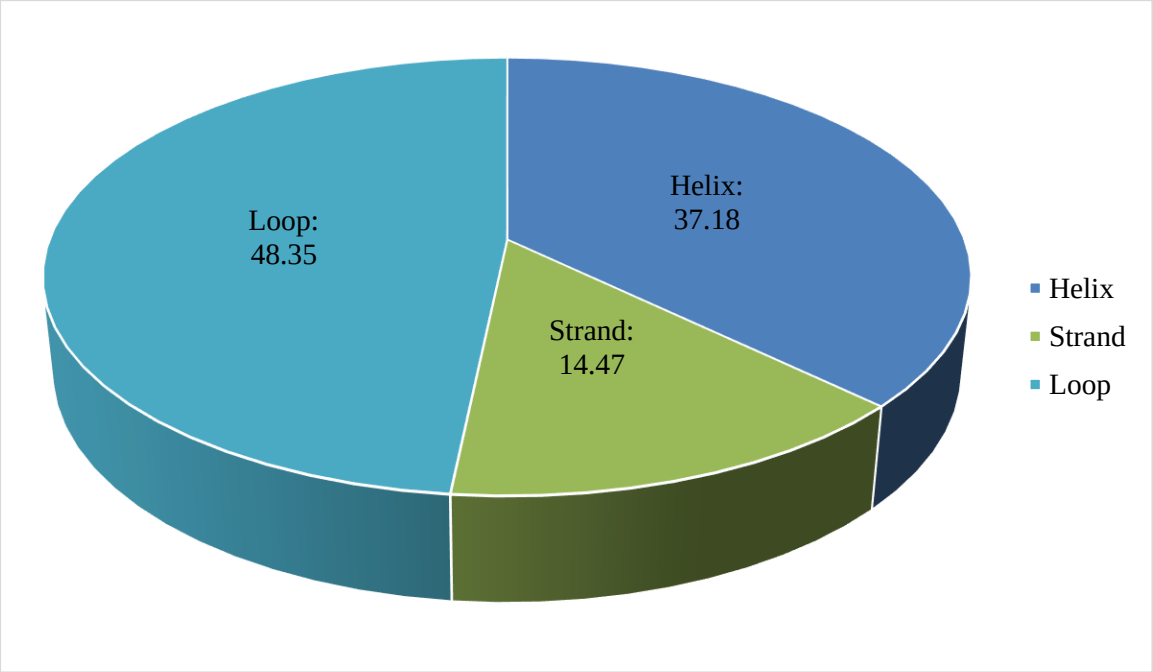

Figure 4.27: Secondary structure composition of HcGS protein indicating percentage proportion of helix, loops and strands involved in protein confirmation.

Most of the conserved domains identified in these fungal γ-GCS proteins were found to be conserved even in plants, yeasts, parasites and invertebrates. The conserved glycine and cysteine rich motif ‘‘IYLDAMGFGMGCCCLQ’’ 249–268 amino acid from both Lbγ-GCS and Hcγ-GCS has also been reported to be conserved in invertebrate *Ciona intestinalis*, *Chorispora bungeana*, and *S. cerevisiae* (Ohtake and Yabuuchi 1991; Franchi *et al.*, 2012; Nair *et al.*, 2013). The amino acid E52, E101, C260, Q264, R309, I319, R435 involved in substrate

(L-glutamate) binding site were found to be conserved not only in fungi but also in invertebrates (Franchi *et al.,* 2012). This shows that the catalytic unit of Lbγ-GCS and Hcγ-GCS is highly conserved. However, the cysteine binding moiety has not been identified in the both Lbγ-GCS and Hcγ-GCS tertiary structure. The same has also been reported in *Leishmania donovani* γ-GCS (Agnihotri *et al.,* 2016).

4.8 Real time PCR analysis

The induction of glutathione biosynthesis in response to Cd and As was further validated by studying the expression of *γ-GCS* and *GS* genes under metal(loid) stress. The ECM fungi, *L. bicolor* and *H. cylindrosporum* was stressed with different concentrations of As and Cd and the expression of *γ-GCS* and *GS* genes under each stress concentration was monitored using quantitative real time PCR. Firstly, all three reference genes α-actin, β-tubulin and adenosine kinase were amplified from the fungal cDNAs isolated at different stress treatments of Cd and As using the reverse transcription PCR. The genes were then normalized using their respective Ct values in the NormFinder software and the stability values were calculated for each reference gene (Table 4.21).

Table 4.21 Stability values of different reference genes in *L. bicolor* and *H. cylindrosporum* calculated by using NormFinder.

L. bicolor		***H. cylindrosporum***	
Reference Gene	**Stability Value**	**Reference Gene**	**Stability Value**
Lb α-actin	0.050	*Hc α-actin*	0.058
Lb β-tubulin	0.143	*Hc β-tubulin*	0.122
Lb adenosine kinase	0.085	*Hc adenosine kinase*	0.092

Since the stability value of α-actin was minimum therefore it was selected as the most stable gene for studying the relative expression of *γ-GCS* and *GS* genes in both *L. bicolor* and *H. cylindrosporum* (Table 4.21). The relative expression of both *γ-GCS* and *GS* genes with respect to α-actin in *L. bicolor* and *H. cylindrosporum* was calculated as the fold increase in expression using the comparative threshold (Ct) method with following formula:

$$Fold\ increase\ in\ expression = 2^{(\Delta Ct(target\ gene) - \Delta Ct\ (Reference\ gene))}$$

$$\text{Where,} \quad \Delta Ct = Ct\ (\text{without treatment}) - Ct\ (\text{with treatment})$$

When exposed to Cd stress, the ECM fungus *L. bicolor* responded with immediate increase in the fold expression of both *Lbγ-GCS* and *LbGS* genes (Figure 4.28). At 10 µM of Cd stress, almost 10-fold increase in expression was observed for *Lbγ-GCS* and 3-fold increase was observed for *LbGS*. Further, increasing the Cd stress to 30 µM, increased the expression of *Lbγ-GCS* by 13.6-fold and that of *LbGS* by 12-fold. When the Cd stress was elevated 40 µM, the expression of *Lbγ-GCS* increased by 18.9 folds, whereas that of *LbGS* increased only by 10.3 folds (Table 4.22).

Table 4.22: Fold increase in the relative expression of *Lbγ-GCS* and *LbGS* genes when stressed with increasing concentrations of Cd ($CdSO_4$: 10, 20, 30, 40 µM) for 48 h at 25 ˚C. Actin was normalized as an internal reference gene. The experiment was performed in triplicates and the readings indicated are mean ± S.D under each stress condition.

Cadmium concentrations (µM)	**Fold increase in expression**	
	Lbγ-GCS	***LbGS***
10	10.33±0.015c	3.01±0.125d
20	9.53±0.869c	6.25±0.129c
30	13.63±0.220b	12.11±0.352a
40	18.96±0.150a	10.38±0.956b

Values (Mean±SD) sharing a common letter within the column are not significantly different at $P<0.05(n=3)$

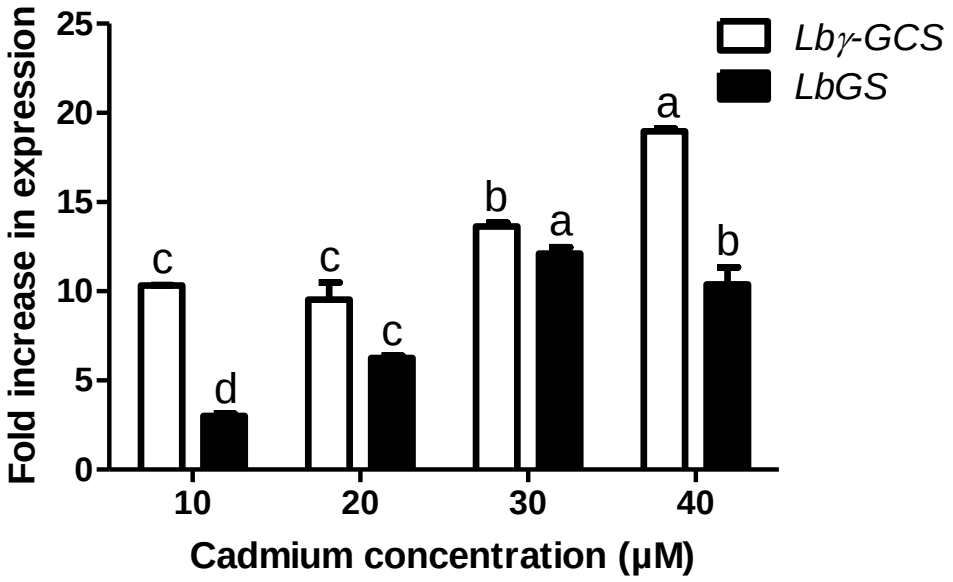

Figure 4.28: Fold increase in expression of *Lbγ-GCS* and *LbGS* in response to different concentrations of Cd. Values plotted are referred to the control condition (expression level in free living fungus without metal treatment) and represent an average of three biological replicates. Values sharing a common letter within the gene are not significantly different at $P < 0.05$. Error bars are ± SD.

The expression of both *Lbγ-GCS* and *LbGS* genes also increased when the fungus was subjected to varying concentrations of As stress (Figure 4.29). When stressed with 5 mM of external As, *L. bicolor* responded by increasing the expression of both *Lbγ-GCS* and *LbGS* by 3.8-fold and 2.15-fold respectively. Similarly, at 10 mM of external As the expression of both *Lbγ-GCS* and *LbGS* increased by 4.8 and 3.4 fold respectively. Further, increasing the stress to 15 mM of As, increased the expression of *Lbγ-GCS* by 8.3-fold and that of *LbGS* by 4.8-fold. At 20 mM As, the expression further increased by 10.8-fold for *Lbγ-GCS* and 6.6-fold for *LbGS* (Table 4.23).

Table 4.23: Fold increase in the relative expression of *Lbγ-GCS* and *LbGS* genes when stressed with increasing concentrations of As (Na_2HAsO_4: 5, 10, 15, 20 mM) for 48 h at 25˚C. Actin was normalized as an internal reference gene.

Arsenic concentrations (mM)	Fold increase in expression	
	Lbγ-GCS	***LbGS***
5	3.86±0.147d	2.15±0.125d
10	4.79±0.158c	3.44±0.885c
15	8.33±0.214b	4.88±0.635b
20	10.85±0.658a	6.58±0.758a

Values (Mean±SD) sharing a common letter within the column are not significantly different at P<0.05(n=3).

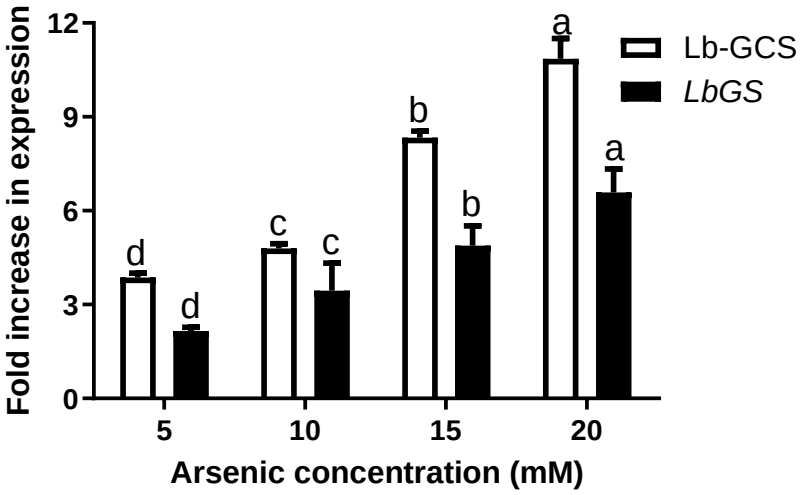

Figure 4.29: Fold increase in expression of *Lbγ-GCS* and *LbGS* in response to different concentrations of As. Values plotted are referred to the control condition (expression level in free living fungus without metal(loid) treatment) and represent an average of three biological replicates. Values sharing a common letter within the gene are not significantly different at P < 0.05. Error bars are ± SD.

Similar observations were made in case of *H. cylindrosporum*, where the expression of both *Hcγ-GCS* and *HcGS* genes was induced with the increase in external metal(loid) stress (Figure 4.30). When stressed with 5 mM Cd, 6.2-fold increase was recorded in the expression of *Hcγ-*

GCS and 4.2 folds increase in expression of *HcGS*. Further, increasing the metal stress to 20 µM and 30 µM, increased the mRNA accumulation of *Hcγ-GCS* by 8.9-fold and 9.7-fold, respectively and that of *HcGS* by 6.5-fold and 8.9-fold respectively. When stressed with 40 µM of Cd, 11.3-fold increase in expression was recorded for *Hcγ-GCS* and 9.6-fold increase was recorded for *HcGS* (Table 4.24).

Table 4.24: Fold increase in the relative expression of *Hcγ-GCS* and *HcGS* genes when stressed with increasing concentrations of Cd ($CdSO_4$: 10, 20, 30, 40 µM) for 48 h at 25 ˚C. Actin was normalized as an internal reference gene.

Cadmium concentrations (µM)	Fold increase in expression	
	Hcγ-GCS	***HcGS***
10	6.2±0.75d	4.2±0.41d
20	8.9±0.89c	6.5±0.48c
30	9.7±0.60b	8.9±0.33b
40	11.3±0.23a	9.6±0.81a

Values (Mean±SD) sharing a common letter within the column are not significantly different at P<0.05

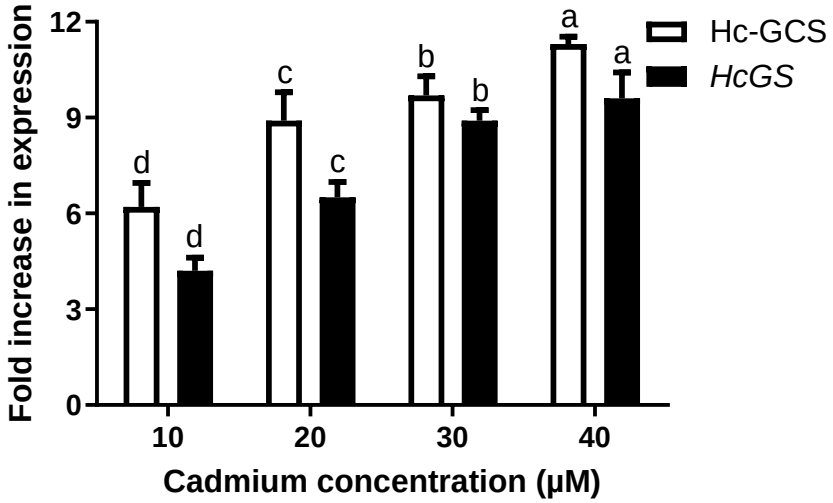

Figure 4.30: Fold increase in expression of *Hcγ-GCS* and *HcGS* in response to different concentrations of Cd. Values plotted are referred to the control condition (expression level in free living fungus without metal treatment) and represent an average of three biological replicates. Values sharing a common letter within the gene are not significantly different at P < 0.05. Error bars are ± SD.

The mRNA accumulation of both *Hcγ-GCS* and *HcGS* also increased in response to external As stress (Figure 4.31). At 5 mM of As exposure, the expression of both *Hcγ-GCS* and *HcGS* increased by 6.5 and 4.21 fold respectively. Increasing the external As concentration to 10 mM, increased the expression of both *Hcγ-GCS* and *HcGS* by 8.12 and 7.16 fold respectively, which was further increased to 9.18 and 8.54 fold, respectively at 15 mM. Further, increasing the As concentration to 20 mM escalated the expression of both *Hcγ-GCS* and *HcGS* genes by 12.8 and 11.25 fold respectively (Table 4.25).

Table 4.25: Fold increase in the relative expression of *HCγ-GCS* and *HcGS* genes when stressed with increasing concentrations of As (Na_2HAsO_4: 5, 10, 15, 20 mM) for 48 h at 25˚C. Actin was normalized as an internal reference gene.

Arsenic concentrations (mM)	**Fold increase in expression**	
	Hcγ-GCS	***HcGS***
5	6.54±0.12d	4.21±0.25d
10	8.12±0.15c	7.16±0.12c
15	9.18±0.55b	8.54±0.63b
20	12.80±0.63a	11.25±0.85a

Values (Mean±SD) sharing a common letter within the column are not significantly different at P<0.05(n=3)

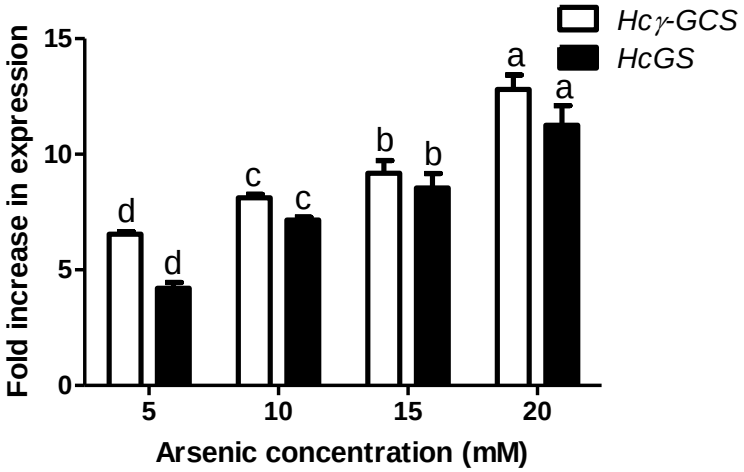

Figure 4.31: Fold increase in expression of *Hcγ-GCS* and *HcGS* in response to different concentrations of As. Values plotted are referred to the control condition (expression level in free living fungus without metal(loid) treatment) and represent an average of three biological

replicates. Values sharing a common letter within the gene are not significantly different at P < 0.05. Error bars are ± SD.

It was observed that the expression of glutathione biosynthesis genes (*γ-GCS* and *GS*) increased spontaneously in both ECM fungi, *L. bicolor* and *H. cylindrosporum* when exposed to As and Cd. The fold increase in expression of *γ-GCS* was more than that of *GS* gene. This might be due to the fact that *γ-GCS* is a rate limiting enzyme and is therefore more effected under stress conditions. A 2.5 folds increase in the relative expression of *γ-GCS* was recorded in *Brassica chinensis* when exposed to 10 µM Cd (Lou *et al.,* 2017). In *Chironomus riparius* exposure to Cd resulted in 1.5-3.5 folds increase in expression of *γ-GCS* and 1.3-2.3 folds increase in expression of *GS* (Nair *et al.,* 2013). The increase in expression of both glutathione biosynthesis genes has also been reported in *Laeonereis acuta* (Sandrini *et al.,* 2006), *Triticum aestivum* (Sun *et al.,* 2005) and *Arabidopsis thaliana* (Chen *et al.,* 2016). *Arabidopsis thaliana* on exposure to Cd, resulted in 2-3.5 folds increase in expression of *γ-GCS* and 3-9 folds increase in expression of *GS* (Chen *et al.,* 2016). Similar observations were made by Jozefczak *et al.,* (2014) in *Arabidopsis thaliana*, where the expression of both *γ-GCS* and *GS* up-regulated under Cd stress.

γ-GCS has been well characterized in various plants and mammals for its active role in mitigating the As toxicity (Schuliga *et al.,* 2002; Liao and Yu, 2005; Guo *et al.,* 2008), but very meagre information is available for its activity in fungal systems under As stress. In plants like *Lens culinaris* Medik, the expression of GSH biosynthesis genes was upregulated when exposed to 25 mM and 40 mM of As (Talukdar and Talukdar, 2014). Similarly, in *Arabidopsis thaliana*, 2-6 folds increase in the expression of *γ-GCS* gene was reported when exposed to As stress (Dhankher *et al.,* 2002; Li *et al.,* 2006). These observations clearly depict that glutathione plays the central role in Cd and As detoxification and is actively induced under stress. The overexpression of these genes (*γ-GCS* and *GS*) results in more glutathione production, leading to higher tolerance for heavy metals (He *et al.,* 2015a; Martin *et al.,* 2018). However, the inhibition of these genes generates metal(loid) sensitive strains (Han *et al.,* 2019).

The amplification of all reference genes (α-actin, β-tubulin and adenosine kinase) along with the glutathione biosynthesis genes (*γ-GCS* and *GS*) after qPCR analysis was further validated by visualizing it through the agarose gel electrophoresis (Figure 4.32).

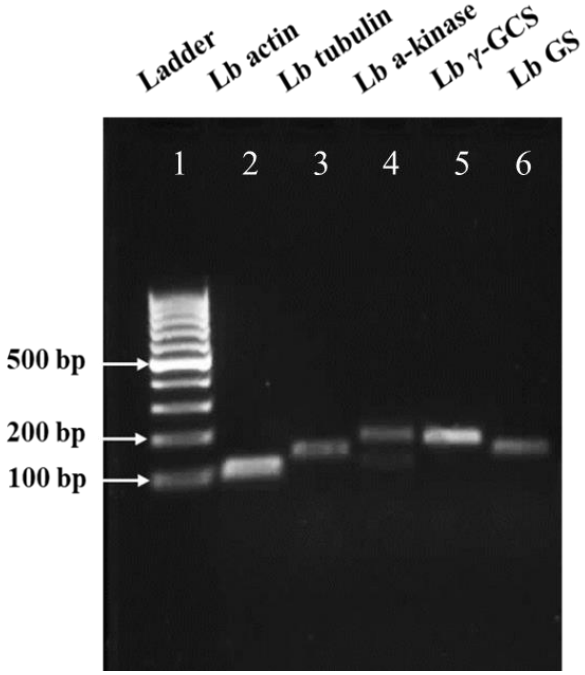

Figure 4.32: Validation of qPCR amplified genes through agarose gel electrophoresis. Lane 1: 100 kb ladder, lane 2: Lb α-actin, lane 3: Lb β-tubulin, lane 4: Lb adenosine kinase, lane 5: Lb *γ-GCS* and lane 6: *LbGS*.

4.9 Plasmid isolation, digestion and ligation

The yeast shuttle vector - pFL61 was isolated using the Quiagen (Figure 4.33) having the concentration of 1958 ng/µl with $A_{260/280}$ of 1.89 (measured by nanodrop). The isolated plasmid along with the gene of interest (*Lbγ-GCS*, *LbGS*, *Hcγ-GCS* and *HcGS*) were subjected to double digestion with their respective restriction enzymes and visualized on 0.8% agarose gel (Figure 4.34). The digested plasmid was excised from the agarose gel using the "GeneJET Gel Extraction Kit - Thermo Fisher Scientific". The digested plasmid and gene were then ligated using the T4 ligase (Figure 4.25).

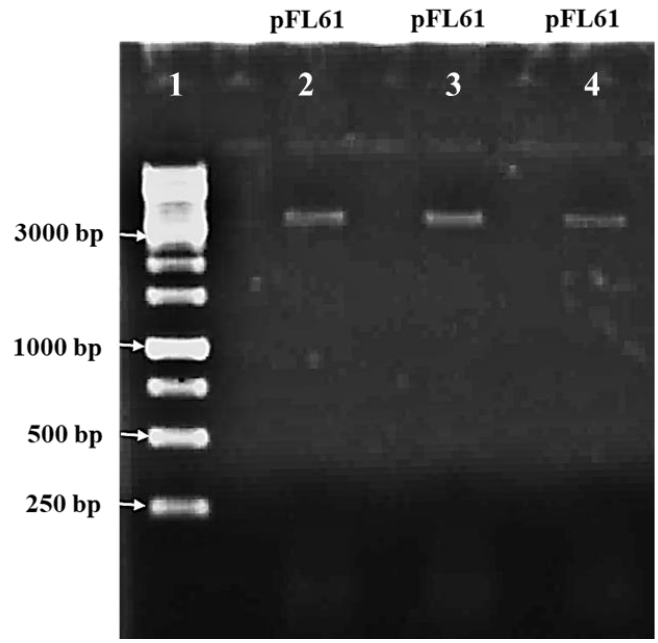

Figure 4.33: pFL61 plasmid isolated from the bacterial cell with approximate size 5 kb. Lane 1: ladder 1kb, Lane 2,3,4: plasmid pFL61.

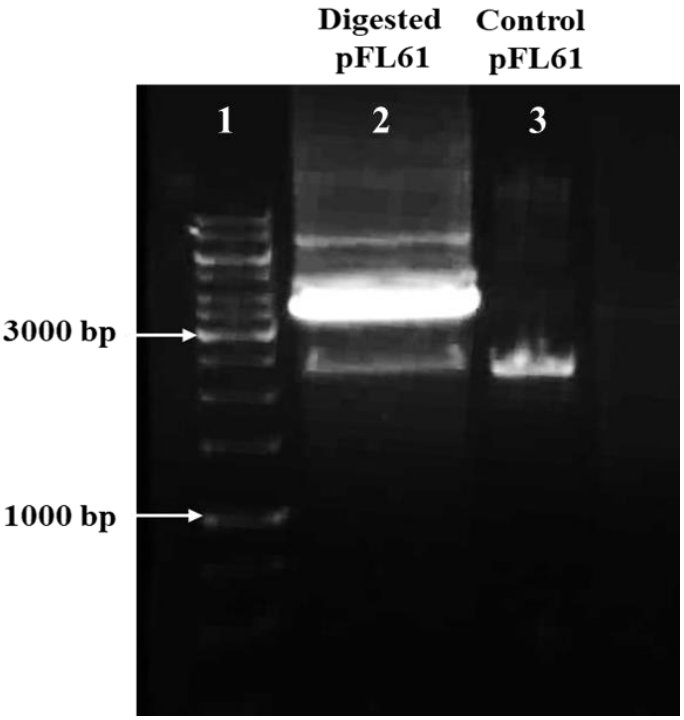

Figure 4.34: pFL61 digested with restriction enzymes along with the undigested control. Lane1: ladder, lane 2: digested pFL61, lane 3: undigested pFL61.

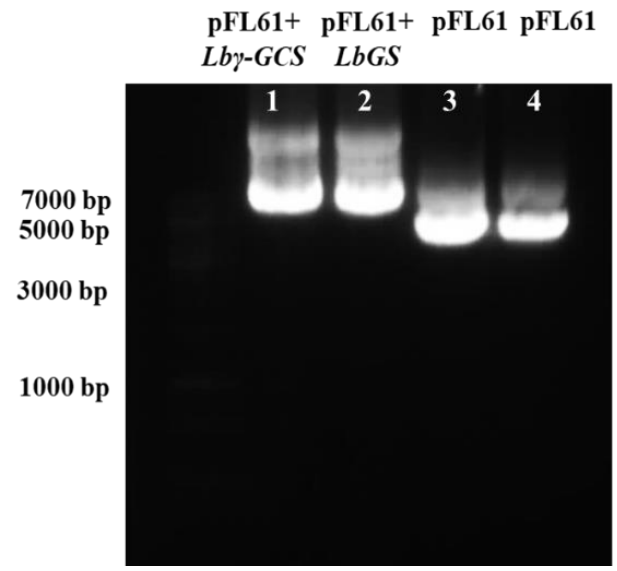

Figure 4.35: Ligation of pFL61 with *L. bicolor* genes. lane 1: pFL61+ *Lbγ-GCS*, lane 2: pFL61+*LbGS*, Lane 3,4: pFL61 control.

4.10 Bacterial transformation and colony PCR

The ligated plasmid+genes (pFL61+*Lbγ-GCS*, pFL61+*LbGS*, pFL61+*Hcγ-GCS* and *HcGS*) were then transformed into the *E. coli* DH10β cells and the positive clones were selected through colony PCR (Figure 4.36).

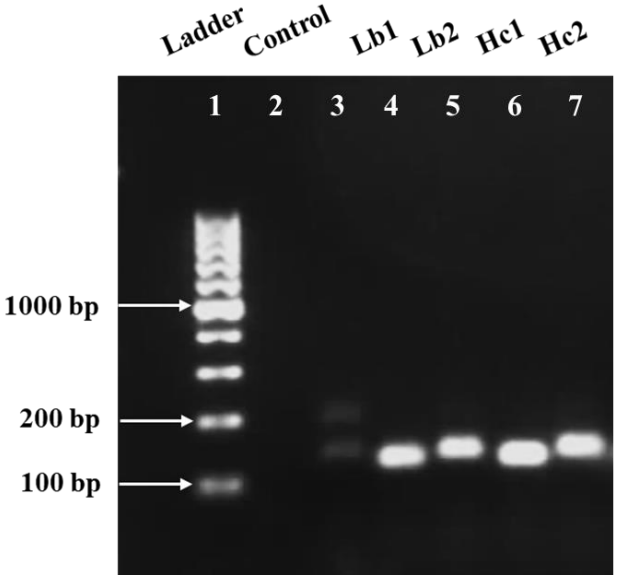

Figure 4.36: Positive clones selected by colony PCR of *E. coli* DH10β cells. Lane 1: 1 kb ladder, Lane 2: control, Lane 3: blank, Lane 4, 5, 6,7: positive clones of *Lbγ-GCS, LbGS, Hcγ-GCS* and *HcGS*, respectively.

4.11 Yeast complementation assay

The function of both *γ-GCS* and *GS* genes in mitigating Cd and As toxicity was studied using the method proposed by Daghino *et al.*, (2016). The functional complementation of *Lbγ-GCS/Hcγ-GCS* and *LbGS/HcGS* genes was carried out by expressing them in their respective *S. cerevisiae* yeast mutants, *gsh1*$^{\Delta}$ and *gsh2*$^{\Delta}$ (sensitive to both Cd and As).

The plasmid isolation was carried out on the positive clones so obtained in section 4.10. The isolated plasmids were then transformed into their respective yeast mutants *gsh1*$^{\Delta}$ (pFL61+*Lbγ-GCS*, pFL61+*Hcγ-GCS*) and *gsh2*$^{\Delta}$ (pFL61+*Lb-GS*, pFL61+*HcGS*). The positive yeast clones so obtained were further used for the functional complementation studies using the drop test analysis and the liquid growth assay.

4.11.1 Drop test analysis

In the drop test analysis, the growth of both mutants *gsh1*$^{\Delta}$ and *gsh2*$^{\Delta}$ transformed with their respective genes (pFL61+*Lbγ-GCS*/pFL61+*Hcγ-GCS* and pFL61+*LbGS*/pFL61+*HcGS*) and empty vector (EV) pFL61 along with the wild type BY4741 carrying pFL61, was monitored on SD-Ura medium supplemented with and without Cd (40 µM) and As (100 µM).

The *S. cerevisiae* metal(loid) sensitive mutants, *gsh1*$^{\Delta}$ and *gsh2*$^{\Delta}$ when transformed with empty vector (EV) pFL61 could grow on normal SD-Ura medium but not on SD-Ura medium supplemented with Cd (40 µM) (Figure 4.37, 4.39) and As (100 µM) (Figure 4.38, 4.40). However, the same mutant cells (*gsh1*$^{\Delta}$ and *gsh2*$^{\Delta}$) when transformed with their respective glutathione synthesis gene (*Lbγ-GCS/Hcγ-GCS* and *LbGS/HcGS*) successfully restored their metal(loid) tolerance tendencies analogous to their wild type BY4741 cells. The wild type BY4741 could successfully grew on both SD-Ura medium supplemented with and without Cd and As. The results are presented as 5 µl drops on SD-Ura plates supplemented with and without Cd and As. Both *gsh1*$^{\Delta}$ and *gsh2*$^{\Delta}$ were highly sensitive to both Cd and As and could not survive when grown on the metal(loid) supplemented SD mediums. However, when both mutants were complemented with their respective mutant genes isolated from ECM fungi, could successfully grow on the metal(loid) supplemented SD-Ura plates. This shows that the GSH biosynthesis genes isolated form *L. bicolor* and *H. cylindrosporum* plays an important role in generating Cd and As tolerance.

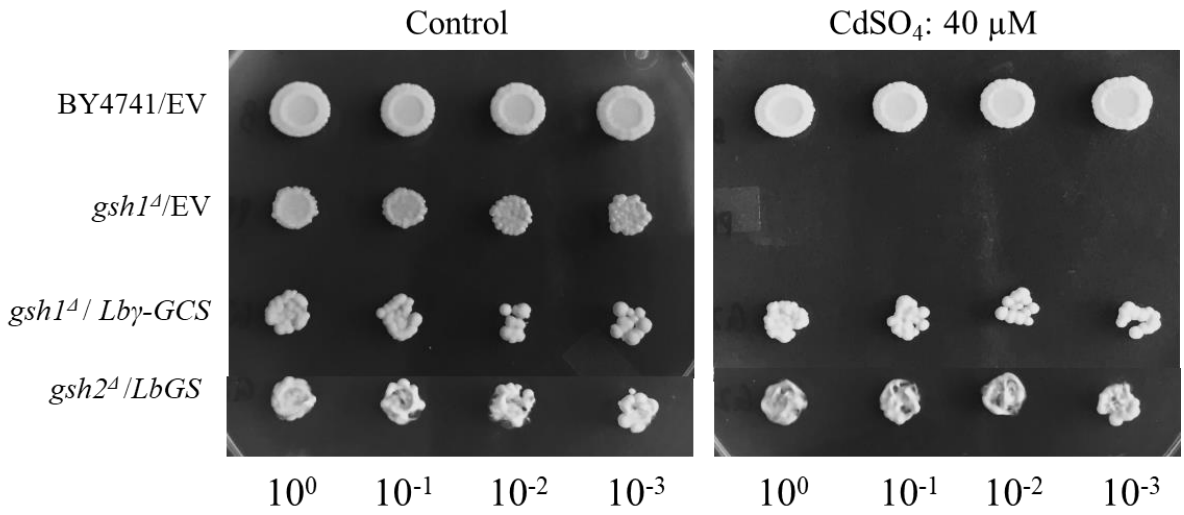

Figure 4.37: Functional complementation of *S. cerevisiae* mutant *gsh1*$^{\Delta}$ and *gsh2*$^{\Delta}$ transformed with empty vector pFL61 (EV) and their respective glutathione biosynthesis genes *Lbγ-GCS* and *LbGS* in response to Cd. BY4741 cells transformed with EV were used as positive control. The 5 µl drop of each culture diluted 10^{-1}, 10^{-2}, 10^{-3} times was spotted on SD- Ura plated supplemented with and without Cd.

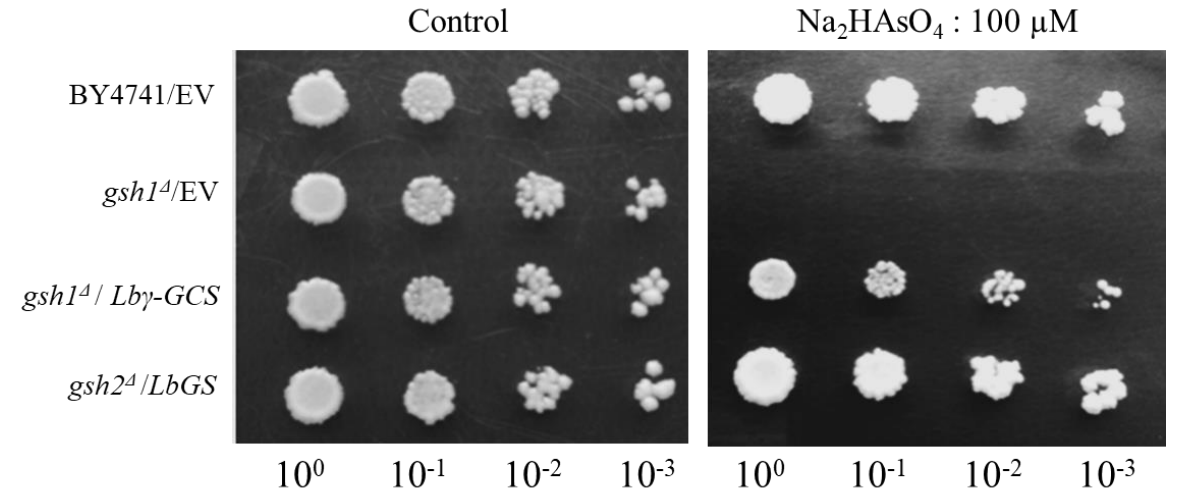

Figure 4.38: Functional complementation of *S. cerevisiae* mutant *gsh1*$^{\Delta}$ and *gsh2*$^{\Delta}$ transformed with empty vector pFL61 (EV) and their respective glutathione biosynthesis genes *Lbγ-GCS* and *LbGS* in response to As (100 µM). BY4741 cells transformed with EV were used as positive control. The 5 µl drop of each culture diluted 10^{-1}, 10^{-2}, 10^{-3} times was spotted on SD-Ura plated supplemented with and without As.

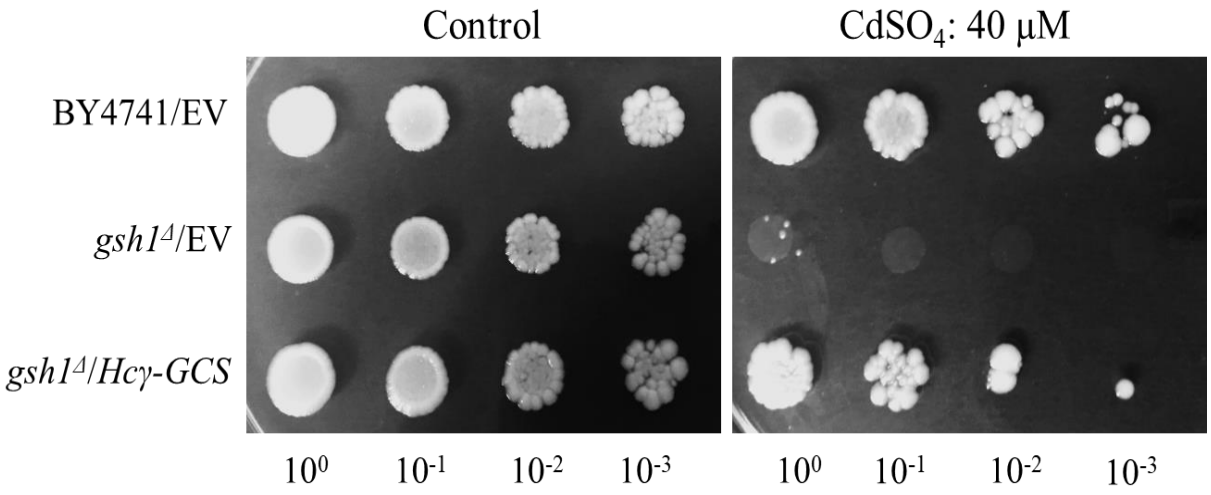

Figure 4.39: Functional complementation of *S. cerevisiae* mutant *gsh1*$^{\Delta}$ and *gsh2*$^{\Delta}$ transformed with empty vector pFL61 (EV) and their respective glutathione biosynthesis genes *Hcγ-GCS* and *HcGS* in response to Cd. BY4741 cells transformed with EV were used as positive control. The 5 µl drop of each culture diluted 10^{-1}, 10^{-2}, 10^{-3} times was spotted on SD-Ura plated supplemented with and without Cd.

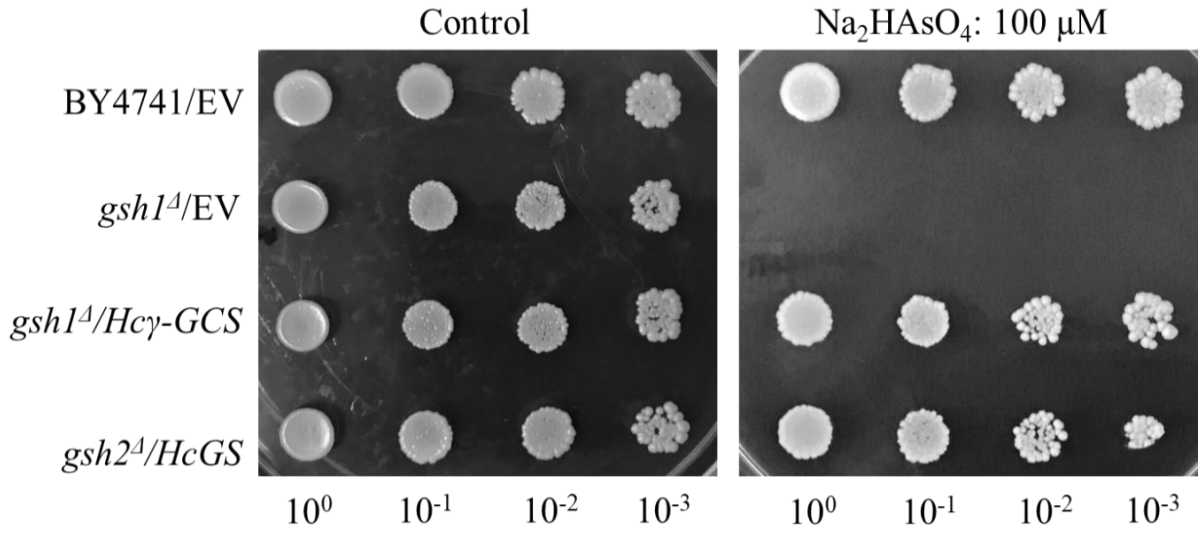

Figure 4.40: Functional complementation of *S. cerevisiae* mutant *gsh1*$^{\Delta}$ and *gsh2*$^{\Delta}$ transformed with empty vector pFL61 (EV) and their respective glutathione biosynthesis genes *Hcγ-GCS* and *HcGS* in response to As. BY4741 cells transformed with EV were used as positive control. The 5 µl drop of each culture diluted 10^{-1}, 10^{-2}, 10^{-3} times was spotted on SD-Ura plated supplemented with and without As.

4.11.2 Liquid Assay:

The function of glutathione biosynthesis genes (*γ-GCS* and *GS*) in mitigating Cd and As toxicity was further validated through liquid assay. The *S. cerevisiae* yeast mutants *gsh1*$^{\Delta}$ and *gsh2*$^{\Delta}$ transformed with *Lbγ-GCS/Hcγ-GCS* and *LbGS/HcGS*, respectively were allowed to grow in SD-Ura broth supplemented with varying concentrations of As (0, 50, 100, 150, 200 µM) and Cd (0, 20, 40, 60, 80 µM) for 24 hours. The response of each transformant along with the wild type BY4741 was recorded as the absorbance of the culture at 600 nm.

The response of yeast mutants carrying GSH biosynthesis genes *(Lbγ-GCS* and *LbGS*) isolated from *L. bicolor* to both Cd and As have been represented graphically in figure 4.41 and 4.42. When exposed to 20 µM Cd, the growth of *gsh1*$^{\Delta}$ carrying empty vector pFL61 declined drastically whereas the mutants carrying *Lbγ-GCS* and *LbGS* could successfully grow equivalent to their wild type BY4741 cells (Figure 4.41). Further, increasing the Cd stress to 40, 60 and 80 µM, completely arrested the growth of *gsh1*$^{\Delta}$(pFL61) and *gsh2*$^{\Delta}$(pFL61), whereas the same mutants carrying GSH genes *gsh1*$^{\Delta}$(pFL61+*Lbγ-GCS*) and *gsh2*$^{\Delta}$(pFL61+ *LbGS*) tolerated the metal(loid) stress and showed growth similar to BY4741 cells (Table 4.26).

Similar observations were made when the mutants were exposed to As stress. The mutants carrying EV pFL61 arrested their growth at 50 µM As, whereas the same mutants carrying GSH genes *gsh1*$^{\Delta}$(pFL61+*Lbγ-GCS*) and *gsh2*$^{\Delta}$(pFL61+ *LbGS*) successfully followed the growth pattern of their wild type BY4741 (Table 4.27) (Figure 4.42).

Table 4.26: Growth assay of yeast mutants *gsh1*$^{\Delta}$ and *gsh2*$^{\Delta}$, transformed with *Lbγ-GCS* and *LbGS* genes, respectively and empty vector pFL61 along with its wild type (BY4741) grown in presence of various concentrations of Cd for 24 h at 30˚C.

Cadmium concentration (µM)	Absorbance (600 nm)			
	BY4741	**pFL61**	**pFL61+*Lbγ-GCS***	**pFL61+*LbGS***
0	1.542±0.010a	1.564±0.012a	1.560±0.018a	1.570±0.020a
20	0.885±0.095b	0.130±0.044b	0.698±0.052b	0.754±0.066b
40	0.654±0.087c	0.109±0.068b	0.347±0.088c	0.489±0.048c
60	0.210±0.012d	0.104±0.099b	0.118±0.020d	0.208±0.015d
80	0.152±0.011d	0.100±0.010b	0.104±0.014d	0.110±0.002d

Values (Mean±SD) sharing a common letter within the column are not significantly different at P<0.05(n=3)

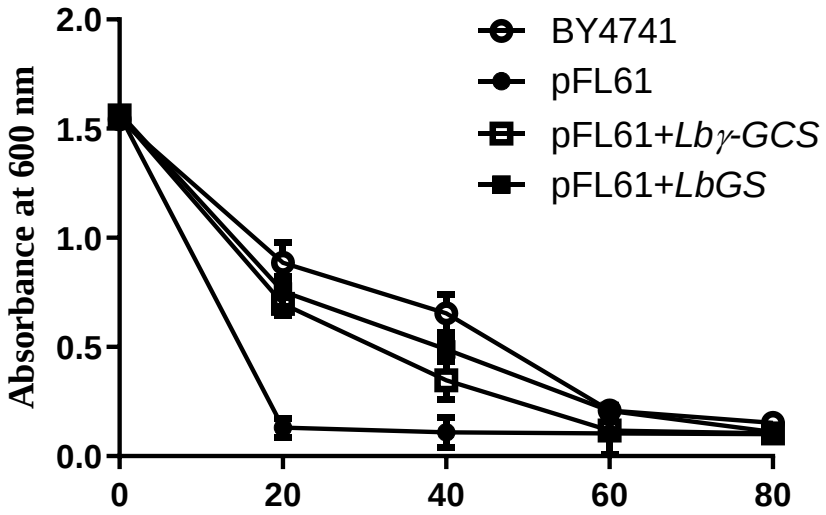

Figure 4.41: Growth assay of yeast mutants *gsh1*$^{\Delta}$ and *gsh2*$^{\Delta}$, transformed with *Lbγ-GCS* and *LbGS* genes, respectively and empty vector pFL61 along with its wild type (BY4741) grown in presence of various concentrations of Cd for 24 h at 30˚C. Values represent an average of three biological replicates with ±SD.

Table 4.27: Growth assay of yeast mutants *gsh1*$^{\Delta}$ and *gsh2*$^{\Delta}$, transformed with *Lbγ-GCS* and *LbGS* genes, respectively and empty vector pFL61 along with its wild type (BY4741) grown in presence of various concentrations of As for 24 h at 30˚C.

Arsenic concentration (mM)	Absorbance (600 nm)			
	BY4741	**pFL61**	**pFL61+*Lbγ-GCS***	**pFL61+*LbGS***
0	1.685±0.016a	1.632±0.120a	1.612±0.019a	1.620±0.023a
50	0.985±0.086b	0.180±0.074b	0.795±0.094b	0.704±0.052b
100	0.662±0.045c	0.110±0.066c	0.658±0.055c	0.592±0.041c
150	0.287±0.032d	0.104±0.025c	0.150±0.042d	0.159±0.013d
200	0.156±0.011e	0.100±0.009c	0.104±0.015d	0.110±0.007d

Values (Mean±SD) sharing a common letter within the column are not significantly different at P<0.05(n=3)

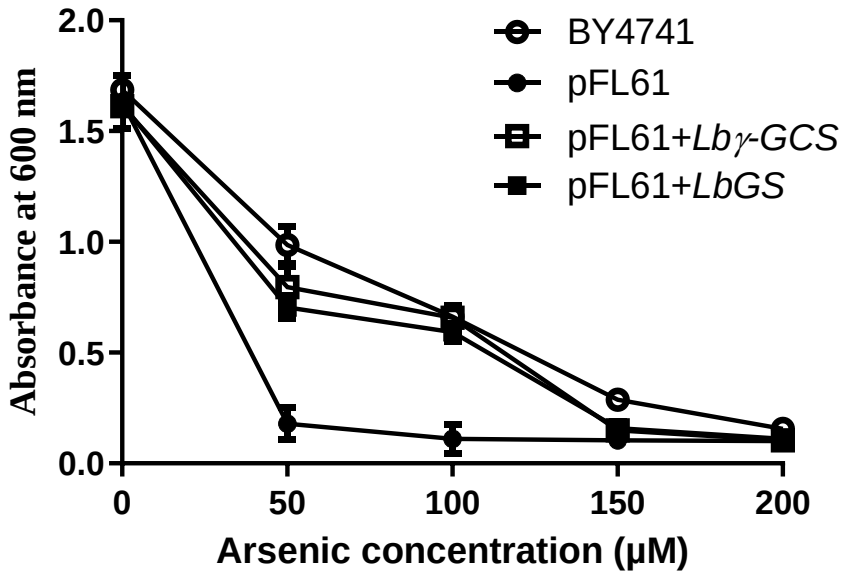

Figure 4.42: Growth assay of yeast mutants *gsh1*$^{\Delta}$ and *gsh2*$^{\Delta}$, transformed with *Lbγ-GCS* and *LbGS* genes, respectively and empty vector pFL61 along with its wild type (BY4741) grown in presence of various concentrations of As for 24 h at 30˚C. Values represent an average of three biological replicates with ±SD.

Further, the function of *Hcγ-GCS* and *HcGS* genes isolated from *H. cylindrosporum* was also validated through the liquid assay. Similarly, the mutants carrying empty vector pFL61 ceased its growth when exposed to 20 µM Cd (Table 4.28) and 50 µM As (Table 4.29), whereas the same mutants when transformed with *Hcγ-GCS* and *HcGS* successfully grew even at 40 µM Cd and 100 µM As similar to their wild type BY4741 (Figure 4.43, 4.44). This shows that the both *γ-GCS* and *GS* genes plays a significant role in inducing heavy metal(loid) tolerance in ECM fungi.

Table 4.28: Growth assay of yeast mutants *gsh1*$^{\Delta}$ and *gsh2*$^{\Delta}$, transformed with *Hcγ-GCS* and *HcGS* genes, respectively and empty vector pFL61 along with its wild type (BY4741) grown in presence of various concentrations of Cd for 24 h at 30˚C.

Cadmium concentration (µM)	**Absorbance (600 nm)**			
	BY4741	**pFL61**	**pFL61+*Hcγ-GCS***	**pFL61+*HcGS***
0	1.956±0.010s	1.998±0.012a	1.985±0.018a	1.914±0.011a
20	1.065±0.089b	0.215±0.052b	0.965±0.055b	0.885±0.042b
40	0.779±0.052c	0.196±0.015b	0.651±0.099c	0.569±0.054c
60	0.315±0.042d	0.142±0.033b	0.296±0.056d	0.198±0.067d
80	0.162±0.020e	0.100±0.008b	0.154±0.026e	0.115±0.039d

Values (Mean±SD) sharing a common letter within the column are not significantly different at $P<0.05$(n=3)

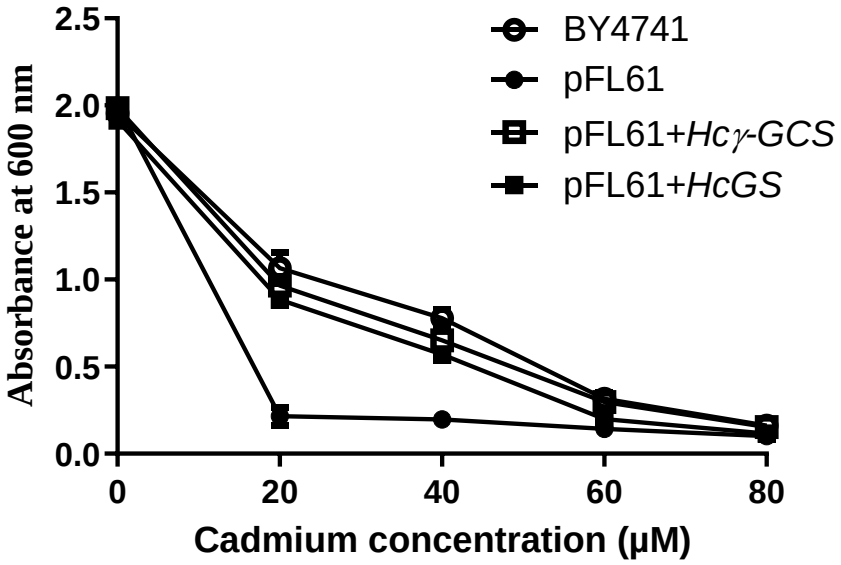

Figure 4.43: Growth assay of yeast mutants *gsh1*$^{\Delta}$ and *gsh2*$^{\Delta}$, transformed with *Hcγ-GCS* and *HcGS* genes, respectively and empty vector pFL61 along with its wild type (BY4741) grown in presence of various concentrations of Cd for 24 h at 30˚C. Values represent an average of three biological replicates with ±SD.

Table 4.29: Growth assay of yeast mutants *gsh1*$^{\Delta}$ and *gsh2*$^{\Delta}$, transformed with *Hcγ-GCS* and *HCGS* genes, respectively and empty vector pFL61 along with its wild type (BY4741) grown in presence of various concentrations of As for 24 h at 30˚C.

Arsenic concentration (mM)	**Absorbance (600 nm)**			
	BY4741	**pFL61**	**pFL61+*Hcγ-GCS***	**pFL61+*HcGS***
0	1.880±0.018a	1.850±0.015a	1.890±0.014a	1.810±0.011a
50	1.105±0.095b	0.315±0.069b	0.956±0.054b	0.854±0.095b
100	0.743±0.080c	0.221±0.041c	0.621±0.052c	0.452±0.051c
150	0.448±0.041d	0.185±0.013c	0.335±0.022d	0.289±0.025d
200	0.164±0.016e	0.099±0.012c	0.087±0.014e	0.084±0.011e

Values (Mean±SD) sharing a common letter within the column are not significantly different at P<0.05(n=3)

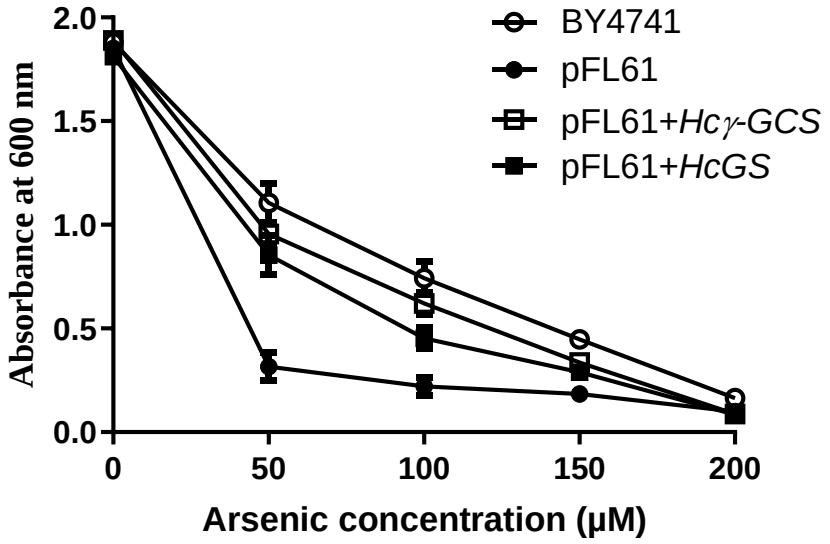

Figure 4.44: Growth assay of yeast mutants *gsh1*$^{\Delta}$ and *gsh2*$^{\Delta}$, transformed with *Hcγ-GCS* and *HcGS* genes, respectively and empty vector pFL61 along with its wild type (BY4741) grown in presence of various concentrations of As for 24 h at 30˚C. Values represent an average of three biological replicates with ±SD.

The transformation of both genes *Lbγ-GCS/Hcγ-GCS* and *LbGS/HcGS* in their respective yeast mutants successfully restored their metal(loid) tolerance ability. Similar observations have been reported by Saunders and McLellan, (2000), where the functional complementation of *γ-GCS* gene isolated from *Drosophila melanogaster* in *S. cerevisiae γ-GCS* mutant partially restored the glutathione levels and conferred resistance to Cd and methylglyoxal (Saunders and McLellan, 2000). Similarly, *Hansenula polymorpha* mutant for *GSH1* (*γ-GCS*) was highly sensitive to Cd, however the same mutant when transformed with *GSH1* gene successfully restored the Cd tolerance tendencies (Ubiyvovk *et al.*, 2011). The transformation of *GSH1* (*γ-GCS*) gene isolated from aresnite-resistant *Leishmania tarentolae* into the wild type increased the glutathione production and conferred arsenite resistance (Grondin *et al.*, 1997). These observations clearly validate the active role of both *γ-GCS* and *GS* in inducing Cd and As tolerance in ECM fungi, *L. bicolor* and *H. cylindrosporum*.

In the light of these evidence, it can be clearly concluded that the ECM fungi, *L. bicolor* and *H. cylindrosporum* can be a good metal(loid) accumulators and detoxifiers, highlighting the role of GSH defense system in both Cd and As sequestration and thus preventing its transfer to the host plant.

4.12 Protein isolation

In order to study the total proteome of ECM fungus *L. bicolor* in response to Cd, the fungus was stressed with 40 µM of Cd for 48 hours. After 48 hours, the mycelium was crushed with liquid nitrogen and the total protein was isolated. The isolated proteins were visualized through SDS-PAGE (Figure 4.46) and quantified through Bradford assay (Table 4.30). A standard plot for protein estimation was prepared using the known concentrations of BSA (Figure 4.45). The linear equation was calculated and used for estimation of LbCd-0 and LbCd-40.

Table 4.30: Protein estimation by Bradford method using BSA standard.

S. No.	Concentration of BSA µg/100 µl	Absorbance (595 nm)
1	0	0.000
2	1.56	0.001
3	3.12	0.020
4	6.25	0.036
5	12.5	0.072
6	25	0.159
7	50	0.293
8	100	0.493
9	LbCd-0	1.240
10	LbCd-40	1.259

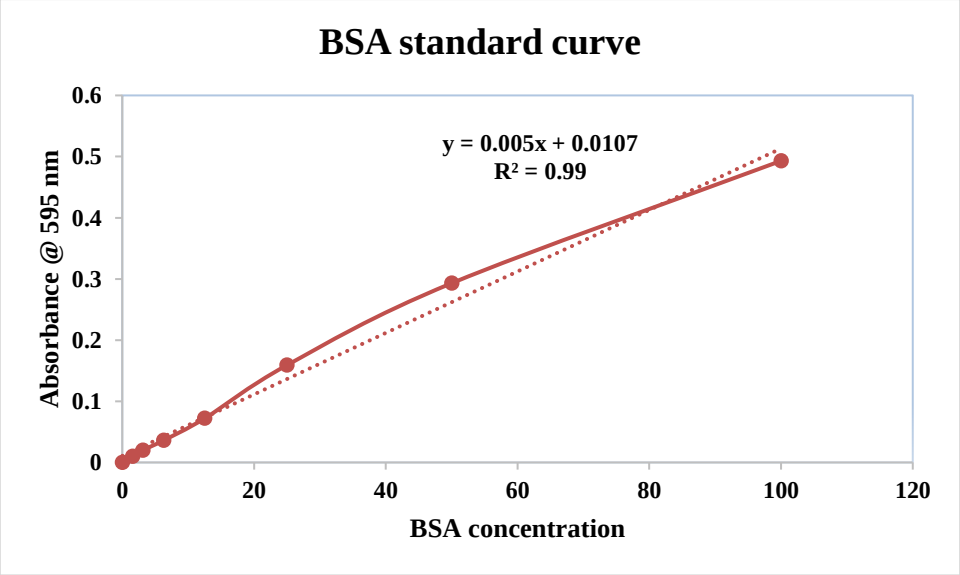

Figure 4.45: Standard plot of BSA for protein estimation through Bradford method.

The concentration of unknown protein samples was calculated using the equation derived from standard curve, i.e., y=0.005x + 0.0107. The concentrations so obtained were 2.45 mg/ml for LbCd-0 and 2.49 mg/ml for LbCd-40.

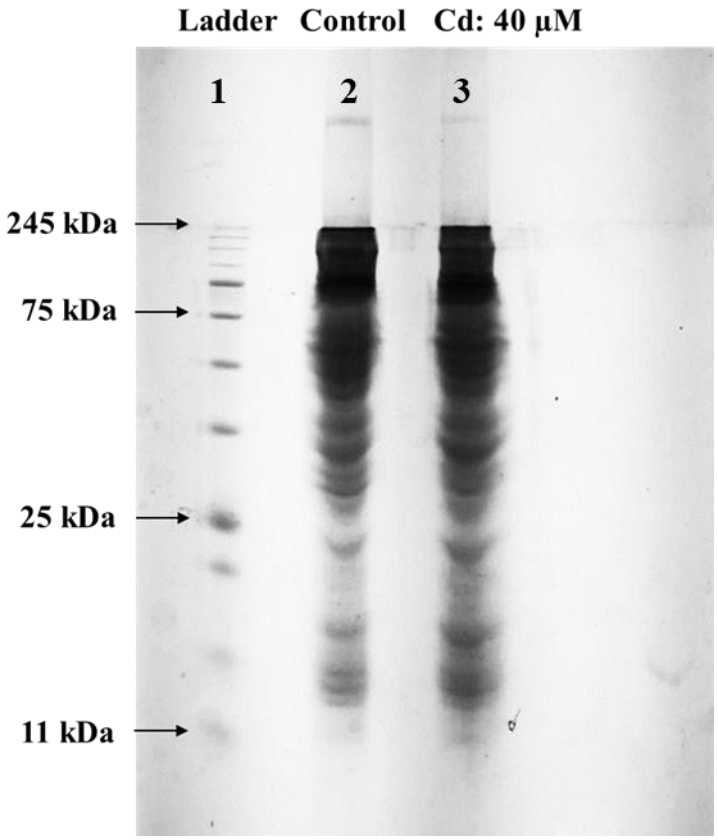

Figure 4.46: Agarose gel electrophoresis of total protein samples isolated from *L. bicolor* with and without Cd stress. Lane 1: ladder, lane 2: control (unstressed sample), lane 3: mycelium stressed with 40 µM Cd.

4.13 RP-LC ESI Q-TOF MSMS

The liquid chromatography mass spectroscopy using Electron spray ionizer and Quadrupole Time-of-flight analyzer was performed for both *L. bicolor* samples stressed with Cd 40 µM (LbCd-40) and unstressed (LbCd-0). The analysis resulted in isolating and identifying 1048 proteins in LbCd-0 and 1050 proteins in LbCd-40. Amongst them, 997 protein samples overlapped in both LbCd-0 and LbCd-40 and were used for comparative proteomic analysis. The fold change in the expression of each protein was calculated as the ratio of its quantities LbCd40:LbCd0. Amongst all the 997 proteins, the proteins with fold change more than 1.5 (upregulated) or less than -1.5 (down-regulated) were selected for proteomic analysis as "differentially expressed proteins" in response to Cd stress.

The differentially expressed proteins so obtained were then annotated through Gene Ontology (GO) analysis and their related metabolic pathways were studied using the KEGG classifications. The detected proteins were classified into various groups/categories based on their relative metabolic pathways as shown in Figure 4.47.

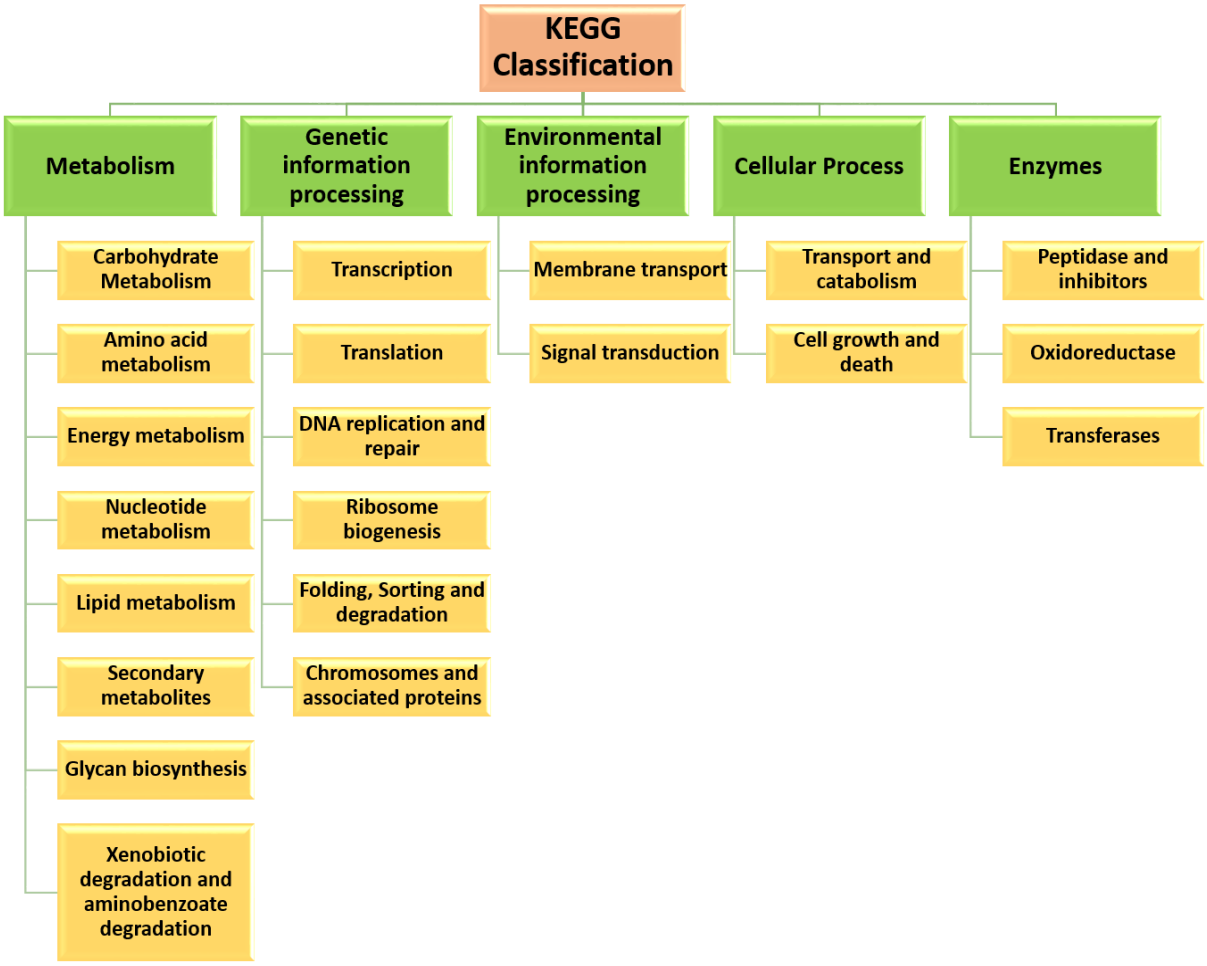

Figure 4.47: Different categories of KEGG classification based on the molecular functions of proteins.

The differentially expressed proteins were then classified into different categories based upon their annotated function in UniProt database and KEGG metabolic pathway.

4.13.1 Metabolism

a) Carbohydrate Metabolism

Carbohydrate metabolism is the fundamental process ensuring the constant supply of energy in living beings. Cd stress imposed various deleterious effects on the carbohydrate metabolism in ECM fungus *L. bicolor*. The expression of most of the enzymes involved in carbohydrate metabolism was down-regulated under Cd stress (Table 4.31). Glycolysis/gluconeogenesis pathway, pentose phosphate pathway, inositol phosphate metabolism, glyoxylate and dicarboxylate metabolism and starch and sucrose metabolism, were severely impaired under Cd stress. The down-regulation in these pathways indicate that the exposure to Cd induces energy stress in the ECM fungi and most of the energetic reserves are depleted to counter this stress. On the contrary, two enzymes involved in galactose pathway were up-regulated. Galactose is an important part of complex glycoproteins and polysaccharides involved in cell wall and cell membrane structures. The increase in galactose metabolism could be to support the energy demand and may contribute in rigidification of cell wall (Le Gall *et al.,* 2015). This imbalance between the increasing energy demand and weakness of glycolysis/gluconeogenesis pathway can be one of the major causes of Cd toxicity in ECM fungi.

Similar observations have been reported in *Lactobacillus plantarum* exposed to Cd (Zhai *et al.,* 2017). The comparative proteomic analysis of the bacteria in response to Cd, revealed a drastic downregulation in 24 proteins involved in carbohydrate metabolism, and only 2 proteins were found to be up-regulated (Zhai *et al.,* 2017). The impaired carbohydrate metabolism under Cd stress has also been reported in many fishes like *Cyprinus carpio, Rhamdia quelen, Sinopotamon yangtsekiense* (CiCiK and ENGiN, 2005; Xuan *et al.,* 2011; Pretto *et al.,* 2014; Yallapa and Nzhat, 2018) and plants like bean seeds, *Beta vulgaris* (Greger and Bertell, 1992; Sfaxi-Bousbih *et al.,* 2010). Apart from carbohydrate metabolism, the carbohydrate reserves are also depleted under Cd stress leading to high metabolic imbalance and failure of metabolic homeostasis (Zhai *et al.,* 2017; Yallappa and Nzhat, 2018). Therefore, we can say that the impairment in carbohydrate metabolism is one of the significant cause of Cd toxicity and growth inhibition.

Table 4.31: Differentially expressed proteins involved in carbohydrate metabolism

S.No.	Protein Id	Protein Name	Function	Fold change
1	POC034	Inositol-pentakis-phosphate 2-kinase	Inositol phosphate metabolism	-12.5
2	Q711G1	Glucose-6-phosphate isomerase	Glycolysis/Gluconeogenesis Pentose phosphate pathway Starch and Sucrose metabolism	-2.04
3	Q96UV5	Glutamine synthetase	Glyoxylate and dicarboxylate metabolism	-1.82
4	P32636	Glyceraldehyde-3-phosphate dehydrogenase	Glycolysis/Gluconeogenesis Pentose phosphate pathway	-1.73
5	O13439	Isocitrate lyase	Glyoxylate and dicarboxylate metabolism	-1.68
6	O94123	Phosphoglycerate kinase	Glycolysis/Gluconeogenesis	-1.64
7	W8QRE4	Beta-xylosidase	Amino sugar and nucleotide sugar metabolism	-1.63
8	P32861	UTP--glucose-1-phosphate uridylyltransferase	Starch and sucrose metabolism Galactose metabolism Amino sugar and nucleotide sugar metabolism	-1.59
9	P54424	Endoglucanase	Starch and sucrose metabolism	-1.58
10	P0CP76	Chitin deacetylase	Amino sugar and nucleotide sugar metabolism	-1.54
11	P0CL98	Probable actetate kinase	Pyruvate metabolism	-1.52
12	O13395	Chitin synthase	Amino sugar and nucleotide sugar metabolism	-1.50
13	P32895	Ribose-phosphate pyrophosphokinase 1	Pentose phosphate pathway	+1.51
14	Q870B9	Enolase	Glycolysis/Gluconeogenesis	+1.53
15	P29064	Alpha-glucosidase	Galactose metabolism	+1.55

16	P0CN77	Galactose-1-phosphate uridylyltransferase	Galactose metabolism	+1.61

b) Amino acid metabolism

Most of the differentially expressed proteins involved in amino acid metabolism were up regulated under Cd stress (Table 4.32). Cysteine, methionine, tyrosine, arginine, tryptophan, glycine, valine, leucine, isoleucine, lysine, phenylalanine, aspartate and glutamate metabolisms were actively induced in *L. bicolor* under Cd stress. Similar observations were made in a recent study to monitor the effect of Cd on amino acid profile of maize grains. Most of the amino acids like proline, valine, leucine, isoleucine, arginine, aspartate, tyrosine, threonine, glycine, alanine and phenylalanine were actively induced under Cd stress (Kato *et al.*, 2020).

Cysteine plays an important role in Cd tolerance. It is the precursor molecule in glutathione biosynthesis. The induction in cysteine biosynthesis genes has also been reported in *Arabidopsis* under Cd stress (Jia *et al.,* 2016). Increase in cysteine availability is a prerequisite for Cd tolerance and accumulation (Domínguez-Solís *et al.*, 2004).

In compositae plants *Ageratum conyzoides* L. and *Crassocephalum crepidioides,* high accumulation of free amino acids glutamine (Gln) and asparagine (Asn) have been associated with higher Cd tolerance and accumulation (Zhu *et al.*, 2018). Similar observations have also been recorded in tomato roots, where asparagine, glutamine and branched chain amino acids like valine, phenylalanine, isoleucine and tryptophan accumulated in response to Cd stress (Zoghlami *et al.*, 2011) and in *Noccaea* metallophytes, phenylalanine, tryptophan, threonine and ornithine accumulated in response to Cd stress (Zemanová *et al.*, 2017).

Amino acid metabolism has a significant role in providing heavy metal resistance (Zhu *et al.*, 2018). Cd toxicity perturbs the amino acid metabolism and the change in amino acid levels further plays a significant role in mitigating Cd stress (Zhu *et al.,* 2018). The possible reasons for this include: in plants, amino acids under stress conditions, serves as signaling molecules and plays other important roles like radical scavenger, osmolyte, ion transport regulators and modulates the stomatal openings to detoxify heavy metals (Sharma and Dietz, 2006; Xu *et al.,* 2012; Pavlíková *et al.,* 2014). In *Solanum nigrum* and *Solanum torvum,* high accumulation of hydroxyproline prevented Cd translocation form roots to the aerial parts (Xu *et al.,* 2012). Amino acids are also involved in synthesis of important metal binding ligands like glutathione

and phytochelatins involved in metal detoxification and homeostasis (Dave *et al.,* 2013; Asgher *et al.,* 2017). Amino acids also regulate the activity of enzymes, gene expression and redox-homeostasis (Chaffei-Haouari *et al.*, 2009; Islam *et al.,* 2009). According to Xuan *et al.*, (2011), during chronic period of stress, when there is limited amount of carbohydrates, proteins may be utilized to meet the increasing energy demands. Amino acids can be used as precursors for gluconeogenesis (Felig *et al.,* 1970).

Table 4.32: Differentially expressed proteins involved in amino-acid metabolism

S.No.	Protein Id	Protein Name	Function	Fold change
1	QO1752	Aryl-alcohol dehydrogenase	Tyrosine metabolism Phenylalanine metabolism	2.90
2	P09575	Multifunctional tryptophan biosynthesis protein	Tryptophan, phenylalanine and tyrosine metabolism	2.66
3	P0CO52	Kynureninase	Tryptophan metabolism	1.90
4	P78568	Delta-1-pyrroline-5-carboxylate dehydrogenase	Alanine, aspartate and glutamate metabolism	1.84
5	A8NEP3	Tryptophan synthase	Glycine, serine, threonine and tryptophan metabolism	1.83
6	B0DOU4	Methylthioribose-1-phosphate isomerase	Cysteine and methionine metabolism	1.81
7	B0CR45	Amino-acid acetyltransferase	Arginine biosynthesis	1.68
8	P0CS23	Urease	Arginine biosynthesis	1.65
9	Q5KPJ5	Acetolactate synthase	Valine, leucine and isoleucine metabolism	1.65
10	P35669	Glutathione synthetase	Cysteine and methionine metabolism	1.64
11	Q5KD76	1,2-dihydroxy-3-keto-5-methylthiopentene dioxygenase	Cysteine and methionine metabolism	1.54
12	Q4P521	Homoaconitase	Lysine biosynthesis	1.52
13	A7BHQ9	Tyrosinase	Tyrosine metabolism	1.51

14	A8NAN2	Arginine biosynthesis bifunctional protein ArgJ	Arginine biosynthesis	-1.53
15	Q01772	Aldehyde oxidase	Valine, leucine and isoleucine metabolism	-2.5

c) Nucleotide metabolism

Cd stress also impaired the nucleotide metabolism in *L. bicolor*. Most of the proteins involved in nucleotide biosynthesis were upregulated under Cd stress (Table 4.33). Out of the 9 differentially expressed proteins under Cd stress, 8 proteins were up-regulated whereas one protein was downregulated. This upregulation may support more DNA and mRNA biosynthesis in-order to cope up with Cd stress. The increased biosynthesis of nucleic acids under Cd stress has also been reported in that *Stigeocloni tenue,* where the concentration of nucleic acids increased under Cd stress (Vanaja *et al.,* 2000). Cd impaired both purine and pyrimidine metabolism in *L. bicolor*. The comparative proteomic analysis of *Lactobacillus plantarum* under Cd stress also highlighted the impairment in nucleotide metabolism. Most of the proteins involved in purine and pyrimidine metabolism were up-regulated under Cd stress. However, there is insufficient data to explain it on molecular basis.

Table 4.33: Differentially expressed proteins involved in nucleotide metabolism

S.No	Protein Id	Protein Name	Function	Fold change
1	P31301	Dihydroorotase	Pyrimidine metabolism	2.83
2	Q4P7R2	Adenylosuccinate synthetase	Purine metabolism	2.41
3	P15188	Orotidine 5'-phosphate decarboxylase	Pyrimidine metabolism	2.16
4	Q5KP44	Inosine 5'-monophosphate dehydrogenase	Purine metabolism	1.78
5	POCS23	Urease	Purine metabolism	1.65
6	Q4P763	GMP synthase [Glutamine-hydrolyzing]	Purine metabolism	1.56
7	A8PAA1	Adenylate kinase	Purine metabolism	1.54

8	O42644	CTP synthase	Pyrimidine metabolism	1.50
9	O59845	UMP-CMP Kinase	Pyrimidine metabolism	-1.53

d) Energy metabolism

The Cd exposure also affected the energy metabolism in *L. bicolor*. The up-regulation in proteins from nitrogen metabolism and oxidative phosphorylation implicated their contribution in Cd resistance of ECM fungi, whereas the ATP synthesis was down-regulated under Cd stress (Table 4.34). Three proteins involved in oxidative phosphorylation- NADH-ubiquinone oxidoreductase, Succinate dehydrogenase and V-type proton ATPase were upregulated under Cd stress. The change in oxidative phosphorylation proteins, might be the molecular mechanism for meeting the energy demand under Cd stress. The overexpression in energy metabolism proteins like NADH-dehydrogenase, succinate reductase and cytochrome C reductase under Cd stress has also been reported in *Lactococcus lactis* and *Pardosa pseudoannulata* (Sheng *et al.,* 2016; Yang *et al.,* 2018). The metatranscriptomic analysis of *Pardosa pseudoannulata* in response to Cd stress revealed 19 differentially expressed genes involved in oxidative phosphorylation so as to meet the increasing energy consumption and energy metabolism under Cd stress (Yang *et al.,* 2018). However, the ATP synthetase was highly down-regulated under Cd stress, thus limiting the ATP production. The decrease in ATP content has been directly linked to Cd accumulation in *Arabidopsis* (He *et al.,* 2019).

Table 4.34: Differentially expressed proteins involved in energy metabolism

S.No	**Protein Id**	**Protein Name**	**Function**	**Fold change**
1	Q96UJ9	NADP-specific glutamate dehydrogenase	Nitrogen metabolism	2.86
2	Q70KF8	Succinate dehydrogenase [ubiquinone] iron-sulfur subunit	Oxidative phosphorylation	1.68
3	QOH8X6	NADH-ubiquinone oxidoreductase chain 4	Oxidative phosphorylation	1.65
4	P53615	Carbonic anhydrase	Nitrogen metabolism	1.58

5	Q59PT0	V-type proton ATPase subunit B	Oxidative phosphorylation	1.52
6	POCN04	Sulfate adenylyl transferase	ATP synthesis and sulfur metabolism	-1.62
7	Q92196	ATP synthase subunit delta	ATP synthesis	-6.25

e) Glutathione metabolism

Upregulation in all proteins involved in glutathione biosynthesis and metabolism was recorded in *L. bicolor* under Cd stress (Table 4.35). Glutathione is the first line of defense against Cd toxicity in plants, mammals, bacteria, yeast and fungi (Garg and Aggarwal, 2011; Tarhan and Kavakcioglu, 2016; Ding *et al.,* 2017; Lou *et al.,* 2017; Nikolić *et al.,* 2019). Glutathione biosynthesis is immediately induced when the cell is exposed to Cd stress (Zheng *et al.,* 2018). The expression of glutathione synthetase increased by 1.6 folds under Cd stress thus inducing the glutathione synthesis and accumulation in *L. bicolor* so as to mitigate Cd toxicity.

Glutathione shows a dual protection mechanism under metal stress- it acts as a metal scavenger during metal homeostasis and as an antioxidant during oxidative stress. As a metal scavenger, GSH binds Cd forming a $Cd(GSH)_2$ complex by the enzyme glutathione-S-transferase, which is compartmentalized into the vacuoles (Adamis *et al.,* 2007; Mendoza-Cózatl *et al.,* 2011; Oestreicher and Morgan, 2018). As an antioxidant, it eliminates ROS by reducing the harmful free radicals and itself gets oxidized to GSSG. This reduction of free radicals and oxidation of GSH to GSSG is mediated by glutathione peroxidase. The oxidized GSSG is then again converted to GSH by glutathione reductase. Both glutathione-S-transferase and glutathione reductase/glutathione peroxidase were up regulated in *L. bicolor* under Cd stress. Glutathione-S-transferase significantly increased by 1.7 folds, glutathione reductase by 1.8 folds and peroxidase by 1.7 folds under Cd stress. This shows that in *L. bicolor*, GSH mitigates Cd toxicity by eliminating the ROS and sequestering the metal away into the vacuoles.

Table 4.35: Differentially expressed proteins involved in glutathione metabolism

S.No	Protein Id	Protein Name	Function	Fold change
1	Q02784	Monothiol glutaredoxin-5	Glutathione metabolism	1.84
2	Q6BPI1	Glutathione reductase (NADPH)	Glutathione metabolism	1.83
3	C9SG98	L-ascorbate peroxidase	Glutathione metabolism	1.75
4	P30102	Glutathione-S-transferase	Glutathione metabolism	1.71
5	P35669	Glutathione synthetase	Glutathione metabolism	1.64

f) Metabolism of terpenoids and polyketides

Terpenoids and polyketides are the bioactive secondary metabolites with antitumor, antibacterial, hypoglycemic, immunosuppressive and neuroprotective effects. The Cd toxicity down regulated the metabolisms involved in terpenoid and polyketide biosynthesis in *L. bicolor* under Cd stress (Table 4.36), thus, making the ECM fungi feeble.

Table 4.36: Differentially expressed proteins involved in metabolism of terpenoids and polyketides

S.No	Protein ID	Protein Name	Function	Fold change
1	A0A2L0VXR5	Geranylgeranyl pyrophosphate synthase	Terpenoid backbone biosynthesis	-1.50
2	S0DQN6	FAD-dependent monooxygenase fsr3	Polyketide biosynthesis	-1.50
3	A0A0U3C228	Flavin-dependent halogenase armH5	Biosynthesis of enediyne antibiotics	-1.52
4	A0A286LEZ6	4-hydroxytryptamine kinase	Indole alkaloid biosynthesis	-1.63
5	Q4WB01	Cytochrome P450 monooxygenasepsoD	Diterpenoid biosynthesis	-1.64
6	G9BIY1	Diphosphomevalonate decarboxylase	Terpenoid backbone biosynthesis	-2.03

7	O42641	Isopentenyl-diphosphate Delta-isomerase	Terpenoid backbone biosynthesis	-2.78

4.13.2 Genetic information processing

Genetic information processing includes transcription, translation, DNA replication, DNA repair, protein folding and sorting and chromosome formation. Cd stress altered all the mechanisms involved in genetic information processing in ECM fungus *L. bicolor*.

a) Trascription and translation

Cd toxicity uncouples the transcription and translation process in plant cell (Sormani *et al.*, 2011). This is one of the major causes of Cd induced carcinogenesis (Waisberg *et al.*, 2003). In *L. bicolor*, most of the proteins involved in transcription machinery were down-regulated under Cd stress, whereas the proteins involved in translation machinery were up-regulated (Table 4.37, Table 4.38). The imbalance so created can be a possible cause of Cd toxicity in *L. bicolor*. Even in *E. coli*, the transcription machinery was highly disrupted under Cd stress (Wang and Crowley, 2005). The higher expression of translation factors in mice has also been associated with the Cd carcinogenesis (Joseph *et al.*, 2009). However, the up-regulation in translation machinery may also be related to more protein biosynthesis to mitigate the toxic effects of Cd. The up-regulation in proteins involved in RNA biogenesis also supports the induction of translation machinery.

Table 4.37: Differentially expressed proteins involved in translation process

S.No	Protein ID	Protein Name	Function	Fold change
1	Q4P7G1	Eukaryotic translation initiation factor 3	mRNA biogenesis	3.56
2	A8N8S3	Glutamyl-tRNA(Gln) amidotransferase subunit A	Aminoacyl-tRNA biosynthesis	2.69
3	P0CQ55	37S ribosomal protein S10	Ribosome	2.36
4	P0CN33	Elongation factor Ts	Translation factors	1.88

5	P0CN33	Elongation factor G	Translation factors	1.73
6	P0CQ45	RNA exonuclease 4	Ribosome biogenesis	1.59
7	Q4P8R9	Polyadenylate-binding protein	RNA transport	1.55
8	A8Q513	Exportin-T	RNA transport	-1.85

Table 4.38: Differentially expressed proteins involved in transcription process

S.No	**Protein ID**	**Protein Name**	**Function**	**Fold change**
1	Q4P2Q5	U1 small nuclear ribonucleoprotein C	Spliceosome	1.73
2	Q01877	Heat shock protein HSS1	Spliceosome	1.68
3	P0CO39	Transcription factor IWS1	Transcription machinery	-1.58
4	A8PT44	Ribosome biogenesis protein YTM1	Ribosome biogenesis	-1.67
5	Q4P101	RNA polymerase II holoenzyme cyclin-like subunit	Transcription machinery	-2.00
6	Q12753	Transcriptional activator HAA1	Transcription machinery	-2.23
7	P54785	Transcriptional activator/repressor MOT3	Transcription machinery	-2.41
8	B5VGZ3	Transcription factor STP1	Transcription machinery	-2.50

b) DNA replication and repair

Cd also impairs DNA replication and repair machinery, thus inducing genomic instability and leading to carcinogenesis (Wang *et al.,* 2016; Hartwig, 2018). Cd interfere with the DNA repair system and also inactivates the tumor suppressor genes. Proteins with zinc-binding structures, like transcription factors, tumor suppressor protein p53 and DNA repair proteins are primary sensitive target under Cd stress (Hartwig, 2018). In *L. bicolor* most of the genes involved in DNA replication and repair were impaired under Cd stress (Table 4.39). Cd inhibited nucleotide excision repair mechanisms, base excision repair, gap filling pathways etc, thus decreasing the DNA repair tendencies causing toxicity in the cells. DNA ligase plays an important role in DNA replication and repair by forming phosphodiester bonds in DNA (Yang *et al.,* 1996) and DNA helicase unwinds double stranded DNA during replication. The expression of both helicase and ligase were altered in *L. bicolor* under Cd stress.

The proteomic analysis of *Crassostrea gigas* in response to Cd also highlighted the inhibition of DNA glycosylase, DNA ligation enzymes, gap-filling, base excision repair pathway thus decreasing the DNA repair capacity (Meng *et al.,* 2017). The effect of Cd toxicity on genetic information processing has also been reported in *Triticum urartu* (Qiao *et al.,* 2019). Most of the differentially expressed proteins under Cd stress were related to ribosome biogenesis, DNA replication, DNA repair, DNA binding, DNA conformation, chromatin assembly or disassembly and DNA packaging (Qiao *et al.,* 2019). The expression of genes coding helicase, DNA polymerase, DNA ligase and mini chromosome maintaining protein (MCM) was down-regulated under Cd stress. Cd can also cause single or double strand breakdown in DNA (Zhang *et al.,* 2019).

Table 4.39: Differentially expressed proteins involved in DNA replication and repair

S.No	Protein ID	Protein Name	Function	Fold change
1	P14746	DNA repair exonuclease REC1	DNA repair	2.67
2	P0CQ32	DNA replication complex GINS protein PSF3	DNA replication	1.83

3	P0CO50	ATP-dependent DNA helicase II subunit 1	DNA Replication and repair	1.61
4	A8N936	DNA ligase 4	DNA replication and repair	1.54
5	P10862	Post replication repair E3 ubiquitin protein ligase RAD18	DNA repair	-1.51
6	P0CR93	Topoisomerase 1-associated factor 1	DNA repair	-1.55
7	P41511	DNA topoisomerase 1	DNA replication	-1.55
8	P26659	General transcription and DNA repair factor IIH helicase	DNA repair	-1.55
9	P0CN25	DNA polymerase epsilon subunit B	DNA replication Nucleotide excision repair	-1.68
10	Q4P1V1	Flap endonuclease 1	DNA replication Base excision repair	-2.54

c) Chromosomal assemblies

Cd induces abnormalities in chromosomes have been reported in many studies (Wang *et al.,* 2017; Pizzaia *et al.,* 2019). In *L. bicolor*, the proteins involved in chromosome assembly like chromatin remodeling factors, histone modification proteins and nucleosome assembly factors were impaired under Cd stress (Table 4.40). The proteins involved in centrosome formation, centromeric chromatin formation and chromatin remodeling were up-regulated whereas the proteins involved in Histone modification and nucleosome assembly were down-regulated under Cd stress. Thus, disturbing the chromosomal formations, leading to genetic instability in *L. bicolor* under Cd stress. In a recent study on tomato plant, Cd toxicity caused various chromosomal abnormalities like chromosome lost, polyploidy, bridges and C-metaphase and chromosomal stickiness and effects polarization of spindle fibres, non-uniform tubulin deposition etc (Pizzaia *et al.,* 2019). It also induces mitosis and micronuclei in *Allium cepa* (Wang *et al.,* 2017).

Table 4.40: Differentially expressed proteins involved in Chromosome assemblies

S.No	Protein ID	Protein Name	Function	Fold change
1	**P0CO96**	SWR1-complex protein 4	Chromatin remodeling factors	2.18
2	**P38219**	Obg like ATPase 1	Centrosome formation and ciliogenesis proteins	2.05
3	**P0CP41**	Kinetochore protein NUF2	Centromeric chromatin formation proteins	1.58
4	**P0CO17**	Chromatin-remodeling ATPase IN080	Chromatin remodeling factors	1.58
5	**P0CP02**	Histone acetyltransferase ESA1	Histone modification proteins	-1.50
6	**P0CO98**	Chromatin modification related protein EAF1	Histone modification proteins	-1.51
7	**P0CO05**	Histone H3	Histone modification proteins	-1.52
8	**Q4PBU8**	Histone chaperone ASF1	Nucleosome assembly factors	-3.54

d) Protein folding, sorting and degradation

Cd also impairs the expression of proteins involved in protein folding, sorting and degradation (Tamás *et al.*, 2018). In most of the proteins, Cd induces toxicity by inducing misfolding and aggregation of nascent proteins (Jacobson *et al.*, 2017) by two ways: firstly, it has high affinity for the thiol group of cysteine, therefore binds proteins at cysteine residue causing misfolding. Secondly, it impairs the expression of proteins involved in protein folding, sorting and degradation. Cd damages the endoplasmic reticulum, thus causing protein unfolding or misfolding (Gardarin *et al.*, 2010; Le *et al.*, 2016). Even in *L. bicolor*, most of the proteins involved in "protein processing in endoplasmic reticulum" were down-regulated under Cd stress (Table 4.41), indicating that Cd was also a strong endoplasmic reticulum stress inducer in *L. bicolor*. However, the expression of heat-shock proteins involved in protein folding was up-regulated under Cd stress. Heat shock proteins (Hsp) are the important component of

molecular chaperons and are actively involved in variety of protein folding processes. Therefore, their up-regulation indicate that excess Cd induces protein folding in cytosol, mitochondria and ER in *L. bicolor*. Hsp proteins are also involved in maintaining protein homeostasis (Meng *et al.,* 2017). Therefore, the up-regulation in Hsp70 proteins may also help *L. bicolor* in maintaining cellular homeostasis under Cd stress. Similar observations have been made by Lee *et al.,* (2010) in rice plant exposed to Cd and in *Crassostrea gigas* (Meng *et al.,* 2017).

Table 4.41: Differentially expressed proteins involved in protein folding, sorting and degradation

S.No	Protein ID	Protein Name	Function	Fold change
1	Q4P7G1	Eukaryotic translation initiation factor 3	Protein processing in endoplasmic reticulum	3.56
2	Q4P0V4	Peptidyl-prolyl cis-trans isomerase D	Protein folding catalysts	2.01
3	P0CP92	Peptidyl-prolyl isomerase CWC27	Protein folding catalysts	1.68
4	Q01877	Heat shock protein HSS1	Protein processing in endoplasmic reticulum	1.55
5	Q4P7F2	Hsp70 nucleotide exchange factor FES1	Protein folding	1.51
6	P0CS71	Cytoplasmic tRNA 2-thiolation protein 1	Sulfur relay system	-1.56
7	P0CR40	Protein transport protein SEC24	Protein processing in endoplasmic reticulum	-1.61
8	P0CR30	Small COPII coat GTPase SAR1	Protein processing in endoplasmic reticulum	-1.82

4.13.3 Environmental information processing

a) Signal transduction

Cd induces reactive oxygen species (ROS) formation inside the cells (Heyno *et al.,* 2008; Cuypers *et al.,* 2010). These ROS molecules have been implicated as the initial signal in Cd signal transduction pathway (Rodríguez-Serrano *et al.,* 2009). The ROS induces the redox signaling pathway to transfer signal from different parts of cell to nuclei so as to regulate: Cell growth, proliferation, differentiation and apoptosis (Nemmiche *et al.,* 2016). The most actively induced pathway under Cd stress was "Mitogen activated protein kinase (MAPK) signaling pathway". MAPK pathway also regulates the cell wall integrity and promotes homeostasis in fungi (Esquivel-Naranjo *et al.,* 2016). In *L. bicolor,* most of the proteins involved in MAPK stress were actively induced (up-regulated) in response to Cd stress (Table 4.42). The induction in MAPK pathway lead to higher Cd tolerance in *Schizosaccharomyces pombe* and *Trichoderma atroviride* (Zhou *et al.,* 2010; Guo *et al.,* 2012; Esquivel-Naranjo *et al.,* 2016).

The role of MAPK signaling pathway in generating Cd tolerance was studied in *T. atroviride*, where the MAPK mutants could not grow at 250 mM Cd whereas the wild type grew well (Esquivel-Naranjo *et al.,* 2016). The triggered MAPK pathway under metal stress has also been reported in many plants (Sytar *et al.,* 2013). The up-regulation in MAPK and other signaling pathways has also been related to induction of cellular defense system in response to Cd stress (Bryan *et al.,* 2013; Shinkai *et al.,* 2016). The interaction of thiol molecules with Cd and the build-up of ROS in response to Cd, triggers the activation of MPK3 (mitogen-activated protein kinase 3) and MPK6 (mitogen-activated protein kinase 6) in *Arabidopsis* (Liu *et al.,* 2010). Thus, we can say that the upregulation in signaling pathways can be defense initiative in ECM fungi to mitigate the Cd toxicity.

Table 4.42: Differentially expressed proteins involved in Signal transduction

S.No	Protein ID	Protein Name	Function	Fold change
1	P87033	Guanine nucleotide-binding protein alpha-2	Rap1 signaling pathway Apelin signaling pathway Sphingolipid signaling pathway cAMP signaling pathway cGMP-PKG signaling pathway	6.36
2	M1T7M3	Mitogen-activated protein kinase	MAPK signaling pathway ErbB signaling pathway MAPK signaling pathway - fly Ras signaling pathway Rap1 signaling pathway cGMP-PKG signaling pathway cAMP signaling pathway Chemokine signaling pathway HIF-1 signaling pathway FoxO signaling pathway Sphingolipid signaling pathway Phospholipase D signaling pathway	3.15
3	B0CRU6	Fe-S cluster assembly protein DRE2	Signaling proteins	2.09
4	ATTM15	V-type proton ATPase subunit F	mTOR signaling pathway	2.01
5	Q4P9Q7	High osmolarity signaling protein SHO1	MAPK signaling pathway	1.72
6	Q05659	Pheromone B alpha 2 receptor	MAPK signaling pathway	1.64

7	P33748	Zinc finger protein MSN2	MAPK signaling pathway	1.58
8	P84339	Calmodulin	Ras signaling pathway Rap1 signaling pathway MAPK signaling pathway - plant Calcium signaling pathway cGMP-PKG signaling pathway cAMP signaling pathway Phosphatidylinositol signaling system	1.55
9	Q99078	Dual specificity protein kinase FUZ7	MAPK signaling pathway	1.53
10	P0CM16	ADP-ribosylation factor	Phospholipase D signaling pathway	1.51
11	P18694	Heat shock 70kDa protein	MAPK signaling pathway	1.50
12	Q9UQX0	Superoxide dismutase [Mn]	FoxO signaling pathway	-1.59

b) Membrane transport and trafficking, Cell growth and death

Cd toxicity disturb cell's homeostasis and cellular functions by altering the intracellular transport system, vesicular trafficking, cell growth and death (Wan and Zhang, 2012). Intracellular transport and vesicular trafficking are critical for transport of membrane bound vesicles to different parts of cell, endocytosis and exocytosis. In *L. bicolor*, most of the proteins involved in membrane transport were upregulated under Cd stress. ABC transporters are actively involved in compartmentalizing Cd-$(GSH)_2$ molecules to vacuoles. Thus, up-regulation of ABC transporters in *L. bicolor* helps in mitigating Cd toxicity by compartmentalizing Cd molecules in vacuoles (Table 4.43).

Another most influenced area under Cd stress in *L. bicolor* is Golgi apparatus. The 12.18 folds increase in the expression of Golgi apparatus membrane protein TVP38 along with the Golgi apparatus transporters (GDP-mannose transporter, Protein SEY1) was recorded under Cd stress (Table 4.43). This observation throws light on the fact that apart from vacuoles, Golgi apparatus might be another site for Cd sequestration in *L. bicolor*. There are few reports on localization

of Ca^{2+} and Mn^{2+} into the Golgi apparatus through Ca/Mn-ATPase transporters. Golgi apparatus sequester these metals (Ca/Mn) into secretory vesicles, which subsequently get released (Van Baelen *et al.*, 2004; Xiang *et al.,* 2005). Even in yeast *Saccharomyces cerevisiae*, Ca-ATPase, Pmr1p of Glogi apparatus played a central role in the secretion of Cd through the vesicle secretion pathway (Lauer Júnior *et al.,* 2008). In a recent study on mycorrhizal plants, HMs can be sequestered in cell wall, vacuoles and Golgi apparatus in plants. However, these studies are limited to Mn^{2+} accumulation in Golgi apparatus (Shi *et al.,* 2019). More is to be investigated for Cd sequestration in Golgi apparatus as it can be a powerful tool in mitigating Cd toxicity in ECM fungi.

Cd induced toxicity in *L. bicolor* by upregulating the proteins involved in autophagy, apoptosis, phagosome and peroxisome (Table 4.43). Cd induced autophagy and apoptosis has been well reported in fungus, *Oudemansiella radicata* (Li *et al.,* 2019), mammalin- Mesangial cells (MES-13) (Wang *et al.,* 2008), endothelial cells (Messner *et al.,* 2016;), plants- *Arabidopsis* (Calero-Muñoz *et al.,* 2019), wheat (Yue *et al.,* 2018). Autophagy is the highly sophisticated and well-regulated degradation pathway for degrading or recycling the cytosolic components into the vacuoles. Under Cd stress, autophagy acts like a protective mechanism to help organisms survive the adverse conditions.

Table 4.43: Differentially expressed proteins involved in membrane transport, trafficking, cell growth and death.

S.No	Protein ID	Protein Name	Function	Fold change
1	A8NX72	Golgi apparatus membrane protein TVP38	Vesicular trafficking and spindle migration	12.18
2	B0D0T8	Transcription activator of gluconeogenesis ERT1	Peroxisome	3.71
3	B0DI84	GDP-mannose transporter	Imports GDP-mannose from the cytoplasm into the Golgi lumen	3.15
4	Q6CPE2	Superoxide dismutase [Cu-Zn] family	Peroxisome	2.02

5	Q4P4N1	Autophagy-related protein 18	Autophagy	1.99
6	Q4P4N1	Autophagy-related protein 18	cytoplasm to vacuole transport vesicle formation starvation-induced autophagy	1.94
7	Q8J112	Electron transfer flavoprotein subunit alpha	Exosomes	1.71
8	B0D0N9	Protein SEY1	Endoplasmic reticulum (ER) - Golgi transport	1.70
9	P0CR44	Phosphatidylinositol transfer protein SFH5	Exocytosis	1.69
10	Q10185	ATP-binding cassette transporter abc2	ABC transporter	1.68
11	Q9HFQ3	Tubulin beta chain	Phagosome Apoptosis	1.68
12	P0CO68	Mitochondrial distribution and morphology protein 12	Mitochondrial protein import machinery ER-mitochondria encounter structure (ERMES) complex	1.67
13	P0CM35	Autophagy-related protein 3	Cytoplasm to vacuole transport Autophagy	1.65
14	Q4PA36	Vacuolar fusion protein MON1	Autophagy Lysosome transport	1.61
15	P0CM60	Vacuolar protein 8	Autophagy	1.58
16	P0CM17	ADP-ribosylation factor	Endocytosis	1.55
17	P0CM32	Autophagy-related protein 22	Autophagy	1.54

18	P0CM35	Autophagy-related protein 3	Autophagy	1.52
19	P41909	Peroxisomal long-chain fatty acid import protein 2	ABC transporter	1.52
20	P49742	Tubulin alpha-1B chain	Phagosome Apoptosis	1.52
21	Q99128	AP-1 complex subunit gamma-1	Endosome - Golgi transport	1.51
22	P0CR62	Sorting nexin 4	Endocytosis	-1.51
23	A8NU18	24 kDaRas-like protein	GTP-binding proteins Endocytosis	-1.55
24	Q4P7J4	Mitochondrial fission 1 protein	Mitochondrial quality control factors	-1.74
25	A1A653	Fe-regulated protein 8	Transporter-siderophore	-1.78
26	P0CP32	UDP-galactose transporter homolog	Nucleoside-sugar transporter	-1.96
27	A8Q0M1	ATPase GET3	arsenite/tail-anchored protein-transporting ATPase	-1.96
28	P0CR78	Class E vacuolar protein-sorting machinery protein HSE1	Sorting receptor for ubiquitinated cargo proteins	-3.84

4.13.4 Response to oxidative stress

Oxidative stress is one of the most important mechanism attributed to Cd toxicity. Cd stress leads to accumulation of ROS like superoxide, hydroxyl radical and hydrogen peroxide in cells. These free radicals cause drastic cellular damage. ECM fungi have developed mechanisms to cope with these ROS, by synthesizing various metal scavengers and antioxidants. The antioxidant defense system can be classified into two categories: enzymatic defense system which includes catalases (CAT), peroxidases, superoxide dismutase (SOD), polyphenol oxidase, ascorbate peroxidase (APX) etc., and the non-enzymatic defense system which includes ascorbate, glutathione etc.

The cellular redox homeostasis in cell is basically maintained by SOD by converting O_2^- ions into H_2O_2. The H_2O_2 molecules so formed are subsequently reduced to H_2O by CAT, GSH and APX resulting in oxidation of ascorbate to ASA and GSH to GSSG. The GSH is again regenerated from GSSG by glutathione reductase using NADPH as an electron donor. This process is involved in maintaining the cellular redox equilibrium resulting in high GSH/GSSG ratio (Gill *et al.,* 2013; Hernández *et al.,* 2015). Under metal mediated oxidative stress, all these enzymes involved in maintaining cellular redox are highly affected.

The expression of all the enzymes involved in mitigating oxidative response and maintaining cellular redox homeostasis were found to be highly up-regulated in *L. bicolor* under Cd stress (Table 4.44). Twelve molecules involved in mitigating oxidative stress, which include: Superoxide dismutase [Mn], Polyphenol oxidase (PPO), Monothiol glutaredoxin, Cell surface superoxide dismutase, Carbonic anhydrase, peroxisomal catalase, AP1-like transcription factor YAP2 (cad1), Cytochrome c peroxidase, NADH-ubiquinone oxidoreductase, O-methyltransferase imqG, Glutathione reductase (NADPH) and L-ascorbate peroxidase were up-regulated under Cd stress. Similar results have been reported in many plants like *Arabidopsis thaliana* (Jozefczak *et al.,* 2014), *Lolium perenne* (Luo et al 2011), Rice (Afzal *et al.,* 2019), *Kandelia obovate* (Pan *et al.,* 2020) etc. The activity of glutathione reductase was highly induced by Cd stress in alfalfa plant (Sobrino-Plata *et al.,* 2009) and by As in *Silene vulgaris* (Sobrino-Plata *et al.,* 2013).

The 11.82 folds increase in expression of polyphenol oxidase was recorded in *L. bicolor* under Cd stress (Table 4.44). PPO plays an important role in heavy metal detoxification. In plants, they have been actively involved in metal accumulation (Lavid *et al.,* 2001; Kundu *et al.,* 2018). In *Nymphoides peltate* and *Nymphaeae,* PPO stimulates the trapping of Cd molecules by polymerized phenols thus leading to Cd accumulation in plants (Lavid *et al.,* 2001). Apart from metal accumulation, PPO also plays an important role in phenolic compound synthesis, which are actively involve in heavy metal detoxification, neutralizing free radicals, quenching singlet oxygen and decomposing peroxides (Michalack, 2006; Zheng *et al.,* 2010). Polyphenol accumulation in plants is the robust mechanism to fight and adapt against metal stress (Kováčik and Bačkor, 2007). Under stress conditions, PPO is also involved in repairing damaged cells (Mayer, 2006). The increase in activity of PPO under Cd stress has also been reported in many plants like *Arabidopsis thaliana* (Saffar *et al.,* 2009), *Glycyrrhiza uralensis* (Zheng *et al.,*

2010), *Chamomile* (Kováčik and Bačkor, 2007), *Hydrilla verticillata* and *Ceratophyllum demersun* L. (Li *et al.*, 2018; Zhang *et al.*, 2020).

Apart from these, few metal binding proteins like: Metal binding activator 1, Putative heme-binding peroxidase, Heavy metal tolerance protein hmt1, Multicopper oxidase terE, Cytochrome c peroxidase and Glutathione-S-transferase were also up-regulated under Cd stress (Table 4.44). The ATP binding cassette (ABC) transporter abc2, V-type proton ATPase subunit B, that facilitates the compartmentalization of Cd into the vacuoles were also up-regulated. The ATP binding cassette mediates the transport of GSH sequestered metals into the vacuoles (Song *et al.*, 2014; Basu *et al.*, 2019). The role of ABC transporters vacuolar sequestration of glutathione-metal complex has been reported in *Saccharomyces cerevisiae*, *Schizosaccharomyces pombe* and many plants (Song *et al.*, 2014).

Apart from these various stress responsive proteins like heat shock proteins (70 Kda and HSS1), zinc finger protein MSN2 were also up-regulated in ECM fungi as a response to Cd stress (Table 4.44). Zinc finger proteins regulates the Cd tolerance by directly inducing the glutathione pathway. In a recent study on *Arabidopsis*, zinc finger transcription factor (ZAT6) was characterized for its role in providing Cd tolerance by positively regulating the transcription of *GSH1* and *GSH2* genes. Plants overexpressing ZAT6 genes were accumulated more Cd and were more tolerant to metal stress than the wildtype (Chen *et al.*, 2016).

The up-regulation in all these proteins involved in eliminating the ROS, suppressing the oxidative stress and chelating Cd molecules highlights response of ECM fungus *L. bicolor* in mitigating Cd toxicity.

Table 4.44: Differentially expressed proteins expressed in response to oxidative stress

S.No	Protein ID	Protein Name	Function	Fold change
1	O42713	Polyphenol oxidase	Metal detoxification	11.82
2	Q6C7U1	Putative heme-binding peroxidase	Destroy radicals toxic to biological system	2.29
3	Q6CPE2	Superoxide dismutase [Mn]	Destroy superoxide anion radicals	1.99

4	Q02784	Monothiol glutaredoxin	Protect cells against oxidative damage due to ROS	1.84
5	Q6BPI1	Glutathione reductase (NADPH)	Neutalize free radicals	1.83
6	C9SG98	L-ascorbate peroxidase	Neutralize free radicals	1.75
7	P30102	Glutathione-S-transferase	Help forming GSH-metal complex	1.71
8	Q10185	ATP binding cassette transporter abc2	Vacuolar sequestration of Glutathione-S-conjugates	1.68
9	Q5ACV9	Cell surface superoxide dismutase	Converts superoxides to less damaging peroxides	1.66
10	P35192	Metal binding activator 1	Regulatory protein involved in Cu/Fe utilization and stress resistance	1.59
11	P53615	Carbonic anhydrase	Protection against oxidative stress	1.58
12	Q02592	Heavy metal tolerance protein hmt1	Involved in metal tolerance, transport of metal-bound phytochelatins/glutathione and compartmentalizing Cd in vacuoles	1.58
13	Q0D1P3	Multicopper oxidase terE	Mediate biosynthesis of terrein (fungal metabolite with ecological, antimicrobial and antioxidant activities)	1.56
14	P07820	Peroxisomal catalase	Protect cells from toxic effects of hydrogen peroxide	1.55

15	P24813	AP1-like transcription factor YAP2 (cad1)	Transcription activator involved in oxidative stress response and Cd resistance	1.54
16	B8NI24	O-methyltransferase imqG	Mediate biosynthesis of imizoquins (alkaloids that protect against oxidative stress	1.53
17	Q08422	AN1-type zinc finger protein TMC1	Protect cells from metalloid induced proteotoxicity	1.52
18	Q59PT0	V-type proton ATPase subunit B	Promotes intracellular compartmentalization and protect from various stress	1.52
19	P33748	Zinc finger protein MSN2	Transcription factor for stress responsive system, recognize and bind stress response elements	1.51
20	Q6CAB5	Cytochrome c peroxidase	Destroy toxic radicals	1.50

4.14 Conclusion to proteomic analysis

Cadmium imposes high toxicity in ECM fungi by creating imbalance in carbohydrate metabolism, amino acid metabolism, nucleotide metabolism, energy metabolism and lipid metabolism. It impairs the genetic information processing in ECM fungi by uncoupling the transcription and translation machineries, DNA replication and repair system, protein folding and chromosome formation, thus causing high carcinogenicity. Cd also induces ROS formation in ECM fungi leading to oxidative stress in ECM fungi. The ECM fungi confront this oxidative challenge by up-regulating the expression of various enzymes, antioxidants and glutathione metabolism and by instigating the signaling pathways.

SUMMARY

Ectomycorrhizal (ECM) fungi are well known for protecting the host plant from various biotic and abiotic stresses. They are highly tolerant to heavy metals. They accumulate heavy metals and mitigate them, thus preventing their transfer to the host plant. However, the regulatory mechanisms and the defense strategies involved in metal tolerance in ECM fungi are still unknown. The present study aims at investigating the response to ECM fungi, *L. bicolor* and *H. cylindrosporum* to heavy metals Cadmium (Cd) and Arsenic (As) at molecular level. When exposed to Cd and As, both *L. bicolor* and *H. cylindrosporum* accumulated these metals into the cytosol. The accumulated metals having high affinity for the thiol group of GSH, depletes the active GSH, thus inducing the glutathione biosynthesis pathway. The two enzymes involved in GSH biosynthesis- γ-glutamylcysteine synthetase (γ-GCS) and glutathione synthetase (GS) were actively induced under both Cd and As stress, thus increasing the intracellular GSH concentration. The effect of total GSH accumulation inside the cell increased as the function of external metal stress. The effect of Cd and As on expression of both genes involved in GSH biosynthesis- γ-GCS and GS was studied qPCR. The expression of both genes was actively induced as a function of external Cd and As concentration. The functional complementation of GSH biosynthesis genes in their respective yeast mutants successfully restored their metal tolerance tendencies, thus clearly depicting the central role of GSH biosynthesis in mitigating Cd and As toxicity in both *L. bicolor* and *H. cylindrosporum*.

Further, the proteomic analysis of ECM fungi, *L. bicolor* in response to Cd, provided deep insight into the mechanisms of Cd toxicity, regulatory mechanisms/metabolic pathways associated with Cd stress and the response of ECM fungi in mitigating these toxic effects. The comparative proteomic analysis of *L. bicolor* (LbCd-0 and LbCd-40) using LCMS-ESI-qTOF-MS/MS analysis revealed 997 differentially expressed proteins under Cd stress. The differentially expressed proteins were then subjected to Kyoto Encyclopedia of Genes and Genomes (KEGG) analysis and annotated based on their gene ontology.

The KEGG analysis revealed various metabolisms and pathways influenced by Cd stress. Cd induced toxicity in *L. bicolor* by impairing various metabolism like carbohydrate metabolism, amino acid metabolism, nucleotide metabolism and energy metabolism. Cd down-regulated the carbohydrate metabolism, inducing energy stress and depleting the energetic reserves, leading to metabolic imbalance. It also perturbs the amino acid metabolism. Most of the proteins involved in amino acid metabolism and biosynthesis were up-regulated under Cd

stress. The changes in amino acid levels further plays a significant role in mitigating Cd stress. Cd also up-regulates the nucleotide metabolism so as to support more DNA and RNA biosynthesis under stress conditions. The increasing energy demands under Cd stress were fulfilled by enhancing the proteins involved in energy metabolism. The proteins involved in nitrogen metabolism and oxidative phosphorylation were up-regulated under Cd stress. However, Cd toxicity down-regulated the proteins involved in ATP synthesis.

Cd also altered the genetic information processing in *L. bicolor* by uncoupling the transcription and translation machineries, DNA replication and repair system, protein folding and chromosome formation, thus inducing genetic instability leading to carcinogenesis. The signal transduction pathways were also up-regulated under Cd stress. The up-regulation in signaling pathways can be the defense initiative in ECM fungi to mitigate Cd toxicity.

Cd toxicity also disturb the cell's homeostasis and cellular functions by altering the intracellular transport system, vesicular trafficking, cell growth and death. The up-regulation of ABC transporter mediates vacuolar compartmentalization of Cd molecules so as to detoxify them. The up-regulation in Golgi apparatus transport proteins and membrane proteins throws light on the fact, that apart from vacuoles, Golgi apparatus might be another site for Cd sequestration in *L. bicolor*. Cd also up-regulates the proteins involved in autophagy, apoptosis, phagosomes and peroxisomes so as to protect the fungus under Cd stress.

Cd induces oxidative stress and reactive oxygen species is one of the most important mechanism attributing to Cd toxicity. Most of the enzymes and antioxidants involved in eliminating ROS and metal ions were up-regulated in *L. bicolor*, so as to alleviate Cd toxicity. Both the enzymatic as well as non-enzymatic antioxidants were induced in defense to Cd stress. Glutathione mechanism is the key process involved in Cd detoxification. Glutathione not only chelate the Cd ions into the vacuoles but also alleviate the metal induced oxidative stress by neutralizing the free radicals.

Hence, we can say that Cd induced toxicity in *L. bicolor* by generating oxidative stress and altering various metabolisms like carbohydrate metabolism, energy metabolism, DNA replication process, DNA repair mechanisms and uncoupling transcription/translation machinery. *L. bicolor* confront these oxidative and metabolic challenges by up-regulating the expression of various enzymes and antioxidants involved in mitigating Cd stress, inducing the glutathione metabolism and other metal binding proteins, escalating signal transduction pathways and amino acid/ protein biosynthesis. Therefore, the present study provides deep

insight into the mechanisms of Cd toxicity and its mitigation by *L. bicolor*. The study provides detailed information about various molecular biomarkers for Cd toxicity and target genes involved in Cd uptake and accumulation. The information can be further used in optimizing application of ECM fungi in bioremediation of various metal polluted areas.

REFERENCES

Abdul KS, Jayasinghe SS, Chandana EP, Jayasumana C, De Silva PM. Arsenic and human health effects: A review. Environmental Toxicology and Pharmacology. 2015; 40:828-846.

Aborode FA, Raab A, Voigt M, Costa LM, Krupp EM, Feldmann J. The importance of glutathione and phytochelatins on the selenite and arsenate detoxification in *Arabidopsis thaliana*. Journal of Environmental Sciences. 2016; 49:150-161.

Adamis PD, Panek AD, Eleutherio EC. Vacuolar compartmentation of the cadmium-glutathione complex protects *Saccharomyces cerevisiae* from mutagenesis. Toxicology Letters. 2007; 173:1-7.

Adeyemi AO. Bioaccumulation of arsenic by fungi. American Journal of Environmental Sciences. 2009; 5:364.

Adriaensen K, Vangronsveld J, Colpaert JV. Zinc-tolerant *Suillus bovinus* improves growth of Zn-exposed *Pinus sylvestris* seedlings. Mycorrhiza. 2006; 16:553-568.

Adriaensen K, Vrålstad T, Noben JP, Vangronsveld J, Colpaert JV. Copper-adapted *Suillus luteus*, a symbiotic solution for pines colonizing Cu mine spoils. Applied and Environmental Microbiology. 2005; 71:7279-7284.

Afzal J, Hu C, Imtiaz M, Elyamine AM, Rana MS, Imran M, Farag MA. Cadmium tolerance in rice cultivars associated with antioxidant enzymes activities and Fe/Zn concentrations. International Journal of Environmental Science and Technology. 2019; 16:4241-4252.

Agnihotri P, Singh SP, Shakya AK, Pratap JV. Biochemical and biophysical characterization of *Leishmania donovani* gamma-glutamylcysteine synthetase. Biochemistry and Biophysics Reports. 2016; 8:127-138.

Ahsan N, Lee DG, Alam I, Kim PJ, Lee JJ, Ahn YO, Kwak SS, Lee IJ, Bahk JD, Kang KY, Renaut J. Comparative proteomic study of arsenic-induced differentially expressed proteins in rice roots reveals glutathione plays a central role during As stress. Proteomics. 2008; 8:3561-3576.

Ahsan N, Nakamura T, Komatsu S. Differential responses of microsomal proteins and metabolites in two contrasting cadmium (Cd)-accumulating soybean cultivars under Cd stress. Amino Acids. 2012; 42:317-327.

Aimola P, Carmignani M, Volpe AR, Di Benedetto A, Claudio L, Waalkes MP, Van Bokhoven A, Tokar EJ, Claudio PP. Cadmium induces p53-dependent apoptosis in human prostate epithelial cells. PloS One. 2012; 7:e33647.

Alloway BJ, editor. Heavy metals in soils: trace metals and metalloids in soils and their bioavailability. Springer Science & Business Media. 2012; 22.

Almárcegui RJ, Navarro CA, Paradela A, Albar JP, von Bernath D, Jerez CA. New copper resistance determinants in the extremophile *Acidithiobacillus ferrooxidans*: a quantitative proteomic analysis. Journal of Proteome Research. 2014; 13:946-960.

Altikat S, Uysal K, Kuru HI, Kavasoglu M, Ozturk GN, Kucuk A. The effect of arsenic on some antioxidant enzyme activities and lipid peroxidation in various tissues of mirror carp (*Cyprinus carpio carpio*). Environmental Science and Pollution Research. 2015; 22:3212-3218.

Anahid S, Yaghmaei S, Ghobadinejad Z. Heavy metal tolerance of fungi. Scientia Iranica. 2011; 18:502-508.

Andersen CL, Jensen JL, Ørntoft TF. Normalization of real-time quantitative reverse transcription-PCR data: a model-based variance estimation approach to identify genes suited for normalization, applied to bladder and colon cancer data sets. Cancer Research. 2004; 64:5245-5250.

Andresen E, Küpper H. Cadmium toxicity in plants. InCadmium: from toxicity to essentiality 2013 (pp. 395-413). Springer, Dordrecht.

Anoduadi CO, Okenwa LB, Okieimen FE, Tyowua AT, Uwumarongie-Ilori EG. Metal immobilization in CCA contaminated soil using laterite and termite mound soil. Evaluation by chemical fractionation. Nigerian Journal of Applied Science. 2009; 27:77-87.

Aoshima K. Itai-itai disease: renal tubular osteomalacia induced by environmental exposure to cadmium—historical review and perspectives. Soil Science and Plant Nutrition. 2016; 62:319-326.

Argos M, Kalra T, Rathouz PJ, Chen Y, Pierce B, Parvez F, Islam T, Ahmed A, Rakibuz-Zaman M, Hasan R, Sarwar G. Arsenic exposure from drinking water, and all-cause and chronic-disease mortalities in Bangladesh (HEALS): a prospective cohort study. The Lancet. 2010; 376:252-258.

Asgher M, Khan NA, Khan MI, Fatma M, Masood A. Ethylene production is associated with alleviation of cadmium-induced oxidative stress by sulfur in mustard types differing in ethylene sensitivity. Ecotoxicology and Environmental Safety. 2014; 106:54-61.

Asgher M, Per TS, Anjum S, Khan MI, Masood A, Verma S, Khan NA. Contribution of glutathione in heavy metal stress tolerance in plants. InReactive Oxygen Species and Antioxidant Systems in Plants: Role and Regulation under Abiotic Stress 2017 (pp. 297-313). Springer, Singapore.

Aslam B, Basit M, Nisar MA, Khurshid M, Rasool MH. Proteomics: technologies and their applications. Journal of Chromatographic Science. 2017; 55:182-196.

ATSDR. Draft Toxicological Profile for Cadmium. Agency for Toxic Substances and Disease Registry, US Public Health Services, Atlanta, GA, USA. 2008.

ATSDR. Toxic substances portal [Internet]. Agency for Toxic Substances and Disease Registry. Available from: http://www.atsdr.cdc.gov/toxprofiles/index.asp. 2012.

ATSDR-Agency for toxic substances and Disease Registry. Priority list of hazardous Substances. www.atsdr.cdc.gov/spl/. 2017.

Baiwir D, Nanni P, Müller S, Smargiasso N, Morsa D, De Pauw E, Mazzucchelli G. Gel-free proteomics. InProteomics in Domestic Animals: from Farm to Systems Biology 2018 (pp. 55-101). Springer, Cham.

Balestrini R, Bonfante P. Cell wall remodeling in mycorrhizal symbiosis: a way towards biotrophism. Frontiers in Plant Science. 2014; 5:237.

Barrameda-Medina Y, Montesinos-Pereira D, Romero L, Blasco B, Ruiz JM. Role of GSH homeostasis under Zn toxicity in plants with different Zn tolerance. Plant Science. 2014; 227:110-121.

Basu U, Upadhyaya HD, Srivastava R, Daware A, Malik N, Sharma A, Bajaj D, Narnoliya L, Thakro V, Kujur A, Tripathi S. ABC transporter-mediated transport of glutathione conjugates enhances seed yield and quality in chickpea. Plant Physiology. 2019; 180:253-275.

Bazrafshan E, Zarei AA, Mostafapour FK. Biosorption of cadmium from aqueous solutions by *Trichoderma* fungus: kinetic, thermodynamic, and equilibrium study. Desalination and Water Treatment. 2016; 57:14598-14608.

Bellion M, Courbot M, Jacob C, Blaudez D, Chalot M. Extracellular and cellular mechanisms sustaining metal tolerance in ectomycorrhizal fungi. FEMS Microbiology Letters. 2006; 254:173-181.

Bellion M, Courbot M, Jacob C, Guinet F, Blaudez D, Chalot M. Metal induction of a *Paxillus involutus* metallothionein and its heterologous expression in *Hebeloma cylindrosporum*. New Phytologist. 2007; 174:151-158.

Belyaeva EA. Respiratory complex II in mitochondrial dysfunction-mediated cytotoxicity: Insight from cadmium. Journal of Trace Elements in Medicine and Biology. 2018; 50:80-92.

Benavides MP, Gallego SM, Tomaro ML. Cadmium toxicity in plants. Brazilian Journal of Plant Physiology. 2005; 17:21-34.

Bernard A. Cadmium & its adverse effects on human health. Indian Journal of Medical Research. 2008; 128:557.

Bertagnolli C, Grishin A, Vincent T, Guibal E. Recovering heavy metal ions from complex solutions using polyethylenimine derivatives encapsulated in alginate matrix. Industrial & Engineering Chemistry Research. 2016; 55:2461-2470.

Beyersmann D, Hartwig A. Carcinogenic metal compounds: recent insight into molecular and cellular mechanisms. Archives of Toxicology. 2008; 82:493.

Bhanoori M, Venkateswerlu G. In vivo chitin–cadmium complexation in cell wall of *Neurospora crassa*. Biochimica et Biophysica Acta (BBA)-General Subjects. 2000; 1523:21-28.

Bhattacharjee H, Mukhopadhyay R, Thiyagarajan S, Rosen BP. Aquaglyceroporins: ancient channels for metalloids. Journal of Biology. 2008; 7:33.

Bhowmick D, Srivastava S, D'Silva P, Mugesh G. Highly efficient glutathione peroxidase and peroxiredoxin mimetics protect mammalian cells against oxidative damage. Angewandte Chemie International Edition. 2015; 54:8449-8453.

Bhowmick S, Pramanik S, Singh P, Mondal P, Chatterjee D, Nriagu J. Arsenic in groundwater of West Bengal, India: a review of human health risks and assessment of possible intervention options. Science of the Total Environment. 2018; 612:148-169.

Bianucci E, Furlan A, del Carmen Tordable M, Hernández LE, Carpena-Ruiz RO, Castro S. Antioxidant responses of peanut roots exposed to realistic groundwater doses of arsenate: Identification of glutathione S-transferase as a suitable biomarker for metalloid toxicity. Chemosphere. 2017; 181:551-561.

Binz PA, Kägi JH. Metallothionein: molecular evolution and classification. InMetallothionein Iv 1999 (pp. 7-13). Birkhäuser, Basel.

Blaudez D, Botton B, Chalot M. Cadmium uptake and subcellular compartmentation in the ectomycorrhizal fungus *Paxillus involutus*. Microbiology. 2000; 146:1109-1117.

Blaudez D, Chalot M. Characterization of the ER-located zinc transporter ZnT1 and identification of a vesicular zinc storage compartment in *Hebeloma cylindrosporum*. Fungal Genetics and Biology. 2011; 48:496-503.

Blindauer CA, Harrison MD, Parkinson JA, Robinson AK, Cavet JS, Robinson NJ, Sadler PJ. A metallothionein containing a zinc finger within a four-metal cluster protects a

bacterium from zinc toxicity. Proceedings of the National Academy of Sciences. 2001; 98:9593-9598.

Blindauer CA, Leszczyszyn OI. Metallothioneins: unparalleled diversity in structures and functions for metal ion homeostasis and more. Natural Product Reports. 2010; 27:720-741.

Bojarczuk K, Kieliszewska-Rokicka B. Effect of ectomycorrhiza on Cu and Pb accumulation in leaves and roots of silver birch (*Betula pendula* Roth.) seedlings grown in metal-contaminated soil. Water, Air, and Soil Pollution. 2010; 207:227-240.

Bona E, Cantamessa S, Massa N, Manassero P, Marsano F, Copetta A, Lingua G, D'Agostino G, Gamalero E, Berta G. Arbuscular mycorrhizal fungi and plant growth-promoting pseudomonads improve yield, quality and nutritional value of tomato: a field study. Mycorrhiza. 2017; 27:1-11.

Bonfante P, Genre A. Mechanisms underlying beneficial plant–fungus interactions in mycorrhizal symbiosis. Nature Communications. 2010; 1:48.

Bonfante P. Plants, mycorrhizal fungi and endobacteria: a dialog among cells and genomes. The Biological Bulletin. 2003; 204:215-220.

Bonilla JO, Callegari EA, Estevéz MC, Villegas LB. Intracellular Proteomic Analysis of *Streptomyces* sp. MC1 When Exposed to Cr (VI) by Gel-Based and Gel-Free Methods. Current Microbiology. 2020; 77:62-70.

Bonnell JA. Emphysema and proteinuria in men casting copper-cadmium alloys. British Journal of Industrial Medicine. 1955; 12:181.

Bonneville S, Smits MM, Brown A, Harrington J, Leake JR, Brydson R, Benning LG. Plant-driven fungal weathering: Early stages of mineral alteration at the nanometer scale. Geology. 2009; 37:615-618.

Borges KL, Salvato F, Loziuk PL, Muddiman DC, Azevedo RA. Quantitative proteomic analysis of tomato genotypes with differential cadmium tolerance. Environmental Science and Pollution Research. 2019; 26:26039-26051.

Borovička J, Braeuer S, Sácký J, Kameník J, Goessler W, Trubač J, Strnad L, Rohovec J, Leonhardt T, Kotrba P. Speciation analysis of elements accumulated in *Cystoderma carcharias* from clean and smelter-polluted sites. Science of the Total Environment. 2019; 648:1570-1581.

Bottari E, De Tommaso G, Festa MR, Iuliano M, Zennaro G. Behavior of glutathione as ligand of lead (II). Chemosphere. 2020; 246:125718.

Bradford MM. A rapid and sensitive method for the quantitation of microgram quantities of protein utilizing the principle of protein-dye binding. Analytical Biochemistry. 1976; 72:248-254.

Brearley FQ, Saner P, Uchida A, Burslem DF, Hector A, Nilus R, Scholes JD, Egli S. Testing the importance of a common ectomycorrhizal network for dipterocarp seedling growth and survival in tropical forests of Borneo. Plant Ecology & Diversity. 2016; 9:563-576.

Brundrett MC. Global diversity and importance of mycorrhizal and nonmycorrhizal plants. InBiogeography of mycorrhizal symbiosis 2017 (pp. 533-556). Springer, Cham.

Bryan HK, Olayanju A, Goldring CE, Park BK. The Nrf2 cell defence pathway: Keap1-dependent and-independent mechanisms of regulation. Biochemical Pharmacology. 2013; 85:705-717.

Buée M, Reich M, Murat C, Morin E, Nilsson RH, Uroz S, Martin F. 454 Pyrosequencing analyses of forest soils reveal an unexpectedly high fungal diversity. New Phytologist. 2009; 184:449-56.

Bundschuh J, Litter MI, Parvez F, Román-Ross G, Nicolli HB, Jean JS, Liu CW, López D, Armienta MA, Guilherme LR, Cuevas AG. One century of arsenic exposure in Latin America: a review of history and occurrence from 14 countries. Science of the Total Environment. 2012; 429:2-35.

Cadet J, Wagner JR. Oxidatively generated base damage to cellular DNA by hydroxyl radical and one-electron oxidants: similarities and differences. Archives of Biochemistry and Biophysics. 2014; 557:47-54.

Calderone V, Dolderer B, Hartmann HJ, Echner H, Luchinat C, Del Bianco C, Mangani S, Weser U. The crystal structure of yeast copper thionein: the solution of a long-lasting enigma. Proceedings of the National Academy of Sciences. 2005; 102:51-56.

Calero-Muñoz N, Exposito-Rodriguez M, Collado-Arenal AM, Rodríguez-Serrano M, Laureano-Marín AM, Santamaría ME, Gotor C, Díaz I, Mullineaux PM, Romero-Puertas MC, Olmedilla A. Cadmium induces reactive oxygen species-dependent pexophagy in *Arabidopsis* leaves. Plant, Cell & Environment. 2019; 42:2696-2714.

Campbell PG. Cadmium - a priority pollutant. Environmental Chemistry. 2007; 3:387-398.

Cánovas D, Vooijs R, Schat H, de Lorenzo V. The role of thiol species in the hypertolerance of *Aspergillus* sp. P37 to arsenic. Journal of Biological Chemistry. 2004; 279:51234-51240.

Capdevila M, Bofill R, Palacios O, Atrian S. State-of-the-art of metallothioneins at the beginning of the 21st century. Coordination Chemistry Reviews. 2012; 256:46-62.

Casentini B, Hug SJ, Nikolaidis NP. Arsenic accumulation in irrigated agricultural soils in Northern Greece. Science of the Total Environment. 2011; 409:4802-4810.

Cejpková J, Gryndler M, Hršelová H, Kotrba P, Řanda Z, Synková I, Borovička J. Bioaccumulation of heavy metals, metalloids, and chlorine in ectomycorrhizae from smelter-polluted area. Environmental Pollution. 2016; 218:176-185.

Chaffei-Haouari C, Carrayol E, Ghorbel MH, Gouia H. Physiological and biochemical effects of cadmium toxicity in enzymes involved in nitrogen and amino—acid metabolism in tomato plants. Acta Botanica Gallica. 2009; 156:477-486.

Chandramouli K, Qian PY. Proteomics: challenges, techniques and possibilities to overcome biological sample complexity. Human Genomics and Proteomics: HGP. 2009; 239204.

Chaney RL, Baklanov IA. Phytoremediation and phytomining: status and promise. InAdvances in botanical research. 2017. (Vol. 83, pp. 189-221). Academic Press.

Chen H, Chen J, Guo Y, Wen Y, Liu J, Liu W. Evaluation of the role of the glutathione redox cycle in Cu (II) toxicity to green algae by a chiral perturbation approach. Aquatic Toxicology. 2012; 120:19-26.

Chen J, Yang L, Yan X, Liu Y, Wang R, Fan T, Ren Y, Tang X, Xiao F, Liu Y, Cao S. Zinc-finger transcription factor ZAT6 positively regulates cadmium tolerance through the glutathione-dependent pathway in *Arabidopsis*. Plant Physiology. 2016; 171:707-719.

Chen SH, Tibbett M. Phosphate supply and arsenate toxicity in ectomycorrhizal fungi. Journal of Basic Microbiology. 2007; 47:358-362.

Chen Y, Nara K, Wen Z, Shi L, Xia Y, Shen Z, Lian C. Growth and photosynthetic responses of ectomycorrhizal pine seedlings exposed to elevated Cu in soils. Mycorrhiza. 2015; 25:561-571.

Cheng ZW, Chen ZY, Yan X, Bian YW, Deng X, Yan YM. Integrated physiological and proteomic analysis reveals underlying response and defense mechanisms of *Brachypodium distachyon* seedling leaves under osmotic stress, cadmium and their combined stresses. Journal of Proteomics. 2018; 170:1-3.

Chevalier F. Highlights on the capacities of" Gel-based" proteomics. Proteome Science. 2010; 8:23.

Cho KH, Sthiannopkao S, Pachepsky YA, Kim KW, Kim JH. Prediction of contamination potential of groundwater arsenic in Cambodia, Laos, and Thailand using artificial neural network. Water Research. 2011; 45:5535-5544.

Choma A, Nowak K, Komaniecka I, Waśko A, Pleszczyńska M, Siwulski M, Wiater A. Chemical characterization of alkali-soluble polysaccharides isolated from a *Boletus edulis* (Bull.) fruiting body and their potential for heavy metal biosorption. Food Chemistry. 2018; 266:329-334.

CiCiK B, ENGiN K. The effects of cadmium on levels of glucose in serum and glycogen reserves in the liver and muscle tissues of Cyprinus carpio (L., 1758). Turkish Journal of Veterinary and Animal Sciences. 2005; 29:113-117.

Cobbett CS. Phytochelatins and their roles in heavy metal detoxification. Plant Physiology. 2000; 123:825-832.

Cobine PA, McKay RT, Zangger K, Dameron CT, Armitage IM. Solution structure of Cu6 metallothionein from the fungus *Neurospora crassa*. European Journal of Biochemistry. 2004; 271:4213-4221.

Colpaert JV, Wevers JH, Krznaric E, Adriaensen K. How metal-tolerant ecotypes of ectomycorrhizal fungi protect plants from heavy metal pollution. Annals of Forest Science. 2011; 68:17-24.

Combier JP, Melayah D, Raffier C, Gay G, Marmeisse R. *Agrobacterium tumefaciens*-mediated transformation as a tool for insertional mutagenesis in the symbiotic ectomycorrhizal fungus *Hebeloma cylindrosporum*. FEMS Microbiology Letters. 2003; 220:141-148.

Contu M. Contributo allo studio del genere *Hebeloma* (Basidiomycetes, Cortinariaceae) in Sardegna (Italia). Revista Iberoamericana de Micología. 1991; 8:38-42.

Cope KR, Bascaules A, Irving TB, Venkateshwaran M, Maeda J, Garcia K, Rush TA, Ma C, Labbé J, Jawdy S, Steigerwald E. The ectomycorrhizal fungus *Laccaria bicolor* produces lipochitooligosaccharides and uses the common symbiosis pathway to colonize *Populus* roots. The Plant Cell. 2019; 31:2386-2410.

Courbot M, Diez L, Ruotolo R, Chalot M, Leroy P. Cadmium-responsive thiols in the ectomycorrhizal fungus *Paxillus involutus*. Applied and Environmental Microbiology. 2004; 70:7413-7417.

Cummins I, Dixon DP, Freitag-Pohl S, Skipsey M, Edwards R. Multiple roles for plant glutathione transferases in xenobiotic detoxification. Drug Metabolism Reviews. 2011; 43:266-280.

Cuypers A, Plusquin M, Remans T, Jozefczak M, Keunen E, Gielen H, Opdenakker K, Nair AR, Munters E, Artois TJ, Nawrot T. Cadmium stress: an oxidative challenge. BioMetals. 2010; 23:927-940.

Cvjetko P, Zovko M, Balen B. Proteomics of heavy metal toxicity in plants. Archives of Industrial Hygiene and Toxicology. 2014; 65:1-8.

D'Alessandro A, Taamalli M, Gevi F, Timperio AM, Zolla L, Ghnaya T. Cadmium stress responses in *Brassica juncea*: hints from proteomics and metabolomics. Journal of Proteome Research. 2013; 12:4979-4997.

Daghino S, Martino E, Perotto S. Model systems to unravel the molecular mechanisms of heavy metal tolerance in the ericoid mycorrhizal symbiosis. Mycorrhiza. 2016; 26:263-274.

Dave R, Tripathi RD, Dwivedi S, Tripathi P, Dixit G, Sharma YK, Trivedi PK, Corpas FJ, Barroso JB, Chakrabarty D. Arsenate and arsenite exposure modulate antioxidants and amino acids in contrasting arsenic accumulating rice (*Oryza sativa* L.) genotypes. Journal of Hazardous Materials. 2013; 262:1123-1131.

Davis SR, Cousins RJ. Metallothionein expression in animals: a physiological perspective on function. The Journal of Nutrition. 2000; 130:1085-1088.

Davison K, Cote S, Mader S, Miller WH. Glutathione depletion overcomes resistance to arsenic trioxide in arsenic-resistant cell lines. Leukemia. 2003; 17:931-940.

Debaud JC, Gay G. In vitro fruiting under controlled conditions of the ectomycorrhizal fungus *Hebeloma cylindrosporum* associated with Pinus pinaster. New Phytologist. 1987; 105:429-435.

Degola F, Fattorini L, Bona E, Sprimuto CT, Argese E, Berta G, di Toppi LS. The symbiosis between *Nicotiana tabacum* and the endomycorrhizal fungus *Funneliformis mosseae* increases the plant glutathione level and decreases leaf cadmium and root arsenic contents. Plant Physiology and Biochemistry. 2015; 92:11-18.

Del Águila-Vargas AC, Vázquez-Medina JP, Crocker DE, Méndez-Rodríguez LC, Gaxiola-Robles R, de Anda-Montañez JA, Ramírez-Jirano LJ, Lugo-Lugo O, Zenteno-Savín T. Antioxidant response to cadmium exposure in primary skeletal muscle cells isolated from humans and elephant seals. Comparative Biochemistry and Physiology Part C: Toxicology & Pharmacology. 2020; 227:108641.

Delalande O, Desvaux H, Godat E, Valleix A, Junot C, Labarre J, Boulard Y. Cadmium–glutathione solution structures provide new insights into heavy metal detoxification. The FEBS Journal. 2010; 277:5086-5096.

Dellisanti F, Rossi PL, Valdrè G. In-field remediation of tons of heavy metal-rich waste by Joule heating vitrification. International Journal of Mineral Processing. 2009; 93:239-245.

Dhankhar R, Hooda A. Fungal biosorption–an alternative to meet the challenges of heavy metal pollution in aqueous solutions. Environmental Technology. 2011; 32:467-491.

Dhankher OP, Li Y, Rosen BP, Shi J, Salt D, Senecoff JF, Sashti NA, Meagher RB. Engineering tolerance and hyperaccumulation of arsenic in plants by combining arsenate reductase and γ-glutamylcysteine synthetase expression. Nature Biotechnology. 2002; 20:1140.

Di Palma S, Hennrich ML, Heck AJ, Mohammed S. Recent advances in peptide separation by multidimensional liquid chromatography for proteome analysis. Journal of Proteomics. 2012; 75:3791-3813.

Diagne N, Ngom M, Djighaly PI, Ngom D, Ndour B, Cissokho M, Faye MN, Sarr A, SY MO, Laplaze L, Champion A. Remediation of heavy metal-contaminated soils and enhancement of their fertility with actinorhizal plants. InHeavy Metal Contamination of Soils 2015 (pp. 355-366). Springer, Cham.

Díaz S, Martín-González A, Gutiérrez JC. Evaluation of heavy metal acute toxicity and bioaccumulation in soil ciliated protozoa. Environment International. 2006; 32:711-717.

Ding S, Ma C, Shi W, Liu W, Lu Y, Liu Q, Luo ZB. Exogenous glutathione enhances cadmium accumulation and alleviates its toxicity in *Populus*× *canescens*. Tree Physiology. 2017; 37:1697-712.

Diwakar J, Johnston SG, Burton ED, Shrestha SD. Arsenic mobilization in an alluvial aquifer of the Terai region, Nepal. Journal of Hydrology: Regional Studies. 2015; 4:59-79.

Dixit G, Singh AP, Kumar A, Mishra S, Dwivedi S, Kumar S, Trivedi PK, Pandey V, Tripathi RD. Reduced arsenic accumulation in rice (*Oryza sativa* L.) shoot involves sulfur mediated improved thiol metabolism, antioxidant system and altered arsenic transporters. Plant Physiology and Biochemistry. 2016; 99:86-96.

Dixit R, Malaviya D, Pandiyan K, Singh U, Sahu A, Shukla R, Singh B, Rai J, Sharma P, Lade H, Paul D. Bioremediation of heavy metals from soil and aquatic environment: an overview of principles and criteria of fundamental processes. Sustainability. 2015; 7:2189-2212.

Domínguez-Solís JR, López-Martín MC, Ager FJ, Ynsa MD, Romero LC, Gotor C. Increased cysteine availability is essential for cadmium tolerance and accumulation in *Arabidopsis thaliana*. Plant Biotechnology Journal. 2004; 2:469-476.

Doré J, Perraud M, Dieryckx C, Kohler A, Morin E, Henrissat B, Lindquist E, Zimmermann SD, Girard V, Kuo A, Grigoriev IV. Comparative genomics, proteomics and transcriptomics give new insight into the exoproteome of the basidiomycete *Hebeloma cylindrosporum* and its involvement in ectomycorrhizal symbiosis. New Phytologist. 2015; 208:1169-1187.

Dorta DJ, Leite S, DeMarco KC, Prado IM, Rodrigues T, Mingatto FE, Uyemura SA, Santos AC, Curti C. A proposed sequence of events for cadmium-induced mitochondrial impairment. Journal of Inorganic Biochemistry. 2003; 97:251-257.

Douay F, Pruvot C, Roussel H, Ciesielski H, Fourrier H, Proix N, Waterlot C. Contamination of urban soils in an area of Northern France polluted by dust emissions of two smelters. Water, Air, and Soil Pollution. 2008; 188:247-260.

Egerton-Warburton LM, Griffin BJ. Differential responses of *Pisolithus tinctorius* isolates to aluminum in vitro. Canadian Journal of Botany. 1995; 73:1229-1233.

Ejnik J, Robinson J, Zhu J, Försterling H, Shaw III CF, Petering DH. Folding pathway of apo-metallothionein induced by Zn^{2+}, Cd^{2+} and Co^{2+}. Journal of Inorganic Biochemistry. 2002; 88:144-152.

EPA-Environment Protection agency. Initial List of Hazardous Air Pollutants with Modifications. (https://www.epa.gov/haps/initial-list-hazardous-air-pollutants-modifications). 2007. (Accessed 24 December 2018)

Ercal N, Gurer-Orhan H, Aykin-Burns N. Toxic metals and oxidative stress part I: mechanisms involved in metal-induced oxidative damage. Current Topics in Medicinal Chemistry. 2001; 1:529-539.

Esquivel-Naranjo EU, García-Esquivel M, Medina-Castellanos E, Correa-Pérez VA, Parra-Arriaga JL, Landeros-Jaime F, Cervantes-Chávez JA, Herrera-Estrella A. A *Trichoderma atroviride* stress-activated MAPK pathway integrates stress and light signals. Molecular Microbiology. 2016; 100:860-876.

Farooq MA, Islam F, Ali B, Najeeb U, Mao B, Gill RA, Yan G, Siddique KH, Zhou W. Arsenic toxicity in plants: cellular and molecular mechanisms of its transport and metabolism. Environmental and Experimental Botany. 2016; 132:42-52.

Felig P, Pozefsk T, Marlis E, Cahill GF. Alanine: key role in gluconeogenesis. Science. 1970; 167:1003-10104.

Felten J, Kohler A, Morin E, Bhalerao RP, Palme K, Martin F, Ditengou FA, Legué V. The ectomycorrhizal fungus *Laccaria bicolor* stimulates lateral root formation in Poplar and *Arabidopsis* through auxin transport and signaling. Plant Physiology. 2009; 151:1991-2005.

Fernández-Fuego D, Bertrand A, González A. Metal accumulation and detoxification mechanisms in mycorrhizal *Betula pubescens*. Environmental Pollution. 2017; 231:1153-1162.

Ferraro A, Van Hullebusch ED, Huguenot D, Fabbricino M, Esposito G. Application of an electrochemical treatment for EDDS soil washing solution regeneration and reuse in a multi-step soil washing process: case of a Cu contaminated soil. Journal of Environmental Management. 2015; 163:62-69.

Ferrol N, Tamayo E, Vargas P. The heavy metal paradox in arbuscular mycorrhizas: from mechanisms to biotechnological applications. Journal of Experimental Botany. 2016; erw403.

Figueroa A, Cameselle C, Gouveia S, Hansen HK. Electrokinetic treatment of an agricultural soil contaminated with heavy metals. Journal of Environmental Science and Health, Part A. 2016; 51:691-700.

Filipič M. Mechanisms of cadmium induced genomic instability. Mutation Research/Fundamental and Molecular Mechanisms of Mutagenesis. 2012; 733:69-77.

Finlay RD. Ecological aspects of mycorrhizal symbiosis: with special emphasis on the functional diversity of interactions involving the extraradical mycelium. Journal of Experimental Botany. 2008; 59:1115-1126.

Finnegan P, Chen W. Arsenic toxicity: the effects on plant metabolism. Frontiers in Physiology. 2012; 3:182.

Flora SJ, Mittal M, Mehta A. Heavy metal induced oxidative stress & its possible reversal by chelation therapy. Indian Journal of Medical Research. 2008; 128:501.

Foyer CH, Noctor G. Redox homeostasis and antioxidant signaling: a metabolic interface between stress perception and physiological responses. The Plant Cell. 2005; 17:1866-1875.

Franchi N, Ferro D, Ballarin L, Santovito G. Transcription of genes involved in glutathione biosynthesis in the solitary tunicate *Ciona intestinalis* exposed to metals. Aquatic Toxicology. 2012; 114:14-22.

Frey B, Zierold K, Brunner I. Extracellular complexation of Cd in the Hartig net and cytosolic Zn sequestration in the fungal mantle of *Picea abies–Hebeloma crustuliniforme* ectomycorrhizas. Plant, Cell & Environment. 2000; 23:1257-1265.

Friberg L. Cadmium in the Environment. CRC press; 2018.

Fu R, Wen D, Xia X, Zhang W, Gu Y. Electrokinetic remediation of chromium (Cr)-contaminated soil with citric acid (CA) and polyaspartic acid (PASP) as electrolytes. Chemical Engineering Journal. 2017; 316:601-608.

Galli U, Meier M, Brunold C. Effects of cadmium on non-mycorrhizal and mycorrhizal Norway spruce seedlings [*Picea abies* (L.) Karst.] and its ectomycorrhizal fungus *Laccaria laccata* (Scop, ex Fr.) Bk. & Br.: Sulphate reduction, thiols and distribution of the heavy metal. New Phytologist. 1993; 125:837-843.

Ganguly K, Levänen B, Palmberg L, Åkesson A, Lindén A. Cadmium in tobacco smokers: a neglected link to lung disease?. European Respiratory Review. 2018; 27:170122.

Garcia BA. Quantitative proteomics for understanding modified proteins and proteomes. The FASEB Journal. 2018; 32:474-481.

García-Guzmán OM, Garibay-Orijel R, Hernández E, Arellano-Torres E, Oyama K. Word-wide meta-analysis of Quercus forests ectomycorrhizal fungal diversity reveals southwestern Mexico as a hotspot. Mycorrhiza. 2017; 27:811-822.

Gardarin A, Chédin S, Lagniel G, Aude JC, Godat E, Catty P, Labarre J. Endoplasmic reticulum is a major target of cadmium toxicity in yeast. Molecular Microbiology. 2010; 76:1034-1048.

Garg N, Aggarwal N. Effects of interactions between cadmium and lead on growth, nitrogen fixation, phytochelatin, and glutathione production in mycorrhizal *Cajanus cajan* (L.) Millsp. Journal of Plant Growth Regulation. 2011; 30:286-300.

Georgescu AA, Eliescu A, Nicolescu CM, Bumbac M, Cioateră N, Mureșeanu M, Buruleanu LC. Performance of *Pleurotus ostreatus* Mushrooms and Spent Substrate for the Biosorption of Cd (II) From Aqueous Solution. Analytical Letters. 2019; 52:2007-2027.

Giaginis C, Gatzidou E, Theocharis S. DNA repair systems as targets of cadmium toxicity. Toxicology and Applied Pharmacology. 2006; 213:282-290.

Gietz RD, Schiestl RH. High-efficiency yeast transformation using the LiAc/SS carrier DNA/PEG method. Nature Protocols. 2007; 2:31.

Gill SS, Anjum NA, Hasanuzzaman M, Gill R, Trivedi DK, Ahmad I, Pereira E, Tuteja N. Glutathione and glutathione reductase: a boon in disguise for plant abiotic stress defense operations. Plant Physiology and Biochemistry. 2013; 70:204-212.

Gillet S, Decottignies P, Chardonnet S, Le Maréchal P. Cadmium response and redoxin targets in *Chlamydomonas reinhardtii*: a proteomic approach. Photosynthesis Research. 2006; 89:201-211.

Gonçalves SC, Martins-Loução MA, Freitas H. Evidence of adaptive tolerance to nickel in isolates of *Cenococcum geophilum* from serpentine soils. Mycorrhiza. 2009; 19:221-230.

Gopal S, Borovok I, Ofer A, Yanku M, Cohen G, Goebel W, Kreft J, Aharonowitz Y. A multidomain fusion protein in *Listeria monocytogenes* catalyzes the two primary activities for glutathione biosynthesis. Journal of Bacteriology. 2005; 187:3839-3847.

Gouia H, Ghorbal MH, Meyer C. Effects of cadmium on activity of nitrate reductase and on other enzymes of the nitrate assimilation pathway in bean. Plant Physiology and Biochemistry. 2000; 38:629-638.

Greger M, Bertell G. Effects of Ca^{2+} and Cd^{2+} on the carbohydrate metabolism in sugar beet (Beta vulgaris). Journal of Experimental Botany. 1992; 43:167-173.

Grelet GA, Ba R, Goeke DF, Houliston GJ, Taylor AF, Durall DM. A plant growth-promoting symbiosis between *Mycena galopus* and *Vaccinium corymbosum* seedlings. Mycorrhiza. 2017; 27:831-839.

Grondin K, Haimeur A, Mukhopadhyay R, Rosen BP, Ouellette M. Co-amplification of the γ-glutamylcysteine synthetase gene gsh1 and of the ABC transporter gene pgpA in arsenite-resistant *Leishmania tarentolae*. The EMBO Journal. 1997; 16:3057-3065.

Gryta H, Debaud JC, Effosse AG, Gay G, Marmeisse R. Fine-scale structure of populations of the ectomycorrhizal fungus *Hebeloma cylindrosporum* in coastal sand dune forest ecosystems. Molecular Ecology. 1997; 6:353-364.

Guan C, Ji J, Jia C, Guan W, Li X, Jin C, Wang G. A GSHS-like gene from *Lycium chinense* maybe regulated by cadmium-induced endogenous salicylic acid and overexpression of

this gene enhances tolerance to cadmium stress in *Arabidopsis*. Plant Cell Reports. 2015; 34:871-884.

Guirola M, Pérez-Rafael S, Capdevila M, Palacios Ò, Atrian S. Metal dealing at the origin of the *Chordata* phylum: the metallothionein system and metal overload response in amphioxus. PloS One. 2012; 7:e43299.

Guo J, Dai X, Xu W, Ma M. Overexpressing GSH1 and AsPCS1 simultaneously increases the tolerance and accumulation of cadmium and arsenic in *Arabidopsis thaliana*. Chemosphere. 2008; 72:1020-1026.

Guo L, Ghassemian M, Komives EA, Russell P. Cadmium-induced proteome remodeling regulated by Spc1/Sty1 and Zip1 in fission yeast. Toxicological Sciences. 2012; 129:200-212.

Guo Z, Han J, Yang XY, Cao K, He K, Du G, Zeng G, Zhang L, Yu G, Sun Z, He QY. Proteomic analysis of the copper resistance of *Streptococcus pneumoniae*. Metallomics. 2015; 7:448-454.

Habibul N, Hu Y, Sheng GP. Microbial fuel cell driving electrokinetic remediation of toxic metal contaminated soils. Journal of Hazardous Materials. 2016; 318:9-14.

Haham H, Grinblat J, Sougrati MT, Stievano L, Margel S. Engineering of iron-based magnetic activated carbon fabrics for environmental remediation. Materials. 2015; 8:4593-4607.

Han Y, Fan T, Zhu X, Wu X, Ouyang J, Jiang L, Cao S. WRKY12 represses GSH1 expression to negatively regulate cadmium tolerance in *Arabidopsis*. Plant Molecular Biology. 2019; 99:149-159.

Hänsch R, Mendel RR. Physiological functions of mineral micronutrients (cu, Zn, Mn, Fe, Ni, Mo, B, cl). Current Opinion in Plant Biology. 2009; 12:259-266.

Hansda A, Kumar V. A comparative review towards potential of microbial cells for heavy metal removal with emphasis on biosorption and bioaccumulation. World Journal of Microbiology and Biotechnology. 2016; 32:170.

Harrison MJ. Signaling in the arbuscular mycorrhizal symbiosis. Annual Review of Microbiology. 2005; 59:19-42.

Hartley J, Cairney JW, Meharg AA. Do ectomycorrhizal fungi exhibit adaptive tolerance to potentially toxic metals in the environment?. Plant and Soil. 1997; 189:303-319.

Hartwig A. Cadmium and Its Impact on Genomic Stability. InCadmium Interaction with Animal Cells 2018 (pp. 107-125). Springer, Cham.

Hashem A, Abd_Allah EF, Alqarawi AA, Al-Huqail AA, Wirth S, Egamberdieva D. The interaction between arbuscular mycorrhizal fungi and endophytic bacteria enhances plant growth of *Acacia gerrardii* under salt stress. Frontiers in Microbiology. 2016; 7:1089.

Hassan SE, Hijri M, St-Arnaud M. Effect of arbuscular mycorrhizal fungi on trace metal uptake by sunflower plants grown on cadmium contaminated soil. New Biotechnology. 2013; 30:780-787.

Hawkes SJ. What is a" heavy metal"?. Journal of Chemical Education. 1997; 74:1374.

He J, Li H, Ma C, Zhang Y, Polle A, Rennenberg H, Cheng X, Luo ZB. Overexpression of bacterial γ-glutamylcysteine synthetase mediates changes in cadmium influx, allocation and detoxification in poplar. New Phytologist. 2015; 205:240-254.

He L, Jing Y, Shen J, Li X, Liu H, Geng Z, Wang M, Li Y, Chen D, Gao J, Zhang W. Mitochondrial pyruvate carriers prevent cadmium toxicity by sustaining the TCA cycle and glutathione synthesis. Plant Physiology. 2019; 180:198-211.

He Z, Shentu J, Yang X, Baligar VC, Zhang T, Stoffella PJ. Heavy metal contamination of soils: sources, indicators and assessment. Journal of Environmental Indicator. 2015; 9:17-18.

Heller G, Adomas A, Li G, Osborne J, van Zyl L, Sederoff R, Finlay RD, Stenlid J, Asiegbu FO. Transcriptional analysis of *Pinus sylvestris* roots challenged with the ectomycorrhizal fungus *Laccaria bicolor*. BMC Plant Biology. 2008; 8:19.

Henke C, Jung EM, Kothe E. Hartig'net formation of *Tricholoma vaccinum*-spruce ectomycorrhiza in hydroponic cultures. Environmental Science and Pollution Research. 2015; 22:19394-19399.

Hernández LE, Sobrino-Plata J, Montero-Palmero MB, Carrasco-Gil S, Flores-Cáceres ML, Ortega-Villasante C, Escobar C. Contribution of glutathione to the control of cellular redox homeostasis under toxic metal and metalloid stress. Journal of Experimental Botany. 2015; 66:2901-2911.

Heyno E, Klose C, Krieger-Liszkay A. Origin of cadmium-induced reactive oxygen species production: mitochondrial electron transfer versus plasma membrane NADPH oxidase. New Phytologist. 2008; 179:687-699.

Hibi T, Nii H, Nakatsu T, Kimura A, Kato H, Hiratake J, Oda JI. Crystal structure of γ-glutamylcysteine synthetase: insights into the mechanism of catalysis by a key enzyme for glutathione homeostasis. Proceedings of the National Academy of Sciences. 2004; 101:15052-15057.

Hirano S, Kobayashi Y, Cui X, Kanno S, Hayakawa T, Shraim A. The accumulation and toxicity of methylated arsenicals in endothelial cells: important roles of thiol compounds. Toxicology and Applied Pharmacology. 2004; 198:458-467.

Hložková K, Matěnová M, Žáčková P, Strnad H, Hršelová H, Hroudová M, Kotrba P. Characterization of three distinct metallothionein genes of the Ag-hyperaccumulating ectomycorrhizal fungus *Amanita strobiliformis*. Fungal Biology. 2016; 120:358-369.

Horton BM, Glen M, Davidson NJ, Ratkowsky DA, Close DC, Wardlaw TJ, Mohammed C. An assessment of ectomycorrhizal fungal communities in Tasmanian temperate high-altitude *Eucalyptus delegatensis* forest reveals a dominance of the Cortinariaceae. Mycorrhiza. 2017; 27:67-74.

Hossain MA, Piyatida P, da Silva JA, Fujita M. Molecular mechanism of heavy metal toxicity and tolerance in plants: central role of glutathione in detoxification of reactive oxygen species and methylglyoxal and in heavy metal chelation. Journal of Botany. 2012.

Hossain Z, Hajika M, Komatsu S. Comparative proteome analysis of high and low cadmium accumulating soybeans under cadmium stress. Amino Acids. 2012; 43:2393-2416.

Hou Y, Gao S. Monodisperse nickel nanoparticles prepared from a monosurfactant system and their magnetic properties. Journal of Materials Chemistry. 2003; 13:1510-1512.

Hrynkiewicz K, Szymańska S, Piernik A, Thiem D. Ectomycorrhizal community structure of *Salix* and *Betula* spp. at a saline site in central Poland in relation to the seasons and soil parameters. Water, Air, & Soil Pollution. 2015; 226:99.

Huang G, Su X, Rizwan MS, Zhu Y, Hu H. Chemical immobilization of Pb, Cu, and Cd by phosphate materials and calcium carbonate in contaminated soils. Environmental Science and Pollution Research. 2016; 23:16845-16856.

IARC- International Agency for Research on Cancer. List of classification. 2019. https://monographs.iarc.fr/list-of-classifications, (Accessed on: 22 June, 2019)

IARC. Cadmium and cadmium compounds. 2018. https://monographs.iarc.fr/wp-content/uploads/2018/06/mono100C-8.pdf (Accessed on: 24 December, 2018)

IARC. Arsenic and arsenic compounds. 2018a. https://monographs.iarc.fr/wp-content/uploads/2018/06/mono100C-6.pdf (Accessed on: 24 December, 2018)

Ibemenuga KN. Bioaccumulation and toxic effects of some heavy metals in freshwater fishes. Animal Research International. 2013; 10:1792.

Ilyas S, Rehman A, Coelho AV, Sheehan D. Proteomic analysis of an environmental isolate of *Rhodotorula mucilaginosa* after arsenic and cadmium challenge: Identification of a protein expression signature for heavy metal exposure. Journal of Proteomics. 2016; 141:47-56.

Ilyas S, Rehman A. Oxidative stress, glutathione level and antioxidant response to heavy metals in multi-resistant pathogen, *Candida tropicalis*. Environmental Monitoring and Assessment. 2015; 187:4115.

Islam MM, Hoque MA, Okuma E, Jannat R, Banu MN, Jahan MS, Nakamura Y, Murata Y. Proline and glycinebetaine confer cadmium tolerance on tobacco bright yellow-2 cells

by increasing ascorbate-glutathione cycle enzyme activities. Bioscience, Biotechnology, and Biochemistry. 2009; 0909031637.

Jackson AP, Alloway BJ. The transfer of cadmium from agricultural soils to the human food chain. InBiogeochemistry of Trace Metals 2017 (pp. 121-170). CRC Press.

Jacobson T, Priya S, Sharma SK, Andersson S, Jakobsson S, Tanghe R, Ashouri A, Rauch S, Goloubinoff P, Christen P, Tamás MJ. Cadmium causes misfolding and aggregation of cytosolic proteins in yeast. Molecular and Cellular Biology. 2017; 37:e00490-16.

Jacquart A, Brayner R, Chahine JM, Ha-Duong NT. Cd^{2+} and Pb^{2+} complexation by glutathione and the phytochelatins. Chemico-Biological Interactions. 2017; 267:2-10.

Jan AT, Azam M, Ali A, Haq QM. Prospects for exploiting bacteria for bioremediation of metal pollution. Critical Reviews in Environmental Science and Technology. 2014; 44:519-560.

Janowiak BE, Griffith OW. Glutathione synthesis in *Streptococcus agalactiae* one protein accounts for γ-glutamylcysteine synthetase and glutathione synthetase activities. Journal of Biological Chemistry. 2005; 280:11829-11839.

Jia H, Wang X, Dou Y, Liu D, Si W, Fang H, Zhao C, Chen S, Xi J, Li J. Hydrogen sulfide-cysteine cycle system enhances cadmium tolerance through alleviating cadmium-induced oxidative stress and ion toxicity in *Arabidopsis* roots. Scientific Reports. 2016; 6:1-4.

Jin H, Xu M, Chen H, Zhang S, Han X, Tang Z, Sun R. Comparative proteomic analysis of differentially expressed proteins in *Amaranthus hybridus* L. roots under cadmium stress. Water, Air, & Soil Pollution. 2016; 227:220.

Johansson EM, Fransson PM, Finlay RD, van Hees PA. Quantitative analysis of exudates from soil-living basidiomycetes in pure culture as a response to lead, cadmium and arsenic stress. Soil Biology and Biochemistry. 2008; 40:2225-2236.

John R, Ahmad P, Gadgil K, Sharma S. Heavy metal toxicity: Effect on plant growth, biochemical parameters and metal accumulation by *Brassica juncea* L. International Journal of Plant Production. 2009; 3:65-76.

Jomova K, Jenisova Z, Feszterova M, Baros S, Liska J, Hudecova D, Rhodes CJ, Valko M. Arsenic: toxicity, oxidative stress and human disease. Journal of Applied Toxicology. 2011; 31:95-107.

Joseph P. Mechanisms of cadmium carcinogenesis. Toxicology and Applied Pharmacology. 2009; 238:272-279.

Jourand P, Ducousso M, Loulergue-Majorel C, Hannibal L, Santoni S, Prin Y, Lebrun M. Ultramafic soils from New Caledonia structure *Pisolithus albus* in ecotype. FEMS Microbiology Ecology. 2010; 72:238-249.

Jozefczak M, Keunen E, Schat H, Bliek M, Hernández LE, Carleer R, Remans T, Bohler S, Vangronsveld J, Cuypers A. Differential response of *Arabidopsis* leaves and roots to cadmium: glutathione-related chelating capacity vs antioxidant capacity. Plant Physiology and Biochemistry. 2014; 83:1-9.

Jozefczak M, Remans T, Vangronsveld J, Cuypers A. Glutathione is a key player in metal-induced oxidative stress defenses. International Journal of Molecular Sciences. 2012; 13:3145-3175.

Kaiser C, Mayerhofer W, Dietrich M, Gorka S, Schintlmeister A, Reipert S, Schweiger P, Weidinger M, Wiesenbauer J, Martin V, Richter A. Reciprocal trade of Carbon and Nitrogen at the root-fungus interface in ectomycorrhizal beech plants. InEGU General Assembly Conference Abstracts. 2017. (Vol. 19, p. 15133).

Kalsotra T, Khullar S, Agnihotri R, Reddy MS. Metal induction of two metallothionein genes in the ectomycorrhizal fungus *Suillus himalayensis* and their role in metal tolerance. Microbiology. 2018; 164:868-876.

Katewa SD, Katyare SS. A simplified method for inorganic phosphate determination and its application for phosphate analysis in enzyme assays. Analytical Biochemistry. 2003; 323:180-187.

Kato FH, Carvalho ME, Gaziola SA, Piotto FA, Azevedo RA. Lysine metabolism and amino acid profile in maize grains from plants subjected to cadmium exposure. Scientia Agricola. 2020; 77:e20180095.

Khalid S, Shahid M, Niazi NK, Murtaza B, Bibi I, Dumat C. A comparison of technologies for remediation of heavy metal contaminated soils. Journal of Geochemical Exploration. 2017; 182:247-268.

Khan MA, Chattha MR, Farooq K, Jawed MA, Farooq M, Imran M, Iftkhar M, Kasana MI. Effect of farmyard manure levels and NPK applications on the pea plant growth, pod yield and quality. International Journal of Life Sciences. 2015; 9:3178-3181.

Khan MI, Khan NA, Masood A, Per TS, Asgher M. Hydrogen peroxide alleviates nickel-inhibited photosynthetic responses through increase in use-efficiency of nitrogen and sulfur, and glutathione production in mustard. Frontiers in Plant Science. 2016; 7:44.

Khan MI, Khan NA. Ethylene reverses photosynthetic inhibition by nickel and zinc in mustard through changes in PS II activity, photosynthetic nitrogen use efficiency, and antioxidant metabolism. Protoplasma. 2014; 251:1007-1019.

Khan MI, Nazir F, Asgher M, Per TS, Khan NA. Selenium and sulfur influence ethylene formation and alleviate cadmium-induced oxidative stress by improving proline and glutathione production in wheat. Journal of Plant Physiology. 2015; 173:9-18.

Khan Z, Rehman A, Nisar MA, Zafar S, Zerr I. Biosorption behavior and proteomic analysis of *Escherichia coli* P4 under cadmium stress. Chemosphere. 2017; 174:136-147.

Kim HS, Kim YJ, Seo YR. An overview of carcinogenic heavy metal: molecular toxicity mechanism and prevention. Journal of Cancer Prevention. 2015; 20:232.

Klein M, Mamnun YM, Eggmann T, Schüller C, Wolfger H, Martinoia E, Kuchler K. The ATP-binding cassette (ABC) transporter Bpt1p mediates vacuolar sequestration of glutathione conjugates in yeast. FEBS Letters. 2002; 520:63-67.

Klironomos JN, Hart MM. Food-web dynamics: animal nitrogen swap for plant carbon. Nature. 2001; 410:651.

Kobayashi E, Suwazono Y, Dochi M, Honda R, Kido T. Influence of consumption of cadmium-polluted rice or Jinzu River water on occurrence of renal tubular dysfunction and/or Itai-itai disease. Biological Trace Element Research. 2009; 127:257-268.

Kohler A, Kuo A, Nagy LG, Morin E, Barry KW, Buscot F, Canbäck B, Choi C, Cichocki N, Clum A, Colpaert J. Convergent losses of decay mechanisms and rapid turnover of symbiosis genes in mycorrhizal mutualists. Nature Genetics. 2015; 47:410.

Koller M, Saleh HM. Introductory Chapter: Introducing Heavy Metals. Heavy Metals. 2018:1.

Kolluru V, Tyagi A, Chandrasekaran B, Damodaran C. Profiling of differentially expressed genes in cadmium-induced prostate carcinogenesis. Toxicology and Applied Pharmacology. 2019; 375:57-63.

Komorowicz I, Barałkiewicz D. Determination of total arsenic and arsenic species in drinking water, surface water, wastewater, and snow from Wielkopolska, Kujawy-Pomerania, and Lower Silesia provinces, Poland. Environmental Monitoring and Assessment. 2016; 188:504.

Kopriva S. Regulation of sulfate assimilation in *Arabidopsis* and beyond. Annals of Botany. 2006; 97:479-495.

Koutros S, Baris D, Waddell R, Beane Freeman LE, Colt JS, Schwenn M, Johnson A, Ward MH, Hosain GM, Moore LE, Stolzenberg-Solomon R. Potential effect modifiers of the arsenic–bladder cancer risk relationship. International Journal of Cancer. 2018; 143:2640-2646.

Kováčik J, Bačkor M. Phenylalanine ammonia-lyase and phenolic compounds in chamomile tolerance to cadmium and copper excess. Water, Air, and Soil Pollution. 2007; 185:185-193.

Krupa P, Kozdrój J. Ectomycorrhizal fungi and associated bacteria provide protection against heavy metals in inoculated pine (*Pinus sylvestris* L.) seedlings. Water, Air, and Soil Pollution. 2007; 182:83-90.

Krznaric E, Verbruggen N, Wevers JH, Carleer R, Vangronsveld J, Colpaert JV. Cd-tolerant *Suillus luteus*: a fungal insurance for pines exposed to Cd. Environmental Pollution. 2009; 157:1581-1588.

Kuang Y, Du J, Zhou R, Chen Z, Megharaj M, Naidu R. Calcium alginate encapsulated Ni/Fe nanoparticles beads for simultaneous removal of Cu (II) and monochlorobenzene. Journal of Colloid and Interface Science. 2015; 447:85-91.

Kulikowska D, Gusiatin ZM, Bułkowska K, Klik B. Feasibility of using humic substances from compost to remove heavy metals (Cd, Cu, Ni, Pb, Zn) from contaminated soil aged for different periods of time. Journal of Hazardous Materials. 2015; 300:882-891.

Kundu D, Dey S, Raychaudhuri SS. Chromium (VI)–induced stress response in the plant *Plantago ovata* Forsk in vitro. Genes and Environment. 2018; 40:21.

Kuo CC, Moon KA, Wang SL, Silbergeld E, Navas-Acien A. The association of arsenic metabolism with cancer, cardiovascular disease, and diabetes: a systematic review of the epidemiological evidence. Environmental Health Perspectives. 2017; 125:087001.

Lauer Júnior CM, Bonatto D, Mielniczki-Pereira AA, Zilles Schuch A, Dias JF, Yoneama ML, Henriques JA. The Pmr1 protein, the major yeast Ca^{2+}-ATPase in the Golgi, regulates intracellular levels of the cadmium ion. FEMS Microbiology Letters. 2008; 285:79-88.

Lavid N, Schwartz A, Lewinsohn E, Tel-Or E. Phenols and phenol oxidases are involved in cadmium accumulation in the water plants *Nymphoides peltata* (Menyanthaceae) and *Nymphaeae* (Nymphaeaceae). Planta. 2001; 214:189-195.

Le Gall H, Philippe F, Domon JM, Gillet F, Pelloux J, Rayon C. Cell wall metabolism in response to abiotic stress. Plants. 2015; 4:112-166.

Le QG, Ishiwata-Kimata Y, Kohno K, Kimata Y. Cadmium impairs protein folding in the endoplasmic reticulum and induces the unfolded protein response. FEMS Yeast Research. 2016; 16:fow049.

Lee JY, Kwon TS, Park JY, Choi S, Kim EJ, Lee HU, Lee YC. Electrokinetic (EK) removal of soil co-contaminated with petroleum oils and heavy metals in three-dimensional (3D) small-scale reactor. Process Safety and Environmental Protection. 2016; 99:186-193.

Lee K, Bae DW, Kim SH, Han HJ, Liu X, Park HC, Lim CO, Lee SY, Chung WS. Comparative proteomic analysis of the short-term responses of rice roots and leaves to cadmium. Journal of Plant Physiology. 2010; 167:161-168.

Lee SC, Knowles TJ, Postis VL, Jamshad M, Parslow RA, Lin YP, Goldman A, Sridhar P, Overduin M, Muench SP, Dafforn TR. A method for detergent-free isolation of membrane proteins in their local lipid environment. Nature Protocols. 2016; 11:1149.

Leonhardt T, Sácký J, Šimek P, Šantrůček J, Kotrba P. Metallothionein-like peptides involved in sequestration of Zn in the Zn-accumulating ectomycorrhizal fungus *Russula atropurpurea*. Metallomics. 2014; 6:1693-1701.

Leslie EM. Arsenic–glutathione conjugate transport by the human multidrug resistance proteins (MRPs/ABCCs). Journal of Inorganic Biochemistry. 2012; 108:141-149.

Leung HM, Wu FY, Cheung KC, Ye ZH, Wong MH. Synergistic effects of arbuscular mycorrhizal fungi and phosphate rock on heavy metal uptake and accumulation by an arsenic hyperaccumulator. Journal of Hazardous Materials. 2010; 181:497-507.

Leung HM, Zhen-Wen WA, Zhi-Hong YE, Kin-Lam YU, Xiao-Ling PE, Cheung KC. Interactions between arbuscular mycorrhizae and plants in phytoremediation of metal-contaminated soils: a review. Pedosphere. 2013; 23:549-563.

Levy JL, Stauber JL, Adams MS, Maher WA, Kirby JK, Jolley DF. Toxicity, biotransformation, and mode of action of arsenic in two freshwater microalgae (*Chlorella* sp. and *Monoraphidium arcuatum*). Environmental Toxicology and Chemistry: An International Journal. 2005; 24:2630-2639.

Li D, Zhang L, Chen M, He X, Li J, An R. Defense Mechanisms of Two Pioneer Submerged Plants during Their Optimal Performance Period in the Bioaccumulation of Lead: A Comparative Study. International Journal of Environmental Research and Public Health. 2018; 15:2844.

Li H, Otvos JD. Biphasic kinetics of Zn^{2+} removal from Zn metallothionein by nitrilotriacetate are associated with differential reactivity of the two metal clusters. Journal of Inorganic Biochemistry. 1998; 70:187-194.

Li JT, Baker AJ, Ye ZH, Wang HB, Shu WS. Phytoextraction of Cd-contaminated soils: current status and future challenges. Critical Reviews in Environmental Science and Technology. 2012; 42:2113-2152.

Li X, Xiao K, Ma H, Li L, Tan H, Xu H, Li Y. Mechanisms into the removal and translocation of cadmium by *Oudemansiella radicata* in soil. Environmental Science and Pollution Research. 2019; 26:6388-6398.

Li Y, Dankher OP, Carreira L, Smith AP, Meagher RB. The shoot-specific expression of γ-glutamylcysteine synthetase directs the long-distance transport of thiol-peptides to roots conferring tolerance to mercury and arsenic. Plant Physiology. 2006; 141:288-298.

Liang J, Diao H, Song W, Li L. Tolerance and Bioaccumulation of Arsenate by *Aspergillus Oryzae* TLWK-09 Isolated from Arsenic-Contaminated Soils. Water, Air, & Soil Pollution. 2018; 229:169.

Liang T, Ding H, Wang G, Kang J, Pang H, Lv J. Sulfur decreases cadmium translocation and enhances cadmium tolerance by promoting sulfur assimilation and glutathione metabolism in *Brassica chinensis* L. Ecotoxicology and Environmental Safety. 2016; 124:129-137.

Liao VH, Yu CW. *Caenorhabditis elegans* gcs-1 confers resistance to arsenic-induced oxidative stress. BioMetals. 2005; 18:519-528.

Lin S, Wan W, Tian T, Wang Y, Liu Q, Zhang W, Ai Y, Xue L, He H. Protein complex and proteomic profile in the roots of *Oryza sativa* L. in response to cadmium toxicity. Acta Physiologiae Plantarum. 2015; 37:188.

Liu L, Li W, Song W, Guo M. Remediation techniques for heavy metal-contaminated soils: principles and applicability. Science of the Total Environment. 2018; 633:206-219.

Liu SH, Zeng GM, Niu QY, Liu Y, Zhou L, Jiang LH, Tan XF, Xu P, Zhang C, Cheng M. Bioremediation mechanisms of combined pollution of PAHs and heavy metals by bacteria and fungi: A mini review. Bioresource Technology. 2017; 224:25-33.

Liu W, Song Q, Cao Y, Zhao Y, Huo H, Wang Y, Song Y, Li J, Tu P. Advanced liquid chromatography-mass spectrometry enables merging widely targeted metabolomics and proteomics. Analytica Chimica Acta. 2019; 1069:89-97.

Liu XM, Kim KE, Kim KC, Nguyen XC, Han HJ, Jung MS, Kim HS, Kim SH, Park HC, Yun DJ, Chung WS. Cadmium activates *Arabidopsis* MPK3 and MPK6 via accumulation of reactive oxygen species. Phytochemistry. 2010; 71:614-618.

Liu YL, Shen ZJ, Simon M, Li H, Ma DN, Zhu XY, Zheng HL. Comparative proteomic analysis reveals the regulatory effects of H2S on salt tolerance of mangrove plant *Kandelia obovata*. International Journal of Molecular Sciences. 2020; 21:118.

Livak KJ, Schmittgen TD. Analysis of relative gene expression data using real-time quantitative PCR and the $2^{-\Delta\Delta CT}$ method. Methods. 2001; 25:402-408.

Lloyd JR, Oremland RS. Microbial transformations of arsenic in the environment: from soda lakes to aquifers. Elements. 2006; 2:85-90.

Long R, Li M, Zhang T, Kang J, Sun Y, Yang Q. Comparative proteomic analysis reveals differential root proteins in *Medicago sativa* and *Medicago truncatula* in response to salt stress. The Model Legume Medicago Truncatula. 2019; 27:1102-1111.

Lopez E, Arce C, Oset-Gasque MJ, Canadas S, Gonzalez MP. Cadmium induces reactive oxygen species generation and lipid peroxidation in cortical neurons in culture. Free Radical Biology and Medicine. 2006; 40:940-951.

Lorenzo-Gutiérrez D, Gómez-Gil L, Guarro J, Roncero MI, Fernández-Bravo A, Capilla J, López-Fernández L. Role of the *Fusarium oxysporum* metallothionein Mt1 in resistance to metal toxicity and virulence. Metallomics. 2019; 11:1230-1240.

Lou L, Kang J, Pang H, Li Q, Du X, Wu W, Chen J, Lv J. Sulfur protects pakchoi (*Brassica chinensis* L.) seedlings against cadmium stress by regulating ascorbate-glutathione metabolism. International Journal of Molecular Sciences. 2017;18:1628.

Lu G, Wu H, Ding J. Interactive Effects of copper, fluorene, and fluoranthene on enzymatic biomarkers and metallothionein levels in Crucian Carp (*Carassius auratus*). Environment. 2018; 8:10.

Luo H, Li H, Zhang X, Fu J. Antioxidant responses and gene expression in perennial ryegrass (*Lolium perenne* L.) under cadmium stress. Ecotoxicology. 2011; 20:770-778.

Luo ZB, Wu C, Zhang C, Li H, Lipka U, Polle A. The role of ectomycorrhizas in heavy metal stress tolerance of host plants. Environmental and Experimental Botany. 2014; 108:47-62.

Ma Y, He J, Ma C, Luo J, Li H, Liu T, Polle A, Peng C, LUO ZB. Ectomycorrhizas with *Paxillus involutus* enhance cadmium uptake and tolerance in *Populus*× *canescens*. Plant, Cell & Environment. 2014; 37:627-642.

Magdeldin S, Enany S, Yoshida Y, Xu B, Zhang Y, Zureena Z, Lokamani I, Yaoita E, Yamamoto T. Basics and recent advances of two dimensional-polyacrylamide gel electrophoresis. Clinical Proteomics. 2014; 11:16.

Mahar A, Ping WA, Ronghua LI, ZHANG Z. Immobilization of lead and cadmium in contaminated soil using amendments: a review. Pedosphere. 2015; 25:555-568.

Mahar A, Wang P, Ali A, Awasthi MK, Lahori AH, Wang Q, Li R, Zhang Z. Challenges and opportunities in the phytoremediation of heavy metals contaminated soils: A review. Ecotoxicology and Environmental Safety. 2016; 126:111-121.

Mahmood T, Islam KR. Response of rice seedlings to copper toxicity and acidity. Journal of Plant Nutrition. 2006; 29:943-957.

Majorel C, Hannibal L, Ducousso M, Lebrun M, Jourand P. Evidence of nickel (Ni) efflux in Ni-tolerant ectomycorhizal *Pisolithus albus* isolated from ultramafic soil. Environmental Microbiology Reports. 2014; 6:510-518.

Mandlate JS, Soares BM, Seeger TS, Dalla Vecchia P, Mello PA, Flores EM, Duarte FA. Determination of cadmium and lead at sub-ppt level in soft drinks: An efficient combination between dispersive liquid-liquid microextraction and graphite furnace atomic absorption spectrometry. Food Chemistry. 2017; 221:907-912.

Mao X, Han FX, Shao X, Guo K, McComb J, Arslan Z, Zhang Z. Electro-kinetic remediation coupled with phytoremediation to remove lead, arsenic and cesium from contaminated paddy soil. Ecotoxicology and Environmental Safety. 2016; 125:16-24.

Marano KM, Naufal ZS, Kathman SJ, Bodnar JA, Borgerding MF, Garner CD, Wilson CL. Cadmium exposure and tobacco consumption: Biomarkers and risk assessment. Regulatory Toxicology and Pharmacology. 2012; 64:243-252.

Margis R, Dunand C, Teixeira FK, Margis-Pinheiro M. Glutathione peroxidase family–an evolutionary overview. The FEBS Journal. 2008; 275:3959-3970.

Marmeisse R, Guidot A, Gay G, Lambilliotte R, Sentenac H, Combier JP, Melayah D, Fraissinet-Tachet L, Debaud JC. *Hebeloma cylindrosporum*–a model species to study ectomycorrhizal symbiosis from gene to ecosystem. New Phytologist. 2004; 163:481-498.

Martin F, Abati V, Burel A, Clément-Vidal A, Sanier C, Fabre D, Woraathasin N, Rio M, Besret P, Farinas B, Montoro P. Overexpression of EcGSH1 induces glutathione production and alters somatic embryogenesis and plant development in *Hevea brasiliensis*. Industrial Crops and Products. 2018; 112:803-814.

Martin F, Aerts A, Ahrén D, Brun A, Danchin EG, Duchaussoy F, Gibon J, Kohler A, Lindquist E, Pereda V, Salamov A. The genome of *Laccaria bicolor* provides insights into mycorrhizal symbiosis. Nature. 2008; 452:88.

Martin F, Nehls U. Harnessing ectomycorrhizal genomics for ecological insights. Current Opinion in Plant Biology. 2009; 12:508-515.

Martin F, Selosse MA. The *Laccaria* genome: a symbiont blueprint decoded. New Phytologist. 2008:296-310.

Marty L, Siala W, Schwarzländer M, Fricker MD, Wirtz M, Sweetlove LJ, Meyer Y, Meyer AJ, Reichheld JP, Hell R. The NADPH-dependent thioredoxin system constitutes a functional backup for cytosolic glutathione reductase in *Arabidopsis*. Proceedings of the National Academy of Sciences. 2009; 106:9109-9114.

Mayer AM. Polyphenol oxidases in plants and fungi: going places? A review. Phytochemistry. 2006; 67:2318-2331.

Meharg AA. The mechanistic basis of interactions between mycorrhizal associations and toxic metal cations. Mycological Research. 2003; 107:1253-1265.

Melgar MJ, Alonso J, García MA. Cadmium in edible mushrooms from NW Spain: bioconcentration factors and consumer health implications. Food and Chemical Toxicology. 2016; 88:13-20.

Melin EL. Physiology of mycorrhizal relations in plants. Annual Review of Plant Physiology. 1953; 4:325-346.

Mendes R, Garbeva P, Raaijmakers JM. The rhizosphere microbiome: significance of plant beneficial, plant pathogenic, and human pathogenic microorganisms. FEMS Microbiology Reviews. 2013; 37:634-663.

Mendoza-Cózatl DG, Jobe TO, Hauser F, Schroeder JI. Long-distance transport, vacuolar sequestration, tolerance, and transcriptional responses induced by cadmium and arsenic. Current Opinion in Plant Biology. 2011; 14:554-562.

Meng J, Wang W, Li L, Yin Q, Zhang G. Cadmium effects on DNA and protein metabolism in oyster (*Crassostrea gigas*) revealed by proteomic analyses. Scientific Reports. 2017; 7:11716.

Messner B, Türkcan A, Ploner C, Laufer G, Bernhard D. Cadmium overkill: autophagy, apoptosis and necrosis signalling in endothelial cells exposed to cadmium. Cellular and Molecular Life Sciences. 2016; 73:1699-1713.

Michalak A. Phenolic compounds and their antioxidant activity in plants growing under heavy metal stress. Polish Journal of Environmental Studies. 2006; 15: 523-530.

Mittova V, Theodoulou FL, Kiddle G, Gómez L, Volokita M, Tal M, Foyer CH, Guy M. Coordinate induction of glutathione biosynthesis and glutathione-metabolizing enzymes is correlated with salt tolerance in tomato. FEBS Letters. 2003; 554:417-421.

Mo Y, Wang Y, Yang R, Zheng J, Liu C, Li H, Ma J, Zhang Y, Wei C, Zhang X. Regulation of plant growth, photosynthesis, antioxidation and osmosis by an arbuscular mycorrhizal fungus in watermelon seedlings under well-watered and drought conditions. Frontiers in Plant Science. 2016; 7:644.

Mueller GM, Gardes M. Intra-and interspecific relations within *Laccaria bicolor* sensu lato. Mycological Research. 1991; 95:592-601.

Mukherjee A, Das D, Mondal SK, Biswas R, Das TK, Boujedaini N, Khuda-Bukhsh AR. Tolerance of arsenate-induced stress in *Aspergillus niger*, a possible candidate for bioremediation. Ecotoxicology and Environmental Safety. 2010; 73:172-182.

Muñiz Ortiz JG, Opoka R, Kane D, Cartwright IL. Investigating arsenic susceptibility from a genetic perspective in *Drosophila* reveals a key role for glutathione synthetase. Toxicological Sciences. 2009; 107:416-426.

Murata H, Yamada A, Maruyama T, Neda H. Ectomycorrhizas in vitro between *Tricholoma matsutake*, a basidiomycete that associates with *Pinaceae*, and *Betula platyphylla* var. japonica, an early-successional birch species, in cool-temperate forests. Mycorrhiza. 2015; 25:237-241.

Mustafa G, Sakata K, Komatsu S. Proteomic analysis of flooded soybean root exposed to aluminum oxide nanoparticles. Journal of Proteomics. 2015; 128:280-297.

Nair PM, Park SY, Chung JW, Choi J. Transcriptional regulation of glutathione biosynthesis genes, γ-glutamyl-cysteine ligase and glutathione synthetase in response to cadmium and nonylphenol in *Chironomus riparius*. Environmental Toxicology and Pharmacology. 2013; 36:265-273.

Narendrula-Kotha R, Nkongolo KK. Microbial response to soil liming of damaged ecosystems revealed by pyrosequencing and phospholipid fatty acid analyses. PloS One. 2017; 12:e0168497.

Nath RG, Sonawane BR, Vulimiri SV, Lin YS. Mechanisms of cadmium carcinogenesis. Journal of Cancer Research. 2015; 75:2738.

National Resources Canada. Canadian minerals Yearbook. 2007.

Navarro A, Cardellach E, Cañadas I, Rodríguez J. Solar thermal vitrification of mining contaminated soils. International Journal of Mineral Processing. 2013; 119:65-74.

Nawrot TS, Staessen JA, Roels HA, Munters E, Cuypers A, Richart T, Ruttens A, Smeets K, Clijsters H, Vangronsveld J. Cadmium exposure in the population: from health risks to strategies of prevention. BioMetals. 2010; 23:769-782.

Neilson KA, Ali NA, Muralidharan S, Mirzaei M, Mariani M, Assadourian G, Lee A, Van Sluyter SC, Haynes PA. Less label, more free: approaches in label-free quantitative mass spectrometry. Proteomics. 2011; 11:535-553.

Nemmiche S. Oxidative signaling response to cadmium exposure. Toxicological Sciences. 2016; 156:4-10.

Nersesyan A, Kundi M, Waldherr M, Setayesh T, Mišík M, Wultsch G, Filipic M, Barcelos GR, Knasmueller S. Results of micronucleus assays with individuals who are occupationally and environmentally exposed to mercury, lead and cadmium. Mutation Research/Reviews in Mutation Research. 2016; 770:119-139.

Ngu TT, Stillman MJ. Metal-binding mechanisms in metallothioneins. Dalton Transactions. 2009; 28:5425-5433.

Nguyen H, Rineau F, Vangronsveld J, Cuypers A, Colpaert JV, Ruytinx J. A novel, highly conserved metallothionein family in basidiomycete fungi and characterization of two representative SlMTa and SlMTb genes in the ectomycorrhizal fungus *Suillus luteus*. Environmental Microbiology. 2017; 19:2577-2587.

Nikolić TV, Kojić D, Orčić S, Vukašinović EL, Blagojević DP, Purać J. Laboratory bioassays on the response of honey bee (*Apis mellifera* L.) glutathione S-transferase and acetylcholinesterase to the oral exposure to copper, cadmium, and lead. Environmental Science and Pollution Research. 2019; 26:6890-6897.

Noctor G, Mhamdi A, Chaouch S, Han YI, Neukermans J, Marquez-Garcia BE, Queval G, Foyer CH. Glutathione in plants: an integrated overview. Plant, Cell & Environment. 2012; 35:454-484.

Oestreicher J, Morgan B. Glutathione: subcellular distribution and membrane transport. Biochemistry and Cell Biology. 2018; 97:270-289.

Ohtake Y, Yabuuchi S. Molecular cloning of the γ-glutamylcysteine synthetase gene of *Saccharomyces cerevisiae*. Yeast. 1991; 7: 953-961.

Orłowska E, Godzik B, Turnau K. Effect of different arbuscular mycorrhizal fungal isolates on growth and arsenic accumulation in *Plantago lanceolata* L. Environmental Pollution. 2012; 168:121-130.

Osobová M, Urban V, Jedelský PL, Borovička J, Gryndler M, Ruml T, Kotrba P. Three metallothionein isoforms and sequestration of intracellular silver in the hyperaccumulator *Amanita strobiliformis*. New Phytologist. 2011; 190:916-926.

Outten CE, Darch M, McGee C. Characterization of Glutathione Flux Between Subcellular Compartments. The FASEB Journal. 2017; 31:773-778.

Pagani A, Villarreal L, Capdevila M, Atrian S. The *Saccharomyces cerevisiae* Crs5 metallothionein metal-binding abilities and its role in the response to zinc overload. Molecular Microbiology. 2007; 63:256-269.

Palacios Ò, Atrian S, Capdevila M. Zn-and Cu-thioneins: a functional classification for metallothioneins?. JBIC Journal of Biological Inorganic Chemistry. 2011; 16:991.

Pan C, Lu H, Liu J, Yu J, Wang Q, Li J, Yang J, Hong H, Yan C. SODs involved in the hormone mediated regulation of H2O2 content in *Kandelia obovata* root tissues under cadmium stress. Environmental Pollution. 2020; 256:113272.

Park SJ, Kim S, Lee S, Khim ZG, Char K, Hyeon T. Synthesis and magnetic studies of uniform iron nanorods and nanospheres. Journal of the American Chemical Society. 2000; 122:8581-8592.

Park YH, Lee YM, Kim DS, Park J, Suk K, Kim JK, Han HS. Hypothermia enhances induction of protective protein metallothionein under ischemia. Journal of Neuroinflammation. 2013; 10:21-36.

Pavlíková D, Zemanová V, Procházková D, Pavlík M, Száková J, Wilhelmová N. The long-term effect of zinc soil contamination on selected free amino acids playing an important role in plant adaptation to stress and senescence. Ecotoxicology and Environmental Safety. 2014; 100:166-170.

Pellegrin C, Daguerre Y, Ruytinx J, Guinet F, Kemppainen M, Frey NF, Puech-Pagès V, Hecker A, Pardo AG, Martin FM, Veneault-Fourrey C. *Laccaria bicolor* MiSSP8 is a small-secreted protein decisive for the establishment of the ectomycorrhizal symbiosis. Environmental Microbiology. 2019; 21:3765-3779.

Per TS, Khan S, Asgher M, Bano B, Khan NA. Photosynthetic and growth responses of two mustard cultivars differing in phytocystatin activity under cadmium stress. Photosynthetica. 2016; 54:491-501.

Perfus-Barbeoch L, Leonhardt N, Vavasseur A, Forestier C. Heavy metal toxicity: cadmium permeates through calcium channels and disturbs the plant water status. The Plant Journal. 2002; 32:539-548.

Petrick JS, Ayala-Fierro F, Cullen WR, Carter DE, Aposhian HV. Monomethylarsonous acid (MMAIII) is more toxic than arsenite in Chang human hepatocytes. Toxicology and Applied Pharmacology. 2000; 163:203-207.

Phanthavongsa P, Chalot M, Papin A, Lacercat-Didier L, Roy S, Blaudez D, Bert V. Effect of mycorrhizal inoculation on metal accumulation by poplar leaves at phytomanaged sites. Environmental and Experimental Botany. 2017; 143:72-81.

Pickering IJ, Prince RC, George MJ, Smith RD, George GN, Salt DE. Reduction and coordination of arsenic in Indian mustard. Plant Physiology. 2000; 122:1171-1178.

Pinter IF, Salomon MV, Gil R, Mastrantonio L, Bottini R, Piccoli P. Arsenic and trace elements in soil, water, grapevine and onion in Jáchal, Argentina. Science of the Total Environment. 2018; 615:1485-1498.

Pires C, Franco AR, Pereira SI, Henriques I, Correia A, Magan N, Castro PM. Metal (loid)-contaminated soils as a source of culturable heterotrophic aerobic bacteria for remediation applications. Geomicrobiology Journal. 2017; 34:760-768.

Pizzaia D, Nogueira ML, Mondin M, Carvalho ME, Piotto FA, Rosario MF, Azevedo RA. Cadmium toxicity and its relationship with disturbances in the cytoskeleton, cell cycle and chromosome stability. Ecotoxicology. 2019; 28:1046-1055.

Plett JM, Daguerre Y, Wittulsky S, Vayssières A, Deveau A, Melton SJ, Kohler A, Morrell-Falvey JL, Brun A, Veneault-Fourrey C, Martin F. Effector MiSSP7 of the mutualistic fungus *Laccaria bicolor* stabilizes the *Populus* JAZ6 protein and represses jasmonic acid (JA) responsive genes. Proceedings of the National Academy of Sciences. 2014; 111:8299-8304.

Plett JM, Kemppainen M, Kale SD, Kohler A, Legué V, Brun A, Tyler BM, Pardo AG, Martin F. A secreted effector protein of *Laccaria bicolor* is required for symbiosis development. Current Biology. 2011; 21:1197-1203.

Pluskal T, Sajiki K, Becker J, Takeda K, Yanagida M. Diverse fission yeast genes required for responding to oxidative and metal stress: Comparative analysis of glutathione-related and other defense gene deletions. Genes to Cells. 2016; 21:530-542.

Pócsi I, Prade RA, Penninckx MJ. Glutathione, altruistic metabolite in fungi. Advances in Microbial Physiology. 2004; 49:1-76.

Podila GK, Zheng J, Balasubramanian S, Sundaram S, Hiremath S, Brand JH, Hymes MJ. Fungal gene expression in early symbiotic interactions between *Laccaria bicolor* and red pine. InDiversity and Integration in Mycorrhizas 2002 (pp. 117-128). Springer, Dordrecht.

Pradet-Balade B, Boulmé F, Beug H, Müllner EW, Garcia-Sanz JA. Translation control: bridging the gap between genomics and proteomics?. Trends in Biochemical Sciences. 2001; 26:225-229.

Pretto A, Loro VL, Morsch VM, Moraes BS, Menezes C, Santi A, Toni C. Alterations in carbohydrate and protein metabolism in silver catfish (*Rhamdia quelen*) exposed to cadmium. Ecotoxicology and Environmental Safety. 2014; 100:188-192.

Pyrzyńska K, Bystrzejewski M. Comparative study of heavy metal ions sorption onto activated carbon, carbon nanotubes, and carbon-encapsulated magnetic nanoparticles. Colloids and Surfaces A: Physicochemical and Engineering Aspects. 2010; 362:102-109.

Qiao K, Liang S, Wang F, Wang H, Hu Z, Chai T. Effects of cadmium toxicity on diploid wheat (*Triticum urartu*) and the molecular mechanism of the cadmium response. Journal of Hazardous Materials. 2019; 374:1-10.

Qin R, Ning C, Björn LO, Li S. Proteomic analysis of *Allium cepa* var. agrogarum L. roots under copper stress. Plant and Soil. 2016; 401:197-212.

Quoreshi AM, Timmer VR. Early outplanting performance of nutrient-loaded containerized black spruce seedlings inoculated with *Laccaria bicolor*: a bioassay study. Canadian Journal of Forest Research. 2000; 30:744-752.

Rabilloud T, Chevallet M, Luche S, Lelong C. Two-dimensional gel electrophoresis in proteomics: Past, present and future. Journal of Proteomics. 2010; 73:2064-2077.

Rahman I, Kode A, Biswas SK. Assay for quantitative determination of glutathione and glutathione disulfide levels using enzymatic recycling method. Nature Protocols. 2006; 1:3159.

Ramesh G, Podila GK, Gay G, Marmeisse R, Reddy MS. Different patterns of regulation for the copper and cadmium metallothioneins of the ectomycorrhizal fungus *Hebeloma cylindrosporum*. Applied and Environmental Microbiology. 2009; 75:2266-2274.

Rani A, Kumar A, Lal A, Pant M. Cellular mechanisms of cadmium-induced toxicity: a review. International Journal of Environmental Health Research. 2014; 24:378-399.

Ray P, Adholeya A. Correlation between organic acid exudation and metal uptake by ectomycorrhizal fungi grown on pond ash in vitro. BioMetals. 2009; 22:275.

Reddy MS, Kour M, Aggarwal S, Ahuja S, Marmeisse R, Fraissinet-Tachet L. Metal induction of a *Pisolithus albus* metallothionein and its potential involvement in heavy metal tolerance during mycorrhizal symbiosis. Environmental Microbiology. 2016; 18:2446-2454.

Reddy MS, Prasanna L, Marmeisse R, Fraissinet-Tachet L. Differential expression of metallothioneins in response to heavy metals and their involvement in metal tolerance in the symbiotic basidiomycete *Laccaria bicolor*. Microbiology. 2014; 160:2235-2242.

Reeves RD, Baker AJ, Jaffré T, Erskine PD, Echevarria G, van der Ent A. A global database for plants that hyperaccumulate metal and metalloid trace elements. New Phytologist. 2018; 218:407-411.

Robinson NJ, Tommey AM, Kuske C, Jackson PJ. Plant metallothioneins. Biochemistry Journal 1993; 295:1–10.

Rodríguez-Lado L, Sun G, Berg M, Zhang Q, Xue H, Zheng Q, Johnson CA. Groundwater arsenic contamination throughout China. Science. 2013; 341:866-868.

Rodríguez-Serrano M, Romero-Puertas MC, Pazmino DM, Testillano PS, Risueño MC, Luis A, Sandalio LM. Cellular response of pea plants to cadmium toxicity: cross talk between reactive oxygen species, nitric oxide, and calcium. Plant Physiology. 2009; 150:229-243.

Romagnesi H. Etudes sur le genre *Hebeloma*. Société Mycologique de France; 1965; 81:321-344.

Rosestolato D, Bagatin R, Ferro S. Electrokinetic remediation of soils polluted by heavy metals (mercury in particular). Chemical Engineering Journal. 2015; 264:16-23.

Rousseau JD, Reid CP, English RJ. Relationship between biomass of the mycorrhizal fungus *Pisolithus tinctorius* and phosphorus uptake in loblolly pine seedlings. Soil Biology & Biochemistry. 1992; 24:183-184.

Roy SK, Cho SW, Kwon SJ, Kamal AH, Kim SW, Oh MW, Lee MS, Chung KY, Xin Z, Woo SH. Morpho-physiological and proteome level responses to cadmium stress in sorghum. PloS One. 2016; 11:e0150431.

Rudakiya DM, Iyer V, Shah D, Gupte A, Nath K. Biosorption potential of *Phanerochaete chrysosporium* for arsenic, cadmium, and chromium removal from aqueous solutions. Global Challenges. 2018; 2:1800064.

Ruiz JM, Rivero RM, Romero L. Preliminary studies on the involvement of biosynthesis of cysteine and glutathione concentration in the resistance to B toxicity in sunflower plants. Plant Science. 2003; 165:811-817.

Ruytinx J, Nguyen H, Van Hees M, De Beeck MO, Vangronsveld J, Carleer R, Colpaert JV, Adriaensen K. Zinc export results in adaptive zinc tolerance in the ectomycorrhizal basidiomycete *Suillus bovinus*. Metallomics. 2013; 5:1225-1233.

Sabella E, Nutricati E, Aprile A, Miceli A, Negro C, Rampino P, Lenucci M, De Bellis L. *Tuber borchii* Vitt. mycorrhiza protects *Cistus creticus* L. from heavy metal toxicity. Environmental and Experimental Botany. 2016; 130:181-188.

Sácký J, Leonhardt T, Borovička J, Gryndler M, Briksí A, Kotrba P. Intracellular sequestration of zinc, cadmium and silver in *Hebeloma mesophaeum* and characterization of its metallothionein genes. Fungal Genetics and Biology. 2014; 67:3-14.

Saffar A, Najjar MB, Mianabadi M. Activity of antioxidant enzymes in response to cadmium in *Arabidopsis thaliana*. Journal of Biological Sciences. 2009; 9:44-50.

Sakai Y, Watanabe T, Wasaki J, Senoura T, Shinano T, Osaki M. Influence of arsenic stress on synthesis and localization of low-molecular-weight thiols in *Pteris vittata*. Environmental Pollution. 2010; 158:3663-3669.

Sandrini JZ, Regoli F, Fattorini D, Notti A, Inácio AF, Linde-Arias AR, Laurino J, Bainy AC, Marins LF, Monserrat JM. Short-term responses to cadmium exposure in the estuarine polychaete *Laeonereis acuta* (Polychaeta, Nereididae): Subcellular distribution and oxidative stress generation. Environmental Toxicology and Chemistry: An International Journal. 2006; 25:1337-1344.

Sanger F, Nicklen S, Coulson AR. DNA sequencing with chain-terminating inhibitors. Proceedings of the National Academy of Sciences. 1977; 74:5463-5467.

Sarı A, Tuzen M. Kinetic and equilibrium studies of biosorption of Pb (II) and Cd (II) from aqueous solution by macrofungus (*Amanita rubescens*) biomass. Journal of Hazardous Materials. 2009; 164:1004-1011.

Satarug S, Baker JR, Urbenjapol S, Haswell-Elkins M, Reilly PE, Williams DJ, Moore MR. A global perspective on cadmium pollution and toxicity in non-occupationally exposed population. Toxicology Letters. 2003; 137:65-83.

Saunders RD, McLellan LI. Molecular cloning of *Drosophila* γ-glutamylcysteine synthetase by functional complementation of a yeast mutant. FEBS Letters. 2000; 467:337-340.

Schlunk I, Krause K, Wirth S, Kothe E. A transporter for abiotic stress and plant metabolite resistance in the ectomycorrhizal fungus *Tricholoma vaccinum*. Environmental Science and Pollution Research. 2015; 22:19384-19393.

Schuliga M, Chouchane S, Snow ET. Upregulation of glutathione-related genes and enzyme activities in cultured human cells by sublethal concentrations of inorganic arsenic. Toxicological Sciences. 2002; 70:183-192.

Schutzendubel A, Polle A. Plant responses to abiotic stresses: heavy metal-induced oxidative stress and protection by mycorrhization. Journal of Experimental Botany. 2002; 53:1351-1365.

Schwerdtle T, Ebert F, Thuy C, Richter C, Mullenders LH, Hartwig A. Genotoxicity of soluble and particulate cadmium compounds: impact on oxidative DNA damage and nucleotide excision repair. Chemical Research in Toxicology. 2010; 23:432-442.

Selosse MA, Bouchard D, Martin F, Tacon FL. Effect of *Laccaria bicolor* strains inoculated on Douglas-fir (*Pseudotsuga menziesii*) several years after nursery inoculation. Canadian Journal of Forest Research. 2000; 30:360-371.

Selosse MA, Jacquot D, Bouchard D, Martin F, Le Tacon F. Temporal persistence and spatial distribution of an American inoculant strain of the ectomycorrhizal basidiomycete *Laccaria bicolor* in a French forest plantation. Molecular Ecology. 1998; 7:561-573.

Selosse MA, Roy M. Green plants that feed on fungi: facts and questions about mixotrophy. Trends in Plant Science. 2009; 14:64-70.

Semane B, Cuypers A, Smeets K, Van Belleghem F, Horemans N, Schat H, Vangronsveld J. Cadmium responses in *Arabidopsis thaliana*: glutathione metabolism and antioxidative defence system. Physiologia Plantarum. 2007; 129:519-528.

Semane B, Dupae J, Cuypers A, Noben JP, Tuomainen M, Tervahauta A, Kärenlampi S, Van Belleghem F, Smeets K, Vangronsveld J. Leaf proteome responses of *Arabidopsis thaliana* exposed to mild cadmium stress. Journal of Plant Physiology. 2010; 167:247-254.

Sengupta D, Ramesh G, Mudalkar S, Kumar KR, Kirti PB, Reddy AR. Molecular cloning and characterization of γ-glutamyl cysteine synthetase (VrγECS) from roots of *Vigna radiata* (L.) Wilczek under progressive drought stress and recovery. Plant Molecular Biology Reporter. 2012; 30:894-903.

Seshadri B, Bolan NS, Choppala G, Kunhikrishnan A, Sanderson P, Wang H, Currie LD, Tsang DC, Ok YS, Kim G. Potential value of phosphate compounds in enhancing immobilization and reducing bioavailability of mixed heavy metal contaminants in shooting range soil. Chemosphere. 2017; 184:197-206.

Sfaxi-Bousbih A, Chaoui A, El Ferjani E. Cadmium impairs mineral and carbohydrate mobilization during the germination of bean seeds. Ecotoxicology and Environmental Safety. 2010; 73:1123-1129.

Shakhristova EV, Stepovaya EA, Ryazantseva NV, Nosareva OL, Yakushina VD, Ivanov VV, Novitskii VV. Role of glutathione system redox potential in apoptosis dysregulation in mcf-7 breast adenocarcinoma. Bulletin of Experimental Biology and Medicine. 2016; 160:364-367.

Shanying HE, Xiaoe YA, Zhenli HE, Baligar VC. Morphological and physiological responses of plants to cadmium toxicity: a review. Pedosphere. 2017; 27:421-438.

Sharma SS, Dietz KJ, Mimura T. Vacuolar compartmentalization as indispensable component of heavy metal detoxification in plants. Plant, Cell & Environment. 2016; 39:1112-1126.

Sharma SS, Dietz KJ. The significance of amino acids and amino acid-derived molecules in plant responses and adaptation to heavy metal stress. Journal of Experimental Botany. 2006; 57:711-726.

Sharples JM, Meharg AA, Chambers SM, Cairney JW. Arsenate resistance in the ericoid mycorrhizal fungus *Hymenoscyphus ericae*. New Phytologist. 2001; 151:265-270.

Sheikh-Assadi M, Khandan-Mirkohi A, Alemardan A, Moreno-Jiménez E. Mycorrhizal *Limonium sinuatum* (L.) mill. enhances accumulation of lead and cadmium. International Journal of Phytoremediation. 2015; 17:556-562.

Sheng Y, Yang X, Lian Y, Zhang B, He X, Xu W, Huang K. Characterization of a cadmium resistance *Lactococcus lactis* subsp. lactis strain by antioxidant assays and proteome profiles methods. Environmental Toxicology and Pharmacology. 2016; 46:286-291.

Shi L, Xue J, Liu B, Dong P, Wen Z, Shen Z, Chen Y. Hydrogen ions and organic acids secreted by ectomycorrhizal fungi, *Pisolithus* sp1, are involved in the efficient removal of hexavalent chromium from waste water. Ecotoxicology and Environmental Safety. 2018; 161:430-436.

Shi W, Zhang Y, Chen S, Polle A, Rennenberg H, Luo ZB. Physiological and molecular mechanisms of heavy metal accumulation in nonmycorrhizal versus mycorrhizal plants. Plant, Cell & Environment. 2019; 42:1087-1103.

Shinkai Y, Kimura T, Itagaki A, Yamamoto C, Taguchi K, Yamamoto M, Kumagai Y, Kaji T. Partial contribution of the Keap1–Nrf2 system to cadmium-mediated metallothionein expression in vascular endothelial cells. Toxicology and Applied Pharmacology. 2016; 295:37-46.

Shishkova E, Hebert AS, Coon JJ. Now, more than ever, proteomics needs better chromatography. Cell Systems. 2016; 3:321-324.

Shukla D, Trivedi PK, Nath P, Tuteja N. Metallothioneins and phytochelatins: role and perspectives in heavy metal (loid) s stress tolerance in crop plants. Abiotic stress response in plants. Wiley-VCH Verlag GmbH and Co. KGaA, Weinheim, Germany. 2016; 10: 233-274.

Shukla GS, Chiu JF, Hart BA. Cadmium-induced elevations in the gene expression of the regulatory subunit of γ-glutamylcysteine synthetase in rat lung and alveolar epithelial cells. Toxicology. 2000; 151:45-54.

Singh M, Srivastava PK, Verma PC, Kharwar RN, Singh N, Tripathi RD. Soil fungi for mycoremediation of arsenic pollution in agriculture soils. Journal of Applied Microbiology. 2015; 119:1278-1290.

Singh N, Ma LQ, Srivastava M, Rathinasabapathi B. Metabolic adaptations to arsenic-induced oxidative stress in *Pteris vittata* L and *Pteris ensiformis* L. Plant Science. 2006; 170:274-282.

Singh PK, Tewari RK. Cadmium toxicity induced changes in plant water relations and oxidative metabolism of *Brassica juncea* L. plants. Journal of Environmental Biology. 2003; 24:107-112.

Singh R, Gautam N, Mishra A, Gupta R. Heavy metals and living systems: An overview. Indian Journal of Pharmacology. 2011; 43:246.

Širić I, Humar M, Kasap A, Kos I, Mioč B, Pohleven F. Heavy metal bioaccumulation by wild edible saprophytic and ectomycorrhizal mushrooms. Environmental Science and Pollution Research. 2016; 23:18239-18252.

Širić I, Kasap A, Bedeković D, Falandysz J. Lead, cadmium and mercury contents and bioaccumulation potential of wild edible saprophytic and ectomycorrhizal mushrooms, Croatia. Journal of Environmental Science and Health, Part B. 2017; 52:156-165.

Smičiklas I, Smiljanić S, Perić-Grujić A, Šljivić-Ivanović M, Mitrić M, Antonović D. Effect of acid treatment on red mud properties with implications on Ni (II) sorption and stability. Chemical Engineering Journal. 2014; 242:27-35.

Smirnova GV, Oktyabrsky ON. Glutathione in bacteria. Biochemistry (Moscow). 2005; 70:1199-1211.

Smith AH, Marshall G, Roh T, Ferreccio C, Liaw J, Steinmaus C. Lung, bladder, and kidney cancer mortality 40 years after arsenic exposure reduction. JNCI: Journal of the National Cancer Institute. 2017; 110:241-249.

Smith FA, Smith SE. How harmonious are arbuscular mycorrhizal symbioses? Inconsistent concepts reflect different mindsets as well as results. New Phytologist. 2015; 205:1381-1384.

Smith SE, Read DJ. Mycorrhizal symbiosis. NY: Academic press; 2010.

Soares MA, Quina MJ, Quinta-Ferreira RM. Immobilisation of lead and zinc in contaminated soil using compost derived from industrial eggshell. Journal of Environmental Management. 2015; 164:137-145.

Sobrino-Plata J, Herrero J, Carrasco-Gil S, Pérez-Sanz A, Lobo C, Escobar C, Millán R, Hernández LE. Specific stress responses to cadmium, arsenic and mercury appear in the metallophyte *Silene vulgaris* when grown hydroponically. RSC Advances. 2013; 3:4736-4744.

Sobrino-Plata J, Ortega-Villasante C, Flores-Cáceres ML, Escobar C, Del Campo FF, Hernández LE. Differential alterations of antioxidant defenses as bioindicators of mercury and cadmium toxicity in alfalfa. Chemosphere. 2009; 77:946-954.

Song WY, Park J, Eisenach C, Maeshima M, Lee Y, Martinoia E. ABC transporters and heavy metals. InPlant ABC Transporters 2014 (pp. 1-17). Springer, Cham.

Song Y, Zhang H, Chen C, Wang G, Zhuang K, Cui J, Shen Z. Proteomic analysis of copper-binding proteins in excess copper-stressed rice roots by immobilized metal affinity chromatography and two-dimensional electrophoresis. BioMetals. 2014; 27:265-276.

Sormani R, Delannoy E, Lageix S, Bitton F, Lanet E, Saez-Vasquez J, Deragon JM, Renou JP, Robaglia C. Sublethal cadmium intoxication in *Arabidopsis thaliana* impacts translation at multiple levels. Plant and Cell Physiology. 2011; 52:436-447.

Sousa CA, Hanselaer S, Soares EV. ABCC subfamily vacuolar transporters are involved in Pb (lead) detoxification in *Saccharomyces cerevisiae*. Applied Biochemistry and Biotechnology. 2015; 175:65-74.

Sowjanya TN, Mohan PM. A calcium binding protein from cell wall of *Neurospora crassa*. Journal of Basic Microbiology. 2009; 49:371-376.

Srivastava S, Sharma YK. Impact of arsenic toxicity on black gram and its amelioration using phosphate. ISRN Toxicology. 2013; 2013:340925.

Štefanić PP, Jarnević M, Cvjetko P, Biba R, Šikić S, Tkalec M, Cindrić M, Letofsky-Papst I, Balen B. Comparative proteomic study of phytotoxic effects of silver nanoparticles and silver ions on tobacco plants. Environmental Science and Pollution Research. 2019; 26:22529-22550.

Su S, Zeng X, Bai L, Li L, Duan R. Arsenic biotransformation by arsenic-resistant fungi *Trichoderma asperellum* SM-12F1, *Penicillium janthinellum* SM-12F4, and *Fusarium oxysporum* CZ-8F1. Science of the Total Environment. 2011; 409:5057-5062.

Sun Q, Wang XR, Ding SM, Yuan XF. Effects of interactions between cadmium and zinc on phytochelatin and glutathione production in wheat (*Triticum aestivum* L.). Environmental Toxicology: An International Journal. 2005; 20:195-201.

Suzuki T, Niinae M, Koga T, Akita T, Ohta M, Choso T. EDDS-enhanced electrokinetic remediation of heavy metal-contaminated clay soils under neutral pH conditions. Colloids and Surfaces A: Physicochemical and Engineering Aspects. 2014; 440:145-150.

Sytar O, Kumar A, Latowski D, Kuczynska P, Strzałka K, Prasad MN. Heavy metal-induced oxidative damage, defense reactions, and detoxification mechanisms in plants. Acta Physiologiae Plantarum. 2013; 35:985-999.

Szajko K, Plich J, Przetakiewicz J, Sołtys-Kalina D, Marczewski W. Comparative proteomic analysis of resistant and susceptible potato cultivars during *Synchytrium endobioticum* infestation. Planta. 2020; 251:4.

Tajudin SA, Azmi MA, Nabila AT. Stabilization/solidification remediation method for contaminated soil: a review. InIOP Conference Series: Materials Science and Engineering. 2016 (Vol. 136, No. 1, p. 012043). IOP Publishing.

Talukdar D, Talukdar T. Retracted article: Coordinated response of sulfate transport, cysteine biosynthesis, and glutathione-mediated antioxidant defense in lentil (*Lens culinaris* Medik.) genotypes exposed to arsenic. Protoplasma. 2014; 251:839-855.

Tamás MJ, Fauvet B, Christen P, Goloubinoff P. Misfolding and aggregation of nascent proteins: a novel mode of toxic cadmium action in vivo. Current Genetics. 2018; 64:177-181.

Tang L, Wang W, Zhou W, Cheng K, Yang Y, Liu M, Cheng K, Wang W. Three-pathway combination for glutathione biosynthesis in *Saccharomyces cerevisiae*. Microbial Cell Factories. 2015; 14:139.

Targhetta BL, Oliveira VL, Rossi MJ. Tolerance of ectomycorrhizal fungi and plants associated to toxic levels of metals. Revista Árvore. 2013; 37:825-833.

Tarhan L, Kavakcioglu B. Glutathione metabolism in *Urtica dioica* in response to cadmium based oxidative stress. Biologia Plantarum. 2016; 60:163-172.

Taylor V, Goodale B, Raab A, Schwerdtle T, Reimer K, Conklin S, Karagas MR, Francesconi KA. Human exposure to organic arsenic species from seafood. Science of the Total Environment. 2017; 580:266-282.

Tchounwou PB, Yedjou CG, Patlolla AK, Sutton DJ. Heavy metal toxicity and the environment. InMolecular, Clinical and Environmental Toxicology 2012 (pp. 133-164). Springer, Basel.

Thévenod F. Cadmium and cellular signaling cascades: to be or not to be?. Toxicology and Applied Pharmacology. 2009; 238:221-239.

Thomas DJ. Unraveling arsenic—glutathione connections. Toxicological Sciences. 2009; 107:309-311.

Thorsen M, Jacobson T, Vooijs R, Navarrete C, Bliek T, Schat H, Tamás MJ. Glutathione serves an extracellular defence function to decrease arsenite accumulation and toxicity in yeast. Molecular Microbiology. 2012; 84:1177-1188.

Thorsen M, Lagniel G, Kristiansson E, Junot C, Nerman O, Labarre J, Tamás MJ. Quantitative transcriptome, proteome, and sulfur metabolite profiling of the *Saccharomyces cerevisiae* response to arsenite. Physiological Genomics. 2007; 30:35-43.

Torres-Aquino M, Becquer A, Le Guernevé C, Louche J, Amenc LK, Staunton S, Quiquampoix H, Plassard C. The host plant *Pinus pinaster* exerts specific effects on phosphate efflux and polyphosphate metabolism of the ectomycorrhizal fungus *Hebeloma cylindrosporum*: a radiotracer, cytological staining and 31P NMR spectroscopy study. Plant, Cell & Environment. 2017; 40:190-202.

Townsend DM. S-glutathionylation: indicator of cell stress and regulator of the unfolded protein response. Molecular Interventions. 2007; 7:313.

Tripp SL, Pusztay SV, Ribbe AE, Wei A. Self-assembly of cobalt nanoparticle rings. Journal of the American Chemical Society. 2002; 124:7914-7925.

Turnau K, Przybyłowicz WJ, Mesjasz-Przybyłowicz J. Heavy metal distribution in *Suillus luteus* mycorrhizas–as revealed by micro-PIXE analysis. Nuclear Instruments and Methods in Physics Research Section B: Beam Interactions with Materials and Atoms. 2001; 181:649-658.

Ubiyvovk VM, Blazhenko OV, Zimmermann M, Sohn MJ, Kang HA. Cloning and functional analysis of the GSH1 gene complementing cysteine and glutathione auxotrophy of the methylotrophic yeast *Hansenula polymorpha*. Ukrainskii Biokhimicheskii Zhurnal. 2011; 83:67–81.

Uniprot. Metallothioneins: classification and list of entries. 2019. (https://www.uniprot.org/docs/metallo.txt)

US Geological Survey. Mineral Commodity Summaries. Government Printing Office. 2009.

USEPA. Edition of the Drinking Water Standards and Health Advisories Tables. 2018. https://www.epa.gov/sites/production/files/2018-03/documents/dwtable2018.pdf

Van Baelen K, Dode L, Vanoevelen J, Callewaert G, De Smedt H, Missiaen L, Parys JB, Raeymaekers L, Wuytack F. The Ca^{2+}/Mn^{2+} pumps in the Golgi apparatus. Biochimica et Biophysica Acta (BBA)-Molecular Cell Research. 2004; 1742:103-112.

Van Der Heijden MG, Martin FM, Selosse MA, Sanders IR. Mycorrhizal ecology and evolution: the past, the present, and the future. New Phytologist. 2015; 205:1406-1423.

Vanaja M, Charyulu NV, Rao KV. Effect of cadmium on carbohydrate, nucleic acid, amino acid and phenolic content in *Stigeoclonium tenue* Kutz. Indian Journal of Plant Physiology. 2000; 5:253-256.

Verbruggen N, Hermans C, Schat H. Molecular mechanisms of metal hyperaccumulation in plants. New Phytologist. 2009; 181:759-776.

Vergauwen B, De Vos D, Van Beeumen JJ. Characterization of the bifunctional γ-glutamate-cysteine ligase/glutathione synthetase (GshF) of *Pasteurella multocida*. Journal of Biological Chemistry. 2006; 281:4380-4394.

Verougstraete V, Lison D, Hotz P. Cadmium, lung and prostate cancer: a systematic review of recent epidemiological data. Journal of Toxicology and Environmental Health, Part B. 2003; 6:227-256.

Vido K, Spector D, Lagniel G, Lopez S, Toledano MB, Labarre J. A proteome analysis of the cadmium response in *Saccharomyces cerevisiae*. Journal of Biological Chemistry. 2001; 276:8469-8474.

Waalkes MP, Goering PL. Metallothionein and other cadmium-binding proteins: recent developments. Chemical Research in Toxicology. 1990; 3:281-288.

Wachter A, Wolf S, Steininger H, Bogs J, Rausch T. Differential targeting of GSH1 and GSH2 is achieved by multiple transcription initiation: implications for the compartmentation of glutathione biosynthesis in the *Brassicaceae*. The Plant Journal. 2005; 41:15-30.

Waisberg M, Joseph P, Hale B, Beyersmann D. Molecular and cellular mechanisms of cadmium carcinogenesis. Toxicology. 2003; 192:95-117.

Wan L, Zhang H. Cadmium toxicity: effects on cytoskeleton, vesicular trafficking and cell wall construction. Plant Signaling & Behavior. 2012; 7:345-348.

Wang A, Crowley DE. Global gene expression responses to cadmium toxicity in *Escherichia coli*. Journal of Bacteriology. 2005; 187:3259-3266.

Wang B, Qiu YL. Phylogenetic distribution and evolution of mycorrhizas in land plants. Mycorrhiza. 2006; 16:299-363.

Wang C, Wang CY, Zhao XQ, Chen RF, Lan P, Shen RF. Proteomic analysis of a high aluminum tolerant yeast *Rhodotorula taiwanensis* RS1 in response to aluminum stress. Biochimica et Biophysica Acta (BBA)-Proteins and Proteomics. 2013; 1834:1969-1975.

Wang H, He L, Song J, Cui W, Zhang Y, Jia C, Francis D, Rogers HJ, Sun L, Tai P, Hui X. Cadmium-induced genomic instability in *Arabidopsis*: Molecular toxicological biomarkers for early diagnosis of cadmium stress. Chemosphere. 2016; 150:258-265.

Wang L, Yan B, Liu N, Li Y, Wang Q. Effects of cadmium on glutathione synthesis in hepatopancreas of freshwater crab, *Sinopotamon yangtsekiense*. Chemosphere. 2008; 74:51-56.

Wang P, Chen H, Kopittke PM, Zhao FJ. Cadmium contamination in agricultural soils of China and the impact on food safety. Environmental Pollution. 2019; 249:1038-1048.

Wang QL, Liu DH, Yue JY. The uptake of cadmium by *Allium cepa* var. agrogarum L. and its effects on chromosome and nucleolar behavior in root tip cells. Phyton, International Journal of Experimental Botany. 2017; 85:155-161.

Wang S, Shi X. Molecular mechanisms of metal toxicity and carcinogenesis. Molecular and Cellular Biochemistry. 2001; 222:3-9.

Wang SH, Shih YL, Ko WC, Wei YH, Shih CM. Cadmium-induced autophagy and apoptosis are mediated by a calcium signaling pathway. Cellular and Molecular Life Sciences. 2008; 65:3640-3652.

Wang Y, Qian Y, Hu H, Xu Y, Zhang H. Comparative proteomic analysis of Cd-responsive proteins in wheat roots. Acta Physiologiae Plantarum. 2011; 33:349-357.

Wang Y, Wang S, Xu P, Liu C, Liu M, Wang Y, Wang C, Zhang C, Ge Y. Review of arsenic speciation, toxicity and metabolism in microalgae. Reviews in Environmental Science and Bio/Technology. 2015; 14:427-451.

Watanabe M, Henmi K, Ogawa KI, Suzuki T. Cadmium-dependent generation of reactive oxygen species and mitochondrial DNA breaks in photosynthetic and non-photosynthetic strains of *Euglena gracilis*. Comparative Biochemistry and Physiology Part C: Toxicology & Pharmacology. 2003; 134:227-234.

Waterlot C, Pruvot C, Marot F, Douay F. Impact of a phosphate amendment on the environmental availability and phytoavailability of Cd and Pb in moderately and highly carbonated kitchen garden soils. Pedosphere. 2017; 27:588-605.

Wei M, Chen J, Wang X. Removal of arsenic and cadmium with sequential soil washing techniques using Na_2EDTA, oxalic and phosphoric acid: optimization conditions, removal effectiveness and ecological risks. Chemosphere. 2016; 156:252-261.

Wei X, Qi Y, Zhang X, Gu X, Cai H, Yang J, Zhang Y. ROS act as an upstream signal to mediate cadmium-induced mitophagy in mouse brain. Neurotoxicology. 2015; 46:19-24.

Weng ZX, Wang LX, Tan FL, Huang L, Xing JH, Chen SP, Cheng CL, Chen W. Proteomic and physiological analyses reveal detoxification and antioxidation induced by Cd stress in *Kandelia candel* roots. Trees. 2013; 27:583-595.

Wheeler GL, Trotter EW, Dawes IW, Grant CM. Coupling of the transcriptional regulation of glutathione biosynthesis to the availability of glutathione and methionine via the Met4 and Yap1 transcription factors. Journal of Biological Chemistry. 2003; 278:49920-49928.

Wu AL, Moye-Rowley WS. GSH1, which encodes gamma-glutamylcysteine synthetase, is a target gene for yAP-1 transcriptional regulation. Molecular and Cellular Biology. 1994; 14:5832-5839.

Wu QS, Cao MQ, Zou YN, He XH. Direct and indirect effects of glomalin, mycorrhizal hyphae, and roots on aggregate stability in rhizosphere of trifoliate orange. Scientific Reports. 2014; 4:5823.

Wu Z, Ren H, McGrath SP, Wu P, Zhao FJ. Investigating the contribution of the phosphate transport pathway to arsenic accumulation in rice. Plant Physiology. 2011; 157:498-508.

Wyszkowska J, Borowik A, Kucharski M, Kucharski J. Effect of cadmium, copper and zinc on plants, soil microorganisms and soil enzymes. Journal of Elementology. 2013; 18:2587-2602.

Xiang M, Mohamalawari D, Rao R. A novel isoform of the secretory pathway Ca^{2+}, Mn^{2+}-ATPase, hSPCA2, has unusual properties and is expressed in the brain. Journal of Biological Chemistry. 2005; 280:11608-11614.

Xu J, Zhu Y, Ge Q, Li Y, Sun J, Zhang Y, Liu X. Comparative physiological responses of *Solanum nigrum* and *Solanum torvum* to cadmium stress. New Phytologist. 2012; 196:125-138.

Xu P, Liu L, Zeng G, Huang D, Lai C, Zhao M, Huang C, Li N, Wei Z, Wu H, Zhang C. Heavy metal-induced glutathione accumulation and its role in heavy metal detoxification in *Phanerochaete chrysosporium*. Applied Microbiology and Biotechnology. 2014; 98:6409-6418.

Xu P, Zeng G, Huang D, Liu L, Zhao M, Lai C, Li N, Wei Z, Huang C, Zhang C. Metal bioaccumulation, oxidative stress and antioxidant defenses in *Phanerochaete chrysosporium* response to Cd exposure. Ecological Engineering. 2016; 87:150-156.

Xu X, Xia L, Zhu W, Zhang Z, Huang Q, Chen W. Role of *Penicillium chrysogenum* XJ-1 in the detoxification and bioremediation of cadmium. Frontiers in Microbiology. 2015; 6:1422.

Xu Z, Wang M, Xu D, Xia Z. The Arabidopsis APR2 positively regulates cadmium tolerance through glutathione-dependent pathway. Ecotoxicology and Environmental Safety. 2020; 187:109819.

Xu Z, Wu Y, Jiang Y, Zhang X, Li J, Ban Y. Arbuscular mycorrhizal fungi in two vertical-flow wetlands constructed for heavy metal-contaminated wastewater bioremediation. Environmental Science and Pollution Research. 2018; 25:12830-12840.

Xuan R, Wang L, Sun M, Ren G, Jiang M. Effects of cadmium on carbohydrate and protein metabolisms in the freshwater crab *Sinopotamon yangtsekiense*. Comparative Biochemistry and Physiology Part C: Toxicology & Pharmacology. 2011; 154:268-274.

Xue ZC, Gao HY, Zhang LT. Effects of cadmium on growth, photosynthetic rate and chlorophyll content in leaves of soybean seedlings. Biologia Plantarum. 2013; 57:587-590.

Yadav SK. Heavy metals toxicity in plants: an overview on the role of glutathione and phytochelatins in heavy metal stress tolerance of plants. South African Journal of Botany. 2010; 76:167-179.

Yallappa S, Nuzhat FB. Toxic effect of carbohydrate metabolism changes on carp (*Cyprinus carpio*) exposed to cadmium Chloride. International Journal of Fisheries and Aquatic Studies. 2018; 6:364-371.

Yan Y, Yi W, HU FF, Jiang CY, Zhang YJ, Yang JL, Zhao SW, GU JH, Liu XZ, Bian JC, Liu ZP. Cadmium activates reactive oxygen species-dependent AKT/mTOR and mitochondrial apoptotic pathways in neuronal cells. Biomedical and Environmental Sciences. 2016; 29:117-126.

Yang H, Wang J, Lv Z, Tian J, Peng Y, Peng X, Xu X, Song Q, Lv B, Chen Z, Sun Z. Metatranscriptome analysis of the intestinal microorganisms in *Pardosa pseudoannulata* in response to cadmium stress. Ecotoxicology and Environmental Safety. 2018; 159:1-9.

Yang SW, Becker FF, Chan JY. Inhibition of human DNA ligase I activity by zinc and cadmium and the fidelity of ligation. Environmental and Molecular Mutagenesis. 1996; 28:19-25.

Yang Y, Li X, Yang S, Zhou Y, Dong C, Ren J, Sun X, Yang Y. Comparative physiological and proteomic analysis reveals the leaf response to cadmium-induced stress in poplar (*Populus yunnanensis*). PLoS One. 2015; 10.

Yeh JH, Huang CC, Yeh MY, Wang JS, Lee JK, Jan CR. Cadmium-induced cytosolic Ca^{2+} elevation and subsequent apoptosis in renal tubular cells. Basic & Clinical Pharmacology & Toxicology. 2009; 104:345-351.

Yue JY, Wei XJ, Wang HZ. Cadmium tolerant and sensitive wheat lines: their differences in pollutant accumulation, cell damage, and autophagy. Biologia Plantarum. 2018; 62:379-387.

Yung MC, Ma J, Salemi MR, Phinney BS, Bowman GR, Jiao Y. Shotgun proteomic analysis unveils survival and detoxification strategies by *Caulobacter crescentus* during exposure to uranium, chromium, and cadmium. Journal of Proteome Research. 2014; 13:1833-1847.

Zemanová V, Pavlík M, Pavlíková D. Cadmium toxicity induced contrasting patterns of concentrations of free sarcosine, specific amino acids and selected microelements in two *Noccaea* species. PloS One. 2017; 12:e0177963.

Zhai Q, Xiao Y, Zhao J, Tian F, Zhang H, Narbad A, Chen W. Identification of key proteins and pathways in cadmium tolerance of *Lactobacillus plantarum* strains by proteomic analysis. Scientific Reports. 2017; 7:1-7.

Zhang A, Xu T, Zou H, Pang Q. Comparative proteomic analysis provides insight into cadmium stress responses in brown algae *Sargassum fusiforme*. Aquatic Toxicology. 2015; 163:1-5.

Zhang F, Anasontzis GE, Labourel A, Champion C, Haon M, Kemppainen M, Commun C, Deveau A, Pardo A, Veneault-Fourrey C, Kohler A. The ectomycorrhizal basidiomycete *Laccaria bicolor* releases a secreted β-1, 4 endoglucanase that plays a key role in symbiosis development. New Phytologist. 2018; 220:1309-1321.

Zhang H, Zhang LL, Li J, Chen M, An RD. Comparative study on the bioaccumulation of lead, cadmium and nickel and their toxic effects on the growth and enzyme defence strategies of a heavy metal accumulator, *Hydrilla verticillata* (Lf) Royle. Environmental Science and Pollution Research. 2020; 11: 1-3.

Zhang J, Sun X, Wu J. Heavy metal ion detection platforms based on a glutathione probe: a mini review. Applied Sciences. 2019; 9:489.

Zhang L, Elias JE. Relative protein quantification using tandem mass tag mass spectrometry. InProteomics 2017 (pp. 185-198). Humana Press, New York, NY.

Zhang S, Hao S, Qiu Z, Wang Y, Zhao Y, Li Y, Gao W, Wu Y, Liu C, Xu X, Wang H. Cadmium disrupts the DNA damage response by destabilizing RNF168. Food and Chemical Toxicology. 2019; 133:110745.

Zhang Z, Wu S, Stenoien DL, Paša-Tolić L. High-throughput proteomics. Annual Review of Analytical Chemistry. 2014; 7:427-4254.

Zhao FJ, Ma JF, Meharg AA, McGrath SP. Arsenic uptake and metabolism in plants. New Phytologist. 2009; 181:777-794.

Zhao L, Sun YL, Cui SX, Chen M, Yang HM, Liu HM, Chai TY, Huang F. Cd-induced changes in leaf proteome of the hyperaccumulator plant *Phytolacca americana*. Chemosphere. 2011; 85:56-66.

Zheng C, Zhang L, Chen M, Zhao XQ, Duan Y, Meng Y, Zhang X, Shen RF. Effects of cadmium exposure on expression of glutathione synthetase system genes in *Acidithiobacillus ferrooxidans*. Extremophiles. 2018; 22:895-902.

Zheng G, Lv HP, Gao S, Wang SR. Effects of cadmium on growth and antioxidant responses in *Glycyrrhiza uralensis* seedlings. Plant, Soil and Environment. 2010; 56:508-515.

Zheng W, Yingheng FE, Huang Y. Soluble protein and acid phosphatase exuded by ectomycorrhizal fungi and seedlings in response to excessive Cu and Cd. Journal of Environmental Sciences. 2009; 21:1667-1672.

Zhou C, Zhang X, Chen Y, Liu X, Sun Y, Xiong B. Glutathione alleviates the cadmium exposure-caused porcine oocyte meiotic defects via eliminating the excessive ROS. Environmental Pollution. 2019; 255:113194.

Zhou X, Ma Y, Sugiura R, Kobayashi D, Suzuki M, Deng L, Kuno T. MAP kinase kinase kinase (MAPKKK)-dependent and-independent activation of Sty1 stress MAPK in fission yeast. Journal of Biological Chemistry. 2010; 285:32818-32823.

Zhu G, Xiao H, Guo Q, Zhang Z, Zhao J, Yang D. Effects of cadmium stress on growth and amino acid metabolism in two compositae plants. Ecotoxicology and Environmental Safety. 2018; 158:300-308.

Ziller A, Fraissinet-Tachet L. Metallothionein diversity and distribution in the tree of life: a multifunctional protein. Metallomics. 2018; 10:1549-1559.

Zoghlami LB, Djebali W, Abbes Z, Hediji H, Maucourt M, Moing A, Brouquisse R, Chaïbi W. Metabolite modifications in *Solanum lycopersicum* roots and leaves under cadmium stress. African Journal of Biotechnology. 2011; 10:567-79.

Zong K, Huang J, Nara K, Chen Y, Shen Z, Lian C. Inoculation of ectomycorrhizal fungi contributes to the survival of tree seedlings in a copper mine tailing. Journal of Forest Research. 2015; 20:493-500.

APPENDIX I

Modified Melin-Norkan's Medium (Gay, 1990)

Media Component	Concentration
$(NH_4)HPO_4$	250 mg/L
KH_2PO_4	500 mg/L
$MgSO_4.7H_2O$	150 mg/L
$CaCl_2.H_2O$	50 mg/L
NaCl	25 mg/L
$FeCl_3$ 1 % (w\v)	1.2 ml/L
Thiamine HCl	40 mg/L
Biotine	0.4 mg/L
Glucose	2500 mg/L
Heller's micronutrient (100x)	10 ml/L
Agar	8 g/L

Heller's micronutrients (Heller, 1953)

Component	Concentration
$FeCl_3.6H_20$	100 mg/L
$ZnSO_4.7H_20$	100 mg/L
H_3BO_3	100 mg/L
$MgSO_4.7H_20$	10 mgL
$AlCl_3$	3 mg/L
KI	1 mg/L
$NiCl_3.6H_20$	3 mg/L
$CuSO_4.5H_20$	3 mg/L

Luria Broth

Component	Concentration
Tryptone	10 g/L
Yeast extract	5 g/L
NaCl	5 g/L

Adjust pH to 7.0 and autoclave at 121°C

YPD medium

Component	Concentration
Peptone	20 g/L
Yeast extract	10 g/L
Dextrose	20 g/L

Adjust pH to 6.5 and autoclave at 121°C

SD medium

Component	Concentration
Yeast nitrogen base	6.7 g/L
1% Adenine stock	1 ml/L
1% Tyrosine stock	5 ml/L
DO supplement - ura (Clontech)	0.77 g/L
Glucose	20 g

Adjust pH to 5.6 and autoclave at 121°C

Plasmid isolation Solutions

Solution I		Solution II		Solution III	
Glucose	50 mM	NaoH	0.2 N	5M Potassium acetate	60 ml
EDTA	10 mM	SDS	1%	Glacial acetic acid	11.5 ml
Tris-HCl (pH 8)	25 mM			Water	To make 100 ml

Bradford Reagent

Component	Concentration
Coomassie Brilliant Blue G-250	100 mg
Ethanol (95%)	50 ml
Phosphoric acid (85%)	100 ml
Deionized water	To make 1 litre

TBE Buffer (5X)

Component	**Concentration**
Tris-HCl	54 g (pH 8)
Boric acid	27.5 g
EDTA (0.5 M)	20 ml
Deionized water	To make 1 litre

DNA loading dye (6X)

Component	**Concentration**
Bromophenol blue	0.25%
Xylene cyanol FF	0.25%
Glycerol in water	30.0%

SDS-PAGE

Resolving Gel (12%)	
1.5 M Tris (pH 8.0)	2.0 ml
Acrylamide solution (30%) (29 g acrylamide + 1 g bis-acrylamide in 100 ml H_2O)	3.2 ml
SDS (10%)	80 µl
Distilled H_2O	2.6 ml
TEMED	8 µl
APS (10%) freshly prepared	80 µl

Stacking Gel (4%)	
0.5 M Tris (pH 6.8)	1.25 ml
Acrylamide solution (30%) (29 g acrylamide + 1 g bis-acrylamide in 100 ml H_2O)	1.0 ml
SDS (10%)	50 µl
Distilled H_2O	2.6 ml
TEMED	5 µl
APS (10%) freshly prepared	50 µl

SDS Tank Buffer (pH8.3)	
Tris Base	6.05 g
Glycine	28.8 g
SDS (10%)	10 ml
Distilled water	To make 2 l

Staining solution	
Coomassie Blue (R-250)	0.3 g
Methanol	80 ml
Glacial acetic acid	20 ml
Distilled water	To make 100 ml

Destaining Solution	
Acetic acid	100 ml
Methanol	300 ml
Distilled water	600 ml

APPENDIX II

Laccaria bicolor strain S238N gamma glutamylcysteine synthetase (GSH1) mRNA, complete cds

GenBank: MF766455.1

FASTA Graphics

Go to:

```
LOCUS       MF766455                1854 bp    mRNA    linear   PLN 15-APR-2018
DEFINITION  Laccaria bicolor strain S238N gamma glutamylcysteine synthetase
            (GSH1) mRNA, complete cds.
ACCESSION   MF766455
VERSION     MF766455.1
KEYWORDS    .
SOURCE      Laccaria bicolor
  ORGANISM  Laccaria bicolor
            Eukaryota; Fungi; Dikarya; Basidiomycota; Agaricomycotina;
            Agaricomycetes; Agaricomycetidae; Agaricales; Tricholomataceae;
            Laccaria.
REFERENCE   1 (bases 1 to 1854)
  AUTHORS   Khullar,S. and Reddy,S.M.
  TITLE     Cloning and characterization of glutathione biosynthesis genes from
            ectomycorrhizal fungus Laccaria bicolor in response to cadmium and
            arsenic stress
  JOURNAL   Unpublished
REFERENCE   2 (bases 1 to 1854)
  AUTHORS   Khullar,S. and Reddy,S.M.
  TITLE     Direct Submission
  JOURNAL   Submitted (24-AUG-2017) Department of Biotechnology, Thapar
            University, Bhadson Road, Patiala, Punjab 147004, India
COMMENT     ##Assembly-Data-START##
            Sequencing Technology :: Sanger dideoxy sequencing
            ##Assembly-Data-END##
FEATURES             Location/Qualifiers
     source          1..1854
                     /organism="Laccaria bicolor"
                     /mol_type="mRNA"
                     /strain="S238N"
                     /db_xref="taxon:29883"
     gene            1..1854
                     /gene="GSH1"
     CDS             1..1854
                     /gene="GSH1"
                     /EC_number="6.3.2.2"
```

/note="GSH1; first enzyme involved in ATP-dependent glutathione biosynthesis"
/codon_start=1
/product="gamma glutamylcysteine synthetase"
/protein_id="AVX28161.1"
/translation="MGLLYLGTPLPWDEAKKYADHVRTHGITQFLHIWDRLKDRTGDE
LLWGDEIEYMVVAFDEQEKSAKLSLRQTEILAKLSDIVHDISAGLRYEVDTLMLLTDH
FSVAVPNFHPEYGRYMLESTPGSPYTGYIQDLLSVECNMRYRRALARKHLKPNEIPLT
FTSFPLLGVQGHFTEPYFNPNDAVSSHSFFLPEEITNPHARFPTLTANIRSRRGSKVA
INLPIFFDEKTPRPFVDPTIPWDRNIYKEDSDAKNGAALPDHIYLDAMGFGMGCCCLQ
LTFQACNVSDARRLYDGLIPIGPILLALTGASPIWRGYLADVDCRWNVIAGSVDDRTE
EERGLKVIPKSRYDSVDLYISNDGFNRPEYNDNYLPYDESIYDRLRAHGIDDLLSKHM
SHLFIRDPLVVFSETINQDDTSSSDHFENIQSTNWQTLRFKPPPPNSPIGWRVEFRSM
EVQITDFENAAFAVFVVLLSRAILSFNLNLYIPISKVDENMATAQRRDAAAKAKFHFR
KDVYPPGRSGASSEEYEEMSMDEIINGKGDNFPGLLRLIYAYIDTLDIEPRELAKVGS
YLDLIRRRANGSLITPATWIRNFVRSHPTYKHDSVVSQEINYDLLLAIDEM"

ORIGIN

```
        1 atgggcctct tgtatctcgg cactcctttg ccttgggatg aagctaaaaa atatgctgac
       61 catgtgcgaa cccatggaat cactcagttc cttcatattt gggatcgatt gaaggacaga
      121 actggcgacg agctactatg gggcgatgag atcgaatata tggtggtagc cttcgatgaa
      181 caagaaaaga gtgcaaaact ctcattgagg caaacggaaa ttctcgcaaa actcagtgat
      241 atagtccatg acatttctgc tggcttacgt tacgaggtcg acacattgat gttattaaca
      301 gatcatttca gcgtcgctgt gccgaacttc cacccagagt atggacgata catgcttgag
      361 tctaccccag gttctcccta cactggctat attcaagatc tcttgtcggt tgagtgcaat
      421 atgcgataca gacgagctct tgctcgtaaa catctcaagc cgaatgaaat acctttgacc
      481 tttacttcgt ttcctctttt gggtgtgcaa ggtcacttta cggaaccata tttcaatcca
      541 aacgatgctg tttcaagtca tagctttttt ttacccgaag aaatcacgaa tccgcatgca
      601 cgcttcccca cccttacggc caatatcagg agtcgaagag gttccaaggt tgcaatcaat
      661 ttaccaattt ttttcgacga gaagacccct cgtccatttg tcgacccaac gattccctgg
      721 gaccgcaaca tttacaaaga agattcagat gcgaagaatg gtgcagccct ccccgatcac
      781 atttatcttg acgcgatggg ctttggaatg ggatgttgct gccttcaact cactttccag
      841 gcatgcaatg tttctgacgc caggcgcctg tatgatggtt tgattcctat tggccctatc
      901 ttgctggcgt tgacgggggc cagccctata tggcgtgggt acctcgctga tgtggattgt
      961 cgatggaacg ttattgccgg cagtgtcgat gatcgcacgg aggaagagcg tggcttgaag
     1021 gtgattccaa agtctcgtta cgacagcgtt gatctgtaca tctcaaacga tggattcaac
     1081 cgacccgagt ataacgataa ctatttgccg tacgacgaat ctatttacga ccgcctgcgc
     1141 gcacatggaa tcgatgattt gctctcaaag cacatgtcgc acctcttcat acgcgaccct
     1201 cttgtcgttt tctcagaaac aatcaaccaa gatgacacgt ccagcagtga tcattttgag
     1261 aatatacaat caaccaactg gcagactctc cgattcaaac cccctccgcc caactcaccg
     1321 attggctggc gtgttgaatt tcgtagcatg gaggttcaaa taacggattt cgagaatgcc
     1381 gctttcgctg tatttgttgt gctgctttca cgcgctatcc ttagtttcaa tcttaatctc
     1441 tacattccaa tatcgaaggt cgacgagaat atggccacgg ctcagcgtag ggacgccgct
     1501 gcgaaagcga agttccattt tagaaaagac gtatacccac ccggccgaag tggagcgtca
     1561 agcgaggagt atgaggaaat gagcatggac gaaatcatca atggcaaggg ggacaatttc
     1621 ccaggactcc tgcgacttat ttatgcctat attgacacgt tagatatcga gccgcgagag
```

```
     1681 ttggcaaagg tagggagtta tctagatctc attagacggc gggccaacgg atctctcata
     1741 actcctgcaa cttggatcag aaatttcgta cggtcgcacc cgacttataa acacgactcg
     1801 gttgtttcac aggaaattaa ttacgatcta ttgctggcca tagatgaaat gtga
//
```

Laccaria bicolor strain S238N glutathione synthetase (GSH2) mRNA, partial cds

GenBank: MF766456.1

FASTA Graphics

Go to:

```
LOCUS       MF766456               1593 bp    mRNA    linear   PLN 15-APR-2018
DEFINITION  Laccaria bicolor strain S238N glutathione synthetase (GSH2) mRNA,
            partial cds.
ACCESSION   MF766456
VERSION     MF766456.1
KEYWORDS    .
SOURCE      Laccaria bicolor
  ORGANISM  Laccaria bicolor
            Eukaryota; Fungi; Dikarya; Basidiomycota; Agaricomycotina;
            Agaricomycetes; Agaricomycetidae; Agaricales; Tricholomataceae;
            Laccaria.
REFERENCE   1  (bases 1 to 1593)
  AUTHORS   Khullar,S. and Reddy,S.M.
  TITLE     Cloning and characterization of glutathione biosynthesis genes from
            ectomycorrhizal fungus Laccaria bicolor in response to cadmium and
            arsenic stress
  JOURNAL   Unpublished
REFERENCE   2  (bases 1 to 1593)
  AUTHORS   Khullar,S. and Reddy,S.M.
  TITLE     Direct Submission
  JOURNAL   Submitted (24-AUG-2017) Department of Biotechnology, Thapar
            University, Bhadson Road, Patiala, Punjab 147004, India
COMMENT     ##Assembly-Data-START##
            Sequencing Technology :: Sanger dideoxy sequencing
            ##Assembly-Data-END##
FEATURES             Location/Qualifiers
     source          1..1593
                     /organism="Laccaria bicolor"
                     /mol_type="mRNA"
                     /strain="S238N"
                     /db_xref="taxon:29883"
     gene            1..>1593
                     /gene="GSH2"
     CDS             1..>1593
                     /gene="GSH2"
                     /EC_number="6.3.2.3"
                     /note="GSH2; second enzyme involved in ATP-dependent
                     glutathione biosynthesis"
                     /codon_start=1
```

/product="glutathione synthetase"
/protein_id="AVX28162.1"
/translation="MTTEPFDIPSWPPSLTPIQLEALTLYATTYALSHGLLYLLPGPL
PAISSAAIHAPFSLFPSPFPRKLFEAGQRIQRTYNVLYARIAMDEEFLDRVMGTETGV
GKVDDFIGQLWTGWKQLRDEGLAQHLHLGLFRSDYLLHTLPNQPLSIKQVEFNTISVS
FACLSQKISELHRYLLSSTQYYNCSAQLKPENLPPNRTISGLAEGLAVGHKAYNVQGS
RILFVVQPGERNVFDQRWLEYELLEQHSIHIVRQTFEELAHSAIVDPHTSILRVSCST
DIHPSGSIEISTVYYRAGYMPNEYPTPAHYATRFLLERSKAIKCPTIALQLAGGKKVQ
EVLAQPGVLERFLRDEKRYGKDGIFSEHEVNELRSTFMAMWGLDVGENLLTADYDSIA
SGKEGFGVLKARDDAHALVLKPQREGGGNNVYKEAIPAFLDSLPPQERQAWIAMELIV
PPEGTGNYLVRAGTIQAESQAAAKADVVSELGIFGYALFGGESREIKEKEVGWLVRTK
GKDSDEGGVATGFSVLDSLLLVD"

ORIGIN

```
        1 atgacaacag aaccgtttga catccctagc tggcccccat cactcacacc cattcaattg
       61 gaggcgttga cactatatgc cactacatat gcactatccc acgggctact ttatcttctg
      121 ccaggcccac taccagcaat atcaagcgcg gccatccacg ctcctttctc tcttttccca
      181 tcacctttc ctcgaaagct ttttgaagct ggacagagaa tccagaggac ttacaatgtc
      241 ctttacgcga gaatcgcgat ggatgaagag tttttggata gggtcatggg aacagagacg
      301 ggtgtgggca aggtcgatga ctttattggg caattgtgga ctgggtggaa gcagttgagg
      361 gatgaggggc ttgctcagca cctgcatctt ggcctatttc gttccgacta ccttctccac
      421 accctaccga accagccact ttctatcaag caggtcgagt tcaataccat ctccgtgtcg
      481 ttcgcatgtc tatcccaaaa gatatctgag cttcataggt acctcttatc gtcaacgcaa
      541 tattacaact gctctgcaca actcaaaccc gagaacttgc cgccaaaccg gaccatctct
      601 ggcctagcag aagggcttgc agtagggcat aaagcctata acgttcaagg gtctcgaata
      661 ctatttgtcg ttcaacccgg agaacgcaat gtttttgacc aacgatggct cgagtacgag
      721 ctgctggaac agcattccat ccacattgtc cgccaaactt ttgaagaact cgctcattcg
      781 gccatcgtag acccgcacac atccatcctc cgcgtttcct gctctacgga cattcaccca
      841 tcaggttcca ttgagatatc cacagtatat tatcgcgcgg ggtatatgcc caatgaatac
      901 ccaacccctg cgcactacgc cactcgtttc cttctcgaac gatccaaagc aatcaaatgt
      961 cctactatcg ccctccagct agctggtggg aaaaaagttc aagaggtgct agcccaacct
     1021 ggtgttcttg agcgcttctt acgcgacgag aaaaggtatg gcaaagacgg catattctcc
     1081 gaacacgaag tcaacgagct acggtccacc ttcatggcca tgtggggttt agacgtgggg
     1141 gaaaatctcc taacggccga ttatgactcc atcgcatctg gaaaagaggg attcggagtc
     1201 ctcaaagcta gagatgacgc acatgcgtta gtgctcaagc cgcagaggga aggtggcggc
     1261 aataacgtct ataaagaagc aattcctgct ttcctggaca gcctaccgcc gcaagaacgc
     1321 caggcttgga ttgcgatgga attgattgtc cctcctgagg gcactggaaa ctacctcgtt
     1381 cgcgccggaa caattcaggc ggagagtcaa gcagcggcga aggctgatgt cgtcagcgag
     1441 cttgggatct ttggctatgc gctgtttggg ggcgagtcta gggaaatcaa agaaaaggaa
     1501 gtcggatggt tagtcagaac caaggggaag gacagcgatg agggtggcgt tgcaactgga
     1561 ttttctgtgt tagattcgct gctgttggtg gat
```

//

Hebeloma cylindrosporum strain h7 gammaglutamyl cysteine synthetase 1 (GCS) mRNA, complete cds

GenBank: MH892339.1

FASTA Graphics

Go to:

```
LOCUS       MH892339               2040 bp    mRNA    linear   PLN 09-JAN-2019
DEFINITION  Hebeloma cylindrosporum strain h7 gammaglutamyl cysteine synthetase
            1 (GCS) mRNA, complete cds.
ACCESSION   MH892339
VERSION     MH892339.1
KEYWORDS    .
SOURCE      Hebeloma cylindrosporum
  ORGANISM  Hebeloma cylindrosporum
            Eukaryota; Fungi; Dikarya; Basidiomycota; Agaricomycotina;
            Agaricomycetes; Agaricomycetidae; Agaricales; Cortinariaceae;
            Hebeloma.
REFERENCE   1  (bases 1 to 2040)
  AUTHORS   Khullar,S. and Reddy,M.S.
  TITLE     Cadmium induced glutathione bioaccumulation mediated by
            gamma-glutamylcysteine synthetase in ectomycorrhizal fungus
            Hebeloma cylindrosporum
  JOURNAL   Biometals (2018) In press
   PUBMED   30560539
  REMARK    Publication Status: Available-Online prior to print
REFERENCE   2  (bases 1 to 2040)
  AUTHORS   Reddy,S.M. and Khullar,S.
  TITLE     Direct Submission
  JOURNAL   Submitted (11-SEP-2018) Department of Biotechnology, Thapar
            Institute of Engineering & Technology, Bhadson Road, Patiala,
            Punjab 147004, India
COMMENT     ##Assembly-Data-START##
            Sequencing Technology :: Sanger dideoxy sequencing
            ##Assembly-Data-END##
FEATURES             Location/Qualifiers
     source          1..2040
                     /organism="Hebeloma cylindrosporum"
                     /mol_type="mRNA"
                     /strain="h7"
                     /db_xref="taxon:76867"
     gene            1..2040
                     /gene="GCS"
                     /note="Hcg-GCS"
     CDS             1..2040
                     /gene="GCS"
```

/EC_number="6.3.2.2"
/note="GSH1"
/codon_start=1
/product="gammaglutamyl cysteine synthetase 1"
/protein_id="AZS52301.1"
/translation="MGLLYLGTPLVWDEAKKYADHVRSHGITQFLHIWDRLKDRQGDE
LLWGDEIEYMVVSFDAKEKNAKLSLRQQEILEKINSAVDDISAGAPNNVCVPKFHPEY
GRYMLESTPGAPYTGSIPDLLSVENNMRYRRNLARKHLNPNEIPITITSFPRLGVPGN
LRNPSMIHATPSPATVYFYQKKSQTRTHVSRPCTANIRRRRGSKVAINLPIYFDEKTP
RPFIDPTIPWDRAIYPEDSEAKRGAALPDHIYLDAMGFGMGCCCLQLTFQACNVADAR
RMYDGLIPIGPLLLALTAASPIWRGYLADVDCRWNVIAGSVDDRTEEERGLKPIERKQ
FRTEVSLRQRHLYISDDWVNRPEYNDNPITLRREHLQPFAHTRHISHLFIRDPLVVFS
ETIDQDDTSSSDHFENIQSTNWQTLRFKPPPPNSPIGWRVEFRSMEVQMTDFENAAFA
VFVVLLSRAIFAFNLNFYIPISKVDENMARAQQRDASASKKFFFKKDVYATGRSATIE
RCNQSFGRQNTSAMKCTAEERQKMKNCFPPPPLPENGFAYRGPVEDEYEEMTMKEIMN
GKGDNFPGLLALVDAYLETLEIELRDMEKIQQYLDFVRRRSDGRLLTPATWIRNFVTS
HPDYRKDSVVSQTINYDLLVAVDEIERGVRRAPDLLPADYRGGDKDTRDPLIFIF"

ORIGIN

```
        1 atgggtcttc tctatctcgg aactccgttg gtctgggacg aggctaaaaa gtacgccgat
       61 catgtacgaa gtcatgggat cacccaattt cttcatatat gggaccgcct aaaggacagg
      121 caaggtgatg aactgctctg gggtgacgag attgaatata tggtggtctc cttcgatgct
      181 aaggaaaaaa atgcaaagtt atccttgcga cagcaagaga ttttggaaaa aattaactct
      241 gccgtcgacg acatctccgc tggggctcca aacaacgttt gtgtacccaa gttccaccca
      301 gagtatggcc gctacatgct cgaatctacc cccggcgccc cgtataccgg ttctattcct
      361 gatctgttgt cggttgaaaa taacatgcga tacaggcgaa acctcgcccg caagcatctc
      421 aatcctaacg aaatacccat tacaatcact tccttcccgc gactgggcgt tccgggcaat
      481 ttacggaacc cttctatgat ccatgcgacg ccgtctccag ccacagtcta tttctatcag
      541 aagaaatcac aaacccgcac gcacgtttcc cgaccctgta ctgctaatat tagacggcga
      601 agggggtcaa aggttgcgat caatctcccg atttactttg acgaaaaaac gcctcgacct
      661 ttcattgacc ccactatacc atgggatcgt gcgatatacc cagaagattc agaggcaaag
      721 cgtggggcag ctttgcctga tcatatatac ctggacgcta tgggtttcgg catgggttgt
      781 tgctgtcttc aattaacatt ccaagcttgc aacgttgccg atgctcggag aatgtatgat
      841 gggttgatcc caatcggacc tcttcttttg gcattgacag ctgcgagccc tatctggagg
      901 ggatacctcg ctgatgtcga ctgtcgttgg aacgttatcg caggaagcgt tgacgaccga
      961 accgaggaag aacgtggctt gaaacccatt gaaagaaagc aattccggac cgaagtctcg
     1021 ttacgacagc gtcatctcta catttcggac gattgggtta atcgtccaga atataacgac
     1081 aaccccatta ccttacgacg agaacattta caaccgtttg cgcacacacg gcacatctct
     1141 caccttttca ttcgtgaccc tcttgtagtc ttctccgaga cgatagatca agacgacact
     1201 tccagcagcg atcacttcga gaatatccaa tcgacaaact ggcaaactct ccgctttaaa
     1261 ccgccaccac caaattcacc gatcggatgg agggttgaat tccgatccat ggaggttcaa
     1321 atgacggact ttgagaatgc cgcatttgcg gtctttgtcg tgctcctctc tcgagccatc
     1381 tttgccttca acctcaattt ttatatcccg atatccaaag tcgacgaaaa tatggctagg
     1441 gcacagcaaa gggatgcttc ggcttcaaag aagtttttct ttaagaagga cgtatatgca
     1501 acgggccgaa gtgcgaccat cgagcgctgc aatcaatcct tcgggcgcca gaacacctcc
     1561 gccatgaagt gtaccgcgga agaaagacaa aaaatgaaga attgttttcc tcctccacct
```

```
     1621 cttcccgaga atggtttcgc atatcgcggt ccagtagaag atgaatacga agaaatgact
     1681 atgaaagaaa ttatgaacgg aaagggcgat aatttccctg gtttgcttgc acttgtggat
     1741 gcctatctag agacgctgga aattgagctc cgggatatgg agaagataca gcaatatcta
     1801 gactttgtcc gacgtcgttc tgacggaaga ctcctgaccc cagcgacgtg gatccggaat
     1861 tttgtcacgt ctcatcctga ctacagaaag gattcggttg tttctcaaac catcaactac
     1921 gatctattag tagctgtgga tgaaatcgaa cgaggggttc gtcgggcgcc tgatcttctt
     1981 ccggctgatt acaggggtgg agacaaggat acaagggacc ctttgatatt tatttttaa
//
```

Hebeloma cylindrosporum strain h7 glutathione synthetase (GSH2) mRNA, complete cds

GenBank: MK617301.1

FASTA Graphics

Go to:

```
LOCUS       MK617301               1641 bp    mRNA    linear   PLN 24-JUN-
2019
DEFINITION  Hebeloma cylindrosporum strain h7 glutathione synthetase (GSH2)
            mRNA, complete cds.
ACCESSION   MK617301
VERSION     MK617301.1
KEYWORDS    .
SOURCE      Hebeloma cylindrosporum
  ORGANISM  Hebeloma cylindrosporum
            Eukaryota; Fungi; Dikarya; Basidiomycota; Agaricomycotina;
            Agaricomycetes; Agaricomycetidae; Agaricales; Cortinariaceae;
            Hebeloma.
REFERENCE   1  (bases 1 to 1641)
  AUTHORS   Khullar,S. and Reddy,S.M.
  TITLE     Arsenic toxicity and its mitigation in ectomycorrhizal fungus
            Hebeloma cylindrosporum through glutathione biosynthesis
  JOURNAL   Unpublished
REFERENCE   2  (bases 1 to 1641)
  AUTHORS   Khullar,S. and Reddy,S.M.
  TITLE     Direct Submission
  JOURNAL   Submitted (08-MAR-2019) Department of Biotechnology, Thapar
            Institute of Engineering & Technology, Bhadson Road, Patiala,
            Punjab 147004, India
COMMENT     ##Assembly-Data-START##
            Sequencing Technology :: Sanger dideoxy sequencing
            ##Assembly-Data-END##
FEATURES             Location/Qualifiers
     source          1..1641
                     /organism="Hebeloma cylindrosporum"
                     /mol_type="mRNA"
                     /strain="h7"
                     /db_xref="taxon:76867"
     gene            1..1641
                     /gene="GSH2"
     CDS             1..1641
```

/gene="GSH2"
/EC_number="6.3.2.3"
/codon_start=1
/product="glutathione synthetase"
/protein_id="QDD67718.1"

/translation="MASTFDFASWPPSLTVDQLENLTLYATSYALSHGALYLPPAEPQ

PTVPSAAIHAPISLFPSPFPRQLYEQGRRIQRTYNVLYSRIAMDTEFLDKIMGAEEGV

GKVDDFIGQLWRGWKKLRDAGLAQVRPFSREGTVMRLISGQPLHLGLFRSDYLLHAPR

NEPLSIKQVEFNTISVSFGGLSQKTSELHRYLLAATDYYNSSSYLKPDNFPSNDSIAG

LAQGLAEAHKAYDVEGSRILFVVQSGERNVFDQRLLEYELLEKHSIRIIRQTFSELAL

SASVDPSTCVLRIARSPDLQPSGSIEISTVYFRAGYMPHDYHTPAHYDTRFLLESSKA

IKCPTIALQLAGGKKVQEVLTQAGMLERFLSDEKKYGKNIASMQDIDELRASFMGMWV

LDVSEDLLTPDYAAQAAGSEEFGVRKARDLAQSPVLKPQREGGGNNVYKESIPGFLDA

LAPQERQAWIAMELIDAPENAGNYLVRAGSTDSQSQTPVKTDVVSELGIFGWALFGGP
DKSIDEREVGWLVRTKGKDINEGGVATGFSVLDSLLLV"
ORIGIN
1 atggcatcga ctttcgactt tgccagttgg ccgccatctt tgaccgtgga ccagctcgaa
61 aatttgacgt tatacgcaac gtcatacgcc ctatcgcacg gtgctttgta tctaccacca
121 gctgaaccac aaccgactgt ccccagcgct gctatccatg caccgatttc cctctttcct
181 tcgcctttcc ctcgtcagct ctatgaacaa ggccgccgga tacaacgcac atacaacgtc
241 ttgtattctc ggatcgcgat ggataccgaa tttctggaca agataatggg ggcggaagaa
301 ggagttggca aggtcgacga ttttatcggc cagctttgga gaggttggaa aaagctaaga
361 gatgctgggc ttgcccaagt acgccccttt tctcgagagg ggaccgtaat gcgtctgatc
421 tcagggcaac ccctccatct tggtcttttt cgctcagatt accttcttca tgcaccacgc
481 aatgagccgt tatccatcaa gcaagtggaa tttaacacca tctctgtgtc ttttgggggt
541 ctatctcaaa aaacgtcgga gctgcatcga tacttgctag ccgcgacaga ttactacaat
601 agttcatcct acttaaagcc ggacaacttt ccatcgaatg attcaatcgc agggctggca
661 cagggtttgg cggaggccca taaggcttac gatgtcgaag gctcgcggat cctcttcgtc
721 gtccaatcag gcgagcggaa tgttttcgac caaaggcttt tggaatacga attgctcgaa
781 aagcattcca ttcggattat acggcaaacc ttcagcgaat tggccctctc tgcctctgtg
841 gatccatcaa catgtgttct acgaatagca cggtccccag atctccaacc ttcgggttca
901 atcgaaattt cgacggtgta tttccgtgcc ggatatatgc cgcatgatta ccacactccg

```
 961 gcgcattatg acactcgttt tcttctcgag agttcaaagg cgatcaaatg cccaacaatt
1021 gccctccagc tggccggtgg aaagaaagtc caggaagtgt tgacgcaagc aggcatgctc
1081 gagcgctttt tatctgacga gaaaaagtac gggaagaata ttgctagtat gcaggacatt
1141 gatgagctga gggcaagctt tatgggaatg tgggttctgg acgtcagtga agatttgtta
1201 acgccagatt acgcagctca ggcagctggt tctgaggaat tcggggttcg aaaagccaga
1261 gatcttgcac aatcgccggt cctcaaacca cagcgcgaag gaggtggtaa caatgtttac
1321 aaggagtcaa tacctggctt ccttgatgcc ctggcgcccc aagaacggca ggcttggatt
1381 gccatggaat tgatcgacgc accggaaaat gcaggaaact atcttgtccg agccggctca
1441 acggattctc aaagccaaac cccagttaaa accgacgttg tgagcgagtt gggtattttt
1501 gggtgggcac tgtttggtgg accagacaaa agcattgatg agcgtgaggt gggatggttg
1561 gtacggacta aagggaaaga catcaatgaa ggtggcgtcg caaccggctt ctcggtcttg
1621 gattcattgc tcttggtgta g
```

//

Chemosphere 240 (2020) 124914

Contents lists available at ScienceDirect

Chemosphere

journal homepage: www.elsevier.com/locate/chemosphere

Arsenic toxicity and its mitigation in ectomycorrhizal fungus *Hebeloma cylindrosporum* through glutathione biosynthesis

Shikha Khullar, M. Sudhakara Reddy*

Department of Biotechnology, Thapar Institute of Engineering & Technology, Patiala, 147004, Punjab, India

HIGHLIGHTS

- Glutathione biosynthesizing genes, *Hcγ-GCS* and *HcGS* were characterized in *H. cylindrosporum*.
- Enhanced accumulation and glutathione content were observed due to As exposure.
- Yeast mutants rescued the As sensitivity due to cloning of *Hcγ-GCS* and *HcGS*.
- mRNA accumulation of *Hcγ-GCS* and *HcGS* increased significantly due to As exposure.
- Glutathione play an important role in As detoxification in ECM fungus *H. cylindrosporum*.

GRAPHICAL ABSTRACT

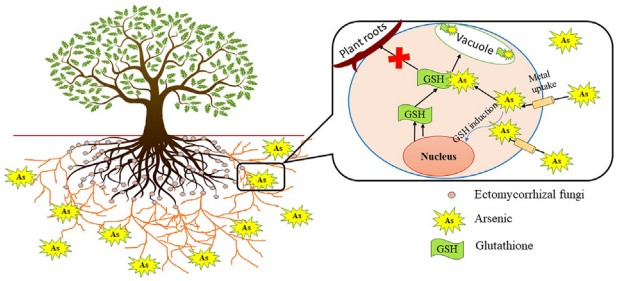

ARTICLE INFO

Article history:
Received 13 March 2019
Received in revised form
16 September 2019
Accepted 18 September 2019
Available online 19 September 2019

Handling Editor: X. Cao

Keywords:
Arsenic
Ectomycorrhizal fungi
Glutathione
γ-glutamylcysteine synthetase
Glutathione synthetase
Hebeloma cylindrosporum

ABSTRACT

Arsenic (As) contamination is one of the most daunting environmental problem bothering the whole world. Exploring a suitable bioremediation technique is an urgent need of the hour. The present study focusses on scrutinizing the ectomycorrhizal (ECM) fungus for its potential role in As detoxification and understanding the molecular mechanisms responsible for its tolerance. When exposed to increasing concentrations of external As, the ECM fungus *H. cylindrosporum* accumulated the metalloid intracellularly, inducing the glutathione biosynthesis pathway. The genes coding for GSH biosynthesis enzymes, γ-glutamylcysteine synthetase (*Hcγ-GCS*) and glutathione synthetase (*HcGS*) were highly regulated by As stress. Arsenic coordinately upregulated the expression of both *Hcγ-GCS* and *HcGS* genes, thus resulting in increased Hcγ-GCS and HcGS protein expressions and enzyme activities, with substantial increase in intracellular GSH. Functional complementation of the two genes (*Hcγ-GCS* and *HcGS*) in their respective yeast mutants (*gsh1*$^{\Delta}$ and *gsh2*$^{\Delta}$) further validated the role of both enzymes in mitigating As toxicity. These findings clearly highlight the potential importance of GSH antioxidant defense system in regulating the As induced responses and its detoxification in ECM fungus *H. cylindrosporum*.

1. Introduction

Arsenic (As) has been ranked first in the toxicity and as the most hazardous metalloid in the environment by the Agency for Toxic Substances and Disease Registry (ATSDR-Agency for toxic substances and Disease Registry, 2017). The International Agency

* Corresponding author. Department of Biotechnology, Thapar Institute of Engineering & Technology, Bhadson Road, Patiala, 147004, Punjab, India.
E-mail address: msreddy@thapar.edu (M.S. Reddy).

https://doi.org/10.1016/j.chemosphere.2019.124914
0045-6535/

for Research on Cancer (IARC) has classified arsenic and its compounds as "Carcinogenic to humans", mostly responsible for lung, bladder, liver, kidney and skin cancer (IARC, 2018). World Health organization (WHO, 2011), United States Environmental Protection Agency (USEPA, 2006), Health Canada and European Union (EU) has restricted the amount of arsenic in drinking water to 10 μg/l. Still there are millions of people across the world especially in India, Bangladesh, Thailand, Argentina, Nepal, Poland, China, Mexico and USA who are in exposure to the concentrations of As much higher than the prescribed value (greater than 100 μg/l) (Argos et al., 2010; Bhowmick et al., 2018; Bundschuh et al., 2012; Cho et al., 2011; Diwakar et al., 2015; Komorowicz and Barałkiewicz, 2016; Pinter et al., 2018; Rodríguez-Lado et al., 2013). Geogenic activities occurring inside the aquifers are the major cause of arsenic mobility into the environment. The use of these As polluted tube-wells for irrigation further pollutes the agricultural topsoil (Casentini et al., 2011). Arsenate (As(V)) is the main As species present in the oxic conditions of aerobic soil. Since As and P belong to same chemical group (Group 15 (V_A) of periodic table), both exhibit similar chemical and geochemical properties. As(V) being analogous to Pi, enters the plants through the phosphorous transporters and thereby pose high threat to the plant establishment (Wu et al., 2011).

Not only cancer, the As exposure also leads to many other notorious diseases like Skin lesions, cardiovascular disease, pulmonary disease, neurological disorders, diabetes, gastrointestinal disturbances, renal disease, liver disease and various reproductive problems (Jomova et al., 2011). Therefore, remediation of soil and drinking water from As contamination is the urgent need of an hour. Although there are many physico-chemical methods for sequestering As such as coagulation-flocculation, adsorption, ion-exchange, membrane filtration etc., but they are very expensive and low in efficiency, as they only mobilize contaminants from one site to the other. Bioremediation using plants and microorganisms on the other hand has proven to (Fazi et al., 2016; Khullar and Reddy, 2019a).

Microorganisms like bacteria, fungi, yeast and algae have proven to be low cost adsorbents for sequestration of As (Dey et al., 2016; Khullar and Reddy, 2019a; Mitra et al., 2017; Singh et al., 2015). Although many studies have documented the response of these microorganisms to As, not much have been explored in ectomycorrhizal fungi (ECM). These fungi thrive inside the soil forming a symbiotic association with the plant roots, thus protecting them from various biotic and abiotic stresses and helping them in nutrient uptake from the deeper soil (Khullar and Reddy, 2019a).

In the previous studies, it has been well established that mycorrhizas being the nutrient absorbing organs for most of the plant, enhances the phosphorus uptake by plant as compared to the non-mycorrhizal plants (Smith et al., 2011; Treseder, 2013). Since As(V) is an analog to Pi and uses the same phosphorus transporters to enter into the cell, it might be expected that mycorrhization may also increase the As(V) uptake by the host plant (DiTusa et al., 2016; Smith et al., 2010). However, a contrast observation has been reported in some studies where it has been reported that mycorrhizal plants showed higher P/As ratio than non-mycorrhizal plants (Chan et al., 2013; Liu et al., 2005; Zhang et al., 2015). This indicates that although ECM fungi accumulate more As but prevent its transfer to the host plant. The underlying mechanism that detoxifies As in ECM fungi and inhibits its transfer to plant is still not clear.

ECM fungi have evolved multifarious mechanisms to survive heavy metals which includes, cell wall binding, cellular efflux, extracellular chelation by extruded ligands, intracellular conjugation with thiols like glutathione (GSH) and metallothioneins (MTs) and vacuolar compartmentalization (Bellion et al., 2006; Khullar and Reddy, 2018). It has been reported that ECM fungi respond differentially to different heavy metals (Khullar and Reddy, 2018). The response of ECM fungi to cadmium, copper, zinc, silver has already been documented many a times (Hložková et al., 2016; Kalsotra et al., 2018; Khullar and Reddy, 2019c, 2019b; Nguyen et al., 2017; Ramesh et al., 2009; Reddy et al., 2014, 2016; Sácký et al., 2019), but there is very meager information on the response of ECM fungi to arsenic. The most credible mechanism known to be responsible for As tolerance or detoxification in plants and other fungi is through its conjugation with GSH (Ahsan et al., 2008; Mukherjee et al., 2010). GSH chelates As through thiolate bonds forming $As(GSH)_3$ complex, which further gets compartmentalized into the vacuoles through the ABC transporters (Verbruggen et al., 2009). The role of arbuscular mycorrhizas in modulating thiols under As stress has been realized but to our knowledge no report is available to study the thiol mechanism in ECM systems (Garg et al., 2015; He and Lilleskov, 2014; Sharma et al., 2017).

Glutathione (L-gamma-glutamyl-L-cysteinyl-glycine) is the multifaceted essential bio-thiol tripeptide synthesized in two ATP dependent steps catalyzed by two enzymes γ-glutamylcysteine synthetase (γ-GCS; E.C.6.3.2.2) and glutathione synthetase (GS; E.C.6.3.2.3). In the first step γ-GCS catalyzes the binding of L-glutamate and L-cysteine resulting in the formation of γ-glutamylcysteine (γ-GC), followed by the addition of L-glycine to the C-terminal of γ-GC by GS resulting in glutathione (Anderson, 1998; Khullar and Reddy, 2018). There are few reports on plants and yeast where the expression of these GSH biosynthesis genes has been found to increase in response to As stress but there is very meager information for its response in ECM fungi (Guo et al., 2012). Since, the ECM fungi provide a cost efficient and environment friendly mitigation to diminish As exposure in plants, it becomes imperative to understand the actual mechanisms involved in extenuation of As toxicity. The current study is based on the hypothesis that amongst different metal detoxification mechanisms of ECM fungi, glutathione biosynthesis is the key mechanism that gets induced under As stress. The intracellular accumulation of As activates the glutathione biosynthesis in ECM fungi thus protecting it from As toxicity.

The present study focuses on studying the effect of As on ECM fungus *Hebeloma cylindrosporum* and provides molecular insight into the mechanisms involved in mitigating the toxic effect of As with special emphasis on GSH biosynthesis. The present study provides information about the effect of As on growth of ECM fungi and studied its response to As like, metalloid accumulation, GSH production and investigate the enzymes involved in GSH biosynthesis (*Hcγ-GCS* and *HcGS*). The effect of As on the expression of both *Hcγ-GCS* and *HcGS* genes was studied by qPCR. Further, the role of both genes in mitigating As stress was studied by functional complementation in yeast using mutants lacking *γ-GCS* ($gsh1^{\Delta}$) and *GS* ($gsh2^{\Delta}$).

2. Materials and methods

2.1. Biological materials and growth parameters

The ECM fungus *Hebeloma cylindrosporum* (strain h7) isolated from the basidiomata associated with *Pinus pinaster* was used in this study. The culture was maintained on Modified Melin-Norkan's medium (MMN) (Melin, 1953) supplemented with Heller's micronutrients (Gay, 1990) at 25 °C in dark. For the functional complementation studies, two *Saccharomyces cerevisiae* (Wild type: BY4741) mutants lacking $gsh1^{\Delta}$ (Accession no: Y07097- BY4741; *MATa; ura3Δ0; leu2Δ0; his3Δ1; met15Δ0; YJL101c::kanMX4*) and $gsh2^{\Delta}$ (Accession no: Y01740- BY4741; *MATa; ura3Δ0; leu2Δ0; his3Δ1; met15Δ0; YOL049w::kanMX4)* for the GSH biosynthesis genes *γ-GCS* and *GS*, respectively were procured from the Indian

Institute of Science Education and Research (IISER), Mohali, Punjab, India.

2.2. Stress treatment and metalloid accumulation

The ECM fungus *H. cylindrosporum* was allowed to grow in 50 ml MMN broth for 48 h at 25 °C. After 48 h, each flask was stressed with increasing concentrations of As ($Na_2HAsO_4 \cdot 7H_2O$: 0, 3, 6, 9, 12, 15 mM) and incubated at 25 °C for 21 days. The mycelium was harvested after 21 days, washed with 0.9% saline water and then with 0.1 M EDTA water, followed by three washings with distilled water. The mycelium was then dried at 50 °C for 24 h and the dry biomass was recorded as the effect of As on the growth of *H. cylindrosporum*. Further, to measure the As accumulation in *H. cylindrosporum* under different stress concentrations, the dried mycelium was digested with nitric acid and perchloric acid (HNO_3/$HClO_4$) in the ratio of 3:1 (v/v) and the metalloid concentrations were determined using Atomic absorption spectroscopy.

2.3. Total GSH production in response to As stress

The total GSH produced by As stressed cultures of *H. cylindrosporum* was estimated spectrophotometrically using the enzymatic recycling method as described by Rahman et al. (2006). The fungus was grown on MMN agar plates overlaid with cellophane sheets for 14 days at 25 °C in dark. After 14 days, the cellophane sheets with mycelium were transferred on to MMN medium supplemented with increasing concentrations of As ($Na_2HAsO_4 \cdot 7H_2O$: 0, 3, 6, 9, 12, 15 mM) for 48 h at 25 °C. The mycelium so obtained was scrapped from the cellophane sheets and crushed using liquid nitrogen. 100 mg of liquid nitrogen crushed mycelium under each stress concentration was further used for GSH estimation. Firstly, the cell extract was prepared by homogenizing the crushed mycelium in sulfosalicylic-TritonX mixture (0.6% sulfosalicylic acid + 0.1% TritonX) in KPE buffer (0.1 M Potassium phosphate buffer with 5 mM EDTA at pH 7.5) followed by centrifugation at 8000*g* for 10 min at 4 °C. The cell extract obtained was further used for estimating the total GSH concentration using sulfhydryl reagent DTNB (5,5′-dithio-bis(2-nitrobenzoic acid). Then, 100 µl of cell extract was mixed with 700 µl of KPE buffer and 120 µl of DTNB-Glutathione reductase mix (freshly prepared) and incubated at room temperature for 30 s. Sixty microliters of freshly prepared β-NADPH solution (1 mg β-NADPH in 1.5 ml KPE buffer) was added to the above mixture and the absorbance was recorded at 412 nm. The absorbance so obtained is directly proportional to the amount of GSH present in the solution. The amount of GSH produced was further quantified by comparing with the standard curve of GSH (Sigma-Aldrich; St. Louis, USA) prepared using the same protocol.

2.4. Hcγ-GCS and HcGS enzyme activity in response to As stress

The activity of both the GSH biosynthesizing enzymes Hcγ-GCS and HcGS was assayed according to the method described by Ruiz et al. (2003). The 14-day old culture of *H. cylindrosporum* was stressed with different concentrations of As for 48 h and crushed with liquid nitrogen. The crushed samples (100 mg) from each concentration was homogenized with lysis buffer (100 mM Tris-HCl, pH 8.0, 10 mM $MgCl_2$ and 1 mM DTT) and centrifuged at 1000 g for 10 min at 4 °C. The clear supernatant obtained was used for determining the Hcγ-GCS and HcGS enzyme activity in response to As. For measuring the Hcγ-GCS enzyme activity, 100 µl of supernatant was mixed with 500 µl of assay mix (100 mM Hepes (pH 8.0), 5 mM ATP, 50 mM $MgCl_2$, 5 mM DTT, 5 mM phosphoenolpyruvate, 20 mM glutamate, 1 mM cysteine and 10 U ml^{-1} of pyruvate kinase) and incubated at 37 °C for 1 h. The reaction was then stopped by adding 100 µl of 50% TCA. The mixture was centrifuged, and the supernatant collected was further used for phosphate estimation by phosphomolybdate method. Since both Hcγ-GCS and HcGS are ATP dependent, the amount of phosphate released in the reaction is directly proportional to the enzyme activity. For measuring the HcGS activity the same protocol was used replacing 20 mM glutamate and 1 mM cysteine with 0.5 mM γ-glutamylcysteine and 1 mM glycine.

2.5. RNA isolation, cDNA synthesis and gene amplification

Total RNA was isolated using the QiAzol lysis reagent (Qiagen, Valencia, CA) from the liquid nitrogen crushed two weeks culture of *H. cylindrosporum* stressed with As. cDNA was synthesized using 5 µg of total RNA by 'The PrimeScript first strand cDNA Synthesis Kit' (Takara, Japan) as per the manufacturer's instructions. The single stranded cDNA so obtained was used to amplify genes coding for both *Hcγ-GCS* and *HcGS* using the primers designed by retrieving their specific sequences from JGI portal htt5p://genome.jgi.doe.gov/(Supplementary Table 1). Specific restriction sites were added to the 5′ end of each primer for its effective ligation into the plasmid (Supplementary Table 1 underlined). Both the genes were amplified in a 25 µl PCR reaction constituting 1x reaction buffer, 2 µl dNTPs (2 mM), 1 µl forward primer (10 µM), 1 µl reverse primer (10 µM), 100 ng template DNA, 1.5 U Taq polymerase and nuclease free water to make 25 µl. Amplification was performed in Thermo cycler (Veriti Thermal Cycler, Thermo Fisher Scientific, U.S) with the following program: initial denaturation at 95 °C (3 min) followed by 30 cycles at 94 °C (1 min), 62 °C (1 min), 72 °C (1 min) and final extension at 72 °C (8 min). The amplified genes were purified using the PCR purification kit (Thermo Fisher, U.S) and ligated into pMD20 vector under M13 promoter (TA cloning Kit, Takara, Japan) and sequenced. Analysis of *Hcγ-GCS* and *HcGS* sequences were performed by using BLAST analysis (http://www.ncbi.nlm.nih.gov/Blast.cgi) and were submitted to GenBank of NCBI under the accession numbers, MH892339 and MK617301, respectively.

2.6. Relative expression of Hcγ-GCS and HcGS in response to As by qPCR analysis

The expression or mRNA accumulation of both *Hcγ-GCS and HcGS* genes in response to As was measured using the Real time PCR analysis. The two weeks old culture of *H. cylindrosporum* grown on MMN plates overlaid with cellophane sheets was stressed with different concentrations of As ($Na_2HAsO_4 \cdot 7H_2O$: 0, 3, 6, 9, 12, 15 mM) for 48 h and crushed with liquid nitrogen. Total RNA was isolated, and cDNAs were synthesized from each stressed sample as described above. The relative expression of each gene under As stress was determined using SYBR® Green JumpStart™ Taq ReadyMIX™ (Sigma-Aldrich; St. Louis, USA) in a 25 µl reaction with 12.5 µl SYBR mix, 0.2 µM of each forward and reverse primer (Supplementary Table 1), 0.75 µl template cDNA (20 fold diluted) and nuclease free water. The amplification was carried out in the Mastercycler eprealplex system (Eppendorf, Hamburg, Germany) using the following program: initial denaturation 95 °C (20 s) followed by 35 cycles of 95 °C (15 s), 55 °C (15 s) and 72 °C (20 s). Non-reverse transcribed RNA sample was also run as a negative control, to verify the absence of DNA traces. α-Actin (*HcAct*) (JGI Protein Id: 444180), γ-tubulin (*HcTub*) (JGI Protein Id: 15217) and adenosine kinase (*HcAK*) were used as positive controls. All the three genes were subjected to qPCR analysis using their respective primers (Supplementary Table 1) and normalized using Norm-Finder

(Andersen et al., 2004). Since α-actin showed minimum stability value, it was used further for the comparative analysis of both *Hcγ-GCS* and *HcGS*. Further the qPCR efficiency (E-value) for both genes was calculated by the equation $E = [10^{(-1/slope)}] - 1$. The E values so obtained were in range from 1.35 to 1.52. The E values was further used to calculate the C_{t1} value for each sample using the formula '$C_{t1} = C_{te}$ x [log(1 + E)/log2]'. The C_{t1} values so obtained were used to calculate the relative expression of both *Hcγ-GCS* and *HcGS* by comparative Ct method ($^{\Delta\Delta}$Ct method) (Livak and Schmittgen, 2001). All qPCR measurements were performed on total RNA isolated independently from three biological samples and for each RNA sample, three technical replicates were performed.

2.7. Functional complementation of Hcγ-GCS and HcGS in yeast mutants

The role of both *Hcγ-GCS* and *HcGS* in mitigating the toxic effects of As was validated by transforming them in their respective yeast mutants *gsh1*$^{\Delta}$ and *gsh2*$^{\Delta}$, respectively. The full length *Hcγ-GCS* and *HcGS* genes were amplified from the *H. cylindrosporum* cDNA using the gene specific primers with restriction sites on their 5' end (Supplementary Table 1). Both the genes were digested with their respective restriction enzymes and ligated into the yeast expression vector pFL61 under the PGK promoter from yeast phosphoglycerokinase encoding gene (Minet et al., 1992). The ligated constructs pFL61-*Hcγ-GCS* and pFL61-*HcGS* along with the empty vector pFL61 were then transformed into their respective yeast mutants *gsh1*$^{\Delta}$ and *gsh2*$^{\Delta}$ using the lithium acetate method (Stearns et al., 1990). The positive transformants were then selected by spreading the cells on a synthetic defined medium without uracil (SD-Ura), which is a minimal medium supplemented with 2% glucose (Hi-media laboratories, India) and drop out supplement without uracil (Takara-Clontech, Japan). The positive clones were then subjected to increasing concentrations of As and their response was recorded in both liquid medium and drop test. For the drop test, both *gsh1*$^{\Delta}$ and *gsh2*$^{\Delta}$ transformed with empty vector pFL61 and the respective genes (pFL61-*Hcγ-GCS* and pFL61-*HcGS*) along with wild type BY4741 were pre-grown in SD-Ura medium for 24 h at 30 °C. The intensity of all the five cultures was set at $OD_{600} = 1.0$. All the cultures were serially diluted (10°, 10^{-1}, 10^{-2}, 10^{-3}) and 5 μl of each dilution was spotted on SD-Ura with and without As (100 μM). The spotted plates were then incubated at 30 °C for 3 days and photographed. Further, the tolerance of both transformants to As was also measured in a liquid SD broth. The transformants *gsh1*$^{\Delta}$ (pFL61), *gsh1*$^{\Delta}$ (pFL61- *Hcγ-GCS*), *gsh2*$^{\Delta}$ (pFL61) and *gsh2*$^{\Delta}$ (pFL61-*HcGS*) along with wild type BY4741 were inoculated separately in 50 ml SD-Ura medium with the starting OD_{600} of 0.05 and allowed to grow at 30 °C for 5 h at 220 rpm. After 5 h, the cultures were subjected to different concentrations of As (0, 50, 100, 150, 200 μM) and incubated at 30 °C for 24 h. The effect of As on each culture was recorded as their optical density at 600 nm after 24 h.

2.8. Statistical analyses

All the experiments were performed in triplicates. The data were analyzed by analysis of variance and the means were compared with Tukey's test at $P < 0.05$. All the analyses were performed by using Graph Pad Prism 5.1 software.

3. Results

3.1. Mycelium growth and metalloid uptake

The mycelial growth was significantly affected under As stress. With increase in external concentrations of As, the growth of *H. cylindrosporum* decreased. The half minimum inhibitory concentration (IC_{50}) of As was recorded at approximately 7 mM, where the dry weight of mycelium was reduced to 50% (Fig. 1a). However, the metalloid uptake by the mycelium (per mg of dry weight), increased with increase in external As concentration. The maximum uptake of 0.76 μg As per mg of dry mycelium was observed at 15 mM of external As stress (Fig. 1b).

3.2. GSH production and enzyme activity of Hcγ-GCS and HcGS

The total GSH produced by *H. cylindrosporum* in response to As stress was measured by the DTNB assay. The GSH production increased with increase in external As concentration. When stressed with 3 mM As, the fungus responded by increasing the GSH level from 0.15 to 0.75 nmol mg^{-1} mycelium i.e., almost 5 folds increase in GSH production. However, further increasing the external metalloid stress to 15 mM As, resulted in increasing the GSH production to 1.6 nmol mg^{-1} mycelium i.e. almost 10.7 folds higher than the unstressed culture (Fig. 2a). The increase in GSH production in response to As stress was also justified by measuring the activity of both enzymes (Hcγ-GCS and HcGS) involved in GSH biosynthesis. Since both Hcγ-GCS and HcGS are ATP dependent, they use one ATP molecule each time for catalyzing the synthesis of γ-glutamylcysteine or glutathione, respectively. The ATP so used get converted to ADP, thus liberating one molecule of inorganic phosphorous during each reaction. Thus, the amount of inorganic phosphorus liberated per minute by one mg of protein gives direct evidence of the activity of each enzyme under metalloid stress. In the present study, the total inorganic phosphorous liberated by both enzymes when exposed to increasing concentrations of As was measured using the phosphomolybdate method. When stressed with only 3 mM of As, the amount of phosphorous liberated by Hcγ-GCS increased from 0.30 to 0.88 μmol mg^{-1} protein min^{-1} (almost 3 folds increase in activity) and that of HcGS increased from 0.28 to 0.78 μmol mg^{-1} protein min^{-1} (almost 2.8 folds increase in activity). Further, the activity of both enzymes was found to increase as a function of external As stress. Activity of both Hcγ-GCS and HcGS increased up to 4 folds when the As stress was increased up to 15 mM (Fig. 2b). These results indicate that the activity of both the enzymes was induced by external As stress, thus inducing the GSH biosynthesis.

3.3. Relative expression of Hcγ-GCS and HcGS in response to As stress

When exposed to increasing concentrations of As, induction of both GSH biosynthetic genes, *Hcγ-GCS* and *HcGS* were significantly increased in *H. cylindrosporum*. With increase in external arsenic stress to 3 mM, the relative expression of *Hcγ-GCS* increased by 6 folds and that of *HcGS* by 4 folds. Further, *Hcγ-GCS* and *HcGS* expression levels increased to 12.8 and 11-fold, respectively at 15 mM of As concentration (Fig. 3).

3.4. Functional complementation of Hcγ-GCS and HcGS in yeast mutants

The function of both *Hcγ-GCS* and *HcGS* genes in mitigating As toxicity was validated by expressing both genes in their respective *S. cerevisiae* mutants, *gsh1*$^{\Delta}$ and *gsh2*$^{\Delta}$ and subjecting them to increasing As concentrations. Both mutants, *gsh1*$^{\Delta}$ and *gsh2*$^{\Delta}$ transformed with empty vector (EV) pFL61 and their respective gene pFL61+ *Hcγ-GCS* and pFL61 + *HcGS*, along with wild type BY4741 were allowed to grow on SD-Ura medium with and without As and their growth was monitored by drop test on agar plates and in liquid medium. The drop test on SD-Ura plates with and without

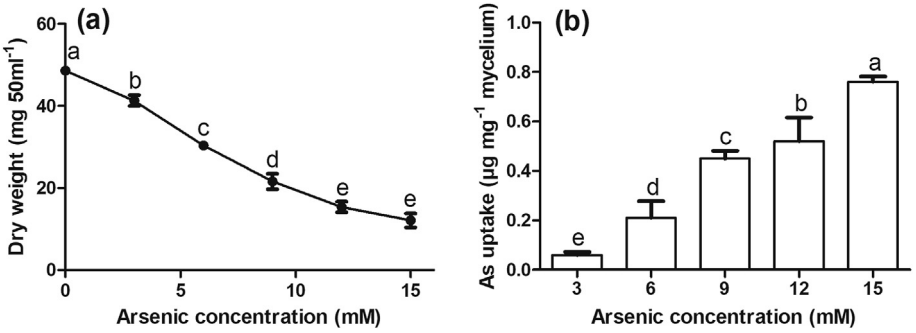

Fig. 1. Effect of different concentrations of As on (a) mycelial growth – recorded as dry weight and (b) metalloid accumulation inside *H. cylindrosporum*. Values sharing a common letter among As concentrations are not significantly different at $P < 0.05$ ($n = 3$). Error bars are ±SD.

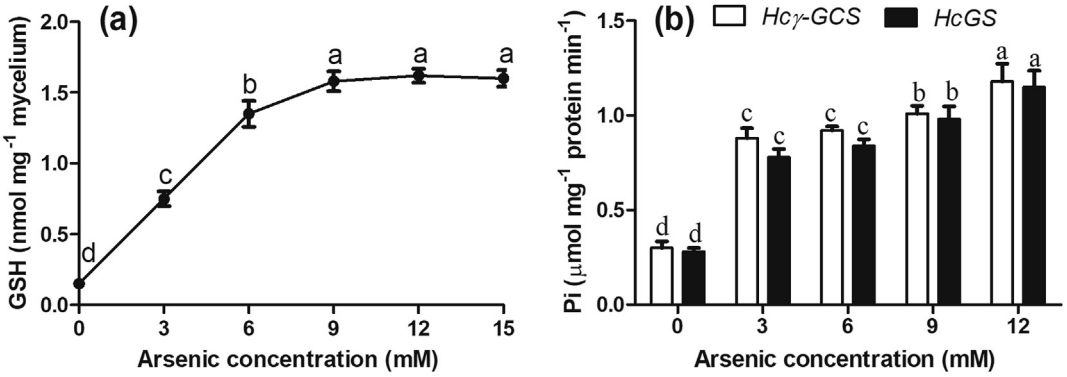

Fig. 2. Effect of different concentration of As on (a) total GSH production and, (b) enzyme activity of both Hcγ-GCS and HcGS, measured as amount of Pi released per mg protein per min. The values sharing a common letter (a) among As concentraqtions and (b) within the gene are not significantly different at $P < 0.05$ ($n = 3$). Error bars are ±SD.

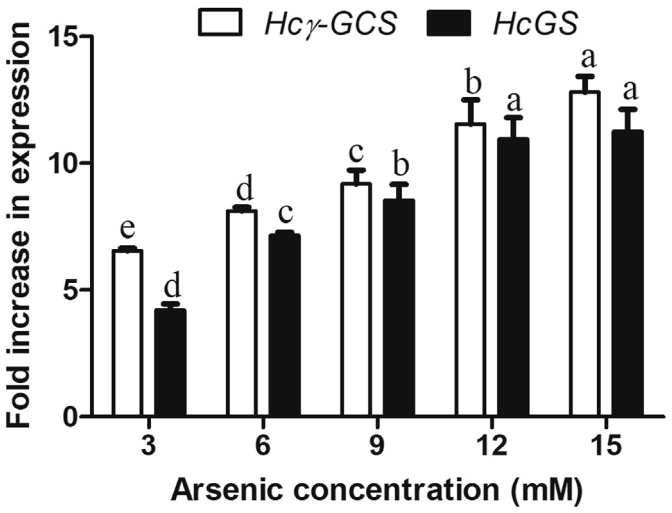

Fig. 3. Fold increase in expression of Hcγ-*GCS* and *HcGS* genes in response to different concentrations of As. Values plotted are referred to the control condition (expression level in free living fungus without metal treatment) and represent an average of three biological replicates. The values sharing a common letter within the gene are not significantly different at $P < 0.05$. Error bars are ± SD.

As (100 µM), clearly affirms that the transformation of yeast mutants *gsh1*$^{\Delta}$ and *gsh2*$^{\Delta}$ with their respective genes from *H. cylindrosporum*, *Hcγ-GCS* and *HcGS*, successfully restored their As tolerance capacity, near to that of their wild-type BY4741 cells. Whereas the yeast mutants transformed with empty vector (pFL61) could not survive the stress (Fig. 4a). Similar observations were made in case of liquid assay, where the yeast mutants *gsh1*$^{\Delta}$ and *gsh2*$^{\Delta}$ transformed with *Hcγ-GCS* and *HcGS*, showed higher tolerance to different concentrations of As, that the mutants transformed with empty vector, thus restoring the wild-type phenotype for metalloid tolerance (Fig. 4b).

4. Discussion

Arsenic toxicity is one of the most daunting issue concerning the world today. Since As has been identified as the most carcinogenic metalloids, it becomes imperative to find a suitable detoxification mechanism. ECM fungi have been well known to protect the host plant from various biotic as well as abiotic stresses (Khullar and Reddy, 2019a). They have proven to be good metal accumulators and detoxifiers, therefore holds a potential application in bioremediation of heavy metals. However, till date not many reports are available on the response of ECM fungi to As toxicity. Mechanistic understanding of the molecular processes involved in As detoxification in ECM fungi can provide new tools for bioremediation of As. In the present study, we explored the response of ECM fungus *H. cylindrosporum* to As and the molecular mechanisms involved in its detoxification. When subjected to increasing concentrations of As, the fungal biomass decreased. At 7 mM As, the fungal biomass was reduced to almost half of the unstressed culture. Similar observations were reported in *Hebeloma crustuliniforme*, *Suillus variegatus* and *Cenococcum geophilum* where the growth was completely inhibited at 8 mM As (Chen and Tibbett, 2007). Ericoid mycorrhizal fungus *Hymenoscyphus ericae* also showed curtailed growth in response to increasing As concentrations (Sharples et al., 2001). *Aspergillus oryzae* isolated from the As contaminated soil showed half minimum inhibition of its growth at 8 mM As and the

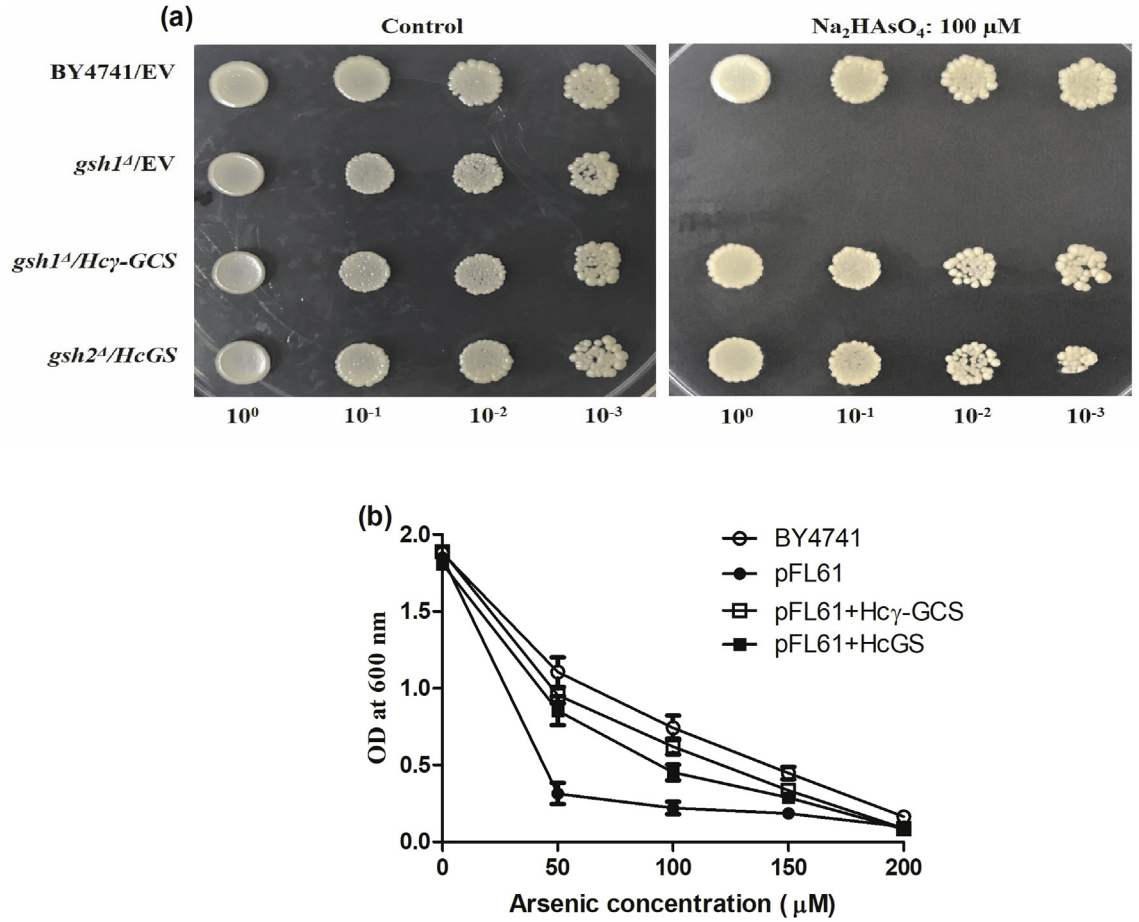

Fig. 4. Functional complementation of *Saccharomyces cerevisiae* mutants *gsh1*$^{\Delta}$ and *gsh2*$^{\Delta}$ transformed with empty vector (EV) pFL61 and their respective genes pFL61+*Hcγ-GCS* and pFL61 + *HcGS* along with their wild type BY4741. The tolerance of all the transformants and wild type BY4741 to different concentrations of As measured by (a) drop test on selective media SD-ura plates supplemented with and without As and (b) liquid broth test on SD-ura broth where the growth was recorded as O.D at 600 nm. The values represented are an average of three biological replicated with ±SD.

growth almost ceased at 13 mM As (Liang et al., 2018). Although the fungal biomass was found to decrease with increase in As concentration, the As accumulation increased in *H. cylindrosporum*. Binding of As to fungal cell wall and intracellular transport are the main responses of fungi to As stress (Singh et al., 2015). Bioaccumulation and biomethylation have been suggested as the key detoxification mechanisms in microbes existing in As polluted areas (Su et al., 2011; Singh et al., 2015). In ECM fungus, *H. cylindrosporum*, the metalloid accumulation increased with increase in As stress, whereas in case of *Aspergillus niger*, the As accumulation increased up to 0.5 mM (75 mg/l) As followed by its decrease (Mukherjee et al., 2010). Similar observations were reported in *Serpula himantioides* and *Trametes versicolor*, where the increase in As accumulation has been reported as a function of external As stress (Adeyemi, 2009). This observation throws light on the fact that not only extracellular but intracellular mechanisms are responsible for generating As tolerance in ECM fungi.

The role of glutathione in As tolerance has been reported on some plants, fungi and yeast. The comparative proteomics of As-induced differentially expressed proteins in rice plant revealed that glutathione played a central role during As stress (Ahsan et al., 2008). Therefore, the response of glutathione to different concentrations of As was analyzed in ECM fungus *H. cylindrosporum*. It was observed that with increase in As accumulation, the GSH concentrations increased in *H. cylindrosporum*. The GSH concentration increased as a function of external As stress. This indicates that the GSH defense system gets promptly induced in ECM fungus when subjected to external As stress. This observation has been supported by various researches on plants (*Arabidopsis thaliana, Nicotiana tabacum*), fungi (*Laccaria bicolor, Aspergillus niger*), yeast (*Candida tropicalis, Saccharomyces cerevisiae*) etc. (Aborode et al., 2016; Degola et al., 2015; Ilyas and Rehman, 2015; Khullar and Reddy, 2019c, 2019b; Mukherjee et al., 2010; Thorsen et al., 2007; Yadav, 2010). When exposed to intracellular As, glutathione provides a dual protection mechanism. It acts both as an antioxidant and as a metal scavenger. As an antioxidant, glutathione reduces the free radicals generated by As stress thus neutralizing their harmful effects and itself gets oxidized to GSSG (Davison et al., 2003). Glutathione also reduces pentavalent As to trivalent As (Muñiz Ortiz et al., 2008). This trivalent As further binds glutathione forming As-$(GSH)_3$ complex which actively gets transported to vacuoles through the ABC transporters (Klein et al., 2002; Leslie, 2012). The As-GSH conjugate has been identified in various mammals, plants and fungi when exposed to heavy metals (Cánovas et al., 2004; Pickering et al., 2000; Thomas, 2008; Verbruggen et al., 2009). However, it is worth noting that the ABC proteins serve as As(III) transporters only when As is complexed with the thiol group (Zhao et al., 2009). Therefore, when exposed to As, the active glutathione present inside the cell gets immediately utilized, leading to the induction in glutathione biosynthesis pathway (Davison et al., 2003). However, the study is still fragmentary in ECM systems. To justify the induction of GSH biosynthesis pathway

in ECM fungus *H. cylindrosporum*, qPCR analysis was performed, which revealed that the expression of both genes was highly induced under As stress. γ-*GCS* has been well characterized in various plants and mammals for its active role in mitigating the As toxicity (Guo et al., 2008; Liao and Yu, 2005; Schuliga et al., 2002), but very meager information is available for its activity in fungal systems under As stress. In plants like *Lens culinaris Medik*, the expression of GSH biosynthesis genes was upregulated when exposed to 25 μM and 40 μM of As (Talukdar and Talukdar, 2014). Similarly, in *Arabidopsis thaliana,* 2–6 folds increase in the expression of γ-GCS gene was reported when exposed to As stress (Li et al., 2006; Dhankher et al., 2002).

Further, the activity of both enzymes (Hcγ-GCS and HcGS) also increased in response to external As stress. This clearly throws light on the fact that GSH biosynthesis is the first line of defense in ECM fungus *H. cylindrosporum*, when exposed to As stress. As proposed by Daghino et al. (2016), the functional characterization of both *Hcγ-GCS* and *HcGS* genes was attained by expressing them their respective *S. cerevisiae* yeast mutants $gsh1^{\Delta}$ and $gsh2^{\Delta}$ (sensitive to As). The transformation of both genes in their respective yeast mutants successfully restored their metal tolerance ability. This observation clearly validates the active role of both *Hcγ-GCS* and *HcGS* in inducing As tolerance in ECM fungus *H. cylindrosporum*. In the light of these evidence, it can be clearly concluded that the ECM fungus *H. cylindrosporum* can be a good metalloid accumulator and detoxifier, highlighting the role of GSH defense system in As sequestration and thus preventing its transfer to the host plant.

5. Conclusion

The present study unequivocally justifies the central role of GSH in protecting the ECM fungus *H. cylindrosporum* from As stress. The GSH biosynthesis genes were actively induced when the mycelium was exposed to As stress, thus providing a pivotal contribution to As tolerance in ECM fungi. The above findings clearly demonstrate that the enhanced GSH biosynthetic tendency promotes the tolerance to As toxicity in ECM fungi. Therefore, we can say that when in an As contaminated soil, these ECM fungi forms a symbiotic association with the plant roots, protecting the host plant from As stress. They filter the transfer of soil As to plant roots by conjugating it with glutathione and accumulating inside the vacuoles. We may also conclude that *H. cylindrosporum* is efficient in dealing with As stress and may offer global potential in its bioremediation.

Acknowledgements

Authors are thankful to Department of Biotechnology, Govt. of India for sponsoring the research project (BT/PR8339/BCE/8/1045/2013) to carry out the present work.

Appendix A. Supplementary data

Supplementary data to this article can be found online at https://doi.org/10.1016/j.chemosphere.2019.124914.

Conflicts of interest

The authors declare that there are no conflicts of interest.

Declarations of interest

None.

References

Aborode, F.A., Raab, A., Voigt, M., Costa, L.M., Krupp, E.M., Feldmann, J., 2016. The importance of glutathione and phytochelatins on the selenite and arsenate detoxification in *Arabidopsis thaliana*. J. Environ. Sci. 49, 150–161.
Adeyemi, A.O., 2009. Bioaccumulation of arsenic by fungi. Am. J. Environ. Sci. 5, 364–370.
Ahsan, N., Lee, D.G., Alam, I., Kim, P.J., Lee, J.J., Ahn, Y.O., Kwak, S.S., Lee, I.J., Bahk, J.D., Kang, K.Y., Renaut, J., 2008. Comparative proteomic study of arsenic-induced differentially expressed proteins in rice roots reveals glutathione plays a central role during As stress. Proteomics 8, 3561–3576.
Andersen, C.L., Jensen, J.L., Ørntoft, T.F., 2004. Normalization of real-time quantitative reverse transcription-PCR data: a model-based variance estimation approach to identify genes suited for normalization, applied to bladder and colon cancer data sets. Cancer Res. 64, 5245–5250.
Anderson, M.E., 1998. Glutathione: an overview of biosynthesis and modulation. Chem. Biol. Interact. 111, 1–14.
Argos, M., Kalra, T., Rathouz, P.J., Chen, Y., Pierce, B., Parvez, F., Islam, T., Ahmed, A., Rakibuz-Zaman, M., Hasan, R., Sarwar, G., 2010. Arsenic exposure from drinking water, and all-cause and chronic-disease mortalities in Bangladesh (HEALS): a prospective cohort study. The Lancet 376, 252–258.
ATSDR-Agency for toxic substances and Disease Registry, 2017. Priority list of hazardous Substances. www.atsdr.cdc.gov/spl/. (Accessed 24 December 2018).
Bellion, M., Courbot, M., Jacob, C., Blaudez, D., Chalot, M., 2006. Extracellular and cellular mechanisms sustaining metal tolerance in ectomycorrhizal fungi. FEMS Microbiol. Lett. 254, 173–181.
Bhowmick, S., Pramanik, S., Singh, P., Mondal, P., Chatterjee, D., Nriagu, J., 2018. Arsenic in groundwater of West Bengal, India: a review of human health risks and assessment of possible intervention options. Sci. Total Environ. 612, 148–169.
Bundschuh, J., Litter, M.I., Parvez, F., Román-Ross, G., Nicolli, H.B., Jean, J.S., Liu, C.W., López, D., Armienta, M.A., Guilherme, L.R., Cuevas, A.G., 2012. One century of arsenic exposure in Latin America: a review of history and occurrence from 14 countries. Sci. Total Environ. 429, 2–35.
Cánovas, D., Vooijs, R., Schat, H., de Lorenzo, V., 2004. The role of thiol species in the hypertolerance of *Aspergillus* sp. P37 to arsenic. J. Biol. Chem. 279, 51234–51240.
Casentini, B., Hug, S.J., Nikolaidis, N.P., 2011. Arsenic accumulation in irrigated agricultural soils in Northern Greece. Sci. Total Environ. 409, 4802–4810.
Chan, W.F., Li, H., Wu, F.Y., Wu, S.C., Wong, M.H., 2013. Arsenic uptake in upland rice inoculated with a combination or single arbuscular mycorrhizal fungi. J. Hazard Mater. 262, 1116–1122.
Chen, S.H., Tibbett, M., 2007. Phosphate supply and arsenate toxicity in ectomycorrhizal fungi. J. Basic Microbiol. 47, 358–362.
Cho, K.H., Sthiannopkao, S., Pachepsky, Y.A., Kim, K.W., Kim, J.H., 2011. Prediction of contamination potential of groundwater arsenic in Cambodia, Laos, and Thailand using artificial neural network. Water Res. 45, 5535–5544.
Daghino, S., Martino, E., Perotto, S., 2016. Model systems to unravel the molecular mechanisms of heavy metal tolerance in the ericoid mycorrhizal symbiosis. Mycorrhiza 26, 263–274.
Davison, K., Cote, S., Mader, S., Miller Jr., W.H., 2003. Glutathione depletion overcomes resistance to arsenic trioxide in arsenic-resistant cell lines. Leukemia 17, 931.
Degola, F., Fattorini, L., Bona, E., Sprimuto, C.T., Argese, E., Berta, G., di Toppi, L.S., 2015. The symbiosis between *Nicotiana tabacum* and the endomycorrhizal fungus *Funneliformis mosseae* increases the plant glutathione level and decreases leaf cadmium and root arsenic contents. Plant Physiol. Biochem. 92, 11–18.
Dey, U., Chatterjee, S., Mondal, N.K., 2016. Isolation and characterization of arsenic-resistant bacteria and possible application in bioremediation. Biotechnol. Rep. 10, 1–7.
Dhankher, O.P., Li, Y., Rosen, B.P., Shi, J., Salt, D., Senecoff, J.F., Sashti, N.A., Meagher, R.B., 2002. Engineering tolerance and hyperaccumulation of arsenic in plants by combining arsenate reductase and γ-glutamylcysteine synthetase expression. Nat. Biotechnol. 20, 1140.
DiTusa, S.F., Fontenot, E.B., Wallace, R.W., Silvers, M.A., Steele, T.N., Elnagar, A.H., Dearman, K.M., Smith, A.P., 2016. A member of the Phosphate transporter 1 (Pht1) family from the arsenic-hyperaccumulating fern *Pteris vittata* is a high-affinity arsenate transporter. New Phytol. 209, 762–772.
Diwakar, J., Johnston, S.G., Burton, E.D., Shrestha, S.D., 2015. Arsenic mobilization in an alluvial aquifer of the Terai region, Nepal. J. Hydrol. 4, 59–79.
Fazi, S., Amalfitano, S., Casentini, B., Davolos, D., Pietrangeli, B., Crognale, S., Lotti, F., Rossetti, S., 2016. Arsenic removal from naturally contaminated waters: a review of methods combining chemical and biological treatments. Rend. Lincei 27, 51–58.
Garg, N., Singla, P., Bhandari, P., 2015. Metal uptake, oxidative metabolism, and mycorrhization in pigeonpea and pea under arsenic and cadmium stress. Turk. J. Agric. For. 39, 234–250.
Gay, G., 1990. Effect of the ectomycorrhizal fungus *Hebeloma hiemale* on adventitious root formation in derooted *Pinus halepensis* shoot hypocotyls. Can. J. Bot. 68, 1265–1270.
Guo, J., Xu, W., Ma, M., 2012. The assembly of metals chelation by thiols and vacuolar compartmentalization conferred increased tolerance to and accumulation of cadmium and arsenic in transgenic *Arabidopsis thaliana*. J. Hazard

Mater. 199, 309–313.
Guo, J., Dai, X., Xu, W., Ma, M., 2008. Overexpressing GSH1 and AsPCS1 simultaneously increases the tolerance and accumulation of cadmium and arsenic in *Arabidopsis thaliana*. Chemosphere 72, 1020–1026.
He, X., Lilleskov, E., 2014. Arsenic uptake and phytoremediation potential by arbuscular mycorrhizal fungi. In: Mycorrhizal Fungi: Use in Sustainable Agriculture and Land Restoration. Springer, Berlin, Heidelberg, pp. 259–275.
Hložková, K., Matěnová, M., Žáčková, P., Strnad, H., Hršelová, H., Hroudová, M., Kotrba, P., 2016. Characterization of three distinct metallothionein genes of the Ag-hyperaccumulating ectomycorrhizal fungus *Amanita strobiliformis*. Fungal Biol. 120, 358–369.
IARC, 2018. Arsenic and arsenic compounds. https://monographs.iarc.fr/wp-content/uploads/2018/06/mono100C-6.pdf. (Accessed 24 December 2018).
Ilyas, S., Rehman, A., 2015. Oxidative stress, glutathione level and antioxidant response to heavy metals in multi-resistant pathogen, *Candida tropicalis*. Environ. Monit. Assess. 187, 4115–4121.
Jomova, K., Jenisova, Z., Feszterova, M., Baros, S., Liska, J., Hudecova, D., Rhodes, C.J., Valko, M., 2011. Arsenic: toxicity, oxidative stress and human disease. J. Appl. Toxicol. 31, 95–107.
Kalsotra, T., Khullar, S., Agnihotri, R., Reddy, M.S., 2018. Metal induction of two metallothionein genes in the ectomycorrhizal fungus *Suillus himalayensis* and their role in metal tolerance. Microbiology 164, 868–876.
Khullar, S., Reddy, M.S., 2019a. Cadmium induced glutathione bioaccumulation mediated by γ-glutamylcysteine synthetase in ectomycorrhizal fungus *Hebeloma cylindrosporum*. Biometals 32, 101–110.
Khullar, S., Reddy, M.S., 2019b. Ectomycorrhizal diversity and tree sustainability. In: Microbial Diversity in Ecosystem Sustainability and Biotechnological Applications. Springer, Singapore, pp. 145–166.
Khullar, S., Reddy, M.S., 2018. Ectomycorrhizal fungi and its role in metal homeostasis through metallothionein and glutathione mechanisms. Curr. Biotechnol. 7, 231–241.
Khullar, S., Reddy, M.S., 2019c. Cadmium and arsenic responses in the ectomycorrhizal fungus *Laccaria bicolor*: glutathione metabolism and its role in metal(-loid) homeostasis. Environ. Microbiol. Rep. 11, 53–61.
Klein, M., Mamnun, Y.M., Eggmann, T., Schüller, C., Wolfger, H., Martinoia, E., Kuchler, K., 2002. The ATP-binding cassette (ABC) transporter Bpt1p mediates vacuolar sequestration of glutathione conjugates in yeast. FEBS Lett. 520, 63–67.
Komorowicz, I., Barałkiewicz, D., 2016. Determination of total arsenic and arsenic species in drinking water, surface water, wastewater, and snow from *Wielkopolska, Kujawy-Pomerania*, and Lower Silesia provinces, Poland. Environ. Monit. Assess. 188, 504.
Leslie, E.M., 2012. Arsenic–glutathione conjugate transport by the human multidrug resistance proteins (MRPs/ABCCs). J. Inorg. Biochem. 108, 141–149.
Li, Y., Dankher, O.P., Carreira, L., Smith, A.P., Meagher, R.B., 2006. The shoot-specific expression of γ-glutamylcysteine synthetase directs the long-distance transport of thiol-peptides to roots conferring tolerance to mercury and arsenic. Plant Physiol. 141, 288–298.
Liang, J., Diao, H., Song, W., Li, L., 2018. Tolerance and bioaccumulation of arsenate by *Aspergillus Oryzae* TLWK-09 isolated from arsenic-contaminated soils. Water Air Soil Pollut. 229, 169.
Liao, V.H.C., Yu, C.W., 2005. *Caenorhabditis elegans* gcs-1 confers resistance to arsenic-induced oxidative stress. Biometals 18, 519–528.
Liu, Y., Zhu, Y.G., Chen, B.D., Christie, P., Li, X.L., 2005. Influence of the arbuscular mycorrhizal fungus *Glomus mosseae* on uptake of arsenate by the As hyperaccumulator fern *Pteris vittata* L. Mycorrhiza 15, 187–192.
Livak, K.J., Schmittgen, T.D., 2001. Analysis of relative gene expression data using real-time quantitative PCR and the $2^{-\Delta\Delta CT}$ method. Methods 25, 402–408.
Melin, E.L.I.A.S., 1953. Physiology of mycorrhizal relations in plants. Annu. Rev. Plant Physiol. 4, 325–346.
Minet, M., Dufour, M.E., Lacroute, F., 1992. Complementation of *Saccharomyces cerevisiae* auxotrophic mutants by *Arabidopsis thaliana* cDNAs. Plant J. 2, 417–422.
Mitra, A., Chatterjee, S., Gupta, D.K., 2017. Potential role of microbes in bioremediation of arsenic. In: Arsenic Contamination in the Environment. Springer, Cham, pp. 195–213.
Mukherjee, A., Das, D., Mondal, S.K., Biswas, R., Das, T.K., Boujedaini, N., Khuda-Bukhsh, A.R., 2010. Tolerance of arsenate-induced stress in *Aspergillus niger*, a possible candidate for bioremediation. Ecotoxicol. Environ. Saf. 73, 172–182.
Muñiz Ortiz, J.G., Opoka, R., Kane, D., Cartwright, I.L., 2008. Investigating arsenic susceptibility from a genetic perspective in *Drosophila* reveals a key role for glutathione synthetase. Toxicol. Sci. 107, 416–426.
Nguyen, H., Rineau, F., Vangronsveld, J., Cuypers, A., Colpaert, J.V., Ruytinx, J., 2017. A novel, highly conserved metallothionein family in basidiomycete fungi and characterization of two representative *SlMTa* and *SlMTb* genes in the ectomycorrhizal fungus *Suillus luteus*. Environ. Microbiol. 19, 2577–2587.
Pickering, I.J., Prince, R.C., George, M.J., Smith, R.D., George, G.N., Salt, D.E., 2000. Reduction and coordination of arsenic in Indian mustard. Plant Physiol. 122, 1171–1178.
Pinter, I.F., Salomon, M.V., Gil, R., Mastrantonio, L., Bottini, R., Piccoli, P., 2018. Arsenic and trace elements in soil, water, grapevine and onion in Jáchal, Argentina. Sci. Total Environ. 615, 1485–1498.
Rahman, I., Kode, A., Biswas, S.K., 2006. Assay for quantitative determination of glutathione and glutathione disulfide levels using enzymatic recycling method. Nat. Protoc. 1, 3159–3165.
Ramesh, G., Podila, G.K., Gay, G., Marmeisse, R., Reddy, M.S., 2009. Different patterns of regulation for the copper and cadmium metallothioneins of the ectomycorrhizal fungus *Hebeloma cylindrosporum*. Appl. Environ. Microbiol. 75, 2266–2274.
Reddy, M.S., Kour, M., Aggarwal, S., Ahuja, S., Marmeisse, R., Fraissinet-Tachet, L., 2016. Metal induction of a *Pisolithus albus* metallothionein and its potential involvement in heavy metal tolerance during mycorrhizal symbiosis. Environ. Microbiol. 18, 2446–2454.
Reddy, M.S., Prasanna, L., Marmeisse, R., Fraissinet-Tachet, L., 2014. Differential expression of metallothioneins in response to heavy metals and their involvement in metal tolerance in the symbiotic basidiomycete *Laccaria bicolor*. Microbiology 160, 2235–2242.
Rodríguez-Lado, L., Sun, G., Berg, M., Zhang, Q., Xue, H., Zheng, Q., Johnson, C.A., 2013. Groundwater arsenic contamination throughout China. Science 341, 866–868.
Ruiz, J.M., Rivero, R.M., Romero, L., 2003. Preliminary studies on the involvement of biosynthesis of cysteine and glutathione concentration in the resistance to B toxicity in sunflower plants. Plant Sci. 165, 811–817.
Sácký, J., Beneš, V., Borovička, J., Leonhardt, T., Kotrba, P., 2019. Different cadmium tolerance of two isolates of *Hebeloma mesophaeum* showing different basal expression levels of metallothionein (*HmMT3*) gene. Fungal Biol. 123, 247–254.
Schuliga, M., Chouchane, S., Snow, E.T., 2002. Upregulation of glutathione-related genes and enzyme activities in cultured human cells by sublethal concentrations of inorganic arsenic. Toxicol. Sci. 70, 183–192.
Sharma, S., Anand, G., Singh, N., Kapoor, R., 2017. Arbuscular mycorrhiza augments arsenic tolerance in wheat (*Triticum aestivum* L.) by strengthening antioxidant defense system and thiol metabolism. Front. Plant Sci. 8, 906.
Sharples, J.M., Meharg, A.A., Chambers, S.M., Cairney, J.W., 2001. Arsenate resistance in the ericoid mycorrhizal fungus *Hymenoscyphus ericae*. New Phytol. 151, 265–270.
Singh, M., Srivastava, P.K., Verma, P.C., Kharwar, R.N., Singh, N., Tripathi, R.D., 2015. Soil fungi for mycoremediation of arsenic pollution in agriculture soils. J. Appl. Microbiol. 119, 1278–1290.
Smith, S.E., Christophersen, H.M., Pope, S., Smith, F.A., 2010. Arsenic uptake and toxicity in plants: integrating mycorrhizal influences. Plant Soil 327, 1–21.
Smith, S.E., Jakobsen, I., Grønlund, M., Smith, F.A., 2011. Roles of arbuscular mycorrhizas in plant phosphorus nutrition: interactions between pathways of phosphorus uptake in arbuscular mycorrhizal roots have important implications for understanding and manipulating plant phosphorus acquisition. Plant Physiol. 156, 1050–1057.
Stearns, T., Ma, H., Botstein, D., 1990. Manipulating yeast genome using plasmid vectors. Methods Enzymol. 185, 280–297.
Su, S., Zeng, X., Bai, L., Li, L., Duan, R., 2011. Arsenic biotransformation by arsenic-resistant fungi *Trichoderma asperellum* SM-12F1, *Penicillium janthinellum* SM-12F4, and *Fusarium oxysporum* CZ-8F1. Sci. Total Environ. 409, 5057–5062.
Talukdar, D., Talukdar, T., 2014. Retracted article: coordinated response of sulfate transport, cysteine biosynthesis, and glutathione-mediated antioxidant defense in lentil (*Lens culinaris* Medik.) genotypes exposed to arsenic. Protoplasma 251, 839–855.
Thomas, D.J., 2008. Unraveling arsenic—glutathione connections. Toxicol. Sci. 107, 309–311.
Thorsen, M., Lagniel, G., Kristiansson, E., Junot, C., Nerman, O., Labarre, J., Tamás, M.J., 2007. Quantitative transcriptome, proteome, and sulfur metabolite profiling of the *Saccharomyces cerevisiae* response to arsenite. Physiol. Genom. 30, 35–43.
Treseder, K.K., 2013. The extent of mycorrhizal colonization of roots and its influence on plant growth and phosphorus content. Plant Soil 371, 1–13.
USEPA, 2006. Drinking water arsenic rule history. . (Accessed 24 December 2018). https://www.epa.gov/dwreginfo/drinking_water_arsenic_rule_history.
Verbruggen, N., Hermans, C., Schat, H., 2009. Mechanisms to cope with arsenic or cadmium excess in plants. Curr. Opin. Plant Biol. 12, 364–372.
WHO, 2011. Edition F. Guidelines for Drinking-Water Quality, vol. 38. WHO chronicle, pp. 104–108.
Wu, Z., Ren, H., McGrath, S.P., Wu, P., Zhao, F.J., 2011. Investigating the contribution of the phosphate transport pathway to arsenic accumulation in rice. Plant Physiol. 157, 498–508.
Yadav, S.K., 2010. Heavy metals toxicity in plants: an overview on the role of glutathione and phytochelatins in heavy metal stress tolerance of plants. South Afr. J. Bot. 76, 167–179.
Zhang, X., Ren, B.H., Wu, S.L., Sun, Y.Q., Lin, G., Chen, B.D., 2015. Arbuscular mycorrhizal symbiosis influences arsenic accumulation and speciation in *Medicago truncatula* L. in arsenic-contaminated soil. Chemosphere 119, 224–230.
Zhao, F.J., Ma, J.F., Meharg, A.A., McGrath, S.P., 2009. Arsenic uptake and metabolism in plants. New Phytol. 181, 777–794.

environmental microbiology reports

Environmental Microbiology Reports (2018) **00**(00), 00–00 doi:10.1111/1758-2229.12712

Cadmium and arsenic responses in the ectomycorrhizal fungus *Laccaria bicolor*: glutathione metabolism and its role in metal(loid) homeostasis

Shikha Khullar and M. Sudhakara Reddy*
Department of Biotechnology, Thapar Institute of Engineering and Technology, Patiala, Punjab, 147004, India.

Summary

Ectomycorrhizal fungi play an important role in protecting their host plant from metal(loid) stresses by synthesizing various thiol rich compounds like metallothioneins and glutathione. We investigated the effect of cadmium (Cd) and arsenic (As) stress with a specific interest on glutathione (GSH) in the ectomycorrhizal fungus *Laccaria bicolor*. The total GSH levels inside the cell were significantly increased with increase in external metal(loid) stress. An analysis of the transcript levels of genes responsible for GSH synthesis, γ-glutamylcysteine synthetase *(Lbγ-GCS)* and glutathione synthetase *(LbGS)*, using qPCR revealed that expression of both genes increased as a function of external metal(loid) concentration. The enzyme activity of both *Lbγ-GCS* and *LbGS* were increased with increase in external Cd and As concentration. Further, the functional role of *Lbγ-GCS* and *LbGS* genes in response to Cd and As stress was studied using their respective yeast mutant strains *gsh1*$^{\Delta}$ and *gsh2*$^{\Delta}$. The mutant strains successfully expressed the two genes resulting in wild-type phenotype restoration of Cd and As tolerance. From these results, it was concluded that GSH act as a core component in the mycorrhizal defence system under Cd and As stress for metal(loid) homeostasis and detoxification.

Introduction

Heavy metals constitute a major environmental hazard to human health. Metal(loid)s like cadmium (Cd), arsenic (As), lead (Pb), mercury (Hg), zinc (Zn) and so forth, are continuously being mobilized into the atmosphere through natural processes like weathering of metalliferous rocks and anthropogenic activities like combustion of fossil fuels, mining and industry, use of phosphate fertilizers and so forth. These metal(loid)s are highly toxic to living organisms affecting various physiological processes (John *et al*., 2012). In order to cope with this toxic effect caused by metal(loid)s, organisms possess different defence mechanisms like: reduced uptake of metals by extracellular chelators, binding to the cell wall or increased efflux, intracellular chelation of metals in the cytosol by ligands like glutathione, metallothioneins and compartmentalization into the vacuoles (Bellion *et al.,* 2006). Synthesis of specific chelators and subsequent sequestration of metal complexes are of major importance to limit free metal concentrations. The main molecules responsible for the sequestration of metal(loid)s include glutathione (γ-Glu-Cys-Gly, GSH), small metal-binding peptides known as phytochelatins $(\gamma\text{-Glu-Cys})_n$Gly, PCs), and metallothioneins (small cysteine-rich proteins, MTs) (Cobbett and Goldsbrough, 2002). Glutathione (GSH) plays an important role in metal(loid) scavenging due to the high affinity of metal(loid)s to its thiol (-SH) group and as a precursor of phytochelatins (PCs). Besides metal homeostasis, organisms possess antioxidative defence systems to manage the metal-imposed oxidative challenge (Smeets *et al.,* 2009). In addition to its primary antioxidant capacities, GSH also acts as a substrate for the regeneration of other essential antioxidants (Foyer and Noctor 2005).

Glutathione, a tripeptide (γ-glutamyl-cysteinyl-glycine) is the most abundant non-protein thiol present in the living system (Pócsi *et al*., 2004). GSH sequesters the toxic metal(loid)s (X) by forming non-toxic $(GSH)_nX$ conjugates, which are further compartmentalized into the vacuoles through ABC (ATP-binding cassette) transporters (Schlunk *et al*., 2015). In plants, both Cd and As show high affinity for the thiol (–SH) group of glutathione, thus, forming a metal(loid)-$(GSH)_2$ complex, which gets subsequently sequestered into the vacuoles (Verbruggen *et al.,* 2009). GSH is biosynthesized in two sequential ATP dependent reactions, mediated by two enzymes, γ-glutamylcysteine synthetase (*γ-GCS*; E.C.6.3.2.2) and glutathione synthetase (*GS*; E.C.6.3.2.3). In the first step, γ-glutamylcysteine synthetase catalyses the formation of γ-glutamylcysteine

Received 6 July, 2018; accepted 2 November, 2018. *For correspondence. E-mail msreddy@thapar.edu; Tel. +911752393350; Fax +911752393005.

using L-glutamate and L-cysteine, followed by the second step catalysed by glutathione synthetase, where L-glycine is added to the C-terminal of γ-glutamylcysteine, forming glutathione. Studies have reported the induction of GSH biosynthesis pathway by different metal(loid)s like As, Cd, Hg and Cr (Thorsen *et al*., 2007; Jozefczak *et al.,* 2012). GSH biosynthesis is the primary rapidly responsive line of defence against Cd exposure (Clemens and Simm, 2003). Studies on *Paxillus involutus, Phanerochaete chrysosporium* and *Penicillium chrysogenum* also demonstrated the significant upregulation in GSH biosynthesis in response to Cd stress (Xu *et al*., 2015; Xu *et al*., 2016).

Ectomycorrhizal fungi (ECM) are the rhizospheric fungi that form a symbiotic association with the plant roots (woody plants like birch, dipterocarp, myrtle, beech, willow, pine and rose families), protecting them from various biotic and abiotic stresses. The ECM fungi benefit the host plant by improving nutrient and water uptake and protecting against various stresses like drought, salinity, pests and toxic metal(loid)s (Leung *et al*., 2013). The ECM fungi have developed an extensive defence mechanism against metal(loid)s toxicity (Bellion *et al*., 2006). They prevent the uptake of metal(loid)s into the cytosol by extracellular chelation through extruded ligands like tricarboxylic acid, oxalic acid (Xu *et al*., 2015) or by biosorption of these metal(loid)s to the fungal cell wall through chitin and glucosamine (Bellion *et al*., 2006). Further, the metal(loid) accumulated in the cytosol is detoxified by synthesizing thiol rich ligands like GSH and MTs (Khullar and Reddy, 2018). In many ECM fungi such as *L. bicolor, Hebeloma cylindrosporum, Pisolithus albus, P. involutus, Suillus luteus, S. himalayensis* and so forth, MTs have been found highly expressive under copper stress (Bellion *et al*., 2007; Ramesh *et al*., 2009; Reddy *et al*., 2014; 2016; Nguyen *et al.,* 2017; Kalsotra *et al.,* 2018). However, very little induction of MTs have been reported in response to Cd stress. It has been hypothesized that Cd detoxification in ECM fungi might be operated through GSH chelation because, the concentrations of GSH in ECM fungi are reported in millimolar range in response to Cd stress (Courbot *et al*., 2004). These observations show that different mechanisms are induced by different metal(loid)s in ECM fungi.

The aim of the present work was therefore to gain insight into the molecular basis of Cd and As tolerance in *L. bicolor* by investigating enzymes of GSH metabolism. The relative expression of both *Lbγ-GCS* and *LbGS* genes was studied by qPCR under different Cd and As stress conditions. Further, the functional characterization of both genes in response to Cd and As stress was carried out using their respective yeast mutants, *gsh1*$^{\Delta}$ and *gsh2*$^{\Delta}$.

Results

Growth and metal(loid) uptake

The growth of *L. bicolor* decreased with increase in external concentration of Cd and As in the media. The half minimum inhibitory concentration (IC_{50}) of Cd and As was found to be 8 μM and 7 mM respectively (Fig. 1A and B). The metal(loid) uptake by *L. bicolor* increased as a function of external metal(loid) stress. In case of Cd, maximum uptake of 0.869 μg mg^{-1} mycelium was observed at 9 μM Cd concentration and decreased at higher concentrations. In case of As, maximum uptake of 0.667 μg As mg^{-1} mycelium was recorded at 15 mM of As concentration (Fig. 1C and D).

Glutathione production and *Lbγ-GCS* and *LbGS* enzyme activities

Total GSH production increased as a function of external metal(loid) stress. When exposed to Cd and As, a rapid increase in GSH content was observed. Even at the lower concentrations used (10 μm Cd and 3 mM As), the GSH concentration increased by fivefold and sixfold respectively. Maximum GSH production of 1.4 nmol mg^{-1} mycelium (about 13 folds higher than the control) was observed at 40 μM Cd and 1.6 nmol mg^{-1} (about 15 folds higher than the control) at 15 mM As (Fig. 2A and B). Since both *Lbγ-GCS* and *LbGS* are ATP dependent enzymes, they liberate one molecule of inorganic phosphorous every time they catalyse the synthesis of γ-glutamylcysteine and glutathione, respectively, converting ATP to ADP. The total inorganic phosphorous liberated by both enzymes per minute per mg of protein increased with increase in external Cd and As concentrations, resulting in the increased activity of both enzymes. The total phosphate liberated increased from 0.2 to 1 μmol mg^{-1} min^{-1} when the Cd concentration was increased 0 to 40 μM and As concentration from 0 to 30 mM (Fig. 2C and D). These results indicated that both enzymes involved in GSH synthesis were induced in response to external Cd and As concentrations.

Relative expression of *Lbγ-GCS* and *LbGS* genes by qPCR

The mRNA accumulation of both *Lbγ-GCS* and *LbGS* increased with increase in metal(loid) stress. In case of Cd, maximum expression of *Lbγ-GCS* was observed at 40 μM (18 fold increase) while *LbGS* at 30 μM Cd (12 fold increase) compared to control (Fig. 3A). Similarly, at 20 mM of As, the expression of *Lbγ-GCS* and *LbGS* increased by 10 fold and sixfold respectively (Fig. 3B).

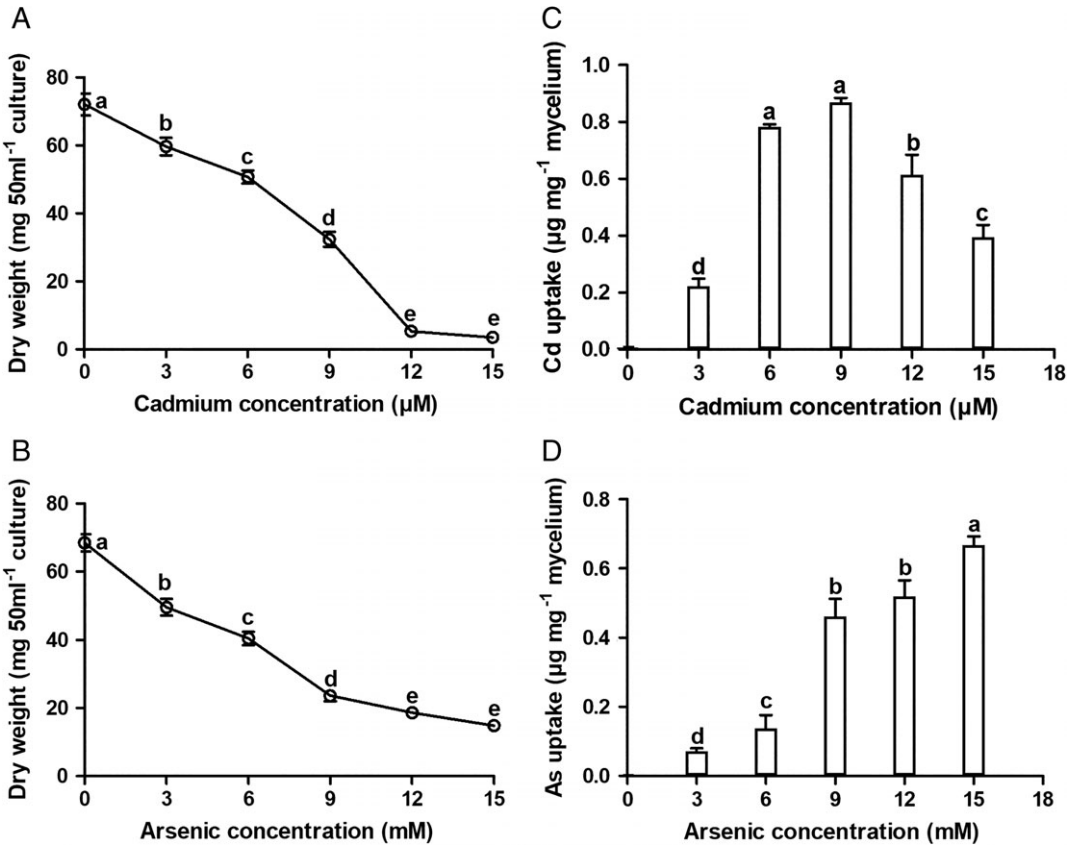

Fig. 1. Effect of different concentrations of Cd and As on the mycelial growth (A, B) and metal uptake (C, D) by *L. bicolor.* Values sharing a common letter among treatments are not significantly different at $P < 0.05$ ($n = 3$). Error bars are ±SD.

Functional complementation of *Lbγ-GCS* and *LbGS* genes in *S. cerevisiae*

The growth of both yeast mutants carrying pFL61 or pFL61-*Lbγ-GCS*/pFL61-*LbGS* along with the wild type strain was monitored on SD-Ura medium with and without Cd and As. Drop test analysis revealed that, the growth of both mutants, *gsh1*$^{\Delta}$ and *gsh2*$^{\Delta}$ carrying pFL61 was inhibited at 40 μM Cd and 100 μM As. However, the mutants transformed with *Lbγ-GCS* and *LbGS* genes were able to grow on metal(loid) supplemented medium similar to the wild type strain BY4741 (Fig. 4). Further, the restoration of metal(loid) tolerance by yeast mutants was verified by growing these *Lbγ-GCS* and *LbGS* transformed mutants in liquid SD-Ura medium with various concentrations of Cd and As. The transformation of yeast mutants with *Lbγ-GCS* and *LbGS* successfully restored the wild-type phenotype for metal(loid) tolerance (Fig. 5).

Sequence analysis of *Lbγ-GCS* and *LbGS* genes

The *Lbγ-GCS* cDNA contains an 1854 bp ORF encoding 617 amino acids with predicted molecular mass of 70.5 kDa and pI 5.3. The ATP binding sites in the primary sequence were identified using the ATP interacting site prediction server 'ATPint: Prediction of ATP interacting protein residues' (http://www.imtech.res.in/raghava/atpint/) (Chauhan *et al.,* 2009). A unique ATP binding domain 'MGFGMGCCCLQLT' rich in glycine and cysteine was found to be conserved throughout the nine selected basidiomycetes (Supporting Information Table 2). The protein was predicted to be a membrane protein with amino acids 1 to 459 as non-cytoplasmic domain, 460 to 482 as transmembrane domain and 483 to 617 as cytoplasmic domain. The *LbGS* cDNA consists of 1596 bp ORF encoding 531 amino acids with molecular mass 58.9 kDa and pI 5.59. A conserved glycine rich domain 'KPQREGGGNN' involved in ATP binding has been observed between 413 and 422 amino acids. Other predicted ATP binding amino acids E_{153}, K_{331}, Y_{424}, E_{480}, K_{508}, E_{514} were also found to be conserved throughout 11 selected basidiomycetes (Supporting Information Table 2).

Discussion

The present study was aimed at characterizing the GSH biosynthesis genes in response to Cd and As stress in the ectomycorrhizal fungus *L. bicolor* and its possible

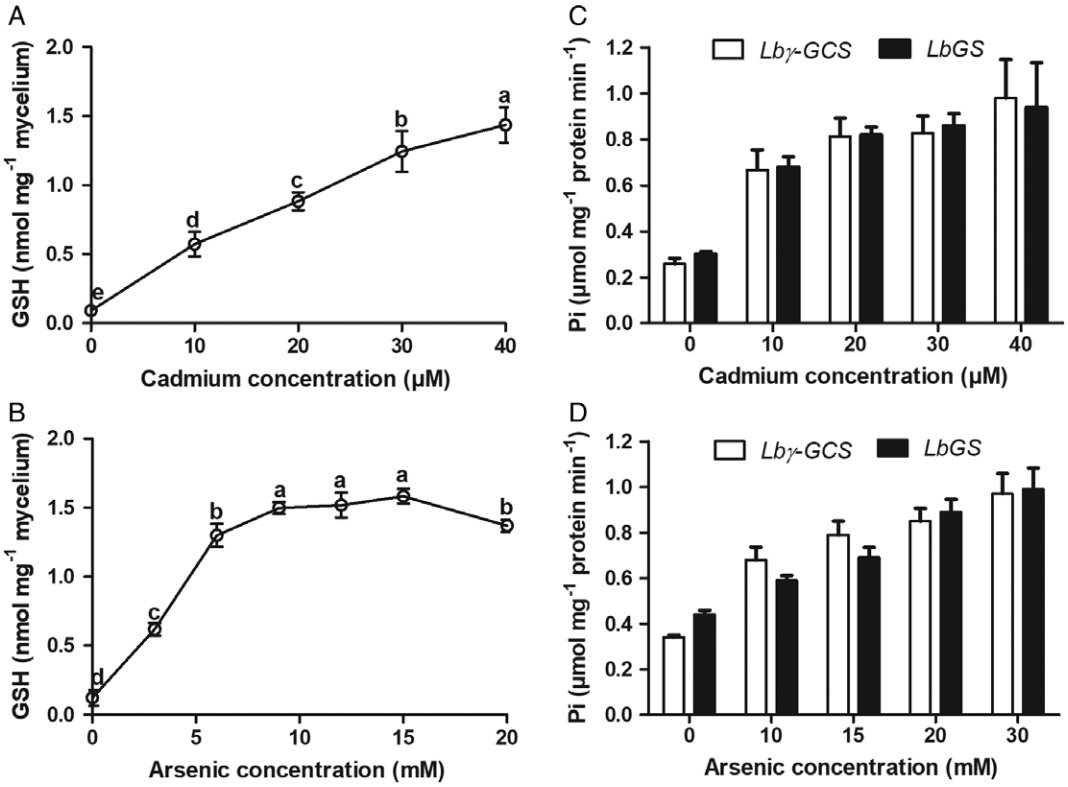

Fig. 2. Effect of increasing concentrations of Cd and As on total glutathione production (A, B) and enzyme activity of *Lbγ-GCS* and *LbGS* (C, D) in *L. bicolor*. The Values sharing a common letter within the metal are not significantly different at $P < 0.05$ ($n = 3$). Error bars are ±SD.

functional role in detoxification of metal(loid)s such as Cd and As. In the present study, with increase in concentration of metal(loid)s, a decrease in the growth of *L. bicolor* was observed. In case of Cd, the half minimum inhibitory concentration (IC_{50}) was recorded at 8.0 μM whereas the IC_{50} of Cd reported for other ectomycorrhizal fungi, *P. tinctorius, Cenococcum geophilum, P. involutus,* and *S. luteus* were 89.0, 9.0, 2.2 and 0.4 μM respectively (Hartley *et al*., 1997). In case of As, *L. bicolor* showed IC_{50} value of 7.0 mM. Sharples and colleagues (2000) reported a higher resistance to As compounds for an ericoid mycorrhizal strain belonging to the *Hymenoscyphus ericae* (now *Rhizoscyphus ericae*) species isolated from an As/Cu mine site when compared to a *H. ericae* strain coming from an uncontaminated heathland site. The growth of the heathland isolate was completely inhibited at 1.33 mM $H_2AsO_4^-$, whereas the mine isolate was able to grow up to 13.3 mM $H_2AsO_4^-$, with its growth being inhibited by only 40% at this concentration. Considering literature data, our results do not place *L. bicolor* among Cd and As resistant fungi.

The GSH content increased with increase in concentration of Cd and As in this study. About 1.5 nmol mg^{-1} of total GSH was produced per mg of mycelium in response to Cd and As stress, indicating that GSH biosynthesis is highly inducible by external metal(loid) stress. Similar GSH levels have also been reported in *P. involutus* where approximately 1.2 nmol mg-1 GSH was produced in response to 64 μM Cd stress (Courbot *et al.,* 2004). However, *P. chrysosporium* produced about 2.5 nmol mg-1 GSH at Cd stress of 162 μM (Xu *et al.,* 2016). Similar observations have also been reported in various plants, fungi and other living systems (Sun *et al*., 2007; Thorsen *et al*., 2007; Eroglu *et al*., 2015). GSH also protects potentially susceptible cysteine-rich proteins from binding free metal(loid) ions and consecutively affecting their function. After forming nontoxic complexes with metal(loid)s, GSH facilitates their sequestration away from sensitive sites in cells (Verbruggen *et al.,* 2009).

GSH biosynthesis involves two sequential ATP dependent reactions, mediated by two enzymes γ-glutamylcysteine synthetase (*γ-GCS)* and glutathione synthetase (*GS).* Analysis of the transcript levels of genes responsible for GSH synthesis (*Lbγ-GCS* and *LbGS* genes), using real-time PCR revealed that expression of both genes increased as a function of external metal(loid) concentration (Fig. 3). Expression level of *Lbγ-GCS* was significantly higher than *LbGS* gene in both Cd and As treated mycelium. The involvement of both enzymes (*Lbγ-GCS* and *LbGS*) in Cd and As tolerance mechanisms has been corroborated by quantifying the activity of each enzyme in response to metal(loid)

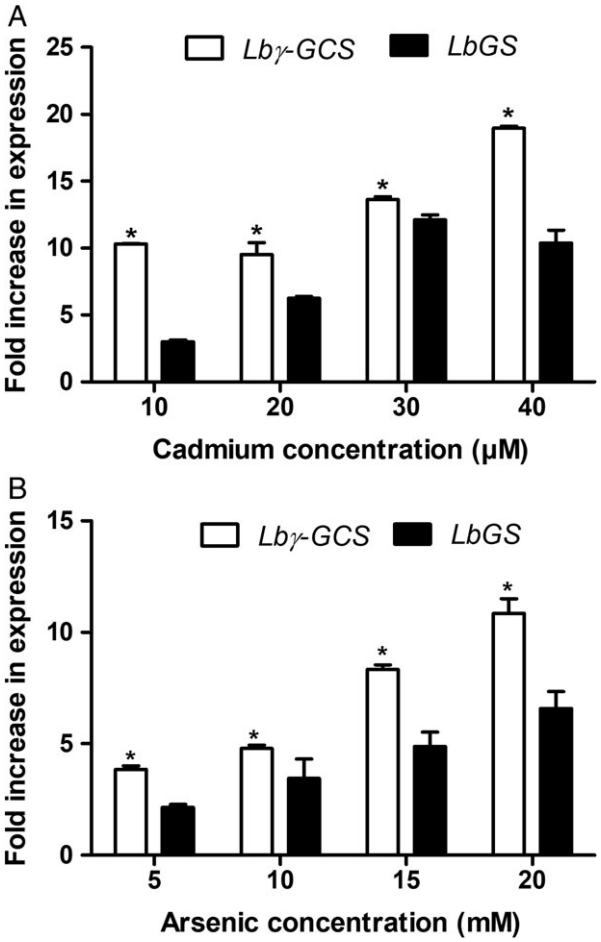

Fig. 3. Fold increase in expression level of *Lbγ-GCS* and *LbGS* genes in *L. bicolor* after 48 h of incubation in medium supplemented with different concentrations of (A) Cd and (B) As. Values plotted are referred to the control condition (expression level in free living fungus without metal treatment) and represent an average of three biological replicates ± standard deviation. Bars showing '*' are significantly different at $P < 0.05$ ($n = 3$).

exposure (Fig. 2C and D). Similar response has also been reported in various hyper accumulating plants (Pickering *et al*., 2000; Dhankher *et al*., 2002).

The functional characterization of two genes in their respective yeast mutants *gsh1*$^{\Delta}$ and *gsh2*$^{\Delta}$, revelled the actual function of these genes in metal(loid) homeostasis. The yeast mutants *gsh1*$^{\Delta}$ and *gsh2*$^{\Delta}$ when transformed with their respective *Lbγ-GCS* and *LbGS* genes successfully restored their metal(loid) tolerance tendencies (Figs 4 and 5). This observation clearly demonstrates that GSH biosynthesis is one of the key mechanisms involved in Cd and As tolerance in the ectomycorrhizal fungus *L. bicolor.* Both the genes were also characterized using various bioinformatics tools and various ATP and substrate binding domains were identified (Chauhan *et al*., 2009). The conserved glycine and cysteine rich motif 'IYLDAMGFGMGCCCLQLTFQ' 249–268 amino acid from *Lb-γGCS* has also been reported to be conserved in invertebrate (*Ciona intestinalis*), plant *(Chorispora bungeana*) and yeast (*S. cerevisiae*) (Ohtake and Yabuuchi, 1991; Franchi *et al.,* 2012; Nair *et al.,* 2013).

Conclusions

In the present study, the ECM fungus *L. bicolor* showed sensitivity to both Cd and As. The GSH concentration increased in the mycelium in response to Cd and As stress. The two genes involved in GSH biosynthesis (*Lbγ-GCS* and *LbGS*) were actively induced in response to metal(loid) stress. The enzyme activity of both *Lbγ-GCS* and *LbGS* also increased with increase in external Cd and As concentration. The yeast mutants *gsh1*$^{\Delta}$ and *gsh2*$^{\Delta}$ transformed with *Lbγ-GCS* and *LbGS* genes respectively, rescued their metal(loid) sensitivity. According to our results, it can be concluded that GSH biosynthesis is one of the key mechanisms responsible for Cd and As detoxification in the ECM fungus *L. bicolor.*

Experimental procedure

Biological material and stress treatment

The ectomycorrhizal fungus *L. bicolor* S238 N was maintained on Modified Melin-Norkrans medium (MMN) (Melin, 1953) supplemented with Heller's micronutrients (Gay, 1990), at 25 °C in dark. The tolerance of *L. bicolor* to different metal(loid)s was tested by growing the fungus on liquid MMN medium supplemented with different concentrations of Cd ($3CdSO_4.8H_2O$: 0, 3, 6, 9, 12 and 15 μM) and As ($Na_2HAsO_4.7H_2O$: 0, 5, 10, 12, 15 mM) for 21 days at 25 °C in dark. After 21 days, the mycelium was harvested and washed with saline water (0.9% NaCl) and 0.1 M EDTA water followed by three washings with distilled water and dried at 60 °C for 24 h. The dried mycelium was further digested with nitric acid and perchloric acid ($HNO_3/HCLO_4$) and the total metal(loid) uptake by mycelium at different metal(loid) concentrations was determined using atomic absorption spectroscopy.

For the functional complementation, two *S. cerevisiae* mutants *gsh1*$^{\Delta}$-Y07097 (BY4741; *MATa; ura3Δ0; leu2Δ0; his3Δ1; met15Δ0; YJL101c::kanMX4*) and *gsh2*$^{\Delta}$-Y01740 (BY4741; *MATa; ura3Δ0; leu2Δ0; his3Δ1; met15Δ0; YOL049w::kanMX4)* for *γ-GCS* and *GS* genes, respectively, were procured from Indian Institute of Science Education and Research, Mohali, Punjab, India.

Glutathione production and *Lbγ-GCS* and *LbGS* enzyme activities

In order to measure the total amount of glutathione produced by *L. bicolor* in response to Cd and As, the mycelium was grown on MMN agar plates overlaid with cellophane

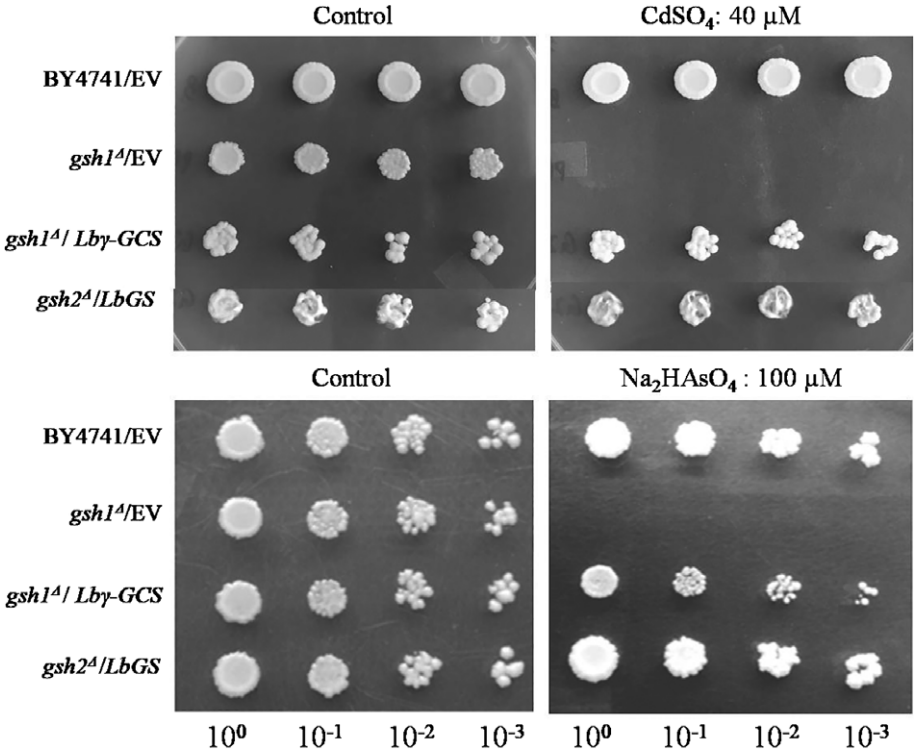

Fig. 4. Functional complementation of *gsh1*$^{\Delta}$ and *gsh2*$^{\Delta}$ yeast mutants transformed with empty vector pFL61 (EV) and with their respective genes *Lbγ-GCS* and *LbGS* on selective media SD-Ura. BY4741 wild type strain was used as a positive control.

sheets for 14 days at 25 °C. These were then transferred on MMN medium supplemented with increasing concentrations of Cd ($3CdSO_4.8H_2O$: 0, 10, 20, 30, 40 μM) and As ($Na_2HAsO_4.7H_2O$: 0, 3, 6, 9, 12, 15, 20 mM) for 48 h. After 48 h, the mycelium was scrapped from the cellophane sheets and crushed with liquid nitrogen. Total glutathione was estimated from these crushed samples by enzymatic recycling in two steps: Cell extract preparation and GSH detection. Cell extract was prepared by homogenizing the mycelium in sulfosalicylic acid-TritonX solution (0.6% sulfosalicylic acid and 0.1% TritonX solution in 0.1 M Potassium phosphate buffer with 5 mM EDTA disodium salt at pH 7.5 (KPE)) (Rahman *et al*., 2006), followed by the centrifugation of homogenized sample at 8000*g* for 10 min at 2–4 °C. Clear supernatant was collected and used for glutathione estimation. The amount of glutathione produced by the mycelium under various stress conditions was quantified spectrophotometrically by enzymatic recycling method, using the sulfydryl reagent 5,5′-dithio-bis(2-nitrobenzoic acid) (DTNB) to form the yellow coloured derivative 5′-thio-2-nitrobenzoic acid (TNB) measurable at 412 nm (Rahman *et al*., 2006).

Lbγ-GCS and *LbGS* activities were assayed according to Ruiz and colleagues (2003) and Sengupta and colleagues (2012). The liquid nitrogen crushed samples of *L. bicolor* stressed with different concentrations of Cd and As were homogenized with lysis buffer consisting of 100 mM Tris–HCl (pH 8.0), 10 mM $MgCl_2$ and 1 mM DTT. The supernatant collected after centrifugation was used for *Lbγ-GCS* and *LbGS* assay. *Lbγ-GCS* activity was assayed by mixing 100 μl of supernatant with 500 μl of assay mix consisting of 100 mM Hepes (pH 8.0), 50 mM $MgCl_2$, 5 mM ATP, 5 mM phosphoenolpyruvate, 5 mM DTT, 20 mM gluatamate, 1 mM cysteine, and 10 U ml^{-1} pyruvate kinase. The mixture was incubated at 37 °C for 60 min followed by addition of 100 μl of 50% TCA to stop the reaction. The mixture was centrifuged, and the supernatant was used for phosphate estimation by phosphomolybdate method. The amount of phosphate released is directly proportional to the enzyme activity. For *LbGS* activity the same assay was performed replacing glutamate and cysteine with 1 mM glycine and 0.5 mM γ-glutamylcysteine.

RNA isolation, cDNA synthesis and qPCR analysis

Total RNA was isolated from the liquid nitrogen crushed samples treated with Cd and As using the QiAzol lysis reagent (Qiagen; Valencia, CA) and cDNAs were synthesized using 'The RevertAID™ First Strand cDNA synthesis Kit, (Thermo Fisher Scientific, Waltham, USA)' as per the manufacturer's instructions. The relative expression of both *Lbγ-GCS* and *LbGS* was studied by qPCR analysis using SYBR® Green JumpStart™TaqReadyMix™

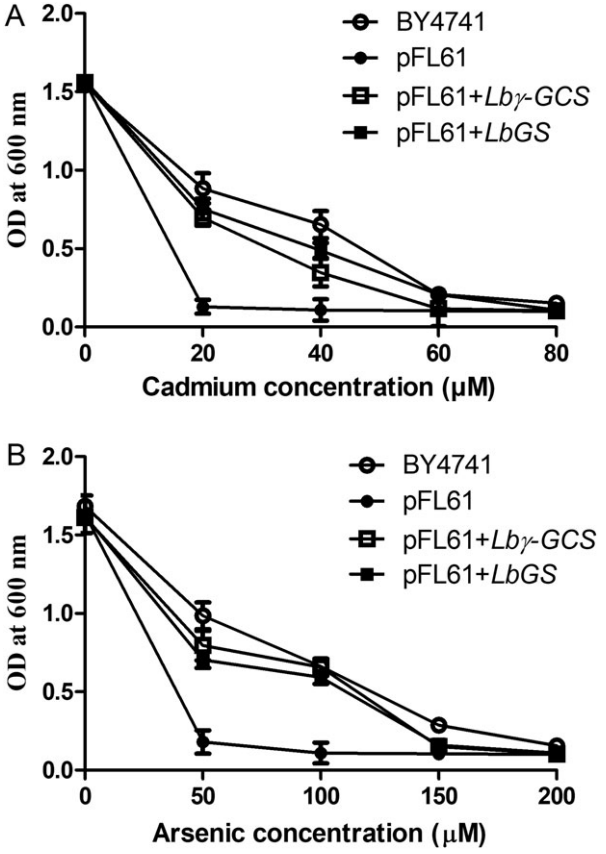

Fig. 5. Growth curve of yeast mutants *gsh1*$^{\Delta}$ and *gsh2*$^{\Delta}$, transformed with their respective genes *Lbγ-GCS* and *LbGS*, and empty vector pFL61 along with its wild type (BY4741) grown in presence of various concentrations of Cd and As for 24 h at 30 °C. The values represent an average of three biological replicates with ±SD.

(Sigma-Aldrich; St. Louis, USA) in Mastercycler®eprealplex system (Eppendorf; Hamburg, Germany) using the following program: initial denaturation at 95 °C for 20 s followed by 40 cycles of 95 °C for 15 s, 55 °C for 15 s and 72 °C for 20 s. The *E* value was obtained in the range of 1.08 to 1.28 using the equation $E\ [10_{(-1/\text{slope})}] - 1$. The *E* value was used to calculate C_{t1} value using the equation $C_{t1} = C_{te} \times [\log (1 + E)/\log 2]$. The reference gene was selected using NormFinder algorithm (Andersen *et al*., 2004). Since the stability value of α-actin was minimum, it was used as the reference gene for further calculating the relative gene expression of *Lbγ-GCS* and *LbGS* genes using 'the comparative C_T Method (ΔΔCT Method) - $2^{-\Delta\Delta Ct1}$, (Livak and Schmittgen, 2001).

The full length sequence of *Lbγ-GCS* and *LbGS* genes was obtained using gene specific primers designed from the sequences retrieved from JGI portal http://genome.jgi.doe.gov/ (Supporting Information Table 1). PCR amplification of *Lbγ-GCS* and *LbGS* genes were carried out in a 25 μl reaction consisting of 1 X reaction buffer, 2 mM dNTPs, 1 μl (forward primer, 10 μM), 1 μl (reverse primer, 10 μM), template DNA (100 ng), 1.5 U Advantage 2 polymerase (Takara, CA, USA) and nuclease free water to make 25 μl. The PCR program was set as: initial denaturation at 95 °C for 3 min followed by 30 cycles of 1 min at 94 °C, 1 min at 62 °C, 1 min at 72 °C and final extension at 72 °C for 8 min. The amplified PCR products were sequenced. The sequences were analysed by using various bioinformatics tools. The sequences obtained were submitted to GenBank of NCBI as *GSH1* and *GSH2* for *Lbγ-GCS* and *LbGS*, respectively, under the accession number MF766455 and MF766456.

Expression of *Lbγ-GCS* and *LbGS* genes in *S. cerevisiae*

The two genes *Lbγ-GCS* and *LbGS* were amplified from *L. bicolor* cDNA using the primers Lbam1F/Leco1R and Lbam2F/Leco2R respectively (Supporting Information Table 1). Restriction sites *BamH1* and *EcoR1* were added to the 5′ end of forward and reverse primer respectively. The amplified PCR products were ligated into the yeast expression vector pFL61 under the control of the PGK promoter from the yeast phosphoglycerokinase encoding gene (Minet *et al*., 1992). For the functional complementation, two *S. cerevisiae* mutants *gsh1*$^{\Delta}$ (*γ-GCS* mutant) and *gsh2*$^{\Delta}$ (*GS* mutant) were transformed with empty vector pFL61, and pFL61-*Lbγ-GCS*/pFL61-*LbGS*, respectively by lithium acetate method (Stearns *et al*., 1990). All the four transformants along with wild type BY4741 were then pre-grown on SD-ura medium for 24 h. The function of each gene in metal(loid) tolerance was studied by analysing their growth on both liquid and solidified SD-Ura supplemented with $CdSO_4$ ($3CdSO_4.8H_2O$: 40 μM) and As ($Na_2HAsO_4.7H_2O$: 100 μM) as described in Kalsotra *et al.,* 2018. In liquid SD-Ura medium (with and without Cd and As), the growth of each transformant was recorded as their optical density at 600 nm.

The data collected from this study followed homoscedasticity. Analysis of variance (ANOVA) was performed to test the significant differences among the treatments and the means were compared with Tukey's test at $P < 0.05$. All the analysis was performed by using Graph Pad Prism 5.1 software.

Acknowledgements

Authors are thankful to Department of Biotechnology, Govt. of India for sponsoring the research project (BT/PR8339/BCE/8/1045/2013) to carry out the present work.

References

Andersen, C.L., Jensen, J.L., and Ørntoft, T.F. (2004) Normalization of real-time quantitative reverse transcription-PCR data: a model-based variance estimation approach to identify genes suited for normalization, applied to bladder and colon cancer data sets. *Cancer Res* **64**: 5245–5250.

Bellion, M., Courbot, M., Jacob, C., Blaudez, D., and Chalot, M. (2006) Extracellular and cellular mechanisms sustaining metal tolerance in ectomycorrhizal fungi. *FEMS Microbiol Lett* **254**: 173–181.

Bellion, M., Courbot, M., Jacob, C., Guinet, F., Blaudez, D., and Chalot, M. (2007) Metal induction of a *Paxillus involutus* metallothionein and its heterologous expression in *Hebeloma cylindrosporum*. *New Phytol* **174**: 151–158.

Chauhan, J.S., Mishra, N.K., and Raghava, G.P. (2009) Identification of ATP binding residues of a protein from its primary sequence. *BMC Bioinformatics* **10**: 434–443.

Clemens, S., and Simm, C. (2003) *Schizosaccharomyce spombe* as a model for metal homeostasis in plant cells: the phytochelatin-dependent pathway is the main cadmium detoxification mechanism. *New Phytol* **159**: 323–330.

Cobbett, C., and Goldsbrough, P. (2002) Phytochelatins and metallothioneins: roles in heavy metal detoxification and homeostasis. *Annu Rev Plant Biol* **53**: 159–182.

Courbot, M., Diez, L., Ruotolo, R., Chalot, M., and Leroy, P. (2004) Cadmium-responsive thiols in the ectomycorrhizal fungus *Paxillus involutus*. *Appl Environ Microbiol* **70**: 7413–7417.

Dhankher, O.P., Li, Y., Rosen, B.P., Shi, J., Salt, D., Senecoff, J.F., *et al*. (2002) Engineering tolerance and hyperaccumulation of arsenic in plants by combining arsenate reductase and γ-glutamy-lcysteinesynthetase expression. *Nat Biotechnol* **20**: 1140–1145.

Eroglu, A., Dogan, Z., Kanak, E.G., Atli, G., and Canli, M. (2015) Effects of heavy metals (Cd, Cu, Cr, Pb, Zn) on fish glutathione metabolism. *Environ Sci Pollut Res* **22**: 3229–3237.

Foyer, C., and Noctor, G. (2005) Oxidant and antioxidant signalling in plants: a re-evaluation of the concept of oxidative stress in a physiological context. *Plant Cell Environ* **28**: 1056–1071.

Franchi, N., Ferro, D., Ballarin, L., and Santovito, G. (2012) Transcription of genes involved in glutathione biosynthesis in the solitary tunicate *Ciona intestinalis* exposed to metals. *Aquat Toxicol* **114**: 14–22.

Gay, G. (1990) Effect of the ectomycorrhizal fungus *Hebeloma hiemale* on adventitious root formation in derooted *Pinus halepensis* shoot hypocotyls. *Can J Bot* **68**: 1265–1270.

Hartley, J., Cairney, J.W., and Meharg, A.A. (1997) Do ectomycorrhizal fungi exhibit adaptive tolerance to potentially toxic metals in the environment? *Plant Soil* **189**: 303–319.

John, R., Ahmad, P., Gadgil, K., and Sharma, S. (2012) Heavy metal toxicity: effect on plant growth, biochemical parameters and metal accumulation by *Brassica juncea* L. *Int J Plant Prod* **3**: 65–76.

Jozefczak, M., Remans, T., Vangronsveld, J., and Cuypers, A. (2012) Glutathione is a key player in metal-induced oxidative stress defenses. *Int J Mol Sci* **13**: 3145–3175.

Kalsotra, T., Khullar, S., Agnihotri, R., and Reddy, M.S. (2018) Metal induction of two metallothionein genes in the ectomycorrhizal fungus *Suillus himalayensis* and their role in metal tolerance. *Microbiology* **164**: 868–876.

Khullar, S., and Reddy, M.S. (2018) Ectomycorrhizal fungi and its role in metal homeostasis through metallothionein and glutathione mechanisms. *Curr Biotechnol* **7**: 231–241.

Leung, H.M., Wang, Z.-W., Ye, Z.-H., Yung, K.-L., Peng, X.-L., and Cheung, K.C. (2013) Interactions between arbuscular mycorrhizae and plants in phytoremediation of metal-contaminated soils: a review. *Pedosphere* **23**: 549–563.

Livak, K.J., and Schmittgen, T.D. (2001) Analysis of relative gene expression data using real-time quantitative PCR and the 2− ΔΔCT method. *Methods* **25**: 402–408.

Melin, E.L.I.A.S. (1953) Physiology of mycorrhizal relations in plants. *Annu Rev Plant Physiol* **4**: 325–346.

Minet, M., Dufour, M.E., and Lacroute, F. (1992) Complementation of mutants by *Arabidopsis thaliana* cDNA. *Plant J* **32**: 417–422.

Nair, P.M., Park, S.Y., Chung, J.W., and Choi, J. (2013) Transcriptional regulation of glutathione biosynthesis genes, γ-glutamyl-cysteine ligase and glutathione synthetase in response to cadmium and nonylphenol in *Chironomus riparius*. *Environ Toxicol Pharmacol* **36**: 265–273.

Nguyen, H., Rineau, F., Vangronsveld, J., Cuypers, A., Colpaert, J.V., and Ruytinx, J. (2017) A novel, highly conserved metallothionein family in basidiomycete fungi and characterization of two representative SlMTa and SlMTb genes in the ectomycorrhizal fungus *Suillus luteus*. *Environ Microbiol* **19**: 2577–2587.

Ohtake, Y., and Yabuuchi, S. (1991) Molecular cloning of the γ-glutamylcysteine synthetase gene of *Saccharomyces cerevisiae*. *Yeast* **7**: 953–961.

Pickering, I.J., Prince, R.C., George, M.J., Smith, R.D., George, G.N., and Salt, D.E. (2000) Reduction and coordination of arsenic in Indian mustard. *Plant Physiol* **122**: 1171–1178.

Pócsi, I., Prade, R.A., and Penninckx, M.J. (2004) Glutathione, altruistic metabolite in fungi. *Adv Microb Physiol* **49**: 1–76.

Rahman, I., Kode, A., and Biswas, S.K. (2006) Assay for quantitative determination of glutathione and glutathione disulfide levels using enzymatic recycling method. *Nat Protoc* **1**: 3159–3165.

Ramesh, G., Podila, G.K., Gay, G., Marmeisse, R., and Reddy, M.S. (2009) Different patterns of regulation for the copper and cadmium metallothioneins of the ectomycorrhizal fungus *Hebeloma cylindrosporum*. *Appl Environ Microbiol* **75**: 2266–2274.

Reddy, M.S., Kour, M., Aggarwal, S., Ahuja, S., Marmeisse, R., and Fraissinet-Tachet, L. (2016) Metal induction of a *Pisolithus albus* metallothionein and its potential involvement in heavy metal tolerance during mycorrhizal symbiosis. *Environ Microbiol* **18**: 2446–2454.

Reddy, M.S., Prasanna, L., Marmeisse, R., and Fraissinet-Tachet, L. (2014) Differential expression of metallothioneins in response to heavy metals and their involvement in metal tolerance in the symbiotic basidiomycete *Laccaria bicolor*. *Microbiology* **160**: 2235–2242.

Ruiz, J.M., Rivero, R.M., and Romero, L. (2003) Preliminary studies on the involvement of biosynthesis of cysteine and glutathione concentration in the resistance to B toxicity in sunflower plants. *Plant Sci* **165**: 811–817.

Schlunk, I., Krause, K., Wirth, S., and Kothe, E. (2015) A transporter for abiotic stress and plant metabolite resistance in the ectomycorrhizal fungus *Tricholoma vaccinum*. *Environ Sci Pollut Res* **22**: 19384–19393.

Sengupta, D., Ramesh, G., Mudalkar, S., Kumar, K.R.R., Kirti, P.B., and Reddy, A.R. (2012) Molecular cloning and characterization of γ-glutamyl cysteine synthetase (VrγECS) from roots of *Vigna radiata* (L.) Wilczek under progressive drought stress and recovery. *Plant Mol Biol* **30**: 894–903.

Sharples, J.M., Meharg, A.A., Chambers, S.M., and Cairney, J.W. (2000) Mechanism of arsenate resistance in the ericoid mycorrhizal fungus *Hymenoscyphus ericae*. *Plant Physiol* **124**: 1327–1334.

Smeets, K., Opdenakker, K., Remans, T., Van Sanden, S., Van Belleghem, F., Semane, B., *et al*. (2009) Oxidative stress-related responses at transcriptional and enzymatic levels after exposure to Cd or Cu in a multipollution context. *J Plant Physiol* **166**: 1982–1992.

Stearns, T., Ma, H., and Botstein, D. (1990) Manipulating yeast genome using plasmid vectors. *Methods Enzymol* **185**: 280–297.

Sun, Q., Ye, Z.H., Wang, X.R., and Wong, M.H. (2007) Cadmium hyperaccumulation leads to an increase of glutathione rather than phytochelatins in the cadmium hyperaccumulator *Sedum alfredii*. *J Plant Physiol* **164**: 1489–1498.

Thorsen, M., Lagniel, G., Kristiansson, E., Junot, C., Nerman, O., Labarre, J., and Tamás, M.J. (2007) Quantitative transcriptome, proteome, and sulfur metabolite profiling of the *Saccharomyces cerevisiae* response to arsenite. *Physiol Genomics* **30**: 35–43.

Verbruggen, N., Hermans, C., and Schat, H. (2009) Mechanisms to cope with arsenic or cadmium excess in plants. *Curr Opin Plant Biol* **12**: 364–372.

Xu, P., Leng, Y., Zeng, G., Huang, D., Lai, C., Zhao, M., *et al*. (2015) Cadmium induced oxalic acid secretion and its role in metal uptake and detoxification mechanisms in *Phanerochaete chrysosporium*. *Appl Microbiol Biotechnol* **99**: 435–443.

Xu, P., Zeng, G., Huang, D., Liu, L., Zhao, M., Lai, C., *et al*. (2016) Metal bioaccumulation, oxidative stress and antioxidant defenses in *Phanerochaete chrysosporium* response to Cd exposure. *Ecol Eng* **87**: 150–156.

Supporting Information

Additional Supporting Information may be found in the online version of this article at the publisher's web-site:

Table S1. Different primers used for gene amplification from *L. bicolor* cDNA. *Lbγ-GCS* and *LbGS* primers were used for amplification of γ-glutamylcysteine synthetase and glutathione synthetase genes respectively. Actin, tubuline, adenosine kinase, *Lbγ-GCS* -RT and *LbGS*-RT primers were used to amplify the genes for RT-PCR analysis. Lbam1F, Leco1R, Lbam2F and Leco2R primers were used for yeast complementation studies. The restriction sites were added to the 5′ end of primers (underlined) [a]NdeI, [b]XhoI, [c]BamHI, [d]EcoRI.

Table S2. Conserved domains in *Lbγ-GCS* and *LbGS* genes identified for their potential role in ATP binding. The *L. bicolor γ-GCS* gene MF766455 were aligned with different basidiomycetes *Rhodotorula* KWU43246, *Serendipita indica* CCA66352, *Daedalea quercina* EPT04524, *Paxillus rubicundulus* KIK91183, *Pisolithus microcarpus* KIK27695, *Fistulina hepatica* KIY44398, *Gymnopus luxurians* KIK67150, *Agaricus bisporus* XP_006460756, *Hebeloma cylindrosporum* KIM45296 and *LbGS* gene MF766456 was aligned with *Coniophora puteana* XP_007768870, *Stereum hirsutum* XP_007305063, *Lentinula edodes* GAW08968, *Obba rivulosa* OCH89932, *Pycnoporus coccineus* OSC99094, *Trametes versicolor* XP_008045264, *Laccaria amethystina* KIK06216, *Galerina marginata* KDR82535, *Hebeloma cylindrosporum* KIM43057, *Hypsizygus marmoreus* KYQ41889, *Termitomyces* KNZ73319 and the conserved ATP binding domains were identified.

Biometals (2019) 32:101–110
https://doi.org/10.1007/s10534-018-00164-2

Cadmium induced glutathione bioaccumulation mediated by γ-glutamylcysteine synthetase in ectomycorrhizal fungus *Hebeloma cylindrosporum*

Shikha Khullar · M. Sudhakara Reddy

Received: 24 September 2018 / Accepted: 3 December 2018 / Published online: 17 December 2018

Abstract Ectomycorrhizal fungi hold a potential role in bioremediation of heavy metal polluted areas because of its metal accumulation and detoxification property. We investigated the cadmium (Cd) induced bioaccumulation of glutathione (GSH) mediated by γ-glutamylcysteine synthetase (γ-GCS) in the ectomycorrhizal fungus *Hebeloma cylindrosporum*. In *H. cylindrosporum*, a demand driven synthesis of GSH has been observed in response to Cd. The expression and enzyme activity of *H. cylindrosporum* γ-GCS (*Hcγ-GCS*) increased as a function of external Cd stress resulting in increased GSH production. The function of *Hcγ-GCS* in providing heavy metal tolerance to *H. cylindrosporum* was justified by complementing the gene in *gsh1*$^{\Delta}$ mutant of *Saccharomyces cerevisiae*. The metal sensitive mutant *gsh1*$^{\Delta}$ successfully restored its metal tolerance ability when transformed with *Hcγ-GCS* gene. Sequence analysis of *Hcγ-GCS* showed homology with most of the reported γ-GCS proteins from basidiomycetes family. The active site of the *Hcγ-GCS* protein is composed of amino acids that were found to be conserved not only in fungi, but also in plants and mammals. From these results, it was concluded that *Hcγ-GCS* plays an important role in bioaccumulation of GSH, which is a core component in the mycorrhizal defense system under Cd stress for Cd homeostasis and detoxification.

Keywords Ectomycorrhizal fungi · Metal homeostasis · γ-Glutamylcysteine synthetase · *Hebeloma cylindrosporum* · Glutathione · Cadmium

Introduction

Cadmium (Cd) is considered as the global environmental threats due to its high bioaccumulation and biomagnifications into the diverse ecosystems (Dietz et al. 2000). It is toxic to living systems even at low concentrations and interferes with many metabolic pathways resulting in cellular damage because of its strong affinity for the sulphydryl residues (Gallego et al. 2012). Cd is the potent inducers of oxidative stress inside the cells and these oxidative damages in cell are usually caused by the imbalance between accumulation of reactive oxygen species (ROS) and the protective cellular antioxidant system (Foyer and Noctor 2011). Therefore it is crucial to maintain adequate level of ROS in the cell. This is attained by the complex antioxidant homeostatic system

Electronic supplementary material The online version of this article (https://doi.org/10.1007/s10534-018-00164-2) contains supplementary material, which is available to authorized users.

S. Khullar · M. S. Reddy (✉)
Department of Biotechnology, Thapar Institute of Engineering & Technology, Bhadson Road, Patiala, Punjab 147004, India
e-mail: msreddy@thapar.edu

composed of metabolites like glutathione (GSH) and ascorbate (ASC) (Foyer and Noctor 2011).

Glutathione is a ubiquitous intracellular peptide with multifarious functions like detoxification of various heavy metals and xenobiotics, antioxidant defense, sulfur assimilation; cell signaling and regulate cell growth and death (Lu 2009; Khullar and Reddy 2016). GSH is a key component in metal scavenging, due to the high affinity of metals for its thiol (–SH) group and also as a precursor of phytochelatins (PCs). GSH is reported as the most abundant thiol present in the living system, with the average concentration in millimoles (Pócsi et al. 2004). It is a tripeptide (L-γ-glutamyl-L-cysteinyl-glycine) ($\sim$ 307 Da) composed of three amino acids, glutamate, cysteine and glycine. GSH is synthesized in two sequential ATP dependant reactions mediated by two enzymes, γ-glutamylcysteine synthetase (γGCS; E.C.6.3.2.2) and glutathione synthetase (GS; E.C.6.3.2.3). In the first reaction, γGCS catalyzes the formation of γ-glutamylcysteine by combining L-glutamate and L-cycteine, followed by the condensation of glycine to the C-terminal of γ-glutamylcysteine by GS, resulting in the formation of glutathione. Both reactions are ATP dependant. The two major determinants of GSH biosynthesis in the cell are: availability of cysteine (the sulfur amino acid precursor), and the activity of γ-glutamylcysteine synthetase (the rate limiting enzyme) (Lu 2009). During the metal stress, both factors increase in order to cope with the desired GSH demand for the detoxification and survival (Jozefczak et al. 2012). γGCS is a rate limiting enzyme in GSH synthesis and its activity is enhanced by Cd, As, Hg, Cr ions (Vido et al. 2001; Thorsen et al. 2007; Galant et al. 2011; Sobrino-Plata et al. 2014). It has also been reported that the mutation in the γGCS gene resulted in increasing metal sensitivity in *Arabidopsis thaliana* and *Candida glabrata* (Sobrino-Plata et al. 2014; Gutiérrez-Escobedo et al. 2013). Many studies have reported the GSH-mediated induction of the transcription of genes involved in Cd transport and detoxification (Sengupta et al. 2012; He et al. 2015).

The response of ectomycorrhizal (ECM) fungi to toxic metals is important, since these organisms are present at contaminated sites, participate in crucial symbiotic relationships with plants that grow at these sites, and alleviate metal toxicity for their host plants (Jentschke and Goldbold 2000). The mechanisms that are involved in metal homeostasis and detoxification of heavy metals in ECM fungi includes extracellular mechanisms such as precipitation, chelation and cell-wall binding and intracellular mechanisms such as binding to organic acids, sulfur compounds, polyphosphates, peptides and transport into intracellular compartments (Bellion et al. 2006). The main molecules responsible for the sequestration of metals include glutathione, phytochelatins and metallothioneins (Cobbett and Goldsbrough 2002). It has been reported that in ECM fungi, metallothioneins have been induced in response to copper stress than Cd (Reddy et al. 2014, 2016; Khullar and Reddy 2016). However, accumulation of GSH in ECM fungi was reported when exposed to Cd suggesting the role of GSH in Cd detoxification (Courbot et al. 2004).

The aim of the present study was therefore to gain insight into the molecular basis of Cd detoxification in the ectomycorrhizal fungus *Hebeloma cylindrosporum* by investigating enzyme *Hcγ-GCS* of GSH metabolism. The relative expression of *Hcγ-GCS* gene was studied by qPCR under different Cd stress conditions. Further, the functional characterization of *Hcγ-GCS* gene in response to Cd stress was carried out using yeast mutant *gsh1*$^{\Delta}$.

Materials and methods

Biological material, stress treatment and metal accumulation

The ectomycorrhizal fungus *Hebeloma cylindrosporum* was maintained on modified Melin-Norkrans medium (MMN) (Melin 1953) supplemented with Heller's micronutrients (Gay 1990) at 25 °C. The tolerance of *H. cylindrosporum* to cadmium was monitored by growing the fungus in MMN broth supplemented with different concentrations of cadmium (0, 3, 6, 9, 12 and 15 μM) for 21 days at 25 °C. After 21 days, the mycelium was harvested and washed with saline water (0.9% NaCl) and 0.1 M EDTA water followed by three washings with distilled water and dried at 60 °C for 24 h. The dry weight of each sample was recorded and the dried mycelium was further digested with nitric acid and perchloric acid (HNO_3/$HCLO_4$) in the ratio 3:1 (Kalsotra et al. 2018) and the total metal uptake by mycelium at different Cd

concentrations was determined using atomic absorption spectroscopy.

For the functional complementation, *S. cerevisiae* mutant *gsh1*$^{\Delta}$-Y07097 (BY4741; *MATa*; *ura3Δ0*; *leu2Δ0*; *his3Δ1*; *met15Δ0*; *YJL101c::kanMX4*) *γ-GCS* was procured from Indian Institute of Science Education and Research (IISER, Mohali, Punjab, India).

Total glutathione production and *Hcγ-GCS* activity

Total glutathione produced by *H. cylindrosporum* in response to the elevated levels of Cd was determined by the method described in Rahman et al. (2006). The fungus was grown on MMN agar plates overlaid with cellophane sheets for 14 days at 25 °C. The cellophane sheets were then transferred on MMN medium supplemented with increasing concentrations of cadmium ($CdSO_4$: 0, 10, 20, 30, 40 µM) for 48 h. After 48 h, the mycelium was scrapped from the cellophane sheets and crushed with liquid nitrogen. Total glutathione was estimated from these crushed samples by enzymatic recycling. Firstly, the cell extract was prepared by homogenizing the mycelium in sulfosalicylic acid-TritonX solution (0.6% sulfosalicylic acid and 0.1% Triton-X solution in 0.1 M Potassium phosphate buffer) with 5 mM EDTA disodium salt at pH 7.5 (KPE) followed by the centrifugation of homogenized sample at 8000×*g* for 10 min at 4 °C. Clear supernatant obtained was used for GSH estimation. The amount of GSH produced by the mycelium under various stress conditions was quantified spectrophotometrically by enzymatic recycling method, using the sulfydryl reagent 5,5′-dithio-bis(2-nitrobenzoic acid) (DTNB) to form the yellow colored derivative 5′-thio-2-nitrobenzoic acid (TNB) measurable at 412 nm (Rahman et al. 2006). Cell extract (100 µl) was mixed with 700 µl of KPE buffer followed by addition of 120 µl of freshly prepared DTNB and glutathione reductase (GR) mix. The mixture was kept at room temperature for 30 s. 60 µl of β-NADPH (2 mg β-NADPH in 3 ml KPE buffer) was added to the above mix and absorbance was measured at 412 nm. The amount of GSH produced was measured using the GSH (Sigma-Aldrich; St. Louis, USA) standard curve prepared by the same procedure.

Hcγ-GCS activity was determined according to the method described in Ruiz et al. (2003) and Sengupta et al. (2012). The liquid nitrogen crushed samples of *H. cylindrosporum* stressed with different concentrations of Cd (0, 10, 20, 30, 40 µM) were homogenized with lysis buffer (100 mM Tris–HCl (pH 8.0), 1 mM DTT and 10 mM $MgCl_2$). *Hcγ-GCS* activity was assayed by mixing 100 µl of supernatant with 500 µl of assay mix consisting of 100 mM Hepes (pH 8.0), 50 mM $MgCl_2$, 5 mM ATP, 5 mM phosphoenolpyruvate, 5 mM DTT, 20 mM glutamate, 1 mM cysteine, and 10 U ml^{-1} pyruvate kinase. The mixture was incubated at 37 °C for 60 min followed by addition of 100 µl of 50% TCA to stop the reaction. The mixture was centrifuged and the supernatant was used for phosphate estimation by phosphomolybdate method. The amount of phosphate released is directly proportional to the enzyme activity.

RNA isolation, cDNA synthesis and gene amplification

Total RNA was isolated from the liquid nitrogen crushed samples of *H. cylindrosporum* using the QiAzol lysis reagent (Qiagen; Valencia, CA), followed by the RNase free DNase I treatment. cDNA was synthesized from approximately 5 µg of total RNA using "The RevertAID^{TM} First Strand cDNA synthesis Kit, (Thermo Fisher Scientific, Waltham, USA)" as per the manufacturer's instructions. The cDNA so obtained was used to amplify the *Hcγ-GCS* gene using the gene specific primers. The gene specific primers were designed using the sequence retrieved from JGI portal http://genome.jgi.doe.gov/ (Supplementary Table 1). Restriction sites NdeI (CATATG) and NotI (GCGGCCGC) were added to the 5′ end of the forward and reverse primer respectively. PCR amplification of *Hcγ-GCS* gene was carried out in a 25 µl reaction consisting of 1 X reaction buffer, 2 µl (dNTPs, 2 mM), 1 µl (forward primer, 10 µM), 1 µl (reverse primer, 10 µM), template DNA (100 ng), 1.5 U *Taq* polymerase and nuclease free water to make 25 µl. The PCR program was set as: initial denaturation at 95 °C for 3 min followed by 30 cycles of 1 min at 94 °C, 1 min at 62 °C, 1 min at 72 °C and final extension at 72 °C for 8 min. The amplified product so obtained was purified and sequenced. The sequence was submitted to GenBank of NCBI under the Accession Number MH892339.

Expression of *γ-GCS* by real time PCR (RT-PCR) analysis

Total RNA was isolated from the liquid nitrogen crushed samples treated with Cd using the QiAzol lysis reagent (Qiagen; Valencia, CA) and cDNAs were synthesized using "The RevertAID^{TM} First Strand cDNA synthesis Kit, (Thermo Fisher Scientific, Waltham, USA)" as per the manufacturer's instructions. The relative expression of *Hcγ-GCS* was determined by Real time PCR analysis using SYBR® Green JumpStart^{TM}TaqReadyMix^{TM} (Sigma-Aldrich; St. Louis, USA) in Mastercycler®eprealplex system (Eppendorf; Hamburg, Germany) using the following program: initial denaturation at 95 °C for 20 s followed by 40 cycles of 95 °C for 15 s, 55 °C for 15 s and 72 °C for 20 s. The E value was obtained in the range of 0.97 to 1.08 using the equation E $[10_{(-1/\text{slope})}] - 1$. The E value was used to calculate C_{t1} value using the equation $C_{t1} = C_{te} \times [\log (1 + E)/\log 2]$. Among the three reference genes α-actin, β-tubulin and adenosine kinase, α-actin showed minimum stability value with NormFinder algorithm (Andersen et al. 2004). Hence α-actin was used as a reference gene for studying the relative gene expression of *Hcγ-GCS* using the comparative C_T Method (ΔΔCT Method) $- 2^{-\Delta\Delta Ct1}$" (Livak and Schmittgen 2001).

Functional complementation of *Hcγ-GCS* in *S. cerevisiae*

The *Hcγ-GCS* gene was amplified from cDNA using primers Hcbam1F and Hceco1R. BamH1 and EcoR1 restriction sites were added to the 5′ end of both forward and reverse primer respectively (Supplementary Table 1). The amplified PCR product was ligated into the yeast expression vector pFL61 under the control of the PGK promoter from the yeast phosphoglycerokinase encoding gene (Minet et al. 1992). For the functional complementation, *S. cerevisiae* mutant $gsh1^{\Delta}$ (*γ-GCS* mutant) was transformed with empty vector pFL61 and pFL61-*Hcγ-GCS* by lithium acetate method (Stearns et al. 1990). The transformants along with wild type BY4741 were then pre-grown on SD-ura medium for 24 h at 30 °C with constant shaking at 220 rpm. The OD_{600} of each culture was adjusted to 1.0. For each culture 4 serial dilutions were made 10^0, 10^{-1}, 10^{-2} and 10^{-3}. 5 µl serial dilutions of each culture was spotted on SD-Ura plates with and without Cd ($CdSO_4$: 40 µM). The plates were incubated at 30 °C for 3 days and photographed. In a consecutive experiment, all the three cultures, $gsh1^{\Delta}$ (pFL61 + *Hcγ-GCS*), $gsh1^{\Delta}$ (pFL61) and wild type BY4741 were inoculated in 50 ml SD-ura broth and allowed to grow at 30 °C till the OD_{600nm} reached 0.05. The cultures were then subjected to different concentrations of Cd and allowed to grow for next 24 h and the OD at 600 nm was recorded.

Sequence analysis and structure prediction of *Hcγ-GCS*

The ORF of the sequence was identified using ORF finder and subjected to BLAST (http://www.ncbi.nlm.nih.gov/BLAST) for homology search. The homologous sequence so obtained were aligned by ClustalW. Phylogenetic tree was reconstructed by using MEGA software. Further, Expasy tool was used to calculate the molecular weight and pI of *Hcγ-GCS* protein. The protein domains were identified using Interpro (http://www.ebi.ac.uk/interpro/sequence-search). Various conserved domains like catalytic domain, ATP binding domains, glycosylation sites, phosphorylation sites were identified by Motif-Scan and ATPint (crdd.osdd.net/raghava/atpint/index.html). The secondary structure of Hcγ-GCS protein was predicted using PSSpred (http://zhanglab.ccmb.med.umich.edu/PSSpred), where all the possible α-helix, β-sheets and coils were identified. The tertiary structure of Hcγ-GCS protein was constructed by I-TASSER. The structure template was identified using threading program LOMETS from PDB library with Normalized Z-score greater than 1. I-TASSER generated 5 predicted models and the model with highest confidence value (C value) was selected. The structure so obtained was verified by aligning it with all structures in PDB library using TM-align. Various ligand binding sites in the predicted structure were identified using COFACTOR and COACH programs.

The data were analyzed by One way analysis of variance the significant differences among the means were compared with Tukey's test at $P < 0.05$. All the analysis was performed by using Graph Pad Prism 5.1 software.

Results

Metal tolerance and accumulation

The growth of *H. cylindrosporum* decreased significantly with increasing concentrations of Cd. The half minimum inhibitory (IC_{50}) of Cd was recorded at 8 μM (Fig. 1a). However, the Cd accumulated inside the fungus was found to increase with increase in external metal concentrations. Maximum Cd accumulation of 0.9 μg mg^{-1} dry mycelium was recorded at 9 μM and decreased hereafter (Fig. 1b).

Glutathione production and *Hcγ-GCS* activity

The total GSH production increased as a function of external Cd stress. Total GSH production increased significantly from 0.118 to 0.85 nmol mg^{-1} mycelium when the stress was increased from 0 to 40 μM (Fig. 2a). Approx. 8.4 folds increase in glutathione concentration was observed, when the Cd stress was increased from 0 to 40 μM. Since *Hcγ-GCS* is an ATP

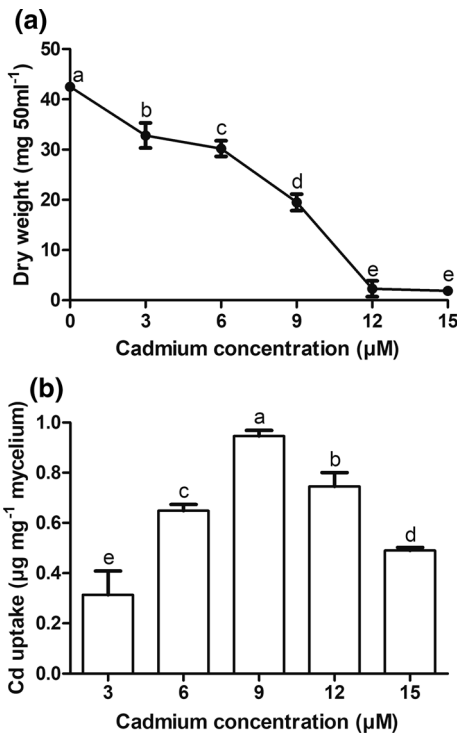

Fig. 1 Effect of increasing concentrations of Cd on the growth (**a**) and total metal uptake (**b**) by *H. cylindrosporum*. Values sharing a common letter among treatments are not significantly different at $P < 0.05$ ($n = 3$). Error bars are ± SD

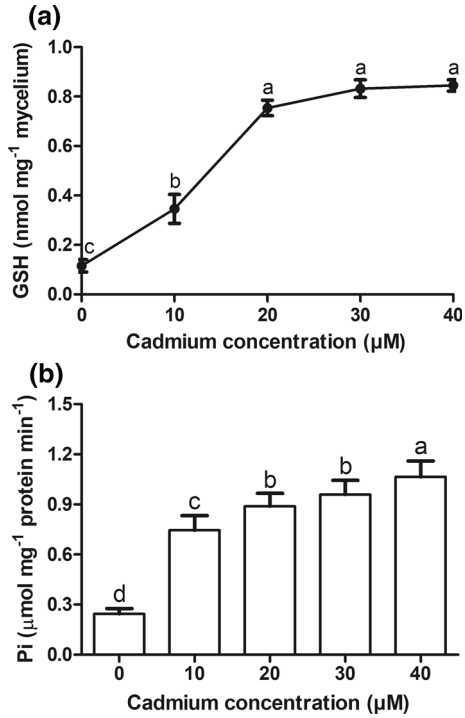

Fig. 2 Effect of increasing concentrations of Cd on **a** total glutathione (GSH) production and **b** the enzyme activity of *Hcγ-GCS*. The activity was measured as the amount of inorganic phosphorous released by the enzymes using ATP per mg of isolated protein per minute. Values sharing a common letter among same metals are not significantly different at $P < 0.05$ ($n = 3$). Error bars are ± SD

dependant enzyme, it liberated one molecule of inorganic phosphorus every time it catalyze the synthesis of γ-glutamylcysteine, converting ATP to ADP. Therefore the amount of inorganic phosphorus liberated per minute per mg of protein gives direct evidence of the enzyme activity of *Hcγ-GCS*. The 10 μM Cd stressed mycelium liberated 0.75 μmol mg^{-1} min^{-1} of inorganic phosphorus, which is three times the phosphorus liberated by control mycelium (0.25 μmol mg^{-1} min^{-1}). At 40 μM Cd stress, the concentration of inorganic phosphorous increased to 1.06 μmol mg^{-1} min^{-1}, which is 5 times that of control mycelium (Fig. 2b).

Real time PCR analysis

The mRNA accumulation of *Hcγ-GCS* gene in *H. cylindrosporum* increased when exposed to increasing concentrations of Cd. The 10 folds increase in mRNA accumulation of *Hcγ-GCS* gene was observed at

10 μM Cd stress, whereas it increased to 22 folds at 40 μM Cd (Fig. 3). This clearly depicts that *Hcγ-GCS* gene is highly inducible by Cd stress, resulting in more glutathione biosynthesis.

Functional complementation of *Hcγ-GCS* gene in yeast mutant

The role of *Hcγ-GCS* in inducing heavy metal tolerance in ectomycorrhizal fungus *H. cylindrosporum* was validated by expressing the gene in *S. cerevisiae* mutant for *γGCS* (*gsh1*$^{\Delta}$). The growth of *gsh1*$^{\Delta}$ yeast mutant cells transformed with empty vector pFL61 (EV) and pFL61 + *Hcγ-GCS* was monitored on SD-Ura medium supplemented with and without Cd. The Drop test analysis of all the three cultures BY4741, *gsh1*$^{\Delta}$/EV and *gsh1*$^{\Delta}$/*Hcγ-GCS*, clearly revealed that the growth of *gsh1*$^{\Delta}$/EV inhibited at Cd 40 μM, whereas the same mutant when transformed with *Hcγ-GCS* gene successfully grew under Cd stress like their wild type BY4741 cells (Fig. 4a). Further, the restoration of metal tolerance ability by yeast mutant *gsh1*$^{\Delta}$ was validated by growing all the three cultures BY4741, *gsh1*$^{\Delta}$/EV and *gsh1*$^{\Delta}$/*Hcγ-GCS* in SD-Ura liquid medium supplemented with increasing concentrations of Cd. When subjected under metal stress, *gsh1*$^{\Delta}$/EV did not show any tolerance to Cd. However *gsh1*$^{\Delta}$/*Hcγ-GCS* successfully grew under Cd stress like their parent BY4741 cells (Fig. 4b). This clearly shows that the metal tolerance ability was successfully restored in *gsh1*$^{\Delta}$, when transformed with *Hcγ-GCS* gene.

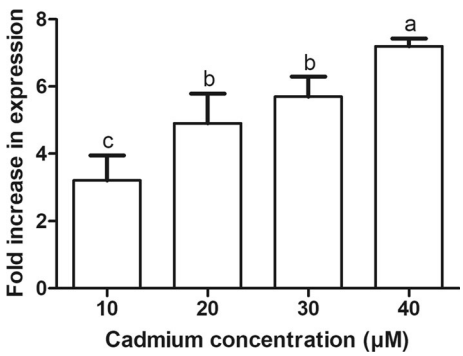

Fig. 3 Fold increase in the relative expression of *Hcγ-GCS* gene when stressed with increasing concentrations of Cd ($CdSO_4$: 0, 10, 20, 30, 40 μM) for 48 h at 25 °C. Actin was normalized as an internal reference gene. Values sharing a common letter within the gene are not significantly different at $P < 0.05$ (n = 3). Error bars are ± SD

Sequence analysis of *Hcγ-GCS* gene

The full length cDNA sequences of *Hcγ-GCS* consists of 2040 bp long open reading frame encoding 679 amino acids with predicted molecular weight of 78.09 kDa and pI of 6.6. The protein is a transmembrane protein with three membrane domains: N-terminal from amino acid 1 to 446 forms a non-cytoplasmic domain; amino acids from 447 to 469 are embedded in the membrane forming a transmembrane domain and at the C-terminal from amino acid 470 to 679 forms a cytoplasmic domain. The putative Hcγ-GCS protein showed maximum homology with most of the basidiomycetes displaying 71%, 70%, 69% and 68% sequence similarity with the γGCS protein sequence form *Coprinopsis cinerea* (XP001830305), *Armillaria gallica* (PBK91420), *Agaricus bisporus* (XP006460756) and *Laccaria bicolor* (XP001877753), respectively. The Phylogenetic tree forms three different clusters of basidiomycetes, mucoromycetes and ascomycetes each sharing common evolutionary history (Fig. 5).

The multiple sequence alignment of different homologous sequences revealed many domains that were found to be conserved in many fungi. Amino acids 249–649 were identified as a conserved glutamylcysteine synthetase catalytic subunit and amino acids 26–84 were identified as 30S ribosomal protein S1. Both the sequences were found to be highly conserved. Most of the predicted ATP binding domains in the primary sequence of Hcγ-GCS protein were found to be conserved. This includes amino acids 188–204 "HVSRPCTANIRRRRGSK", amino acids 249–268 "IYLDAMGFGMGCCCLQLTFQ", amino acids 299–316 "WRGYLADVDCRWNVIAGS" (Supplementary Fig. 1). *N*-glycosylation motifs were also predicted at site N^{163}, N^{511} and N^{518}. The secondary structure of the predicted Hcγ-GCS protein consists of about 37% α-helices, 15% β-strands and 49% coils.

For generating the tertiary structure, the structures homologous to Hcγ-GCS protein sequence were identified in PDB library. Four PBD hits were observed 3ig5, 3ig8, 3ivv and 3ivw. Since 3ig5 (*Saccharomyces cerevisiae* glutamate cysteine ligase) showed maximum identity of 42%, it was selected as a

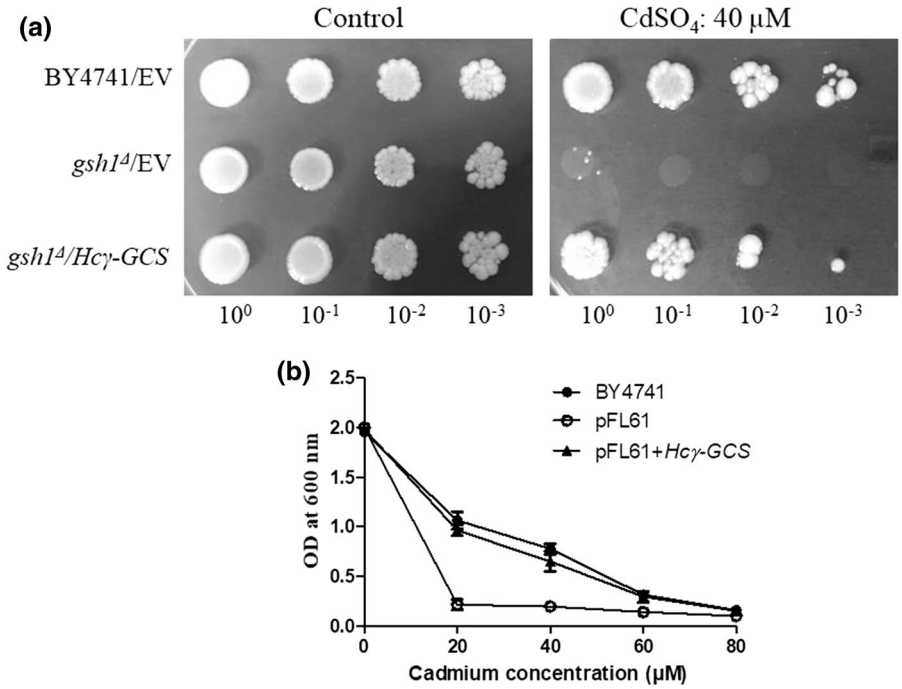

Fig. 4 Drop test analysis (**a**) and liquid broth test (**b**) of the metal sensitive *Saccharomyces cerevisiae* mutant *gsh1*$^{\Delta}$ (Accession Number: Y07097), transformed with empty vector pFL61 (EV) and pFL61 + *Hcγ-GCS* gene on selective media SD-Ura supplemented with and without Cd. BY4741 wild type strain was used as a positive control. For liquid broth test, growth was recorded as optical density at 600 nm after 24 h of incubation at 30 °C and 200 rpm. The values represent an average of three biological replicated with ± SD

template for homology modeling (Fig. 6). Various ligand binding sites were identified on the generated 3D model by COACH. Most of the substrate binding sites like E^{52}, E^{101}, C^{260}, C^{261}, C^{262}, Q^{264}, R^{309}, I^{313}, R^{435} and ADP binding sites L^{46}, W^{47}, G^{48}, D^{49}, E^{50}, H^{99}, E^{108}, P^{114}, T^{266}, F^{267}, Q^{268}, R^{431}, E^{433} were found conserved throughout the selected basidiomycetes.

Discussion

Ectomycorrhizas have been exploited for their potential role in alleviating the metal stress in their host plants but the molecular and cellular mechanisms underlying this substantial metal tolerance are largely unknown. The potential application of ectomycorrhizal fungi in bioremediation of metal polluted areas makes it necessary to have deep insight into their metal binding properties. The present study reports bioaccumulation of heavy metal Cd by ectomycorrhizal fungus *H. cylindrosporum* when exposed to its external stress. The concentration of accumulated Cd is directly proportional to the dose of external metal. However, the dry weight plummeted in response to the increasing concentrations of external Cd. The IC_{50} value observed in this study was at 8.0 µM of Cd. The IC_{50} for Cd reported for other ectomycorrhizal fungi, *Pisolithus tinctorius*, *Cenococcum geophilum*, *Paxillus involutus*, and *Suillus luteus* were 89.0, 9.0, 2.2 and 0.4 µM, respectively (Hartley et al. 1997). These results suggested that the ectomycorrhizal fungus *H. cylindrosporum* is sensitive to Cd.

Since Cd is a sulfhydryl reactive metal with high affinity for the thiols, its bioaccumulation inside the cell results in high demand for the thiol rich compounds. In *H. cylindrosporum*, the amount of glutathione produced was found to be directly dependent upon the external Cd stress. The amount of total GSH produced increased with increase in metals stress. About 0.85 nmol mg^{-1} of total GSH was produced per mg of mycelium in response to Cd stress, indicating that GSH biosynthesis is highly inducible by external Cd stress. Increase in GSH levels have also been reported in ectomycorrhizal fungus *Paxillus involutus* where approximately 1.2 nmol mg^{-1} GSH was produced in response to 50 ppm Cd stress (Courbot et al. 2004). Further, the burgeoning response of glutathione to heavy metal stress in *H. cylindrosporum* was justified by studying the expression level of rate limiting *Hcγ-GCS* gene when exposed to increasing metal concentrations. A significant increase in the expression of *Hcγ-GCS* gene

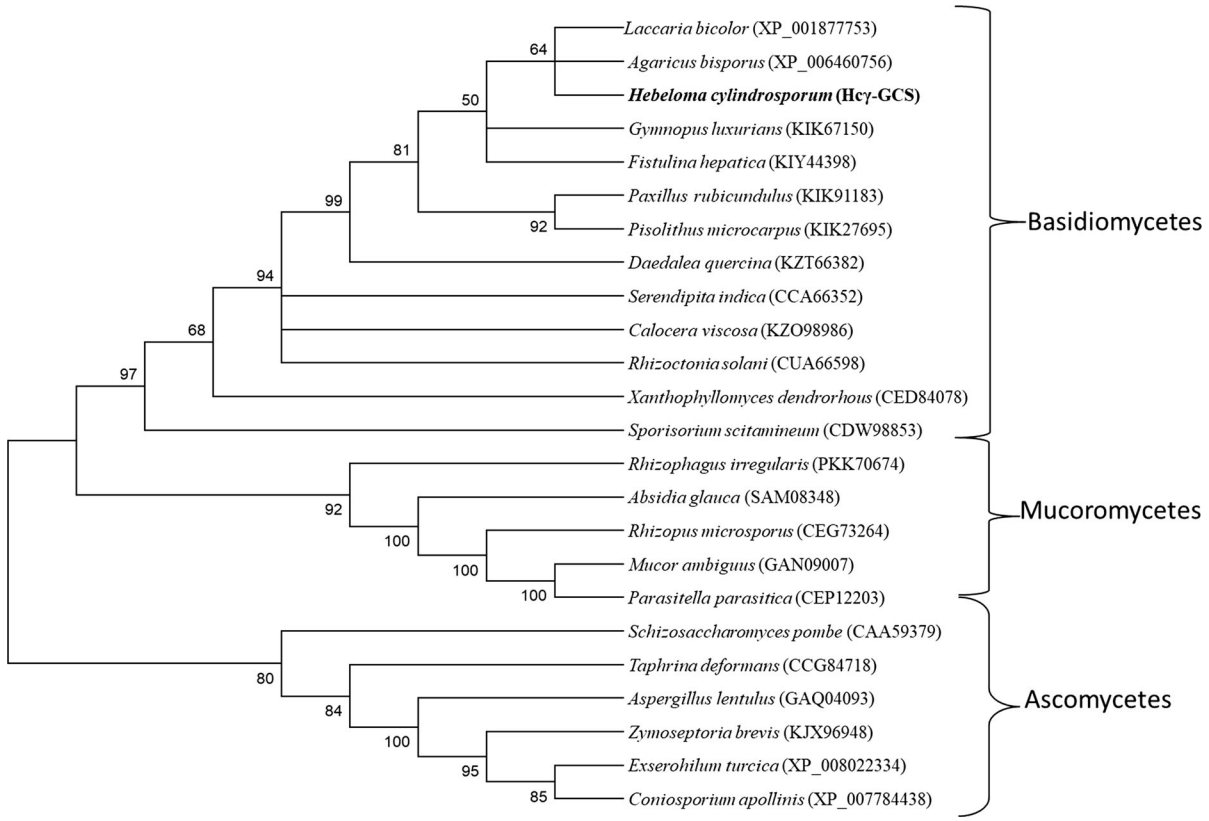

Fig. 5 The maximum parsimony tree constructed using MEGA 7. *γGCS* enzymes from three different classes of fungi were clustered separately into basidiomycetes, mucoromycetes and ascomycetes, showing their common evolutionary history. The tree was constructed using 1000 bootstrap test. Accession number of each protein has been mentioned in parenthesis

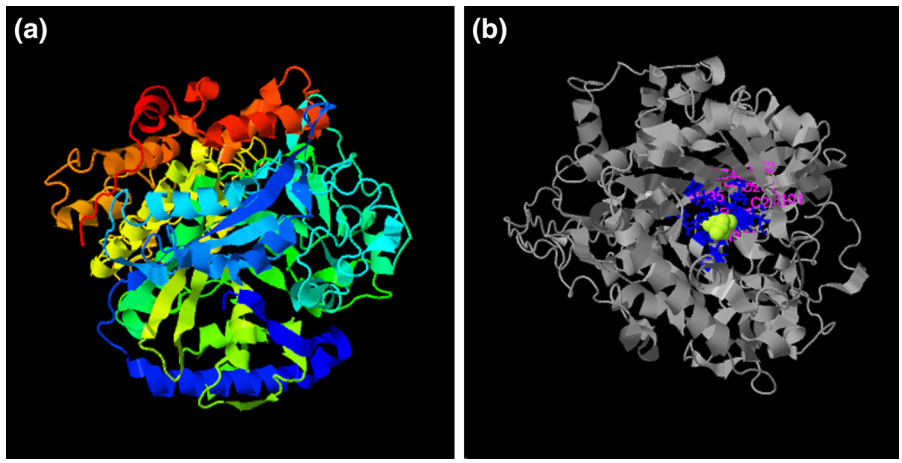

Fig. 6 Tertiary structure of *Hcγ-GCS* enzyme generated by I-TASSER **a** constructed by homology modeling using PBD structure 3ig5 as template. **b** The putative substrate and ADP binding site in the active site have been highlighted in green and blue color respectively. The active site amino acids were highlighted in pink

was observed in response to Cd stress. Similar response has also been reported in various hyper accumulating plants (Pickering et al. 2000; Dhankher et al. 2002). These observations throw light on the fact that the process of GSH biosynthesis triggers immediately on exposure to Cd stress. The functional characterization of *Hcγ-GCS* gene in Cd hypersensitive *S. cerevisiae* mutant for γ-glutamylcysteine synthetase ($gsh1^{\Delta}$) further validates the role of this gene in protecting the organism under metal stress.

The sequence analysis of Hcγ-GCS protein showed homology with many reported γGCS proteins from different fungal species. Hcγ-GCS protein showed close relationship with γGCS protein from various basidiomycetes *Laccaria bicolor*, *Agaricus bisporus* and *Gymnopus luxurians*. Most of the conserved domains identified in these fungal γGCS proteins were found to be conserved even in plants, yeasts, parasites and invertebrates. The conserved glycine and cysteine rich motif "IYLDAMGFGMGCCCLQLTFQ" 249–268 amino acid from Lb-γGCS has also been reported to be conserved in invertebrate *Ciona intestinalis*, *Chorispora bungeana*, and *S. cerevisiae* (Ohtake and Yabuuchi 1991; Franchi et al. 2012; Nair et al. 2013). The aminoacid E52, E101, C260, Q264, R309, I319, R435 involved in substrate (L-glutamate) binding site were found to be conserved not only in fungi but also in invertebrates (Franchi et al. 2012). This shows that the catalytic unit of Hcγ-GCS is highly conserved. However the cysteine binding moiety has not been identified in the Hcγ-GCS tertiary structure. The same has also been reported in *Leishmania donovani* γGCS (Agnihotri et al. 2016).

Conclusion

This is the first report on cloning and characterization of γ-glutamylcysteine synthetase gene isolated from ectomycorrhizal fungus *H. cylindrosporum*. The gene has been successfully characterized using various molecular and bioinformatic approaches. It was observed that the exposure to Cd causes up-regulation of *Hcγ-GCS* gene resulting in increased glutathione production. The functional complementation of the *Hcγ-GCS* in *S. cerevisiae* mutant further justifies its role in heavy metal tolerance. This study provides a deep insight into the role of GSH biosynthesis in ameliorating heavy metal accumulation and detoxification in ectomycorrhizal fungus *H. cylindrosporum*, which may hold a potential application in bioremediation of contaminated sites.

Acknowledgements Authors are thankful to Department of Biotechnology, Govt. of India for sponsoring the research Project (BT/PR8339/BCE/8/1045/2013) to carry out the present work.

Funding The authors report no financial interest or benefit arising from the direct application of this work.

Compliance with ethical standards

Conflict of interest The authors report no conflict of interest.

References

Agnihotri P, Singh SP, Shakya AK, Pratap JV (2016) Biochemical and biophysical characterization of *Leishmania donovani* gamma-glutamylcysteine synthetase. Biochem Biophys Rep 8:127–138

Andersen CL, Jensen JL, Ørntoft TF (2004) Normalization of real-time quantitative reverse transcription-PCR data: a model-based variance estimation approach to identify genes suited for normalization, applied to bladder and colon cancer data sets. Cancer Res 64:5245–5250

Bellion M, Courbot M, Jacob C, Blaudez D, Chalot M (2006) Extracellular and cellular mechanisms sustaining metal tolerance in ectomycorrhizal fungi. FEMS Microbiol Lett 254:173–181

Cobbett C, Goldsbrough P (2002) Phytochelatins and metallothioneins: roles in heavy metal detoxification and homeostasis. Annu Rev Plant Biol 53:159–182

Courbot M, Diez L, Ruotolo R, Chalot M, Leroy P (2004) Cadmium-responsive thiols in the ectomycorrhizal fungus *Paxillus involutus*. Appl Environ Microbiol 70:7413–7417

Dhankher OP, Li Y, Rosen BP, Shi J, Salt D, Senecoff JF, Sashti NA, Meagher RB (2002) Engineering tolerance and hyperaccumulation of arsenic in plants by combining arsenate reductase and γ-glutamylcysteine synthetase expression. Nat Biotechnol 20:1140–1145

Dietz R, Riget F, Cleemann M, Aarkrog A, Johansen P, Hansen JC (2000) Comparison of contaminants from different trophic levels and ecosystems. Sci Total Environ 245:221–231

Foyer CH, Noctor G (2011) Ascorbate and glutathione: the heart of the redox hub. Plant Physiol 155:2–18

Franchi N, Ferro D, Ballarin L, Santovito G (2012) Transcription of genes involved in glutathione biosynthesis in the solitary tunicate *Ciona intestinalis* exposed to metals. Aquat Toxicol 114:14–22

Galant A, Preuss ML, Cameron J, Jez JM (2011) Plant glutathione biosynthesis: diversity in biochemical regulation and reaction products. Front Plant Sci 2:45

Gallego SM, Pena LB, Barcia RA, Azpilicueta CE, Iannone MF, Rosales EP, Zawoznik MS, Groppa MD, Benavides MP (2012) Unravelling cadmium toxicity and tolerance in plants: insight into regulatory mechanisms. Environ Exp Bot 83:33–46

Gay G (1990) Effect of the ectomycorrhizal fungus *Hebeloma hiemale* on adventitious root formation in derooted *Pinus halepensis* shoot hypocotyls. Can J Bot 68:1265–1270

Gutiérrez-Escobedo G, Orta-Zavalza E, Castaño I, De Las Peñas A (2013) Role of glutathione in the oxidative stress response in the fungal pathogen *Candida glabrata*. Curr Genet 59:91–106

Hartley J, Cairney JW, Meharg AA (1997) Do ectomycorrhizal fungi exhibit adaptive tolerance to potentially toxic metals in the environment? Plant Soil 189:303–319

He J, Li H, Ma C, Zhang Y, Polle A, Rennenberg H, Cheng X, Luo ZB (2015) Overexpression of bacterial γ-glutamylcysteine synthetase mediates changes in cadmium influx, allocation and detoxification in popular. New Phytol 205:240–254

Jentschke G, Goldbold DL (2000) Metal toxicity and ectomycorrhizas. Physiol Plant 109:107–116

Jozefczak M, Remans T, Vangronsveld J, Cuypers A (2012) Glutathione is a key player in metal-induced oxidative stress defenses. Int J Mol Sci 13:3145–3175

Kalsotra T, Khullar S, Agnihotri R, Reddy MS (2018) Metal induction of two metallothionein genes in the ectomycorrhizal fungus *Suillus himalayensis* and their role in metal tolerance. Microbiol 64:868–876

Khullar S, Reddy MS (2016) Ectomycorrhizal fungi and its role in metal homeostasis through metallothionein and glutathione mechanisms. Curr Biotechnol 5:1–11

Livak KJ, Schmittgen TD (2001) Analysis of relative gene expression data using real-time quantitative PCR and the $2^{-\Delta\Delta CT}$ method. Methods 25:402–408

Lu SC (2009) Regulation of glutathione synthesis. Mol Aspects Med 30:42–59

Melin ELIAS (1953) Physiology of mycorrhizal relations in plants. Ann Rev Plant Physiol 4:325–346

Minet M, Dufour ME, Lacroute F (1992) Complementation of mutants by *Arabidopsis thaliana* cDNA. Plant J 32:417–422

Nair PM, Park SY, Chung JW, Choi J (2013) Transcriptional regulation of glutathione biosynthesis genes, γ-glutamylcysteine ligase and glutathione synthetase in response to cadmium and nonylphenol in *Chironomus riparius*. Environ Toxicol Pharmacol 36:265–273

Ohtake Y, Yabuuchi S (1991) Molecular cloning of the γ-glutamylcysteine synthetase gene of *Saccharomyces cerevisiae*. Yeast 7:953–961

Pickering IJ, Prince RC, George MJ, Smith RD, George GN, Salt DE (2000) Reduction and coordination of arsenic in Indian mustard. Plant Physiol 122:1171–1178

Pócsi I, Prade RA, Penninckx MJ (2004) Glutathione, altruistic metabolite in fungi. Adv Microb Physiol 49:1–76

Rahman I, Kode A, Biswas SK (2006) Assay for quantitative determination of glutathione and glutathione disulfide levels using enzymatic recycling method. Nat Protoc 1:3159–3165

Reddy MS, Prasanna L, Marmeisse R, Fraissinet-Tachet L (2014) Differential expression of metallothioneins in response to heavy metals and their involvement in metal tolerance in the symbiotic basidiomycete *Laccaria bicolor*. Microbiol 160:2235–2242

Reddy MS, Kour M, Aggarwal S, Ahuja S, Marmeisse R, Fraissinet-Tachet L (2016) Metal induction of a *Pisolithus albus* metallothionein and its potential involvement in heavy metal tolerance during mycorrhizal symbiosis. Environ Microbiol 18:2446–2454

Ruiz JM, Rivero RM, Romero L (2003) Preliminary studies on the involvement of biosynthesis of cysteine and glutathione concentration in the resistance to B toxicity in sunflower plants. Plant Sci 165:811–817

Sengupta D, Ramesh G, Mudalkar S, Kumar KRR, Kirti PB, Reddy AR (2012) Molecular cloning and characterization of γ-glutamylcysteine synthetase (VrγECS) from roots of *Vigna radiata* (L.) Wilczek under progressive drought stress and recovery. Plant Mol Biol 30:894–903

Sobrino-Plata J, Meyssen D, Cuypers A, Escobar C, Hernández LE (2014) Glutathione is a key antioxidant metabolite to cope with mercury and cadmium stress. Plant Soil 377:369–381

Stearns T, Ma H, Botstein D (1990) Manipulating yeast genome using plasmid vectors. Methods Enzymol 185:280–297

Thorsen M, Lagniel G, Kristiansson E, Junot C, Nerman O, Labarre J, Tamás MJ (2007) Quantitative transcriptome, proteome, and sulfur metabolite profiling of the *Saccharomyces cerevisiae* response to arsenite. Physiol Genom 30:35–43

Vido K, Spector D, Lagniel G, Lopez S, Toledano MB, Labarre J (2001) A proteome analysis of the cadmium response in *Saccharomyces cerevisiae*. J Biol Chem 276:8469–8474

Ectomycorrhizal Diversity and Tree Sustainability

6

Shikha Khullar and M. Sudhakara Reddy

Abstract

Ectomycorrhizal (ECM) association of fungi with plants involves diverse category of fungi. They form a mutualistic association with the host plant, nourishing them with minerals and protecting them from various biotic and abiotic stresses. Their long thin hyphae fetch water and minerals from the deepest core of soil and transport them to the plants. In exchange, ECM fungi are rewarded with photosynthates and carbohydrates. They also protect the host plant from drought, salinity, heavy metals, pests and pathogens and extreme environments, thus enhancing their growth and development and helping them to sustain under diverse conditions. Colonization with ECM fungi modulates various cellular, physiological and molecular processes in host plant, thus protecting them under extreme environments. ECM fungi play a significant role in protecting the forest ecology by connecting different trees through a dense network of hyphae forming a wood-wide web of common mycorrhizal networks. However, each mycorrhizal fungus responds differently under different stress conditions through diverse mechanisms. The current study provides deep insight into different mechanisms used by different ECM fungi for facilitating host tree sustainability.

Keywords

Ectomycorrhizal fungi · Mineral nutrition · Tree sustainability · Salinity · Metal tolerance · Metallothioneins · Drought tolerance · Diversity

S. Khullar · M. S. Reddy (✉)
Department of Biotechnology, Thapar Institute of Engineering & Technology, Patiala, Punjab, India
e-mail: msreddy@thapar.edu

T. Satyanarayana et al. (eds.), *Microbial Diversity in Ecosystem Sustainability and Biotechnological Applications*, https://doi.org/10.1007/978-981-13-8487-5_6

6.1 Introduction

Mycorrhizal fungi are mutualistic root symbionts with heterogeneous fungal taxa that thrive in the rhizospheric soil. In this association, both plant and fungi assist each other with various nutritional and non-nutritional benefits. Mycorrhizas form a dense filamentous network that draws water and nutrients from the deeper soil and delivers to the plant roots, thus accelerating plant growth and root development. It is estimated that every kilometre of soil contains at least 200 km of fungal strands, accessing the smallest pore of the soil (Bonneville et al. 2009). Apart from providing nutrition, mycorrhizal fungi also protect the plant from drought and salinity, pests and pathogens, heavy metal toxicity and extreme environments (Smith and Smith 2015). In exchange to all these benefits, the mycorrhizas are awarded with photosynthates or carbohydrates like glucose by the plants. The fungi utilize these carbohydrates for their growth and synthesis of glycoprotein glomalin which is released into the soil that improves the soil structure and organic content (Wu et al. 2014). In the soil, the mycorrhizal hyphae form an extensive network of wood-wide web, which connect all surrounding plant communities promoting horizontal nutrition transfer (Harrison 2005). They are the source of carbon to many achlorophyllous heterotrophic plants. Alpines and boreal zones, tropical forests, grasslands and croplands are the most commonly mycorrhizal colonized areas (Selosse and Roy 2009).

These mycorrhizal fungi are more than 450 million years old. About 80% of all land plants with more than 92% plant families are mycorrhizal (Wang and Qiu 2006). They are most prevalent symbionts involving about 6000 fungal species in the *Glomeromycotina*, *Ascomycotina* and *Basidiomycotina* and 240,000 plant species (Bonfante 2003). Mycorrhizas are cosmopolitan and abundant even in the highly degraded areas. They are classified into five groups based on their characteristic interaction with the host cells. Among the five associations, arbuscular mycorrhizas (AM) and ectomycorrhizas (ECMs) are the two most abundant associations. Orchid, ericoid and arbutoid mycorrhizas are confined to the genera within the Orchidaceae, Ericaceae and Arbutoideae families, respectively (Brundrett 2017). Arbuscular, orchid, ericoid and arbutoid mycorrhizas establish an intracellular symbiosis by penetrating their hyphae into the root cells, whereas the ectomycorrhizal hyphae remain extracellular (Bonfante and Genre 2010). Till date, mycorrhizas have garnered vast attention owing to the new genetic, cellular and molecular techniques along with the genome sequencing of various mycorrhizal plants and fungi (Martin et al. 2008).

6.2 Ectomycorrhizas

Ectomycorrhizal fungi is a symbiotic association of fungi to the plant roots, where the fungi ensheath its hyphae around the root tip forming the thick hyphal mantle of nearly 40 μm. Inside the mantle, the hyphae penetrate into the cell wall and grow in between epidermal cells and cortical cells. They never penetrate inside the cell

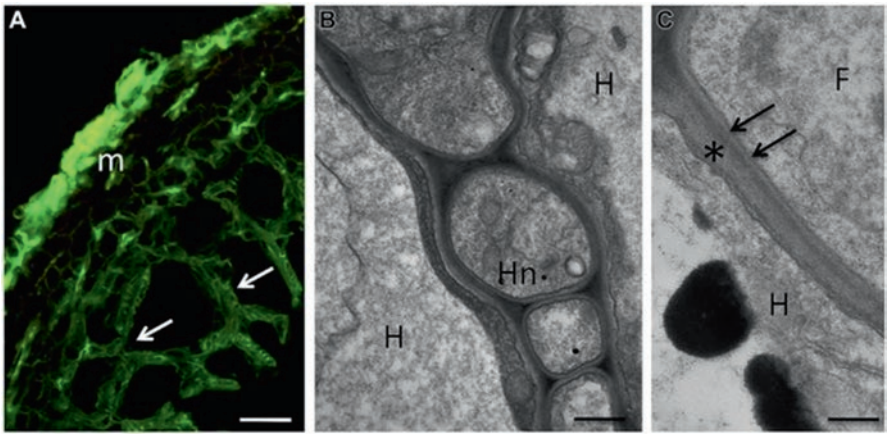

Fig. 6.1 The hyphae of ECM fungi colonizing epidermal and cortical cell layer. (**a**) The confocal micrograph of ECM *Tuber melanosporum* colonizing hazelnut, indicating the mantle (m) formed by the dense hyphae and Hartig net (arrows) surrounding epidermal and cortical cells. (**b**) Hartig net (Hn) developed in a fully truffle developed mycorrhiza. (**c**) Magnification of the contact zone between plant (∗) and fungal cell wall (arrows). *F* fungus, *H* host cell (Balestrini and Bonfante 2014)

lumen of roots, hence forming a Hartig net (Fig. 6.1). This Hartig net is the region of juxtaposition where exchange of water, nutrients and other components between both fungi and the plant roots takes place (Bonfante and Genre 2010; Balestrini and Bonfante 2014; Henke et al. 2015).

On the other end outside the fungal mantle, hyphae extend into the soil called extraradical mycelium and act like an extension to the plant roots so as to have access to the nutrients from deeper parts in soil. In pine seedlings, extraradical mycelium of *Pisolithus tinctorius* contributes 99% of the nutrient-absorbing surface of roots (Rousseau et al. 1992). Thus, ectomycorrhizal fungi provide water, mineral and nutrients to the plant and are rewarded with the photosynthates or stored carbohydrates by the host plant (Fig. 6.2) [Martin and Nehls 2009; Bonfante and Genre 2010]. These fungi have a dual lifestyle, form symbiosis with the plant roots and act as facultative saprotrophs in soil (Martin and Nehls 2009). At laboratory conditions they can be cultured without host (unlike AMF), but under field conditions they depend on their host for carbohydrates (Van Der Heijden et al. 2015).

Ectomycorrhizal fungi belong to the family of *Basidiomycota* (252 genera), *Ascomycota* (84 genera) and *Mucoromycota-Endogonales* (Van Der Heijden et al. 2015). More than 10,000 fungal species have been estimated to form ectomycorrhiza with the host plants (Finlay 2008). They can form a visible reproductive structure of epigeous mushroom and hypogeous truffles at the feet of trees they colonize. The most popular edible mushrooms 'Tuber' fungus, deadly caps destroying angels *Amanita*, also belong to ectomycorrhizas. Trees hosts for ectomycorrhizal fungi include families like Pinaceae, Fagaceae, Betulaceae, Dipterocarpaceae and Caesalpiniaceae, distributed in the sub-tropic, temperate and boreal forests (Smith

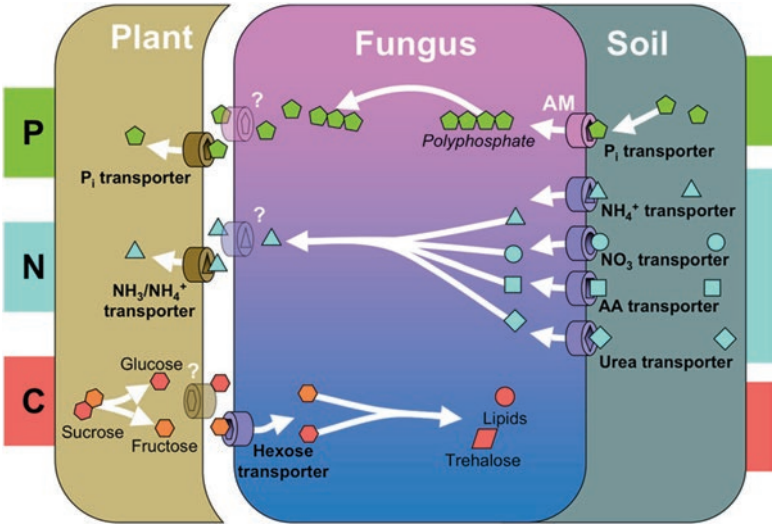

Fig. 6.2 Nutrient exchange mechanism between ECM fungi and their host plant (Bonfante and Genre 2010)

and Read 2010). Birch (*Betula*), dipterocarp (*Pakaraimaea*), beech (*Fagus*), willows (*Salix*), pine (*Pinus*), oaks (*Quercus*) and eucalypts (*Eucalyptus*) are the common host species for ectomycorrhizal symbiosis (Chen et al. 2015; Hrynkiewicz et al. 2015; Murata et al. 2015; Brearley et al. 2016; García-Guzmán et al. 2017; Horton et al. 2017; Kaiser et al. 2017).

It has been estimated that more than 50,000 plant species are involved in ectomycorrhizal association. Most of the ectomycorrhizas have colonized northern temperate forest soils, whereas arbuscular mycorrhizas are commonly found in tropical forests. *Agaricomycetes* were found to be the most dominant class of ectomycorrhizal fungi in the soil (Buée et al. 2009). Ascomycetes have been reported showing higher stress tolerance as compared to basidiomycetes. Many authors have observed the dominance of ascomycetes in heavily polluted areas, whereas basidiomycetes were observed in less polluted and control plots. The genera *Phialophora*, *Phialocephala* and *Leptodontidium* and many other ascomycetes have been reported to have adaptive metal tolerance (Colpaert et al. 2011). Similarly many basidiomycetes have also been reported to have complete defence mechanisms against heavy metals like *Laccaria bicolor* (Reddy et al. 2014), *Hebeloma cylindrosporum* (Ramesh et al. 2009), *Pisolithus albus* (Reddy et al. 2016), *Suillus bovinus* (Ruytinx et al. 2013), *Suillus luteus* (Nguyen et al. 2017), *Paxillus involutus* (Bellion et al. 2007), *Amanita strobiliformis* (Osobová et al. 2011), etc.

There has been a tremendous advancement in research concerning identification of ectomycorrhizal fungi and studying their ecological importance. Such studies have provided a deep insight into ectomycorrhizal diversity and their role in tree sustainability.

6.3 Ectomycorrhiza and Tree Sustainability

6.3.1 ECM and Tree Sustainability Under Drought

Drought is one of the most daunting factors limiting the plant growth in both dry and irrigated agriculture. The change in climatic conditions and increasing demand of water by municipal and residential consumption have worsened the soil water levels. This water deficiency affects various morphological and biochemical processes in plants. However, ECM fungi improve the water and nutrient uptake during drought conditions (Lehto and Zwiazek 2011). The colonization of drought-affected plants with ectomycorrhizal fungus can profoundly modulate the plant's response in improving its water availability and growth by increasing stomatal conductance and shoot water potential, enhancing photosynthesis, increasing hydraulic conductance and increasing aquaporin function (Lehto and Zwiazek 2011). When subjected to drought conditions, *Populus canescens* inoculated with *Paxillus involutus* showed higher predawn water potential and maintained almost full photosynthetic activities, whereas the non-mycorrhizal plants were severely affected by drought in hydrogel-amended soil (Beniwal et al. 2010). The *Populus canescens* plants showed higher stomatal conductance and nitrogen uptake when colonized with *Paxillus involutus* (Danielsen and Polle 2014). Switchgrass (*Panicum virgatum L.*) when inoculated with ectomycorrhizal fungus *Sebacina vermifera* showed enhancement in biomass and macronutrient content under drought conditions (Ghimire and Craven 2011). Even in *Pinus muricata* seedlings inoculated with *Rhizopogon* spp., the plant showed improved shoot biomass, photosynthesis and total leaf nitrogen at low moisture (13%). However both plant and ECM were severely affected when the moisture was reduced to 7% (Kennedy and Peay 2007).

There are several mechanisms by which the ECM fungi can promote drought tolerance. Different studies have reported different mechanisms. Firstly, the ECM fungi increase the surface area of root for absorption of water. Its extensive extraradical hyphae absorb water from the deeper soil and transport it to the host plant roots, resulting in higher root conductance and increased carbon assimilation under drought stress (Plamboeck et al. 2007; Sebastiana et al. 2018). Up-regulation in aquaporin (transporter facilitating water uptake) expression under drought conditions has been observed in many cases (Marjanović et al. 2005). Cork oak when inoculated with *Pisolithus tinctorius* resulted in improved plant height, shoot biomass, shoot basal diameter and root growth than their non-mycorrhizal plants under drought conditions (Sebastiana et al. 2018). Another indirect mechanism would be by facilitating the nutrient acquisition. The mineral nutrients improve the plants photosynthetic machinery facilitating quick recovery after stress. This has been reported in case of *Pinus tabulaeformis* seedlings and *Nothofagus dombeyi*, where the ECM fungal hyphae promoted the plants resistance to drought by facilitating N and P uptake (Wu et al. 1999; Alvarez et al. 2009). Another indirect mechanism involved is by suppressing the reactive oxygen species (ROS) generated during drought conditions by activating the plants antioxidant system (Porcel and Ruiz-Lozano 2004; Alvarez et al. 2009). Many other indirect mechanisms have also been

reported including altered carbohydrate assimilation by stomatal function mediated by change in growth regulators, increased sink strength and change in osmotic adjustments in ectomycorrhizal roots (Lehto and Zwiazek 2011). However a detailed mechanism on how ECM protects the host plant from drought stress is still unexplored.

6.3.2 ECM and Tree Sustainability in Saline Soils

Salt salinity is one of the major constraints limiting plant growth and ecosystem productivity. It is a major issue for both agriculture and forestry in nearly all climatic regions and on all populated continents. More than 6% of the world's total land area is affected by salinity, and the figures are increasing rapidly due to the intensive use of land, irrigation and clearing. Saline salt can be defined as the salt with electrolyte concentration more than 4 dS m^{-1} which is equivalent to 40 mM or higher concentration of sodium chloride (Munns and Tester 2008). High salt concentrations can alter the basic texture of soil, resulting in decreased soil porosity leading to reduced soil aeration and water conductance (Porcel et al. 2012). This creates a low water potential zone, making it difficult for plants to acquire water as well as nutrients. Thus, salinity stress usually overlaps drought and nutritional deficiencies. The higher salt concentrations in soil affect the plant growth, photosynthesis, protein synthesis and energy and lipid metabolism (Chen and Polle 2010). Symbiotic association of the plants with mycorrhiza has proven to be the most effective remedy to salt stress. The mycorrhizas are well known to protect the host plant from various biotic and abiotic stresses. However, the role of ectomycorrhizal fungi has not yet been explored adequately.

Mycorrhizal plants exposed to osmotic constraints have been reported to perform better than the non-mycorrhizal plants (Langenfeld-Heyser et al. 2007). The ectomycorrhizal symbiosis has been demonstrated to increase resistance to saline conditions in many plants including *Populus canescens*, *Populus tremuloides*, *Populus euphratica*, *Pinus tabulaeformis*, *Betula papyrifera*, *Coccoloba uvifera*, etc. (Bandou et al. 2006; Yi et al. 2008; Luo et al. 2011; Jie et al. 2011; Chen et al. 2014). The reduced Na^+ accumulation in ectomycorrhizal roots under salt stress has also been reported in *Picea mariana*, *Pinus banksiana* and *Picea glauca* when colonized with *Hebeloma crustuliniforme* (Muhsin and Zwiazek 2002; Nguyen et al. 2006) and in *Populus canescens* colonized with *P. involutus*. This is due to the fact that the mycelial hyphae exhibit steady Na^+ efflux under salt stress (Li et al. 2012). Although ECM colonization has been reported to reduce with increase in salt concentrations, the ECM dependency of the plant increased under saline conditions (Bandou et al. 2006). Sea grapes (*Coccoloba uvifera*) when colonized with *Scleroderma bermudense* under salt stress led to reduced Na and Cl uptake along with a concomitant increase in P, K and water absorption than the non-mycorrhizal plants (Bandou et al. 2006). Similarly, in case of *Populus canescens*, the colonization with *Paxillus involutus* increased root cell volume and nutrition uptake reducing the Na accumulation. The ECM roots showed higher accumulation of myoinositol, abscisic acid and

salicylic acid and decreased concentrations of jasmonic acid and auxin than the non-mycorrhizal roots. These observations are in contrast to that of arbuscular mycorrhiza, suggesting that ectomycorrhizal and arbuscular mycorrhizas follow different signaling pathways to influence the salt stress response to plants (Luo et al. 2009). Not only roots, the colonization of *Populus canescens* with *Paxillus involutus* also modulates the leaf physiology towards improving salt tolerance (Luo et al. 2011). The leaves of ECM plant displayed increased concentrations of phosphorus and potassium, stress metabolite γ-amino butyric acid, abscisic acid, glucose and fructose and decreased concentrations of galactose and unsaturated to saturated fatty acids than the non-mycorrhizal plants. The ECM-plant leaves under salinity showed alleviation in leaf chlorosis, improved water status and K^+ to Na^+ ratio (Langenfeld-Heyser et al. 2007; Luo et al. 2011).

It has been found that the K^+/Na^+ homeostasis in plants under salt stress has been influenced by the calcium (Ca^{2+}) enrichment in the fungal hyphae (Li et al. 2012;Chen et al. 2014). Under salt stress, Ca^{2+} is replaced by Na^+, and the released Ca^{2+} contributes to the amelioration of K^+/Na^+ ratio. The Ca^{2+} ions also inhibit KORCs and NSCCs (depolarization-activated) to reduce K^+ efflux in *Populus* (Sun et al. 2009; Li et al. 2012) and *Arabidopsis* (Shabala et al. 2005). Thus, we can say that salt stress induces Ca^{2+}/Na^+ exchange, resulting in availability of free Ca^{2+} from ectomycorrhizal roots, which favours the establishment of K^+/Na^+ homeostasis in plants (Li et al. 2012). This indicates that ectomycorrhizal symbiosis plays a significant role in tree sustainability under osmotic stress conditions.

6.3.3 ECM-Mediated Tree Sustainability Against Pests and Pathogens

Plant diseases are a serious risk to the global food security costing 10–16% loss of total crop harvest annually to pests and pathogens (Strange and Scott 2005; Oerke 2006). Fungi, oomycetes, bacteria, viruses, viroids, phytoplasmas, protozoa, insects, mites, weeds, nematodes and parasitic plants are among the most common plant pathogens. Although there are many methods to control plant diseases like using fungicides, bactericide, chemical pesticides, different irrigation practices, etc., they all cause notorious environmental and health consequences (Tilman et al. 2002). However, 'biocontrol' using mycorrhizal fungi has proven to be the most effective and efficient method of protecting the plant from pests and pathogens. Both ECM and AM have proven to protect the plant from various pests and pathogens. These fungi not only protect the plant from pathogens but also improve the plant health, growth and nutrition availability. Studies have reported numerous mechanisms by which the ectomycorrhizal fungi protect the host plant from different pests and pathogens (Ghorbanpour et al. 2018). The first mechanism that is widely reported is the barrier action of ECM fungi. ECM fungi penetrate into the root forming a thick mantle, which acts like a mechanical barrier against the penetration of various pathogens. *Castanea sativa* colonized with four different ECM fungi – *Laccaria laccata*, *Hebeloma sinapizans*, *H. crustuliniforme* and *Paxillus involutus* – showed

no sign of infection when inoculated with ink disease factors *Phytophthora cambivora* and *P. cinnamomi*, whereas the same seedlings without mycorrhization showed significant effect on leaf area, root and shoot weight (Branzanti et al. 1999; Blom et al. 2009). Apart from physical barrier, the ECM fungi also have an antagonistic property, where they chemically inhibit the pathogens. The ECM fungi *Suillus laricinus*, *Suillus tomentosus* and *Amanita vaginata* inhibited the growth of *Rhizoctonia solani* by synthesizing a hydrolytic enzyme chitinase (Tang et al. 2008). In a recent study, the antagonistic potential of eight ECM fungi including *Alnicola* sp., *Russula parazurea*, *Lycoperdon perlatum*, *Laccaria fraterna*, *Pisolithus albus*, *Suillus subluteus*, *Scleroderma citrinum* and *Suillus brevipes* was studied against various plant pathogenic fungi like *Alternaria solani*, *Lasiodiplodia theobromae*, *Botrytis* sp., *Fusarium oxysporum*, *Pythium* sp., *Rhizoctonia solani*, *Phytophthora* sp., *Sclerotium rolfsii* and *Subramaniospora vesiculosa.* All the eight ECM fungal isolates showed inhibitory effect to the selected plant pathogens. *Suillus brevipes* showed maximum inhibition of 60.31% producing maximum chitinase (111.6 μg/ml) followed by *S. subluteus* exhibiting 49.46% inhibition producing 101.7 μg/ml chitinase (Mohan et al. 2015). Similar observations have been made by Vaidya et al. (2005), where the ECM fungi *Pisolithus* and *Scleroderma* showed antifungal and antibacterial activity against plant pathogens *Pythium* sp., *Rhizoctonia solani*, *Fusarium* sp., *Agrobacterium tumefaciens*, *Pseudomonas solanacearum*, *Klebsiella* sp., *Staphylococcus aureus*, *Shigella dysenteriae* and *E. coli* (Vaidya et al. 2005). The ECM fungi *Pisolithus tinctorius* and *Pisolithus arhizus* have been reported to synthesize two antibiotic compounds *p*-hydroxybenzoylformic acid and (*R*)-(−)-*p*-hydroxymandelic acid which inhibited spore germination and caused hyphal lysis in significant number of phytopathogenic and dermatogenic fungi. Both the compounds were effective in inhibiting germination of conidia of *Truncatella hartigii* (Kope et al. 1991; Tsantrizos et al. 1991). *Paxillus involutus* also produced a fungitoxic compound while growing on *Pinus resinosa* roots, which inhibited 80% sporulation of *Fusarium oxysporum* (Duchesne et al. 1988).

Apart from the antagonistic properties, the ECM fungi alter the soil chemical properties in their close vicinity by lowering the soil pH and acidification, thus repressing the growth of pathogen such as *Cylindrocarpon* sp. and protecting the plant from various pathogens (Schelkle and Peterson 1997). Another indirect mechanism of protecting the host plant from pathogens includes competing with pathogens for niche and nutrition. The ECM fungi create a specific niche by colonizing the rhizosphere, thus depriving pathogens of space and nutrients. The ECM fungi create niche either by remaining in high population density or by forming symbiosis with different bacterial communities having antibiosis effect on plant pathogens (Frey-Klett et al. 2005). Schelkle and Peterson (1997) reported the presence of *Bacillus subtilis* in ECM rhizosphere as a biocontrol against *Fusarium oxysporum* and *Cylindrocarpon* sp.

The ECM fungi also protect the host plant from various insects and nematode herbivores. *Betula pubescens* seedlings colonized with ECM fungi *Paxillus involutus*, *Phialophora finlandia*, *Cenococcum geophilum* and *Thelephora terrestris* reduced the *Otiorhynchus* spp. larval root herbivory in birch forest and eroded sites

(Oddsdottir et al. 2010a, b). The effect of ECM fungi on herbivores may be due to the secretion of terpenes or polyphenolic compounds (Fitter and Garbaye 1994).

6.3.4 ECM and Tree Sustainability Under Heavy Metal Stress

Heavy metals contamination is one of the most daunting factors concerning the world today. Most of the agricultural soil is slightly to moderately contaminated with heavy metals like Cd, Cu, Cr, Zn, Ni, Co, As and Pb. Both natural and anthropogenic activities like weathering of metalliferous rocks, volcanoes, erosion, combustion of fossil fuels, mining and industrial activities, use of phosphate fertilizers, sewage sludge, dust from smelters and bad watering practices in agricultural lands contribute to the heavy metal accumulation in the ecosystem (Yadav 2010; Su et al. 2014). The excess of heavy metals in soil affects the plant growth and root development. Roots significantly absorb higher amounts of heavy metals than the aboveground biomass and are thus more affected by heavy metals. There are mainly four mechanisms by which heavy metals exert toxicity in plants: (i) generating reactive oxygen species (ROS) in the plant cells which can damage various macromolecules (Møller et al. 2007; Pena et al. 2012); (ii) heavy metals having similarity with the nutrient cations compete with the nutrient molecules for absorption at root surface and interfere with cellular mechanisms, e.g. As and Cd show similarity with P and Zn, respectively, for absorption at the root surface (Monnet et al. 2001); (iii) heavy metals show high affinity for the sulfhydryl (-SH) group of various functional proteins, thus disrupting the structure and function and rendering them inactive; and (iv) heavy metals displace essential cations from their specific binding sites leading to cellular malfunctioning (Sharma and Dietz 2009; DalCorso et al. 2013; Singh et al. 2016). Inside the plant, these heavy metals interfere with various biological processes like reducing the photosynthesis, water and nutrient uptake and plant chlorosis growth inhibition, disturbing the metabolism of essential elements, disrupting the electron transport chain, disorder in cell membrane functions, suppressing root growth by decreasing the mitotic activities, etc. (Qadir et al. 2004; Yadav 2010). The level of toxicity depends upon various factors like concentration of heavy metals, duration of metal exposure and genotype of associated mycorrhiza and plant (Rajkumar et al. 2012).

Ectomycorrhizal fungi have been proven to protect the plants against the heavy metal stresses. The presence of ECM symbionts on plant roots significantly reduces the heavy metal uptake (Degola et al. 2015; Reddy et al. 2016). ECMs are not only capable of surviving under metalliferous soil but also promote the growth of host plant under metal stress. These fungi have developed specialized mechanisms to cope with heavy metals in the soil, thus protecting their host plant (Fig. 6.3). Primarily, ECM fungi restrict the entry of heavy metals through extracellular precipitation by excreting di-/tricarboxylic acids and oxalic acids, by biosorption of metal ions to the cell wall through chitin and glucosamine or by increasing the cellular efflux (Fig. 6.3). In spite of the restricted entry of these heavy metals, 20–30% of heavy metals could still be found in the cytosol and vacuoles (Blaudez et al.

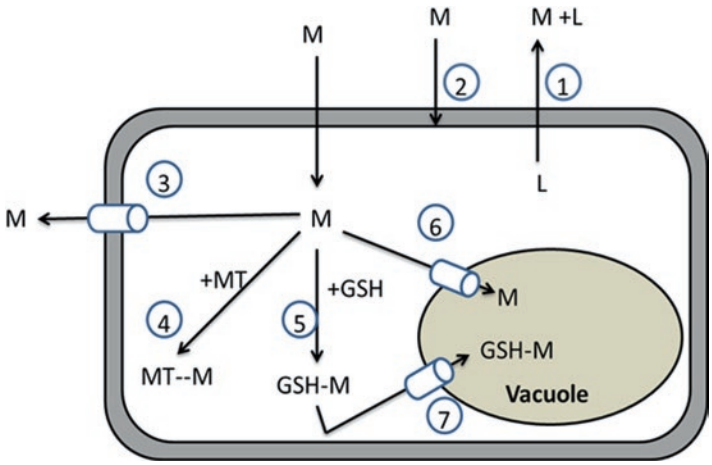

Fig. 6.3 Mechanisms of heavy metal tolerance in ectomycorrhizal fungi. (*1*) Extracellular chelation by secreted ligands, (*2*) cell wall binding, (*3*) enhanced efflux, (*4*) intracellular chelation by metallothioneins (MTs), (*5*) intracellular chelation by glutathione (GSH), (*6*) subcellular compartmentation, (*7*) compartmentation of GSH-M in vacuoles (Bellion et al. 2006)

2000). The heavy metals that enter inside the cell are chelated intracellularly through various thiol-rich compounds like metallothioneins (MTs), glutathione (GSH) and phytochelatins (PCs) (Fig. 6.3). Heavy metals have high affinity for the thiol group (-SH) of these chelators and form metal-MT, metal-(GSH) complex, which actively gets transported into the vacuoles (Sharma et al. 2016; Khullar and Reddy 2018). The role of ectomycorrhizal fungi in metal homeostasis has been clearly reviewed by Bellion et al. (2006), Luo et al. (2014) and Khullar and Reddy (2018).

ECM fungi modulate the heavy metal transfer into the host plants. The fungal mantle acts as an effective barrier or filter for the heavy metals to enter into the plant cells. The heavy metal concentration decreases from the rhizomorphs-hyphal mantle-cortical cells to vascular tissues. This has been clearly demonstrated in case of *Pinus sylvestris* colonized with *Suillus luteus* under zinc stress, where the concentration of zinc declined from 12,830 μg/g in rhizomorph to 2040–3820 μg/g in hyphal mantle, to 280–675 μg/g in cortical cells and to 430 μg/g in the vascular tissues (Turnau et al. 2001). Similar results were reported in case of Cu and Mn by Turnau et al. (2001), where the Cu concentration decreases from 420 μg/g in rhizomorphs to 17 μg/g in hyphal mantle and 6 μg/g in vascular tissues and Mn concentrations decreased from 490 μg/g in rhizomorphs to 88 μg/g in hyphal mantle and to 13–26 μg/g in cortical cells and 14 μg/g in vascular tissues (Turnau et al. 2001). *Betula pendula* seedlings inoculated with ECM fungi reduced the concentration of Cu and Pb in the above-ground parts of plant, thus protecting the plant from elevated metal stress (Bojarczuk and Kieliszewska-Rokicka 2010). Similar results have been reported in *Pinus sylvestris*, where the plants inoculated with *Suillus luteus*, *Suillus bovinus*, *Scleroderma citrinum*, *Amanita muscaria* and *Lactarius rufus* showed better plant protection and nutrient uptake, transferring less Cd, Cu,

Pb and Zn to the above-ground plants than non-mycorrhizal plants (Adriaensen et al. 2005, 2006; Krupa and Kozdrój 2007; Krznaric et al. 2009).

The reduced uptake of heavy metals by ECM fungi is due to the induction of efflux mechanism under heavy metal stress. Majorel et al. (2014) reported low accumulation of Ni in *P. albus* tissues, when exposed to high Ni concentrations, due to the metal efflux mechanisms. Similar observations were made in *S. bovinus*, *P. involutus* and *H. cylindrosporum*, where the increase in metal efflux resulted in low metal accumulation in the fungal tissue. This metal exclusion in fungal symbionts results in lower metal influx by the host plant, thus protecting from metal stress (Blaudez et al. 2000; Blaudez and Chalot 2011; Ruytinx et al. 2013). In contrast to the above observations, few studies have reported increase in metal bioaccumulation in both ECM and its associated host when exposed to high metal stress (Ma et al. 2014; Širić et al. 2016). ECM fungi *Paxillus involutus* significantly increased the net Cd^{2+} influx in the root apical region of *Populus canescens* when exposed to high cadmium stress (Ma et al. 2014).

ECM fungi have been reported to secrete various exudates in the rhizosphere in response to metal stress. These exudates like oxalic acid, formic acid, malic acid and succinic acid can alter the bioavailability of toxic metals in the rhizosphere, thus protecting the host plant from metal toxicity (Meharg 2003; Bellion et al. 2006; Ray and Adholeya 2009; Colpaert et al. 2011; Targhetta et al. 2013). Johansson et al. (2008) reported oxalate exudation in six ectomycorrhizal fungi *Hebeloma velutipes*, *Piloderma byssinum*, *Paxillus involutus*, *Rhizopogon roseolus*, *Suillus bovinus* and *Suillus variegatus*, when exposed to Pb, Cd and As stress (Johansson et al. 2008). In addition to fungal exudates, ECMs also induce plant exudates in the rhizosphere. *P. tabulaeformis* when colonized with ectomycorrhizal fungus *Xerocomus chrysenteron* showed enhanced activity of soluble proteins and acid phosphatases in root exudates than their non-mycorrhizal roots under Cu and Cd stress (Zheng et al. 2009). Bellion et al. (2006) reported up to 85% reduction in Cd uptake by oxalic acid exudation in cadmium-stressed *Paxillus involutus*. In a similar study, Shi et al. (2018) reported 99% removal of chromium Cr(VI) by *Pisolithus* sp1 by secreting H^+ ions and organic acids. The H^+ ions secreted by *Pisolithus* reduced the pH of medium, thus reducing Cr(VI). After 12 days of treatment with *Pisolithus*, it was observed that 75% Cr was removed due to extracellular reduction and 24% was removed by adsorption on cell wall (Shi et al. 2018).

Colpaert et al. (2011) reported development of adaptive heavy metal tolerance in different ECM fungi isolated from metal-polluted areas. *Suillus luteus* and *Suillus bovinus* isolated from metal-polluted areas showed better tolerance to heavy metals like Zn, Cu and Cd when colonized with *Pinus sylvestris* than the same fungus isolated from non-polluted areas (Adriaensen et al. 2005, 2006; Krznaric et al. 2009; Colpaert et al. 2011). Similar observations have also been made with *Pisolithus tinctorius*, *Pisolithus albus* and *Cenococcum geophilum* where the isolates from metal-polluted areas showed higher metal tolerance than the isolated from non-polluted areas (Egerton-Warburton and Griffin 1995; Gonçalves et al. 2009; Jourand et al. 2010).

ECM fungi have developed an intense intracellular mechanism to cope with the heavy metals accumulated inside the cell, so as to prevent their transfer to host plant. ECM fungi synthesize various thiol-rich ligands like metallothioneins and glutathione in response to metal stress (Khullar and Reddy 2018). Heavy metals having high affinity for the thiol group of these ligands bind them forming a strong metal-MT or metal-$(GSH)_2$ complex, rendering them nontoxic and subsequently sequestering into the vacuoles, thus protecting the host plant from metal stress. Differential expression of different metallothioneins and glutathione has been reported in response to different heavy metals. Reddy et al. (2014) characterized two MTs (*LbMT1* and *LbMT2*) out of six putative metallothionein genes from the genome of *Laccaria bicolor* and observed differential expression in response to copper, cadmium and zinc. Both metallothionein genes were induced under Cu stress, whereas only *LbMT1* was induced under Cd stress, and none of them was expressive under Zn stress (Reddy et al. 2014). Similarly in *Suillus himalayensis*, characterization of two metallothionein genes (*ShMT1* and *ShMT2*) revealed their potential role in Cu homeostasis, whereas no response was observed under cadmium stress (Kalsotra et al. 2018). This differential response of different metallothionein isoforms to different metals has also been reported in *Hebeloma cylindrosporum*, *Hebeloma mesophaeum*, *Amanita strobiliformis*, *Suillus luteus*, *Pisolithus albus*, *Russula atropurpurea* and *Paxillus involutus* (Bellion et al. 2007;Ramesh et al. 2009; Leonhardt et al. 2014; Sácký et al. 2014; Hložková et al. 2016; Reddy et al. 2016; Nguyen et al. 2017). However it was observed that most of the metallothioneins are responsive for Cu and Zn tolerance, showing very little response to Cd. However glutathione biosynthesis has been actively reported in response to Cd and As. Ilyas and Rehman (2015) reported that glutathione biosynthesis in ECM is mainly triggered by Cd and As followed by Cr, Pb and Cu. Courbot et al. (2004) reported increased production of glutathione in ECM *Paxillus involutus*, when exposed to cadmium stress. Similar observations were also made in *Laccaria laccata*, *Glomus mosseae*, *Funneliformis mosseae*, *Phanerochaete chrysosporium* and *Penicillium chrysosporium* (Gallie et al. 1993; Garg and Aggarwal 2011; Degola et al. 2015; Xu et al. 2015, 2016). Hence we can say that both metal chelators – metallothioneins and glutathione – play a key role in metal homeostasis in ECM fungi, thus protecting the host plant. However, a detailed study on what effect these chelators have on the metal toxicity in their host plant is still unexplored. These observations clearly demonstrate that the mechanisms involved in ECM protection of host plants are diverse. The heavy metal tolerance mechanism in ectomycorrhizal plants depends on various factors like type of plant, ectomycorrhizal strain and the type of heavy metal.

6.3.5 ECM in Nutrient Cycling in Host Tree

In the current scenario, bioavailability of inorganic nutrients like nitrogen, phosphorus and water in the forest soil is rapidly diminishing, resulting in retarded plant growth, poor photosynthesis and the loss of plant vitality. Most of the forest trees

rely on mycorrhizal symbiosis for fulfilling their nutritional requirements. The ECM fungi colonize the host plant, helping them to fetch nutrients from the deeper parts of the soil, which are otherwise inaccessible. There are mainly two pathways by which the mycorrhizal plants can uptake nutrients from the soil. First is 'the plant pathway' where the plant roots directly uptake nutrients from the soil through root epidermis and root hairs. This pathway is often limited by low mobility of nutrients in soils. The second pathway is 'the mycorrhizal pathway' where the nutrient uptake is mediated by the extraradical mycelium of fungus and transported to host plant through Hartig net (Bücking et al. 2012). However in ectomycorrhizal tree species, majority of the plant root is covered with thick mantle; therefore, the major nutrient uptake by plant is indirectly through the ECM. As reported in case of *Pinus*, 99% of the nutrition-absorbing root surface is covered with thick fungal mantle of ECM fungi (Taylor and Peterson 2000). However, the nutrient uptake mechanism in mycorrhizal plants depends upon the permeability of fungal mantle, its structure and other properties. If the fungal mantle is permeable, the roots can directly absorb the nutrients from soil, whereas if the fungal mantle is impermeable to nutrient ions, the underlying plant roots get completely isolated from the soil, extensively relying on the mycorrhizal pathway for nutrient uptake (Coelho et al. 2010).

During symbiosis, some ECM fungi secrete hydrophobins, which are small cysteine-rich amphiphilic proteins that foster the adhesion of hyphae to the surface and formation of aerial hyphae (Raudaskoski and Kothe 2015). ECM fungi *Pisolithus tinctorius*, *Laccaria bicolor*, *Tricholoma terreum*, *Tricholoma vaccinum* and *Paxillus involutus* have been reported synthesizing hydrophobins during ectomycorrhization (Tagu et al. 2001; Rajashekar et al. 2007; Plett et al. 2012; Sammer et al. 2016). Being hydrophobic, these protein molecules increase the water repellency of fungal mantle, thereby making it impermeable to both water and nutrients. The fungal mantle of *Hebeloma cylindrosporum* colonizing *Pinus banksiana* was found impermeable to sulphates, whereas that of *Pisolithus tinctorius* and *Suillus bovinus* colonizing *Pinus sylvestris* was poorly permeable showing retarded movement of nutrients across the membrane. However, the nutritional uptake by the host plants of all the three ECMs is completely under fungal control (Bücking et al. 2002; Taylor and Peterson 2005). The ECM pines are highly dependent on their fungal symbiont for both nutrition and water uptake (Ouahmane et al. 2009).

Phosphorus is the most important macronutrient required by plants for various cellular and metabolic activities; the availability of P in plants is highly dependent on the soil. ECM fungi facilitate the P uptake from the soil and transport it to the host plant. Due to the smaller hyphal diameter, ECM can scavenge orthophosphates (Pi) from the smallest core of soil and transport them to plant cortical cells. They also secrete various organic acids, phosphatases and phytases into the soil so as to facilitate P release from organic complexes (Alvarez et al. 2011; Plassard et al. 2011). The uptake of P from soil is facilitated by various phosphorus transporters. The expression of P transporters in ECM cell is regulated by various factors like availability of external P and demand in fungal cells (Bucher 2007; Plassard et al. 2011). Various phosphorus transporters have been identified in ectomycorrhizal fungi, which include five Pi transporters in *L. bicolor* (LbPht1;1 to LbPht1;5), two

in *H. cylindrosporum* (*HcPT1* and *HcPT2*) and seven in *Tuber melanosporum* (Tatry et al. 2009). ECM fungi have the tendency to store excessive P in the form of polyphosphates with average size from 10 to 20 Pi molecules, which allows the fungus to keep internal P concentration low, allowing efficient transfer from extraradical mycelium to the Hartig net (Viereck et al. 2004). Thus, the ECM fungi protect the host plant from P deficiencies.

The nitrogen transfer in mycorrhizal plants is also facilitated by their symbiotic fungi. ECM fungi can efficiently take organic and inorganic N from the soil and transfer it to the host plant. Many ECM fungi can mobilize and utilize amino acids and amides like glutamine, glutamate and alanine as N source for various metabolic pathways (Chalot et al. 1994). However, the inorganic nitrogen in soil is present in the form nitrate (NO^{3-}) and ammonium (NH^{4+}) ions. Among the two, ammonium ions are more efficiently taken up by the ECM than nitrate ions (Gachomo et al. 2009). It has been reported in ECM fungus *Hebeloma cylindrosporum* that the presence of NH^{4+} downregulates the expression of NO^{3-} transporters and nitrate reductase and up-regulates NH^{4+} transporters (*AMT1* and *AMT2*) (Javelle et al. 2003). This shows that uptake of NH^{4+} is preferred over NO^{3-}. Inside the fungal system, NO^{3-} is converted into NH^{4+} by nitrite reductase, which is further assimilated into amino acids by GS/GOGAT pathway (Tian et al. 2010). Earlier it was believed that the N can be transferred across the mycorrhizal interface in the form of amino acids or organic N. However Selle et al. (2005) identified high-affinity ammonium importer from *Populus trichocarpa* (*PttSMT1.2*), whose expression increased significantly when colonized with *Amanita muscaria*. This observation throws light on the fact that ammonium could be a major N source to be transported to plant by ectomycorrhizal fungi (Selle et al. 2005). The N transport mechanism from ECM fungi to the host plant was further explained in *Amanita muscaria*, where the exposure of NH^{4+} up-regulated the expression of high-affinity NH^{4+} importer (*AmAMT2*) in the extraradical hyphae but downregulated in Hartig net and fungal mantle (Willmann et al. 2007). The high expression of *AmAMT2* importer in extraradical hyphae indicates high NH^{4+} intake by the extraradical hyphae, whereas the lower expression at Hartig net would prevent the reabsorption of NH^{4+} by fungal hyphae from the root cells, thus increasing the net transport of NH^{4+} to the host (Willmann et al. 2007).

In exchange to all the nutrients, host plant rewards ECM fungi with its photosynthates. The ECM fungi form a strong carbon sink during the early symbiosis, thus receiving 20–30% of the total plant carbohydrate (Hobbie et al. 2008; Menkis et al. 2011). However the ECM fungi are not able to utilize the sucrose synthesized by the host plant due to lack of invertase gene which hydrolyses sucrose to glucose and fructose. In the *L. bicolor* genome, 15 genes encoding putative hexose transporters have been annotated; however, the genome lacks gene coding for invertase (Martin et al. 2008; Bonfante and Genre 2010). This clearly demonstrates that ECM fungi could not hydrolyse sucrose; therefore it depends upon the host plant to release glucose and fructose. It has been reported that *L. bicolor* could uptake only glucose from the host plant, whereas *Amanita muscaria* and *Hebeloma cylindrosporum* could even metabolize fructose (Bonfante and Genre 2010). Nehls et al. (2001)

reported that glucose is mainly taken up at the Hartig net, whereas fructose is taken up by hyphae of inner mantle layer. During symbiosis, the expression of hexose transporters increases immediately, indicating that the fungus is highly dependent on glucose from mycorrhizal interface (Lopez et al. 2008; Bonfante and Genre 2010). It has been observed that the P and N uptake in ECM fungi is stimulated by the supply of carbon from plant host. The Pi and N efflux from the fungus could directly be linked with the glucose uptake by the mycorrhizal fungi (Bücking and Heyser 2003; Bücking 2004; Kytöviita 2005).

6.4 Conclusions

Ectomycorrhizal fungi are a heterogeneous group of diverse fungal taxa, associated with more than 50,000 plant species. These symbiotic fungi play an important role in tree sustainability and ecosystem development. They protect the host trees from various biotic and abiotic stresses like heavy metals, salinity, drought, nutritional imbalance, pathogens and pests. Different ectomycorrhizal fungi respond differently to different stresses, thus balancing the whole ecosystem. The high taxonomic and functional diversity of these ECM fungi delivers a reliable support to trees in tolerating large spectrum of ecological niches.

References

Adriaensen K, Vrålstad T, Noben JP, Vangronsveld J, Colpaert JV (2005) Copper-adapted *Suillus luteus*, a symbiotic solution for pines colonizing Cu mine spoils. Appl Environ Microbiol 71:7279–7284

Adriaensen K, Vangronsveld J, Colpaert JV (2006) Zinc-tolerant *Suillus bovinus* improves growth of Zn-exposed *Pinus sylvestris* seedlings. Mycorrhiza 16:553–558

Alvarez M, Huygens D, Olivares E, Saavedra I, Alberdi M, Valenzuela E (2009) Ectomycorrhizal fungi enhance nitrogen and phosphorus nutrition of *Nothofagus dombeyi* under drought conditions by regulating assimilative enzyme activities. Physiol Plant 136:426–436

Alvarez M, Huygens D, Diaz LM, Villanueva CA, Heyser W, Boeckx P (2011) The Spatial distribution of acid phosphatase activity in Ectomycorrhizal tissues depends on soil fertility and morphotype, and relates to host plant phosphorus uptake. Plant Cell Environ 35:126–135

Balestrini R, Bonfante P (2014) Cell wall remodeling in mycorrhizal symbiosis: a way towards biotrophism. Front Plant Sci 5:237

Bandou E, Lebailly F, Muller F, Dulormne M, Toribio A, Chabrol J, Courtecuisse R, Plenchette C, Prin Y, Duponnois R, Thiao M (2006) The ectomycorrhizal fungus *Scleroderma bermudense* alleviates salt stress in seagrape (*Coccoloba uvifera* L.) seedlings. Mycorrhiza 16:559–565

Bellion M, Courbot M, Jacob C, Blaudez D, Chalot M (2006) Extracellular and cellular mechanisms sustaining metal tolerance in ectomycorrhizal fungi. FEMS Microbiol Lett 54:173–181

Bellion M, Courbot M, Jacob C, Guinet F, Blaudez D, Chalot M (2007) Metal induction of a *Paxillus involutus* metallothionein and its heterologous expression in *Hebeloma cylindrosporum*. New Phytol 174:151–158

Beniwal RS, Langenfeld-Heyser R, Polle A (2010) Ectomycorrhiza and hydrogel protect hybrid poplar from water deficit and unravel plastic responses of xylem anatomy. Environ Exp Bot 69:189–197

Blaudez D, Chalot M (2011) Characterization of the ER-located zinc transporter ZnT1 and identification of a vesicular zinc storage compartment in *Hebeloma cylindrosporum*. Fungal Genet Biol 48:496–503

Blaudez D, Botton B, Chalot M (2000) Cadmium uptake and subcellular compartmentation in the ectomycorrhizal fungus *Paxillus involutus*. Microbiology 146:1109–1117

Blom JM, Vannini A, Vettraino AM, Hale MD, Godbold DL (2009) Ectomycorrhizal community structure in a healthy and a *Phytophthora*-infected chestnut (*Castanea sativa* Mill.) stand in central Italy. Mycorrhiza 20:25–38

Bojarczuk K, Kieliszewska-Rokicka B (2010) Effect of ectomycorrhiza on Cu and Pb accumulation in leaves and roots of silver birch (*Betula pendula* Roth.) seedlings grown in metal-contaminated soil. Water Air Soil Pollut 207:227–240

Bonfante P (2003) Plants, mycorrhizal fungi and endobacteria: a dialog among cells and genomes. Biol Bull 204:215–220

Bonfante P, Genre A (2010) Mechanisms underlying beneficial plant–fungus interactions in mycorrhizal symbiosis. Nat Commun 1:48–58

Bonneville S, Smits MM, Brown A, Harrington J, Leake JR, Brydson R, Benning LG (2009) Plant-driven fungal weathering: early stages of mineral alteration at the nanometer scale. Geology 37:615–618

Branzanti MB, Rocca E, Pisi A (1999) Effect of ectomycorrhizal fungi on chestnut ink disease. Mycorrhiza 9:103–109

Brearley FQ, Saner P, Uchida A, Burslem DF, Hector A, Nilus R, Scholes JD, Egli S (2016) Testing the importance of a common ectomycorrhizal network for dipterocarp seedling growth and survival in tropical forests of Borneo. Plant Ecol Divers 9:563–576

Brundrett MC (2017) Global diversity and importance of mycorrhizal and nonmycorrhizal plants. In: Biogeography of mycorrhizal symbiosis. Springer, Cham, pp 533–556

Bucher M (2007) Functional biology of plant phosphate uptake at root and mycorrhiza interfaces. New Phytol 173:11–26

Bücking H (2004) Phosphate absorption and efflux of three ectomycorrhizal fungi as affected by external phosphate, cation and carbohydrate concentrations. Mycol Res 108:599–609

Bücking H, Heyser W (2003) Uptake and transfer of nutrients in ectomycorrhizal associations: Interactions between photosynthesis and phosphate nutrition. Mycorrhiza 13:59–68

Bücking H, Kuhn AJ, Schröder WH, Heyser W (2002) The fungal sheath of ectomycorrhizal pine roots: an apoplastic barrier for the entry of calcium, magnesium, and potassium into the root cortex? J Exp Bot 53:1659–1669

Bücking H, Liepold E & Ambilwade P (2012) The role of the mycorrhizal symbiosis in nutrient uptake of plants and the regulatory mechanisms underlying these transport processes. In Plant science in Tech

Buée M, Reich M, Murat C, Morin E, Nilsson RH, Uroz S, Martin F (2009) 454 Pyrosequencing analyses of forest soils reveal an unexpectedly high fungal diversity. New Phytol 184:449–456

Chalot M, Brun A, Finlay RD, Söderström B (1994) Metabolism of C-14 Glutamate and C-14 Glutamine by the Ectomycorrhizal Fungus *Paxillus involutus*. Microbiol (UK) 140:1641–1649

Chen S, Polle A (2010) Salinity tolerance of *Populus*. Plant Biol 12:317–333

Chen S, Hawighorst P, Sun J, Polle A (2014) Salt tolerance in *Populus*: significance of stress signaling networks, mycorrhization, and soil amendments for cellular and whole-plant nutrition. Environ Exp Bot 107:113–124

Chen Y, Nara K, Wen Z, Shi L, Xia Y, Shen Z, Lian C (2015) Growth and photosynthetic responses of ectomycorrhizal pine seedlings exposed to elevated Cu in soils. Mycorrhiza 25:561–571

Coelho ID, de Queiroz MV, Costa MD, Kasuya MCM, de Araujo EF (2010) Identification of differentially expressed genes of the fungus *Hydnangium* sp during the pre-symbiotic phase of the ectomycorrhizal association with *Eucalyptus grandis*. Mycorrhiza 20:531–540

Colpaert JV, Wevers JH, Krznaric E, Adriaensen K (2011) How metal-tolerant ecotypes of ectomycorrhizal fungi protect plants from heavy metal pollution. Ann For Sci 68:17–24

Courbot M, Chalot M, Diez L, Leroy P, Ruotolo R (2004) Cadmium responsive thiols in the ectomycorrhizal fungus *Paxillus involutus*. Appl Environ Microbiol 70:7413–7417

DalCorso G, Manara A, Furini A (2013) An overview of heavy metal challenge in plants: from roots to shoots. Metallomics 5:1117–1132

Danielsen L, Polle A (2014) Poplar nutrition under drought as affected by ectomycorrhizal colonization. Environ Exp Bot 108:89–98

Degola F, Fattorini L, Bona E, Sprimuto CT, Argese E, Berta G, di Toppi LS (2015) The symbiosis between *Nicotiana tabacum* and the endomycorrhizal fungus *Funneliformis mosseae* increases the plant glutathione level and decreases leaf cadmium and root arsenic contents. Plant Physiol Biochem 92:11–18

Duchesne LC, Peterson RL, Ellis BE (1988) Pine root exudate stimulates the synthesis of antifungal compounds by the ectomycorrhizal fungus *Paxillus involutus*. New Phytol 108:471–476

Egerton-Warburton LM, Griffin BJ (1995) Differential responses of *Pisolithus tinctorius* isolates to aluminum in vitro. Can J Bot 73:1229–1233

Finlay RD (2008) Ecological aspects of mycorrhizal symbiosis: with special emphasis on the functional diversity of interactions involving the extraradical mycelium. J Exp Bot 59:1115–1126

Fitter AH, Garbaye J (1994) Interactions between mycorrhizal fungi and other soil organisms. Plant Soil 159:123–132

Frey-Klett P, Chavatte M, Clausse ML, Courrier S, Roux CL, Raaijmakers J, Martinotti MG, Pierrat JC, Garbaye J (2005) Ectomycorrhizal symbiosis affects functional diversity of rhizosphere fluorescent pseudomonads. New Phytol 165:317–328

Gachomo E, Allen JW, Pfeffer PE, Govindarajulu M, Douds DD, Jin HR, Nagahashi G, Lammers PJ, Shachar-Hill Y, Bücking H (2009) Germinating Spores of *Glomus* intraradices can use internal and exogenous nitrogen sources for de novo biosynthesis of amino acids. New Phytol 184:399–411

Gallie U, Meire M, Brunold C (1993) Effect of cadmium on nonmycorrhizal and mycorrhizal Norway spruce seedlings *Picea abies* (L) Karst and its ectomycorrhizal fungi *Laccaria laccata* (Scop ex Fr) Bk and Br- sulfate reduction, thiols and distribution of the heavy-metals. New Phytol 125:837–843

García-Guzmán OM, Garibay-Orijel R, Hernández E, Arellano-Torres E, Oyama K (2017) Wordwide meta-analysis of Quercus forests ectomycorrhizal fungal diversity reveals southwestern Mexico as a hotspot. Mycorrhiza 27:811–822

Garg N, Aggarwal N (2011) Effects of interactions between cadmium and lead on growth, nitrogen fixation, phytochelatin, and glutathione production in mycorrhizal *Cajanus cajan* (L.) Millsp. J Plant Growth Regul 30:286–300

Ghimire SR, Craven KD (2011) Enhancement of switchgrass (*Panicum virgatum* L.) biomass production under drought conditions by the ectomycorrhizal fungus *Sebacina vermifera*. Appl Environ Microbiol 77:7063–7067

Ghorbanpour M, Omidvari M, Abbaszadeh-Dahaji P, Omidvar R, Kariman K (2018) Mechanisms underlying the protective effects of beneficial fungi against plant diseases. Biol Control 117:147–157

Gonçalves SC, Martins-Loução MA, Freitas H (2009) Evidence of adaptive tolerance to nickel in isolates of *Cenococcum geophilum* from serpentine soils. Mycorrhiza 19:221–230

Harrison MJ (2005) Signaling in the arbuscular mycorrhizal symbiosis. Annu Rev Microbiol 59:19–42

Henke C, Jung EM, Kothe E (2015) Hartig' net formation of *Tricholoma vaccinum*-spruce ectomycorrhiza in hydroponic cultures. Environ Sci Pollut Res 22:19394–19399

Hložková K, Matěnová M, Žáčková P, Strnad H, Hršelová H, Hroudová M, Kotrba P (2016) Characterization of three distinct metallothionein genes of the Ag-hyperaccumulating ectomycorrhizal fungus *Amanita strobiliformis*. Fungal Biol 120:358–369

Hobbie EA, Colpaert JV, White MW, Ouimette AP, Macko SA (2008) Nitrogen form, availability, and mycorrhizal colonization affect biomass and nitrogen isotope patterns in *Pinus sylvestris*. Plant Soil 310:121–136

Horton BM, Glen M, Davidson NJ, Ratkowsky DA, Close DC, Wardlaw TJ, Mohammed C (2017) An assessment of ectomycorrhizal fungal communities in Tasmanian temperate high-altitude *Eucalyptus delegatensis* forest reveals a dominance of the *Cortinariaceae*. Mycorrhiza 2(7):67–74

Hrynkiewicz K, Szymańska S, Piernik A, Thiem D (2015) Ectomycorrhizal community structure of *Salix* and *Betula* spp. at a saline site in central Poland in relation to the seasons and soil parameters. Water Air Soil Pollut 226:1–15

Ilyas S, Rehman A (2015) Oxidative stress, glutathione level and antioxidant response to heavy metals in multi-resistant pathogen, *Candida tropicalis*. Environ Monit Assess 187:1–7

Javelle A, Morel M, Rodriguez-Pastrana BR, Botton B, Andr, B, Marini AM, Brun A, Chalot M (2003) Molecular characterization, function and regulation of ammonium transporters (Amt) and ammonium-metabolizing enzymes (GS, NADP-GDH) in the ectomycorrhizal fungus *Hebeloma cylindrosporum*. Mol Microbiol 47:411–430

Jie WA, Huang Y, Jiang XY (2011) Influence of ectomycorrhizal fungi on absorption and balance of essential elements of *Pinus tabulaeformis* seedlings in saline soil. Pedosphere 21:400–406

Johansson EM, Fransson PM, Finlay RD, van Hees PA (2008) Quantitative analysis of exudates from soil-living basidiomycetes in pure culture as a response to lead, cadmium and arsenic stress. Soil Biol Biochem 40:2225–2236

Jourand P, Ducousso M, Loulergue-Majorel C, Hannibal L, Santoni S, Prin Y, Lebrun M (2010) Ultramafic soils from New Caledonia structure *Pisolithus albus* in ecotype. FEMS Microbiol Ecol 72:238–249

Kaiser C, Mayerhofer W, Dietrich M, Gorka S, Schintlmeister A, Reipert S, Schweiger P, Weidinger M, Wiesenbauer J, Martin V, Richter A (2017) Reciprocal trade of Carbon and Nitrogen at the root-fungus interface in ectomycorrhizal beech plants. InEGU General Assembly Conf Abst 19:15133

Kalsotra T, Khullar S, Agnihotri R, Reddy MS (2018) Metal induction of two metallothionein genes in the ectomycorrhizal fungus *Suillus himalayensis* and their role in metal tolerance. Microbiology 164:868–876

Kennedy PG, Peay KG (2007) Different soil moisture conditions change the outcome of the ectomycorrhizal symbiosis between *Rhizopogon* species and *Pinus muricata*. Plant Soil 291:155–165

Khullar S, Reddy MS (2018) Ectomycorrhizal fungi and its role in metal homeostasis through metallothionein and glutathione mechanisms. Curr Biotechnol 7:231–241

Kope HH, Tsantrizos YS, Fortin JA, Ogilvie KK (1991) p-Hydroxybenzoylformic acid and (R)-(−)-p-hydroxymandelic acid, two antifungal compounds isolated from the liquid culture of the ectomycorrhizal fungus *Pisolithus arhizus*. Can J Microbiol 37:258–264

Krupa P, Kozdrój J (2007) Ectomycorrhizal fungi and associated bacteria provide protection against heavy metals in inoculated pine (*Pinus sylvestris* L.) seedlings. Water Air Soil Pollut 182:83–90

Krznaric E, Verbruggen N, Wevers JH, Carleer R, Vangronsveld J, Colpaert JV (2009) Cd-tolerant *Suillus luteus*: a fungal insurance for pines exposed to Cd. Environ Pollut 157:1581–1588

Kytöviita MM (2005) Role of nutrient level and defoliation on symbiotic function: experimental evidence by tracing 14C/15N exchange in mycorrhizal *Birch* seedlings. Mycorrhiza 15:65–70

Langenfeld-Heyser R, Gao J, Ducic T, Tachd P, Lu CF, Fritz E, Gafur A, Polle A (2007) *Paxillus involutus* mycorrhiza attenuate NaCl-stress responses in the salt-sensitive hybrid poplar *Populus canescens*. Mycorrhiza 17:121–131

Lehto T, Zwiazek JJ (2011) Ectomycorrhizas and water relations of trees: a review. Mycorrhiza 21:71–90

Leonhardt T, Sacký J, Šimek P, Šantrucek J, Kotrba P (2014) Metallothionein-like peptides involved in sequestration of Zn in the Zn accumulating ectomycorrhizal fungus *Russula atropurpurea*. Metallomics 6:1693–1701

Li J, Bao S, Zhang Y, Ma X, Mishra-Knyrim M, Sun J, Sa G, Shen X, Polle A, Chen S (2012) *Paxillus involutus* strains MAJ and NAU mediate K+/Na+ homeostasis in ectomycorrhizal *Populus*× *canescens* under NaCl stress. Plant Physiol 159:1771–1786

Lopez MF, Dietz S, Grunze N, Bloschies J, Weiss M, Nehls U (2008) The sugar porter gene family of *Laccaria bicolor*: function in ectomycorrhizal symbiosis and soil-growing hyphae. New Phytol 180:365–378

Luo ZB, Li K, Jiang X, Polle A (2009) Ectomycorrhizal fungus (*Paxillus involutus*) and hydrogels affect performance of *Populus euphratica* exposed to drought stress. Ann For Sci 66:1

Luo ZB, Li K, Gai Y, Göbel C, Wildhagen H, Jiang X, Feußner I, Rennenberg H, Polle A (2011) The ectomycorrhizal fungus (*Paxillus involutus*) modulates leaf physiology of poplar towards improved salt tolerance. Environ Exp Bot 72:304–311

Luo ZB, Wu C, Zhang C, Li H, Lipka U, Polle A (2014) The role of ectomycorrhizas in heavy metal stress tolerance of host plants. Environ Exp Bot 108:47–62

Ma Y, He J, Ma C, Luo J, Li H, Liu T, Polle A, Peng C, Luo ZB (2014) Ectomycorrhizas with *Paxillus involutus* enhance cadmium uptake and tolerance in *Populus*× *canescens*. Plant Cell Environ 37:627–642

Majorel C, Hannibal L, Ducousso M, Lebrun M, Jourand P (2014) Evidence of nickel (Ni) efflux in Ni-tolerant ectomycorrhizal *Pisolithus albus* isolated from ultramafic soil. Environ Microbiol Rep 6:510–518

Marjanović Ž, Uehlein N, Kaldenhoff R, Zwiazek JJ, Weiß M, Hampp R, Nehls U (2005) Aquaporins in poplar: what a difference a symbiont makes! Planta 222:258–268

Martin F, Nehls U (2009) Harnessing ectomycorrhizal genomics for ecological insights. Curr Opin Plant Biol 12:508–515

Martin F, Aerts A, Ahrén D, Brun A, Danchin EG, Duchaussoy F, Gibon J, Kohler A, Lindquist E, Pereda V, Salamov A (2008) The genome of *Laccaria bicolor* provides insights into mycorrhizal symbiosis. Nature 452:88–92

Meharg AA (2003) The mechanistic basis of interactions between mycorrhizal associations and toxic metal cations. Mycol Res 107:1253–1265

Menkis A, Bakys R, Lygis V, Vasaitis R (2011) Mycorrhization, establishment and growth of outplanted *Picea abies* seedlings produced under different cultivation systems. Silva Fenn 45:283–289

Mohan V, Nivea R, Menon S (2015) Evaluation of ectomycorrhizal fungi as potential bio-control agents against selected plant pathogenic fungi. JAIR 3:408–412

Møller IM, Jensen PE, Hansson A (2007) Oxidative modifications to cellular components in plants. Annu Rev Plant Biol 58:459–481

Monnet F, Vaillant N, Vernay P, Coudret A, Sallanon H, Hitmi A (2001) Relationship between PSII activity, CO2 fixation, and Zn, Mn and Mg contents of *Lolium perenne* under zinc stress. J Plant Physiol 158:1137–1144

Muhsin TM, Zwiazek JJ (2002) Colonization with *Hebeloma crustuliniforme* increases water conductance and limits shoot sodium uptake in white spruce (*Picea glauca*) seedlings. Plant Soil 238:217–225

Munns R, Tester M (2008) Mechanisms of salinity tolerance. Annu Rev Plant Biol 59:651–681

Murata H, Yamada A, Maruyama T, Neda H (2015) Ectomycorrhizas in vitro between *Tricholoma matsutake*, a basidiomycete that associates with Pinaceae, and *Betula platyphylla* var. japonica, an early-successional birch species, in cool-temperate forests. Mycorrhiza 25:237–241

Nehls U, Mikolajewski S, Magel E, Hampp R (2001) Carbohydrate metabolism in ectomycorrhizas: gene expression, monosaccharide transport and metabolic control. New Phytol 150:533–341

Nguyen H, Calvo Polanco M, Zwiazek JJ (2006) Gas exchange and growth responses of ectomycorrhizal *Picea mariana*, *Picea glauca*, and *Pinus banksiana* seedlings to NaCl and Na2SO4. Plant Biol 8:646–652

Nguyen H, Rineau F, Vangronsveld J, Cuypers A, Colpaert JV, Ruytinx J (2017) A novel, highly conserved metallothionein family in basidiomycete fungi and characterization of two representative SlMTa and SlMTb genes in the ectomycorrhizal fungus *Suillus luteus*. Environ Microbiol 19:2577–2587

Oddsdottir ES, Eilenberg J, Sen R, Halldorsson G (2010a) The effects of insect pathogenic soil fungi and ectomycorrhizal inoculation of birch seedlings on the survival of *Otiorhynchus larvae*. Agric For Entomol 12:319–324

Oddsdottir ES, Eilenberg J, Sen R, Harding S, Halldorsson G (2010b) Early reduction of *Otiorhynchus* spp. larval root herbivory on *Betula pubescens* by beneficial soil fungi. Appl Soil Ecol 45:168–174

Oerke EC (2006) Crop losses to pests. J Agric Sci 144:31–43
Osobová M, Urban V, Jedelský PL, Borovička J, Gryndler M, Ruml T, Kotrba P (2011) Three metallothionein isoforms and sequestration of intracellular silver in the hyperaccumulator *Amanita strobiliformis*. New Phytol 190:916–926
Ouahmane L, Revel JC, Hafidi M, Thioulouse J, Prin Y, Galiana A, Dreyfus B, Duponnois R (2009) Responses of *Pinus halepensis* growth, soil microbial catabolic functions and phosphate-solubilizing bacteria after rock phosphate amendment and ectomycorrhizal inoculation. Plant Soil 320:169–179
Pena LB, Barcia RA, Azpilicueta CE, Méndez AA, Gallego SM (2012) Oxidative post translational modifications of proteins related to cell cycle are involved in cadmium toxicity in wheat seedlings. Plant Sci 196:1–7
Plamboeck AH, Dawson TE, Egerton-Warburton LE, North M, Bruns TD, Querejeta JI (2007) Water transfer via ectomycorrhizal fungal hyphae to conifer seedlings. Mycorrhiza 17:439–447
Plassard C, Louche J, Ali MA, Duchemin M, Legname E, Cloutier-Hurteau B (2011) Diversity in phosphorus mobilisation and uptake in ectomycorrhizal fungi. Ann For Sci 68:33–43
Plett JM, Gibon J, Kohler A, Duffy K, Hoegger PJ, Velagapudi R, Han J, Kües U, Grigoriev IV, Martin F (2012) Phylogenetic, genomic organization and expression analysis of hydrophobin genes in the ectomycorrhizal basidiomycete *Laccaria bicolor*. Fungal Genet Biol 49:199–209
Porcel R, Ruiz-Lozano JM (2004) Arbuscular mycorrhizal influence on leaf water potential, solute accumulation, and oxidative stress in soybean plants subjected to drought stress. J Exp Bot 55:1743–1750
Porcel R, Aroca R, Ruiz-Lozano JM (2012) Salinity stress alleviation using arbuscular mycorrhizal fungi. A review. Agron Sustain Dev 32:181–200
Qadir S, Qureshi MI, Javed S, Abdin MZ (2004) Genotypic variation in phytoremediation potential of Brassica juncea cultivars exposed to Cd stress. Plant Sci 167:1171–1181
Rajashekar B, Samson P, Johansson T, Tunlid A (2007) Evolution of nucleotide sequences and expression patterns of hydrophobin genes in the ectomycorrhizal fungus *Paxillus involutus*. New Phytol 174:399–411
Rajkumar M, Sandhay S, Prasad MNV, Freitas H (2012) Perspectives of plant-associated microbes in heavy metal phytoremediation. Biotechnol Adv 30:1562–1574
Ramesh G, Podila GK, Gay G, Marmeisse R, Reddy MS (2009) Different patterns of regulation for the copper and cadmium metallothioneins of the ectomycorrhizal fungus *Hebeloma cylindrosporum*. Appl Environ Microbiol 75:2266–2274
Raudaskoski M, Kothe E (2015) Novel findings on the role of signal exchange in arbuscular and ectomycorrhizal symbioses. Mycorrhiza 25:243–252
Ray P, Adholeya A (2009) Correlation between organic acid exudation and metal uptake by ectomycorrhizal fungi grown on pond ash in vitro. Biometals 22:275–281
Reddy MS, Prasanna L, Marmeisse R, Fraissinet-Tachet L (2014) Differential expression of metallothioneins in response to heavy metals and their involvement in metal tolerance in the symbiotic basidiomycete *Laccaria bicolor*. Microbiology 160:2235–2242
Reddy MS, Kour M, Aggarwal S, Ahuja S, Marmeisse R, Fraissinet-Tachet L (2016) Metal induction of a *Pisolithus albus* metallothionein and its potential involvement in heavy metal tolerance during mycorrhizal symbiosis. Environ Microbiol 18:2446–2454
Rousseau JVD, Reid CPP, English RJ (1992) Relationship between biomass of the mycorrhizal fungus *Pisolithus tinctorius* and phosphorus uptake in loblolly pine seedlings. Soil Biol Biochem 24:183–194
Ruytinx J, Nguyen H, Van Hees M, De Beeck MO, Vangronsveld J, Carleer R, Colpaert JV, Adriaensen K (2013) Zinc export results in adaptive zinc tolerance in the ectomycorrhizal basidiomycete *Suillus bovinus*. Metallomics 5:1225–1233
Sácký J, Leonhardt T, Borovička J, Gryndler M, Briksí A, Kotrba P (2014) Intracellular sequestration of zinc, cadmium and silver in *Hebeloma mesophaeum* and characterization of its metallothionein genes. Fungal Genet Biol 67:3–14
Sammer D, Krause K, Gube M, Wagner K, Kothe E (2016) Hydrophobins in the life cycle of the ectomycorrhizal basidiomycete *Tricholoma vaccinum*. PLoS One 11:e0167773

Schelkle M, Peterson RL (1997) Suppression of common root pathogens by helper bacteria and ectomycorrhizal fungi in vitro. Mycorrhiza 6:481–485
Sebastiana M, da Silva AB, Matos AR, Alcântara A, Silvestre S, Malhó R (2018) Ectomycorrhizal inoculation with *Pisolithus tinctorius* reduces stress induced by drought in cork oak. Mycorrhiza 28:247–258
Selle A, Willmann M, Grunze N, Gessler A, Weiss M, Nehls U (2005) The high-affinity Poplar ammonium importer *PttAMT1.2* and its role in ectomycorrhizal symbiosis. New Phytol 168:697–706
Selosse MA, Roy M (2009) Green plants that feed on fungi: facts and questions about mixotrophy. Trends Plant Sci 14:64–70
Shabala L, Cuin TA, Newman IA, Shabala S (2005) Salinity-induced ion flux patterns from the excised roots of *Arabidopsis* sos mutants. Planta 222:1041–1050
Sharma SS, Dietz KJ (2009) The relationship between metal toxicity and cellular redox imbalance. Trends Plant Sci 14:43–50
Sharma SS, Dietz KJ, Mimura T (2016) Vacuolar compartmentalization as indispensable component of heavy metal detoxification in plants. Plant Cell Environ 39:1112–1126
Shi L, Xue J, Liu B, Dong P, Wen Z, Shen Z, Chen Y (2018) Hydrogen ions and organic acids secreted by ectomycorrhizal fungi, *Pisolithus* sp1, are involved in the efficient removal of hexavalent chromium from waste water. Ecotoxicol Environ Saf 161:430–436
Singh S, Parihar P, Singh R, Singh VP, Prasad SM (2016) Heavy metal tolerance in plants: role of transcriptomics, proteomics, metabolomics, and ionomics. Front Plant Sci 6:1143
Širić I, Humar M, Kasap A, Kos I, Mioč B, Pohleven F (2016) Heavy metal bioaccumulation by wild edible saprophytic and ectomycorrhizal mushrooms. Environ Sci Pollut Res 23:18239–18252
Smith SE, Read DJ (2010) Mycorrhizal symbiosis. Academic, Amsterdam
Smith FA, Smith SE (2015) How harmonious are arbuscular mycorrhizal symbioses? Inconsistent concepts reflect different mindsets as well as results. New Phytol 205:1381–1384
Strange RN, Scott PR (2005) Plant disease: a threat to global food security. Annu Rev Phytopathol 43:83–116
Su C, Jiang L, Zhang W (2014) A review on heavy metal contamination in the soil worldwide: situation, impact and remediation techniques. Environ Skeptics Critics 3:24–38
Sun J, Dai S, Wang R, Chen S, Li N, Zhou X, Lu C, Shen X, Zheng X, Hu Z, Zhang Z, Song J, Xu Y (2009) Calcium mediates root K+/Na+ homeostasis in poplar species differing in salt tolerance. Tree Physiol 29(9):1175–1186
Tagu D, De Bellis R, Balestrini R, De Vries OM, Piccoli G, Stocchi V, Bonfante P, Martin F (2001) Immunolocalization of hydrophobin HYDPt-1 from the ectomycorrhizal basidiomycete *Pisolithus tinctorius* during colonization of *Eucalyptus globulus* roots. New Phytol 149:127–135
Tang M, Zhang RQ, Chen H, Zhang HH, Tian ZQ (2008) Induced hydrolytic enzymes of ectomycorrhizal fungi against pathogen *Rhizoctonia solani*. Biotechnol Lett 30:1777–1782
Targhetta BL, Oliveira VL, Rossi MJ (2013) Tolerance of ectomycorrhizal fungi and plants associated to toxic levels of metals. Revista Árvore 37:825–833
Tatry MV, El Kassis E, Lambilliotte R, Corratgé C, Van Aarle I, Amenc LK, Alary R, Zimmermann S, Sentenac H, Plassard C (2009) Two differentially regulated phosphate transporters from the symbiotic fungus *Hebeloma cylindrosporum* and phosphorus acquisition by ectomycorrhizal *Pinus pinaster*. Plant J 57:1092–1102
Taylor JH, Peterson CA (2000) Morphometric analysis of *Pinus banksiana* Lamb. root anatomy during a 3-month field study. Trees 14:239–247
Taylor JH, Peterson CA (2005) Ectomycorrhizal impacts on nutrient uptake pathways in woody roots. New For 30:203–214
Tian C, Kasiborski B, Koul R, Lammers PJ, Bücking H, Shachar-Hill Y (2010) Regulation of the nitrogen transfer pathway in the arbuscular mycorrhizal symbiosis: gene characterization and the coordination of expression with nitrogen flux. Plant Physiol 153:1175–1187
Tilman D, Cassman KG, Matson PA, Naylor R, Polasky S (2002) Agricultural sustainability and intensive production practices. Nature 418:671–677

Tsantrizos YS, Kope HH, FoRTIN JA, Ogilvie KK (1991) Antifungal antibiotics from *Pisolithus tinctorius*. Phytochemistry 30:1113–1118

Turnau K, Przybyłowicz WJ, Mesjasz-Przybyłowicz J (2001) Heavy metal distribution in *Suillus luteus* mycorrhizas–as revealed by micro-PIXE analysis. Nucl Instrum Methods Phys Res, Sect B 181:649–658

Vaidya GS, Shrestha K, Wallander H (2005) Antagonistic study of ectomycorrhizal fungi isolated from Baluwa forest (Central Nepal) against with pathogenic fungi and bacteria. Sci World 3:49–52

Van Der Heijden MG, Martin FM, Selosse MA, Sanders IR (2015) Mycorrhizal ecology and evolution: the past, the present, and the future. New Phytol 205:1406–1423

Viereck N, Hansen PE, Jakobsen I (2004) Phosphate pool dynamics in the arbuscular mycorrhizal fungus *Glomus intraradices* studied by in vivo 31P NMR spectroscopy. New Phytol 162:783–794

Wang B, Qiu YL (2006) Phylogenetic distribution and evolution of mycorrhizas in land plants. Mycorrhiza 16:299–363

Willmann A, Weiss M, Nehls U (2007) Ectomycorrhiza-mediated repression of the highaffinity ammonium importer gene amamt2 in *Amanita muscaria*. Curr Genet 51:71–78

Wu B, Watanabe I, Hayatsu M, Nioh I (1999) Effect of ectomycorrhizae on the growth and uptake and transport of 15N-labeled compounds by *Pinus tabulaeformis* seedlings under water-stressed conditions. Biol Fertil Soils 28:136–148

Wu QS, Cao MQ, Zou YN, He XH (2014) Direct and indirect effects of glomalin, mycorrhizal hyphae, and roots on aggregate stability in rhizosphere of trifoliate orange. Sci Rep 4:5823

Xu X, Xia L, Zhu W, Zhang Z, Huang Q, Chen W (2015) Role of *Penicillium chrysogenum* XJ-1 in the detoxification and bioremediation of cadmium. Front Microbiol 6:1–10

Xu P, Zeng G, Huang D, Liu L, Zhao M, Lai C, Li N, Wei Z, Huang C, Zhang C (2016) Metal bioaccumulation, oxidative stress and antioxidant defenses in *Phanerochaete chrysosporium* response to Cd exposure. Ecol Eng 87:150–156

Yadav SK (2010) Heavy metals toxicity in plants: an overview on the role of glutathione and phytochelatins in heavy metal stress tolerance of plants. South Afr J Bot 76:167–179

Yi H, Polanco MC, MacKinnon MD, Zwiazek JJ (2008) Responses of ectomycorrhizal *Populus tremuloides* and *Betula papyrifera* seedlings to salinity. Environ Exp Bot 62:357–363

Zheng W, Yingheng FE, Huang Y (2009) Soluble protein and acid phosphatase exuded by ectomycorrhizal fungi and seedlings in response to excessive Cu and Cd. J Environ Sci 21:1667–1672

Send Orders for Reprints to reprints@benthamscience.ae

Current Biotechnology, **2016,** *5,* **000-000**

REVIEW ARTICLE

Ectomycorrhizal Fungi and Its Role in Metal Homeostasis through Metallothionein and Glutathione Mechanisms

Shikha Khullar and M. Sudhakara Reddy*

Department of Biotechnology, Thapar University, Patiala-147004, Punjab, India

M. Sudhakara Reddy

ARTICLE HISTORY

Received: March 8, 2016
Revised: May 26, 016
Accepted: May 27, 2016

DOI:
10.2174/2211550105666160531145544

Abstract:

Background: Heavy metals are continuously being mobilized into the biosphere either through natural mechanisms or through anthropogenic activities. Ectomycorrhizal fungi forms a symbiotic association with the plant roots and helps them in enhancing growth and protects the plant from various biotic as well as abiotic stresses.

Objective: The focus of this review is to comprehend the role of metallothioneins and glutathione metabolism in heavy metal detoxification in ectomycorrhizal fungi.

Method: Numerous research papers, articles and chapters have been reviewed to study the mechanisms involved in heavy metal chelation in different organisms. Ectomycorrhizal fungi chelate the metals intracellularly by producing metallothioneins and glutathione. The chelation mechanism has been broadly studied.

Results: Ectomycorrhizal fungi play an important role in metal homeostasis by producing intracellular chelators like metallothioneins and glutathione. These chelators are rich in cysteine, having high affinity for binding heavy metals and detoxify them.

Conclusion: Since ectomycorrhizal fungi thrive on the metal polluted soil, they become the most potent candidates for bioremediation of the metal polluted soil. Therefore it is necessary to understand the key mechanisms involved in this detoxification process.

Keywords: Heavy metals, Metal homeostasis, Ectomycorrhizal fungi, Intracellular chelation, Metallothioneins, Glutathione.

1. INTRODUCTION

Heavy metal contamination is the pre-dominant environmental hazard concerning the world today. Heavy metals are continuously being mobilized and dispersed into the biosphere either through natural mechanisms like weathering of metalliferous rocks, volcanos or through the anthropogenic activities like agriculture, mining and industry, combustion of fossil fuels, phosphate fertilizers etc.[1]. For some cellular mechanisms, heavy metals like copper (Cu^{2+}), cobalt (Co^{2+}), iron (Fe^{3+}), manganese (Mn^{2+}), zinc (Zn^{2+}) etc., are essential in trace amount, whereas other heavy metals like cadmium (Cd^{2+}), lead (Pb), mercury (Hg), arsenic (As), are highly toxic and hazardous to both environment and health. But above a certain threshold concentration, all heavy metals are toxic. They enter inside the cell through same transport system as for essential ions and alter the cellular functions [2]. Excess heavy metals in the soil hinder the vegetation by interfering with the functioning of the plants and the soil biota. The toxicity of a heavy metal depends upon certain factors like concentration of the heavy metal, time for which the organism is exposed to heavy metal, the physiochemical properties of metal and the environmental factors [3]. Heavy metals enter inside the cell and interact with the carboxyl and thiol groups of the proteins through their ionophoretic properties and generate free radicals, which induces oxidative stress inside the cell [4]. Many studies have reported the generation of oxidative stress and inducing antioxidant defense mechanisms in plants [5,6], algae and white-rot fungi [7] in response to heavy metal stress.

Metal polluted soil is the major source of heavy metals in the environment. There are many techniques for removal of heavy metals from soil which includes conventional methods like thermal processes, physical separation, electrochemical methods, excavation, extraction, washing, solidification and vitrification and biological methods like bioremediation/phytoremediation in which plants and their microbial rhizosphere organisms sequester or immobilize pollutants for cleaning not only soils but also water contaminated with heavy metals or organic pollutants [8].

*Address correspondenc to this author at the Department of Biotechnology, Thapar University, Patiala-147004, Punjab, India; E-mail: msreddy@thapar.edu

2211-5501/16 $58.00+.00

Phytoremediation involves five processes (i) phytoextraction (absorption of heavy metals) (ii) phytodegradation (decomposition by plants and microorganism) (iii) rhizofilteration (absorption of metals from water) (iv) phytostabilization (immobilization of metals in soil by plants and microorganisms) and (v) phytovolatilization (volatilization into the atmosphere) [9,10].

The conventional methods for removing heavy metals are very expensive and applicable only on small area. They also damage the soil microflora. On the other hand bioremediation is a simple, inexpensive and more reliable method for large areas. Plants that actively remove heavy metals from soil are called hyperaccumulators. Phytoremediation has recently been reviewed in detail by Rahman *et al*. (2016) [11].

Although many plants are proven to have great potential for phytoextraction, most metalophytes have small size and slow growth, long reproductive cycle, which limits their usability in the large-scale operations [12]. They may take decades to remove significant amount of heavy metals from the polluted soil. An alternate to this problem is the use of specific microorganisms like bacteria, fungi, yeast etc., isolated from heavy metal contaminated sites, known to sequester and detoxify the heavy metals.

Many microorganisms have been reported to have specialized mechanisms for not only tolerating the heavy metal stress but also detoxifying them. Plant associated microbes play a very significant role in heavy metal detoxification [13]. Many rhizosphere bacteria have been reported for playing an important role in improving the phytoremediation process by affecting the soil bioavailability through different mechanisms like altering the soil pH, release of various chelators like organic acids and siderophores or by the oxidation/reduction reactions [14,15,16,17]. *Pseudomonas aeruginosa*, *Pseudomonas fluorescens* and *Ralstonia metallidurans* enhances the chromium and lead uptake by plants by producing siderophores like pyroverdine, pyrochelin and alcaligin E [18], *Pseudomonas putida* reduces the cadmium and lead accumulation in *Phaseolus vulgaris* by producing pyroverdine [19], *Burkholderia cepacia*, *Pseudomonas fluorescens* mobilize metals like zinc, lead by producing organic acids like oxalic acid, tartaric acid, citric acid, formic acid etc. so as to enhance phytoextraction [20,21]. Other important metal tolerant microorganisms found in the rhizosphere are the mycorrhizal fungi. The mycorrhizal fungi form a symbiotic association with the plant roots and protect the plant from various biotic as well as abiotic stresses. They are cosmopolitan and abundant, even in the highly degraded areas. There are mainly two types of mycorrhizal fungi depending on whether the fungus colonize the intercellular spaces of roots or develop inside the cell: endomycorrhizal (arbuscular mycorrhizal fungi) and ectomycorrhizal fungi (ECM) (Fig.1). Endomycorrhizal fungi are those mycorrhizal fungi which penetrate the cortical cells of the roots of a vascular plant forming highly branched shrubby structure called arbuscules. They belong to the phylum Glomeromycota, whereas ectomycorrhizal fungi do not penetrate inside the host cell wall instead forms intracellular hyphae known as Hartig's net. Many studies have demonstrated the role of mycorrhizal fungi in protecting the plants from heavy metal polluted soil and also in extracting the metal contaminants from soil [22,23]. There are many mechanisms through which these ectomycorrhizal fungi protect the plant from heavy metals including extracellular chelation, cell wall binding, increase efflux and production of thiol rich chelators like metallothioneins (MT) and glutathione (GSH). Among these mechanisms metallothioneins and glutathione are the key components involved in heavy metal homeostasis. Although both MT and GSH contain cysteine and play similar role in metal detoxification, they are chemically very different. Metallothioneins are low molecular weight proteins coded by specific genes, whereas glutathione is a non-protein thiol, produced by two step enzymatic reaction using ATP molecules. The focus of this review is to provide an insight into these two mechanisms through which ectomycorrhizal fungi detoxify heavy metals and protect the host plants.

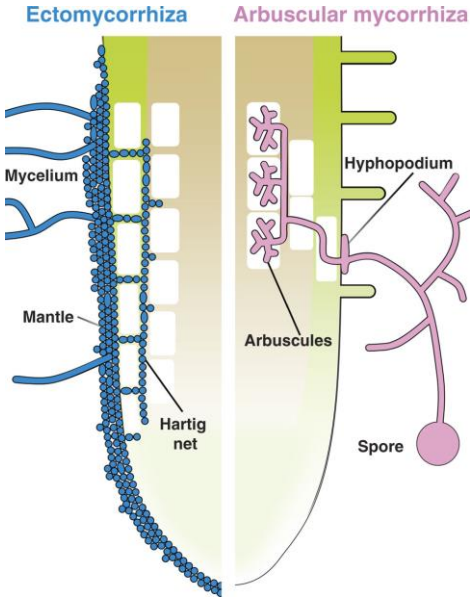

Fig. (1). Schematic view of ectomycorrhizal and endomycorrhizal fungi indicating the formation of Hartig net and arbuscules respectively [24].

2. ECTOMYCORRHIZAL FUNGI

Ectomycorrhizal fungi mainly belong to Ascomycetes or Basidiomycetes. It has been estimated that more than 10,000 fungal species can form ectomycorrhiza with the host plants [25]. Trees families like Pinaceae, Fagaceae, Dipterocarpaceae and Caesalpinoidaceae, distributed in the tropic, sub-tropic, temperate and boreal forests are mainly the hosts for ectomycorrhizal fungi [26]. Agaricomycetes were found to be the most dominant class of ectomycorrhizal fungi in the soil [27]. These fungi have a dual lifestyle, form symbiosis with the plant roots and as facultative saprotrophes in soil [28].

The ectomycorrhizal fungi ensheath its hyphae around the root tip forming the hyphae mantle. Inside the mantle the hyphae penetrate into the cell wall and grow in between epidermal cells and cortical cells. They never penetrate inside the cell lumen of roots, hence forming a Hartig net (Fig. **2**). This Hartig net is an interface for exchange of

water, nutrients and other components between both fungi and the plant roots [24]. On the other end outside the fungal mantle, hyphae extend into the soil so as to have access to the nutrients unavailable to the plant roots. Thus ectomycorrhizal fungi provide water, mineral and nutrients to the plant and are rewarded with the photosynthates or stored carbohydrates by the host plant [28]. They also develop an extensive network by spreading their hyphae in the soil forming a wood-wide web which can connect all surrounding plant communities and promote horizontal nutrition transfer [29].

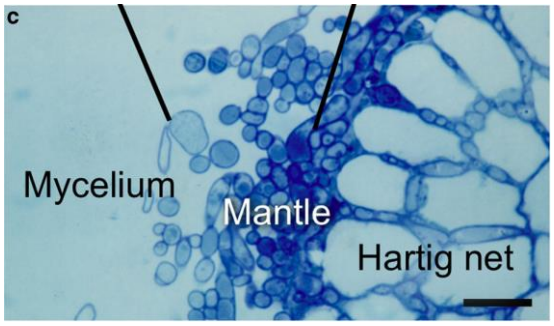

Fig. (2). Formation of Hartig net by the ectomycorrhizal fungi. Mycelium spreads its hyphae in the intercellular space without penetrating the cell lumen [24].

In the symbiosis, host plants provide carbon for mycorrhizal fungi in return for several benefits like, promoting nutrient uptake, tolerating drought and salt stress, resisting pathogens and herbivores, etc. (Fig. **3**) [26]. Fifteen putative genes have been annotated in the *Laccaria bicolor* genome that encodes for hexose transporters. These genes were found to be up-regulated during the symbiosis. This clearly depicts that *L.bicolor* feed on the glucose provided by the host plant [30]. Other ectomycorrhizal fungi like *Amanita muscaria* and *Hebeloma cylindrosporum* also metabolize on glucose and fructose.

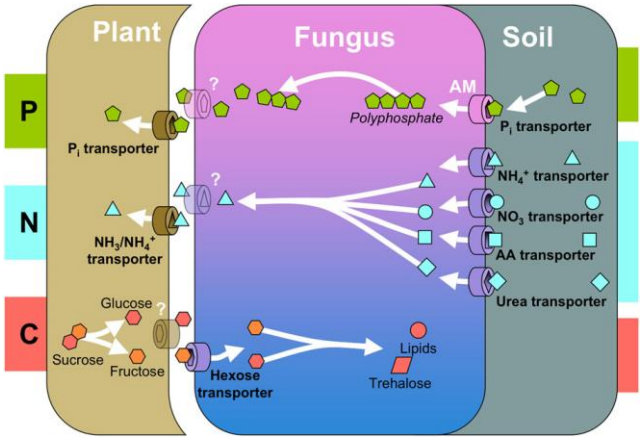

Fig. (3). Nutrient exchange process in soil, mycorrhizal fungi and host plant, P-phosphorous and N-nitrogen being transported by ECM from soil to host plant in exchange of C-carbon [24].

Ectomycorrhizal fungi protect the host plant from various abiotic and biotic stresses like nutrient deficiency, drought, salinity, heavy metals and pests. *Paxillus involutus* enhances cadmium and salt tolerance in *Populus canescens* [31,32], *Pisolithus albus* exhibits enhanced growth of *Eucalyptus tereticornis* under copper and cadmium stress [22], *Suillus bovines and Rhizopogon roseolus* showed cadmium tolerance in *Pinus pinaster* seedlings [33], *Rhizopogon buenoi*, *Tomentella ellisii*, *Inocybe curvipes*, and *Suillus granulatus* protects Masson pine from lead and zinc [34], *Suillus luteus* provides metal tolerance to pines [35] and many more.

Ascomycetes shows higher stress tolerance as compared to basidomycetes. Many authors have observed the dominance of ascomycetes in heavily polluted areas whereas basidomycetes were observed in less polluted and control plots. The genera *Phialophora*, *Phialocephala* and *Leptodontidium* and many other ascomycetes have been reported to have adaptive metal tolerance [36]. Similarly many basidomycetes have also been reported to have complete defense mechanisms against heavy metals like *Laccaria bicolor* [37], *Hebeloma cylindrosporum* [48], *Pisolithus albus* [22], *Suillus bovinus* [38], *Suillus luteus* [35], *Paxillus involutus* [39], *Amanita strobiliformis* [40] etc.

Ectomycorrhizal fungi are highly tolerant to heavy metal stress. They have developed full mechanism to interact with heavy metals either by "Avoidance" when the organism is able to restrict the metal uptake or by developing "Tolerance" when the fungi survive in the presence of high internal metal concentration. In avoidance mechanism the organism inhibit the metal entry by: extracellular precipitation by excreting di- and tricarboxylic acids, oxalic acids, biosorption to cell wall through chitin and glucosamine, reduced uptake, or increase efflux (Fig.4). Inspite of these avoidance mechanisms 20-30% of metal could be found in the cytosol and vacuoles [41], which clearly depicts the presence of intracellular tolerance mechanisms. In case of tolerance, metals entered inside cell are chelated intracellularly through the synthesis of thiol rich chelators such as metallothioneins, glutathione, phytochelatins and compartmentation within vacuoles. These peptides bind the heavy metals present in the cytosol and form metal-peptide complexes (metal-MT, metal-$(GSH)_2$), which actively get transported to the vacuoles (Fig.4) [42].

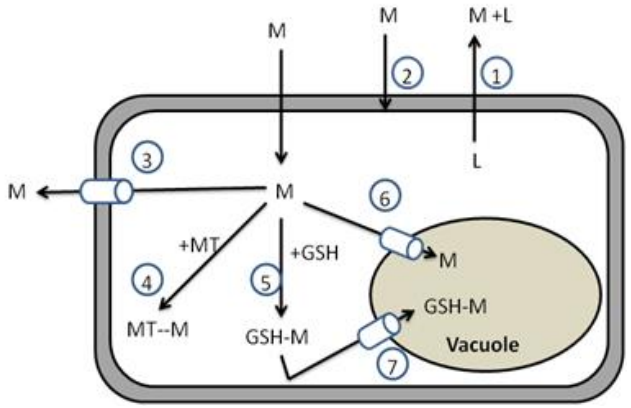

Fig. (4). Mechanisms of heavy metal tolerance in ectomycorrhizal fungi. 1) extracellular chelation by secreted ligands 2) cell wall binding 3) enhanced efflux 4) intracellular chelation by metallothioneins (MT) 5) intracellular chelation by glutathione (GSH) 6) subcellular compartmentation 7) compartmentation of GSH-M in vacuoles [46].

Many studies have reported the absence of phytochelatins in ectomycorrhizal fungi like Paxillus involutus [39], Suillus bovines [43] and genome of Laccaria bicolor [30]. This gives a clear idea about the lack of phytochelatins in ectomycorrhizal fungi. On the contrary many yeasts like Saccharomyces cerevisiae [44], Candida globrata, Schizosaccharomyyces pombe [45], have been reported of synthesizing phytochelatins in response to cadmium and arsenic.

3. METALLOTHIONEINS

Metallothioneins are intracellular, low molecular weight (usually below 7 kDa), cysteine rich (up to 33%) proteins having high affinity for binding metals and xenobiotics. They lack aromatic amino acids. They also protect cells by trapping reactive oxygen species (ROS). MTs are heterogeneous proteins with diverse amino acid and nucleotide sequences. They are named metallothionein for the ability of their thiol group to bind metal, resulting in a metalloprotein complex which is accumulated into vacuole and later released as metallic complex [47]. Metallothioneins are characterized with recurring C-X-C, C-X-X-C or C-X-Y-C motifs in their primary structure (Fig. **5**) [37].

Metallothioneins bind both essential as well as non-essential heavy metals like copper, cadmium, zinc, arsenic, lead, mercury, silver and forming metal-thiolate complex resulting in metal homeostasis and metal detoxification [48,37]. They form γ-mercaptide bonds with the metal. MT genes are induced by the same metal ions that bind to the MT protein, thus providing a direct activation of the defense mechanism [49]. The most common inducers of metallothioneins are Zn, Cu, Cd and Hg. Among these copper and zinc are the primary inducers of metallothioneins.

3.1. Classification of Metallothioneins

Numerous studies have reported the presence of metallothioneins in almost all organisms including prokaryotes, fungi, sea urchins, mammals to plants. UniProt data till date records 15 metallothionein families and 38 subfamilies including vertebrates (12), mollusc (4), crustacean (3), echinodermata (2), diptera (2), nematoda (2), ciliate (1), fungi (6), prokaryota (1) and plant (5) (Released: 20th January, 2016) [50].

Metallothioneins are classified into 3 classes based on their heterogeneous amino acid sequence. Class I metallothioneins comprises of all metallothioneins having sequence similarity with horse kidney MTs. MTs from various vertebrates and mammals fall in this class. Class II metallothioneins consists of all MTs with sequence different from that of Class I metallothioneins. They mainly include metallothioneins from plant, fungi, yeast and nonvertebrate animals. Class III metallothioneins are basically phytochelatins, which is an entirely different class now [51]. So broadly we can say that metallothioneins can be classified into two classes Class I and Class II. In case of plants, Class II is further classified into four types based on the distribution of cysteine motifs on both N-terminal and C-terminal domain [52].

A new functional classification system has been proposed by Palacios *et al.* (2011), in which metallothioneins are classified into two groups Cu-thioneins and Zn-thioneins based on their metal binding ability [53]. Zn-thioneins (also Cd-thioneins) are those which form a homometallic Zn-MT or Cd-MT complexes when exposed to zinc or cadmium-enriched media. They exhibit high degree of folding with expected stoichiometry. But when exposed to copper-supplemented media, they form various heteronuclear complexes like Zn-MT/Cu-MT with a lower degree of folding and high thiol group oxidation resulting in disulfide formation. Similarly Cu-thioneins forms homometallic Cu-MT complexes when exposed to copper-enriched media and shows heteronuclear complexes of Cu/Zn-MT when exposed to zinc supplemented media. Cu-thioneins when exposed to cadmium-supplemented media, forms heterometallic complex of Cd-MT containing sulfide ligands (S^{2-}) [53]. Two MTs in *Saccharomyces cerevisae* Cup1 and Crs5 are identified as Cu-thioneins and Zn-thioneins respectively, where Cup1 isoform has been classified as the strict Cu-thionein and Crs5 can be defined as a dual

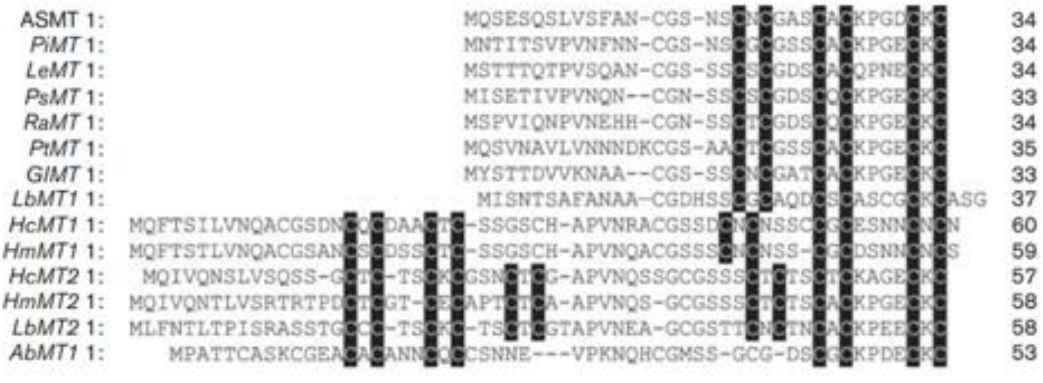

Fig. (5). Multiple sequence alignment of different MT genes from different fungal sources showing C-X-C motifs. Amanita strobiliformis (AsMT), Paxillus involutus (PiMT), Lentinula edodes (LeMT), Piriformospora indica (PsMT), Pisolithus tinctorius (PtMT), Ganoderma lucidum (GlMT), Laccaria bicolor (LbMT1 & 2), Hebeloma cylindrosporum (HcMT1 & 2), Hebeloma mesophaeum (HmMT1 & 2); Agaricus bisporus (AbMT1) [37].

metal binding MT more expressive for zinc than copper. Most of the Zn-thioneins exhibit dual behavior [54]. In different organisms MTs occur in different isoforms, depending on their different metal binding tendencies. One organism can code for many MTs having differential expression for different metals as explained in para 3.4.

3.2. Structure of Metallothioneins

MTs in its apoform (native form without metal ions) are devoid of any tertiary structures. When exposed to metal ions, MTs bind the metal coordinates and form metal-thiolate clusters. Hence we can say that metallothioneins undergo metal-induced protein folding [55]. Since different metal ions require different coordinate geometry, depending on whether they are monovalent or divalent, a single MT protein can be folded into different three dimensional conformations. Hence the three dimentional structure of the metallothionein depends upon the metal ion bound to it. In case of plants, mammals and other higher organisms, metal-MT complexes are reported of having two-domain structure (C-terminal α-domain and N-terminal β-domain). The α-domain consists of 11 cysteine molecules and can bind 4 divalent metal ions ($M_4(Cys)_{11}$), whereas β-domain consists of 9 cysteine molecules which can bind 3 divalent metal ions ($M_3(Cys)_9$) (Fig. **6 A,B**)[56]. Whereas in case of lower organisms like bacteria, yeast, fungi single domain MTs have been reported. *Neurospora crassa*, *Agaricus bisporus*, *Saccharomyces cerevisae*, Cynobacterium *Synechococcus* are reported of having a single domain metallothioneins (Fig. **6 C,D**) [57,58,59]. Metallothionein from *Neurospora crassa* has 25 amino acid residues containing seven cysteines. These seven cysteines can coordinate six Cu^+ atoms forming $Cu_6(Cys)_7$ complex [57]. Cup1 of *Saccharomyces cerevisae* consists of ten cysteine residues which can coordinate 8 Cu^+ ions forming $Cu_8(Cys)_{10}$ complex. Bacterial zinc metallothionein SmtA has also been reported in cynobacteria *Synechococcus* forming $Zn_4(Cys)_9(His)_2$ complex. This is for the first time that metallothioneins have been reported of having Histidine molecules. Inspite of diversities, a conserved sequence segment has been reported in mammals, sea-urchins and many single domain MTs, which clearly signals for the common ancestory.

3.3 Metalation by Metallothioneins

Inspite of devoting more than three decades on the study of metallothioneins the information on true mechanisms involved in the metalation process are still incomplete. Metallation can be achieved either by binding of metals to the apo-MT or by the substitution of metalated-MT with the metal with higher binding constant [61]. There are three reasons behind this paucity, firstly the metallation reactions are generally fast to be completed in milliseconds, secondly metallothioneins are very sensitive to oxidation and thirdly lack of proper chromophores [55]. Earlier studies on Co^{2+} metalation with metallothioneins concluded that the initial binding of the cobalt ions to metallothioneins occur randomly followed by rearrangement to form unique metal-thiolate clusters [62] but recently Ngu and Stillman (2009) reported the metalation process using arsenic instead of copper and zinc by electrospray ionization mass spectrometry (ESI-MS) [55]. As^{3+} metalation process is slow and takes minutes to process, whereas copper and zinc metalation occur in milliseconds. The process explains that metals are bound in a non-cooperative manner to the MT peptide. As the first As^{3+} ion binds to the MT, the rate constant value for the second As^{3+} ion decreases and the process becomes slow. Similarly the rate constant keep on decreasing as the metal ions keep on binding and the process becomes slow. The rate constant for binding first As^{3+} is 6.8 times greater than that for the last As^{3+}. So it can be observed that the rate binding values depend upon the number of binding sites in the MT peptide. Since single domain MTs have lesser metal binding sites than double-domain MTs, the metalation process in single domains is slower than in double domains [55].

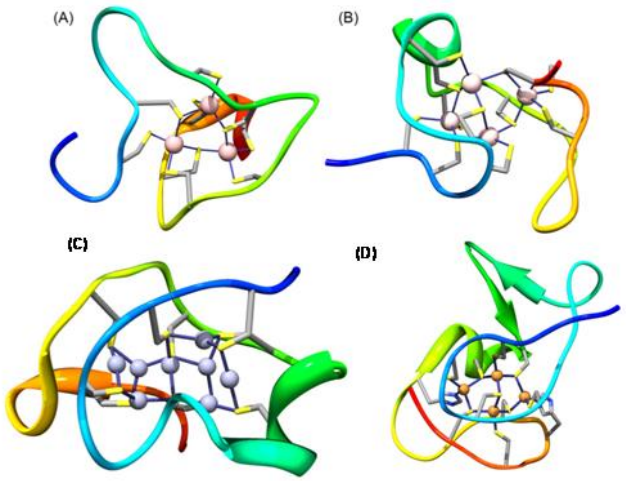

Fig. (6). Structure of metal-MT complexe in different organisms. Mammalian MTs have two domains α and β-domain A) β-domain in mammalian MTs showing Cd3(Cys)9 complex B) α-domain in mammalian MTs showing Cd4(Cys)11 complex C) S. cerevisiae Cu8-Cup1, showing the Cu8(Cys)10 complex D) S. elongatus Zn4–SmtA, showing the Zn4(Cys)9(His)2 complex [60].

3.4 Regulation of Metallothionein Genes

MT genes are mostly induced under stress conditions like heavy metal stress, oxidative stress, heat shock, etc. Copper, zinc and cadmium are the most active inducers of metallothioneins. Many studies have reported high expression of MT genes under copper and zinc stress [37]. This upregulation is controlled by the various cis-acting elements like metal response elements (MREs), antioxidant response elements (AREs), glucocorticoid responsive elements (GREs), heat shock elements (HSEs), etc located in the promoter region [63]. When exposed to metal stress, metal transcription factor-1(MTF-1) binds MREs and induces the metallothionein expression. Hence we can say that MT genes are regulated at transcriptional level [64].

3.5 Metallothioneins and Ectomycorrhizal Fungi

It is very essential to study the role of metallothioneins in ectomycorrhizal fungi, since they thrive on the metal polluted soil and posses a significant role in bioremediation. Although many reports are available till date on metallothionein genes isolated from prokaryotic bacteria

[65], plants [66], animals [67] and fungal species [22] etc., but not much have been reported in ectomycorrhizal fungi.

The metal binding tendency of metallothioneins varies for different metals and host species. Different metallothionein isoforms express differentially in different ectomycorrhizal fungi in response to different metals. In case of *Amanita strobiliformis*, three isoforms of metallothionein genes (*AsMT1, AsMT2, AsMT3*) have been characterized. Among these *AsMT1*is up-regulated in the presence of copper and silver, *AsMT2* is up-regulated in the presence of cadmium and *AsMT3* is up-regulated by zinc [68]. Reddy *et al.* (2014) characterized two (*LbMT1 and LbMT2*) out of six putative metallothionein genes in *Laccaria bicolor* genome and reported their differential expression to copper, cadmium and zinc stress. The expression of both *LbMT1 and LbMT2* were found to increase as a function of increasing external copper concentration, whereas only *LbMT1* responded to cadmium. The expression of both the genes was unaffected by zinc [37]. Reddy *et al.* (2014) also studied the functional complementation of both *LbMT1* and *LbMT2* genes in yeast mutants cup1 (*S.cerevisae* mutant for copper) and yap1 (*S. cerevisae* mutant for cadmium) through drop assay on SD media supplemented with heavy metal (Fig. **7**). The results clearly demonstrated the role of *LbMT1* and *LbMT2* genes in providing copper and cadmium tolerance. *LbMT1* was expressive in both cadmium and copper stress whereas *LbMT2* was mainly expressive in copper stress [37]. Also in case of *Hebeloma mesophaeum*, three MT isoforms (*HmMT1, HmMT2, HmMT3*) have been identified and characterized, among which HmMT1 is induced by zinc and cadmium whereas HmMT2 is induced by silver [69]. Similarly in case of *Hebeloma cylindrosporum* two metallothionein genes (*HcMT1* and *HcMT2*) have been characterized. Where *HcMT1* was expressive only in response to copper and *HcMT2* was expressive in response to both cadmium and copper [48]. The expression level of both *HcMT1* and *HcMT2* genes in response to different concentrations of cadmium and copper also also analyzed by RT-PCR analysis.The *HcMT1* transcription was induced by copper and *HcMT2* transcription was induced by cadmium [48]. This clearly shows that different isoforms of MT genes express differentially to different metals in different ECMs. In other studies on *Pisolithus albus* [22] and *Paxillus involutus* [71], only one metallothionein coding gene has been identified which is induced by both cadmium and copper stress.Many other metallothionein isoforms were also identified in other ectomycorrhizal fungi as listed in Table **1**.

4. GLUTATHIONE

Glutathione is a tripeptide (L-γ-glutamyl-L-cysteinyl-glycine) (307 Da) composed of 3 amino-acids, glutamate, cysteine and glycine. It is synthesized endogeneously and plays an important part in various cellular processes [72].

Glutathione is the most abundant non-protein thiol present in living systems. The normal glutathione concentration in yeast and fungi is approximately 10 mM [73]. Gluathione production has been reported in both prokaryotes and eukaryotes. Bacteria [74], algae [75], yeast [76], fungi [73], plants [77], mammals [78] all produce glutathione. Glutathione plays multiple roles in the cell; it is an efficient redox buffer [79], xenobiotic detoxifier [80], sulphur assimilator [81], heavy metal detoxifier [82], cell signaling component [79], and antioxidant [83]. Glutathione functions as an antioxidant in two ways: firstly, it oxidizes its thiol group in the presence of reactive oxygen species leading to the formation of oxidized glutathione (GSSG); secondly, it acts as an substrate for the enzymes like glutathione peroxidase which scavenges peroxides using glutathione as the reducing factor. Glutathione is a key component in metal scavenging, due to the high affinity of metals for its thiol (-SH) group and also as a precursor of phytochelatins (PCs).

4.1. Biosynthesis of Glutathione

The biosynthesis of GSH consists of 2 sequential ATP dependent reactions mediated by two enzymes γ-glutamylcysteinesynthetase (γECS; E.C.6.3.2.2) and glutathionesynthetase (GS; E.C.6.3.2.3).

Firstly, γ-glutamylcysteine (γ-EC) is formed from L-glutamate and L-cycteine by γ-glutamylcysteinesynthetase and then glycine is added to the C-terminal of γ-EC by glutathione synthetase (GS) forming Glutathione. Both the reactions require ATP as substrate (Fig.8). The γ-ECS is a rate limiting enzyme for GSH synthesis. In cell the γ-ECS activity is enhanced by Cd^{2+} ions and the expression of genes in GSH biosynthesis pathways is stimulated by As, Cd, Hg, Cr [84,85]. In plants γ-EC is restricted to plastids, whereas GS is localized in cytosol [86]. Two important factors affecting GSH synthesis are sulfur availability and γ-ECS

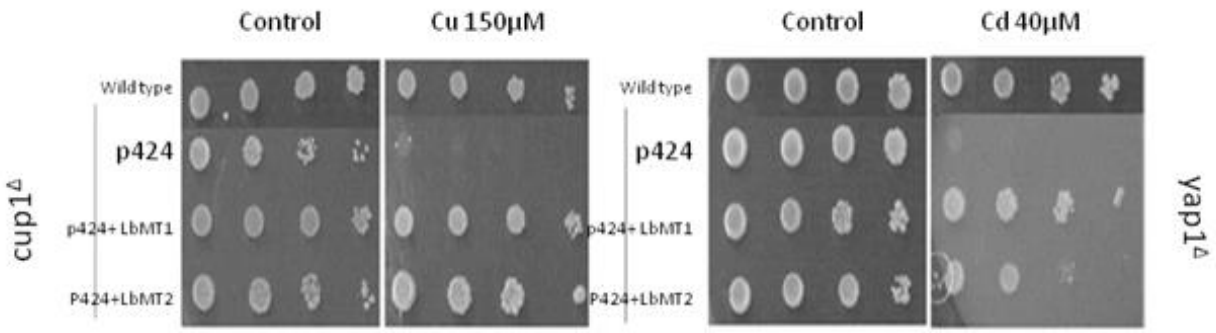

Fig. (7). Functional complementation of LbMT1 and LbMT2 in yeast Cu and Cd mutants, cup1Δ and yap1Δ respectively [37].

Table 1. Differential expression of different metallothionein isoforms in ectomycorrhizal fungi in response to different metal stress.

S.No	Ectomycorrhizal fungi	Metallothionein genes	Inducing metal	References
1.	*Pisolithus albus*	*PaMT1*	Copper, Cadmium	[22]
2.	*Laccaria bicolor*	*LbMT1*	Copper, Cadmium	[37]
		LbMT2	Copper	
3.	*Amanita strobiliformis*	*AsMT1a*	Silver	[40]
		AsMT1b	Silver, Cadmium	
		AsMT1c	Silver, Copper	
4.	*Amanita strobiliformis*	*AsMT1*	Silver, Copper	[68]
		AsMT2	Cadmium	
		AsMT3	Zinc	
5.	*Hebeloma cylindrosporum*	*HcMT1*	Copper	[48]
		HcMT2	Cadmium Copper	
6.	*Hebeloma mesophaeum*	*HmMT1*	Zinc Cadmium	[69]
		HmMT2	Silver	
		HmMT3	Silver	
7.	*Russula atropurpurea*	*RaZBP1*	Zinc	[70]
		RaZBP2	Zinc	
8.	*Paxillus involutus*	*PiMT*	Cadmium, Copper	[71]

activity (rate limiting). During metal toxicity both factors increase in order to meet the desired GSH demand for detoxification and survival [87]. The GSH synthesis in cell is controlled by the feedback inhibition, where GSH itself act as an inhibitor to γ-ECS activity. During metal stress, GSH inside the cell is oxidized and consumed in phytochelatin synthesis, resulting in depleting cellular GSH level which results in releasing the feedback inhibition and increasing GSH synthesis [88].

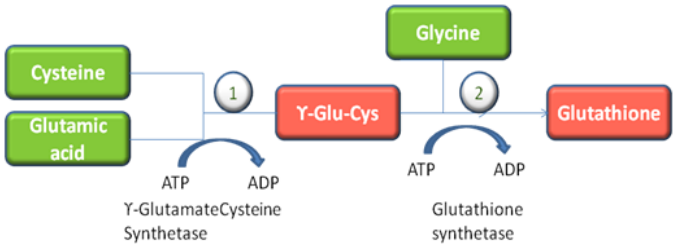

Fig. (8). Biosynthesis of glutathione - a two step reaction catalyzed by two ATP dependent enzymes γ-Glutamatecysteine synthetase and Glutathione synthetase.

Recently, studies have reported two more pathways named F-pathway and P-pathway for glutathione production in different organisms (Fig. **9**) [89]. Few organisms lacking genes for γ-ECS and GS were reported of producing glutathione. This observation threw light on the new pathway known as F-pathway for the synthesis of glutathione. In few strains of Gram-positive bacteria *Listeria monocytogenes*, *Streptococcus agalactiae*, *Streptococcus thermophilus* and *Pasteurella multocida* a novel bifunctional enzyme GshF was identified [90, 91, 92]. GshF functions both as γ-ECS and GS and performs complete synthesis of glutathione.

The third pathway identified is P-pathway. Bioinformatic analysis of some glutathione producing strains of yeast and *E.coli* revealed the absence of gene coding for γ-ECS but presence of GS in their genome. This observation gave rise to a new compensatory pathway for glutathione production. The gene *Pro1* in proline biosynthesis pathway encodes γ-Glutamyl kinase (GK) which catalyzes the formation of γ-glutamylphosphate which reacts with cysteine to form γ-

glutamylcysteine. Glutathione synthetase catalyzes the addition of glycine to produce glutathione.

4.2. Glutathione and Heavy Metal Detoxification

Glutathione has a dual protection mechanism. It acts as a metal scavenger during metal homeostasis and as an antioxidant during oxidative stress. As an antioxidant, it reacts non-enzymatically with different ROS. Cells under heavy metal stress generated ROS such as hydrogen peroxide (H_2O_2), superoxides ($O_2^{\bullet -}$) and hydroxyl radicals (•OH) which are the major contributors of oxidative damage. Glutathione in cell is present in both reduced-GSH and oxidized-GSSG. In reduced state, the thiol group of cysteine has the tendency to donate an electron to the unstable ROS like H_2O_2 and free radicals and neutralize them, but GSH itself becomes reactive and reacts with another reactive GSH to form oxidized GSSG [73]. This electron transfer is mediated by an enzyme glutathione peroxidase [93]. Glutathione reductase (a FAD-containing protein) further converts this GSSG to GSH using NADPH as an electron donator [94], thus maintaining the redox balance (Fig. **10**). The ratio of reduced to oxidized glutathione in a cell is used as a measure of cellular toxicity or oxidative stress.

The GSH/GSSG plays an important role in maintaining cell homeostasis. Qualitative and quantitative alterations in this ratio are considered as the indices of oxidative damage. If the ratio favors GSSG production, it signifies that the apoptosis may have triggered [95].

Glutathione act as sequester for various heavy metals and xenobiotics like fungicides, insecticides etc. (X). The GSH bind these toxic metal/xenobiotics forming a non-toxic GSH-X complex. This conjugation is catalyzed by the enzyme Glutathione-S-transferase. These GSH-X conjugates are then transported to vacuoles through the ABC (ATP-binding cassette) transporters [96]. The MRP (multidrug resistance related protein) transporters of ABC type undergo ATP hydrolysis to transport these conjugates across the vacuolar membrane [97]. The two ABC transporters, ABCC1 and ABCC2 have been identified as the major GSH-X complex transporters [98].

4.3. Regulation of Glutathione Synthesis

As explained earlier, glutathione is synthesized in a two step process, where synthesis of gamma glutamylcysteine is the rate limiting step. Hence the key regulator of glutathione synthesis is the gene coding for γECS. Like metallothioneins, γECS gene expression is also regulated on the transcriptional level. γECS in its promoter region carries AREs like sequences that match 11 out of 12 positions [99]. Two transcription factors, yAP-1 and Met-4, controls the

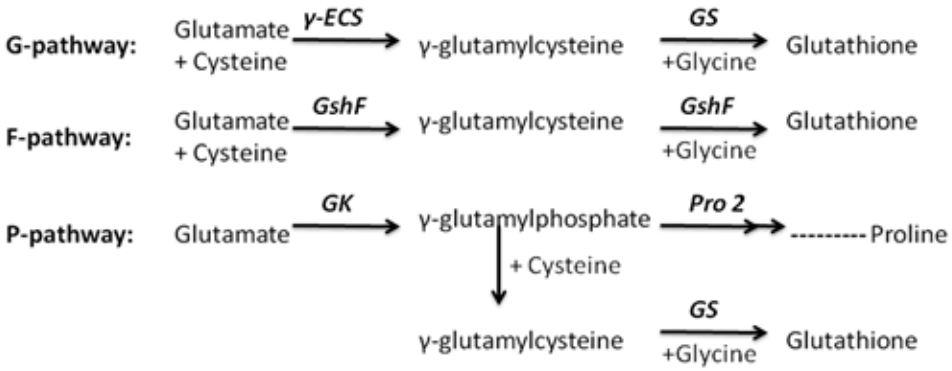

Fig. (9). Different pathways of glutathione production. G-pathway involves two enzymes γ-ECS and GS, F-pathway involves only one enzyme GshF and P-pathway involves GK and GS.

Fig. (10). Glutathione in alleviating oxidative stress by hydrogen peroxide. Role of glutathione peroxide and glutathione reducatse in maintaining cellular redox homeostasis.

expression of γECS gene. Under stress conditions, cellular glutathione gets depleted, which further activate yAP-1 and Met-4 target gene through oxidation of thioredoxin (which otherwise downregulate the yAP-1 mediated response [100]. In case of yeast, yAP-1 response elements (YREs) were recognized by yAP-1 protein [99]. Hence we can say that when an organism is exposed to stress, glutathione is depleted and oxidized thioredoxin is accumulated, which leads to the activation of yAP-1/Met-4 dependent transcriptional response of γECS [100].

4.4 Glutathione in Ectomycorrhizal Fungi

Many ectomycorrhizal fungi have been reported of producing glutathione in response to heavy metal stress. Courbot *et al.* (2004) reported no metallothionein but the increase in glutathione concentration in *Paxillus involutus* in response to cadmium stress [39]. Similar results were observed in case of *Laccaria laccata* [101]. Glutathione production in mycorrhizal fungi is mainly triggered by cadmium and arsenic stress followed by chromium, lead and copper [76]. Numerous studies have now confirmed the dominant role of glutathione as a cadmium chelator. *Glomus mosseae* also produced glutathione in response to cadmium whereas no glutathione was reported under lead stress [102]. *Funneliformis mosseae* was also reported to have increased glutathione levels in response to cadmium and arsenic [23]. *Phanerochaete chrysosporium* and *Penicillium chrysogenum* also clearly demonstrated the role of glutathione as an intracellular cadmium chelator [7, 103]. Putative genes encoding for the γ-Glutamylcysteine synthetase and glutathione synthetase have been reported in the genome of *Laccaria bicolor*, *Hebeloma cylindrosporum*, *Paxillus involutus* [46]. Detailed studies on glutathione metabolism in these fungi are still coming.

5. CONCLUSION

Since ectomycorrhizal fungi sustain in the heavy metal polluted soil, they have developed a full mechanism for tolerating and avoiding the heavy metals. They produce intracellular metal chelators 'glutathione and metallothioneins' which bind these heavy metals, rendering them detoxic and compartmentalize them into the cell vacuoles. Unlike other yeast and fungi, ectomycorrhizal fungi lacks phytochelatins. Metallothioneins are primarily induced by copper and zinc whereas glutathione responds actively to cadmium and arsenic. Since these ectomycorrhizal fungi thrive in a highly polluted soil it becomes inevitable to study the tolerance mechanisms in detail. They are the most potential candidates to be used in bioremediation of heavy metal contaminated soil.

GLOSSARY

Term	Definition
Bioremediation	Use of biological organisms to remove or detoxify the contaminants
Biosorption	Property of biomass to bind contaminants (heavy metals) on their cellular surface
Excavation	Physically removing the heavy metals by digging
Phytoremediation	Using plants for removing pollutants from contaminated soil
Vitrification	Melting soil at extremely high temperatures (1600–2000°C) and crystallizing the impurities
Phytoextraction	Use of hyperaccumulator plants that take up heavy metals from soil and store in a harvestable form.
Rhizofilteration	Plants absorb heavy metals from contaminated water and concentrate in roots
Phytostabilization	Plants stabilize the heavy metals in soil and prevention them from erosion
Phytovolatilization	Plants take up conatminants from the soil and volatize them in gaseous form

CONFLICT OF INTEREST

The authors confirm that this article content has no conflict of interest.

ACKNOWLEDGEMENTS

Declared none.

REFERENCES

[1] Su C, Jiang L, Zhang W. A review on heavy metal contamination in the soil worldwide: Situation, impact and remediation techniques. Environ Skep Crit 2014; 3: 24-38.

[2] Clemens S. Molecular mechanisms of plant metal tolerance and homeostasis. Planta 2001; 212: 475-486.

[3] Järup L. Hazards of heavy metal contamination. Brit Med Bull 2003; 68: 167-182.

[4] Hall JL. Cellular mechanisms of heavy metals detoxification and tolerance. J Exp Bot 2002; 53: 1-11.

[5] Gomes MP, Soares AM, Garcia QS. Phosphorus and sulfur nutrition modulate antioxidant defence in *Myracrodruom urundeuva* plants exposed to arsenic. J Hazard Mater 2014; 276: 97-104.

[6] Yadav SK, Dhote M, Kumar P, Sharma J, Chakrabarti T, Juwarkar AA. Differential antioxidative enzyme response of *Jatropha curcas* L. to chromium stress. J Hazard Mater 2013; 180: 609-615.

[7] Xu P, Zeng G, Huang D, *et al.* Metal bioaccumulation, oxidative stress and antioxidant defenses in *Phanerochaete chrysosporium* response to Cd exposure. Ecol Eng 2016; 87: 150-156.

[8] Raymond AW and Felix EO. Heavy metals in contaminated soils: A review of sources, chemistry, risks and best available strategies for remediation. ISRN Ecol 2011; 1:1-20.

[9] Khan FI, Husain T, Hejazi R. An overview and analysis of site remediation technologies. J Environ Manage 2004; 71: 95-122.

[10] Meier S, Borie F, Bolan N, Cornejo P. Phytoremediation of metal polluted soils by arbuscular mycorrhizal fungi. Crit Rev Env Sci Tec 2012; 42: 741-775.

[11] Rahman MA, Reichman SM, De Filippis L, Sany SB, Hasegawa H. Phytoremediation of Toxic Metals in Soils and Wetlands: Concepts and Applications. In: Environmental Remediation Technologies for Metal-Contaminated Soils 2016; 161-195.

[12] Prasad MNV. Metal hyperaccumulation in plants-biodiversity protecting from phytoremediation technology. Electron J Biotechnol 2003; 6: 285-321.

[13] Rajkumar M, Sandhay S, Prasad MNV, Freitas H. Perspectives of plant-associated microbes in heavy metal phytoremediation. Biotechnol Adv 2012; 30: 1562-1574.

[14] Ma Y, Prasad MNV, Rajkumar M, Freitas H. Plant growth promoting rhizobacteria and endophytes accelerate phytoremediation of metalliferous soils. Biotechnol Adv 2011; 29: 248-258.

[15] Schalk IJ, Hannauer M, Braud A. New roles of bacterial siderophores in metal transport and tolerance. Appl Environ Microbiol 2011; 13: 2844-2854.

[16] Rajkumar M, Ae N, Prasad MNV, Freitas H. Potential of siderophore-producing bacteria for improving heavy metal phytoextraction. Trends Biotechnol 2010; 28: 142-149.

[17] Wenzel WW. Rhizosphere processes and management in plant-assisted bioremediation (phytoremediation) of soils. Plant soil 2009; 321: 385-408.

[18] Braud A, Geoffroy V, Hoegy F, Mislin GLA, Schalk IJ. The siderophores pyoverdine and pyochelin are involved in *Pseudomonas aeruginosa* resistance against metals: Another biological function of these two siderophores. Environ Microbiol Rep 2010; 2: 419-425.

[19] Tripathi M, Munot HP, Shouche Y, Meyer JM, Goel R. Isolation and functional characterization of siderophore-producing lead and chromium resistant *Pseudomonas putida* KNP9. Curr Microbiol 2005; 50: 233-237.

[20] Li WC, Ye ZH, Wong MH. Metal mobilization and production of short-chain organic acids by rhizosphere bacteria associated with a Cd/Zn hyperaccumulating plant *Sedum alfredii*. Plant Soil 2010; 326: 453-467.

[21] Sheng XF, Xia JJ, Jiang CY, He LY, Qian M. Characterization of heavy metal-resistant endophytic bacteria from rape (*Brassica napus*) roots and their potential in promoting the growth and lead accumulation of rape. Environ Pollut 2008; 156: 1164-1170.

[22] Reddy MS, Kour M, Aggarwal S, Ahuja S, Marmeisse R, Fraissinet-Tachet L. Metal induction of a *Pisolithus albus* metallothionein and its potential involvement in heavy metal tolerance during mycorrhizal symbiosis. Environmental Microbiology 2016.

[23] Degola F, Fattorini L, Bona E, *et al*. The symbiosis between *Nicotiana tabacum* and the endomycorrhizal fungus *Funneliformis mosseae* increases the plant glutathione level and decreases leaf cadmium and root arsenic contents. Plant Physiol Bioch 2015; 92: 11-18.

[24] Bonfante P, Genre A. Mechanisms underlying beneficial plant-fungus interactions in mycorrhizal symbiosis. Nat Commun 2010; 1:48.

[25] Finlay RD. Ecological aspects of mycorrhizal symbiosis: with special emphasis on the functional diversity of interactions involving the extraradical mycelium. J Exp Biol 2008; 59: 1115-1126.

[26] Smith SE, Read DJ. Mycorrhizal symbiosis, 3rd edition, Academic press, San Diego 2010.

[27] Buee M, Reich M, Murat C, *et al*. 454 Pyrosequencing analyses of forest soils reveal an unexpectedly high fungal diversity. New Phytol 2009; 184: 449-456.

[28] Martin F, Nehls U. Harnessing ectomycorrhizal genomics for ecological insights. Curr Opin Plant Biol 2009; 12: 508-515.

[29] Harrison MJ. Signalling in the arbuscular mycorrhizal symbiosis. Annu Rev Microbiol 2005; 59: 19-42.

[30] Martin F, Aerts A, Ahren D, *et al*. The genome of *Laccaria bicolor* provides insight into mycorrhizal symbiosis. Nature 2008; 452: 88-92.

[31] Ma Y, He J, Ma C, *et al*. Ectomycorrhizas with *Paxillus involutus* enhance cadmium uptake and tolerance in *Populus canescens*. Plant Cell Environ 2014; 37: 627-642.

[32] Luo ZB, Li K, Gai Y, *et al*. The ectomycorrhizal fungi (*Paxillus involutus*) modulates leaf physiology of poplar towards improved salt tolerance. Environ Exper Bot 2011; 72: 304-311.

[33] Sousa NR, Ramos MA, Marque A, Castro PML. The effect of ectomycorrhizal fungi forming symbiosis with *Pinus pinaster* seedlings exposed to cadmium. Sci Total Environ 2012; 414: 63-67.

[34] Huang J, Nara K, Lian CL, *et al*. Ectomycorrhizal fungal communities associated with Masson pine (*Pinus massoniana Lamb.*) in Pb-Zn mine sites of central south China. Mycorrhiza 2012; 22: 589-602.

[35] Krznaric E, Verbruggen N, Wevers JHL, Carleer R, Vangronsveld J, Colpaert JV. Cd-tolerant *Suillus luteus*: a fungal insurance for pines exposed to cadmium. Environ Pollut 2009; 157: 1581-1588.

[36] Colpaert JV, Wevers JHL, Krznaric E, Adriaensen K. How metal-tolerant ecotypes of ectomycorrhizal fungi protect plant from heavy metal pollution. Ann For Sci 2011; 68: 17-24.

[37] Reddy MS, Prasanna L, Marmeisse R, Fraissinet-Tachet L. Differential expression of metallothioneins in response to heavy metals and their involvement in metal tolerance in the symbiotic basidiomycete *Laccaria bicolor*. Microbiology 2014; 160: 2235-2242.

[38] Ruytinx J, Nguyen H, Hees MV, *et al*. Zinc export results in adaptive zinc tolerance in the ectomycorrhizal basidomycetes *Suillus bovinus*. Metallomics 2013; 5: 1225-1233.

[39] Courbot M, Chalot M, Diez L, Leroy P, Ruotolo R. Cadmium responsive thiols in the ectomycorrhizal fungus *Paxillus involutus*. Appl Environ Microbiol 2004; 70: 7413-7417.

[40] Osobova M, Urban V, Jedelsky PL, *et al*. Three metallothionein isoforms and sequestration of intracellular silver in the hyperaccumulator *Amanita strobiliformis*. New Phytol 2011; 190: 916-926.

[41] Blaudez D, Botton B, Chalot M. Cadmium uptake and subcellular compartmentation in the ectomycorrhizal fungi *Paxillus involutus*. Microbiology 2000; 146: 1109-1117.

[42] Mendoza-Cózatl DG, Jobe TO, Hauser F, Schroeder JI. Long distance transport, vacuolar sequestration, tolerance, and transcriptional responses induced by cadmium and arsenic. Curr Opin Plant Biol 2011; 14: 554–562.

[43] Fomina MA, Alexander IJ, Colpaert JV, Gadd GM. Solubilization of toxix metal minerals and metal tolerance of mycorrhizal fungi. Soil Biol Biochem 2005; 37: 851-866.

[44] Wünschmann J, Beck A, Meyer L, Letzel T, Grill E, Lendzian KJ. Phytochelatins are synthesized by two vacuolar serine carboxypeptidases in *Saccharomyces cerevisiae*. FEBS lett 2007; 581: 1681-1687.

[45] Clemens S, Simm C. *Schizosaccharomyces pombe* as a model for metal homeostasis in plant cells: the phytochelatin-dependent pathway is the main cadmium detoxification mechanism. New Phytol 2003; 159: 323-30.

[46] Bellion M, Courbot M, Jacob C, Blaudez D, Chalot M. Extracellular and cellular mechanisms sustaining metal tolerance in ectomycorrhizal fungi. FEMS Microbiol Lett 2006; 254: 173-181.

[47] Diaz S, Martin-Gonzalez A, Gutierrez JC. Evaluation of heavy metal acute toxicity and bioaccumulation in soil ciliated protozoa. Environ Int 2006; 711-717.

[48] Ramesh G, Podila GK, Gay G, Marmeisse R, Reddy MS. Differential pattern of regulation for the copper and cadmium induced metallothioneins of the ectomycorrhizal fungus *Hebeloma cylindrosporum*. Appl Environ Microbiol 2009; 75: 2266-2274.

[49] Waalkes MP, Goering PL. Metallothionein and other cadmium-binding proteins: recent developments. Chem Res Toxicol 1990; 3: 281-288.

[50] http://www.uniprot.org/docs/metallo.txt; Date of access: 20th Jan 2016.

[51] Binz PA, Kägi JH. Metallothionein: molecular evolution and classification. In: Metallothionein IV. Birkhäuser Basel 1999; pp. 7-13.

[52] Robinson NJ, Tommey AM, Kuske C, Jackson PJ. Plant metallothioneins. Biochem J 1993; 295: 1–10.

[53] Palacios Ò, Atrian S, Capdevila M. Zn-and Cu-thioneins: a functional classification for metallothioneins?. J Biol Inorg Chem 2011; 16: 991-1009.

[54] Pagani A, Villarreal L, Capdevila M, Atrian S. The *Saccharomyces cerevisiae Crs*5 metallothionein metal-binding abilities and its role in the response to zinc overload. Mol Microbiol 2007; 63: 256–269.

[55] Ngu TT, Stillman MJ. Metal-binding mechanisms in metallothioneins. Dalton Trans 2009; 28: 5425-5433.

[56] Blindauer CA, Leszczyszyn OI. Metallothioneins: unparalleled diversity in structures and functions for metal ion homeostasis and more. Nat Prod Rep 2010; 27: 720-741.

[57] Cobine PA, McKay RT, Zangger K, Dameron CT, Armitage IM. Solution structure of Cu6 metallothionein from the fungus *Neurospora crassa*. Eur J Biochem 2004; 271: 4213-4221.

[58] Calderone V, Dolderer B, Hartmann HJ, *et al*. The crystal structure of yeast copper thionein: the solution of a long-lasting enigma. Proc Natl Acad Sci USA 2005; 102: 51-56.

[59] Blindauer CA, Harrison MD, Parkinson JA, *et al*. A metallothionein containing a zinc finger within a four-metal cluster protects a bacterium from zinc toxicity. Proc Natl Acad Sci 2001; 98: 9593-9598.

[60] Capdevila M, Bofill R, Palacios O, Atrian S. State-of-the-art of metallothioneins at the beginning of the 21st century. Coord Chem Rev 2012; 256: 46-62.

[61] Li H, Otvos JD. Biphasic kinetics of Zn^{2+} removal from Zn metallothionein by nitrilotriacetate are associated with differential reactivity of the two metal clusters. J Inorg Biochem 1998; 70: 187-194.

[62] Ejnik J, Robinson J, Zhu J, Försterling H, Shaw CF, Petering DH. Folding pathway of apo-metallothionein induced by Zn^{2+}, Cd^{2+} and Co^{2+}. J Inorg Biochem 2002; 88: 144-152.

[63] Guirola M, Pérez-Rafael S, Capdevila M, Palacios Ò, Atrian S. Metal dealing at the origin of the Chordata phylum: the metallothionein system and metal overload response in *Amphioxus*. PloS one 2012; 7: e43299.

[64] Park YH, Lee YM, Kim DS, *et al.* Hypothermia enhances induction of protective protein metallothionein under ischemia. J Neuroinflammation 2013; 10: 21-36.

[65] Jan AT, Azam M, Ali A, Haq QM. Prospects for exploiting bacteria for bioremediation of metal pollution. Crit Rev Env Sci Tec 2014; 44: 519-560.

[66] Shukla D, Trivedi PK, Nath P, Tuteja N. Metallothioneins and Phytochelatins: Role and Perspectives in Heavy Metal (loid) s Stress Tolerance in Crop Plants. In: Abiotic Stress Response in Plants 2016; pp. 233-274.

[67] Davis SR, Cousins RJ. Metallothionein expression in animals: a physiological perspective on function. J Nutr 2000; 130: 1085-1088.

[68] Hložková K, Matěnová M, Žáčková P, *et al*. Characterization of three distinct metallothionein genes of the Ag-hyperaccumulating ectomycorrhizal fungus *Amanita strobiliformis*.FungalBiol 2015; doi:10.1016/j.funbio.2015. 11.007.

[69] Sácký J, Leonhardt T, Borovička J, Gryndler M, Briksí A, Kotrba P. Intracellular sequestration of zinc, cadmium and silver in *Hebeloma mesophaeum* and characterization of its metallothionein genes. Fungal Genet Biol 2014; 67: 3-14.

[70] Leonhardt T, Sácký J, Šimek P, Šantrůček J, Kotrba P. Metallothionein-like peptides involved in sequestration of Zn in the Zn-accumulating ectomycorrhizal fungus *Russula atropurpurea*. Metallomics 2014; 6: 1693-1701.

[71] Bellion M, Courbot M, Jacob C, Guinet F, Blaudez D, Chalot M. Metal induction of a *Paxillus involutus* metallothionein and its heterologous expression in *Hebeloma cylindrosporum*. New Phytol 2007; 174: 151-158.

[72] Townsend DM. S-Gluathionylation: indicator of cell stress and regulator of the unfolded protein response. Mol Interventions 2007; 7: 313-324.

[73] Pócsi I, Prade RA, Penninckx MJ. Glutathione, altruistic metabolite in fungi. Adv Microb Physiol 2004; 49: 1-76.

[74] Smirnova GV, Oktyabrsky ON. Glutathione in bacteria. Biochemistry (Moscow) 2005; 70: 1199-1211.

[75] Chen H, Chen J, Guo Y, Wen Y, Liu J, Liu W. Evaluation of the role of the glutathione redox cycle in Cu (II) toxicity to green algae by a chiral perturbation approach. Aquat Toxicol 2012; 120: 19-26.

[76] Ilyas S, Rehman A. Oxidative stress, glutathione level and antioxidant response to heavy metals in multi-resistant pathogen, *Candida tropicalis*. Environ Monit Assess 2015; 187: 1-7.

[77] Noctor G, Mhamdi A, Chaouch S, *et al*. Glutathione in plants: an integrated overview. Plant Cell Environ 2012; 35: 454-484.

[78] Bhowmick D, Srivastava S, D'Silva P, Mugesh G. Highly efficient glutathione peroxidase and peroxiredoxin mimetics protect mammalian cells against oxidative damage. Angew Chem 2015; 127: 8569-8573.

[79] Foyer CH, Noctor G. Redox homeostasis and antioxidant signaling: a metabolic interface between stress perception and physiological responses. Plant Cell 2005; 17: 1866-1875.

[80] Cummins I, Dixon DP, Freitag-Pohl S, Skipsey M, Edwards R. Multiple roles for plant glutathione transferases in xenobiotic detoxification. Drug Metab Rev 2011; 43: 266-280.

[81] Kopriva S. Regulation of sulfate assimilation in Arabidopsis and beyond. Ann Bot 2006; 97: 479-495.

[82] Cobbett CS. Phytochelatins and their roles in heavy metal detoxification. Plant Physiol 2000; 123: 825-832.

[83] Mittova V, Theodoulou FL, Kiddle G, *et al*. Coordinate induction of glutathione biosynthesis and glutathione-metabolizing enzyme is correlated with salt tolerance in tomato. FEBS Lett 2003; 554: 417-421.

[84] Vido K, Spector D, Lagniel G, Lopez S, Toledano MB, Labarre J. A proteome analysis of the cadmium response in *Saccharomyces cerevisiae*. J Biol Chem 2001; 276: 8469-8474.

[85] Thorsen M, Lagniel G, Kristiansson E, *et al*. Quantitaive transcriptome, proteome, and sulfur metabolite profiling of the *Saccharomyces cerevisiae* response to arsenite. Physiol Genomics 2007; 30: 35-43.

[86] Wachter A, Wolf S, Steininger H, Bogs J, Rausch T. Differential targeting of GSH1 and GSH2 is achieved by multiple transcription initiation: Implications for the compartmentation of glutathione biosynthesis in the *Brassicaceae*. Plant J 2005; 41: 15–30.

[87] Jozefczak M, Remans T, Vangronsveld J, Cuypers A. Glutathione is a key player in metal-induced oxidative stress defenses. Int J Mol Sci 2012; 13: 3145-3175.

[88] Hibi T, Nii H, Nakatsu T, *et al*. Crystal structure of gamma-glutamylcysteine synthetase: insights into the mechanism of catalysis by a key enzyme for glutathione homeostasis. Proc Natl Acad Sci USA 2004; 101: 15052–15057.

[89] Tang L, Wang W, Zhou W, *et al*. Three-pathway combination for glutathione biosynthesis in *Saccharomyces cerevisiae*. Microb Cell Fact 2015; 14: 1-12.

[90] Gopal S, Borovok I, Ofer A, *et al*. A multidomain fusion protein in *Listeria monocytogenes* catalyzes the two primary activities for glutathione biosynthesis. J Bacteriol 2005; 187: 3839–3847.

[91] Janowiak BE, Griffith OW. Glutathione synthesis in *Streptococcus agalactiae* one protein accounts for γ-glutamylcysteine synthetase and glutathione synthetase activities. J Biol Chem 2005; 280: 11829–11839.

[92] Vergauwen B, De Vos D, Van Beeumen JJ. Characterization of the bifunctional γ-glutamate–cysteine ligase/glutathione synthetase (GshF) of *Pasteurella multocida*. J Biol Chem 2006; 281: 4380–4394.

[93] Margis R, Dunand C, Teixeira FK, Margis-Pinheiro M. Glutathione peroxidase family–an evolutionary overview. Febs Journal 2008; 275: 3959-3970.

[94] Marty L, Siala, W, Schwarzlander M, *et al*. The NADPH-dependent thioredoxin system constitutes a functional backup for cytosolic glutathione reductase in Arabidopsis. Proc Natl Acad Sci USA 2009; 106: 9109–9114.

[95] Shakhristova EV, Stepovaya EA, Ryazantseva NV, *et al*. Role of glutathione system redox potential in apoptosis dysregulation in mcf-7 breast adenocarcinoma. Bull Exp Biol Med 2016; 160: 364-367.

[96] Schlunk I, Krause K, Wirth S, Kothe E. A transporter for abiotic stress and plant metabolite resistance in the ectomycorrhizal fungus *Tricholoma vaccinum*. Environ Sci Pollut Res 2015; 1: 1-10.

[97] Klein M, Mamnun YM, Eggmann T, *et al*. The ATP-binding cassette (ABC) transporter Bpt1p mediates vacuolar sequestration of glutathione conjugates in yeast. FEBS lett 2002; 520: 63-70.

[98] Song WY, Park J, Eisenach C, Maeshima M, Lee Y, Martinoia E. ABC Transporters and Heavy Metals. In Plant ABC Transporters 2014; 22: 1-17.

[99] Wu AL, Moye-Rowley WS. GSH1, which encodes gamma-glutamylcysteine synthetase, is a target gene for yAP-1 transcriptional regulation. Mol Cell Biol 1994;14:5832-5839.

[100] Wheeler GL, Trotter EW, Dawes IW, Grant CM. Coupling of the transcriptional regulation of glutathione biosynthesis to the availability of glutathione and methionine via the Met4 and Yap1 transcription factors. J Biol Chem 2003; 278: 49920-49928.

[101] Gallie U, Meire M, Brunold C. Effect of cadmium on nonmycorrhizal and mycorrhizal Norway spruce seedlings *Picea abies* (L) Karst and its ectomycorrhizal fungi *Laccaria laccata* (Scop ex Fr) Bk and Br- sulfate reduction, thiols and distribution of the heavy-metals. New Phytol 1993; 125: 837-843.

[102] Garg N, Aggarwal N. Effects of interactions between cadmium and lead on growth, nitrogen fixation, phytochelatin, and glutathione production in mycorrhizal *Cajanus cajan* (L.) Millsp. J Plant Growth Regul 2011; 30: 286-300.

[103] Xu X, Xia L, Zhu W, Zhang Z, Huang Q, Chen W. Role of *Penicillium chrysogenum* XJ-1 in the detoxification and bioremediation of cadmium. Front Microbiol 2015; 6: 1-10.